Studies on Abiotic Stress Tolerance in *Hordeum vulgare* L. Genotypes from Arid and Temperate Regions

Muhammad Naeem Shahwani

Thesis Submitted for the Degree of
Doctor of Philosophy

College of Medical, Veterinary and Life Sciences,
School of Life Sciences
University of Glasgow
U.K.

July, 2011

ABSTRACT

Plants growing in arid regions often suffer from high shoot temperatures, low shoot water concentrations, low turgor pressures, and high salinity in the rhizosphere. To investigate which traits confer tolerance on plants in these areas a range of genotypes was studied. These included Local (an uncharacterized landrace grown in south western Pakistan), Soorab-96 and Awaran-2002 (both elite cultivars developed by ICARDA and commercially grown in Pakistan), and Optic (an elite European cultivar). Measurements on germination, growth, and yield suggested that landrace Local is significantly least affected by high salinity ($p < 0.05$) compared with lines Soorab-96, Awaran-2002 and Optic. Further investigations on ion profiling established that landrace Local could maintain low Na^+/K^+ ratios. This appeared to arise from Local's ability to prevent Na^+ accumulation in the roots and shoots by enhanced exclusion or efflux or both. Probably this unique characteristic of landrace Local helped in maintaining its photosynthetic efficiency, plant water status, and stomatal conductance, which resulted in its better performance and survival in high salinity. There was no evidence that high tissue solute concentrations, high proline levels or life cycle strategies played a role in salt stress tolerance. In addition, there was no evidence that osmotic stress was responsible for the observed suppression of growth in any of the genotypes. The main conclusion from this study is that for glycophytes (which do not complete a full life cycle above 100 mM NaCl; this includes all of the world's major crops), it is the ionic component of salinity stress that impairs growth processes and yield, not the osmotic component. Further research on salinity stress in crops should focus on understanding the processes that control ionic balance rather than osmoregulation. There is some evidence that long term exposure of plants in the preceding generations to moderately high salt concentrations (*e.g.* 100 mM NaCl) improves barley halotolerance in succeeding generations, *i.e.* halotolerance has a transgenerational, epigenetic basis, but there was also evidence that the improved halotolerance in the Local genotype was partly genetic.

In another series of experiments the importance of short periods of high leaf temperatures (T_{leaf}) on photosynthetic efficiency of barley genotypes Local, Optic, and Soorab-96 was investigated. In all three genotypes light saturated carbon dioxide assimilation rates (A_{sat}) and the carboxylation coefficients (Φ_{CO2}, a measure of the efficiency of CO_2 fixation) in the fourth fully expanded leaves were equally suppressed to approximately 20 % of their pre-treatment levels immediately after a short period of

heat stress ($T_{leaf} > 40.0 \pm 0.5$ °C for 20 minutes). Parallel measurements using a range of techniques confirmed that the suppression of A_{sat} and Φ_{CO2} was not attributable to changes in the light harvesting capacity (leaf absorptance and *chla* excitation spectra), maximum quantum efficiency of PSII (Φ_{PSII}, Fv/Fm), and to stomatal conductance (g_s). It is unlikely that the suppression arose from damage to the electron transport chain, or to the capacity to develop or maintain non-photochemical quenching (NPQ, which is dependent on the transthylakoid ΔpH), but these possibilities cannot be dismissed. LC-MS and enzymic analysis of leaf metabolite levels showed that the pools of metabolites feeding into RuBisCO are not affected by heat stress whilst those of the metabolites flowing away from RuBisCO were significantly depleted. The implication is that short periods of heat stress severely impairs RuBisCO, RuBisCO Activase, or processes close to the carboxylation step. Five days after heat stress A_{sat} and ΦCO$_2$ had significantly recovered to approximately 40 % ($p < 0.05$) of their pre-stress levels in landrace Local, but no significant recovery was observed in any of the elite lines including those distributed by ICARDA for arid land production. These findings provide evidence that thermal damage may play a significant role in yield suppressions in arid regions and that there is a genetic basis for thermotolerance in barley[1].

---

[1] Some of the work presented in this thesis has been given as oral presentations at two international scientific meetings.
1. International Conference on Food Security and Climate Change in the Dry Areas, by ICARDA in Amman-Jordan from 1-4th February 2010.
2. SEB Annual Conference, Prague, 30th June-3rd July 2010.

بِسْمِ اللَّهِ الرَّحْمَٰنِ الرَّحِيمِ

In the Name of Almighty Allah (God), Most Gracious, Most Merciful

ACKNOWLEDGEMENTS:

TABLE OF CONTENTS

List of Figures

List of Tables

List of Abbreviations

α	Quantum Yield of Photosynthesis.
A	CO_2 Assimilation Rate.
ABA	Abscisic Acid.
ADP	Adenosine diphosphate.
ADPG	ADP-glucose.
AMP	Adenosine monophosphate.
A_{max}	Maximum Photosynthesis Rate.
A_{sat}	Light Saturated Photosynthesis Rate.
A_n	Net Photosynthesis Assimilation.
ATP	Adenosine Tri Phosphate.
bp	Base pair.
C_a	Air CO_2 Concentration.
Cc	Chloroplast CO_2 Concentration.
C_i	Internal CO_2 Concentration.
Chl*a* and Chl*b*	Chlorophyll a and b.
cDNA	Complementary Deoxyribonucleic Acid.
CDPK	Calcium Dependent Protein Kinase.
CRC	CO_2 Response Curve.
dS m^{-1}	DeciSiemens per meter.
DHAP	Di Hydrogen Adenosine Phosphate.
2D LC-MS	2 Dimensional Liquid Chromatography / Mass spectrometry.
DTT	Dithiothreitol.
D Wt	Dry Weight.
E	Transpiration Rate.
EC	Electrical Conductivity.
EDTA	Ethylenediamine tetra acetic acid.
ETR	Photosynthetic Electron Transport Rate.
FAO	Food and Agricultural Organization of the United Nation.
FBP	Fructose Bisphosphate.
F6P	Fructose 6 Phosphate.
F_0	Base Fluorescence.
Fm	Maximum Fluorescence.

Fv	Variable Fluorescence.
FSC & RD	Federal Seed Certification and Registration Department.
F Wt	Fresh Weight.
GABA	γ-4-aminobutyric acid.
GAD	Glutamate Decarboxylase.
GB	Glycinebetaine.
G1P, G3P and G6P	Glucose 1, 3 and 6 Phosphate.
gDNA	genomic Deoxyribonucleic acid.
gs	Stomatal Conductance.
gm	Mesophyll Conductance.
HSPs	Heat Shock Proteins.
ICARDA	International Centre for Agricultural Research in the Dry Areas.
ICP-OES	Inductively Coupled Plasma Optical Emission Spectroscopy.
IRGA	Infra Red Gas Analyzers.
kDa	Kilo Daltons.
kHz	Kilo Hertz.
LRC	Light Response Curve.
LHCP	Light Harvesting Chlorophyll–Protein Complexes.
LS & SS	Large Subunits & Small Subunits.
MAPK	Mitogen Activated Protein Kinases.
MPa	Mega Pascal.
mRNAs	Messenger Ribonucleic acids.
NADPH	Nicotinamide Adenine Dinucleotide Phosphate-Oxidase.
NPQ	Non-Photochemical Quenching.
OEC	Oxygen Evolving Complex.
PAR	Photosynthetic Active Radiation.
PEP	Phosphoenol pyruvate.
PGA	Phosphoglyceric Acid.
pH	Hydrogen Ion Concentration Unit.
ppm	Part Per Million.
psi	Pounds Per Square inch.
PPFD	Photosynthetic Photon Flux Density.
PSI & PSII	Photosystem 1 & 2.

Rd	Dark Respiration.
$^{mit}R_L$ & $^{mit}R_D$	Mitochondrial Photorespiration and Dark Respiration.
$^{Tot}R_L$	Total Photorespiration.
ROSs	Reactive Oxygen Species.
Rl	Photorespiration.
rpm	Revolution Per Minute.
R5P	Ribulose 5 Phosphate.
RuBiCO	Ribulose Bisphosphate Carboxylase-Oxygenase.
RuBP	Ribulose Bisphosphate.
S7P	Sedhabtulose 7 Phosphate.
spp	Species.
T_{leaf} and T_{air}	Leaf and Air Temperature, respectively.
UDPG	UDP-glucose.
V_0	Apparent Photorespiration.
VPDs	Vapour Pressure Deficits.
X5P	Xylulose 5 Phosphate.
Γ	CO_2 Compensation Point.
Φ_{CO2}	Carboxylation Efficiency.
Φ_{PSII}	Maximum Quantum Efficiency of PSII (Fv/Fm).
ψ_{H2O}	Water Potential.
ψ_P	Turgor Pressure.
$^{Cyt}\psi_s$	Cytoplasm Solute Potential.
$^{Tissue}\psi_s$	Tissue Cell Sap Water Potential.
$^{vac}\psi_s$	Vacuole Solute Potential.
$^{xylem}\psi_s$	Exuded Xylem Fluid Water Potential.

Declaration

I declare that this thesis for the degree of Doctor of Philosophy has been edited entirely by me and the work presented herein was performed by me unless stated otherwise.

Signature .... Date ....

Chapter 1: Introduction

1.1 *Food Supply and Population Growth in the 21st Century*

Over the last century global food production (agricultural production) has increased dramatically due to the application of better agronomic practices, integrated pest control methods, classical plant breading, and advance bioengineering technologies. (Huang *et al.*, 2006; Pretty, 2008). In particular cereal crop yields have literally doubled during the last 50 years since the Green Revolution (Fischer and Edmeades, 2010; Kishore and Shewmaker, 1999; Toenniessen *et al.*, 2003). These achievements are attributed to the efforts of farmers, agronomists, and plant biologists (Mann, 1999). It is likely, however, that both increased yields and the acquisition of new arable land will be required to meet the needs of the 21st Century. Whatever technologies are developed and used, they must be sustainable in the long term (Bassett, 2010).

Food production is not uniformly distributed across the globe due to the diversity of terrain, local climatic conditions, and the available agricultural expertise. Clearly, there is a limit to the amount of land available for food production, and to the theoretical limit on the maximum attainable yield of any given crop (Barrett, 2010). At present, global food production is unbalanced; 183 nations in the world depend on food from outside their borders (food imports) and this food comes from those countries with relatively low populations that practice intensive agriculture. Eighty percent of cereal export is from the United States, Canada, Australia, and Argentina (Bureau, 2004; Marchione and Messer, 2010), but this will not be the case in the next 60 years if the World population continues to rise.

Overall, based on realistic trends in food supply, on one hand these countries may no longer be in a position to export food by 2050 (Beddington, 2010; Brown, 2000). On the other hand the World's population doubled between 1900 and 1960; by 2000, the population had reached 6.8 billion citizens, more than three-and-a-half times the population of 1900 (U.S. Census Bureau - World POP Clock Projection). The World Bank and the United Nations FAO documented that 1 to 2 billion people are now malnourished due to a combination of the inadequate food supply, low income, and unfair food distribution (Pimental *et al.*, 1997). Most of these live in developing countries, and includes one third of the population of sub-Saharan Africa. To meet the rising global demand for food it will be necessary to both increase yields on land currently cultivated,

and to appropriate new land for arable production. For the long term protection of the environment new production will have to be achieved on marginal lands that hitherto have been considered too uneconomical for the production of the major cereals (Lang, 2010; Turner *et al*., 2005). Large tracts of marginal land are available at high latitudes in the Americas and Asia (Gardner *et al*., 2010); here spring rainfall and temperatures are adequate, but sporadic early spring frosts prove catastrophic for the production of maize and wheat (Porter, 2005). In addition, at lower latitudes there are extensive tracts of arid land (e.g. in the Americas, Asia, Africa, and Australia) but here cereal production is limited by a range of abiotic stress factors and plants are faced with a number of different challenges (Lobell and Asner, 2003). Extractable soil water content may be low, and the water potential of what is available may also be low (more negative than -1.3 MPa) due to the presence of high levels of electrolytes. For crops to grow well in these regions several complex traits are required including the uptake and compartmentation, or exclusion, of electrolyte (Zhang *et al*., 2010), and the extraction of moisture from soils with low field capacities (Yoshida *et al*., 2010). In addition to these rhizosphere stresses, high vapour pressure deficits (VPDs) are normal in these regions leading to excessive water loss through transpiration resulting in an initial loss of turgor pressure, and in very extreme cases, of desiccation to low tissue water concentrations that impair metabolism (Way and Oran, 2010). Loss of turgor has several important consequences for plant growth and survival such as reductions in cell expansion (growth), stomatal conductance (g_s) which will in turn prevent carbon dioxide assimilation and evaporative cooling of leaves (Cornic, 2000; Lu and Huang, 2008; Radin *et al*., 1994), and the transport to the shoot of nutrient ions via the transpiration stream (Benlloch-Gonzalez *et al*., 2010). Again, a large number of genes will be required to encode the proteins that carry out these various processes. These include those associated with the following: g_s (signalling, stomatal density and morphology, etc.); heat tolerance (heat shock proteins, dissipation of absorbed light energy); the acquisition, synthesis, and compartmentation of inorganic and compatible organic solutes for regaining turgor pressure (Wahid *et al*., 2007).

1.2 *Abiotic Stress: A Worldwide Problem in Agriculture*

The greatest challenge for humanity in the next few decades will be how to increase and sustain arable production without degrading land. Land degradation is proceeding rapidly. The Global Assessment of Land Degradation (GLASOD) estimate that a total of 1964 million hectares have degraded, 910 million hectare to at least a moderate degree (with

significantly reduced productivity), and 305 million hectare strongly degraded (no longer suitable for agriculture). Based on these data, water erosion was the most common problem, affecting almost 1,100 million hectare (Bossio *et al.*, 2010; Sanders, 1992).

1.2.1 Soil Salinity

Figure 1-1: Salt-affected Soils are Visible on Rangelands in Tropics (Thomas, 2009).

Salinity affects 15% of the world's land area, which amounts to 930 million hectares (Rengasamy, 2006). However, land suffering from various degrees of soil salinity has increased from about 48 % of the total irrigated lands in 1990, to 64 % in 2000 (Egamberdieva *et al.*, 2010). Irrigation is important for agriculture; irrigated land, which accounts for 15 % of total arable land, produces at least double that of rain-fed land. In total irrigated arable land produces 1/3 of the world food supply (Munns, 2002). Salinization can cause yield decreases of 10 to 25 percent for many crops, and may prevent cropping altogether when it is severe (Grattan, 2010). Salinity also occurs through natural processes from the accumulation of salts over long periods of time in the soil or groundwater. It is caused by two natural processes: (1) the weathering of parent materials containing soluble salts, and (2) the deposition of oceanic salt carried in wind and rain. Salinization caused by natural or human-induced processes also results in the accumulation of dissolved salts in the soil water and subsequently inhibits plant growth (Munns, 2009).

1.2.1.1 The Effect of Salinity on Agriculture

More than 99 % of the world's food supply comes from land and less than 1 % is from seas, oceans, and other aquatic habitats (FAO, 1991). The total arable land on the earth is approximately 13 billion hectares of which 6 billion hectares are located in arid and semiarid regions, and about 17 % of this is severely affected by salt. In irrigated areas, which constitute 230 million hectares world-wide, 33 % is affected by salt (Ashraf, 1994). Thus, the magnitude and the seriousness of the problem cannot be understated. Moreover, 40000 hectares of land world-wide is being lost every year from agriculture due to salinity (Al-Khatib *et al.*, 1993). It is also estimated that 250000 hectares of cultivated area in South Western Australia has become unproductive because of soil salinity (Malcolm, 1982).

The FAO also reported (FAO, 1991) that 20-30 million hectares of cultivated land is severely affected by salinity, and an additional 60-80 million hectares are affected to some extent. Only about 10 % of total arable land on the Earth can be considered as free from salt stress (Ashraf, 1994). In a survey on the distribution of 323 million hectares of saline soils throughout the World, 54 million hectares of the total is located in Africa, 17 million hectares in Australia, 20 million in Mexico and Central America, 60 million hectares in North America, 69 million hectares in South America, 83 million hectares in Southern Asia, and 20 million hectares in Southeast Asia (Massoud, 1974). In general, there is a strong correlation between global agriculture yields and soil salinity.

1.2.1.2 Classification of Plants According to Their Tolerance of Salinity

Plants can be broadly classified into two groups according to their tolerance of salinity: (1) the salt sensitive plants, termed as 'glycophytes': (2) the salt tolerant plants, or 'halophytes'. Unfortunately, the major crops of the world are glycophytes that can not grow in saline habitats where salt concentrations are above approximately100 mM NaCl. These plants do not appear to possess mechanisms for adapting to the harmful effects of salinity. These glycophytes have evolved in habitats with very low soil Na^+ content, and may never have possessed the mechanisms or features to enable them to cope with the water deficits and ion levels prevailing in saline habitats (Greenway and Munns, 1980). Some classifications categorize plants as follows: tolerant, moderately tolerant, moderately sensitive, and sensitive, with respect of their response to salinity (Maas and Grieve, 1987). For instance barley, cotton, and sugar beet are considered tolerant because they can grow in the salinity range of 6.9 to 8.0 dS m^{-1} (77-88 mM NaCl) without any apparent loss of

yields, whereas most fruit trees, carrot, and onion are considered sensitive with yield loss thresholds of less than 2.0 dS m^{-1} (22 mM NaCl; Flowers, 2004). What is required is the development of major crop varieties that can grow in saline soils without losing their ability to produce high usable yields. The US Laboratory of Salinity define a saline soil as one with a saturation extract (the solution extracted from a soil at its saturation water content) electrical conductivity (EC) of greater than 4 dS m^{-1}, (equivalent to approximately 45 mM NaCl; Corwin *et al.*, 2003). The growth of many glycophytes is significantly limited in concentrations as low as 25-50 mM NaCl (Lessani and Marschner, 1978). In contrast, many halophytes grow well in high concentrations of NaCl, and complete their life cycle in full-strength sea water (*ca.* 560 mM NaCl). Clearly, halophytes have the ability to avoid and/or get rid of toxic ions by mechanisms preventing them from accumulating at metabolic sites and impairing growth; many have specialized organs such as glands and bladders (Yeo, 1998). NaCl inhibits the *in vitro* activity of many enzymes (Flowers *et al.*, 1977; Greenway and Munns, 1980). The cytoplasm of plant cells typically contain about 100 mM K^{+}, and plant metabolism has, therefore, evolved to work efficiently at this concentration. Increased levels of Na^{+} disrupt the ionic balance of the cytoplasm: "the physicochemical properties of K^{+} and Na^{+} are similar, but not identical". As Na^{+} levels in the cytoplasm raise, the ionic interactions within and between proteins, their co-factors, and substrates alters so that metabolism is no longer optimized. As a result, the activities of many enzymes operating in different pathways are perturbed (Flowers *et al.*, 1977).

1.2.1.3 The Deleterious Effects of High Salinity on Plants

Upon exposure, the primary effect of salt on plants is an osmotic stress (Jones, 1993) which causes dehydration and loss of turgor (within 1 hr). Subsequently, ingression of ions into cells can result in ion toxicity. Munns and co-workers (Munns *et al.*, 1995) tested wheat and barley genotypes for salt tolerance and noticed that there were two stages of growth response to salt stress. Initially, they identified a large decrease in growth rate, which arises from the loss of cell turgor. If the plant can regain turgor there is the potential to resume growth, but there is often a second reduction due to salt specific responses that originate from the accumulation of salt at toxic levels within the cell. This may arise through disruption in the normal hormonal signals from roots. Under salt stress conditions, endogenous levels of a plant hormone, abscisic acid (ABA) increase (Gómez *et al.*, 1988), which appears to act as a signal to promote tissue acclimation (Chandler and Robertson, 1994). Elevated ABA levels have been correlated with increased tolerance to salt (Singh *et*

al., 1987), and exogenous application of ABA accelerated the adaptation of cultured tobacco cells to salt (Larosa *et al.*, 1987), which provide further support for a role of ABA in the acclimation of plants to salinity and osmotic stress. The correlation between osmotic stress and change in the ABA levels have been well established at the molecular level (Shinozki and Shinozaki-Yamaguchi, 1996).

In some plants, for example citrus, salt toxicity is due to Cl^- instead of Na^+ (Fernandez-Ballester *et al.*, 2003; Moya *et al.*, 2003). In plants chloride has two main roles: one as a counter anion for cation transport (Ca^{+2}, K^+, Mg^{+2}, NH_4^+ *etc*) for maintaining membrane potential; the second as a major osmotically active solute which maintains both turgor and osmoregulation. Chloride is also a micronutrient essential for healthy plant growth. A minimal requirement for crop growth of 1g .Kg^{-1} dry weight has been suggested, a quantity that can generally be supplied by rainfall (White and Broadley, 2001).

1.2.1.4 Strategies for Coping with High Salinity

Until recently, strategies for solving the salinity problem in agriculture has tended to focus on soil reclamation. However, this has proved to be extremely expensive and untenable. In practice, land has been cultivated until salinity renders production uneconomic, at which point cultivation is switched to new areas. Recently, with the development of breeding and bioengineering, the focus has turned more towards developing salt-tolerant crops. However, this approach has its own drawbacks (Morpurgo, 1991). There is a view that salt tolerance in plants is a polygenic trait involving the co-ordinate expression of many genes, and that the prospects for bioengineering are therefore remote (Glenn *et al.*, 1999). However, recently this view has been challenged: salt resistant tomato (Zhang and Blumwald, 2001) and *Arabidopsis* (Apse *et al.*, 1999) plants have been produced by transformation with a single gene. Therefore, the prospects for overcoming salinity stress in crop plants using information derived from model system such as *Arabidopsis* and rice (*Oryza sativa* L), may not be as bleak as once thought.

Plants exposed to saline environments encounter three basic problems: (1) specific ion (Na^+, Cl^-, *etc*) toxicity; (2) the need to maintain a favorable cell turgor pressure: (3) the need to obtain essential nutrient ions (*e.g.* K^+, NO_3^-) in spite of the predominance of other chemically similar, potentially toxic ions (*e.g.* Na^+, Cl^-) in the growth medium.

Salt tolerance in plants not only varies considerably among species, but also depends very much on the conditions under which the crop is grown (Maas and Grieve, 1987). There are several factors that influence salt tolerance in plants. These include temperature, the composition and levels of salts, the growth phase of the plant, and the Leaching Fraction

(LF; Fageria, 1992; Hanson and Ayars, 2002; USDA, 2002; Western Fertilizer Handbook, 1995).

1.2.1.5 The Importance of Turgor

Soft plant tissues (non-lignified) are supported by the pressure of cell contents against the cell walls. This is known as turgor pressure and is induced by the uptake of water into cytoplasm of the cells so that pressure is exerted by the plasma membrane on the cell wall. Water tends to move into the cell because of the osmotic effect of the low molecular weight solutes in the cytoplasm and vacuole. Water movement from the soil, through the plant, and into the air can best be understood from the concept of water potential, which is measured in pressure units (bars, Pascals *etc*.). Water always moves from high to low water potential whatever the cause of the difference in potential. By definition, pure water at S.T.P. (standard temperature and pressure) and air at 100 % relative humidity has a water potential of zero. Because the growth (expansion) of cells of plants depend totally on turgor, decreased turgor is the factor most likely to inhibit plant growth when they are exposed to high salt (Ashraf, 1994). As a result, transfer of a salt-sensitive plants from their original habitat to a high salt medium will produce a rapid water loss and wilting. Recently the plant cell vacuoles have gained a lot of attention because of their multifaceted role in plant metabolism (*e.g.* recycling of cell components, regulation of turgor pressure, detoxification of xenobiotics, and accumulation of many storage substances; (Maeshima, 2001). Moreover, the space-filling function of the vacuole is essential for cell growth, because cell growth is driven by the expansion of vacuole rather than that of the cytoplasm (Taiz, 1992). Osmotic adjustment by halophytes and other salt-tolerant plants to tolerate high saline conditions is a key strategy for survival and this can be achieved by ion uptake from the soil solution and sequestration in the vacuole, and by internal synthesis of compatible organic solutes in the cytoplasm. A desiccated plant cell must reverse the water to potential gradient to survive, by forcing water to flow back into the cell. Therefore, for plant cells to thrive in concentrations above approximately120 mM NaCl (approximately -0.6 MPa, the water potential of plants in a well watered field), plants must develop a strategy to re-establish turgor pressure. Halophytes achieve this by accumulating enough osmotically-active solute in their vacuoles to reverse the osmotic gradient so that water can be re-absorbed from the external medium. An energetically cheap way of accomplishing this is to take up Na^+ and Cl^- ions from the external medium and sequester them in the vacuole. If the solute potential (Ψ_s, or osmotic potential) of the vacuole ($^{vac}\Psi_s$) becomes more negative than that in the soil solution, water will flow into the cell and turgor will

rise. However, for the cytoplasm to absorb water, it is necessary for the solute potential of the cytoplasm ($^{cyt}\Psi_s$) to decrease in parallel with $^{vac}\Psi_s$, and this can be achieved by the accumulation of non-toxic compatible solutes (*e.g.* glycine betain, proline, and sugars; Flowers *et al.*, 1977).

1.2.1.6 Na$^+$ Uptake Mechanisms

A high K$^+$/Na$^+$ ratio in the cytosol is a very important and essential feature for normal cellular function in plants. Since living cells are not completely impermeable to Na$^+$, the low concentration of Na$^+$ in the cytoplasm requires its continuous exclusion normally against an electrochemical gradient (Rodriguez-Navarro *et al.*, 1994). Therefore, active exclusion of Na$^+$ occurs either by a primary active Na$^+$-pumping ATPases or by a secondary active Na$^+$/H$^+$ antiporter mechanisms coupled to an electrochemical proton gradient (Figure 1-2; Serrano and Gaxiola, 1994). Due to the physio-chemical similarity between K$^+$ and Na$^+$, it is generally assumed that K$^+$ and Na$^+$ compete for common absorption sites in the root. High affinity transporters are effective at very low external K$^+$ concentrations and saturate when external K$^+$ concentrations rise to 1 mM (Fu and Luan, 1998). Sodium, even in 20-fold excess, fails to compete significantly with K$^+$ for binding sites on High Affinity transporters. At higher concentrations of K$^+$ (> 1 mM), Low Affinity transporters become important, and some of these transporters do not discriminate well between K$^+$ and Na$^+$, and thus Na$^+$ can competitively inhibit the absorption of K$^+$ (Amtmann and Sanders, 1998).

Sodium uptake in plants is believed to be primarily through Low Affinity transporters. Recently Kin (inward rectifying K$^+$ channels) channels have been reported in different root cells, including cortical, root hair, stellar and xylem parenchymatous cells, that can sense external K$^+$ concentrations (Haro *et al.*, 2005; Laurie *et al.*, 2002). These ion channels transport at rates between 106 and 108 ions per second per channel protein. Transport is 'passive', where the diffusion of ions through the channel is a function of both the membrane voltage and the concentration difference across the membrane; thus uptake is not directly coupled to the input of other forms of free energy (Blumwald *et al.*, 2000). Some argue, plants should be termed according to their ability to absorb Na$^+$ and translocate it freely to the shoot. 'Natrophiles' take up and translocate Na$^+$ freely, whereas 'Natrophobes' show a strong preference to absorb K$^+$ over Na$^+$ (Figure 1-2; Apse *et al.*, 1999; Gaxiola *et al.*, 2001).
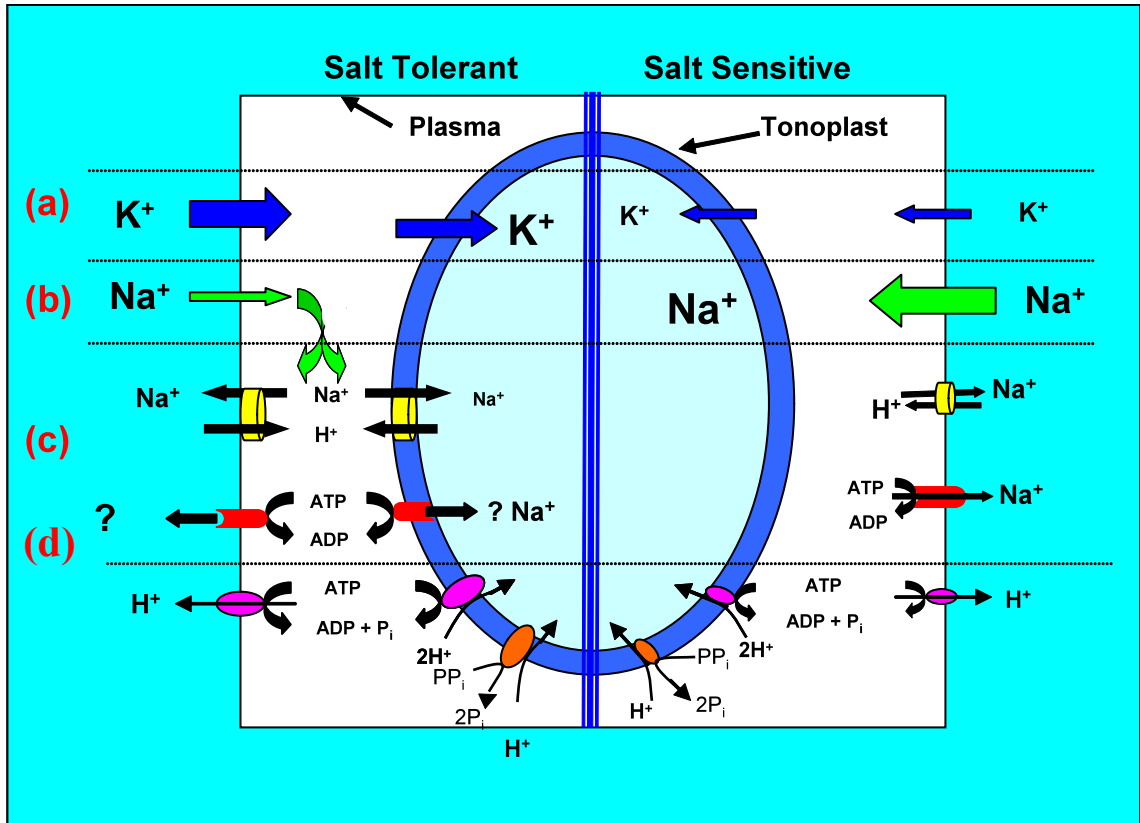
Figure 1-2: Possible Mechanisms Maintaining Ion Balance across the Plasma Membrane and Tonoplast of Salt-Tolerant and Salt-Sensitive Plant Cells (Figure from Attumi, 2007).

When compared with salt-sensitive plants, salt-resistant plants are believed to show **(a):** increased levels of potassium uptake, **(b):** decreased levels of sodium uptake, and **(c):** more efficient methods of sodium efflux by Na^+- ATPase or Na^+/ H^+ antiporters, **(d)** , H^+ pumping activity.

Na^+, the major toxic cation found in saline soils, has a similar physiochemical structure to K^+ and competes for uptake, interfering with K^+ nutrition. There are two mechanisms of K^+ uptake in plants, the high affinity mechanism (K_m of 10-30μM) to allow uptake at low external K^+ concentrations, (believed to be unaffected by external Na^+), and the low affinity mechanism that mediates K^+ uptake at high external K^+ concentrations (> 300μM, K_m of >200μM; Buchanan *et al.*, 2000).

The mechanism for Na^+ uptake into plant cells is unknown, but has been assumed to occur through the K^+ pathway(s) or non-specific cation channels such as LCT1. Na^+ efflux might occur through a Na^+-ATPase (*cf. S. cerevisiae ENA1-4* system) or by a Na^+/H^+ antiporter (*e.g.* SOS1; Kamei *et al.*, 2005).

High K^+/Na^+ can be maintained by the controlled movement of these ions across the plasma membrane. Therefore, it is feasible that salt-resistant cells can discriminate more efficiently between K^+ and Na^+ with a stronger preference for K^+ uptake against Na^+, or also, with effective Na^+ expulsion mechanisms.

The maintenance of favorable ion balance is dependent on the activity of H^+ pumps that drive active transport processes. These include the plasma membrane P-type H^+ ATPase, and tonoplast V-type H^+ ATPase and H^+ pyrophosphatase (Magnotta and Gogarten, 2002). Salt tolerance may depend on high densities and/or activities of these pumps.

1.2.1.7 Salt Stress Sensing in Plants

Plants sense salt stress through ionic (Na^+) and osmotic stress signals. Therefore, excess Na^+ can be sensed either on the surface of the plasma membrane by a transmembrane protein or within the cell by membrane proteins or Na^+ sensitive proteins. In addition to its role as an antiporter, the plasma membrane Na^+/H^+ antiporter SOS1 (Salt Overly Sensitive 1), having 10 to 12 transmembrane domains and a long cytoplasmic tail, may act as a Na^+ sensor (Zhu, 2003). This dual role would be analogous to the sugar permease BglF in *Escherichia coli* and the yeast ammonium transporter Mep2p. When expressed in *Xenopus laevis* oocytes $Na^+–K^+$ co-transporters from *Eucalyptus camaldulensis* (Dehnh) show an increased ion uptake under hypo-osmotic conditions while the *Arabidopsis* homolog did not show this osmosensing capacity (Liu *et al.*, 2001).

1.2.1.8 Na^+ Sequestration.

A positive turgor is very important and essential for expansion-induced growth of plant, and for stomatal functioning. When plants are exposed to high salinity they desiccate, resulting in turgor loss. Plants have evolved an osmotic adjustment mechanism (active solute accumulation) that maintains water uptake and turgor under osmotic stress conditions. For osmotic adjustment, plants use inorganic ions such as Na^+ and K^+ and/or synthesize organic compatible solutes such as proline and soluble sugars. Vacuolar sequestration of Na^+ is an important and cost-effective strategy for osmotic adjustment, which also reduces the Na^+ concentration in the cytosol. Na^+ sequestration into the vacuole depends on expression and activity of Na^+/H^+ antiporters as well as on V-type V-H^+-ATPases and V-H^+-PPases on the tonoplast. These phosphatases generate the necessary proton gradient required for activity of the Na^+/H^+ antiporters.

Over expression of AVP1, a gene that encodes the vacuolar H^+-pyrophosphatase (H^+-PPase) in *Arabidopsis,* enhanced sequestration of Na^+ into the vacuole and maintained higher relative water content in leaves. These plants also show higher salt and drought stress tolerance than that of wild type (Gaxiola *et al.*, 2001). The gene encoding tonoplast Na^+/H^+ antiporter (NHX1) is induced by both salinity and ABA in *Arabidopsis* (Shi and Zhu, 2002), and rice (Fukuda *et al.*, 1999). The AtNHX1 promoter contains a putative ABA responsive element (ABRE) between −736 and −728 from the initiation codon. AtNHX1 expression under salt stress is partially dependent on ABA biosynthesis and ABA signalling through ABA insensitive (ABI1). Salt-stress induced up-regulation of AtNHX1 expression is lower in ABA deficient mutants (*aba2-1 and aba3-1*) and in the ABA

10

insensitive mutant, *abi1-1* (Shi and Zhu, 2002). Comparing tonoplast Na^+/H^+-exchange activity (mainly due to AtNHX1) between wild type and mutants (SOS1, SOS2 and SOS3) shows that SOS2 also regulates tonoplast Na^+ exchange (Chinnusamy *et al.*, 2005).

1.2.2 Thermal Stress

Figure 1-3: Sudden Bout of Hot Weather and its Effects on Plants (Gardens, 2009).

Beside the salinity problem, agronomists world-wide are also greatly concerned with the threat of rising temperatures due to global warming which will impact on achieving maximum yield output from crop plants. High surface temperatures are a common problem faced by agriculture especially during periods of drought or in many arid and semi-arid regions in the world. Normally, plants grow in environments with sufficient water supply to maintain leaf temperatures at or below air temperatures through transpiration. However, in arid areas, or when the plants are exposed to drought conditions, plants experience stomatal closure and reduced transpiration. As a consequence of reduced transpiration, leaf temperatures increase above the temperature of the surrounding air and the elevated temperatures may limit dry matter accumulation because of increased respiration, reduced photosynthesis, and cellular damage (Stone, 2001). High temperatures are frequently experienced in seedlings, which leads to a reduction in the yield (Carr, 1972; Kalra, *et al*., 2007). In a study on Kentucky bluegrass, a combination of heat and drought stress significantly reduced root dry weight (Jiang and Huang, 2000). Maize kernel fresh and dry matter accumulation were severely disrupted by the long-term heat stress (8 days at 35 °C) and did not recover when transferred back to 25 °C, resulting in the abortion of 97 % of the kernels (Cheikh and Jones, 1994).

1.2.2.1 Effects of Heat Stress on Plants

The rise in temperature beyond a threshold level for a period of time is sufficient to cause irreversible damage to plant growth and development. Transient elevations in temperature above ambient is considered a heat shock or heat stress (Wahid *et al.*, 2007). However, heat stress is a complex function of intensity (temperature in degrees), duration, and the rate of increase in temperature. Heat tolerance is generally defined as the ability of plants to grow and produce economic yield under high temperatures (i.e. >35 °C day and >30 °C night). However, the concept of heat stress in plants is some what controversial. Some believe that an increase in night temperatures (> 30 °C) is a major limiting factor in decreasing the yield of tomato (Willits and Peet, 1998), whilst in another study on soybean it was observed that an increase in day temperature > 35 °C resulted in a significant reduction in soybean seed, but moderate to high night temperatures had no effect (Gibson and Mullen, 1996; Willits and Peet, 1998). Heat stress due to high ambient temperature is a serious threat to crop production worldwide (Hall, 2001). High temperatures effects start from impairing photosynthesis which leads to severe cellular injury to foliar tissues and above-ground meristems, which can result in cell death with in a few minutes of exposure. This in turn can result in the collapse and death of the whole plant (Schoffl *et al.*, 1998). The organization of microtubules may also be affected causing a splitting and/or elongation of spindles, formation of microtubule asters in mitotic cells, and elongation of phragmoplast microtubules (Smertenko *et al.*, 1997). Taken together these perturbations will lead to starvation, inhibition of growth, altered ion flux and production of toxic compounds and reactive oxygen species (ROS; Schoffl, 1998; Howarth, 2005). When plants are exposed to high temperatures signalling mechanisms are activated that cause changes in the expression of genes, thereby leading to the synthesis of stress-related proteins (Suzuki and Mittler, 2006). Amongst the first proteins to be synthesized are heat shock proteins (HSPs; Feder and Hoffman, 1999). These HSPs range in molecular mass from about 10 to 200 KDa, and have chaperone-like functions. As a result of HSP expression tolerance mechanisms are activated that confer improved physiological responses upon photosynthesis, assimilate partitioning, water and nutrient use efficiency, and membrane stability (Camejo *et al.*, 2005; Momcilovic and Ristic, 2007). Such improvements make plant growth and development possible under heat stress. The responses, however, vary between species and genotypes within a specie. This variation provides opportunities to improve crop heat-stress tolerance through genetic means. Some

attempts to develop heat-tolerant genotypes via conventional plant breeding protocols have been successful (Ehlers and Hall, 1998; Camejo *et al*., 2005).

Recent advances in molecular breeding, genetic engineering, and tissue culture have raised the prospect that plants with improved tolerance of abiotic stress can be developed. To achieve this, however, the efforts of plant physiologists, geneticists and crop breeders will be required.

1.2.2.2 Plant Responses to Heat Stress

1.2.2.2.1 Morpho-Anatomical Responses

There is a significant morpho-anatomical effect of heat stress on crop plants leading to severe reduction in yield and dry matter production. (Iglesias-Acosta *et al*., 2010). High temperatures may cause severe reduction in the first internode length resulting in premature death of plants (Hall, 1992). Heat stress, alone or with drought, is a common constraint during anthesis and the grain filling stages in many cereal crops (Guilioni *et al*., 1997). Reductions in starch, protein, and oil contents of the maize kernel were also observed due to heat stress (Wilhelm *et al.*, 1999). Grain quality is also effected under heat stress (Maestri *et al*., 2002.). High temperature also adversely affects the reproductive processes, which included meiosis in both male and female organs, pollen germination and pollen tube growth, ovule viability, stigmatic and style positions, number of pollen grains retained by the stigma, fertilization and post-fertilization processes, growth of the endosperm and maturation of the pro embryo and fertilized embryo (Gross and Kigel, 1994). In short, reproductive processes are markedly affected by high temperatures in most plants, which ultimately affect fertilization and post-fertilization processes leading to reduced crop yields. At the whole plant level, heat stress causes reduced cell size, closure of stomata and reduced water loss, change in stomatal and trichome densities, and alterations in xylem vessels structure of both root and shoot (Bañon *et al*., 2004). At the sub-cellular level, major modifications occur in chloroplasts, leading to significant changes in photosynthesis. For example, high temperatures reduce photosynthesis by changing the structural organization of thylakoids (Karim *et al*., 1999). Specific effects of high temperatures on photosynthetic membranes result in the loss of grana stacking and thylakoid swelling. In response to heat stress, chloroplasts in the mesophyll cells became round in shape, stromal lamellae swell, and the contents of vacuoles formed clumps, whilst the cristae are disrupted and mitochondria become leaky (Zhang *et al.*, 2005). In general, it is evident that high temperature considerably affects anatomical structures not only at the

tissue and cellular levels but also at the sub-cellular level. The cumulative effects of all these changes under high temperature stress may result in poor plant growth and productivity.

1.2.2.2.2 Physiological Responses

Water Relations

Plant water status changes drastically under changing ambient temperatures, particularly under field conditions (Mazorra *et al.*, 2002). Experiments with well watered sugar cane showed that increasing air temperature resulted in leaf desiccation (Wahid and Close, 2007). These results suggest that as leaf temperature rises, transpiration rates increase to cool the leaf, but at a critical level water loss from the stomata exceeds then water supply to the shoot and dehydration occurs. In general, in the field, and particularly in hot arid regions, decreased transpiration occurs presumably accompanied by an increase in leaf temperature (Tsukaguchi *et al.*, 2003).

Accumulation of Compatible Solutes

Under different stress conditions including heat, different plant species may accumulate a variety of compatible solutes such as sugars and sugar alcohols (polyols), proline, tertiary and quaternary ammonium compounds, and tertiary sulphonium compounds (Sairam and Tyagi, 2004). Accumulation of such solutes may contribute to enhanced stress tolerance of plants. Glycinebetaine (GB), an amphoteric quaternary amine, plays an important role as a compatible solute in plants under various stresses, such as salinity or high temperature (Sakamoto and Murata, 2002). Some plant species have a greater capacity to synthesize GB, when exposed to desiccating conditions or high temperature, compared with others (Ashraf and Foolad, 2007; Wahid, 2007; Wahid and Close, 2007) Moreover, the introduction of GB-biosynthetic pathways into GB-deficient species is possible through genetic engineering (Sakamoto and Murata, 2002). Proline accumulation is also known to occur widely in higher plants in response to environmental stresses, like glycinebetaine (Kishore *et al.*, 2005). Among other compatible solutes is γ-4-aminobutyric acid (GABA), a non-protein amino acid that is widely distributed throughout the biological world to act as a compatible solute. GABA is synthesized from glutamic acid by a single step reaction catalyzed by glutamate decarboxylase (GAD). Acidic pH activates GAD, a key enzyme in the biosynthesis of GABA. Episodes of high temperatures increase the cytosolic level of

Ca^{2+}, which leads to calmodulin-mediated activation of GAD (Riadh *et al*., 2010). It is clear that plants synthesize compatible solutes in response to stress as a sign of stress, but the mechanism by which they confer stress tolerance is unknown.

Photosynthesis

The most severe effects of heat stress on plants are reported to be on photosynthesis, which can be a good indicator of thermotolerance. Carbon assimilation rates can be disrupted through perturbation of the light reactions, the enzymatic kinetics of the Calvin cycle, or the supply of CO_2 to the chloroplast (stomatal conductance). It is suggested that high temperature affects the three critical processes of photosynthesis (Figure 1-4).

1)   Photochemical reactions in the thylakoid membrane have been implicated as the primary sites of injury at high temperatures (Wise *et al*., 2004). Chlorophyll fluorescence, the ratio of variable fluorescence to maximum fluorescence (Fv/Fm), and the base fluorescence (F_o) are physiological parameters that have been shown to correlate with heat tolerance (Yamada *et al*., 1996). Increasing leaf temperatures and photosynthetic photon flux density influence thermotolerance adjustments of PSII, indicating their potential to optimize photosynthesis under varying environmental growth conditions as long as the upper thermal limits are not exceeded (Salvucci and Crafts-Brandner, 2004a; Marchand *et al.*, 2005).
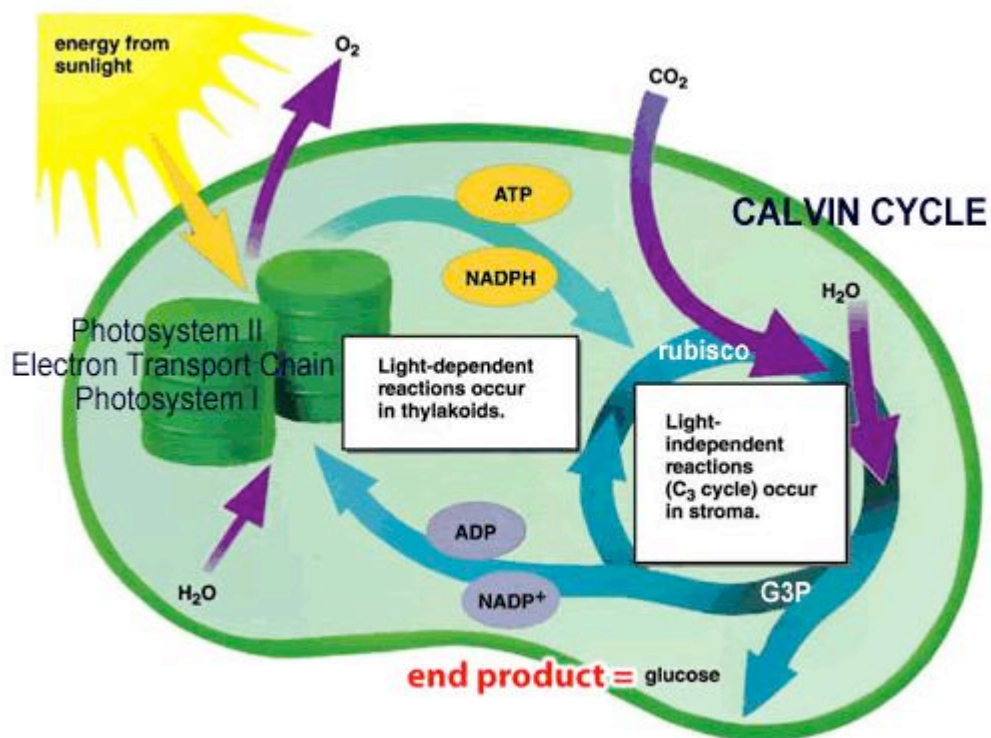
Figure 1-4: Schematic Diagram of Photosynthetic Processes (Lee *et al*., 2009).

Degradation of chlorophyll a and b is more pronounced in developed compared with developing leaves under high temperatures. These effects on the photosynthetic apparatus were suggested to be associated with the production of reactive oxygen species (Camejo *et al.*, 2005; Guo *et al.*, 2006). PSII is considered highly thermo labile, and its activity is greatly reduced due to alterations in the thylakoid membrane under high temperatures (Camejo *et al.*, 2005). It is supposed that heat stress may lead to the dissociation of the oxygen evolving complex (OEC), resulting in an imbalance between the electron flow from the OEC toward the acceptor side of PSII in the direction of PSI reaction centre (Figure 1-5; De Ronde *et al.*, 2004). Due to heat stress a dissociation of the manganese (Mn^{2+}) stabilizing 33-kDa protein in PSII reaction centre complex occurs (Yamane *et al.*, 1998). Along with this, heat stress may also impair other parts of the reaction centre, *e.g.* the D1 and/or the D2 proteins (De Las Rivas and Barber, 1997).
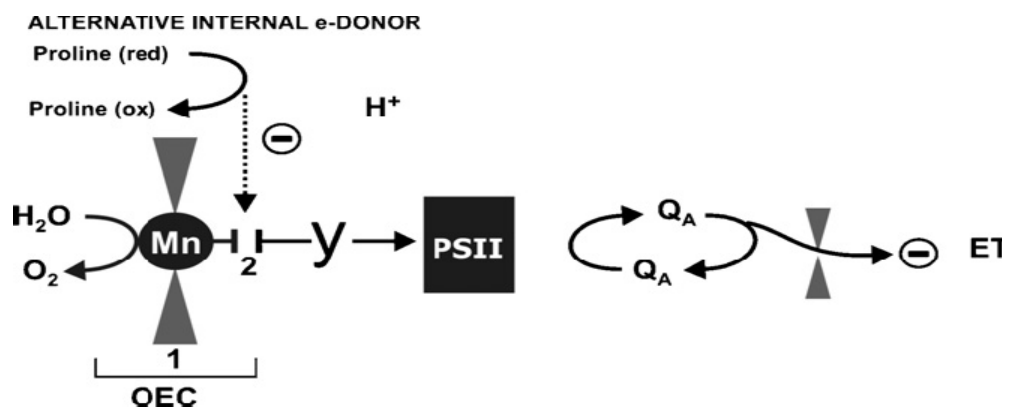
Figure 1-5: Heat induced inhibition of oxygen evolution and PSII activity.

Heat induced inhibition of oxygen evolution and PSII activity. Heat stress leads to either (1) dissociation or (2) inhibition of the oxygen evolving complexes (OEC). This enables an alternative internal e^--donor such as proline instead of H_2O to donate electrons to PSII (De Ronde *et al.*, 2004).

In barley, the PSII units are rapidly damaged by a 4 hour heat stress due mainly to a loss of their capacity for oxygen evolution (To´th *et al.*, 2005).

2)   Secondly under high temperatures, leaf photosynthesis is limited by ribulose-1,5-bisphosphate (RuBP) regeneration capacity of the Calvin cycle, but not RuBisCO activity itself (Wise *et al.*, 2004). High temperature influences the photosynthetic capacity of C_3 plants more strongly than C_4 plants. It alters the energy distribution and changes the activities of carbon metabolism enzymes, particularly RuBisCO, thereby altering the rate of RuBP regeneration by the disruption of electron transport and inactivation of the oxygen evolving enzymes of PSII (Salvucci and Crafts-Brandner, 2004b). Heat shock reduces the

amount of photosynthetic pigments (Todorov *et al.*, 2003), soluble proteins, RuBisCO binding proteins (RBP) and large subunits (LS) and small subunits (SS) of RuBisCO in darkness but increases them in light, indicating their roles as chaperones and HSPs (Demirevska-Kepova, *et al.*, 2005). Transgenic lines of *Arabidopsis thaliana* with thermostable RuBisCO Activase (RCA1) showed higher photosynthetic rates, improved developmental patterns, higher biomass, and increased seed yields when subjected to heat stress of 26ºC and 30ºC when compared with wild type lines expressing thermolabile RuBisCO Activase (RCA) confirming the hypothesis that at high temperatures photosynthesis rates are linked to RuBisCO activity (Kurek *et al.,* 2007)

3)   In any plant species, the ability to sustain leaf gas exchange under heat stress has a direct relationship with heat tolerance. During the vegetative stage, high day temperatures can cause damage to leaf photosynthesis, reducing CO_2 assimilation rates (Hall, 1992). For example, in maize the net photosynthesis rate (Pn) was inhibited at leaf temperatures above 38 ºC and inhibition was much more severe when temperature was increased abruptly rather than gradually. However, this inhibition was independent of stomatal responses to high temperature (Crafts-Brander and Salvucci, 2002).

Nonetheless, photosynthesis is considered by many to be the physiological process most sensitive to high temperatures, and that rising atmospheric CO_2 content will drive temperature increases in many already stressful environments.

1.2.2.3 Mechanisms of Thermotolerance

Plants adopt different structural and functional adaptations including acclimation processes (such as changing leaf orientation, transpirational cooling, or alteration of membrane lipid composition) for surviving under elevated temperatures. In many crop plants, high temperature-induced early floral maturation is closely correlated with smaller yields, which may be attributed to mechanisms that have evolved to avoid thermal damage to reproductive processes (Adams *et al.*, 2001). The sessile nature of plants places a strong emphasis on the evolution of cellular and physiological mechanisms of adaptation and protection. Also plants may experience different types of stress at different developmental stages and their mechanisms of response to stress may vary in different tissues (Chi *et al.*, 2009). The initial stress signals (*e.g.*, osmotic, ionic effects, or changes in shoot temperature) trigger downstream signalling processes that affect gene transcription, and activate stress-responsive mechanisms to re-establish homeostasis and protect and repair damaged proteins and membranes. Inadequate responses at one or more steps in the signalling and gene activation processes might ultimately result in irreversible damages in

cellular homeostasis and destruction of functional and structural proteins and membranes, leading to cell death (Bohnert *et al.*, 2006; Vinocur and Altman, 2005). A tentative heat stress sensing and response pathway has been proposed that better enables plants to cope with the adversaries of high temperature (Figure 1-6; Sung *et al.*, 2003; Wahid *et al.*, 2007).

Heat stress effects are detectable at various levels, including the physical properties of the plasma membrane, and various biochemical pathways in the cytosol or organelles (Sung *et al.*, 2003). According to some models, the initial effects of heat stress start from the plasmalemma, which shows increased fluidity of the lipid bilayer under stress. This is termed as membrane fluidity in Figure 1-6, which leads to the induction of Ca^{2+} influx and cytoskeletal reorganization, resulting in the up-regulation of mitogen activated protein kinases (MAPK) and calcium dependent protein kinase (CDPK). These cascades then signal to the nucleus and results in the production of antioxidants and compatible solutes for cell water balance and osmotic adjustment. Production of ROS in the organelles (*e.g.*, chloroplast and mitochondria) is of great significance for signalling as well as the production of antioxidants (Bohnert *et al.*, 2006). The antioxidant defense mechanism is a part of heat-stress adaptation, and its strength is correlated with acquisition of thermotolerance (Maestri *et al.*, 2002.). One of the most closely studied mechanisms of thermotolerance is the induction of HSPs which, as described above, comprise several evolutionarily conserved protein families. However, each major HSP family has a unique biological role. The protective effects of HSPs can be attributed to the network of the chaperone machinery, in which many chaperones act in concert. An increasing number of studies suggest that the HSPs/chaperones interact with other stress-response mechanisms (Wang *et al.*, 2004). The HSPs/chaperones can play a role in stress signal transduction and gene activation (Nollen and Morimoto, 2002). They also interact with other stress-response mechanisms such as production of compatible solutes (Diamant *et al.*, 2001) and antioxidants (Panchuk *et al.*, 2002; Figure 1-6).

An important aspect of thermotolerance is the rapid change in the pattern of gene expression (Yang *et al.*, 2005). The mRNAs encoding non heat- stress-induced proteins are destabilized during heat stress. Heat stress may also inhibit splicing of some mRNAs (Vogel *et al.*, 1995). Some HSP-encoding genes have introns, and under heat-stress conditions their mRNAs are correctly spliced (Visioli *et al.*, 1997). However, the mechanism of preferential post-transcriptional modification and translation of HSP-encoding mRNA under heat stress is yet to be established.
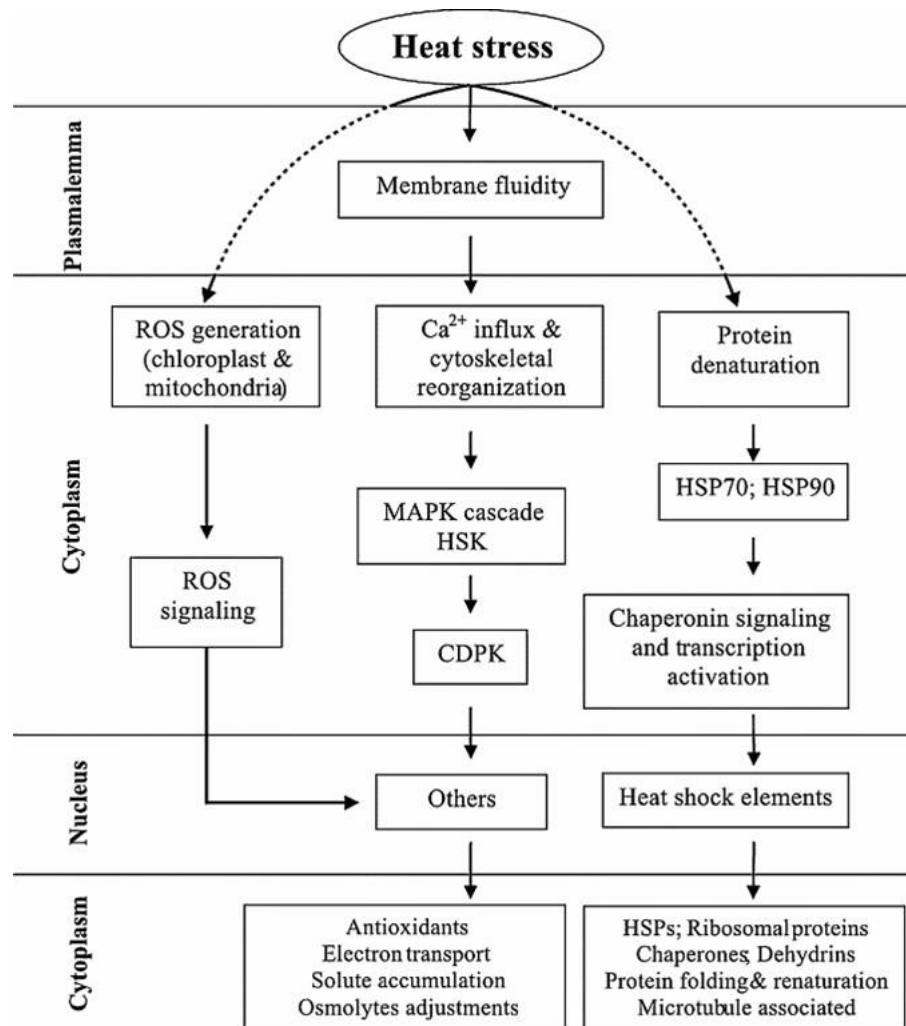
Figure 1-6: Proposed heat-stress tolerance mechanisms in plants (Sung *et al*., 2003; Wahid *et al*., 2007).

Integrated model depicting temperature perception, signal transduction, transcriptional activation and components of temperature stress tolerance. Temperature stresses invoke either a rise of cytoplasmic calcium ions or dehydrative stresses inside the cell that conveys stress-induced signals to response genes through different pathways. These pathways often converge and/or diverge from one another. However, for the sake of clarity, the pathways for cross-talks are not indicated. Abbreviations: CDPK, calcium-dependant protein kinase; HAMK, heat shock-activated MAPK, His kinase, histidine kinase; HSE, heat-shock element; HSP, heat-shock protein; MAPK, mitogen-associated protein kinase; sHSPs, small heat-shock proteins; SFR, sensitive to freezing; ROS, Reactive Oxygen Species; HSE: Heat Shock Element (Sung *et al*., 2003).

1.3 *Thermotolerance Studies in Barley*

Barley (*Hordeum vulgare L.*) is the fourth most important cereal crop in the world after wheat, rice and maize (Schulte *et al*., 2009). It is an annual cereal grain, which serves as a major animal feed crop, with smaller amounts used for malting and human consumption. It is a member of the grass family *Poaceae*. There are two forms of barley, domesticated barley (*H. vulgare*) and wild barley (*H. spontaneum*). The former is descended from the later but both are diploid (2n=14 chromosomes). As wild barley and domesticated barley are sexually compatible, the two forms are often treated as one species, *H. vulgare,* which is divided into subspecies *spontaneum* (wild) and subspecies *vulgare* (domesticated; Zohary *et al*., 2000). The main difference between the two forms is the brittle rachis of the former, which enables seed dispersal in the wild. Barley along with rye and *Triticale spp*., are grown in harsher environments and cover almost twice the area sown with maize or rice. Although barley and rye show significant levels of tolerance to many abiotic stresses, well above those of maize or rice (Maccaferri *et al*., 2009), relatively little known about the molecular basis for tolerance in these species and there is still ample scope for improvement (Langridge *et al*., 2006).

Figure 1-7: Barley Production in South East Asia (Cooper *et al*., 1987).

1.4 *Background of the Study*

1.4.1 Plant Material and Area

Several barley lines are grown in Balochistan (South western Pakistan) and these have been selected or bred due to their perceived drought tolerance. This area (marked on Fig 1-8) is characterized by high temperatures during mid summer (>40 ^{o}C) and approximately 200 mm rainfall *per annum* (Un-published data from Meteorological Department, Pakistan) In Balochistan several uncharacterized 'drought tolerant' lines named 'Local' are cultivated. Two other lines, Awaran-2002 and Soorab-96 are also used extensively; these were bred by the International Centre for Agricultural Research in the Dry Areas (ICARDA, Syria) and further refined by Agriculture Research Institute (ARI) Sariab-Quetta. However the landrace Local is not a variety approved by the Federal Seed Certification and Registration Department (FSC & RD) of Pakistan. It has a "tall stature" (>1.2 m) and "six row" phenotype and therefore is probably not derived from the dwarf lines developed during the Green Revolution (Waines *et al*., 2007). The reason behind selection and adoption of these varieties in the climatic conditions of Balochistan is their ability to withstand and perform well in the hot, dry conditions. Generally it is considered that these lines are drought tolerant, and this enables them to survive in harsher conditions (Khan *et al*., 1999; Rashid *et al*., 2006), but this contention is unproven. These three lines from tropical areas of Pakistan were compared with a genetically well-characterized elite European line 'Optic' bred purely for its malting qualities, with the assumption that this will give a good contrast of characteristics regarding halo and thermotolerance ability.

Figure 1-8: Areas under Rain fed Barley Cultivation in Balochistan (marked) an arid region located in the Iranian Plateau in South Asia, between Iran, Pakistan and Afghanistan (Rees *et al*., 1991).

1.4.2 Hypothesis Behind Current Study

Plants growing in arid regions, however, are also usually exposed to high air temperatures and increased soil salinity. What traits should plant biologists focus on; water conservation, salinity tolerance, or thermotolerance?

Do these lines thrive here because they are drought tolerant, or because they are thermotolerant? it is perhaps instructive to ask the question "why do plants need water?"

Water is the matrix in which all bio-catalytic processes occur. It is required to maintain the three-dimensional structure of bio-molecules, and to transport cargo within and between cells from one metabolic site to another. Water is required in plants for cell growth through the mechanisms of turgor-driven cell expansion in the zones of elongation adjacent to the meristems where cell division occurs. Water is also required to establish turgor pressure in guard cells to open the stomatal pore thereby enabling plants to acquire CO_2 for growth. In addition, turgor is also required to establish an erect habit, particularly in herbaceous, non-

23

woody plants. Without the ability to stand erect, a plant may, in the long term, become out-competed for light once a closed canopy forms above. The rate of water and nutrient ion transport through the xylem from the root to the shoot (transpiration) is also regulated by the turgor pressure of the guard cells, and so the acquisition of mineral ions and other simple solutes is dependent on water. Finally, water evaporation from the stomatal pores cools the leaf due to the latent heat of evaporation. What happens when plants cannot gain sufficient water to maintain an optimal level of hydration? This occurs in many habitats, but is a particularly acute problem for plants growing in high temperatures in arid and semi-arid zones.

Numerous investigations have shown that when most herbaceous plants lose 10-20 % of their tissue water they show signs of serious wilting, and most crops will not recover upon re-watering. One might predict that upon mild desiccation (> 90% hydration state), the guard cells might lose their turgor resulting in stomatal closure thereby minimizing further transpirational losses. Under these conditions the majority of crop plants partly close their stomata but some water loss to the atmosphere continues, resulting in severe wilting. The reason for this can be determined by monitoring leaf temperature as leaves begin to desiccate. Leaf temperature (T_{leaf}) of well watered plants in high air temperatures (>35 °C) is often 5-10 °C below air temperature (T_{air}) due to transpiration (Vitale *et al*., 2007), but as the rate slows T_{leaf} rises. The plant is now faced with several short-term and long-term dilemmas regarding its need for water. Partial desiccation will result in an increase in the cytoplasm /vacuole volume ratio and this will decrease the concentration of solutes in the cytoplasm; metabolic flux will slow although it is difficult to asses by how much, and this may have longer term consequences for growth and survival (Taiz and Zeiger, 2003). Water loss will also cause a slowing of turgor-driven growth, and the onset of visible wilting symptoms (loss of erect stature); again all of these factors will compromise the plant in the medium-to-long term, but are unlikely to affect the plant survival in the short term.

Increasing leaf temperature, however, is a serious threat to plant survival in both the short and long term. Experiments have shown that elevating leaf temperature of some plants to 40 °C for just ten minutes effectively 'cooks' the leaf (Zaragoza-Castells *et al*., 2008). Re-watering and placement in optimal growth temperatures does not lead to a recovery; the leaf fully desiccates, turns brown and dies. Therefore, it is reasonable to assert that leaf temperatures of >40 ºC for a few hours irreversibly damage leaves, causing symptoms that are mistakenly attributed to 'drought stresses, *i.e.* a failure to maintain tissue water

concentration. If this is the case, research effort should be re-focused to determine the mechanism that confers thermotolerance on some plants, not drought-tolerance.

1.4.3 Aims and Objectives of the Study

As mentioned earlier, man's attempts to impose halotolerance on sensitive model plants such as *Arabidopsis* by bioengineering transgenic lines has met with limited success. Perhaps we do not understand how plants work in sufficient detail and nature is more complex than we have assumed. A different approach may be more successful whereby adopting comparative studies nature may reveal to us which traits are important. The aims of this project were to asses this germplasm with respect to its ability to germinate, grow and yield in saline and hot arid conditions. Secondly, experiments were conducted to establish the physiological and molecular basis for any observed tolerance.

Chapter 2: Materials and Methods

This project included two main studies, halotolerance and thermotolerance in barley from arid and temperate regions.

2.1 *Halotolerance*

2.1.1 Plant Material

Table 2-1 presents the name and key characteristics of the four barley genotypes used in this study. Three genotypes were selected from Balochistan. One was landrace Local and reported to be drought and salinity tolerant (Salim Sheikh, ARI-Sariab, Balochistan, per comm.), but no published data are available to confirm this. The two other lines were Soorab-96 and Awaran-2002, both are elite lines developed by ICARDA for their better drought and salinity tolerance (http://www.icarda.org/ Publications/ Program_Reports/ GP.../ Varieties.pdf). The fourth line was Optic an elite European line listed first in 1995 and developed for its malting quality, and was assumed to be drought and salinity susceptible (http://www.syngenta.com/country/uk/en/Pages/home.aspx/). These genotypes were selected as they provide a range of tolerance to salinity. In addition, some preliminary experiments were undertaken to asses the epigenetic basis for the inheritance of salt stress.

Table 1: Name, Origin and Key Agronomic Characteristics of Four Barley Genotypes used in Salt and Thermal Stress Screening Experiments.

Name	Key Characteristics
Local	Landrace; grown for many years in rain fed conditions of Balochistan, Pakistan, It is a six-row barley with straw height >1.2 meters. It is considered to be drought and salinity tolerant, but susceptible to various diseases, particularly stem rust. Mostly grown under rain fed conditions and for fodder. In Balochistan seeds of landrace are sown in December and harvested June/July (growth period 180-210 days). In rain fed conditions yields approximately 2.7 tons per hectare (Salim Sheikh, ARI-Sariab, Balochistan, per. comm.). Seed procured from ARI-Sariab, Quetta, Balochistan and also bulked in glasshouses in Glasgow.
Soorab-96	ICARDA breeding line registered in 1996 with FSC & RD-Pakistan by ARI-Sariab, Quetta, Balochistan. A two-row winter barley with a

	delayed maturity habit. Developed for better drought and salinity tolerance. Straw height approximately 85 cm with high tillering ability, normally sown in December and harvested in June/July (growth period 180-210 days). It is a line mostly grown in rain fed conditions with approximately 1.8 tons per hectare straw yield and 2.0 tons per hectare grain yield in rain fed conditions (Salim Sheikh, ARI-Sariab, Balochistan, per. comm.). Seed procured from ARI-Sariab, Quetta, Balochistan and also bulked in glasshouses in Glasgow.
Awaran-2002	ICARDA breeding line registered in 2002 with FSC & RD-Pakistan by ARI-Sariab, Quetta, Balochistan. Two-row winter barley reported to be drought and salinity tolerant. It has a straw height of approximately 85 cm and is commercially cultivated for grain. Normally sown in January and harvested in June/July (growth period 150-180 days). Average grain yield 2.1 tons per hectare and straw production of 2.0 tons per hectare in rain fed conditions (Salim Sheikh, ARI-Sariab, Balochistan, per. comm.). Seed procured from ARI-Sariab, Quetta, Balochistan and also bulked in glasshouses in Glasgow.
Optic	European elite, two- row spring barley line. Average reported grain yield approximately 7.0 tons per hectare. Straw height 75 cm, commercially grown for malting purposes. Recommended drilling time January to April in United Kingdom and Early spring line with late maturity habit (http://www.newfarmcrops.co.uk/sb-optic.aspx). Seed procured from Syngenta, Cambridge, UK.

2.1.2 Agronomic Characterization of Barley Genotypes Under High Salt Concentrations

2.1.2.1 Germination

Ten uniform healthy seeds from Local, Awaran-2002, Soorab-96, and Optic were imbibed in moist paper towels sealed in square Petri dishes (12x12 cm^2) with ten replicated plates per treatment per line. Paper towels were moistened with a uniform quantity of sterilized distilled water containing different salt concentrations (*i.e.* 0, 50, 100, 150 mM NaCl). Seeds were germinated for 6 days in growth chambers in 14/10 hours day/night photoperiod at 180 μmol .m^{-2} .s^{-1} PPFD light intensity, 22/18 °C day/night temperature, approximately 60 % humidity. For the first six days of germination seeds were kept in the dark.

2.1.2.1.1 Experimental Design

Experiments were conducted using the common Factorial Randomized Block Design (FRBD). A randomized block design is used to reduce the variance introduced into the data arising from location in the growth cabinets and glass houses. To reduce further differences that might arise from location, plant positions were randomly changed at least twice a week. The Factorial experiment is another commonly used design where several experimental factors are under investigation (here genotype and salt stress, or genotype and heat stress), with this approach all combinations of factor level treatments are include to improve the efficiency of analysis and to test for interaction between the main factors (Caliński *et al*., 2000; Grafen and Hails, 2002; Sokal and Rohlf, 1994).

2.1.2.2 Growth of Mature Plants

After germination plants of each barley genotypes were screened for their ability to grow in high salt conditions.

2.1.2.2.1 Plant Material

One hundred seeds of each barley line were germinated for 6 days on moist paper towels at 20 ^{o}C in the dark. Eighty seedlings were selected for uniformity and then transplanted into aerated hydroponic culture (¼ Hoagland's solutions; see Appendix Table A 3-1). The pH of the solution was adjusted to 5.8 with KOH or HCl and was renewed weekly until the seedlings reached the 4th leaf stage, and then replaced every three days. Seedlings were carefully transplanted into polystyrene 40-cell self-watering propagator trays, and held in

place with polyurethane foam stoppers at a density of 20 plants per tray. The polystyrene trays were suspended over rectangular polypropylene troughs 40 (l) x 30 (b) x 22 (h) cm^3, 20 liters capacity fitted with a drainage tap. The containers were filled with 15 liters of ¼ strength Hoagland's solution supplemented with the appropriate amount of NaCl and aerated at 100 ml .min^{-1} (Figure 2-1).
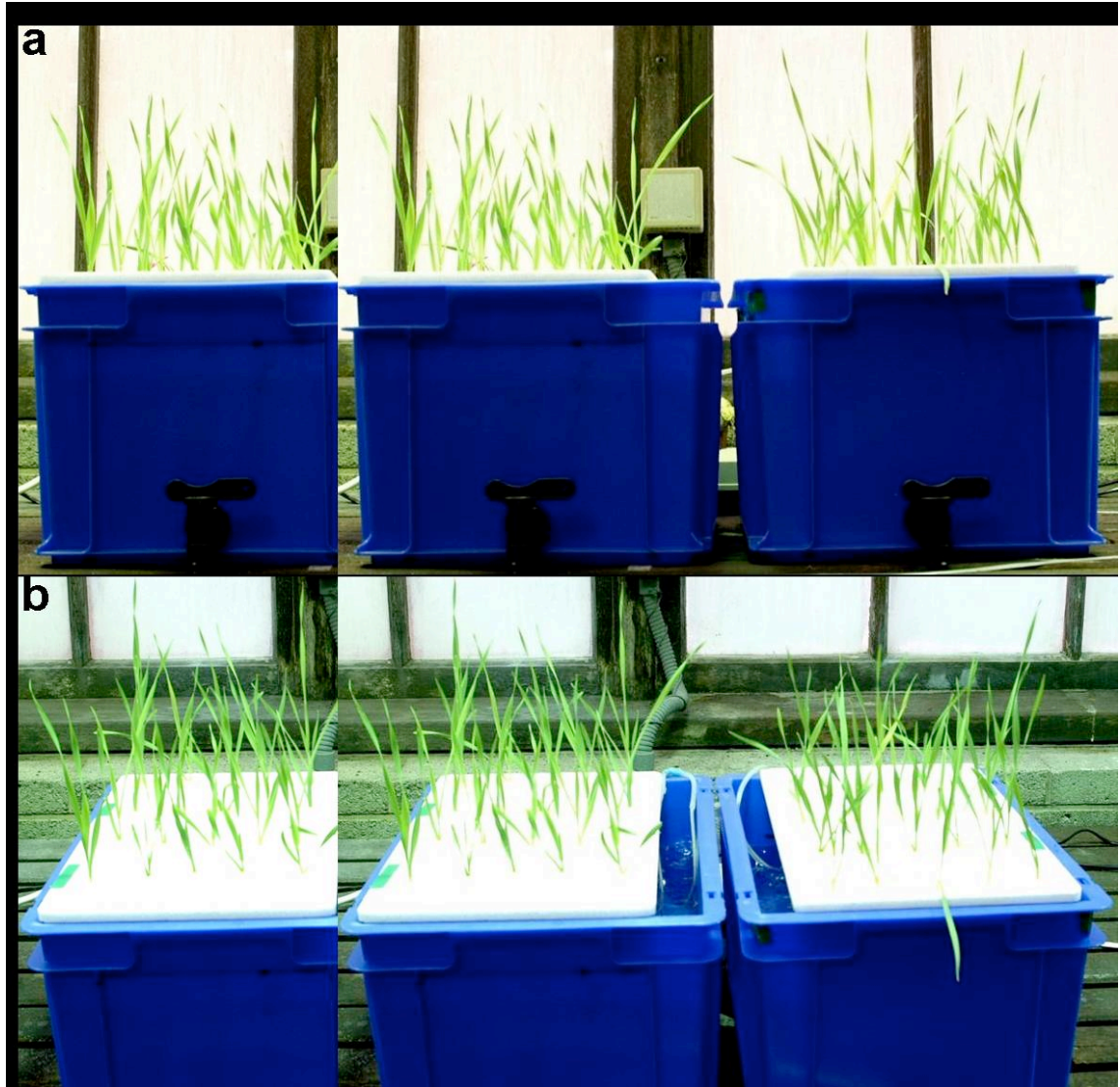
Figure 2-1: Two Views of Barley Plants Growing Hydroponically in Polypropylene Troughs.

Plants were grown in a controlled environment under glass house conditions keeping a 14/10 hour light and dark period, light intensity of 180 μmol .m^{-2}.s^{-1} at the bench surface, and 22/18 °C day/night temperature. The relative humidity was held between 40 – 50 %. From day 22 onward different NaCl concentrations (*i.e.* 0, 50, 100, and 150 mM) were added in Hoagland's medium untill crop harvesting. Data collection for all parameters, *i.e.* agronomic, photosynthetic, water and solute potentials were started on a regular fortnightly basis from day 44 post germination old plants (22 days under salt stress) until crop harvesting.

2.1.2.2.2 Experimental Design for Growth and Yield

The experiment was laid out in a factorial completely randomized design with four harvesting blocks (polypropylene troughs), 4 salt treatments (0, 50, 100, and 150 mM) 4 barley genotypes (Local, Soorab-96, Awaran-2002, and Optic) and 5 replicate plants (4x4x4x5 = 320 plants). The polystyrene trays were re-randomized between the appropriate troughs on a weekly basis to ensure even growth (also see Section 2.1.2.2.1).

2.1.2.2.3 Shoot and Root Length, Fresh and Dry Weight

At each harvest roots were briefly washed three times in ice cold distilled water shoot and root were separated and roots were blotted in sterilized dry paper towels for 10 minutes, after making sure that roots are properly dried. Basic growth parameters were measured, these include shoot/root length, shoot/root fresh weight, and shoot/root dry weight (± 0.1 mg). To obtain shoot and root fresh weight harvested plants were immediately sealed in pre-labeled and weighed 50 ml falcon tubes, and these fresh samples weighed with a micro balance (± 0.1 mg). After determining fresh weights, the falcon tubes were decapped and dried in oven on 70 °C for at least 72 hours. Completely oven dried samples were then re-weighed (± 0.1 mg).

2.1.2.2.4 Tillers, Ears, Grains and Grain Weight Per Plant

The numbers of tillers per plant (inclusive main stem) were recorded fortnightly for each plant of each line under each salt concentration up to maturity. Other yield parameters (*i.e.* number of ears per plant, number of grains per plant, and grain weight) were also recorded at harvest. Mature flower heads were harvested and kept in same glass house for three days, after making sure that the grains are properly dry then spikes were threshed carefully and data were recorded for number of grains per plant, and grain weight per plant (± 0.1 mg).

2.1.2.3 Assessment of Development

Twenty plants of each genotype *i.e.* Local, Optic, Soorab-96, and Awaran-2002, were germinated and grown to maturity in a glass house as described in Section 2.1.2.2.1, during the whole course of development data for development at least on alternate days were recorded for each line according to the Zadoks scale. The Zadoks scale extends from 0 (dry seed), through germination (1-9), seedling growth (10-19), tillering (20-29), stem

elongation (30-39), booting (40-49), inflorescence emergence, heading (50-59), anthesis (60-69), milk stage (70-77), and ripening (80-99); (see Appendix Figure A 3-17, and Table A 3-2).

2.1.2.3.1 Assessment of Ppd-H1 Flowering Locus

Isolating of Genomic DNA for PCR Analysis

A modified protocol for the preparation of plant genomic DNA (gDNA) for PCR analysis was used. The top two-thirds of single section emergent leaves of 14 day old barley seedling (*ca.* 10 mm from the base, and 170 mm in length and approximately 13 mm in width) was harvested and ground to a fine powder under liquid nitrogen using a mortar and pestle. The powder was then transferred into 1.5 ml Eppendorf tubes and 400 µl of extraction buffer (200 mM Tris HCl pH 7.5, 250 mM NaCl, 25 mM EDTA, 0.5% SDS) were added and the sample vortexed for 5 seconds. The extracts were then centrifuged at 12,000 g for 30 seconds and 300 µl of the supernatant transferred to a fresh Eppendorf tube. The supernatant was mixed with 300 µl isopropanol and left at room temperature for 2 minutes. Following this, the sample was then centrifuged at 12,000 g for 8 minutes, rinsed in 75 % ice cold ethanol, and the pellet was air dried before dissolving in 100 µl 1xTE buffer (10 mM Tris-HCl pH 8.0, 1 mM EDTA).

The genomic PCR reaction contained 15 µl of 2x ReddyMix (ABgene, AB-0575-DC-LD), 2-4 µl template genomic DNA, (*ca.* 50 pmol) 2 µl of either the control (CF and CR) or test (TF and TR) primers (Table 2-1), and 7 µl dH$_2$O. Amplification was performed in 30 µl volumes using a MJ Research DYAD, PCR running a program of 94 °C for 2 min followed by 30 cycles of 94 °C for 1 min, 50 °C for 40 seconds and 72 °C for 90 seconds. The resulting PCR products were visualized on 1% agarose gels stained with 10 µg .ml^{-1} ethidium bromide. The gels were run in TBE buffer (45 mM Tris-borate, 1 mM EDTA) at 20 °C using Embi Tec, Run One Electrophoresis cell (Embi-Tec, San Diego, USA). DNA was visualized under UV illumination using Bio RAD Gel Doc 2000 system. The 1 Kb ladder from Promega was used as marker (Figure 3-12; Sambrook and Russell, 2001).

Table 2-2: PCR Primers Used for Amplifying a Fragment Containing SNP 22 of the

Ppd-H1 Flowering Gene

Primer	Sequence	GC Content	Tm	MW	Length bp
HvCF	GAT GAA CAT GAA ACG GG	0.47	50.4	5293	17
HvCR	TAT AGC TAG GTG CGT GGC G	0.58	58.8	5900	19
HvTF	ATG CGA ATG GTG GAT CGG C	0.58	58.8	5909	19
HvTR	TAT AGC TAG GTG CGT GGC G	0.58	58.50	5900	19

Note: Primers and PCR reactions were designed by Turner *et al.* (2005).

2.1.3 Physiological Characterization of Barley Genotypes under high salt concentrations

2.1.3.1 Photosynthesis

Photosynthesis and transpiration are the two basic processes underpinning crop productivity. Accurate estimations of photosynthesis rate and water consumption is important not only in directing irrigation and improving water use efficiency of field crops, but also in studying the interactions between plants and the atmosphere. Photosynthesis has been intensively studied over the past few decades at all levels, from the chloroplast to the canopy level. Salt tolerance in many plant species is reported to be associated with the ability to exclude Na^+ so that high Na^+ concentrations do not occur in leaves, particularly in the leaf blade (Läuchli, 1984; Munns, 2005). High leaf Na^+ concentrations can cause premature leaf senescence and loss of photosynthetic activity (James *et al.*, 2002), which reduces the rate of carbon assimilation and ultimately grain yield (Husain *et al.*, 2003). Photosynthesis rates were determined using Infra Red Gas Analyzers (IRGA), *LCpro+* portable photosynthesis system (*LCpro+*, ADC Bioscientific Ltd., Hoddesdon, Herts., UK) fitted with a rectangular narrow leaf chamber (window area of 5.8 cm^2). The *LCpro+* instruments are fully programmable IRGAs that control ambient temperature, incident light levels, humidity, and CO_2 concentration. A portion of the fully expanded fourth leaf was enclosed in the *LCpro+* ensuring the leaf completely filled the chamber area. The chamber was illuminated with the adjustable *LCpro+* LED unit, and chamber CO_2 (*i.e.* C_{air} or C_a), chamber humidity, and temperature (*i.e.* T_{ch}) were controlled by the *LCpro+* console.

2.1.3.1.1 CO$_2$ Response Curve

Carbon uptake is reduced by environmental stresses that lower transpiration rates, triggered by lowering leaf water potential (Kramer and Boyer, 1995). This is particularly so for water stress (Lawlor, 1995) and also for salinity stress (Munns, 1993), which firstly induces the so-called osmotic or water deficit effect of salinity, and thus impairs the ability of plants for uptake of water. There have been many recent advances in our understanding of the mechanisms by which photosynthesis responds to environmental factors. However, conflicts still arise in the debate on the relative importance of CO_2 diffusive (Griffiths and Parry, 2002) and metabolic (Tezara *et al.,* 1999) factors to the overall control of photosynthesis rates even under mild environmental stress (Flexas and Medrano, 2002).

A rapid rate of CO_2 assimilation (A) requires correspondingly large amounts of many components of the chloroplasts, particularly the light harvesting chlorophyll–protein complexes (LHCP), electron transport and $NADP^+$-reducing (nicotinamide adenine dinucleotide phosphate) components of thylakoids, and the CO_2 assimilating enzyme ribulose 1-5 bisphosphate carboxylase-oxygenase (RuBisCO), plus other enzymes of the C3 cycle for CO_2 assimilation in the stroma.

Only a limited amount of information can be derived directly from an A/C_a curve. But Farquhar *et al*., (1980) *and* Farquhar and Sharkey*,* (1982) have shown how to extract useful photosynthetic parameters by plotting assimilation rate (A) against the CO_2 concentration in the intra cellular leaf space (C_i). A/C_i plots can be constructed from A/C_a plots using simple calculations (Farquhar *et al.,* 1980). The A/C_i plot of a sample represents the CO_2 response when stomatal and boundary layer conductance to CO_2 diffusion have been removed, and thus assimilation rate is limited by the kinetics of the carboxylation processes. At low C_i the A/C_i curve is linear and the slope is an estimate of the carboxylation efficiency ($\Phi\ CO_2$), and the Y intercept estimates the sum of the rates of photorespiration and mitochondrial respiration in the light in a zero CO_2 atmosphere ($^{Tot}R_L = V_0 + {}^{mit}R_L$). The contribution of mitochondrial respiration in the light is often assumed to be the same as that in the dark ($^{mit}R_d$), which can be measured from a light response curve (see Section 2.1.3.1.2). Subtraction of $^{mit}R_d$ from $^{Tot}R_L$ leaves the contribution of photorespiration (V_0), which will be dependent on the oxygenase activity of RuBisCO and the availability of Ribulose 1, 5-bisphosphate (RuBP).

In these experiments the *LCpro+* instruments were programmed to collect CO_2 responses using the following protocols. An area of leaf blade from the 4th emergent leaf (fully expanded by day 60) was sealed in the leaf chamber and the data logger started. The sample was illuminated at 487 µmol photons $.m^{-2}\ .s^{-1}$ (PPFD) and exposed to 0 µmol CO_2 $.mol^{-1}$ air (C_a), 10 mmol $.mol^{-1}$ humidity. After this period, the leaf samples had attained steady state the C_a levels increased incrementally from (0 to 1000 µmol CO_2 $.mol^{-1}$ air) for time periods shown in the Figure 2-2.
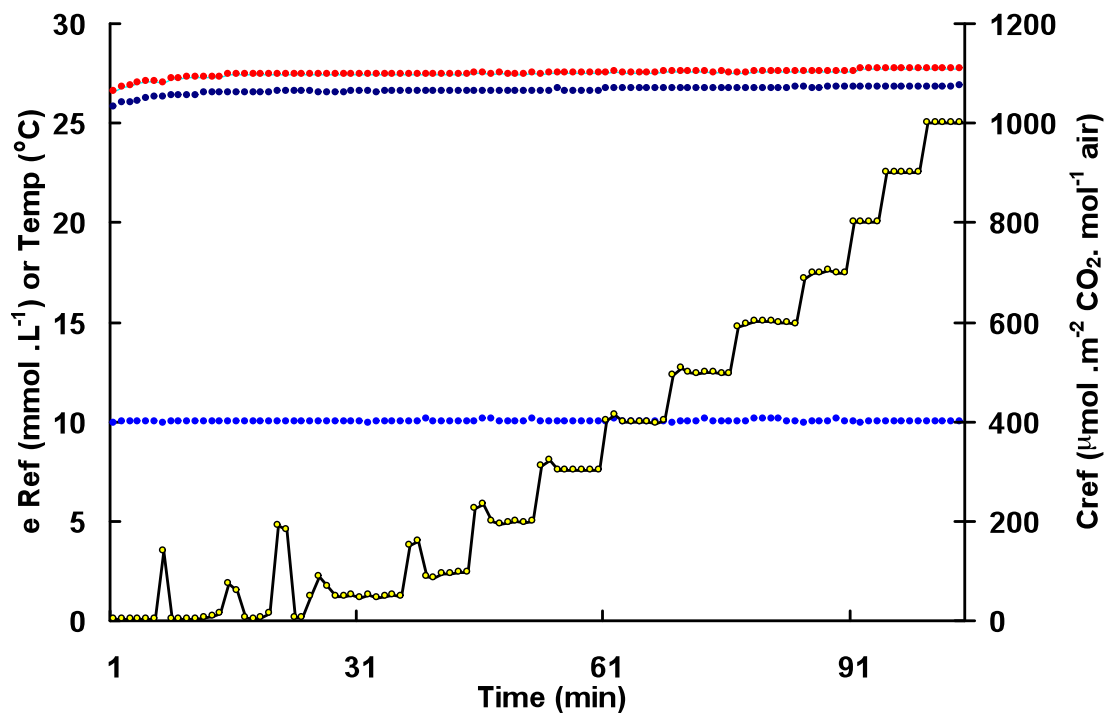
Figure 2-2: Profile of Leaf Chamber Conditions Used to Collect CO₂ Response Curves.

(●), chamber CO₂ (C_a) controlled by the LCpro+ console. C_a levels increased incrementally (from 0 to 1000, μmol CO_2 .mol^{-1} air).
(●), chamber humidity controlled by the LCpro+ console and was set to 10 mmol .mol^{-1}.
(●), chamber temperature controlled by the LCpro+ console and was set to 25 °C.
(●), leaf temperature controlled by the LCpro+ consol and was approximately 27-28 °C.
Readings were taken every one minute. During the course of these experiments light levels were maintained at 487 μmol photons .m^{-2} .s^{-1} (PPFD) using the LCpro+ light emitting diode unit.
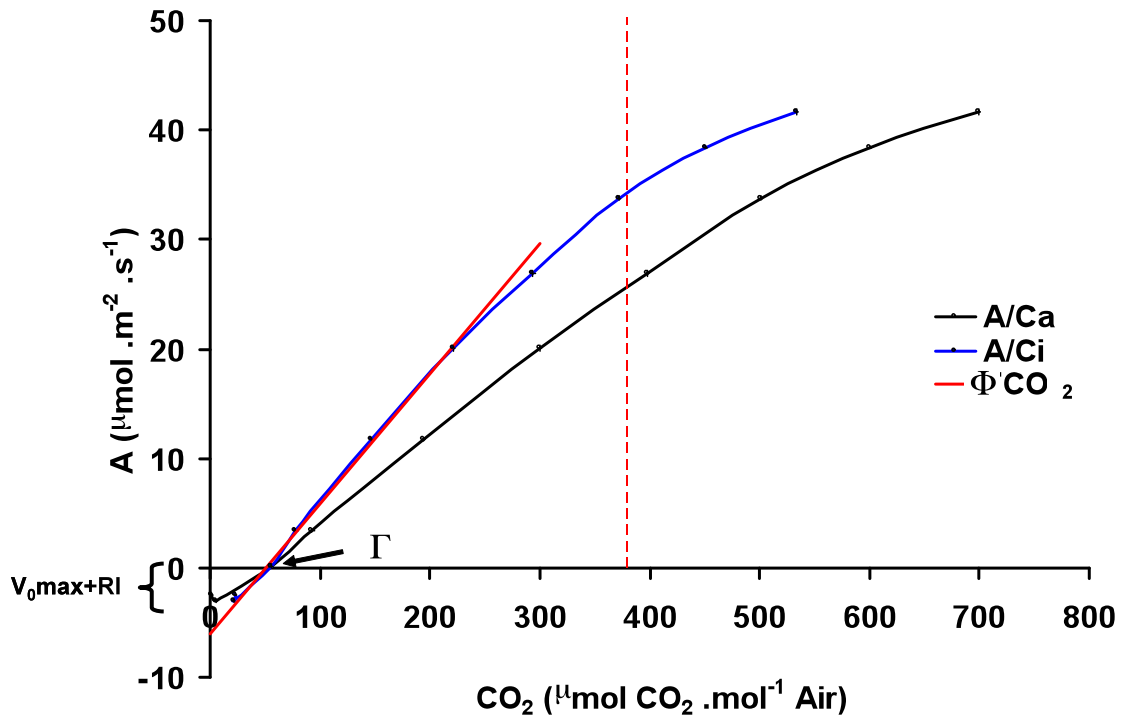
Figure 2-3: CO₂ Response Curve (CRC) of a Barley Leaf.

Barley leaves were sealed in the LCpro+ Narrow Leaf Chamber taking care to avoid damage; leaves were chosen that completely filled the chamber area (5.8 cm^2). Samples were dark adapted at (0 μmol CO_2 .mol^{-1} air, 10 mmol .mol^{-1} humidity, and 25 °C T_{ch}) for 25 minutes prior to running the program shown in Figure 2-2.

Blue solid line ( ) is the relationship between net CO_2 assimilation (A_n) and the internal CO_2 concentration (C_i). Black solid line ( ) is the relationship between net CO_2 assimilation (A_n) and the air CO_2 concentration (C_a). Red Solid line ( ) Φ CO_2 (carboxylation efficiency) from initial slope of the A/C_i curve. Red vertical dashed line ( ) ambient CO_2 (380 μmol CO_2 .mol^{-1} air); Γ, the CO_2 compensation point. Extrapolation of the initial slope of the A/C_i curve to the abscissa gives the total respiration rate (maximum photorespiration V_0max plus mitochondrial respiration in the light, R_L). These data were collected using the program described in Figure 2-2.

2.1.3.1.2 Light Response Curve

CO_2 assimilation rates (A) can be measured as a function of incident light intensity (I or Photosynthetic Photon Flux Density, PPFD). To generate a light response curve (LRC; A versus I), the *LCpro+* was programmed to collect data using the following protocols. Samples were placed in the dark and C_a adjusted to ambient levels (380 μmol CO_2 $.mol^{-1}$ air); chamber humidity was set to 10 mmol $.mol^{-1}$, and chamber temperature to 25 °C. The *LCpro+* data logger was started and the samples left for 20 minutes to dark adapt. After this period the incident light intensity (I) was increased sequentially to provide 15 minutes illumination at each of the following levels (0, 9, 17, 44, 87, 174, 261, 358, 435, 522, 696 and 870 μmol m^{-2} $.s^{-1}$, PPFD). A profile of the chamber conditions used to collect LRC is shown in (Figure 2-4). Figure 2-5 presents a typical light response curve from barley. From this curve several important photosynthetic parameters can be extracted, such as the apparent quantum yield of photosynthesis (α), the maximum photosynthesis rate (A_{max}), light saturated photosynthesis rate (A_{sat}), and the dark respiration rate (Rd).
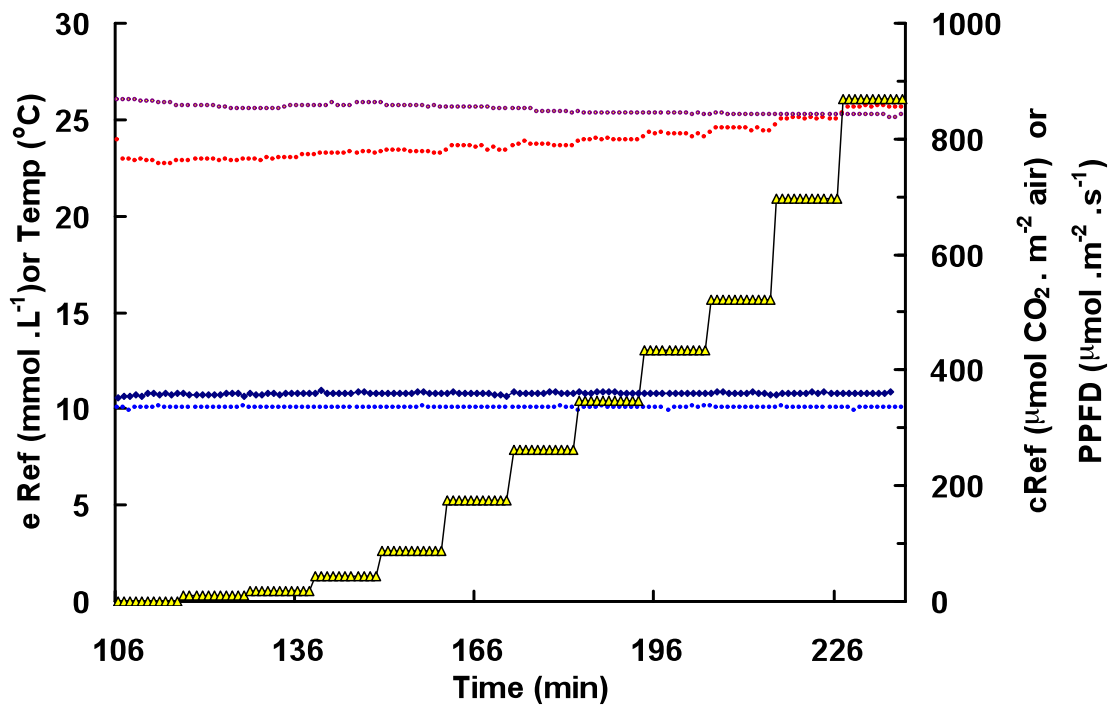
Figure 2-4: Profile of Leaf Chamber Conditions Used to Collect Light Response Curves.

Leaves were carefully sealed in the LCpro+ Narrow Leaf Chamber taking care to avoid damage; leaves were chosen that completely filled the chamber area (5.8 cm^2). A CO_2 response curve was first made on the leaf sample (see Section 2.1.3.1.1) before collecting a light response curve
(●), chamber incident light intensity (Photosynthetic Photon Flux Density, PPFD) was increased sequentially to provide illumination at each of the following levels (0, 9, 17, 44, 87, 174, 261, 358, 435, 522, 696 and 870 μmol .m^{-2} .s^{-1}, PPFD).
(●), chamber humidity controlled by the LCpro+ console was set to 10 mmol .mol^{-1}.
(●), chamber temperature controlled by the LCpro+ console and was set to 25°C.
(●), leaf temperature was measured by the LCpro+ console.
(●), chamber air CO_2 concentration (C_a) was set at ambient (360 μmol .m^{-2} .s^{-1}).
See Section 2.2.3.1 for details. Readings were taken every one minute.
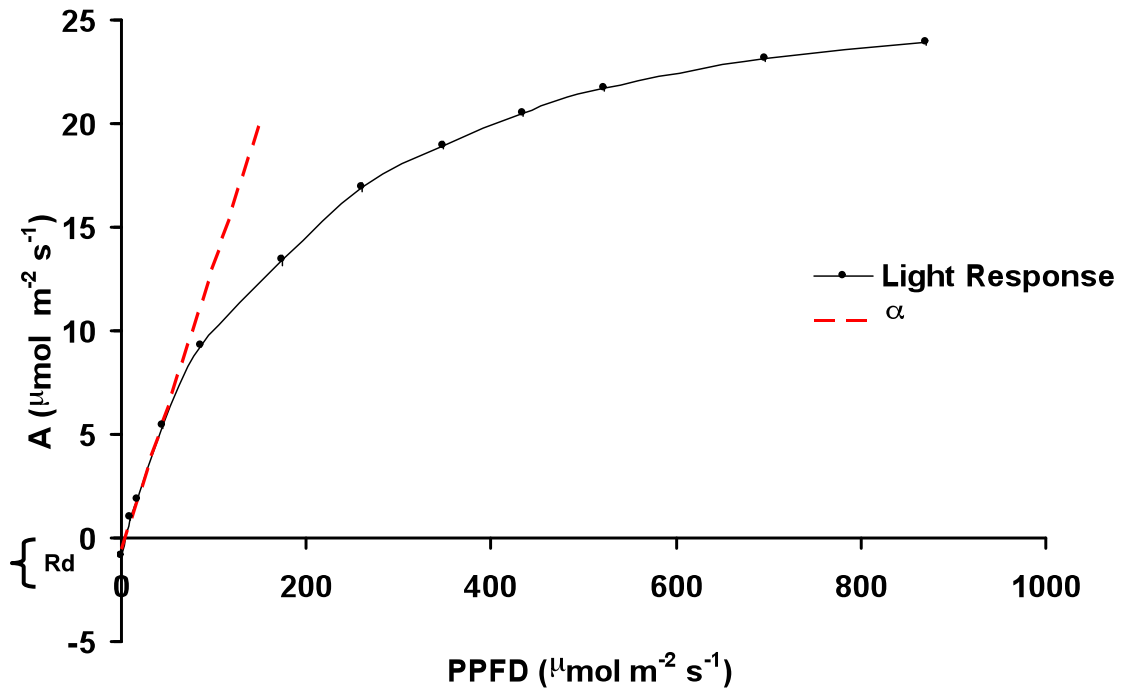
Figure 2-5: Light Response Curve of Barley Leaf.

Leaves were carefully sealed in the LCpro+ Narrow Leaf Chamber taking care to avoid damage; leaves were chosen that completely filled the chamber area (5.8 cm^2). Samples were first exposed to a CO_2-response regime (see Fig 2-3) prior to the light response regime. Carbon dioxide assimilation rate (A) *versus* incident light intensity (PPFD). A typical response is shown from barley line Optic, actual data points are shown as solid circles (●).The quantum efficiency, α (--).

2.1.3.2 Water Potential

Water potentials (ψ_{H2O}) were determined with a pressure chamber (P.M.S. Instruments, Corvallis, Oregon, USA). To measure the water potential of green barley leaves, the 4th emergent fully expanded intact leaves from plants were cut approximately 40 mm from the leaf nodes at exactly 90° from leaf edge. The cut leaf was fixed in the given rubber bung of the pressure chamber's cylinder with the cut end protruding 5mm into the air. After making sure that the cylinder was completely sealed the pressure was slowly increased using the needle valve on the top of pressure chamber and the pressure of air in the chamber was continuously monitored on pressure meter. On increasing pressure the leaf cut edge was continuously observed using a magnifying lens; as soon leaf sap started oozing out from the cut leaf surface the corresponding pressure (Balance Pressure) was recorded instantly from pressure meter.

2.1.3.3 Solute Potential

Solute potentials of tissue cell sap ($^{Tissue}\psi_s$) and exuded xylem fluid ($^{xylem}\psi_s$) were measured using an osmometer (OSMOMAT 030, Gontec GmbH, Germany) and the following protocols.

2.1.3.3.1 Solute Potential of Tissue Cell Sap ($^{Tissue}\psi_s$)

To measure the solute potential of cell sap one gram of fresh healthy leaf tissue was collected from barley leaves of similar age and position and sealed in 10 ml disposable syringes, with the plunger removed and the nozzle plugged with a small piece of 'Blu-Tac'. The syringe containing green leaf tissue was then filled with liquid nitrogen for two minutes. After freezing, the outlet of the syringe was reopened, and the syringe plunger re-inserted and used to squeeze leaf tissue for the extraction of cell sap. The collected cell sap was immediately sealed in eppendorf tubes and diluted to the appropriate concentrations for estimation of cell sap solute potential using the osmometer. The osmometer was calibrated each day with known standards of NaCl concentrations (0-500 mosmol $.kg^{-1}$).

2.1.3.3.2 Solute Potential of Exuded Xylem Sap ($^{xylem}\psi_s$)

For measuring exuded xylem fluid solute potential ($^{xylem}\psi_s$), leaves of approximately the same age were cut and immediately fixed in the rubber bung of a PMS 2000 pressure chamber's cylinder as discussed in Section 2.1.3.2, and air pressure gradually increased

until xylem fluid started oozing out from the leaf veins. The xylem fluid was carefully collected in 0.5 ml eppendorf tubes. Immediately after xylem sap collection, the tubes were sealed tightly to avoid any possible evaporation. Then appropriate dilutions of xylem sap were made using distilled water to measure solute potential by using an osmometer.

2.1.3.3.3 Proline Concentration

Fully expanded leaves from different genotypes of barley plants were sampled. Purified proline was used to produce standards for quantifying samples (0-50 μg .ml^{-1}). Ninhydrin Reagent was prepared by warming 1.25 g ninhydrin in 30 ml glacial acetic acid and 20 ml 6 M phosphoric acid, with agitation, until dissolved. The solution was stored at 4 °C and remained stable for 24 hours. Approximately 0.5 g of plant material was weighed to $\pm$ 0.1 mg precision and then homogenized in 10 ml of 3 % v/v aqueous sulfosalicylic acid and the homogenate filtered through Whatman # 2 filter paper. Two ml of filtrate was reacted with 2 ml Ninhydrin Reagent and 2 ml of glacial acetic acid in a glass test tube for 1 hour at 95 °C, and the reaction terminated by transfer to an ice bath. The reaction mixture was extracted with 4 ml toluene, mixed vigorously with a test tube stirrer for 15-20 seconds and the samples were then left to phase-separate. The chromophore containing (upper toluene phase) was carefully aspirated from the aqueous phase, warmed to room temperature and the absorbance was recorded at 520 nm using toluene for a blank. The proline concentration was determined from a standard curve and values expressed on a dry weight basis (μmol proline .g^{-1} dry weight; Bates, 1973)

2.1.4 Ion Analysis

2.1.4.1 Preparation of Barley Material for ICP-OES Analysis

Barley shoot, root, green and desiccated leaf samples were collected, oven dried for 7 days at 75 °C and ground to a fine powder using a pestle and mortar. The powder was transferred to a pre-weighed 50ml sterile falcon tube, and then reweighed, and the dry weight of the samples was calculated. Thirty grams of 5 % (v/v) analytical reagent grade nitric acid was weighed by a micro balance ($\pm$ 0.1 mg precision) and added to each tube and left to digest for 7 days on a shaking incubator. Ion content (Na, Fe, K, S, P, B, Mn, Mg and Ca) was measured using a Perkin Elmer Inductively Coupled Plasma-Optical Emission Spectrometer (ICP-OES) model Optima 4300 DV (Perkin Elmer, Waltham, USA) controlled by the software package (Win Lab32).

2.1.4.1.1 Standard Solution

Standard solutions were made in 5 % v/v analytical reagent grade HNO_3, exactly equivalent to the final concentration of HNO_3 in the samples. Ion concentrations in the standard solution were chosen based on the expected concentrations in the plant material and the detection limits of the spectrometer. The final concentration of each element in the x1 Standard Solution is shown in Table 2-2. The standard curve was produced by six dilutions of the x1 Standard Solution (0, 0.05, 0.1, 0.3, 0.6 and 1.0). It is important to note that to achieve reproducible results, all analysts, both samples and standards were prepared from the same batch of 5 % v/v HNO_3; this improves the resolution of trace elements as contaminants in the acid can be subtracted. Further, all dilutions were prepared by weighing ($\pm$ 1.0 mg precision), as this is more accurate than pipetting.

2.1.4.1.2 Assessment of Ion Concentration in Plant Material

The intensities of the emission at specific wavelengths from the diluted liquid samples were measured and the signals compared with the standard curve, to determine the concentration of the corresponding elements in the sample. These data were analyzed using Microsoft® EXCEL.

Table 2-3 The Final Concentration of Elements in the times 1 (1x) Standard Solution for Ion Analysis.

Element	K	Na	Ca	P	S	Mn	Mg	Fe	B
Conc. (mg .l^{-1})	46.950	1897.47	361.08	230.42	223.73	1.39	39.45	1.72	1.775

2.2 *High Temperature Thermotolerance*

2.2.1 Plant Material

Seeds were germinated in tap water and after 5 days transplanted into 2 liter pots containing a 1/1 volume mixture of Perlite and Levington's (F2+S grade) compost and placed in a controlled environment growth room (14/10 hour Day/ Night photoperiod, 180 μmoles $.m^{-2}.s^{-1}$ light intensity, 22/18 ºC temperature, 60 % humidity).

2.2.2 Exposure to Heat Stress

In this study two separate experiments were conducted namely Incremental and Temperature Jump heat stress experiments.

2.2.2.1 'Incremental' Heat Stress Experiments

In the 'Incremental' heat stress experiments CO_2 assimilation and transpiration rates were measured continuously from a single leaf using a temperature response profile, whilst T_{air} was increased incrementally. An intact leaf was sealed in the narrow leaf chamber of an IRGA using the following conditions: irradiance 550 μmol $.m^{-2}.s^{-1}$ white light generated from Philips HPLR 400W Mercury Vapour lamps; gas flow rate 200 μmol $.s^{-1}$, C_a 380 μmol $.mol^{-1}$, water vapour 0 mmol $.mol^{-1}$. T_{air} was increased incrementally from 25 °C to 44 °C ($\pm$0.5 °C) and steady state light-saturated rates of assimilation (A_{sat}) and transpiration were measured for at least 10 minutes (*i.e.* 20 minutes at each temperature; Figure 2-6). The *LCPro+* instruments control chamber air temperature up to 40 °C but the additional heat load of the mercury vapour lamps was sufficient to achieve higher T_{air} values.

2.2.2.2 'Temperature Jump' Heat Stress Experiments

In the 'Temperature Jump' heat stress experiments CO_2 assimilation rates, transpiration rates, and chlorophyll fluorescence measurements were made at 25 ºC before, immediately after and 5 days after, whilst an attached leaf was held at a single stress T_{leaf} for three hours. In both experiments fully expanded 4th emergent leaves were used (six to eight weeks after germination). An appropriate piece of fully expanded 4th emergent attached leaf (*ca.* 80 mm from the base of the leaf blade) was identified, lightly marked with a fine indelible marker pen, wrapped in cling film to prevent transpirational cooling, and placed

on an alluminium plate laid upon the heating block of a MJ Machines PTC-200 PCR thermal cycler. The metal plate was thermally insulated with a neoprene gasket to prevent heat loss from the edges, and a neoprene pad to prevent heat loss from the upper surface. Unless stated otherwise, the aluminium plate was heated to 40 °C ± 0.2 °C for 3 hours. Leaf temperatures were continuously monitored by using a bead thermocouple (± 0.1 °C) and data recorded throughout the experiment (Figure 2-7). Every time same labeled and marked leaf was then placed in the IRGA leaf chamber with care to make sure that the section of heat stressed leaf only was used for measurements of the photosynthetic parameters discussed in Section 2.1.3.1, before, immediately after, and 5 days after heat treatment.
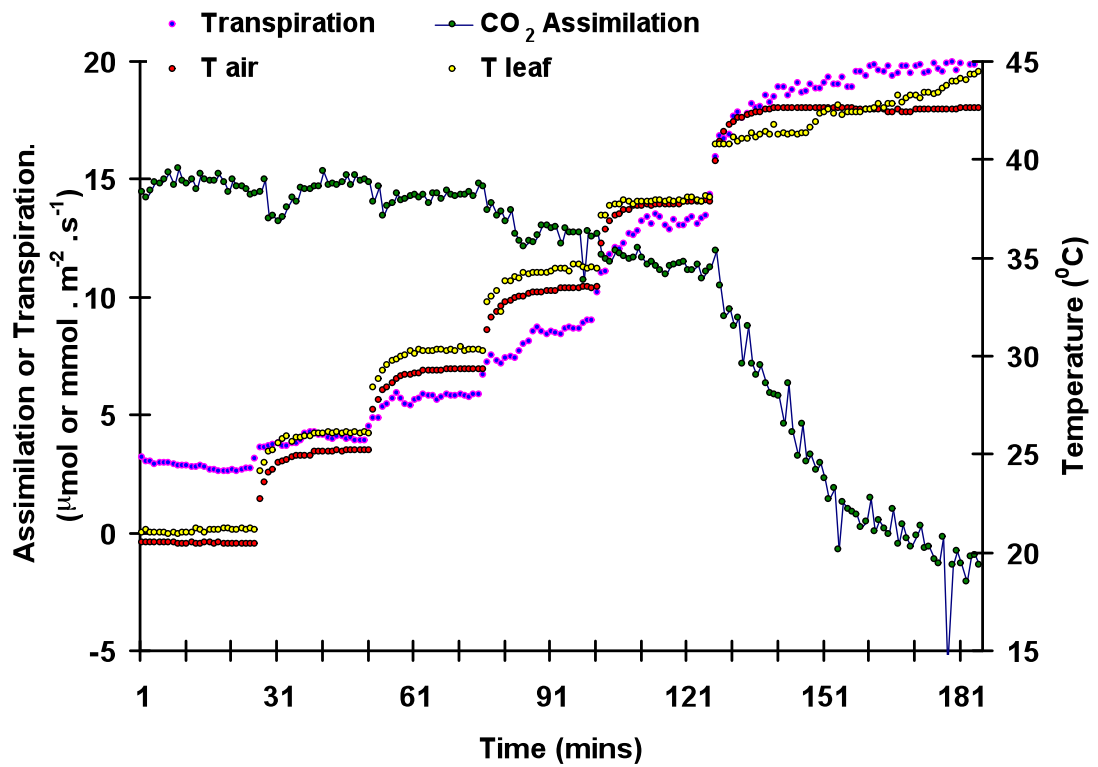
Figure 2-6: Typical Response of Barley Leaf to Increasing Air Temperatures (T_{air}).

Attached 4th emergent leaves were sealed in the leaf chamber of *LCPro+* IRGAs (ADC Bio Scientific, Hoddesdon, Herts, UK) and equilibrated at approximately 23 ºC for 30 minutes. Gas composition flowing through the chamber was 380 μmol CO_2 .mol^{-1} air (*i.e.* ambient) and 5 mmol water vapour .mol^{-1} air. Light intensity was maintained at 550 μmol .m^{-2} .s^{-1} PAR (Photosyntheticaly Active Radiation). Each plot is the continuous record of transpiration rates (E, mmol .m^{-2} .s^{-1}), assimilation rates (A, μmol CO_2 .m^{-2} .s^{-1}), leaf temperature (T_{leaf}, ºC) and air temperature (T_{air}, ºC) against time (minutes).

Figure 2-7: Apparatus for Imposing Thermal Stress on Barley Leaves using a Modified Thermocycler.

Top panel (a): front view; bottom panel (b): top view of the apparatus. Set up used for controlling T_{leaf} to $\pm$ 0.2 °C using a modified thermocycler. Leaves were carefully wrapped in cling film to reduce the cooling effects of transpiration and matched thermocouples placed on either side of the leaf; in all cases, the temperature difference across the leaf was < 0.1 °C, and thermal imaging showed temperature difference across the aluminium plate was < 0.1 °C.

a

Thermocycler

Thermo couple

Intact leaf

b

Insulation
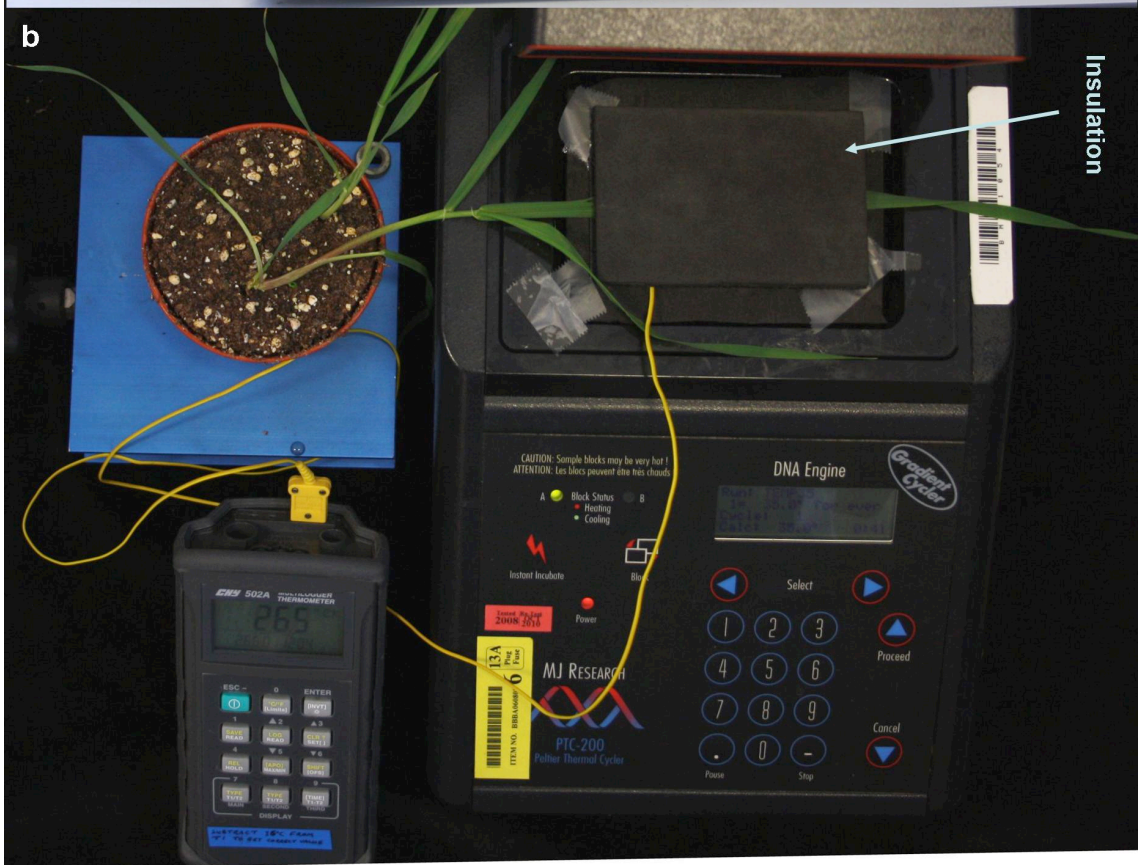
2.2.3 Leaf Absorptance and Fluorescence Measurements

2.2.3.1 Measurement of Leaf Absorptance and Light harvesting Capacity

Leaf absorptance was measured before and after heat stress using a Perkin Elmer λ800 spectrophotometer fitted with a Lab-sphere PELA-1020 Integrated Sphere (2 nm slit widths). The efficiency of light absorption and exciton delivery to PSII reaction centers was assessed from Chl*a* excitation spectra measured at room temperature using a Perkin Elmer LS55 fluorimeter fitted with a fiber-optic attachment (excitation 350-600 nm with 5 nm slit widths; emission 680 nm with 10 nm slit widths). Thirty minutes before measurement, leaves were pre-treated with 50μM DCMU (3-(3,4-dichlorophenyl)-1,1-dimethylurea) to block photosynthetic electron transport and attain the maximal level of fluorescence (F_m).

2.2.3.2 Measurement of Photosystem-II Quantum Yield (ΦPS-II) and Electron Transport Rates (ETR)

Modulated chlorophyll fluorescence measurements were made on intact plants in the growth chamber (at 25 °C) with a PAM fluorimeter (PAM2000H Walz, Effeltrich, Germany) fitted with a 2030-B Leaf Clip and an external actinic light (550 μmol .m^{-2} .s^{-1} delivered by a 50W quartz halogen bulb); these measurements included the maximum quantum yield of photosystem II photochemistry (Fv/Fm of dark adapted leaves, *i.e.* Φ_{PSII}), maximum and steady state rates of photosynthetic electron transport (ETR), and non-photochemical quenching (NPQ) during light induction (Baker, 2008). Before the start of each experiment the leaf was fully dark-adapted for 30 minutes, before the measuring beam was switched on to determine the initial fluorescence (F_0). Maximum fluorescence (F_m) was determined at 100 kHz by providing a 0.4 s saturating pulse of white light (9000 μmol.m^{-2}.s^{-1} PPFD). After determination of 'dark' levels of F_0 and F_m (*i.e.* determination of Φ PSII from (F_m-F_0)/F_m) the actinic light was switched on to drive photosynthesis and the resulting 'light' levels of fluorescence F_m, F'_m. Once steady state rates of F_s. NPQ, and ETR were attained the actinic light was extinguished and the dark induced 'recovery' phase recorded (see Fig 2-8). The important parameters calculated were as follows.

Φ PS II= (F'$_v$/F$_m$), where F'$_v$= F'$_m$-F$_o$ (the maximum quantum efficiency of PSII)

NPQ= F$_m$/F'$_m$ -1   (Non-photochemical quenching)

ETR= ΦPS-II *I* a b   (Electron transport rate)

where I is the irradiance [μmol .m^{-2}.s^{-1} PPFD] supplied to a leaf, assuming the absorbed photons are distributed evenly between the two photosystems, a factor of 2 as absorbed photons are required to process one 0.5 was used (a=0.5) and b is the leaf absorbtance factor (b=0.84). The value of b=0.84 is normally used in these calculations, and measurements on leaf absorbtance confirmed that this was an appropriate value. ETR was measured at its maximum and steady state levels are termed here as ETR$_{max}$, and ETR$_{ss}$, respectively.
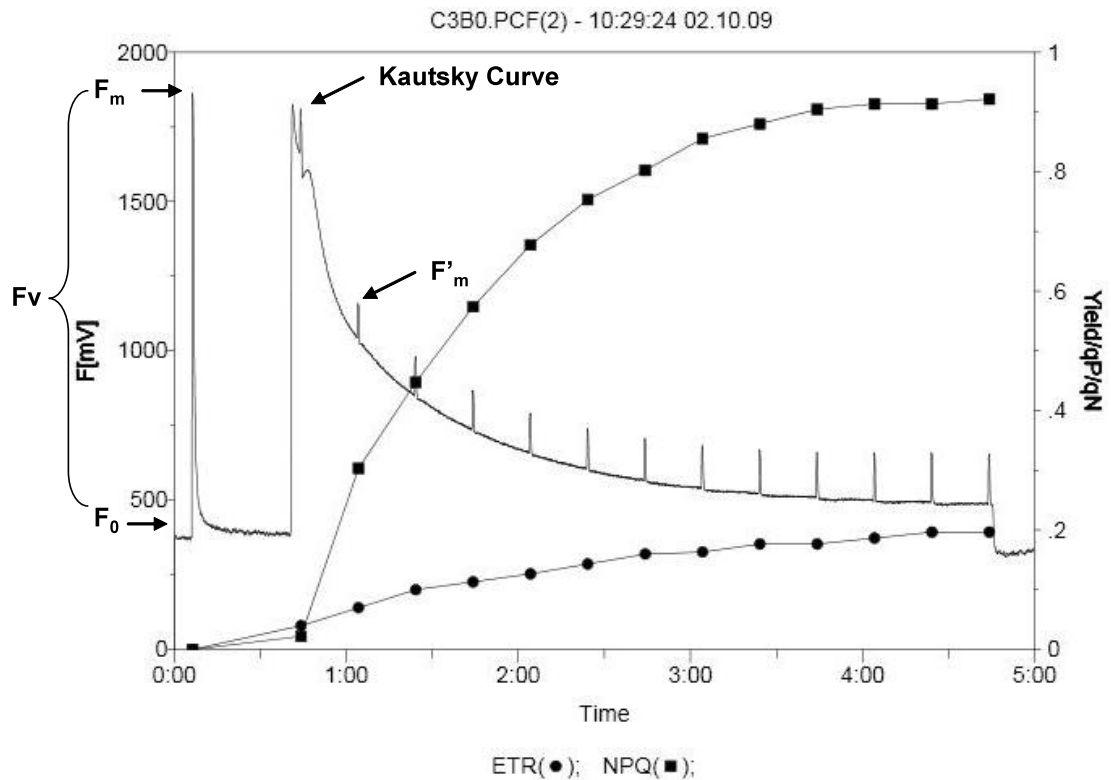
Figure 2-8: Plots of Fluorescence, NPQ, and ETR Collected Using PAM fluorimeter.

Attached 4th emergent leaves were sealed in the Leaf Clip of PAM fluorimeter (PAM2000H Walz, Effeltrich, Germany) and data were collected for the maximum Quantum Efficiency of PSII Photochemistry (Φ_{PSII}; *i.e.* Fv/Fm of fully dark adapted leaves), steady state ETR, maximum ETR determined during the light induction part of the fluorescence measurements and the Non-Photochemical Quenching (NPQ) component measured at steady state.

2.2.4 Gas Exchange Measurements

An appropriate piece of attached leaf (approximately 80 mm from the base of the leaf) was identified, marked and placed in a narrow leaf chamber of an IRGAs (set at T_{air} 25 °C ± 0.5 °C) and CO_2 and light response curves determined (A/Ca and A/Ci; Farquhar and Sharkey, 1982; Farquhar *et al*., 1980) along with the corresponding transpiration rates before, immediately after, and 5 days after a 3 hours heat stress treatment. For complete details see Section 2.1.3.1 of this chapter.

2.2.5 Metabolite Pools Analysis

To asses the C3 cycle activity in control and thermally stressed leaves (40° C ± 0.2 °C for 3 hours) the pool sizes of the intermediates of C3 cycle were quantified. Leaf samples were prepared at University of Glasgow, but metabolite pool analysis was carried out by 2 Dimensional Liquid Chromatography / Mass Spectrometry (2D LC-MS) by Dr. Stéphanie Arrivault, Max Planck Institute of Molecular Plant Physiology, Am Muehlenberg, Germany.

2.2.5.1 Preparation of Plant Extracts

Metabolite fluxes during photosynthesis are often high and many metabolites, including NADP, ATP, ADP, AMP, DHAP, RuBP and FBP, often have turnover rates of the order of seconds or less (Stitt *et al*., 1980, 1983). It is imperative, therefore, that samples adapted to a steady rate of CO_2 assimilation are frozen rapidly. To achieve this a system was built (shown in Figure 2-9), where a high power quartz halogen lamp was used to irradiate attached barley leaves at 580 μ moles .m^{-2}.s^{-1} (saturating light). To prevent the leaf overheating a circulating cold water system was developed using a 500 ml glass bottle. The leaf was kept at 22 °C (± 2 °C) and ambient air (380 μ moles CO_2 .mol^{-1} air) flushed over the leaf (2 liters .min^{-1}). The rate of CO_2 assimilation was estimated using a Walt PAM fluorimeter from the measured values for ETR. When Electron Transport Rate was at its steady state levels for at least 20 minutes, the portion of attached leaf was rapidly frozen by submerging in a pool of liquid nitrogen in a polystyrene container. Thermal stress was applied to leaves just prior to the procedure described above (see Section 2.2.2.2.).
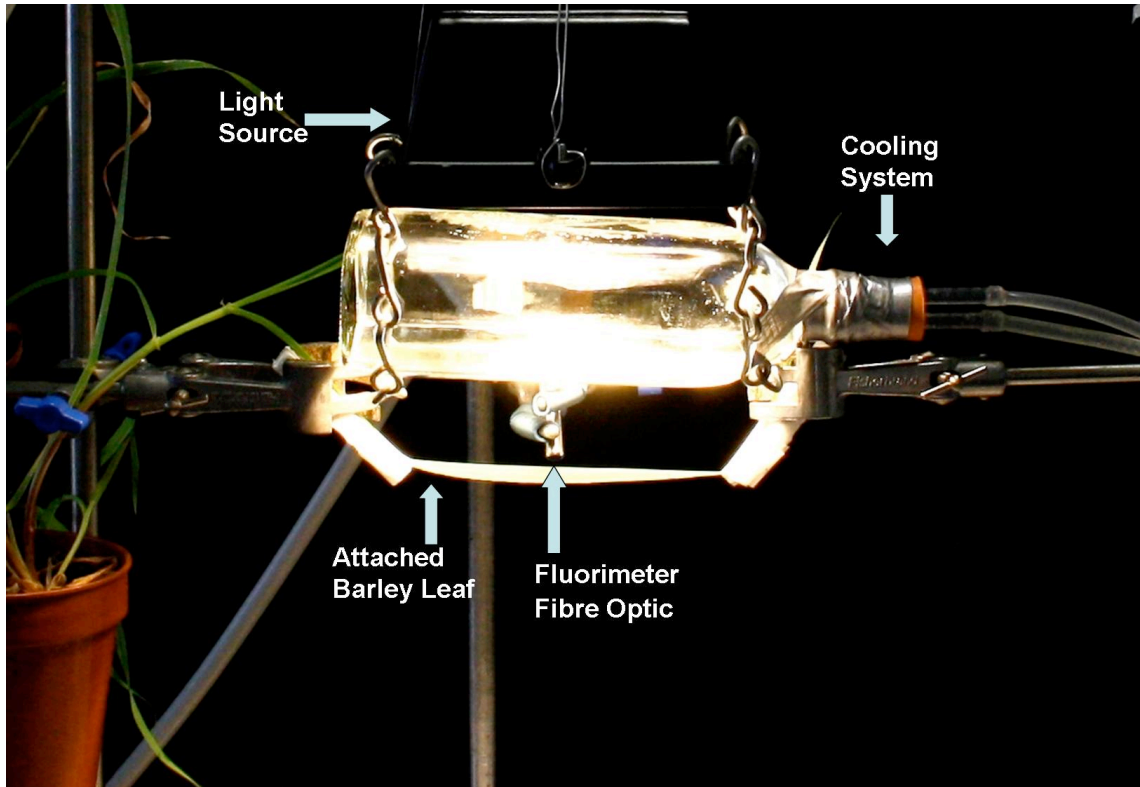
Figure 2-9: View of the Set up Used to Establish Steady State CO_2 Assimilation Rates in Attached Barley Leaves Before Rapid Freezing in Liquid Nitrogen.

Attached leaves were held under the white light source (580 μ moles $.m^{-2} .s^{-1}$) at 22 °C (± 2 °C) in ambient air (380 μ moles $CO_2 .mol^{-1}$ air) for at least 20 minutes to establish steady state rates of CO_2 assimilation; this was confirmed by measurement of *in vivo* photosynthetic ETR using pulse modulated fluorescence. Once steady state had been achieved, a polystyrene box containing liquid nitrogen was raised from beneath the leaf and the leaf Section was rapidly frozen whilst the sample was continually irradiated. It is estimated that the sample cooled to -196 °C within ≤ 1 second.

2.2.5.2 Sample Extraction

For LC-MS/MS analysis, metabolites were extracted using a modification of the method described in (Lunn *et al.,* 2006), except that 400 μl, instead of 200 μl, of water was added in the phase partition and wash. Recovery experiments were carried out by adding authenticated analyte standards to the frozen tissue before adding cold $CHCl_3/CH_3OH$.

2.2.5.3 Analysis of Metabolite Pools

All procedures were carried out by Dr. Stéphanie Arrivault at the Max Planck Institute of Molecular Plant Physiology, Am Muehlenberg, Germany. The following procedures are presented for completeness; full details can be found in (Arrivault *et al*., 2009) Tributylamine and NaOH were purchased from Sigma-Aldrich (http://www.sigmaaldrich.com/), acetic acid (GC standard grade) was purchased from Fluka (Sigma-Aldrich) and methanol (LC gradient grade) was purchased from Merck (http://www.merck.com/). Water was deionized and filtered (0.2 μm filter) in a Purelab-plus system (ELGA LabWater, http://www.elgalabwater.com/). $[2,3,3-^2H_3]$ Aspartic acid, $[2,3,3-^2H_3]$ glutamic acid and $[1,2,3,4-^{13}C_4]$ disodium α-ketoglutarate were purchased from Cil (http://www.isotope.com/), and $[2,3,3-^2H_3]$ malic acid, $[2,2,3,3-^{13}C_4]$ succinic acid and $[2,3,3-^2H_3]$ glyceric acid were purchased from Isotec (Sigma-Aldrich). Metabolite standards were from Sigma-Aldrich or Fluka, except for S7P (GLYCOTEAM GmbH, http://www.glycoteam.com/), SBP (Organix, http://www.essex.ac.uk /guest /organix /research.htm/), ATP, ADP, NAD and NADP (Roche, http://www.roche-applied-science.com/), and X5P (Prof. Fessner, Institute of Organic Chemistry, Darmstadt, Germany). The enzymes were purchased from Roche Diagnostics.

2.2.5.4 Synthesis of Deuterated G6P and G3P

[6,6-2H2] G6P and [1,1,2,3,3-2H5]G3P were synthesized from [6,6-2H2]glucose (Sigma-Aldrich) and [1,1,2,3,3-2H5]glycerol (Isotec). The reactions (final reaction volume 100 μl) contained 1.2 μmol ATP and (for deuterated G6P) 1 μmol [6,6-2H2]glucose, 1.5 U hexokinase, 25 mM Hepes-KOH (pH 7.5) and 5 mM MgCl2, or (for deuterated G3P) 1 μM [1,1,2,3,3-2H5]glycerol, 1.5 U glycerol kinase, 50 mM Hepes-KOH (pH 7.5) and 5 mM MgCl2, and were incubated at 30℃ for 1 h, heated to 99℃ for 2 min, and the precipitated proteins were then removed by centrifugation (18 000 *g* for 2 min).

2.2.5.5 Ion Pair Chromatography – Triple Quadrupole MS

IPC-MS/MS was carried out on a Dionex HPLC system (http://www.dionex.com/) coupled to a Finnigan TSQ Quantum Discovery MS-Q3 (Thermo Scientific, http://www.thermo.com/) equipped with an electrospray (ESI) interface. It was operated in the negative ion mode with selected reaction monitoring (SRM), an ion spray voltage of −4000 V and a capillary temperature of 320°C. Nitrogen was used as the sheath and auxiliary gas, set to 30 and 5 U (arbitrary units), respectively. The argon collision gas pressure was set to 1.1 mTorr, and the quadrupole 1 and quadrupole 3 peak widths were 0.7 m/z. The run was divided into four segments optimized for the detection of each transition, with dwell times of 150 ms or less. Finnigan XCALIBUR 1.4 software (Thermo Scientific) was used for both instrument control and data acquisition.

The major MS/MS fragment patterns of each analyte were determined by direct infusion to the interface of the analyte standard ($c = 3$ mM) dissolved in water at a flow rate of 5 µl min^{-1}.

Chromatographic separation was performed with a modification of the method described by (Luo *et al.*, 2007), by applying each sample both non-diluted and diluted 1/10. Aliquots (100 µl) were passed through a Gemini (C18) 4×2.00 mm pre-column (Phenomenex, http://www.phenomenex.com/), before separation on a Gemini (C18) 150×2.00 mm inner diameter, 5 µm 110 Å particle column (Phenomenex) at 35°C, using a multi-step gradient with online-degassed eluent A (10 mM tributylamine aqueous solution, adjusted to pH 4.95 with 15 mM acetic acid) and eluent B (methanol): 0–5 min, 95 % A; 5–15 min, 95–90 % A; 15–22 min, 90–85 % A; 22–37 min, 85–80 % A; 37–40 min, 80–65 % A, and maintained for 3 min; 43–47 min, 65–40 % A, and maintained for 3 min; 50 min, 10 % A, and maintained for 4 min; 54 min, 95 % A, and maintained for 11 min. The flow rate was 0.2 ml min^{-1} for 0–15 min and 54–65 min, and 0.3 ml min^{-1} for 15–54 min. prior to injection (100 µl); a mixture of eight stable isotope reference compounds of known concentrations was added to the sample to correct for matrix effects on these analytes in the analysis. LC-MS/MS SRM peaks were integrated using the Thermo-Finnigan processing software package LCQuan-2.5. Metabolites were quantified by comparing the integrated signal peak area with a calibration curve obtained using authentic standards. It should be noted that tributylamine is difficult to remove from the MS/MS system, and will interfere with calibration using polytyrosine standards and measurements if the machine is subsequently used in the positive mode.

2.2.5.6 Detection and Validation of Signals in Plant Extracts

Metabolites are present in extracts at a wide range of concentrations, and, at a given dilution, some metabolites may therefore be at or below the detection limit, whereas others are above the range for a linear response. Therefore two runs are always performed. In one, a 1/10 diluted extract was used to measure all metabolites except R5P, G1P, GAP, NAD, AMP, F26BP, FBP, SBP, ADPG, NADP and ADP. These were measured in a second run, using non-diluted extracts.

In complex matrices like plant extracts it is necessary to ensure the detected signal belongs to the suspected target analyte. The identity was first checked by spiking the extract with a standard mixture (data not shown; see also Figure 2-10). As a second check, we included an additional transition for each metabolite in the SRM mode (data not shown), as recommended in (Hernandez *et al.*, 2005). Except for citrate and isocitrate, the second (confirmatory) transition was less sensitive than the transition used for quantification. This allowed us to confirm the identity of each analyte in an Arabidopsis leaf extract (data not shown). For routine measurements, however, we used one transition per analyte. This was because many analytes had similar elution times (for example, ten metabolites eluted between 44 and 46 min). In this situation, the use of two transitions per metabolite requires shorter scan times, and decreases the detection sensitivity for a given fragment ion.

2.2.5.7 Other Metabolite Assays

Glucose, fructose, sucrose and starch were measured by coupled enzymatic assays (Berger, 1985a,b; Merlo *et al.*, 1993; Gibon *et al.*, 2002), taking care to use freshly prepared extracts for ATP, PEP and pyruvate.
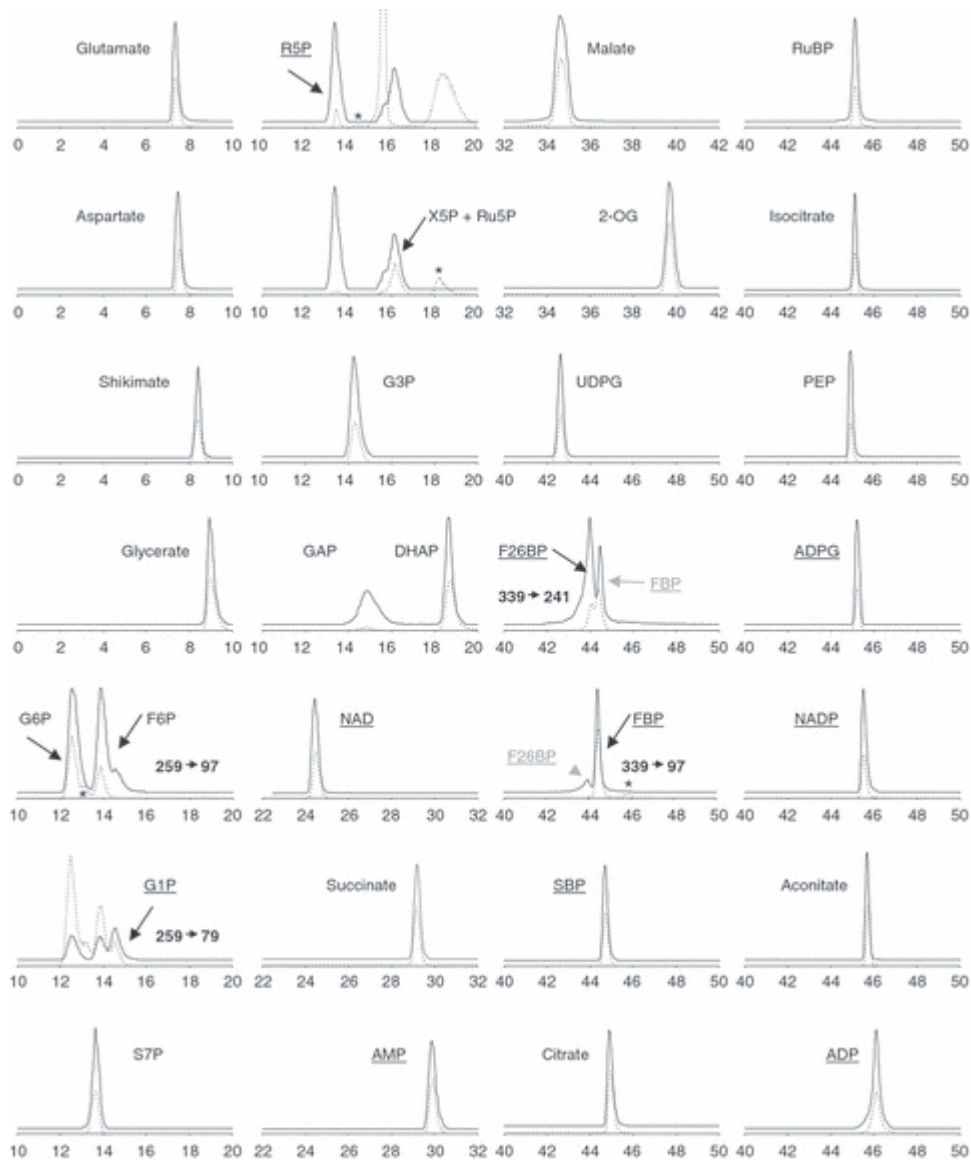
Figure 2-10: Selective Ion Chromatograms for a Standard Mixture (solid lines), and the Corresponding Metabolites in Leaf Extracts (dashed lines), in which the x axis Gives the Retention Time in Minutes.

Underlined metabolites were measured in non-diluted extract. When different transitions are used to distinguish between isomers, these are indicated. *Unidentified metabolite (Figure from Arrivault *et al*., 2009).

2.2.6 Statistical Analysis

Statistical analysis was performed using the General Linear Model ANOVA routine in MINITAB (ver. 16). For halotolerance experiments, Factor 1, Genotype (4 levels; Local, Soorab-96, Awaran-2002, and Optic) 12 replicates (4 x 12 = 48). Factor 2, Salinity (4 levels; 0, 50, 100, 150 mM NaCl) 12 replicates (4 x 12 = 48). Interaction, (4 x 4 = 16) 3 replicates (16 x 3 = 48). For thermotolerance experiments, Factor 1, Genotype (3 levels; Local, Soorab-96, and Optic) 9 replicates (3 x 9 = 27). Factor 2, Temperature (3 levels; before, immediately after, and 5 days after) 9 replicates (3 x 9 = 27). Interaction, (3 x 3) 3 replicates (3 x 3 x 3 = 27). ANOVA tables, residual plots, and interaction plots for each parameter were shown in tables and figures under the Appendix.

Chapter 3: Characterization of Halotolerance in Barley Genotypes: Germination, Growth, Yield, and Development

Four barley genotypes, Local, Optic, Soorab-96, and Awaran-2002 were compared for germination, growth, and yield in a range of hydroponic solution containing increasing levels of NaCl (0, 50, 100 and, 150 mM). The development pattern of the four genotypes was also assessed using the Zadoks scale (Zadoks *et al*., 1974) and by confirming the presence of the dominant Ppd-H1 flowering locus, the major determinant of early flowering spring barleys (Turner *et al*., 2005).

3.1 *Germination*

An experiment was conducted to assess the effects of salinity on germination and early seedling growth of Local, Optic, Soorab-96, and Awaran-2002. Seeds of these genotypes were germinated and grown under control conditions for 14 days on a range of NaCl concentrations (0, 50, 100, and 150 mM; see Material and Methods Section 2.1.2.1 for experimental details). Increasing NaCl concentration inhibited germination of Optic, Soorab-96, and Awaran-2002, but not that of Local, which maintained *ca*.100 % germination irrespective of NaCl concentrations from control levels to 150 mM (Figure 3-1a). Optic, Soorab-96 and Awaran-2002 maintained their germination up to 50 mM. At and above 100 mM NaCl concentrations; however, germination was reduced in all these lines. This reduction was more prominent in Optic (approximately 50 % at 100 mM) at 150 mM NaCl concentration a 85 % reduction was observed. Lines Soorab-96 and Awaran-2002 showed a moderate reduction of approximately 50 to approximately 65 % at 100 and 150 mM NaCl concentrations respectively. Analysis of variance tests revealed that landrace Local showed a significant difference for percentage germination compared with all other lines *i.e.* Optic, Soorab-96, and Awaran-2002, at 100 and 150 mM NaCl concentrations (Figure 3-1a; p<0.05).

All four genotypes showed a significant decline in seedling shoot length with increasing NaCl concentrations. This decline was significant in Optic, Soorab-96 and Awaran-2002 on 100 and 150 mM NaCl concentrations when compared with landrace Local (Figure 3-1b p<0. 05 and Figure 3-2).

Figure 3-1: Effect of NaCl on the Germination and Seedling Shoot Length of Barley Genotypes.

Top panel (a): germination % of control; bottom panel (b): seedling shoot length (cm). Ten seeds from genotypes Local, Optic, Soorab-96, and Awaran-2002, genotypes were imbibed in sealed petri dishes with solutions containing the indicated levels of NaCl (see Material and Methods Section 2.1.2.1 for experimental details). (a) Averages and standard errors of replicates for germination (% of control). (b) Averages and standard errors of replicates for seedling shoot length of the middle two quartiles are presented. ANOVA tests were performed by using a General Linear Model. Tables for ANOVA and grouping information along with Figures for residual and interaction plots are presented in Appendix (Figures A 3-1 & A 3-2).
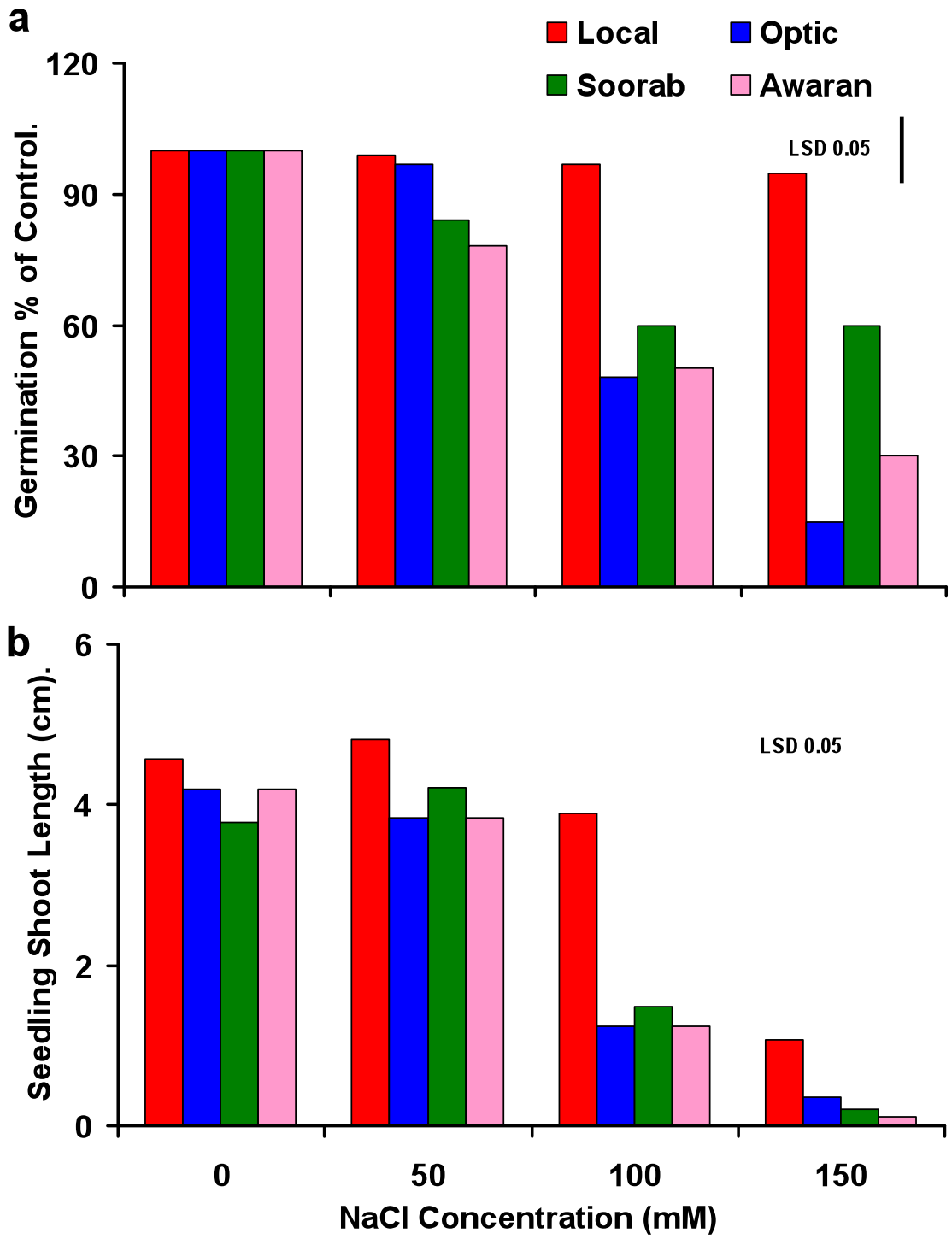
Figure 3-2: Effect of NaCl on the Seedling Shoot Length of Barley Genotypes.

Images of seedlings from landrace Local (a), Optic (b), Soorab-96 (c) and Awaran-2002 (d). The two best developed seedlings germinated and grown on a range of NaCl concentrations i.e. (0, 50, 100, 150 mM) in distilled water are shown; see Section 2.1.2.1 for experimental details.
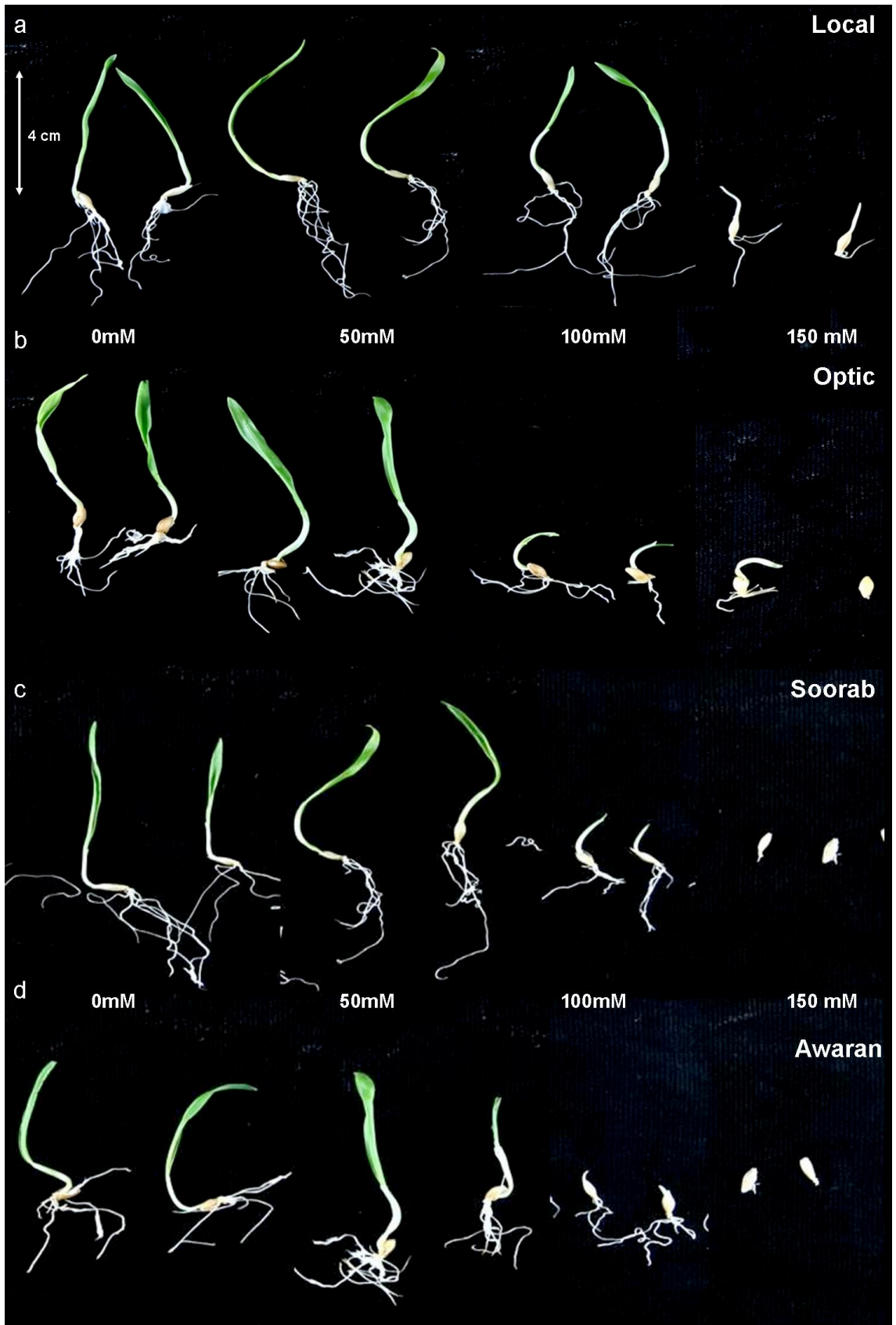
3.2 *Growth Parameters*

All four genotypes Local, Optic, Soorab-96, and Awaran-2002 were assessed for basic growth parameters (*i.e.* shoot and root length, fresh and dry weight) over a range of hydroponic NaCl concentrations. Experiments were conducted for two consecutive years during (October 2008 and June 2009) under controlled glass house conditions (see Section 2.1.2.2 for experimental details). Growth and all physiological parameters were measured at days 31, 45, 60, 74, and harvest. Data for sixty days-old (38 days under salt stress) plants only are presented from here on as at this stage all plants in all genotypes were surviving (even on the highest levels of salinity), and unlike younger plants, where differences between the lines were not so apparent. Increasing salinity produced an apparent decrease in biomass; line Optic (Figure 3-3b) and Awaran-2002 (Figure 3-3d) appeared to be the most sensitive to high salinity and landrace Local (Figure 3-3a) the least. Essentially, the data for the two experiments were very similar; for brevity, only data for the second experiment (June, 2009) are presented as this data set was more complete.

3.2.1 Phenotypic Representation of Barley Genotypes under High Salt Concentrations

Increasing the NaCl concentration in hydroponic solutions impaired the vegetative growth of all genotypes Local, Optic, Soorab-96, and Awaran-2002 (Figure 3-3 a, b, c, and d), from the plant images it is clear that only landrace Local is least affected at the highest salt concentration 150 mM NaCl.
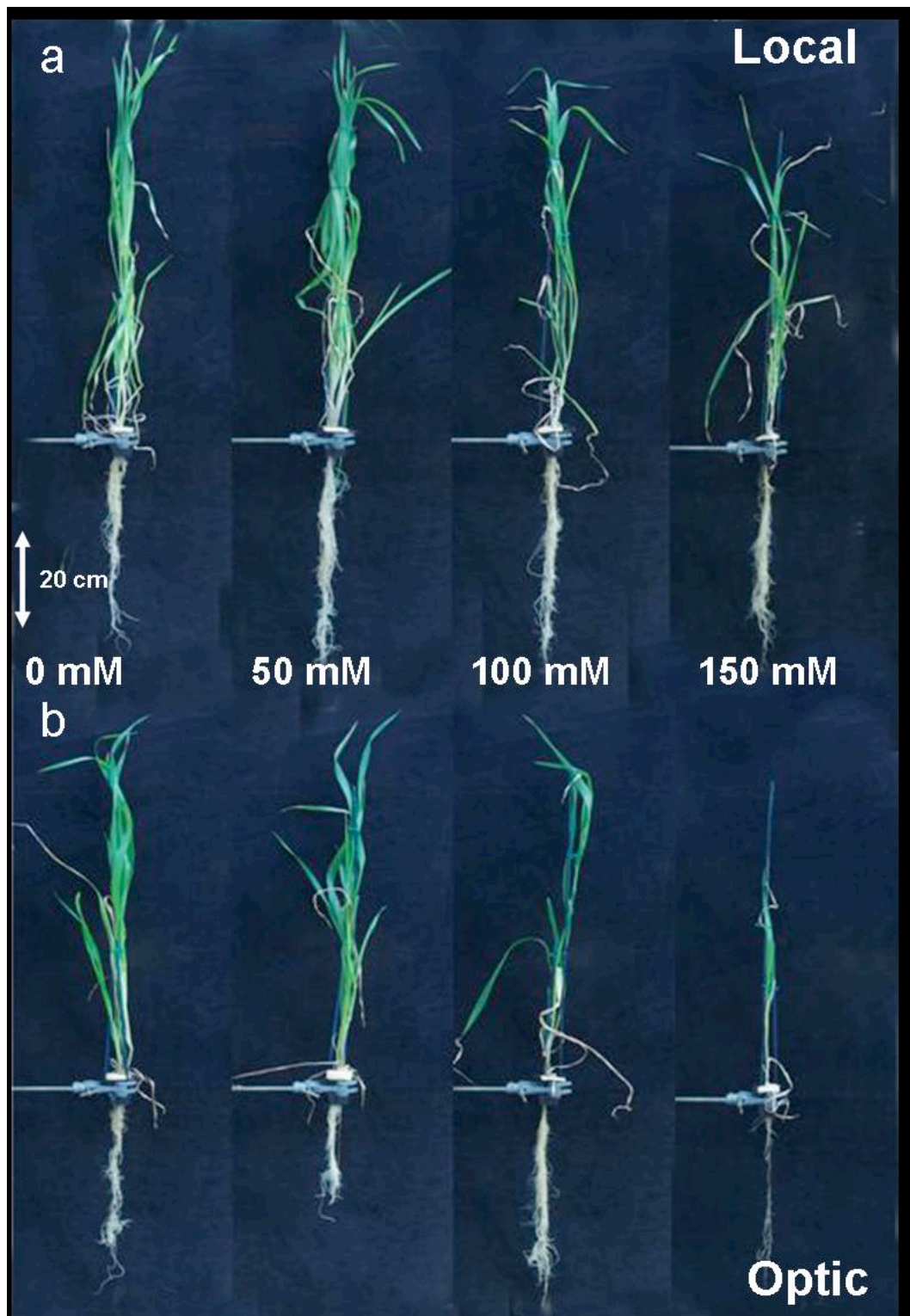
Figure 3-3 a & b: Effect of Salinity on Vegetative Growth on 60 Day Old Barley Genotypes.

Seeds from genotypes Local (a), Optic (b), Soorab-96 (c), and Awaran-2002 (d) were germinated on paper towel pads under sterilized conditions. One week after germination seeds, were shifted to ¼ Hoagland's media and when plants were 21 days old; media was supplemented with NaCl to provide concentrations of 0, 50, 100 and 150 mM; see Section 2.1.2.2 for experimental details.
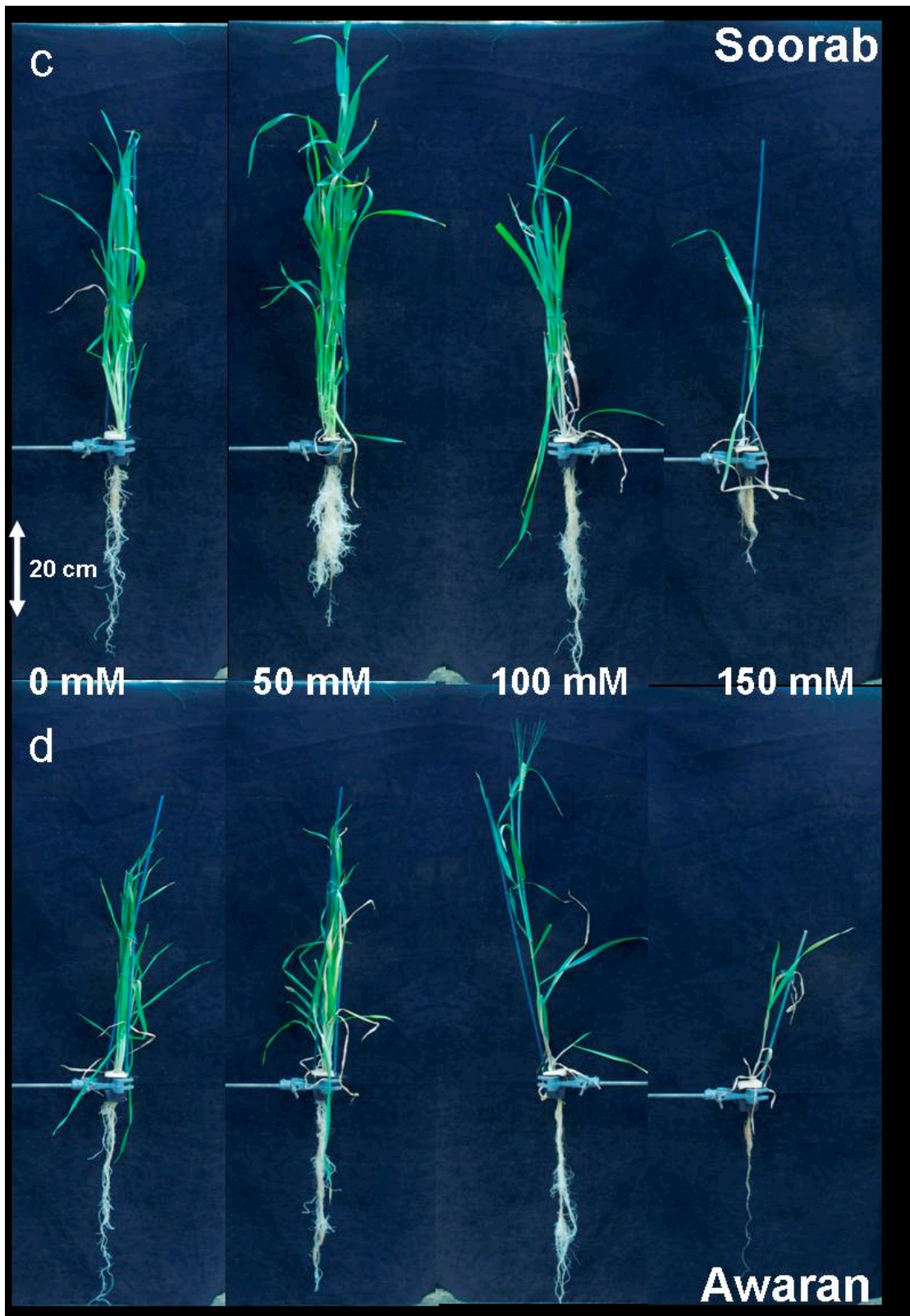
Figure 3-3 c & d: Effect of Salinity on Vegetative Growth on 60 Day Old Barley Genotypes.

Legend continued from (Figure 3-3 a & b; Page-63).

3.2.2 Shoot and Root Length

Comparison of the effects of increasing NaCl concentration from 0 to 100 on shoot length in each of the lines showed no significant differences (p>0.05; Figure 3-4a). However, all genotypes showed a significant decline in shoot length on 150 mM NaCl compared with plants at 0 mM NaCl. This decline was more prominent in the elite lines Optic, Soorab-96, and Awaran-2002 than in Local (p>0.05).

Root length data showed non significant differences for landrace Local, line Optic and Awaran at increasing NaCl from control to 150 mM. While Soorab-96 showed a significant decline compared with control NaCl concentration (p<0.05: Figure 3-4b).

3.2.3 Shoot and Root Fresh Weight

Shoot fresh weight data collected from 60 day old plants (38 days of salt stress) of landrace Local, Optic, Soorab-96, and Awaran-2002 presented in (Figure 3-5a). Shoot fresh weight declined in elite lines with increasing salt concentration (from 0 to 150 mM NaCl), however, landrace maintained shoot fresh weight (p<0.05). The elite lines Awaran-2002, Soorab-96, and Optic showed significant differences for shoot fresh weight values compared with landrace Local at 150 mM NaCl concentration. These data establish that the elite lines are more salt sensitive than Local showing a approximately 80 % decrease in shoot fresh weight biomass at 150 mM NaCl compared with approximately 25 % decrease for landrace Local.

Data for root fresh weight showed a non-significant decline with increasing salt concentration from (0 to 100 mM NaCl) and decline at 150 mM NaCl for all genotypes, however this decline was significant in elite lines Optic, Soorab-96, and Awaran-2002 compared with landrace Local (Figure 3-5b; p≤0.05).

Figure 3-4: Effect of Salinity on Shoot and Root Length of Barley Genotypes.

Top panel (a): shoot length; bottom panel (b): root length. Each data point presents the mean and standard error of five replicates. Measurements were made 60 days after germination (38 days after salt treatment). See Section 2.1.2.2.3 for experimental details. Values are the average (± SE) for 5 replicates per treatment. ANOVA tests were performed by using a General Linear Model. Tables for ANOVA and grouping information along with Figures for residual and interaction plots are presented in Appendix (Figures A 3-3 & A 3-4).
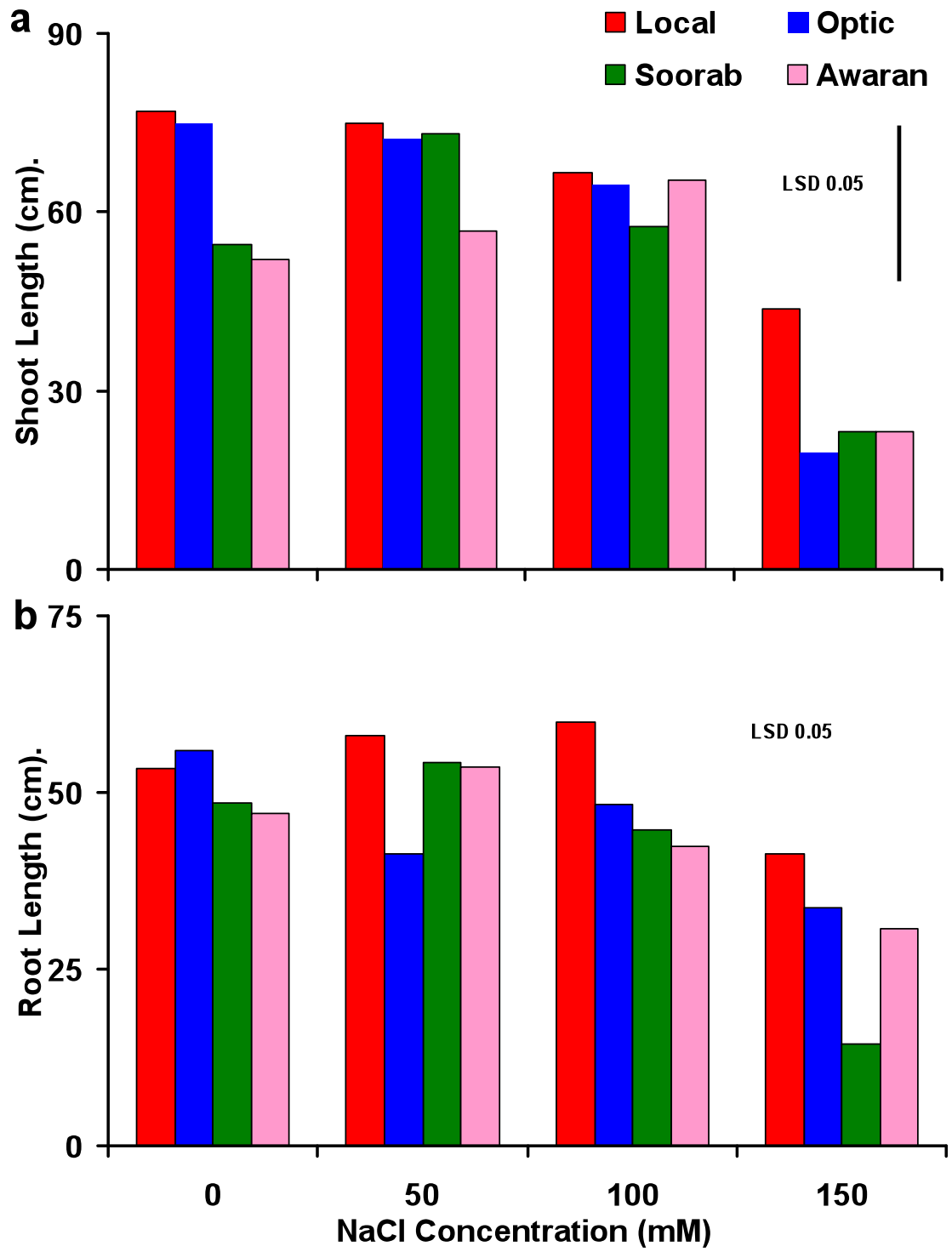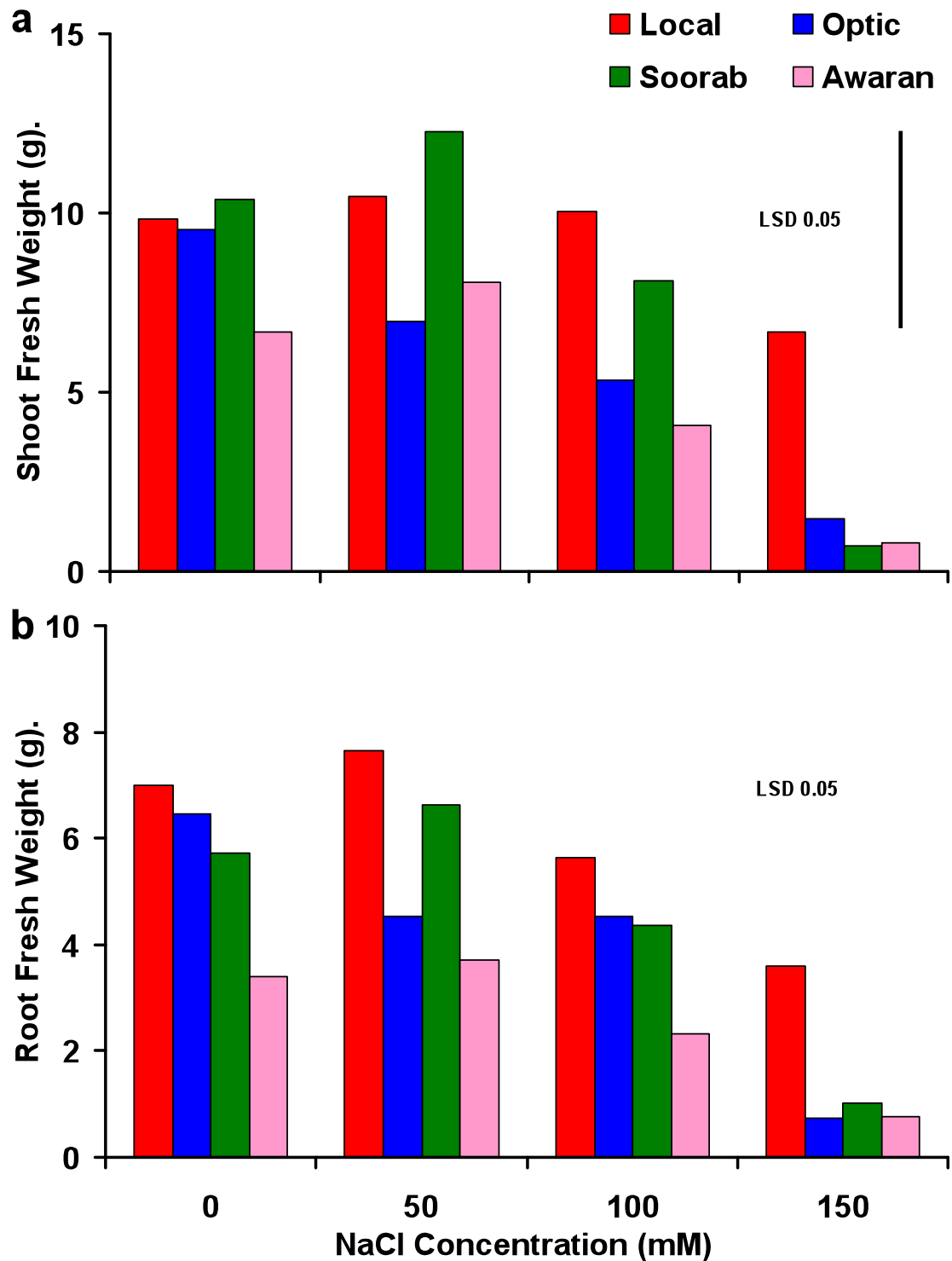
Figure 3-5: Effect of Salinity on Shoot and Root Fresh Weights of Barley Genotypes.

Top panel (a): shoot length; bottom panel (b): root length. Values are the average (± SE) for 5 replicates per treatment see Section 2.1.2.2.4 for experimental details. ANOVA tests were performed by using a General Linear Model. Tables for ANOVA and grouping information along with Figures for residual and interaction plots are presented in Appendix (Figures A 3-5 & A 3-6).

3.2.4 Shoot and Root Dry Weight

Shoot and root dry weights were obtained from oven dried samples of genotypes Local, Optic, Soorab-96, and Awaran-2002 harvested at 60 days from germination (38 days of salt treatment; see Section 2.1.2.2.3 for experimental details). Data for shoot dry weight showed no significant change at 50 mM (*cf* 0 mM) in all genotypes. Local, Soorab-96, and Optic maintained their dry weight values at 100 mM NaCl, but in Awaran-2002 it declined further. At 150 mM NaCl concentrations all three elite lines, Awaran-2002, Soorab-96, and Optic showed a significant decline of approximately 60 to 85 %, compared with controls, but Local showed a decrease of approximately 25 % (Figure 3-6a; $p<0.05$).

For all genotypes root dry weight showed a similar pattern to shoot dry weight, where it maintained its values with increasing external NaCl concentration up to 100 mM. However at 150 mM NaCl root dry weight declined significantly in Optic approximately 80 % compared with controls, whereas Local showed only an approximately 30 % decline (Figure 3-6b; $p<0.05$).
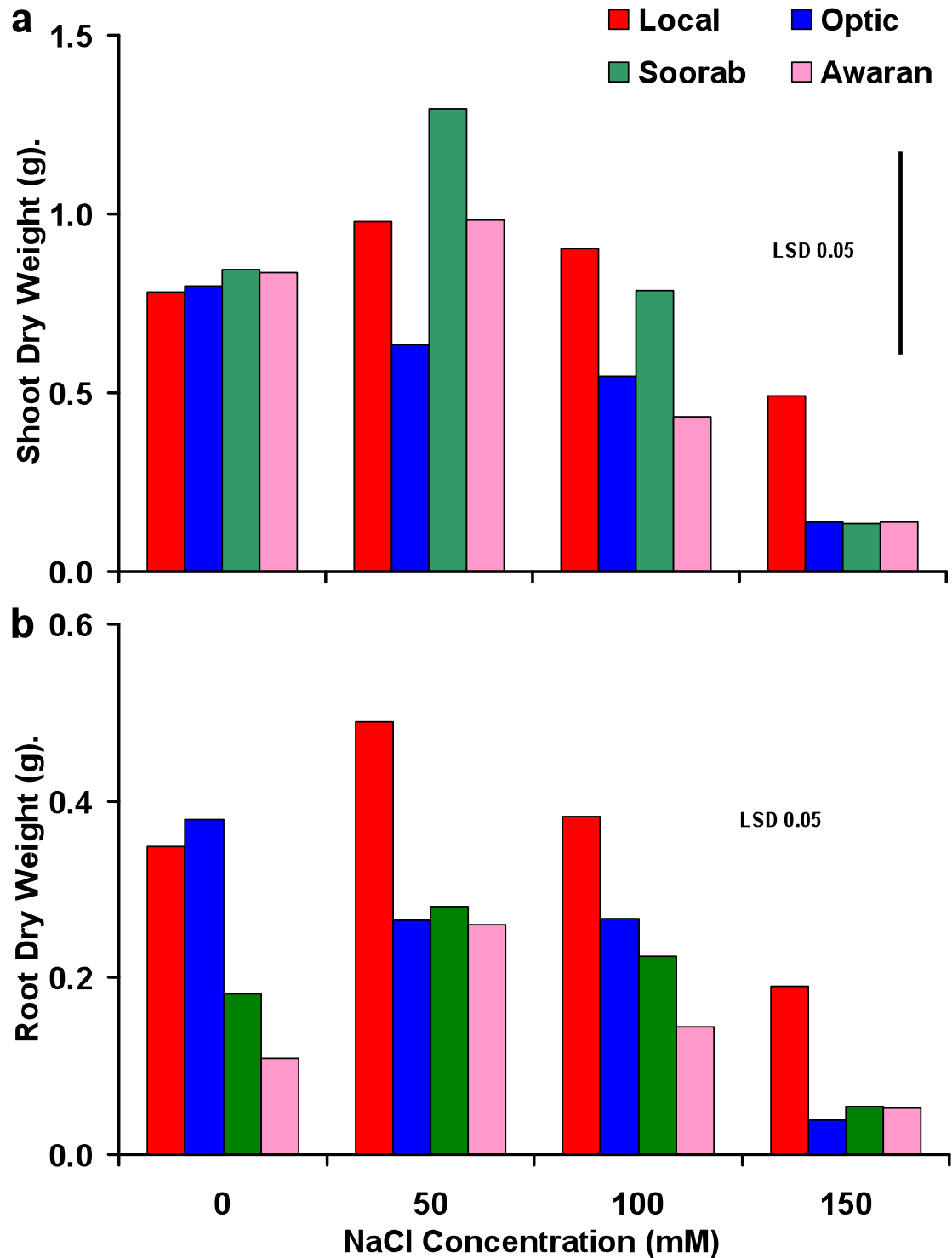
Figure 3-6: Effect of Salinity on Shoot and Root Dry Weights of Barley Genotypes.

Top panel (a): shoot dry weight; bottom panel (b): root dry weight. Values are the average (± SE) for 5 replicates per treatment; see Section 2.1.2.2.4 for experimental details. ANOVA tests were performed by using a General Linear Model. Tables for ANOVA and grouping information along with Figures for residual and interaction plots are presented in Appendix (Figures A 3-7 & A 3-8).

3.2.4.1 Tillering

Data for number of tillers (including the main stem) per plant were recorded from day 45 until day 105 every two weeks.

Landrace Local in 0 and 50 mM NaCl showed a gradual increase in tillers per plant from day 45 to day 105, but this increase was significantly different ($p < 0.05$) only at day 105 (*c.f.* day 45). At 100 and 150 mM NaCl concentrations Local maintained its tillers per plant throughout its developmental period from day 45 to day 105. However, the initiation of new tillers after day 45 was completely suppressed in Local above 50 mM NaCl ($p < 0.05$; Figure 3-7a).

In Optic the number of tillers per plant increased significantly from approximately 3 to 7.5 during the course of vegetative development from day 45 to day 105 at 0 mM NaCl, and from 3 to 4.5 at 50 mM NaCl concentration ($p < 0.05$). At 100 and 150 mM NaCl concentrations the number of tillers per plant decreased with time. The number of tillers per plant started decreasing with time from day 75 at 100mM NaCl and all tillers died after day 75 at 150 mM NaCl concentration ($p < 0.05$; Figure 3-7b).

The number of tillers per plant in line Soorab-96 showed a very similar pattern that observed for landrace Local. At low salt concentrations (0 and 50 mM NaCl) new tillers were produced right up to day 105 ($p < 0.05$), but this was suppressed in concentrations of 100 mM and above ($p < 0.05$; Figure 3-7c). Unlike Local, however, all tillers were killed in 150 mM NaCl at day 105.

The number of tillers in Awaran-2002 did not increase significantly with time when grown in 0 mM and 50 mM NaCl. Higher concentration of NaCl resulted in a decline in living tillers with time ($p < 0.05$) and no tillers survived beyond day 60 at 150 mM NaCl (Figure 3-7d).
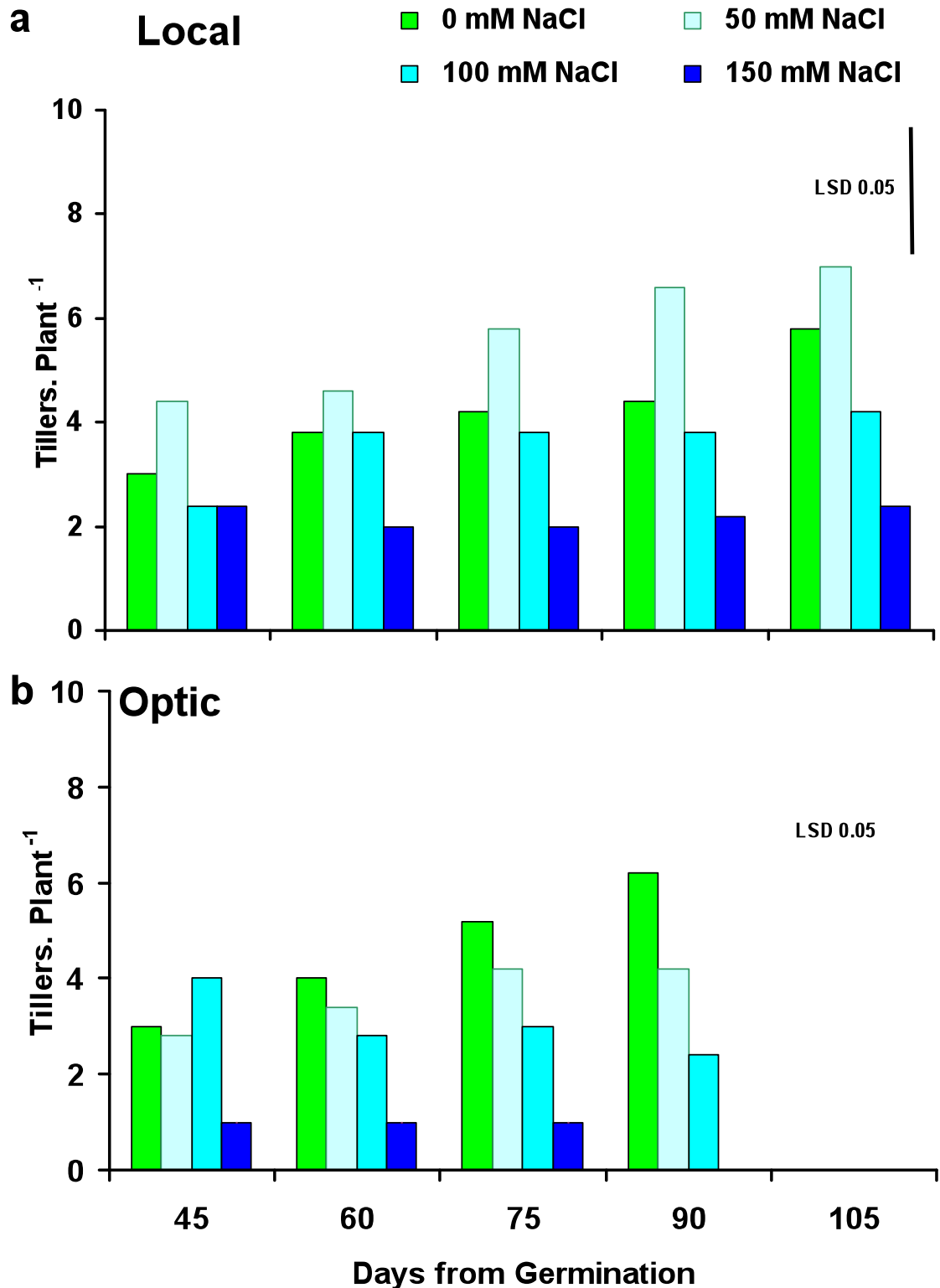
Figure 3-7 a & b: Effect of Salinity on the Number of Tillers per Plant With Time of Barley Genotypes.
Number of living tillers per plant in each genotype was recorded every two weeks. Values are the average (± SE) for 5 replicates per treatment. ANOVA tests were performed by using a General Linear Model. Tables for ANOVA and grouping information along with Figures for residual and interaction plots are presented in Appendix (Figures A 3-9 to A 3-12).
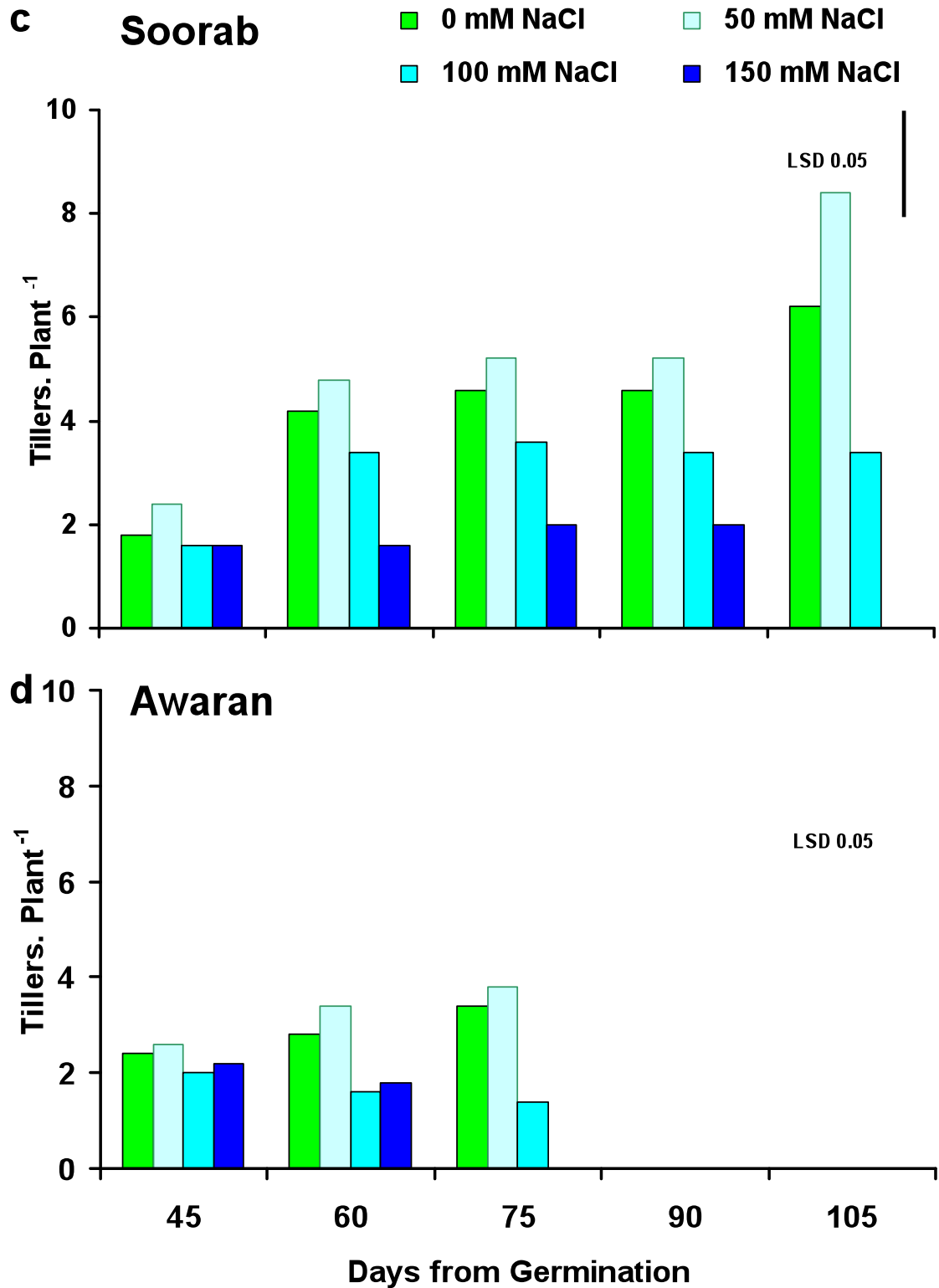
Figure 3-7 c & d: Effect of Salinity on the Number of Tillers per Plant With Time of Barley Genotypes.

Legend continued from (Figure 3-7 a & b; Page-72).

3.3 *Yield Parameters*

In addition to the growth parameters measured during the vegetative phase of growth (Day 60), various yield parameters were also measured at harvest.

3.3.1 Ears and Grains per Plant

Data in Fig 3-8a and 3-8b present the number of ears and number of grains per plant data for the four barley genotypes Local, Optic, Soorab-96 and Awaran-2002 exposed to increasing concentrations of NaCl (0 to 150 mM). An overall decline in ears per plant and grains per plant were observed with increasing salinity (0 to 150 mM NaCl) in genotypes Local, Soorab-96, and Awaran-2002, however, Soorab-96 showed an initial increase in ears per plant followed by a significant decrease of *ca.* 40 to 50 % at higher salt concentrations *i.e.* 100 mM NaCl. In contrast Optic showed a progressive decrease of approximately 30 % at 50 mM NaCl and *ca.* 80 % at 100 mM NaCl, in the number of ears and seeds per plant with incremental external NaCl concentrations from control to 100 mM. This decline in the elite lines Awaran-2002, Soorab-96, and Optic were more dramatic on 150 mM NaCl where they totally failed to produce fertile spikes and seeds (Figure 3-8 a & b; $p<0.05$).
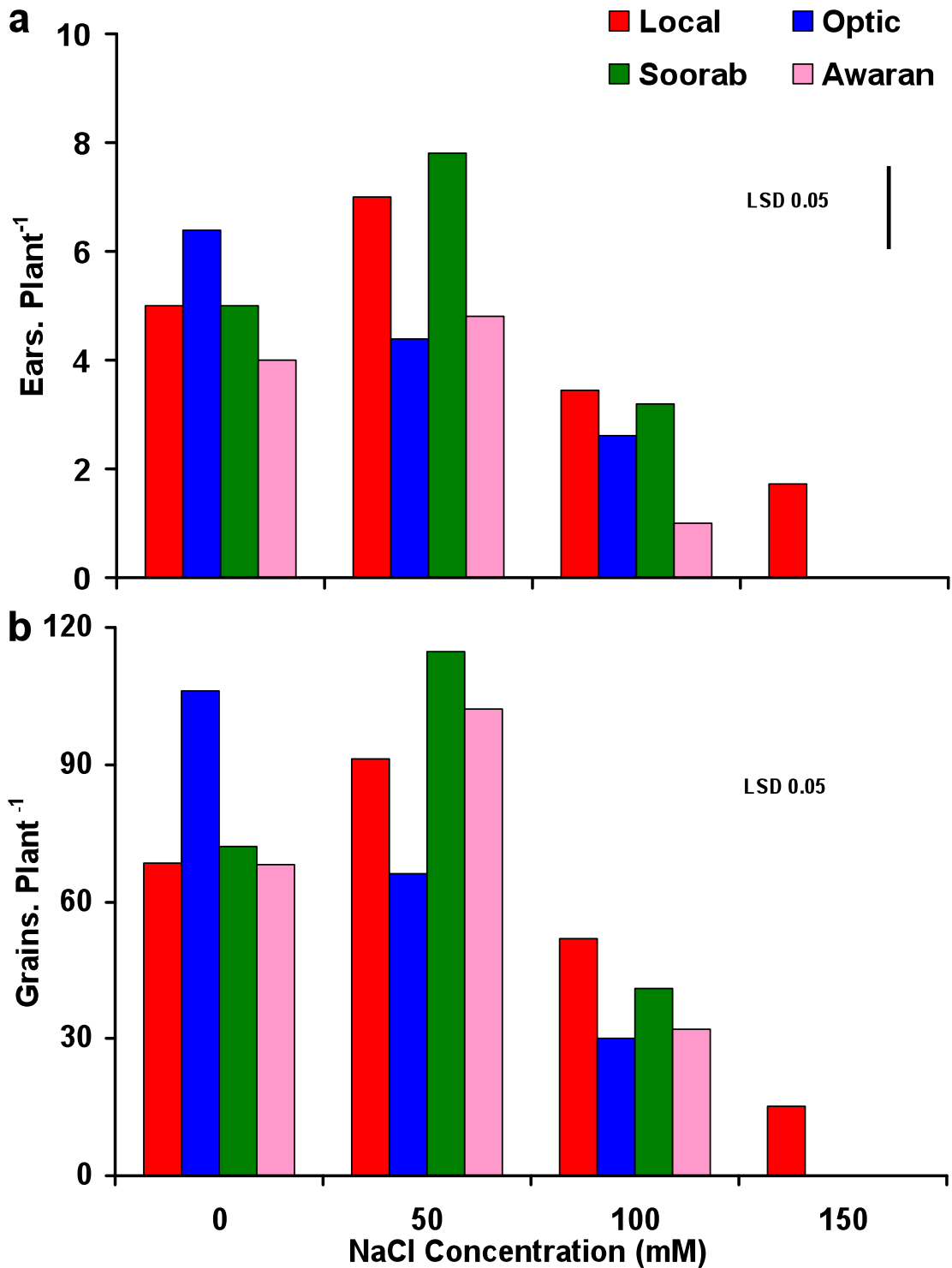
Figure 3-8: Effect of Salinity on Number of Seeds and Ears per Plant in Barley Genotypes.

Top panel (a): ears per plant; bottom panel (b): grains per plant. Values are the average (± SE) for 5 replicates per treatment. ANOVA tests were performed by using a General Linear Model. Tables for ANOVA and grouping information along with Figures for residual and interaction plots are presented in Appendix (Figures A 3-13 & A 3-14).

3.3.2 Grain Weight per Plant and 1000 Grain Weight

All barley genotypes Local, Optic, Soorab-96, and Awaran-2002 showed an overall decline for grain weight per plant at 100 and 150 mM NaCl, when compared with controls (0 mM; Figure 3-9a). Line Soorab-96 showed a significant increase of approximately 25 % at 50 mM NaCl for grain weight per plant values, at 100 mM NaCl concentration line Awaran showed a significant decrease of approximately 80 %. Line Optic showed a progressive and significant decrease of approximately 75 % with increasing salt concentrations to 100 mM NaCl. Landrace Local maintained its grain weight per plant values up to 50 mM NaCl concentration, however, at 100 mM NaCl it showed a significant decline of approximately 40 %. The least affected variety was Local, which managed to produce a few seeds per plant at highest salt concentration of 150 mM NaCl, whereas all other lines failed to produce any (Figure 3-9a; $p<0.05$).

1000 Grain weight (weight of 1000 dry seeds) values in all genotypes were maintained at approximately 40 grams up to 50 mM NaCl, but at 100 mM NaCl concentration these values dropped significantly in lines Awaran-2002, and Soorab-96, but not for landrace Local and line Optic, which maintained their 1000 grain weight values. However, all genotypes showed significant differences for 1000 grain weight compared with controls at 150 mM NaCl concentration (Figure 3-9b; $p \leq 0.05$).
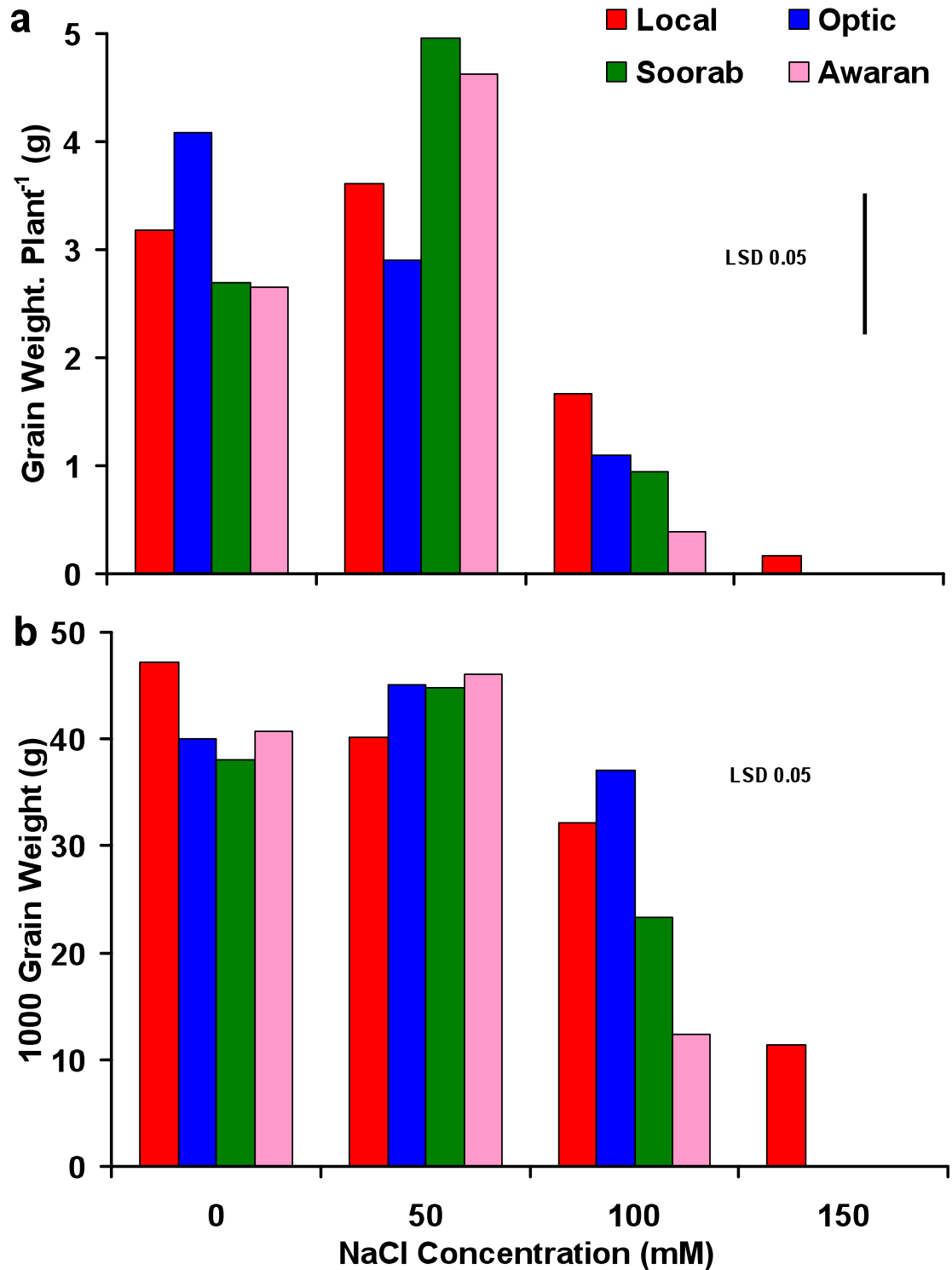
Figure 3-9: Effect of Salinity on Grain Weight per Plant and 1000 Grain Weight in Barley Genotypes.

Top panel (a): seed weight per plant; bottom panel (b): 1000 grain weight. Values are the average (± SE) for 5 replicates per treatment. ANOVA tests were performed by using a General Linear Model. Tables for ANOVA and grouping information along with Figures for residual and interaction plots are presented in Appendix (Figures A 3-15 & 3-16).

3.4 *The Effects of Salt Stress on the Development of Barley Genotypes*

To establish whether the observed significant differences regarding halotolerance between landrace Local and lines Optic, Soorab-96, and Awaran-2002 (elite) could be attributable to the interaction between salinity and development. The development of twenty plants from each genotype in hydroponics supplemented with (0, 50, 100, and 150 NaCl) was recorded using the Zadok's scale (see Section 2.1.2.2.1 and 2.1.2.3 for experimental details).

The effects of salinity on the full developmental program (seed-to-seed) of the four barley genotypes are presented in Figure 3-10. From these data it is clear that across all salt concentrations Awaran completes its life cycle earlier than all other genotypes (65-75 days). In contrast, Soorab takes longest to complete its life cycle in hydroponics (approximately 130 days) although it did not progress to anthesis in 150 mM NaCl. In 0 mM NaCl line Optic completed its life cycle in approximately 88 days, *ca.* 10 days earlier than landrace Local. When grown in 100 mM NaCl, the life cycle of Local accelerates so that seed reaches maturity at the same time as Optic, approximately after 84 days.
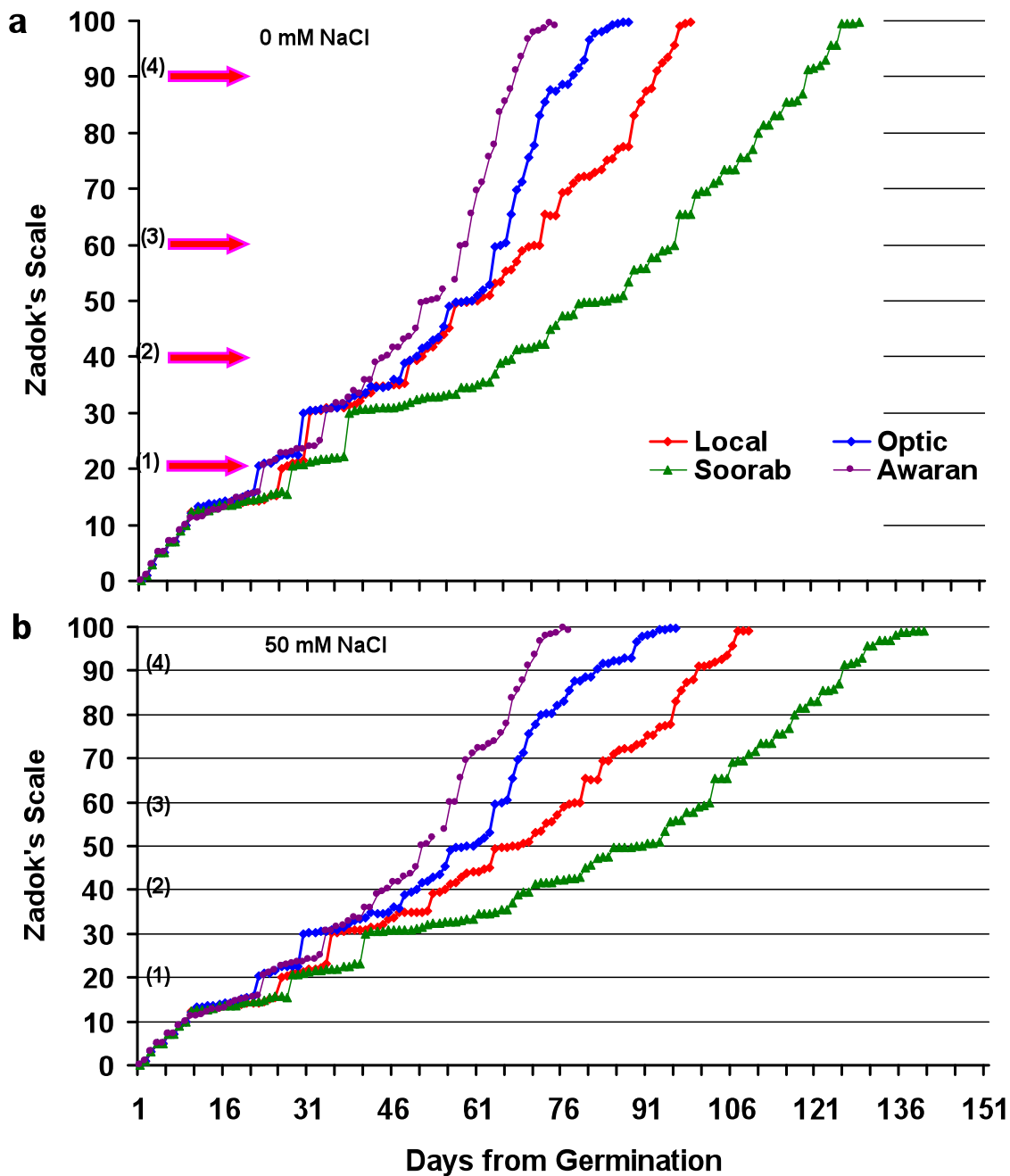
Figure 3-10 a & b: Comparison of the Rate of Development of Barley Genotypes in Hydroponics under Salt Stress.

The Zadoks score (see Section 2.1.2.3) for Local, Optic, Soorab-96, and Awaran-2002 at 0 mM (a), 50 mM (b). 100 mM (c), and 150 mM (d) NaCl concentration. Assessment was made at least every 2nd day. Plants were exposed to NaCl at day 21st (light blue arrow). Important developmental stages are indicated with red arrows for all genotypes as (1) Tillering, (2) Inflorescence Emergence, (3) Anthesis, and (4) Ripening.
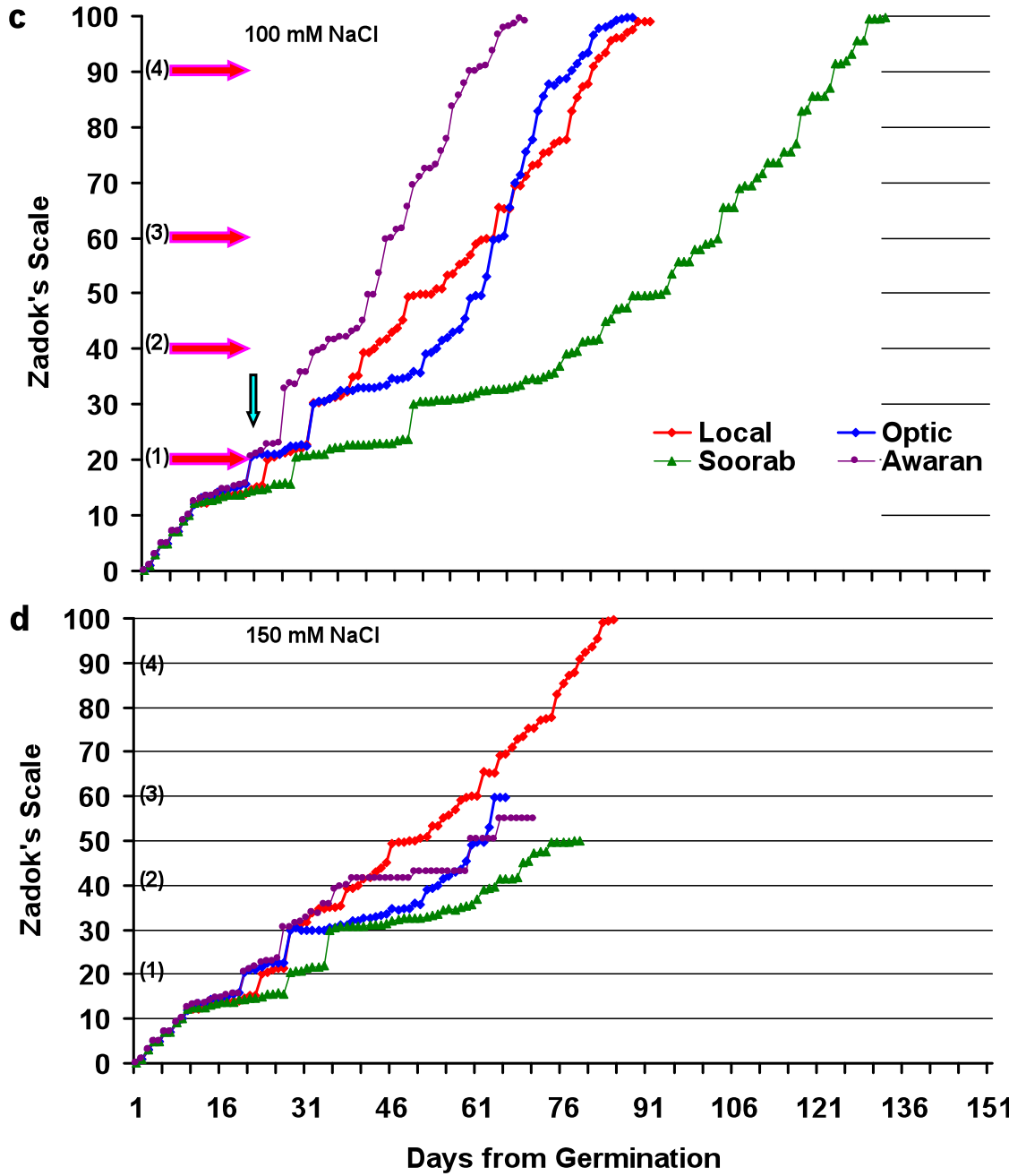
Figure 3-10 c & d: Comparison of the Rate of Development of Barley Genotypes in Hydroponics under Salt Stress.

Legend continued from (Figure 3-10 a & b; Page-80).

3.4.1 The Effects of Salt Stress on Four Key Developmental Stages

In order to assess the effects of salt treatment on the developmental stages of barley genotypes better, the time taken for each genotype to reach four key developmental stages was assessed (Tillering, Inflorescence Emergence, Anthesis and Ripening; Figure 3-11).

From these figures it is evident that salinity had no effect on the timing of the start of tillering in all genotypes when exposed to increasing salt concentrations from 0 to 150 mM NaCl.

Salinity had no effect on spike (inflorescence) emergence in Optic (Figure 3-11b) but caused a significant delay of approximately 12 days in line Soorab when exposed to 100 mM NaCl (*c.f.* 0 mM; $p < 0.05$; Figure 3-11c); higher concentrations, however, removed this delay. Salinity accelerated inflorescence emergence significantly in landrace Local at 150 mM NaCl (*c.f.* 0 mM; $p < 0.05$; Figure 3-11a), and a similar pattern was observed in Awaran ($p < 0.05$; Figure-3-11d).

Salinity prevented flowering in Optic, Soorab-96 and Awaran-2002, but accelerated it significantly in Local at 50 mM NaCl compared with 0, 100, and 150 mM NaCl concentrations ($p < 0.05$; Figure 3-11 a, b, c & d).

Salt concentrations of up to 100 mM NaCl had no effect on the timing of anthesis in lines Soorab and Optic. A similar pattern was observed for line Awaran but there was some evidence that at 100 mM NaCl anthesis was accelerated by approximately 10 days ($p < 0.05$; Figure 3-11d). Anthesis was completely inhibited when Optic, Soorab and Awaran were exposed to 150 mM NaCl (Figure 3-11 b, c & d). High salinity accelerated the time of anthesis in genotype Local from approximately 70 days to 60 days in 150 mM NaCl (Figure 3-11a).

Increasing salinity had little effect on the time to seed maturity in lines Optic, Awaran and Soorab up to 100 mM NaCl, but no seed set was observed in any of these lines at 150 mM NaCl (Figure 3-1 b, c & d). In contrast, seed set was observed in genotype Local at all NaCl concentrations (Figure 3-11a).
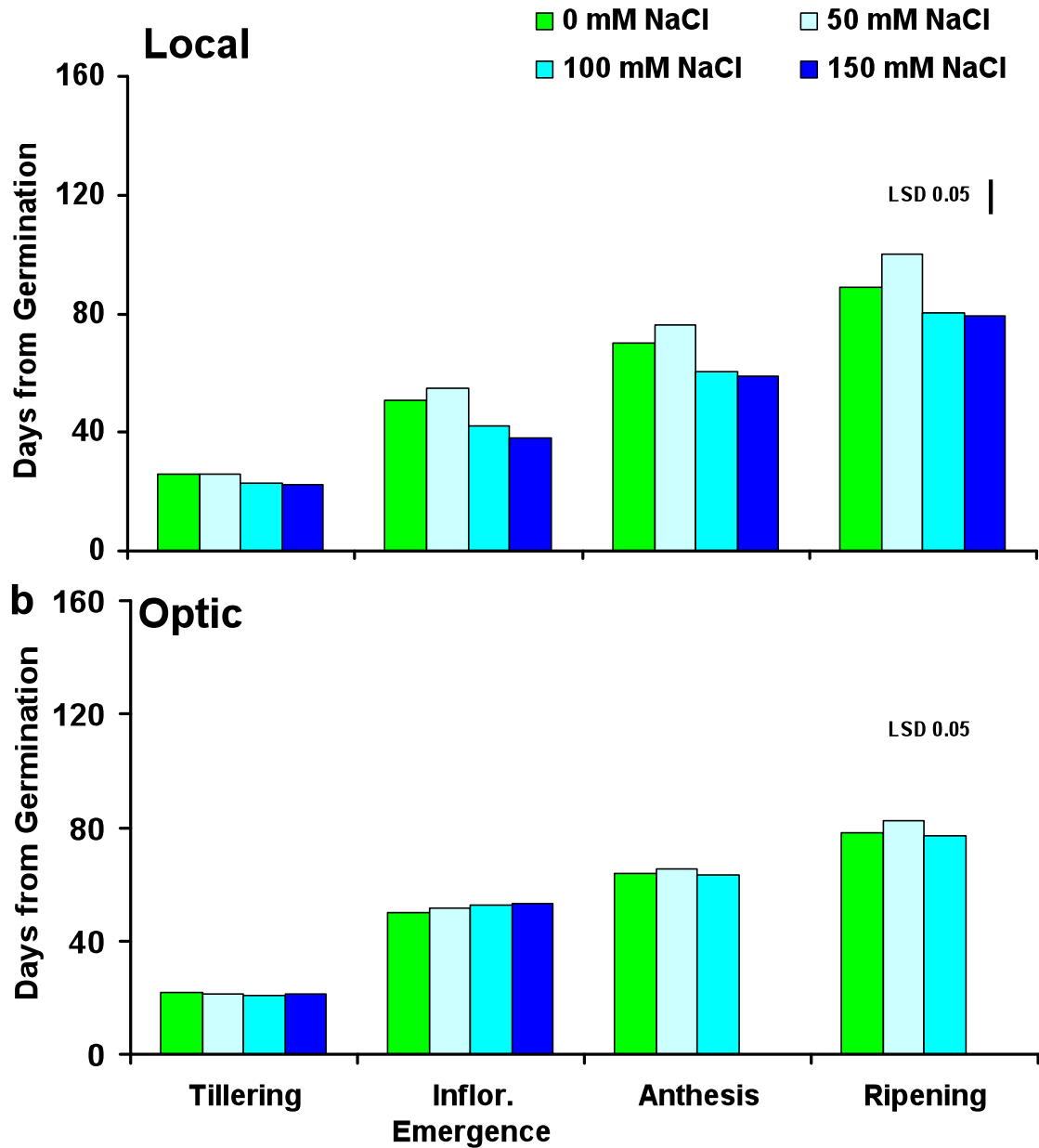
Figure 3-11 a & b: Comparison of Timing of Key Developmental Stages in Barley Genotypes.

The time (Days) to entry into the key Zadoks stages i.e. Tillering (20), Inflorescence Emergence (40), Anthesis (60), and Ripening (90) of four barley genotypes at various NaCl concentrations i.e. 0, 50, 100, and 150 mM NaCl are presented (n=20 plants). ANOVA tests were performed by using a General Linear Model. Tables for ANOVA and grouping information along with Figures for residual and interaction plots are presented in Appendix (Figures A 3-18 to A 3-21).
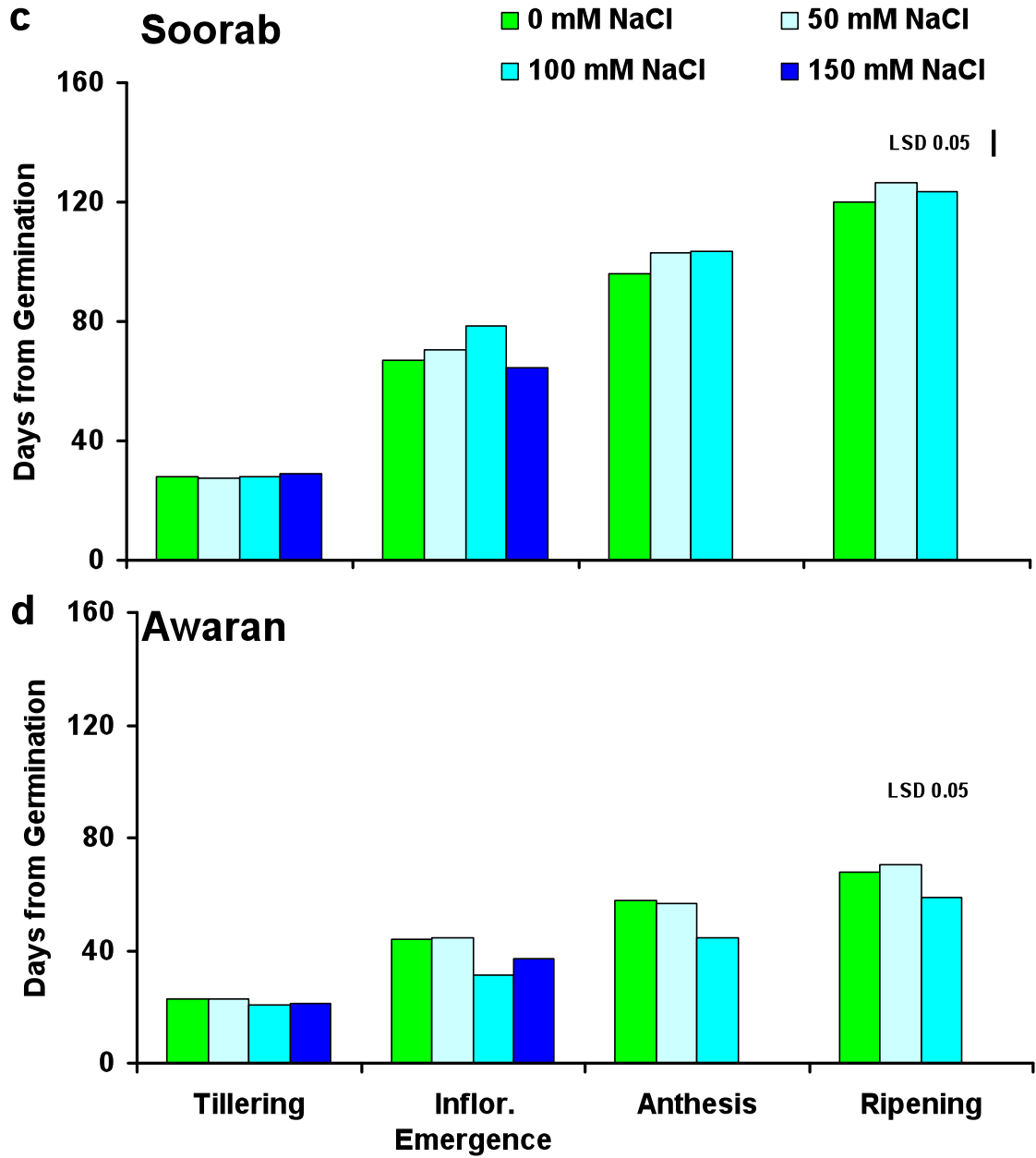
Figure 3-11 c & d: Comparison of Timing of Key Developmental Stages in Barley Genotypes.

Legend continued from (Figure 3-10 a & b; Page-83).

3.4.2 Assessment of Ppd-H1 Flowering Locus

There are two types of barley lines grown commercially *i.e.* winter barley (delayed flowering) and spring barley (early flowering) lines. The locus controlling flowering in barley has been known for many years and named the photoperiod-H1 locus (Ppd-H1) but other loci (*e.g.* VRN 1-3) in cereals have also been implicated (Yan *et al.*, 2004; Yan *et al.*, 2003). Early flowering lines carry a dominant allele, Ppd-H1, whilst delayed flowering lines carry a recessive allele ppd-H1. The identity of the Ppd-H1 gene was revealed by positional cloning and found to encode a 'Pseudo-Response' regulator protein with homology to the *Arabidopsis* clock gene CONSTANS (CO). Further, extensive Single Nucleotide Polymorphism (SNP) analysis with an extensive collection of early and delayed flowering lines identified SNP 22, a G to T (glycine to threonine) substitution (Turner *et al.*, 2005), as the critical SNP causing the observed difference in flowering time.

To assess whether the observed delayed grain filling and kernel hardening in Local line was attributable to a similar substitution, PCR primers were designed to amplify this region of barley genomic DNA. The test interval containing the putative SNP 22 variant was amplified using PCR primers (H*v*TF; ATG CGA ATG GTG GAT CGG C and H*v*CR; TAT AGC TAG GTG CGT GGC G). The 506 bp PCR product from ppd-H1 (late flowering) lines can not be digested with the endonuclease BstUI, whereas the dominant allele (Ppd-H1) is cut to produce a 432 and a 74 bp products. Figure 3-11a shows the digested and undigested PCR products amplified from gDNA from Local and Optic; clearly, in both cases the 506 bp PCR fragment has been restricted indicating both Local and Optic contain the Ppd-H1 (early flowering allele).
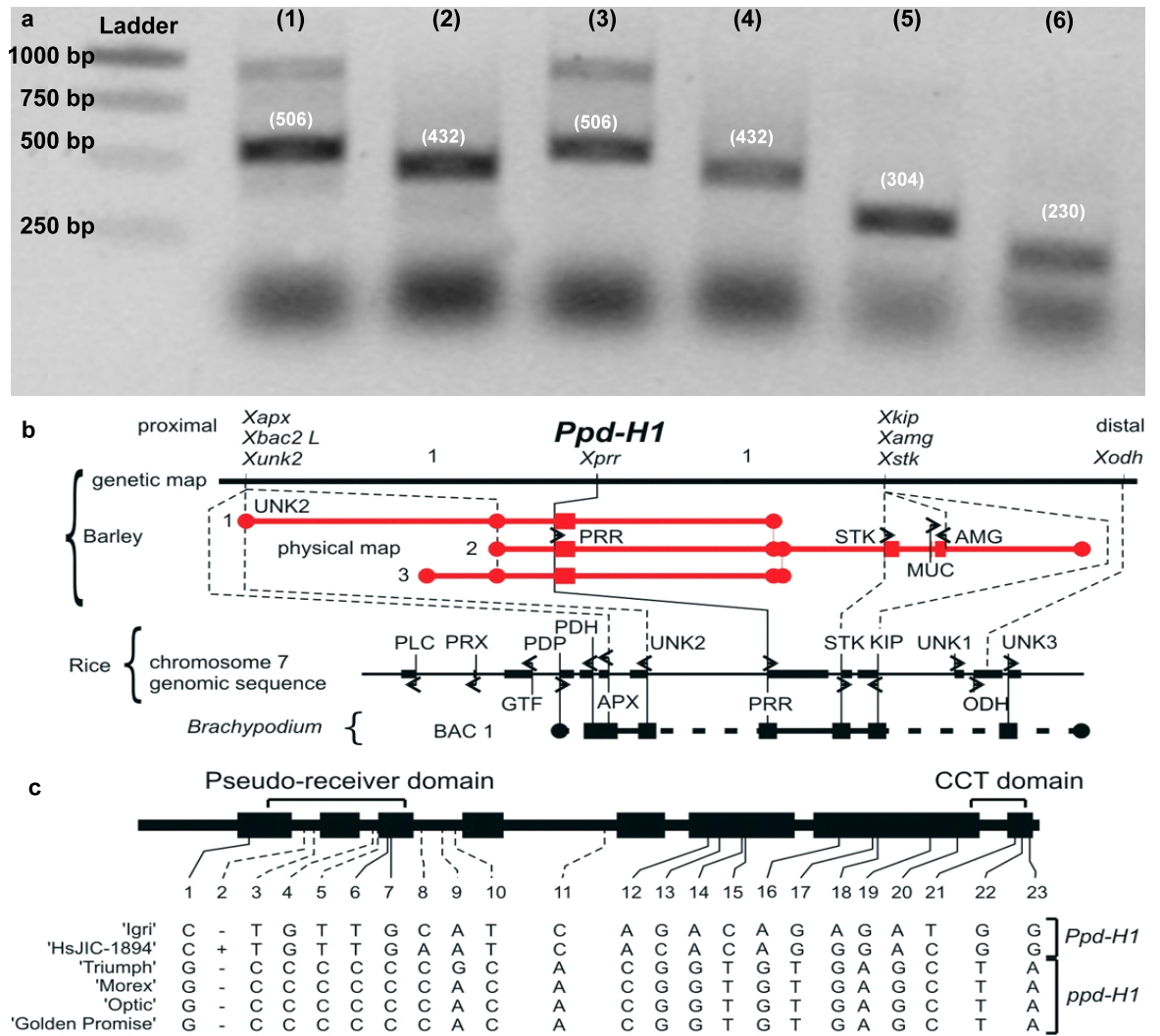
Figure 3-12: Genotyping Local and Optic for the Early Flowering Locus Ppd-H1.

Panel (a): PCR for Ppd-H1 (dominant) and ppd-H1 (recessive) alleles of the early flowering locus in barley. Lanes: (1) Test Local uncut: (2) Test Local cut with BstUI: (3) Test Optic uncut: (4) Test Optic cut with BstUI. PCR primers were used that amplifies a 506 bp product containing SNP 22 (a G/T substitution giving rise to a Glycine/ Threonine substitution). Restriction digests of this 506 bp fragment with BstU1 will generate a 432 bp fragment if the dominant Ppd-H1 alleles is present, but the DNA remains uncut if the recessive ppd-H1 allele is present. It appears that both the Local and Optic 506 bp PCR fragment cut by BstU1 treatment (lane 2 and 4), and therefore both lines carry the dominant early flowering allele, Ppd-H1. Ladder: molecular weight markers; lanes 5 and 6: controls for BstUI activity, (a test sequence of 304 bp amplified from barley genome DNA was included as a positive control for BstUI restriction enzyme activity. Lane 5, uncut 304 bp fragment; lane 6 BstUI digested fragment; Turner *et al.*, 2005a). Panel (b): schematic diagram showing location of Ppd-H1 locus on barley chromosome 3 (Turner *et al.*, 2005b). Panel (c): schematic diagram showing all 23 SNPs between early (Ppd-H1) and late (ppd-H1) flowering lines of barley. SNP 22 has been identified as that associated with the Ppd-H1 locus (Turner *et al.*, 2005).

3.5 *Discussion*

In this Chapter data are presented on the effects of salinity on the germination, vegetative growth, and yield on four barley genotypes Local, Optic, Soorab-96, and Awaran-2002.

Salt stress reduced the germination in the elite barley lines, but had no significant effect on landrace Local even at the highest salt concentration (150 mM NaCl). Germination of Soorab and Awaran were equally affected by salinity, but line Optic was the most sensitive genotype at this growth stage (Figure 3-1).

Measurements of seedling shoot length after 14 days indicated Local was still the most halotolerant of the four genotypes but no differences in the sensitivity of the three elite lines were detected (Figure 3-1 and 3-2). This decrease in the germination of seeds from elite barley lines can be attributable to any one or combination of the toxic effects of Na^+ or Cl^-, nutrient ion imbalances, or osmotic stress (Bliss *et al*., 1986; Welbaum *et al.,* 1990).

High germination rates in Local at high salt concentrations appears to be related its genetic composition and there is evidence to support this from the growth and yield data discussed in Sections 3.2 and 3.3. It has been reported that a decrease in germination is related to salinity-induced disturbance of metabolic processes leading to an increase in phenolic compounds but this was not measured in the present study (Ayaz *et al*., 2000).

With response to vegetative growth, application of salt stress to 21 day-old plants did not produce significant differences between the four genotypes until day 48. By day 60, however, major differences were observed (see Sections 3.2 and 3.3). These significant differences in response to salt stress were apparent through to the harvest stage. Salt stress inhibited shoot and root length above 100 mM NaCl in all four genotypes. This inhibition, however, was more prominent in the elite lines. In lines Optic and Soorab shoot length was more affected by high salt stress than root length. Shoot and root fresh and dry weights also showed a significant suppression with increasing salt concentrations, but once again Local performed better than the elite lines (Local>Soorab>Optic>Awaran). Similar inhibition in the vegetative growth of barley by salinity has been well documented (e.g. Hussain and Rehman, 1997; Razzaque *et al*., 2009).

There was some evidence that, like some halophytes (Greenway and Munns, 1980), line Soorab may show growth stimulation when exposed to 50 mM NaCl although this trend was not significant (Figures 3-5 & 3-6).

The salinity induced reduction in root and shoot development may be due to the toxic effects of Na^+ and/or Cl^- ions or an imbalance in nutrient uptake by the plants. This in turn is dependent on the ability of the root system to control the entry of ions into the cortex, across the endodermis, and into the vasculature as this controls transport to the shoot (Munns and Tester, 2008).

Tillering is also an important parameter that is often correlated with better crop performance under stressed conditions (Semenov and Halford, 2009). In 0 mM NaCl Optic produced the greatest number of tillers per plant (*ca.* 7), followed by genotypes Local and Soorab (ca. 6), while Awaran produced only 3 to 4 tillers per plant. At higher salt concentrations after 24 days in salt stress (>45 day–old plants) both tiller initiation and tiller survival began to decline except for landrace Local which maintained its number of tillers up to the final harvest. There was a positive correlation between the number of tillers per plant with dry weight and grain weight per plant (data not presented). These results on the effects of high salinity on the vegetative growth of barley are consistent with those from earlier studies (Razzaque *et al*., 2009).

A decrease in grain weight per plant could arise from a reduction in grain size or from a decrease in the number of grain per plant, or both. Similarly, the number of grain per plant is determined by the number of floral spikes and the average number of grain per spike. For genotype Local and Soorab it appears that yield reductions per plant (Figure 3-9) were equally attributable to a reduction in seed size (Figure 3-9), seed number, and ear number per plant (Figure 3-8). With line Optic the suppression in grain yield per plant is attributable mainly to a sever reduction in the number of ears per plant (from 6.5 to 2.5, 60 % reduction; Figure 3-8), and the number of grains per plant (*ca.* from 110 to 35; Figure 3-8), but not in the average size of grain (Figure 3-9). From these data it appears that salinity impairs grain production in line Optic mostly by reducing the number of floral spikes, and to a lesser extent by reducing seed size and the number of seed per spike (from approximately 16.9 in 0 mM to 14.0 in 100 mM NaCl). Exposure to 100 mM NaCl suppressed seed production most severely in line Awaran (by approximately 85 %; Figure 3-9) and this was attributable to both a reduction in seed size (Figure 3-9), and the number of spikes per plant (Figure 3-8). These findings are

broadly similar to those of previous studies on the effects of high salinity on cereals (Al-Khatib *et al.,* 1992; Ali *et al.*, 2008; Ashraf and Foolad, 2005; Attumi, 2007).

Comparison of the grain yields achieved in this study (grams/plant) at control salinity levels with those attained in the field (tons/hectare) were calculated by the formula (Recommended density of plants meter^{-2} x 10,000 x grain weight per plant (g) / 1,000,000 = tons per hectare). Approximately 150 plants per meter^2 are recommended for spring barley (Ona *et al.*, 2010). Using this formula it was calculated that in hydroponics at 0 mM NaCl grain yield for the four genotypes (tons/hectare) was approximately Local 4.8, Optic 6.3, Soorab 4.2, and Awaran 4.1. These yields are approximately double those reported for Local, Soorab and Awaran grown in rain-fed field conditions of Pakistan (Khan *et al.*, 1999) and approximately 20 % less than those reported for Optic in the field in the United Kingdom. Presumably these differences in yield arise from the sub-optimal irrigation of plants grown in Pakistan, and the sub-optimal growth conditions of line Optic in hydroponics (nutrient ion balance, light levels, *etc.*). It appears, therefore, that the hydroponic control conditions used in this study provided barley plants with near optimal conditions, and the conclusions drawn above are meaningful and can be attributed to a direct effect of salinity on the germination, growth, and reproduction of barley.

When grown in 0 mM NaCl Awaran was the first genotypes to complete its life cycle within approximately 75 days (seed-to-seed), in contrast Soorab-96 took longest (*ca.* 130 days). Local and Optic were in between these extremes and they took 88 and 98 days respectively, to complete their life cycle (seed-to-seed). Interestingly, in Glasgow all genotypes completed their life cycle at least one to two months earlier than that observed in field conditions even at control salt levels; this occurred in both soil and hydroponics. This might be due to the some what artificial light and temperature conditions used in the glass house and growth rooms (Rahman *et al.*, 2009). The very short life cycle of Awaran implies that this line is probably carrying a functional allele of the Photoperiod-H1 (Ppd-H1) gene (also known as Early maturity 1 (Ea1)). There are other mutations in barley that give rise to a similarly short life cycle, particularly the early maturity (*eam*) mutations. The *eam* mutations are not dependent on long days for their effect (David Laurie, John Innes Institute, Norwich; per. comm.).

The development of barley genotypes at different salt concentrations showed no significant variation between line Optic and Soorab-96 over the 0 to 100 mM NaCl range, however, neither of these entered into the anthesis phase at 150 mM NaCl. In

contrast landrace Local and line Awaran matured approximately two weeks earlier, due to an accelerated entry into the phase of inflorescence emergence at 100 mM NaCl (Figures 3-11 to 3-14). It is clear from these results that there is no relationship between accelerated development (Awaran < Optic = Local < Soorab) and salinity tolerance (Local > Soorab > Optic > Awaran) in these genotypes at 100 mM NaCl, as speculated by earlier workers (Attumi, 2007; Bhatnagar *et al.,* 2008). It is noteworthy that the effects of salinity on the complete developmental program (seed-to-seed) in barley is rarely studied and has not been reported in literature, and therefore these observations are novel.

In conclusion, the experiments reported in this Chapter indicate that high salinity suppresses the germination, vegetative growth, and reproduction in barley and that there are some significant differences in the level of halotolerance shown between genotypes. Landrace Local was the most halotolerant genotype studied, and line Awaran the most sensitive. There may be a genetic basis to account for the improved halotolerance of Local during germination, vegetative growth, and the reproductive phase. There also appears to be differences between the genotypes relating to the effects of salinity on the reproductive processes. Finally, barley grown in controlled environmental conditions show shortened life cycles of as little as 10 weeks; the basis for this is unknown.

Chapter 4: Characterization of Halotolerance in Barley Genotypes: Physiological Responses

To establish whether the salt-induced differences in germination, growth, and yields observed in the four barley genotypes (see Section 3.1, 3.2 and 3.3) were attributable to impaired photosynthetic efficiency, a series of experiments were conducted.

Different parameters reflecting the photosynthetic efficiency of the plants were recorded at each stage of development *i.e.* tillering, anthesis, and grain formation from plants grown in hydroponic solutions containing a range of external NaCl concentration (0, 50, 100, and 150 mM). These parameters included CO_2 assimilation rates at saturating and growth light levels (500 and 180 μmol photons $.m^{-2} .s^{-1}$; A_{sat} and A_{180} respectively) Quantum efficiency (α), apparent photorespiration, dark respiration (Rd), carboxylation efficiency (ΦCO_2), stomatal conductance (**gs**), and mesophyll conductance (**gm**). These were determined from CO_2 Response (A/C_i) and light response (A/Q) curves using an Infra Red Gas Analyzer (IRGA), (see Material and Methods Section 2.1.3.1). Two experiments were conducted (October 2008 and June 2009); the results were similar but for brevity only the more complete June, 2009 data set are discussed further. Data collected from different experiments for all physiological parameters were measured at days 31, 45, 60, 74, and at harvest. Data for sixty day-old (38 days under salt stress) plants of Local (salinity tolerant) and Optic (salinity susceptible) only are presented from here on as differences were greater between these two genotypes. In almost all cases the responses of line Awaran-2002 and Soorab-96 towards salinity were intermediate between those of landrace Local and line Optic. Therefore data for Local and Optic are discussed in this chapter.

4.1 *Carbon Dioxide Supply and Photosynthesis*

Net photosynthesis rate can be affected by the efficiency of light capture, the efficiency of photosynthetic electron transport, the kinetic properties of the C3 cycle and respiration, and by the supply of CO_2 to the chloroplast (see Section 2.1.3.1.1). In this section the effect of salinity on CO_2 supply to the chloroplast is considered.

4.1.1 Stomatal Conductance (gs)

Stomatal conductance (**gs**) is an estimation of stomatal aperture controlling gas exchange across the leaf surface. Data collected for **gs** using an IRGA showed a progressive decline with increasing NaCl concentrations (from 0 to 150 mM NaCl). This decline was more pronounced in Optic (from *ca.* 0.50 to 0.15 mol. m^{-2}. s^{-1}) compared with landrace Local (from *ca.* 0.50 to approximately 0.30 mol .m^{-2}.s^{-1}; $p \leq$ 0.05) as external NaCl concentration increased from 0 to 150 mM NaCl (Figure 4-1a; $p<0.05$).

4.1.2 CO_2 Assimilation Rates and Quantum Efficiency

The effect of salinity on the light-saturated assimilation rate obtained at 380 μmol CO_2 .mol^{-1} air at light saturated (A_{sat}) and 180 μmol .m^{-2} .s^{-1} PAR (A_{180}) for Local and Optic are presented in Figure 4-2a. These data for A_{sat} indicated that values in landrace Local were maintained at control levels (approximately 20 μmol CO_2 .m^{-2} .s^{-1}) up to 100 mM NaCl and were suppressed by approximately 80 % (approximately 3 μmol CO_2 .m^{-2} .s^{-1}) only at the highest concentration of 150 mM NaCl. In contrast, line Optic maintained control levels of A_{sat} only up to 50 mM NaCl, and an approximately 60 % and approximately 90 % suppression was observed at 100 and 150 mM NaCl respectively. A similar pattern was observed with A_{180}, at the average growth light intensity, suggesting the salt-induced suppression in growth reported in Section 3.2.1 may have been attributable to a suppression of photosynthesis.

The quantum efficiency (α) of both genotypes (measured from light response curves, see Section 2.1.3.1.2) decreased with increasing salinity, from approximately 0.11 at 0 mM NaCl to approximately 0.01 at 150 mM NaCl (see Figure 4-2b; $p<0.05$). These data indicate the capacity of leaves to capture and process light energy was severely impaired by the high concentrations of salinity.
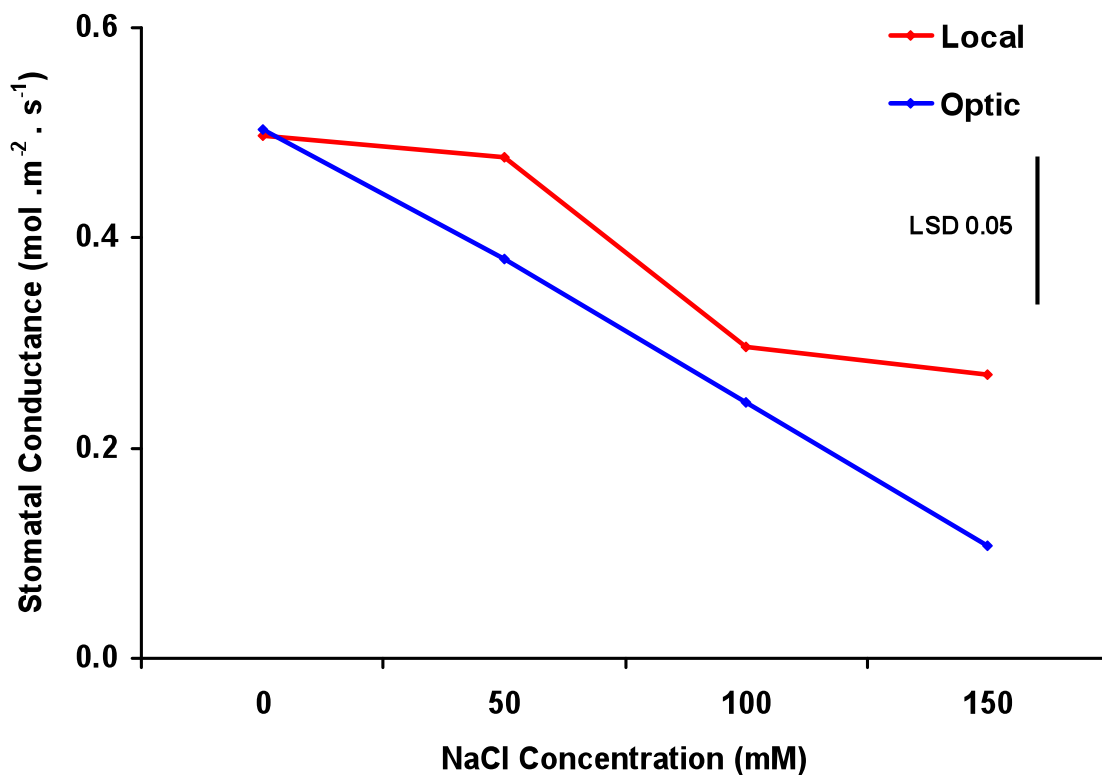
Figure 4-1: The Effects of Salt Treatments on Stomatal Conductance (gs) of Barley Genotypes

Each data point (collected from Light Response Curves; see Section 2.1.3.1.2) and represents the mean and standard error of three replicates. Measurements were made 60 days after germination (38 days into salt treatment) on fully expanded 4th emergent leaves. ANOVA tests were performed using a General Linear Model. Tables for ANOVA and grouping information along with Figures for residual and interaction plots are presented in Appendix (Figure A 4-1).

Figure 4-2: The Effects of Salt Treatments on CO_2 Assimilation and Quantum Efficiency (α) of Barley Genotypes.

Top panel (a): ▬■▬ Local light saturated assimilation rate (A_{sat}); ▬■▬ Local assimilation rate at glass house light levels (180 μmol .m^{-2} .s^{-1} PAR; A_{180}); ▬◆▬ Optic light saturated assimilation rate (A_{sat}); ▬●▬ Optic assimilation rate at 180 μmol .m^{-2} .s^{-1} PAR (A_{180}); bottom panel (b): ▬■▬ Local, ▬◆▬ Optic quantum efficiency. Each data point represents the mean and standard error of three replicates. Measurements were made 60 days after germination (38 days into salt treatment) on fully expanded 4th emergent leaves. Assimilation rates and α value were determined from light response curves, as described in Section 2.1.3.1.2. ANOVA tests were performed using a General Linear Model. Tables for ANOVA and grouping information along with Figures for residual and interaction plots are presented in Appendix (Figures A 4-2 to A 4-4).

a

Legend:
- Local at saturated
- Optic at saturated
- Local at 180
- Optic at 180

y-axis: $A_{sat\ and\ 180}$ (μmol $CO_2 . m^{-2}.s^{-1}$)

LSD 0.05 @ saturated

LSD 0.05 @ 180

b

y-axis: α (mol $CO_2 . mol^{-1}$ photons)

LSD 0.05

x-axis: NaCl Concentration (mM)
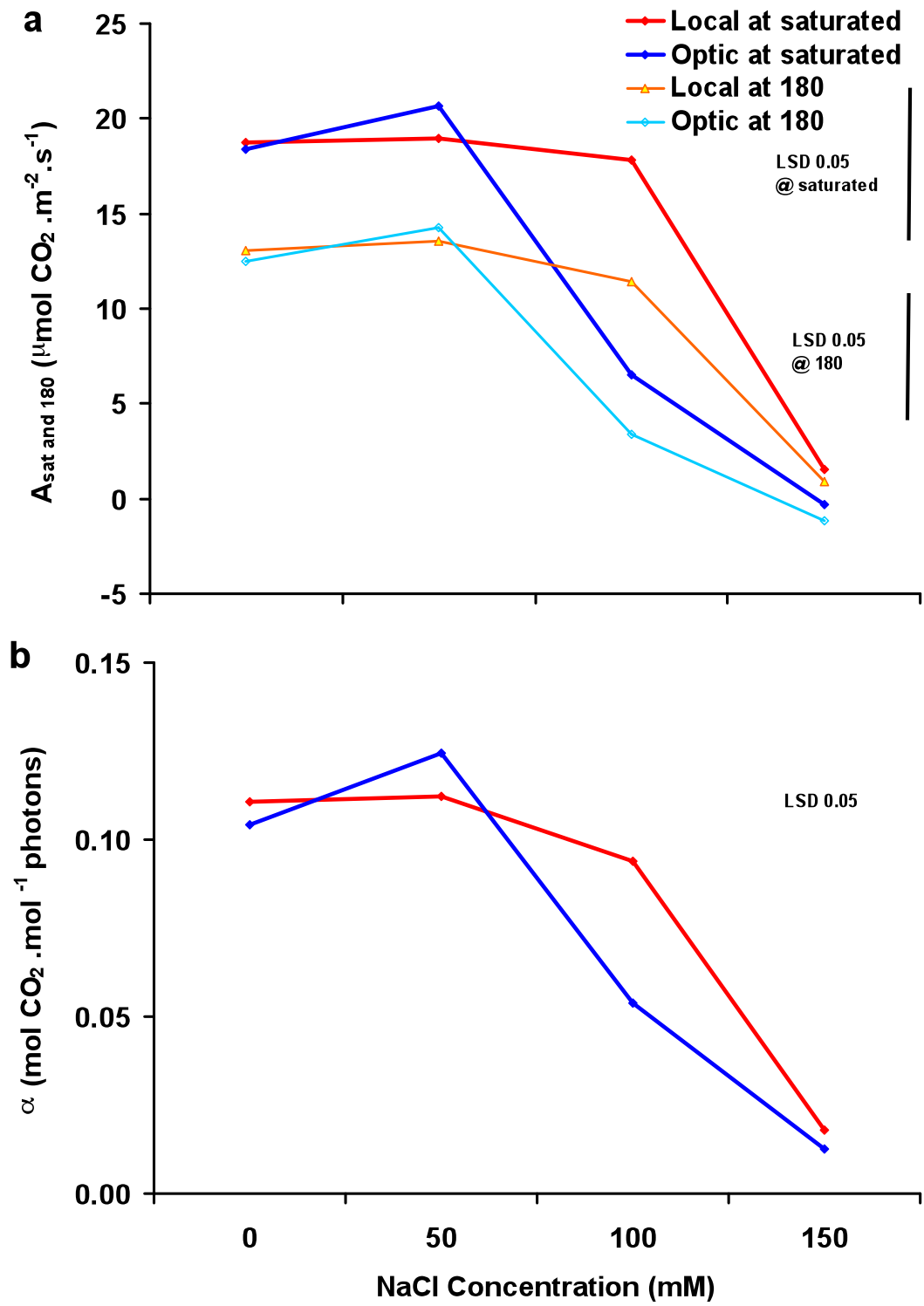
4.1.3 Carboxylation Efficiency (Φ CO$_2$)

The efficiency of the C3 cycle *in vivo* can be estimated from the parameter Φ CO$_2$; as RuBisCO activity is usually the rate limiting step in the C3 cycle, the values of Φ CO$_2$ are often used to estimate the kinetic properties of RuBisCO *in vivo* (Yeo *et al.*, 1994). Increasing NaCl concentration up to 50 mM had no major effect on Φ CO$_2$ values recorded for both lines. These values significantly declined from *ca*. 0.12 to 0.09 mol CO$_2$ .m^{-2} .s^{-1} in landrace Local and to approximately 0.06 mol CO$_2$ .m^{-2} .s^{-1} in line Optic at 100 mM NaCl. At 150 mM NaCl Φ CO$_2$ declined to approximately 0.03 mol CO$_2$ .m^{-2} .s^{-1} in both genotypes (see Figure 4-3; p<0.05). The conclusion is that for both genotypes high levels of salinity at the roots result in a significant impairment of the kinetics of the carboxylation processes in the chloroplast. However this impairment was more pronounced in line Optic than in the landrace Local, at least at 100 mM NaCl.

4.1.4 Apparent Photorespiration (V$_o$) and Dark Respiration (^{mit}Rd)

The intercept of the linear part of A/Ci and A/Q curves with the Y axis provides estimates of the light and dark respiration rates, respectively. By subtraction of ^{mit}Rd from the light respiration rate (^{Tot}R$_L$) provides an estimate of the apparent rate of photorespiration (V$_o$; see Section 2.1.3.1.1). The values for V$_o$ at zero CO$_2$ for the two barley genotypes are presented in Figure 4-4a. No change was observed over the 0 to 50 mM NaCl range; values remained at approximately -6 to -7 µmol CO$_2$ .m^{-2} .s^{-1}. Increasing NaCl concentration above 50 mM produced a decline in apparent photorespiration to from *ca*. -6.0 to -2.5 µmol CO$_2$ .m^{-2} .s^{-1} at 150 mM NaCl. There were no significant differences between the lines at any NaCl concentration.

The interpretation of the physiological significance of the changes in V$_o$ is unclear (see Section 2.1.3.1.1) and may reflect salt-induced changes in the activity of RuBisCO, the supply of the substrate for photorespiration (RuBP), or both.

Dark Respiration (Rd) did not change with increasing NaCl concentration from 0 to 150 mM NaCl (p<0.05; Figure 4-4b).
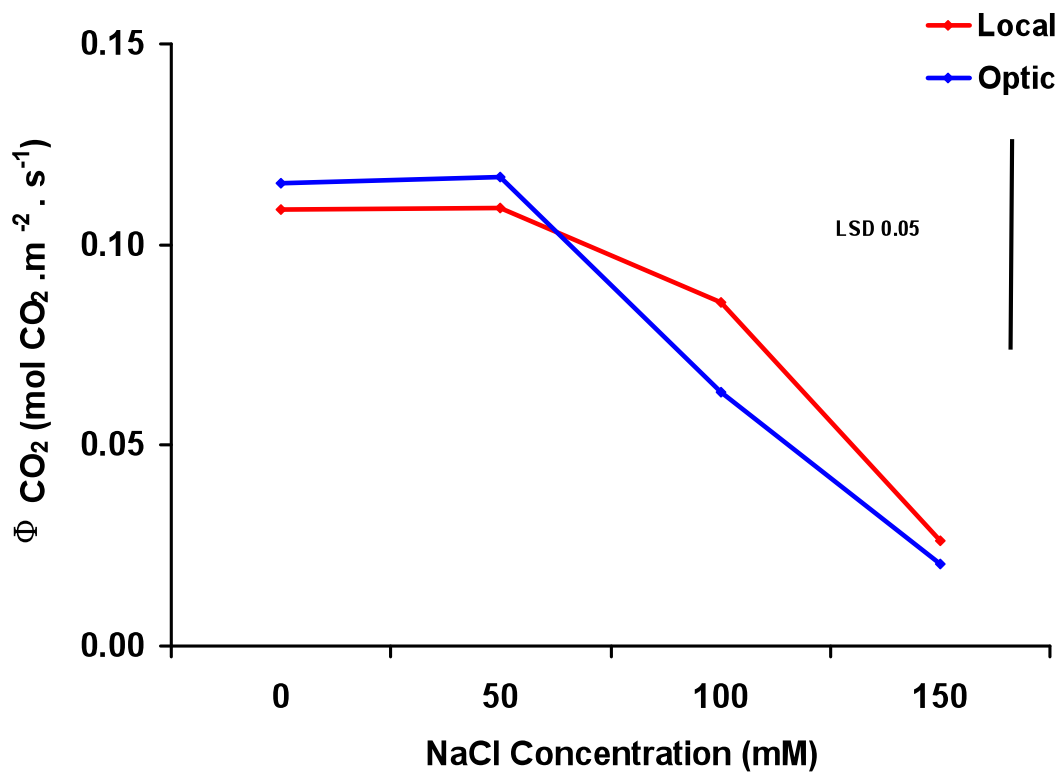
Figure 4-3: The Effects of Salt Treatments on Carboxylation Efficiency (Φ CO$_2$) of Barley Genotypes.

Each data point represents the mean and standard error of three replicates. Measurements were made 60 days after germination (38 days into salt treatment) on fully expanded 4th emergent leaves. Φ CO$_2$ values were determined from the initial slope of the A/C$_i$ response curve (see Material and Methods Section 2.1.3.1.1). ANOVA tests were performed using a General Linear Model. Tables for ANOVA and grouping information along with Figures for residual and interaction plots are presented in Appendix (Figure A 4-5).

Figure 4-4: The Effects of Salt Treatments on Apparent Photorespiration (V_o) and Dark Respiration (Rd) of Barley Genotypes.

Top panel (a): photorespiration; bottom panel (b): dark respiration. Each data point represents the mean and standard error of three replicates. Measurements were made 60 days after germination (38 days into salt treatment) on fully expanded 4th emergent leaves. Photorespiration and dark respiration values were determined from CO_2 and light response curves, as described in Section 2.1.3.1.1 and 2.1.3.1.2. ANOVA tests were performed using a General Linear Model. Tables for ANOVA and grouping information along with Figures for residual and interaction plots are presented in Appendix (Figures A 4-6 & 4-7).

a

NaCl Concentration (mM)

LSD 0.05

b

Local
Optic

LSD 0.05
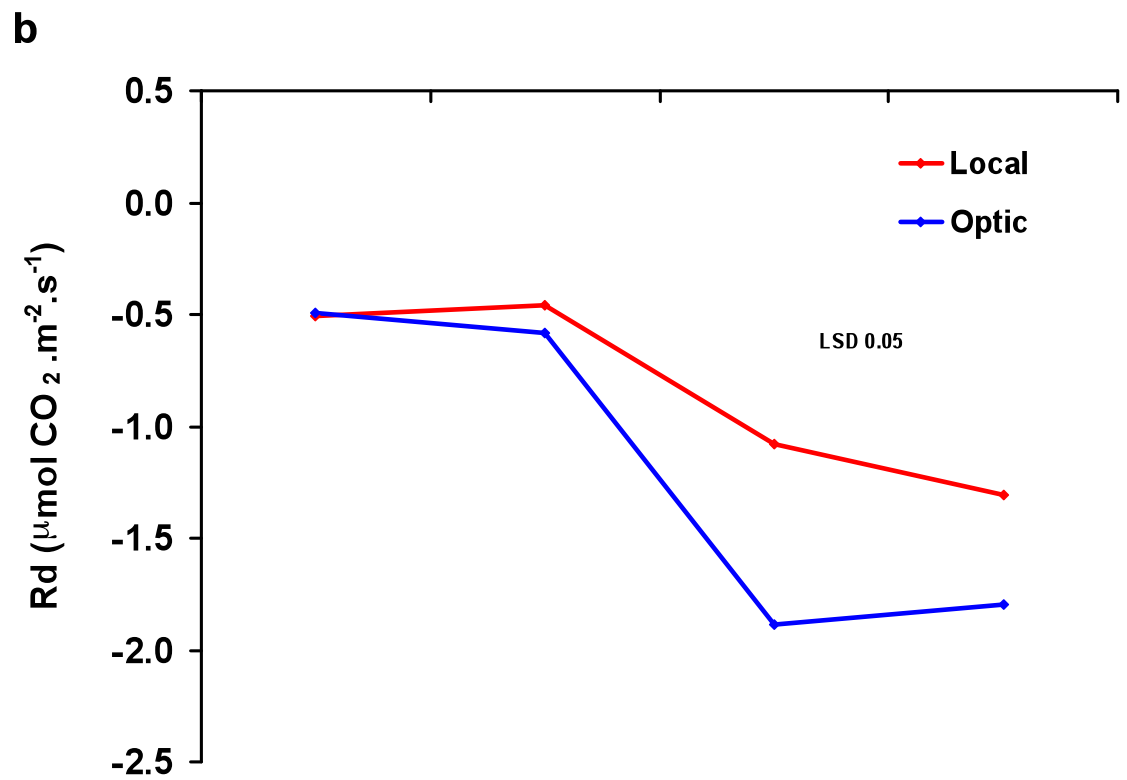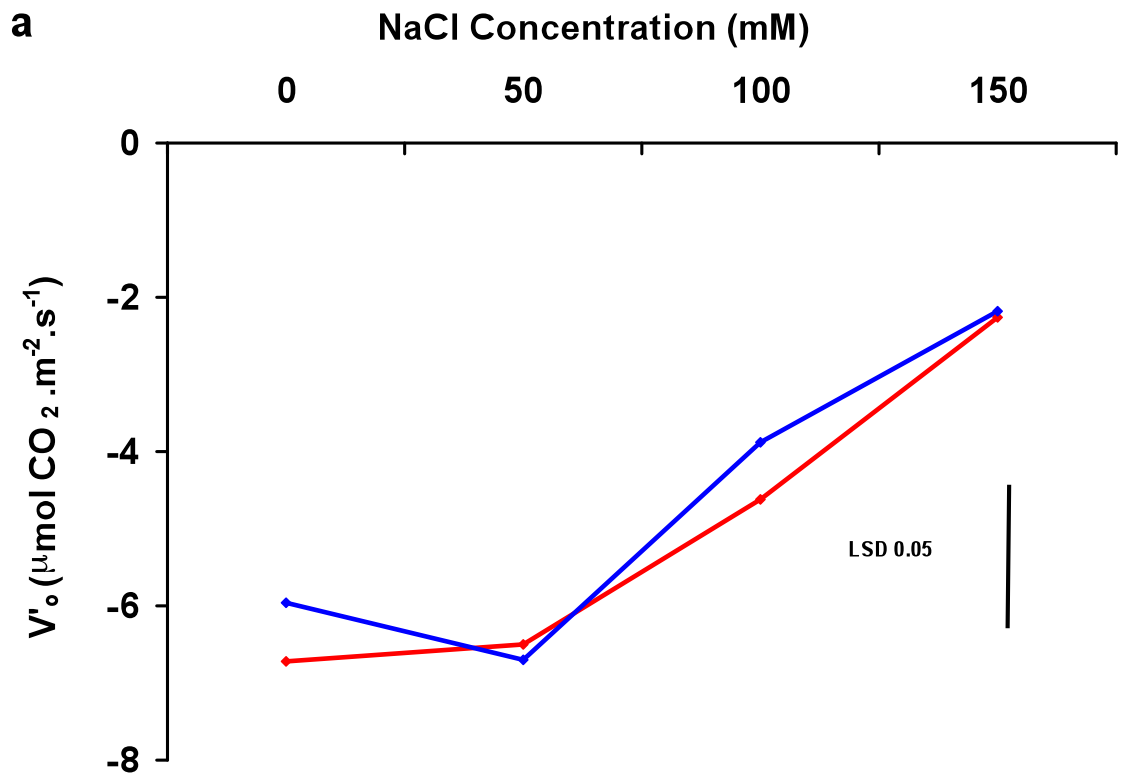
4.1.5 Ratio of Internal CO_2 (C_i) to Atmospheric CO_2 Concentration (C_a), and Assimilation versus Stomatal Conductance

To see whether observed suppression in photosynthetic efficiency of barley leaves could be attributed to its carbon dioxide availability or impairment of C3 cycle following plots were derived from A/Ci curves. Figure 4-5a presenting the ratio of C_i to C_a clearly indicated that this ratio is not changing significantly in both genotypes exposed at increasing salt concentrations from 0 to 150 mM NaCl ($p<0.05$).

A scatter plot of CO_2 assimilation rate *versus* stomatal conductance (A *versus* **gs**) collected from instantaneous measurements of plants exposed to a range of salt stress is presented in Figure 4-5b. Both genotypes showed a positive correlation between CO_2 assimilation and **gs** up to approximately 0.3 $mol.m^{-2}.s^{-1}$, however, at higher values of **gs** the correlation declined. Surprisingly, tests showed the regressions for the two genotypes were significantly different at both low and high values of **gs.**

Figure 4-5: The Effects of Salt Treatments Ci/Ca Ratio and CO₂ Assimilation vs. gs Collected from Instantaneous Photosynthesis Measurements.

Top panel (a): C_i/C_a ratio; each data point represents the mean and standard error of three replicates of C_a/C_i ratio. C_a and C_i collected from CO_2 response curves (see Section 2.1.3.1.1). Measurements were made 60 days after germination (38 days into salt treatment) on fully expanded 4th emergent leaves. ANOVA tests were performed using a General Linear Model. The ANOVA Tables are presented in Appendix (Table A 4-1).

Bottom panel (b): Assimilation rates (A) are plotted against the corresponding values for stomatal conductance (**gs**); both values were obtained from instantaneous measurements at each salt concentration in glass house conditions from 4th emergent leaves of 60-day old plants of Local and Optic barley genotypes grown in 0, 50, 100, and 150 mM NaCl concentration. Second order (quadratic) polynomial regression lines were fitted to the data using Microsoft Excel's LINEST routine with an intercept of 0; the respective equations and their R^2 values are presented on the plot. Tests for significant differences between the coefficients for these plots were performed and these calculations are presented in Appendix (Table A 4-2).

a

Legend: Local (red), Optic (blue)

LSD 0.05

Y-axis: Ci/Ca

X-axis: NaCl Concentration (mM)

b

$A = -49.009gs^2 + 68.467gs \quad R^2 = 0.8252$

$A = -75.499gs^2 + 77.432gs \quad R^2 = 0.9052$

Y-axis: A (μmol $CO_2 .m^{-2} .s^{-1}$)

X-axis: gs (mol $.m^{-2} .s^{-1}$)
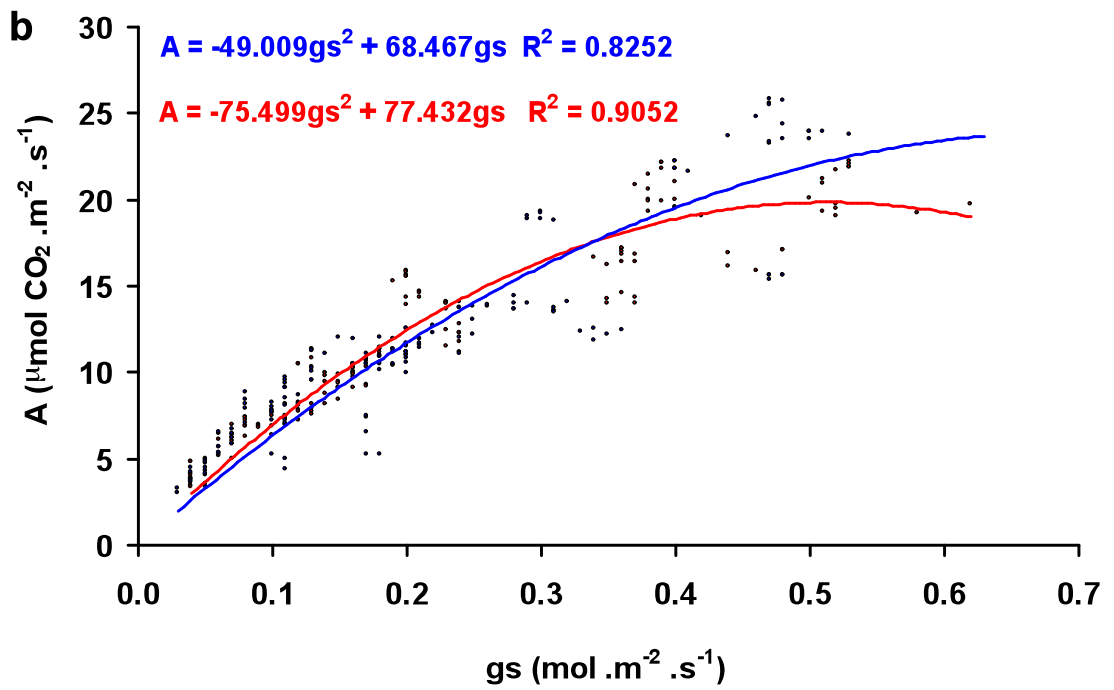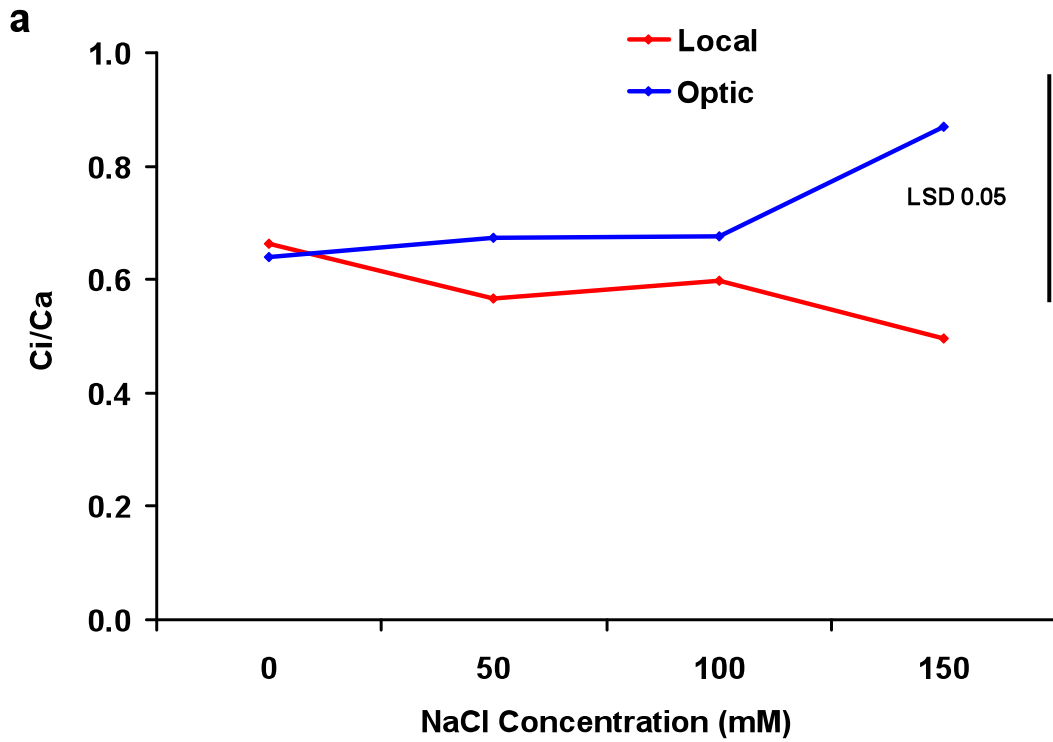
4.2 *Plant Water Status*

To study the effects of high salinity on plant water status several physiological parameters were assessed including water use efficiency, relative water content, leaf water potential, and leaf turgor pressure.

4.2.1 Relative Water Content and Water Use Efficiency

The water status of plants can be estimated from the relative water content (RWC) of shoot and the water potentials (ψ_{H2O}) of green leaves. The RWC of shoot is simply estimated as the ratio of the hydration state of treated plants compared with control plants (RWC = ([g H_2O/g D Wt] ^{treated} / [g H_2O/g D Wt] ^{control}) x100 %). Measurements indicated both lines showed a progressive decline in their shoot RWC values as external NaCl concentration increased from 0 to 150 mM. Local showed a decline of approximately 78 % in its relative water content, whereas Optic showed a steady decline of approximately 86 %. No significant differences in RWC were observed between the two lines at any NaCl concentration although it appears that Local may be more hydrated across this range (Figure 4-6a; $p \leq 0.05$).

Figure 4-6b shows the effects of salinity on the Water Use Efficiency (WUE). These values in landrace Local remained unchanged from 0 to 100 mM external salt concentrations, but declined from approximately 0.24 to approximately 0.2 % at 150 mM NaCl concentration ($p < 0.05$). Line Optic maintained WUE at approximately 0.22 % over the 0 to 100 mM NaCl range, but it declined significantly ($p < 0.05$) to approximately 0.18 % at 150 mM NaCl. Again, landrace Local appeared to be more water use efficient than line Optic and a significant difference in WUE was observed at 100 mM NaCl.
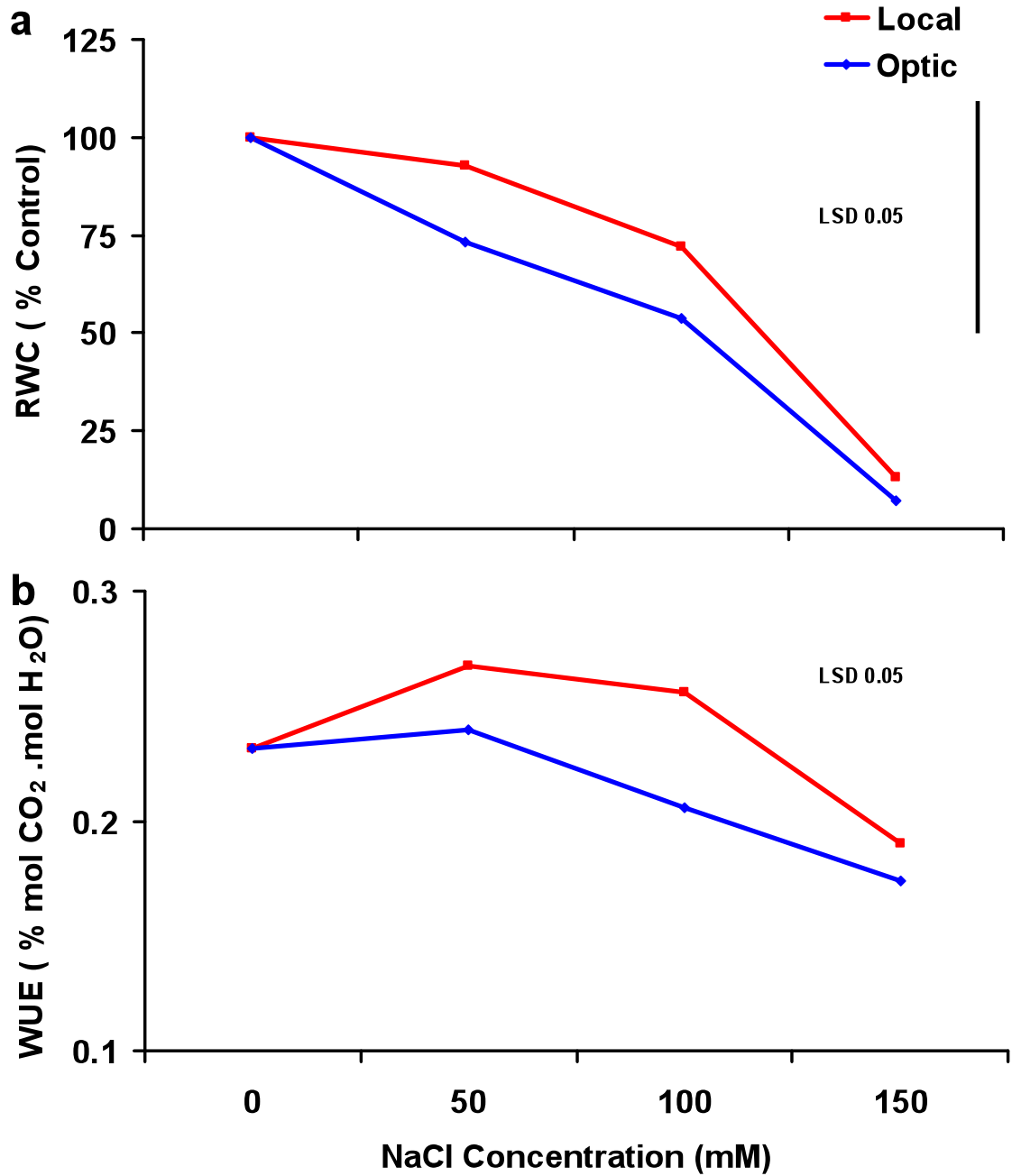
Figure 4-6: The Effects of Salt Treatments on Relative Water Content (RWC) and Water Use Efficiency (WUE) of Barley Genotypes.

Top panel (a): Relative Water Content (RWC); bottom panel (b): Water Use Efficiency (WUE). ■, Local; ◆, Optic. Each data point represents the mean and standard error of five biological replicates for RWC and WUE. Measurements were made 60 days after germination (38 days into salt treatment) on fully expanded 4th emergent leaves. ANOVA tests were performed using a General Linear Model. Tables for ANOVA and grouping information along with Figures for residual and interaction plots are presented in Appendix (Figures A 4-8 & 4-9).

4.2.2 Leaf Water Potential (ψ_{H2O}), Xylem Solute Potential ($^{Xylem}\psi_s$) and Turgor Pressure

Significant errors can be incurred in the estimation of ψ_{H2O} using a pressure chamber unless sufficient attention is paid to the solute potential of the xylem (xylem ψ_s). When used according to the manufacturer's instructions, ψ_s is assumed to be zero. Under these conditions:

$$^{Tissue}\psi_{H2O} = {}^{Tissue}\psi_s + {}^{Tissue}\psi_p = {}^{xylem}\psi_s + {}^{xylem}\psi_p$$

where $^{xylem}\psi_p$ is the negative value of the balance pressure measured by the pressure chamber. When $^{xylem}\psi_s = 0$, $^{Tissue}\psi_{H2O} = {}^{xylem}\psi_p$ (-balance pressure). Whilst this is a reasonable assumption for plants growing in soils with normal, low levels of electrical conductivity (E = 0 to 2 dS $.m^{-1}$), it is clear this is not the case here where significant amounts of NaCl might be present in the transpiration stream. For this reason, $^{xylem}\psi_s$ should be measured along with apparent balance pressure (- $^{xylem}\psi_p$) so that better estimates of tissue water status can be made. Without such corrections measurements of water potential using a pressure chamber incurred significant errors; no significant differences in $^{Tissue}\psi_{H2O}$ were recorded between the genotypes (data not shown). To obtain correct measurements for ψ_{H2O}, $^{xylem}\psi_s$ was measured using an osmometer (see Section 2.1.3.3.2; Fig 4-7b)

Increasing NaCl concentration up to 150 mM did not alter the ψ_{H2O} of green leaf tissue in the landrace Local. In contrast, increasing NaCl concentration above 50 mM NaCl produced a significant dehydration in the green tissues of line Optic; ψ_{H2O} fell well below -2.5 MPa. It is clear that this salt-induced decline in Optic ψ_{H2O} corresponded with a rise in $^{xylem}\psi_s$ (from *ca.* -0.2 to -3.3 MPa; Fig 4-7b), and without this correction ψ_{H2O} for Optic at 150 mM NaCl would have been approximately 3.3 MPa more positive (i.e. approximately -1.4 MPa).

The leaf turgor pressure (ψ_p) was calculated by using the formula

$$(\psi_p) = {}^{leaf}`\psi_{H2O} - {}^{leaf}\psi_s$$

ψ_p values in landrace Local were maintained in the range of +0.3 to +1.0 MPa, while in line Optic it increased significantly from +0.05 to +2.5 MPa (Fig 4-7c; $p < 0.05$)

Figure 4-7: The Effects of Salt Treatments on Leaf Water Potential (Ψ_{H2O}), Xylem Solute Potential ($^{Xylem}\Psi_{H2O}$) and Leaf Turgor Pressure (Ψ_P) of Barley Genotypes.

Top panel (a): corrected leaf water potential ('ψ_{H2O}); middle panel (b): xylem solute potential ($^{Xylem}\psi_{H2O}$); bottom panel (c): leaf turgor pressure, Local; —■— , Optic.—●—

The values for ψ_{H2O} shown are corrected values calculated from pressure chamber balance pressures and xylem solute potential measurement from exuded xylem sap (see Section 2.1.3.2 and 2.1.3.3). Turgor pressure was calculated by subtracting leaf (ψ_s) from corrected leaf (ψ_{H2O}). The values are the average (± SE) for 3 replicates per treatment. ANOVA tests were performed using a General Linear Model. Tables for ANOVA and grouping information along with Figures for residual and interaction plots are presented in Appendix (Figures A 4-10 & A 4-11).

a

Water Potential (MPa)

LSD 0.05

b

Xylem Solute Potential (MPa).

LSD 0.05

c

Turgor Pressure (MPa)

LSD 0.05

NaCl Concentration (mM)
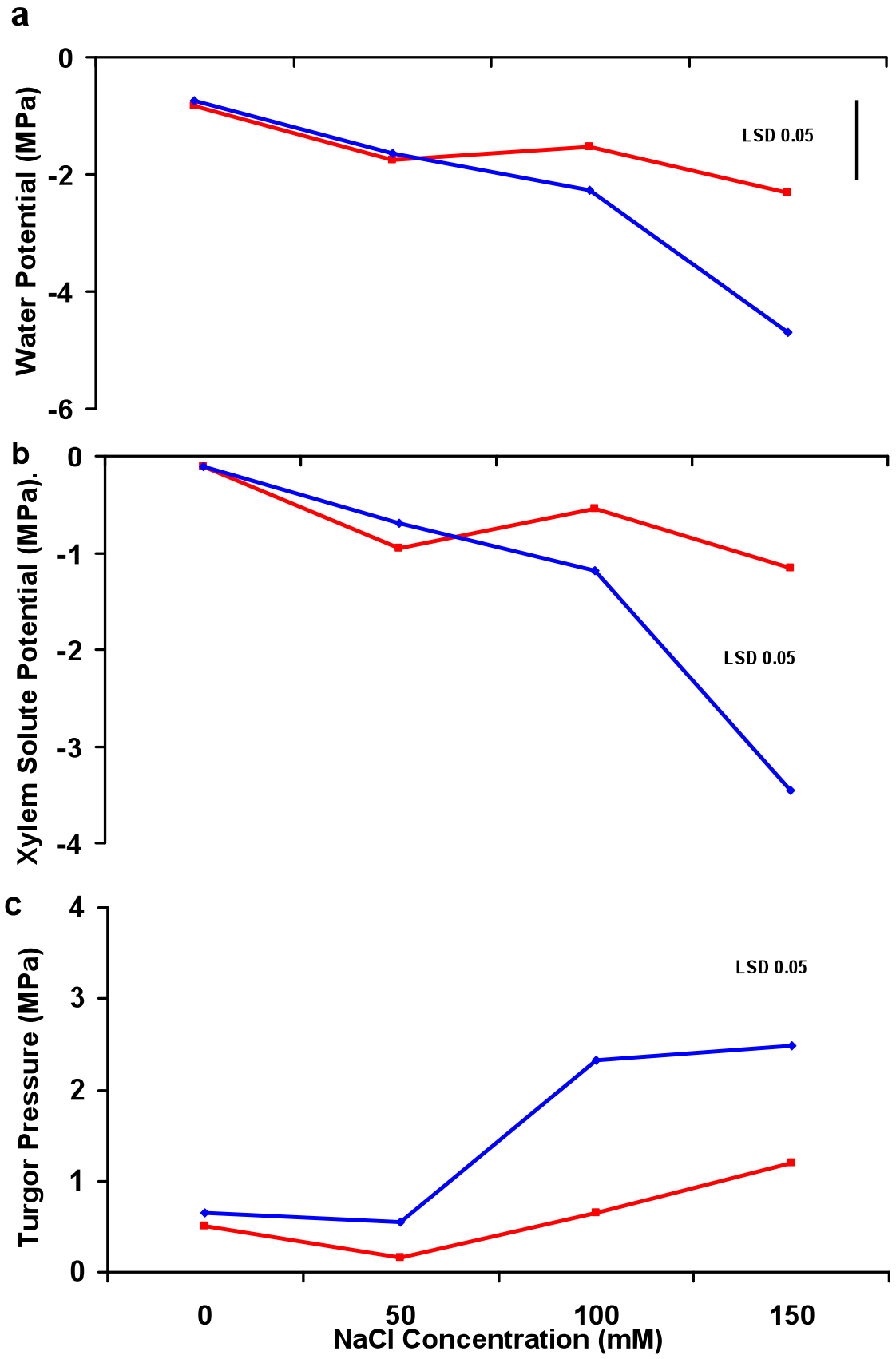
4.2.3 Leaf Tissue Solute Potential and Proline Concentrations

The solute potential (ψ_s) of both lines showed a steady increase with increasing NaCl concentration. This was more prominent from (-1.4 to -6.6 MPa) in Optic (the salinity sensitive line) compared with Local (salinity tolerant line; -1.4 to -3.2). Significant difference in (ψ_s) was apparent between the two genotypes at 100 and 150 mM NaCl (Figure 4-8a; $p \leq 0.05$).

Salt-induced changes in Proline levels, a major compatible solute in barley, showed very similar trends in the two genotypes. Increasing NaCl concentration from 0 to 150 mM produced a significant ($p < 0.05$) increase from approximately 0.6 to 12 μmol .g^{-1} dry weight in line Optic, and a significant increase was also observed in landrace Local (*ca.* 0.7 to 6 μmol .g^{-1} dry weight; but only at 150 mM NaCl; Figure 4-8b; $p < 0.05$). Line Optic showed significantly high tissue proline concentrations compared with landrace Local at all NaCl concentrations above 0 mM.
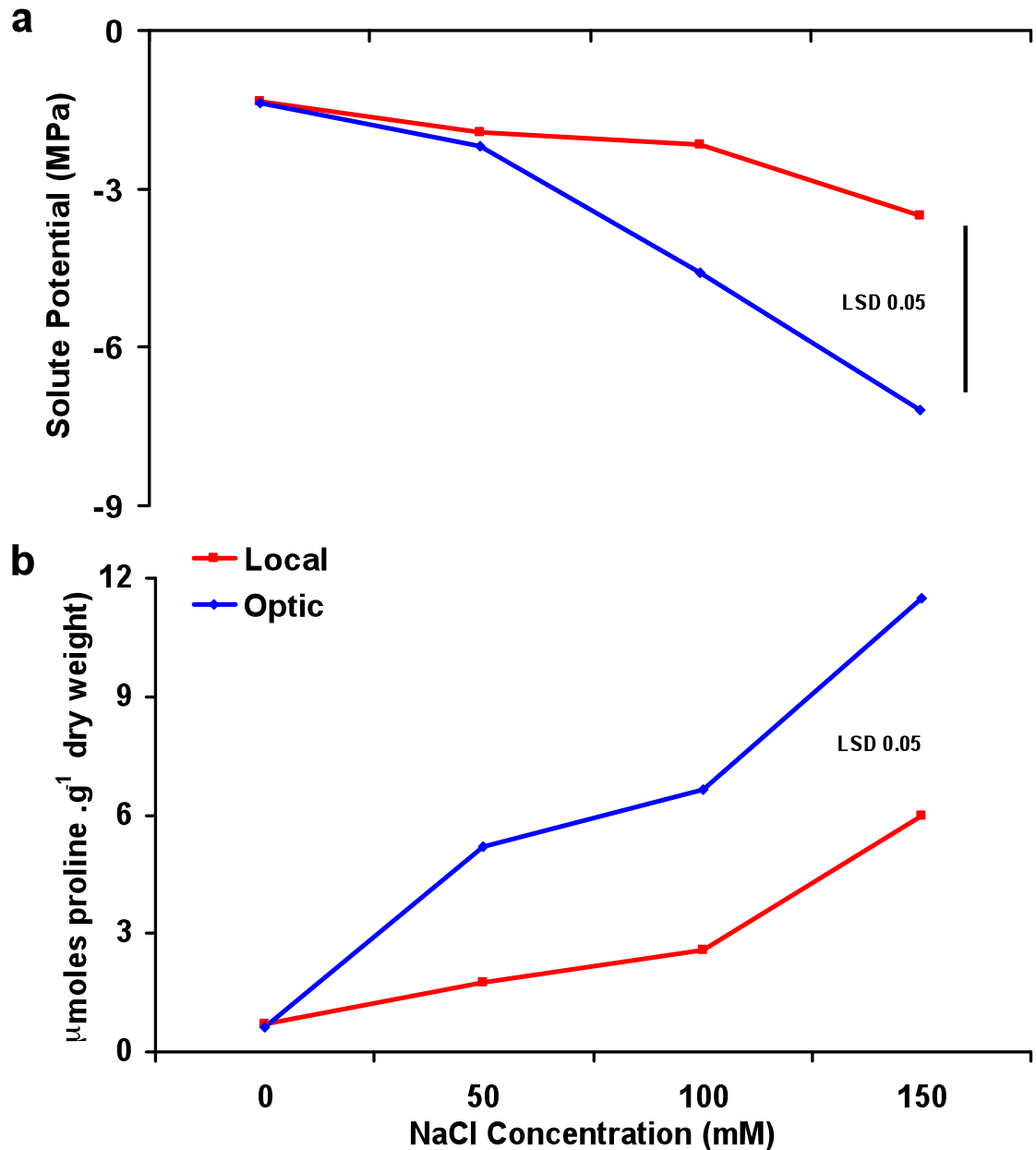
Figure 4-8: The Effects of Salt Treatments on Leaf Solute Potential (ψ_{solute}) and Proline Concentration in Barley Genotypes.

Top panel (a): solute potential (ψ_s); bottom panel (b): proline concentration. Local; ▬■▬ , and Optic; ▬●▬ . Solute potentials were measured from the extracted cell sap of freshly harvested leaves (see Section 2.1.3.3.1) from 60 day old plants growing in hydroponics at the indicated salt concentrations. Proline concentrations were measured from dry leaf samples (see Section 2.1.3.3.3). Values are the average (± SE) for 3 replicates per treatment. ANOVA tests were performed using a General Linear Model. Tables for ANOVA and grouping information along with Figures for residual and interaction plots are presented in Appendix (Figures A 4-12 & 4-13).

4.3 *Ion Content Assessment*

Nutrient ion profiles of stem, green leaf, and dry leaf and root tissues were determined by Inductively Coupled Plasma-Optical Emission Spectrometry; see Section 2.1.4. Different plant tissues like stem, green leaf, desiccated leaf and roots were used to observe any significant salt partitioning by barley plants and its consequences on halotolerance mechanism as mentioned in the literature. Data were collected for the following elements: K, Na, Ca, P, S, Mg, Mn, Fe, and B. No consistent major differences were observed for any of the macro and micronutrients except K^+ and Na^+, therefore, only data for these particular ions are presented.

4.3.1 K^+, Na^+ Content and Na^+/K^+ Ratio of Barley Stem

Increasing NaCl concentration from 0 to 50 mM produced a significant approximately 60 % decline in shoot K^+ levels of both lines. At higher NaCl concentrations the K^+ levels were maintained at approximately 20 mg .g^{-1} dry weight in Local. In contrast Optic showed a significant decline from *ca.* 20 to 5 mg .g^{-1} dry weight in shoot K^+ level (Figure 4-9a p ≤0.05).

Increasing external NaCl concentration from 0 to 150 mM NaCl produced a three fold increase in stem Na^+ levels of landrace Local and seven fold increase in line Optic (Figure 4-9b; p ≤0.05). The data show that stem Na^+ levels did not increase significantly when external NaCl was increased to 50 mM NaCl; above this level line Optic showed a sharp increase in Na^+ levels (from *ca.* 14 to 86 mg .g^{-1} dry weight). Landrace Local also showed an increase in Na^+ levels but this was less dramatic (*ca.* 14 to 38 mg .g^{-1} dry weight). Significant differences between the two lines were observed at 100, and 150 mM NaCl (p<0.05) It appears that both lines adopt a strategy to maintain shoot Na^+ levels below 25 mg .g^{-1} dry weight. Once this threshold level is exceeded, this mechanism may break down as stem Na^+ levels begin to rise abruptly.

The relationship between tissue Na^+ and K^+ content can be revealed by plotting Na^+ / K^+ ratio as a function of external salinity (Figure 4-9c). Both lines Local and Optic maintained their Na^+ / K^+ at approximately 1 to 7 with increasing external NaCl concentrations up to 100 mM. Above 100 mM NaCl concentrations, however, line Optic showed a significant increase (from *ca.* 7 to 75) in the stem Na^+/K^+ ratio, while

landrace Local did not show a significant change in its stem Na^+/K^+ at higher salt concentrations ($p < 0.05$).

Figure 4-9: K$^+$, Na$^+$ Content, and Na$^+$/K$^+$ Ratio of Salt Stressed Barley Stems.

Top panel (a): stem K$^+$ content; middle panel (b): stem Na$^+$ content; bottom panel (c): stem Na/K ratio. Local; ─■─ , Optic; ─◆─ . Samples were harvested at day 60 after germination (38 days into NaCl treatment) and prepared (see Section 2.1.4.1.2). Values are the average (± SE) for 5 replicates per treatment. ANOVA tests were performed using a General Linear Model. Tables for ANOVA and grouping information along with Figures for residual and interaction plots are presented in Appendix (Figures A 4-14 to A 4-16).

a

K$^+$ Content (mg .g^{-1} dry weight)

Local Stem
Optic Stem

LSD 0.05

b

Na$^+$ Content (mg .g^{-1} dry weight)

LSD 0.05

c

Na/K Ratio

LSD 0.05

NaCl Concentration (mM)

112
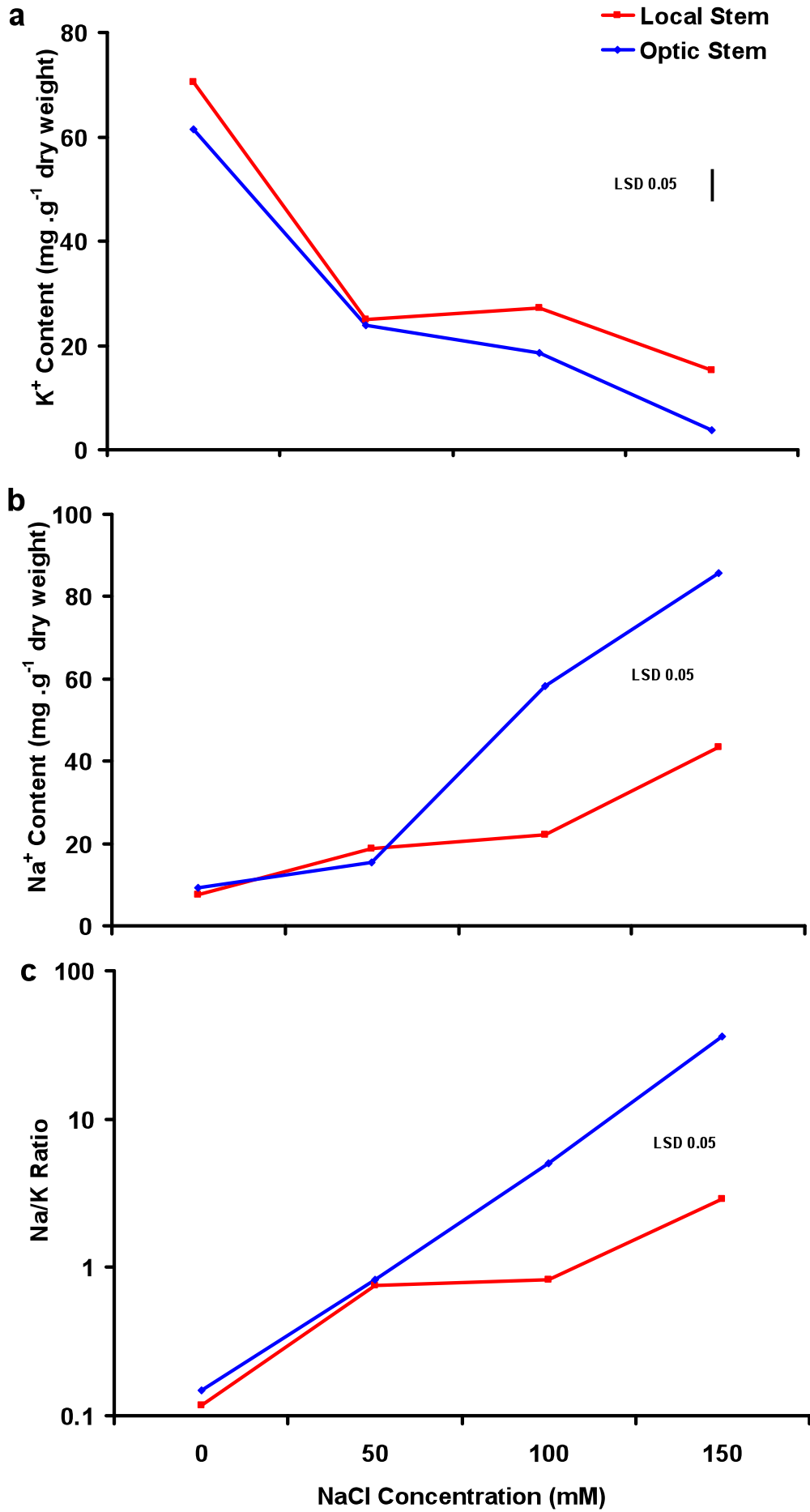
4.3.2 K$^+$, Na$^+$ Content and Na$^+$/K$^+$ Ratio of Barley Root

Both genotypes Local and Optic showed a salinity-induced decline in root tissue K$^+$ content. In Local it progressively declined to approximately 20 % (150 mM NaCl) of the levels of plants in 0 mM NaCl (*ca.* 28 mg .g^{-1} dry weight). In contrast, Optic root K$^+$ levels abruptly declined to approximately 20 % of controls at 50 mM NaCl; Figure 4-10a; p $\leq$0.05). The data presented suggest that Optic partitions proportionately more K$^+$ in the shoot than Local (*cf* Figures 4-9a and 4-10a).

Na$^+$ levels in root tissues of both lines increased abruptly with increasing salinity from 0 to 50 mM; this increase was more prominent in line Optic (from *ca.* 5 to 20 mg .g^{-1} dry weight) than in Local (from *ca.* 4 to 10 mg .g^{-1} dry weight). Above this NaCl concentration, root Na$^+$ levels did not change markedly in both lines. (Figure 4-10b; p $\leq$0.05).

Root Na$^+$/K$^+$ levels showed a similar trend in both genotypes. As external NaCl was increased from control to 150 mM NaCl concentrations Na$^+$/K$^+$ ratio increased from *ca.* 0.2 to 1.6 in Local, and from *ca.* 0.2 to 10 in Optic. It is clear from the data that at higher NaCl concentrations Local maintained a lower Na$^+$/K$^+$ ratio than Optic (Figure 4-10c; p $\leq$0.05).

Figure 4-10: K$^+$, Na$^+$ Content, and Na$^+$/K$^+$ Ratio of Salt Stressed Barley Roots.

Top panel (a): root K$^+$ content; (b): middle panel; root Na$^+$ content; (c): bottom panel: root Na$^+$/K$^+$ Ratio. Local; ━■━ , Optic.━◆━ . Samples were harvested at day 60 after germination (38 days after NaCl treatment) and prepared as described in Section 2.1.4.1.2. Values are the average (± SE) for 5 replicates per treatment. ANOVA tests were performed using a General Linear Model. Tables for ANOVA and grouping information along with Figures for residual and interaction plots are presented in Appendix (Figures A 4-17 to A 4-19).

a

K$^+$ Content (mg .g^{-1} dry weight)

Local Root
Optic Root

LSD 0.05

b

Na$^+$ Content (mg .g^{-1} dry weight)

LSD 0.05

c

Na/K Ratio

LSD 0.05

NaCl Concentration (mM)

115
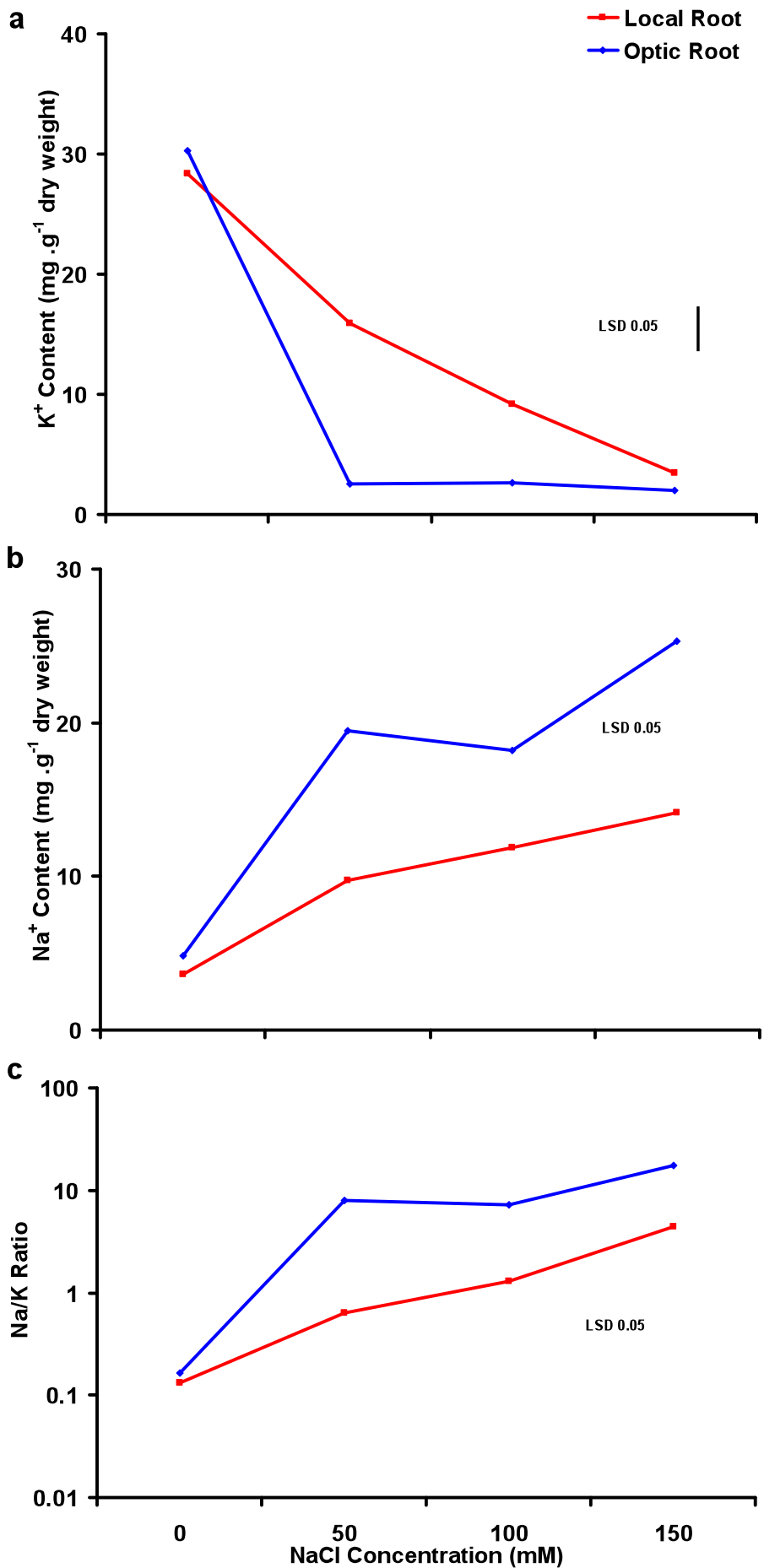
4.3.3 K^+, Na^+ Content and Na^+/K^+ Ratio of Barley Green Leaves

Increasing NaCl concentration to 50 mM produced an approximately 60 % decline in green leaf K^+ levels in landrace Local, but at higher concentrations the levels were maintained at *ca.* 20 mg .g^{-1} dry weight. Optic showed a dramatic and highly significant decline (from *ca.* 55 to 5 mg .g^{-1} dry weight) in green leaf tissue K^+ levels when external NaCl concentrations were increased from 0 to 50 mM, but above this level K^+ content did not change significantly and was maintained at approximately 5 mg .g^{-1} dry weight (Figure 4-11a; $p \le 0.05$).

In case of green leaf tissues Na^+ content of both lines showed an increase with increasing external NaCl concentrations from 0 to 150 mM (Fig 4-11b). Local showed a sharp significant increase in its green leaf Na^+ content (from *ca.* 4 to 14 mg .g^{-1} dry weight), when NaCl concentration increased from 0 to 50 mM. However, Local maintained its Na^+ contents at *ca.* 14 mg .g^{-1} dry weight up to 100 mM NaCl, above this concentration once again a sharp significant increase was observed (from *ca.* 14 to 40 mg .g^{-1} dry weight). Optic showed a highly significant linear increase (of *ca.* 7 fold) for Na^+ contents with increasing external NaCl concentration from 0 to 150 mM NaCl $p \le 0.05$.

In Optic, Na^+/K^+ ratio increased in green leaf tissues from <0.1 to *ca.* 1.5 as external NaCl concentration was increased from 0 to 100 mM NaCl. Beyond this concentration a considerable increase in leaf Na^+ levels was observed (ratio of approximately 70). In contrast, increasing NaCl did not cause a major difference in Na^+/K^+ in landrace Local, and even at the highest level of 150 mM the ratio did not exceed *ca.* 4 (Figure 4-11c; $p<0.05$).

Figure 4-11: K$^+$, Na$^+$ Content, and Na$^+$/K$^+$ Ratio of Salt Stressed Barley Green Leaves.

Top panel (a): Green leaf K$^+$ content; middle panel (b): green leaf Na$^+$ content; bottom panel (c): green leaf Na$^+$/K$^+$ Ratio. Local; ▬■▬ , Optic ▬◆▬. Samples were harvested at day 60 after germination (38 days after NaCl treatment) and prepared as described Section 2.1.4.1.2. Values are the average (± SE) for 5 replicates per treatment. ANOVA tests were performed using a General Linear Model. Tables for ANOVA and grouping information along with Figures for residual and interaction plots are presented in Appendix (Figures A 4-20 to A 4-22).

a

K$^+$ Content (mg .g^{-1} dry weight)

Local Green Leaf
Optic Green Leaf

LSD 0.05

b

Na$^+$ Content (mg .g^{-1} dry weight)

LSD 0.05

c

Na/K Ratio

LSD 0.05

NaCl Concentration (mM)

118
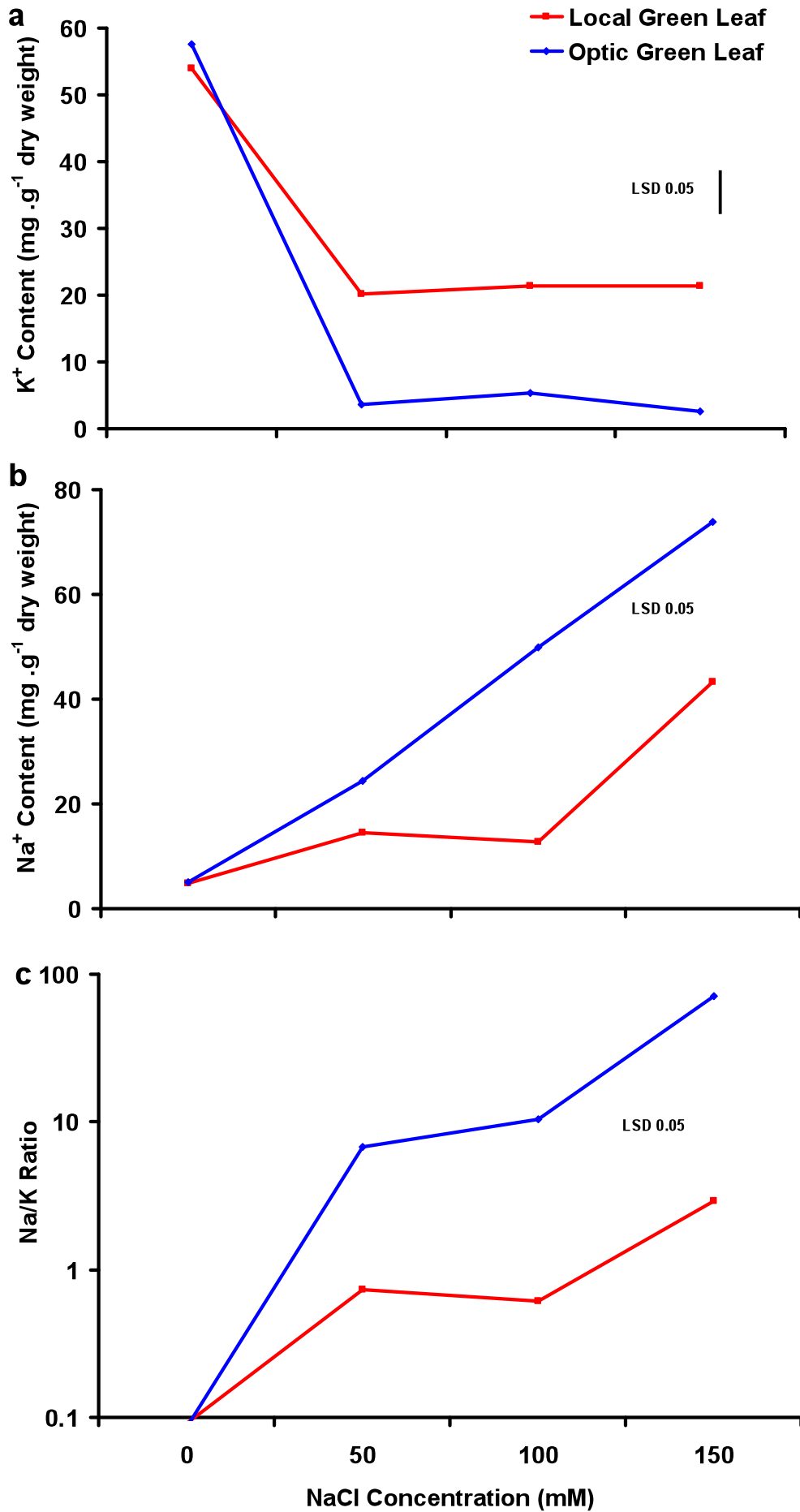
4.3.4 K⁺, Na⁺ Content and Na⁺/K⁺ Ratio of Barley Desiccated Leaves

Both lines Local and Optic showed a significant decline of approximately 66 % to 90 % in their dry leaf K^+ content with increasing NaCl concentration from 0 to 50 mM. However, this decline in line Optic was more prominent (*ca*. 65 to 5 mg .g^{-1} dry weight) than in landrace Local (*ca*. 45 to 18 mg .g^{-1} dry weight). Above this concentration both lines maintained their dry leaf K^+ content (Figure 4-12a; p ≤0.05).

Optic showed a significant increase in Na^+ content of desiccated leaf tissues (from *ca*. 4 to 70 mg .g^{-1} dry weight) with increasing external NaCl concentrations from zero to 100 mM; above this concentration, Optic maintained its Na^+ content levels. A similar pattern was observed in landrace Local, where desiccated leaf Na^+ content levels increased progressively and significantly (from *ca*. 4 to 40 mg .g^{-1} dry weight). This increase was less pronounced in landrace Local compared with line Optic (Figure 4-12b; p ≤0.05).

Optic desiccated leaf material showed a very sharp and significant increase in Na^+/K^+ ratio (>35) with increasing salinity, but values remained below *ca*. 2 in Local (Figure 4-12c; p ≤0.05).

4.3.5 Distribution of K⁺ and Na⁺ Content in Shoots and Roots

Landrace Local showed a decline in K^+ content partitioning to shoot at 50 mM NaCl and an increase in this value at 150 mM (*c.f.* 0 mM). In contrast Optic showed a significantly higher K^+ partitioning to shoot at 50 mM and lower at 150 mM NaCl compared with 0 mM NaCl (p<0.05; Figure 4-13a). Na^+ partitioning between shoots and roots of both genotypes showed a similar trend, where both genotypes at higher salt concentrations started a high Na^+ allocation to shoots, however, these were significant at 100 and 150 mM NaCl in Optic, and only at 150 mM NaCl in Local (*c.f.* 0 mM; p<0.05; Figure 4-13b).

Figure 4-12: K$^+$, Na$^+$ Content, and Na$^+$/K$^+$ Ratio of Salt Stressed Barley Desiccated Leaves.

Top panel (a): desiccated leaf K$^+$ content; middle panel (b): desiccated leaf Na$^+$ content; bottom panel (c): desiccated leaf Na$^+$/K$^+$ ratio. Local; ▬■▬ , Optic ▬◆▬ . Samples were harvested at day 60 after germination (38 days after NaCl treatment) and prepared as described in Section 2.2.3. Values are the average (± SE) for 5 replicates per treatment. ANOVA tests were performed using a General Linear Model. Tables for ANOVA and grouping information along with Figures for residual and interaction plots are presented in Appendix (Figures A 4-23 to A 4-25).
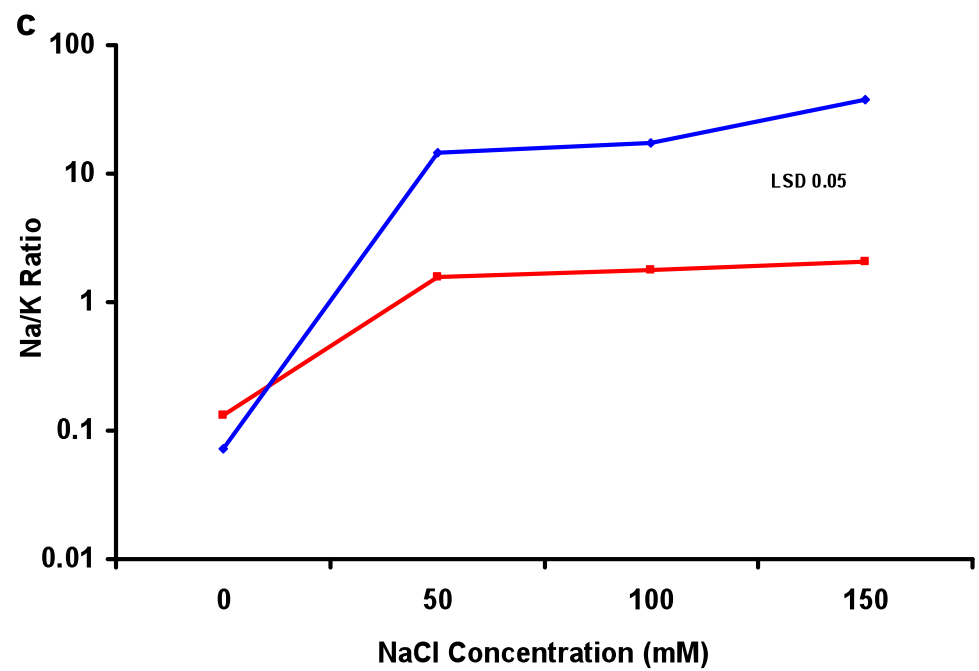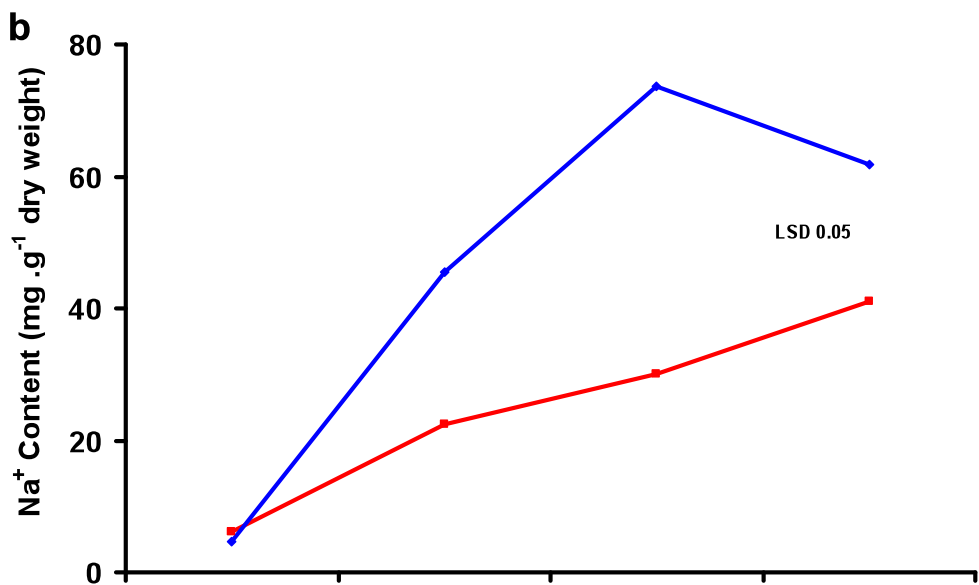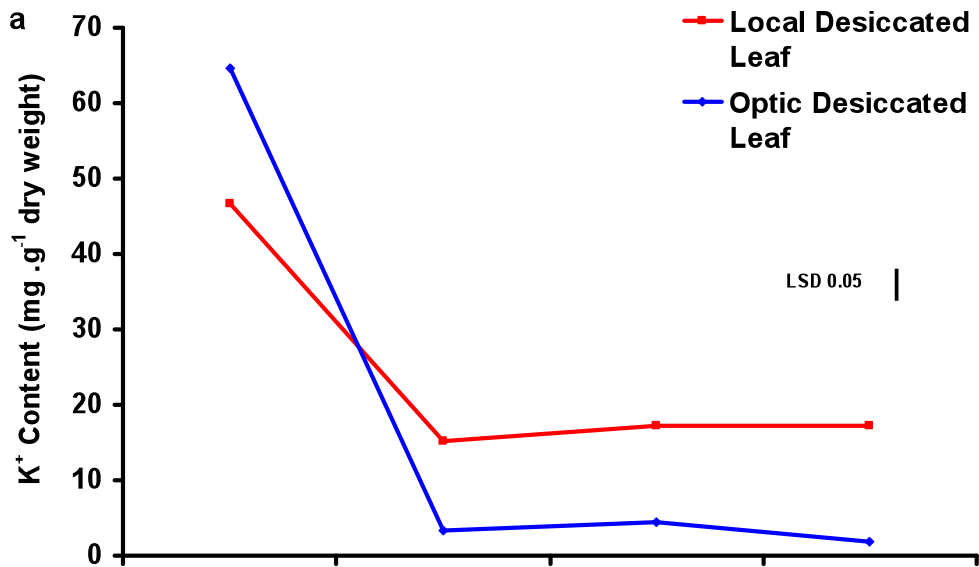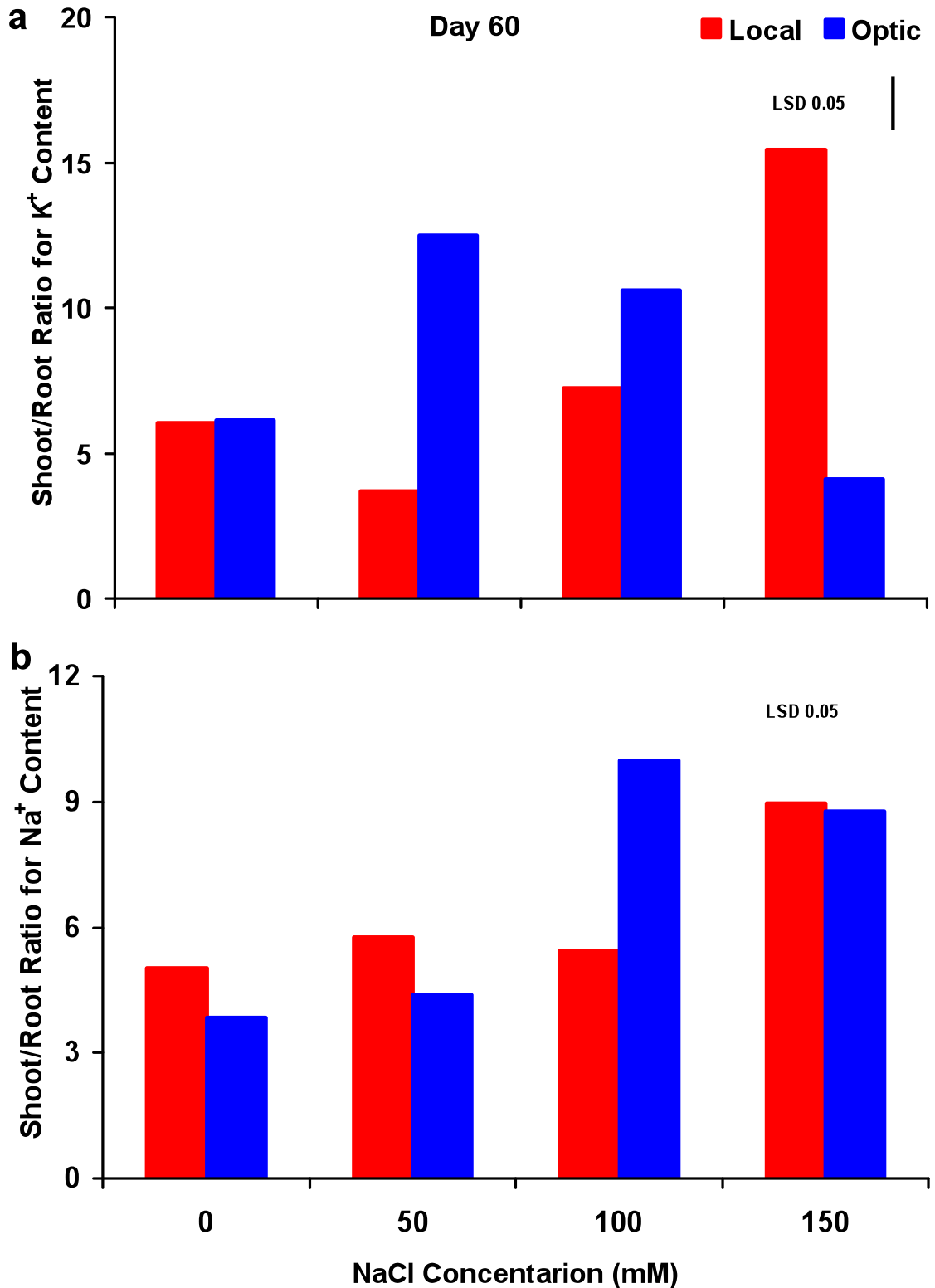
Figure 4-13 a & b: Shoot Root Ratio for K$^+$ and Na$^+$ Content in Barley Genotypes.

Values are the average (± SE) for 5 replicates per treatment of the shoot/root ratio for K$^+$ and Na$^+$ content in barley genotypes Local and Optic under increasing salt concentrations from 0 to 150 mM NaCl. ANOVA tests were performed using a General Linear Model. Tables for ANOVA and grouping information along with Figures for residual and interaction plots are presented in Appendix (Figures A 4-26 & 4-27).

4.4 *Assessment of Sodium Uptake*

The clear differences observed in Na$^+$ content of Local and Optic (see Section 4.3) may have arisen from differences in the rates of Na$^+$ uptake (*i.e.* Na$^+$ discrimination), Na$^+$ exclusion or both. To assess if there were genotypic differences in Na$^+$ discrimination, a series of experiments were conducted. Five day old seedlings were grown in sealed Falcon tubes containing 45.0 ml of ¼ Hoagland's solution plus added NaCl until the fifth leaf had emerged (*ca.* 24 days from germination). Each day the loss of solution due to transpiration was noted (±0.1 ml) and the volume restored to 45.0 ml with the appropriate solution. Ion analysis was performed on the Hoagland's solutions and harvested shoot and root tissue from genotype Local and Optic using Inductively Coupled Plasma-Optical Emission Spectrometry (ICP-OES).

4.4.1 Na$^+$ and K$^+$ Uptake by Barley Shoots

Increasing external NaCl concentration from 0 to 50 mM produced a significant increase (from *ca.* 0 to 10 mg .g^{-1} dry weight) in both barley lines Local and Optic shoot Na$^+$ levels, from 50 to 100 mM NaCl both lines maintained their shoot Na$^+$ levels. However, on increasing NaCl concentration further to 150 mM NaCl landrace Local maintained its shoot Na$^+$ levels, but Optic did not showing a significant increase of (*ca.* 12 to 22 mg .g^{-1} dry weight; Figure 4-14a; $p<0.05$).

Both lines showed a significant progressive decline in their shoot K$^+$ levels from (*ca.* 50 to 10 mg .g^{-1} dry weight) when external NaCl concentration was increased from 0 to 150 mM (Figure 4-14b; $p<0.05$).
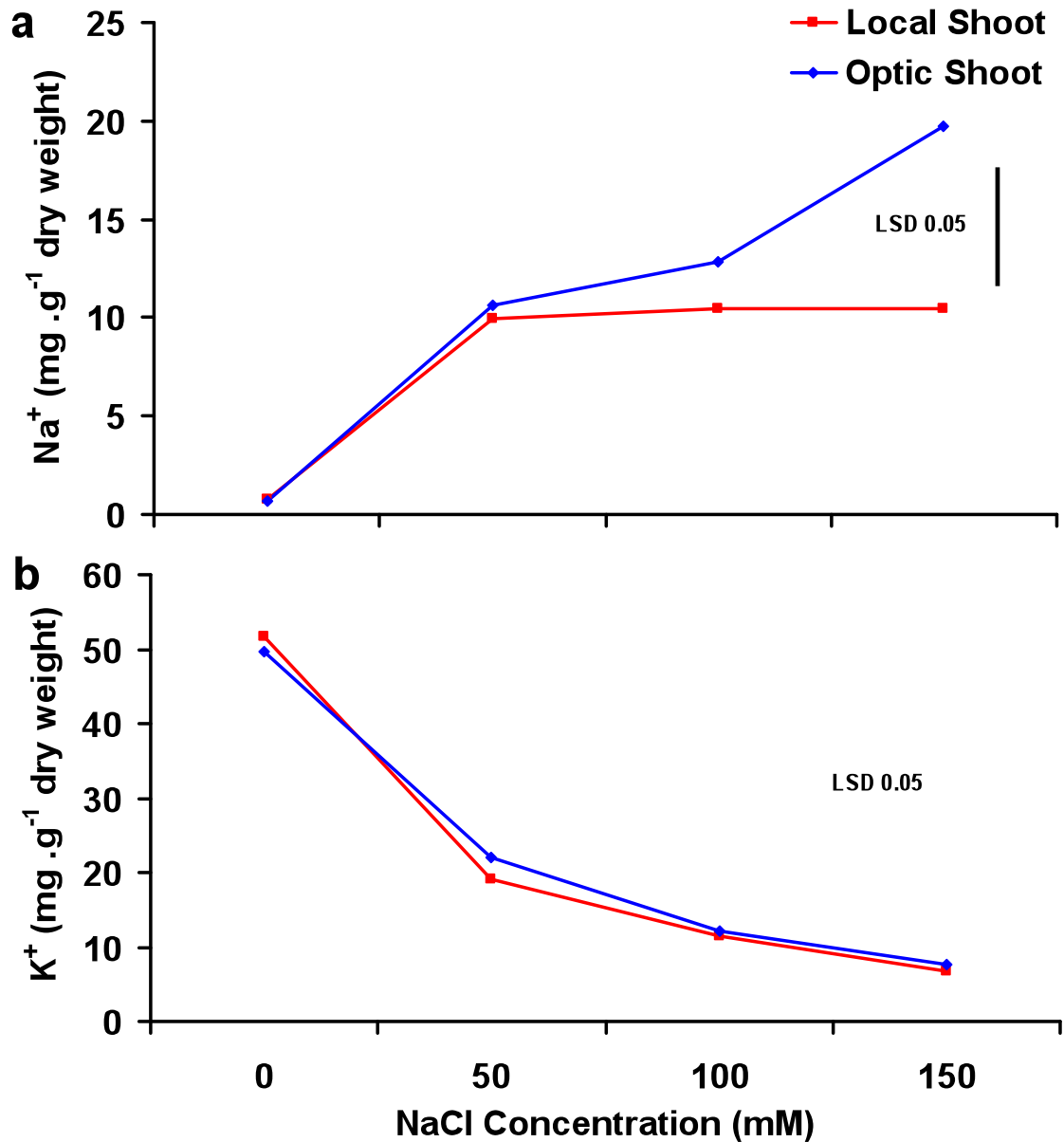
Figure 4-14: Na⁺, K⁺ Contents in the Shoots of Barley Genotypes.

Top panel (a): shoot Na^+ content; bottom panel (b): shoot K^+ content. Local; ▬■▬ , Optic; ▬◆▬ . Samples were harvested at day 24 after germination growing in Falcon tubes at indicated salt concentrations and prepared (see Section 2.1.4.1). Values are the average (± SE) for 5 replicates per treatment. ANOVA tests were performed using a General Linear Model. Tables for ANOVA and grouping information along with Figures for residual and interaction plots are presented in Appendix (Figures A 4-28 & 4-29).

4.4.2 Na$^+$ and K$^+$ Uptake by Barley Roots

Barley lines Local and Optic showed a significant increase in their root Na$^+$ contents (from *ca.* 0 to 5 mg .g^{-1} dry weight) when external NaCl concentration was increased from 0 to 50 mM. Local maintained its root Na$^+$ levels (at approximately 5 mg .g^{-1} dry weight) when its external NaCl concentrations were increased from 50 to 150 mM. However, line Optic showed a similar trend for its root Na$^+$ levels over the 0 to 100 mM range, but values increased significantly from approximately 5 to 10 mg .g^{-1} dry weight when concentrations increased from 100 to 150 mM. (Figure 4-15a; $p<0.05$)

In case of roots K$^+$ levels, line Optic showed a progressive and significant decline from (*ca.* 20 to 4 mg .g^{-1} dry weight) when external NaCl concentration was increased from 0 to 150 mM, while landrace Local maintained its root K$^+$ levels (at *ca.* 20 mg .g^{-1} dry weight) up to 50 mM NaCl concentration; above this concentration it showed a decline, similar to that observed in Optic (Figure 4-15b; $p<0.05$).

4.4.3 Distribution of K$^+$ and Na$^+$ Content in Shoots and Roots

Landrace Local's 24 day old plants diverted most of their K$^+$ content to root at 50 mM NaCl, in contrast Optic diverted most of the K$^+$ content to shoot at 150 mM NaCl ($p<0.05$; Figure 4-16a). While Na$^+$ content partitioning between shoot and root showed no significant differences at all NaCl concentrations from 0 to 150 mM between the both genotypes Local and Optic ($p<0.05$; Figure 4-16b).
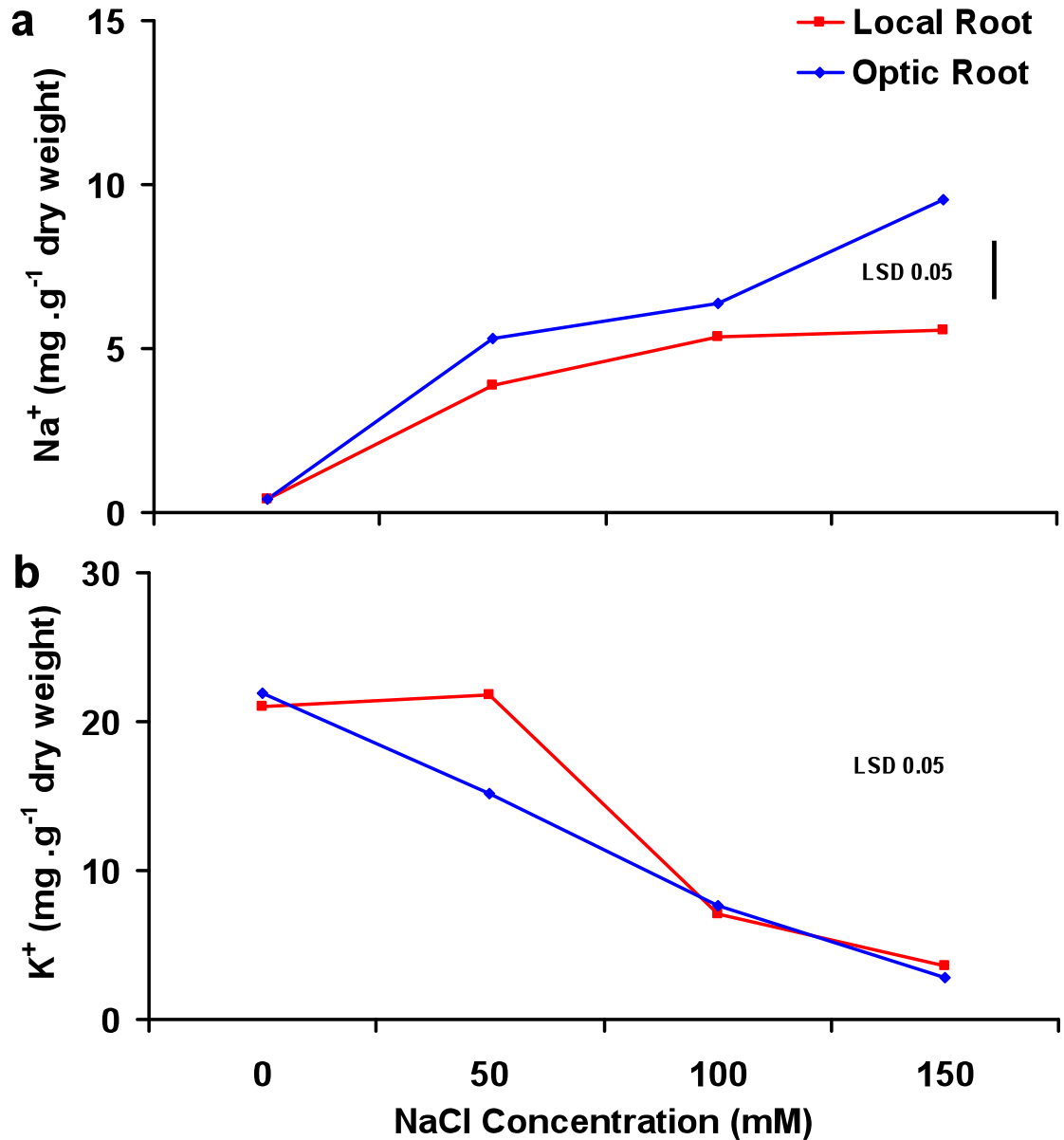
Figure 4-15: Na$^+$, K$^+$ Contents found in the Roots of Barley Genotypes.

Top panel (a): root Na$^+$ content; bottom panel (b): root K$^+$ content. Local; ■ , Optic ◆ . Samples were harvested at day 24 after germination growing in Falcon tubes at indicated salt concentrations and prepared (see Section 2.1.4.1). Values are the average (± SE) for 5 replicates per treatment. ANOVA tests were performed using a General Linear Model. Tables for ANOVA and grouping information along with Figures for residual and interaction plots are presented in Appendix (Figures A 4-30 & 4-31).
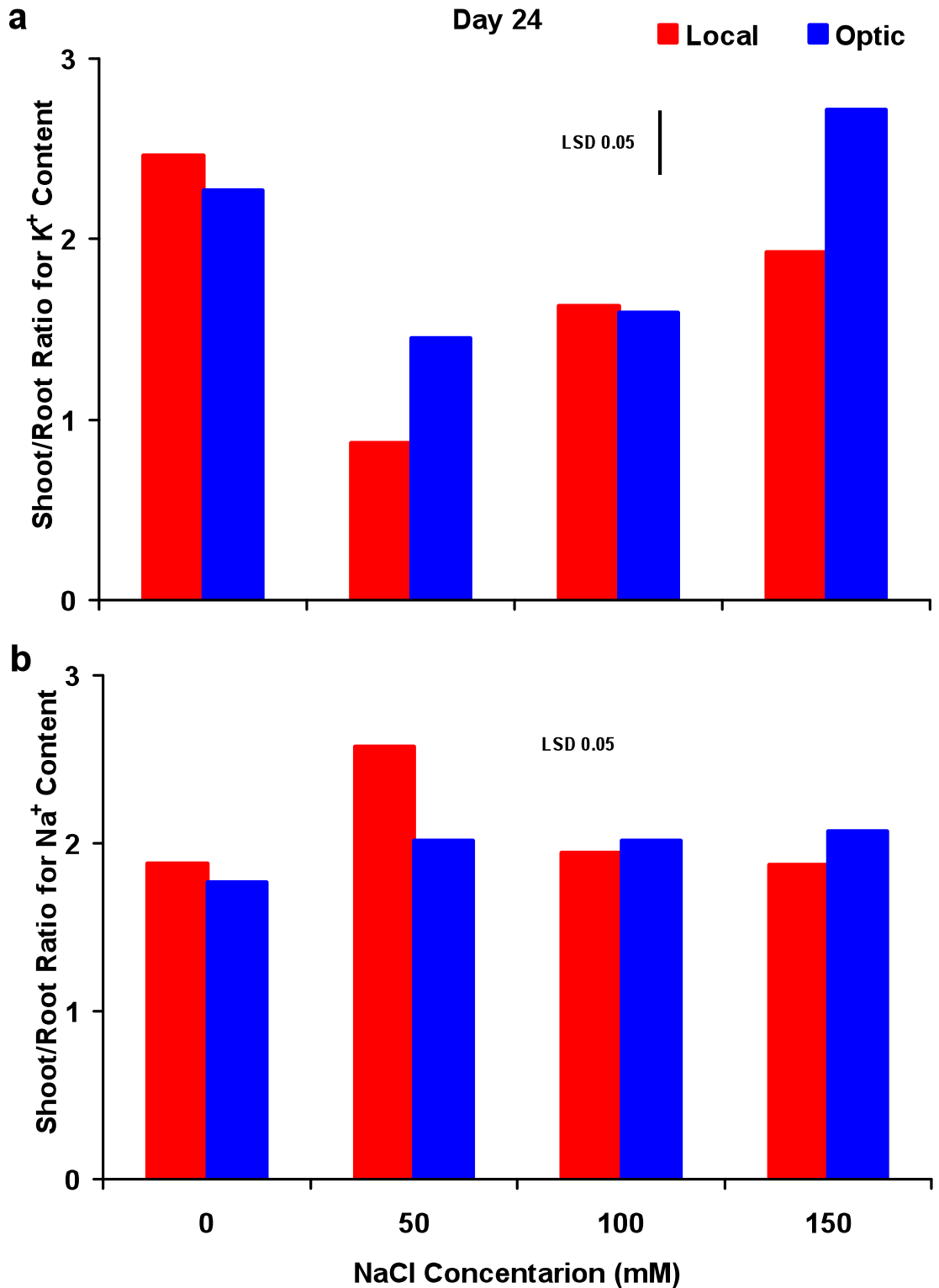
Figure 4-16 a & b: Shoot Root Ratio for K$^+$ and Na$^+$ Content in Barley Genotypes.
Values are the average (± SE) for 5 replicates per treatment of the shoot/root ratio for K$^+$ and Na$^+$ content in barley genotypes Local and Optic under increasing salt concentrations from 0 to 150 mM NaCl. ANOVA tests were performed using a General Linear Model. Tables for ANOVA and grouping information along with Figures for residual and interaction plots are presented in Appendix (Figures A 4-32 & 4-33).

4.5 *Mapping Loci Conferring Tolerance in Landrace Local*

The comparative physiological investigations on salt tolerance in the barley genotypes have confirmed that an underlying genetic variability exists between elite lines and landrace; landrace Local was the most tolerant genotype studied. The project is now at a stage where the genetic basis for improved thermotolerance and halotolerance (see Chapter 3 and 5) in Local should be investigated further. Mapping genes that confer desirable traits to barley can now be undertaken using the Barley Optical Probe Arrays (BOPA) for over 3,000 SNP markers. This will involve crossing Local with a well characterized elite line such as Triumph or Optic and screening *ca.* 3,000 F_2 generation individuals for co-segregation of loci conferring tolerance with specific mapped SNP markers. A critical part of this strategy, therefore, will require scoring the F_2 population as 'tolerant' or 'sensitive' and requires the development of a robust screen. If an incorrect phenotype assignment is made on a few individuals, the analysis can be irrevocably compromised. For this purpose the following experiment was conducted to establish if such a robust screen could be conducted. The ideal situation would be where all plants carrying the Local tolerant loci survive high salt concentrations and all plants carrying the corresponding susceptible Optic loci do not.

To assess whether such a robust screen can be undertaken, 12 Local and 12 Optic plants were grown over a range of high NaCl concentrations. This number was chosen because if a critical threshold NaCl concentration could be found where all Local survive and all Optic do not, this represents a probability of p= $(0.5)^{12}$ = <0.00025 (*i.e.* better than one in 4096 that all Local plants will survive and none of the Optic plants).

Local showed a 40 % higher survivability in 150 mM NaCl and a 16% higher survival in 175 mM NaCl concentration than did Optic (Figure 4-17). Unfortunately, the results do not provide confidence that there are sufficient phenotypic differences between Local and Optic to allow a mapping foundation to proceed further (Figure 4-17; p $\leq$0.05).

It might be that the genetic variance within the pool of Local seed at our disposal is too great and that identification of hyper-tolerant inbred individuals within this seed stock may provide a sound basis to continue with loci mapping. It is suggested a few thousand doubled haploid lines of Local need to be generated for halotolerance screening, and the best of these lines selected for generating a mapping population.
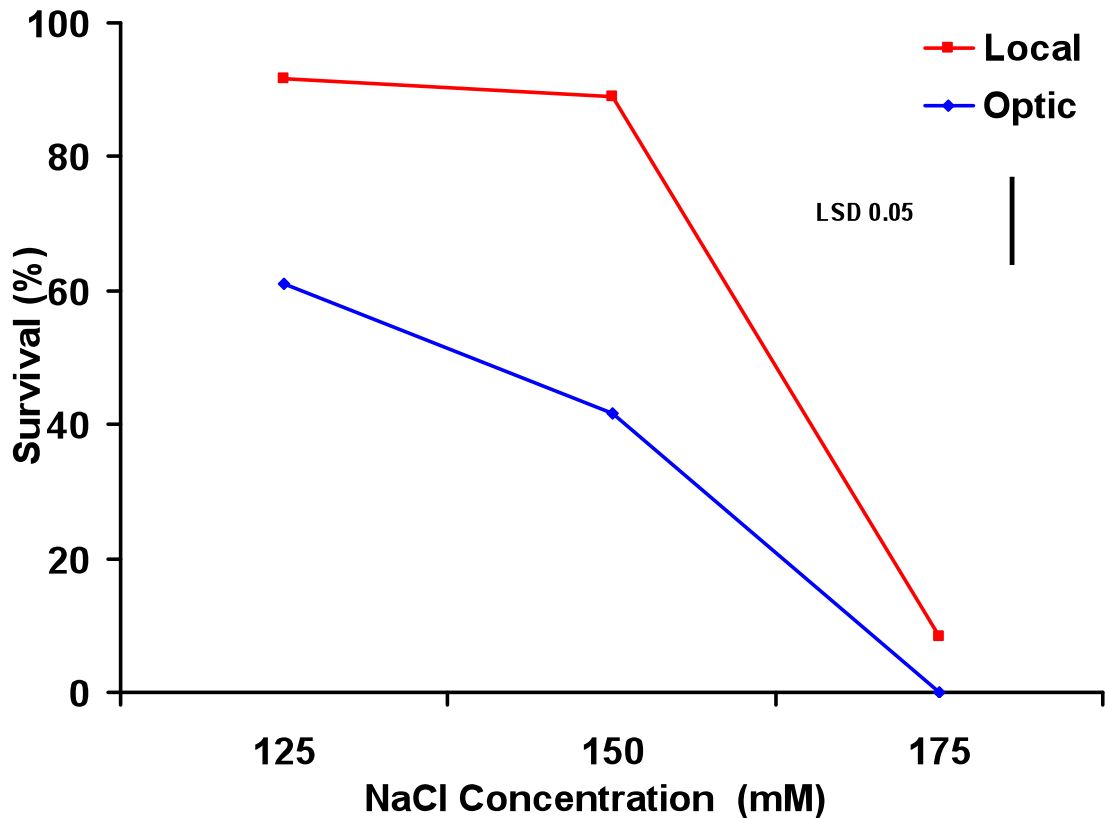
Figure 4-17: Survival of Barley Genotypes Local and Optic under at High Salt Concentrations and Highly Controlled Conditions.

Seeds from Local (salinity tolerant) and Optic (salinity susceptible) lines were germinated on paper towels under sterilized conditions. One week after germination 12 healthy seeds, were shifted to ¼ Hoagland's media and when plants were 21 days old, media was supplemented with NaCl to provide concentrations of 125, 150, and 175 mM; see Section 2.1.2.2 for experimental details. The data points are the averages (± SE) of three replicates in each replicate (twelve independent samples). ANOVA tests were performed using a General Linear Model. Tables for ANOVA and grouping information along with Figures for residual and interaction plots are presented in Appendix (Figure A 4-34).

4.6 *Epigenetic Studies in Barley Genotypes*

An experiment was conducted to asses the effects of parental salt stress on subsequent generations. In this study the first generation F_0 plants were grown until harvest in hydroponics media having either 0 or 100 mM NaCl concentration. The seeds harvested from these two type of plants were then germinated and grown for 12 days in controlled growth chambers (see Section 2.1.2 for experimental details). The only parameter regarding seedling growth measured was their seedling shoot length. Seeds (first generation) F_0 harvested from the plants of genotypes Local and Optic, which were grown to harvest in hydroponics solution having 100mM NaCl concentration, and subsequently these were germinated and grown in their (second generation) F_1 in hydroponics solution containing 100mM NaCl concentrations, indexed as 100(100). Seeds (first generation) F_0 harvested from the plants of genotypes Local and Optic, which were grown to harvest in hydroponics solution having 0 mM NaCl concentration, and subsequently these were germinated and grown in their (second generation) F_1 in hydroponics solution containing 100mM NaCl concentrations, indexed as 0(100). 100(100) grown seedlings showed a significantly higher seedling shoot length during 12 days of growth in 100 mM NaCl compared with the 0(100) seedlings (Figure 4-18 a & b, p ≤0.05).

4.6.1 The Effects of Parental Salt Stress on Seedling Growth

The effects of parental salt stress on seedlings growth were estimated by taking the ratio of seedlings 100(100)/0(100) in both genotypes. This ratio in both genotypes showed non significant differences in genotypes Local and Optic (p<0.05; Figure 4-19).

Figure 4-18: Trans-generational Epigenetic Effects of Salinity in Barley Genotypes Local and Optic.

Genotypes Local (salinity tolerant) and Optic (salinity sensitive) were grown to harvest in hydroponic solution (0 and 100 mM NaCl) and seeds collected; these plants represent the first generation (F_0). Twenty seeds from each line at each NaCl concentration were then germinated both in ¼-strength Hoagland's solution with 0 and 100 mM NaCl and subsequently grown in hydroponic solutions; these plants represent the second generation (F_1). Thus, F_1 seedlings indexed as (0/100) were derived from F_0 plants grown in 0 mM NaCl, and subsequently germinated and grown in 100 mM NaCl; F_1 seedlings indexed as (100/100) were derived from F_0 plants grown in 100 mM NaCl and subsequently germinated and grown in 100 mM NaCl.

Top panel (a): plate showing F_1 seedlings of Local and Optic. The largest and smallest two seedlings, along with four seedlings from quartiles 2 and 3 are presented. Bottom panel (b): average and ± SE of seedling shoot length of quartiles 2 and 3 (n = 20). ANOVA tests were performed using a General Linear Model and different letter codes indicate Tukey's significant differences at $p < 0.05$. The ANOVA Tables and Figures for residual and interaction plots are presented in (Figure A 4-35).

Local 0(100)

Local 100(100)

1 cm

Optic 0(100)

Optic 100(100)

a

b

NaCl Concentration (mM) F_1 Seeds Collected, F_0(Media)
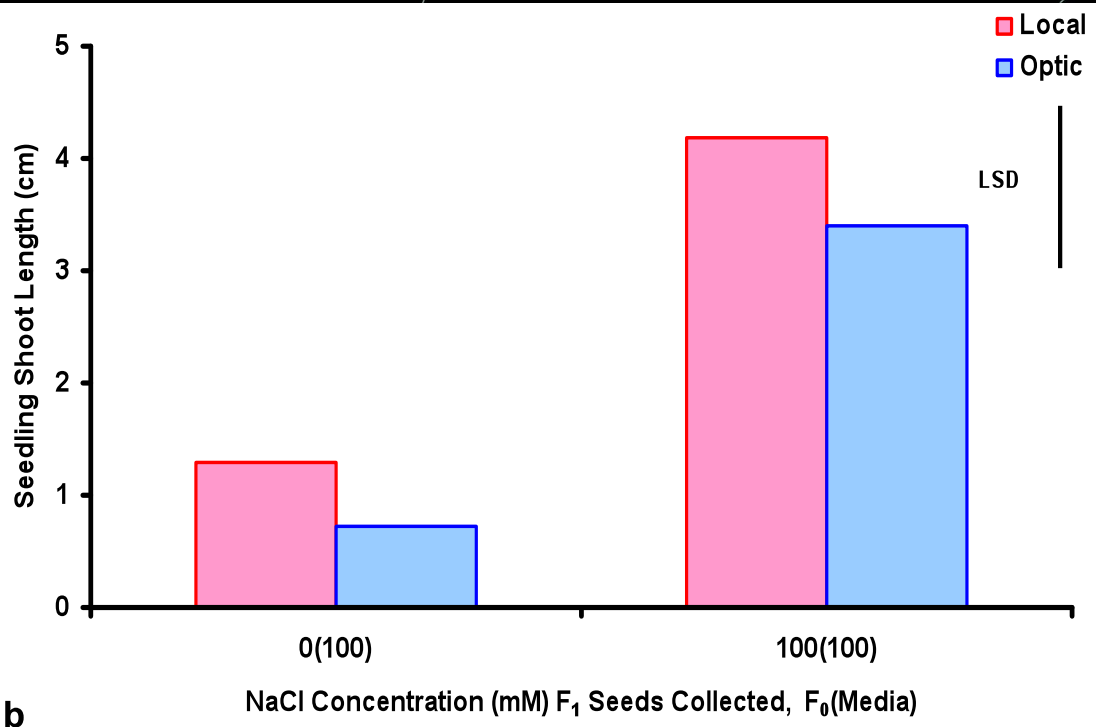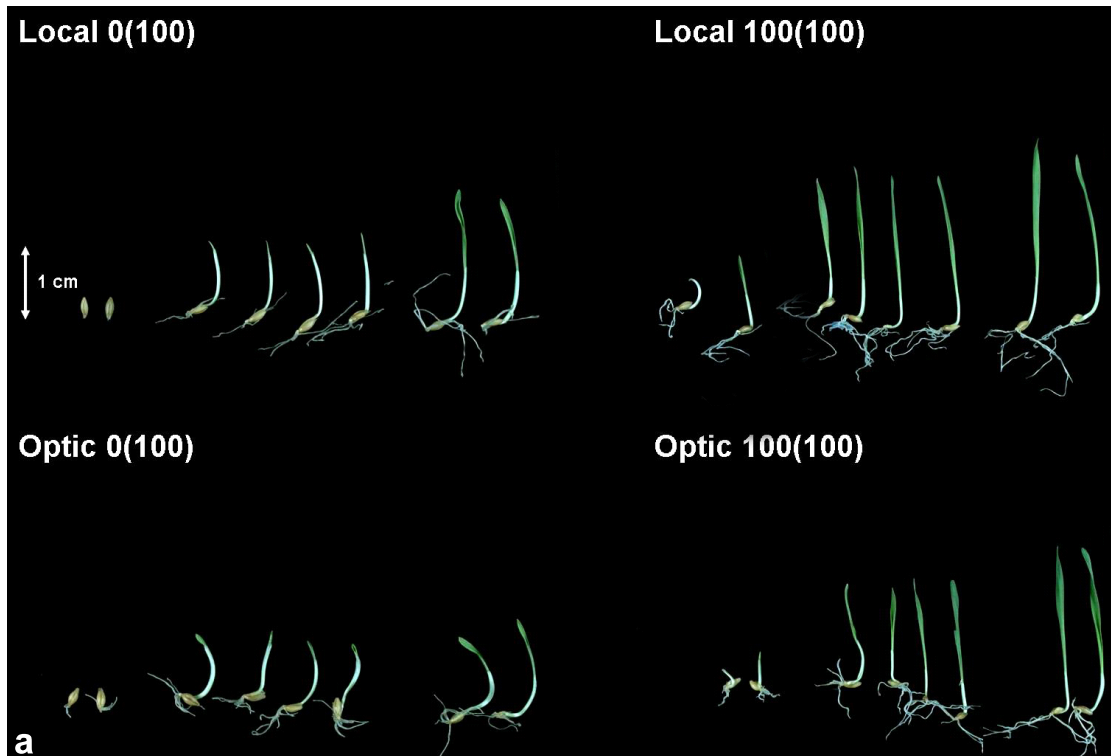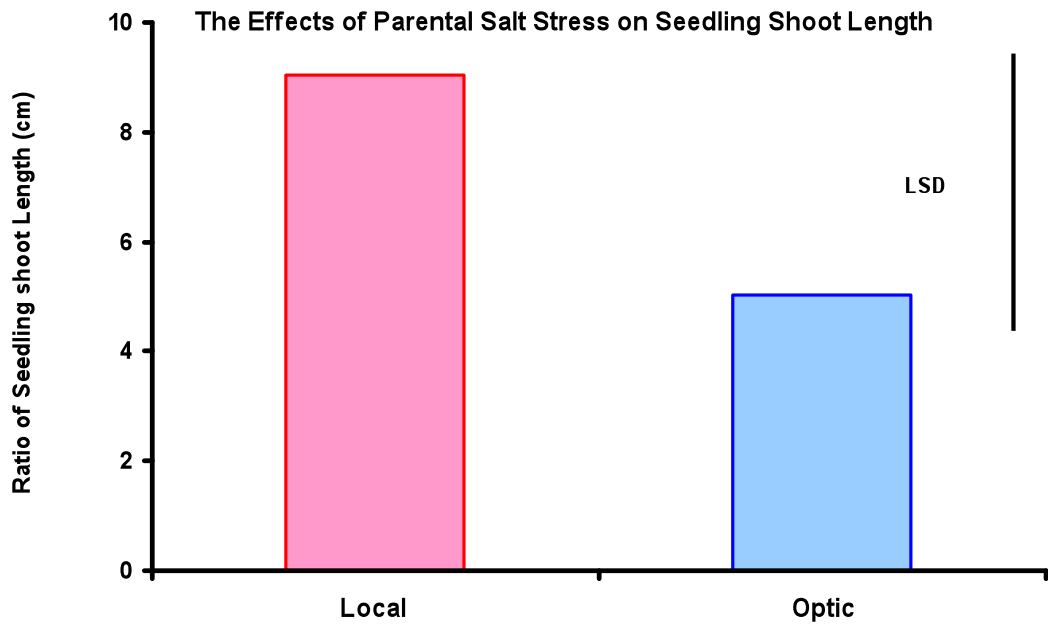
Figure 4-19: Epigenetic Effects of Parental Salt Stress on Seedling Shoot Length of Subsequent Generations in Barley Genotypes Local and Optic.

Ratio of shoot length of second generation seedlings grown in 100 mM NaCl. The ratios were calculated as shoot length of seedlings grown at 100 mM but whose parents were grown 100 mM (100(100), numerator) or 0 mM (0/100), denominator). ANOVA tests were performed using a General Linear Model (n=20).

4.7 *Discussion*

The growth and yield measurements discussed in Chapter 3 indicated that landrace Local shows better salinity tolerance compared with the other three lines; therefore, experiments were designed and undertaken to establish the underlying physiological basis for these differences. In this Chapter results for experiments relating to the physiological characterization obtained from landrace Local and line Optic only are presented; most of the experiments were conducted on all four genotypes, but for brevity the intermediated responses of Soorab-96 and Awaran-2002 have been omitted. The measured parameters include those relating to photosynthesis, water status, and the ionic status of plants growing in different salt concentrations. In addition, experiments were conducted to asses the feasibility of mapping halotolerance quantitative trait loci in the landrace Local. Finally some experiments were conducted to establish if there was an epigenetic basis for the observed halotolerance.

Photosynthetic efficiency (CO_2 assimilation) was impaired significantly in both genotypes at high salt concentrations. Clear and significant differences were observed in genotypes Local and Optic when exposed to a range of salt concentrations from 0 to 150 mM NaCl. Landrace Local maintained control levels of light saturated (A_{sat}) and light limited (180 μmol .m^{-2} .s^{-1} PPFD; A_{180}) CO_2 assimilation up to 100 mM NaCl, and only at 150 mM NaCl showed a significant decline. In contrast, line Optic showed a steep decline for both A_{sat} and A_{180} above 50 mM NaCl. Suppression of CO_2 assimilation in plants by salt stress is not unusual and has been reported previously (Ali *et al.*, 2008; Cramer *et al.* 2007 and Siddiqi *et al.*, 2009). To understand the possible causes of suppression in CO_2 assimilation rates in these barley genotypes parameters estimating the CO_2 supply, the kinetics of C3 cycle, and primary photochemistry were measured; these included quantum efficiency (α), stomatal conductance (**gs**), mesophyll conductance (**gm**), carboxylation coefficient (Φ CO_2), and apparent photorespiration (V'_o) of leaves.

The quantum efficiency (α) declined significantly (*ca.* 80 %) at high salt concentrations in both genotypes confirming that salinity suppresses primary reactions of photosynthesis, however, landrace Local was more tolerant than line Optic (Figure 4-2). With the decrease in CO_2 assimilation **gs** also declined significantly and this decline was more prominent in Optic than Local (Figure 4-1). A salinity-induced decline in **gs** has been reported by others (von Caemmerer *et al.*, 2009). Regression analysis between

CO_2 assimilation and **gs** (Figure 4-5b) showed strong correlations when a second order polynomial (quadratic) equation was fitted to the data; further, the coefficients for Local and Optic were significantly different. Extreme caution should be exercised, however, before firm conclusions can be drawn from such regressions. Whilst it is clear that a salinity-induced decrease in **gs** will result in a decrease in CO_2 assimilation, it is also true that a salinity-induced decrease in CO_2 assimilation will cause stomatal closure. It can be argued that, although often presented in the literature, such plots provide little insight and are of limited value (see Section 6.1 for a further discussion).

Estimates of the effects of salinity on the kinetics of the C3 cycle can be obtained by studying the carboxylation coefficient (ΦCO_2) derived from A/Ci curves. A significant suppression at higher salt concentrations was found and this is consistent with other reports (Wang *et al.*, 2007). Differences between the two genotypes were found, however, ΦCO_2 was suppressed significantly above 50 mM in line Optic, but only above 100 mM NaCl in landrace Local.

A significant decrease in the apparent rate of photorespiration (V'_o) measured at 0 μmol of CO_2 .mole^{-1} of air was observed above 50 mM NaCl concentration (Figure 4-4). This decline in V'_o could be due to a decrease in substrate (RuBP) concentration and/or an impairment in the activity of the enzyme RuBisCO (Munns and Tester, 2008).

Most of the reports attribute suppression of growth in plants to osmotic imbalances at higher salt concentrations (Cramer, 2002; Fricke and Peters, 2002; Munns and Tester, 2008). To asses this contention, the hydration state of barley leaves was assessed by measuring the relative water content (RWC) and the leaf water potential (ψ_{H2O}). RWC values obtained were sensible at up to 50 mM NaCl, however, above this concentration values were low and unreliable (Figure 4-6), probably due to measuring RWC from both green and desiccated tissues. This was a mistake and it is suggested that for accurate measurements on RWC only living green tissues should be included.

Plant leaf water potential (ψ_{H2O}) was measured from green tissues and probably reflects better the hydration state of plant leaves. ψ_{H2O} decreased (*i.e.* more negative) significantly in line Optic above 100 mM NaCl; however, Local did not show any significant decrease at this salt concentration (Figure 4-7). It is worth mentioning here that significant errors can be incurred in the estimation of ψ_{H2O} using a pressure chamber unless sufficient attention is paid to the solute potential of the exuded xylem sap ($^{xylem}\psi_s$). When used according to the manufacturer's instructions, ψ_s is assumed to be zero. This is a reasonable assumption for plants growing in soils with normal, low

levels of electrical conductivity (E = 0 to 2 dS .m^{-1}) it is clear this is not the case here where significant amounts of NaCl might be present in the transpiration stream. For this reason, $^{xylem}\psi_s$ (Figure 4-7b) should be measured along with apparent balance pressure (ψ_{H2O}) so that better estimates of tissue water status can be made (Figure 4-7a). Without such corrections measurements of water potential using a pressure chamber will incur significant errors. When these corrections are made the results presented confirm that landrace Local can maintain a higher ψ_{H2O} than line Optic when exposed to salt stress.

Tissue solute potential also decreased (*i.e.* more negative) significantly in line Optic from approximately -0.7 to -4.5 MPa over the 0 to 150 mM NaCl concentration range, whereas Local maintained its hydration state at approximately -1.5 MPa. This decrease in tissue ψ_s was probably correlated with a significant increase in turgor pressure of leaves and this was greater in Optic than in Local. The turgor pressures of Optic barley leaves calculated from tissue ψ_s and leaf ψ_{H2O} were very high (*ca.* +2.5 MPa) at 100 and 150 mM NaCl. This might be due to errors of measurement of tissue ψ_s, perhaps because it's not possible to extract cell sap without contamination from the aqueous solution in the intercellular spaces and xylem. None-the-less, there is no reason to believe ψ_p in Optic were not at least as high as those in Local indicating both genotypes maintained sufficient turgor in high salinity to support growth and development.

The concentration of proline, the major compatible solute in barley (Ashraf and Foolad, 2007), increased significantly in both Local and Optic with increasing salinity (Figure 4-8b), but at 150 mM NaCl proline levels in Optic were nearly twice those in Local. These data suggest that both genotypes induced proline production in response to salinity but Optic produced more, probably because it was more salt stressed. These data also imply that the higher concentration of compatible solutes in line Optic should be accompanied by a lower (more negative) commensurate tissue ψ_s, and indeed this was the case (Figure 4-8a). An increase in compatible solute levels and decrease in tissue ψ_s are generally considered to occur in response to tissue dehydration. At 150 mM NaCl, however, Optic and Local were exposed to exactly the same water stress at their roots, and if changes in shoot proline levels and ψ_s arose solely from dehydration stress, then similar responses should have been recorded for the two genotypes. As this was not the case it seems that Optic, to a large extent, and Local, to a lesser extent, increased proline levels in response to ionic stress and not water stress. Similar conclusions have been drawn by others (Hasegawa *et al.*, 2000; Sajid *et al.*, 2007).

In this study assessment of the ionic balance of plants showed that Na^+/K^+ ratios increased in both genotypes due mainly to an increase in Na^+ levels and partly to a decrease in K^+ levels. This was a major problem for Optic above 100 mM NaCl where Na^+/K^+ ratio values increased from approximately 4 to 36 (Figure 4-9). The large increase in shoot Na^+ levels in Optic is likely to have contributed to the observed decrease (*i.e.* more negative) in tissue solute potentials, decrease in green leaf water potential, and decrease in exuded xylem sap solute potential which were used to calculate the large increase in turgor pressure (Figure 4-7c). As line Optic appears to have regained high turgor it can also be concluded that water stress caused by high salinity was not responsible for the poor growth in high salinity.

In both genotypes the ion profiles of green and desiccated leaves of salt stressed plants were similar (Figure 4-11 & 4-12) suggesting Na^+ was not re-mobilized from green to senescing tissues; it appears, therefore, that older leaves are not used as a repository for storing toxic levels of sodium. These results are inconsistent with the findings of others (Colmer *et al*., 2005; James *et al*., 2006; Greenway and Munns, 1980), who have suggested that salt tolerance arises in part from transferring excess Na^+ and Cl^- from healthy green tissues to senescing tissues.

Experiments on Na^+ content after a short 14 day exposure period showed Local and Optic accumulated similar levels of shoot Na^+ up to 50 mM NaCl. Increasing the external NaCl concentration to 100 mM did not produce a linear increase in tissue Na^+ content suggesting both genotypes operate a Na^+ exclusion mechanism over this salinity range (Tester and Davenport, 2003), but the mechanism in Local appeared to be more effective that in Optic. At 150 mM NaCl, tissue Na^+ content increased markedly in Optic but to a lesser extent in landrace Local (Figure 4-14). It seems the mechanism of salinity tolerance was beginning to breaking down above 100 mM NaCl in Local, while in Optic this occurred above 50 mM NaCl concentration. These results are consistent with those of others (Munns, 2002; Munns *et al*., 2006).

The experiments reported in Chapter 3 and above indicate there may be a genetic basis for the improved halotolerance observed in landrace Local. It is now important to identify the genes that underpin this halotolerance, and at present this will involve generating a mapping population and identifying quantitative trait loci (QTL) for salinity tolerance. Barley is an excellent system for undertaking these studies as there are over 3,000 mapping SNP markers in the barley genome. The success of such an approach, however, is wholly dependent on developing a robust phenotype (salt

tolerance/sensitivity) screen. Such a screen will require the use of isogenic parental lines with stable quantifiable phenotypes. Unfortunately, experiments reported in this Chapter on the effects of high salinity (125 to 175 mM NaCl) on the survival of Local and Optic plants suggested too much variation exists in these lines. To overcome this problem it is recommended that isogenic lines of the most halotolerant individuals from the Local population are generated along with isogenic hypersensitive lines from a suitable well characterized mapping line. One way to obtain such lines would be to generate plants from microspore (haploid) culture and screen for salt tolerance in this F_0 generation. Seeds (F_1) could then be collected from the most tolerant isogenic Local line and least tolerant isogenic mapping line and crossed to make a mapping population.

Some evidence was found that tolerance of high salinity in both barley lines might be epigenetic. Seedling from parental lines grown in high salinity were more halotolerant than seedlings from parental lines grown in low salinity. These findings suggest that during seed development on salt stressed parents, some 'imprinting' occurred which predisposed these seed to survive better high salinity during their subsequent germination and seedling development. Presumably, this 'imprinting' is related to chromatin re-modeling and DNA methylation and/or acetylation. Further experiments are required to establish the mechanisms and importance of this epigenetic response to high salinity. Similar findings have been reported by others in sorghum (Amzallag, 1999).

In conclusion, it appears that salinity affects CO_2 assimilation in barley and this may account for the effects on growth and yield reported in Chapter 3. Salinity-induced effects on the supply of CO_2 to the chloroplast (**gs** and **gm**), primary photochemical processes, and the kinetic properties of the enzymes of the C3 cycle are implicated, but it is not clear whether there is a primary site of injury. There is experimental evidence that these plants were suffering from ionic stress, not water stress, and there is a sound theoretical basis to support this. Finally, there is evidence that the improved halotolerance recorded in landrace Local has a genetic basis, but may also be partly attributable to epigenetic factors.

Chapter 5: Characterization of Thermotolerance in Barley

In hot arid regions where plants are routinely dehydrated (by drought and/or salinity) air temperatures are high (>40ºC), plants attain hydration states of 80-95%, leaf turgor pressure drops and leaf stomata gradually close to conserve water, resulting in an abrupt increase of leaf temperature. This may cause thermal damage to metabolic processes in the leaf, which undergo irreversible damage and do not recover even if re-watered. On the basis of some unpublished data from collaborators in Pakistan working on salinity and drought tolerance in barley have provided some evidence, which was suggesting that the difference in growth suppression in these barley genotypes may be directly attributable to thermal damage rather than dehydration and/or ionic imbalance *per se*. To confirm this, the following study was conducted using three barley genotypes landrace Local and line Soorab-96 'thermotolerant', and line Optic 'thermo susceptible'. The reason for classifying these genotypes as either 'thermotolerant' and 'thermo susceptible' was the ability of Local and Optic to tolerate salinity as discussed in Chapter 3 & 4, while line Soorab-96 performed better in an experiment conducted in Pakistan to cope with high leaf temperatures (T_{leaf}; data not published).

5.1 *'Incremental' Heat Stress*

In these experiments intact barley leaves from the three genotypes were exposed to different steady-state high leaf temperatures for a short itervals (*ca*. 20 minutes) and several key parameters of photosynthesis were measured.

5.1.1 Gas Exchange Measurements

To assess the effects of short-term high temperature stress on the photosynthetic competence of barley leaves, fully expanded 4th emergent leaves were sealed in the leaf chamber of an Infra Red Gas Analyzer (IRGA). Steady state (light saturated CO_2 assimilation rates at 380 μmol CO_2 .mol^{-1} air; A_{sat}) and transpiration rates (E) were recorded over a range of incrementing T_{air} and T_{leaf} (see Section 2.2.2.1 for experimental details).

5.1.1.1 Light Saturated CO_2 Assimilation Rates (A_{sat})

Figure 5-1 presents the data for steady state A_{sat} from experiments for the three barley genotypes collected by IRGAs. The responses of the three lines to short-term increases in T_{leaf} were similar. Increasing T_{leaf} from *ca.* 23 ℃ to 38 ℃ produced only a minor decrease in A_{sat}, however, beyond this range the values declined rapidly to 25-35 % of their initial values (Figure 5-1; $p<0.05$). There is some evidence that A_{sat} in the European line Optic was more sensitive to increasing T_{leaf} than the Pakistani genotypes Local and Soorab-96, but this may result from the higher initial rates measured in this line.

5.1.1.2 Transpiration Rates (E) and Stomatal Conductance (gs)

Results shown in Section 5.1.1.1 clearly indicate that there is a dramatic suppression in CO_2 assimilation rates of barley leaves caused by a brief exposure to high leaf temperatures (> 38 ℃). To establish whether this suppression could be attributed to the stomatal function, commensurate measurements of leaf transpiration rates (E) and stomatal conductance (**gs**) were obtained. Transpiration rates increased significantly with T_{leaf} particularly at temperatures in excess of 36 ℃, and the rates were always significantly higher in Optic than in the other two genotypes (Figure 5-2a).   The observed increase in E arises partly from the increase in the Vapour Pressure Deficit (VPD) that accompanies an increase in T_{leaf}, but Figure 5-2b also shows that above 36℃ all of the genotypes showed significantly increased stomatal conductance (**g_s**; $p \leq 0.05$).

5.1.1.3 Relationship of CO_2 Assimilation (A) with Stomatal Conductance (gs) under Incremental Heat Stress Events

The relationship between CO_2 assimilation with stomatal conductance showed that all three genotypes responded similarly with increasing T_{leaf} from 23 ℃ to 43 ℃, where CO_2 assimilation decreased significantly, however, on other hand increase in T_{leaf} significantly increased the stomatal conductance ($p<0.05$; Figure 5-3).
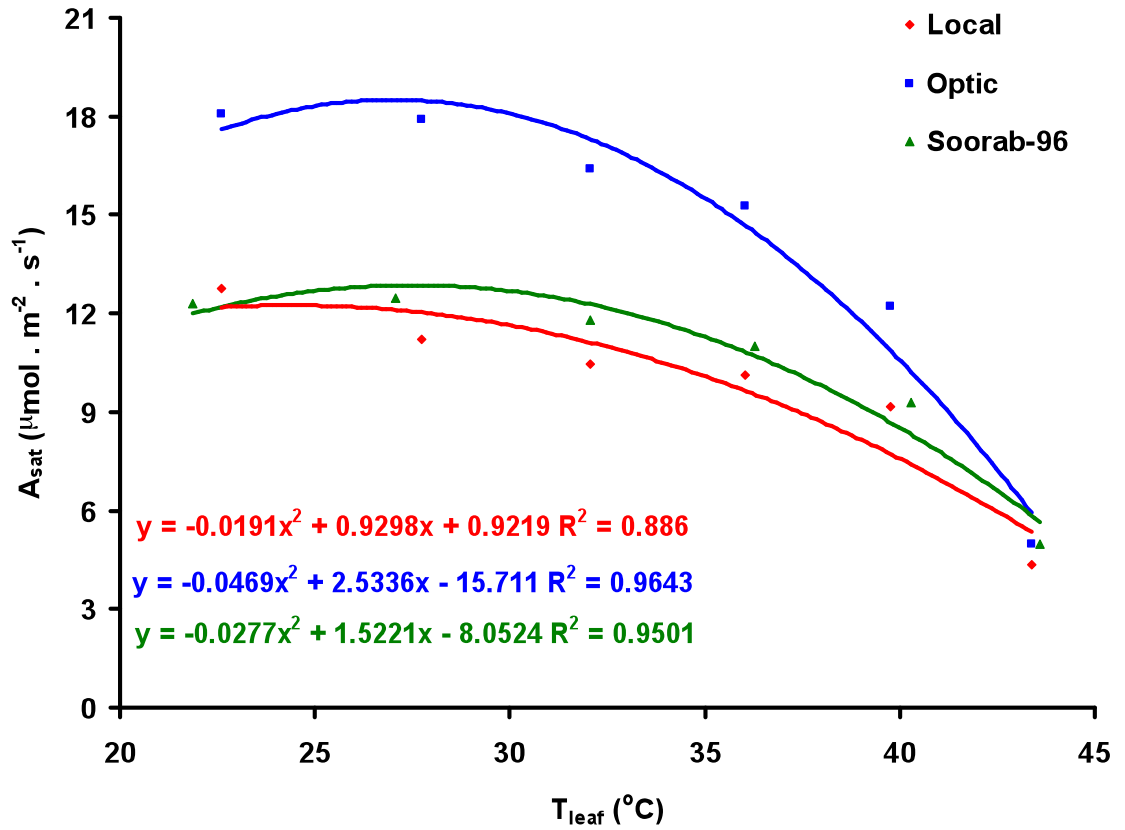
Figure 5-1: Profile of Increasing Leaf Temperature on Photosynthesis in Single Leaves of Barley Genotypes.

Attached fully emerged 4th leaves of the barley genotypes Optic, Local, and Soorab-96 were sealed in leaf chambers and light saturated CO_2 assimilation (A_{sat}), and leaf temperature (T_{leaf}) were recorded (for full details see Materials and Methods Section 2.2.2.1). The values represent the average of 5 independent leaves for each genotype.

Figure 5-2: Profile of Increasing Leaf Temperature on Transpiration Rates (E) and Stomatal Conductance (gs) in Single Leaves of Barley Genotypes.

Top Panel (a): leaf transpiration rate (E); bottom panel (b): stomatal conductance (gs). Attached fully emerged 4th leaves of the barley genotypes Local, Optic, and Soorab-96 were sealed in leaf chambers and steady state rates of transpiration (E), stomatal conductance (**gs**), and leaf temperature (T_{leaf}) were recorded (for full details see Materials and Methods Section 2.2.2.1). The values represent the average 5 independent leaves for each genotype.

$y = 0.0537x^2 - 2.9262x + 43.485 \; R^2 = 0.9893$
$y = 0.0589x^2 - 2.7961x + 39.401 \; R^2 = 0.9943$
$y = 0.05x^2 - 2.4695x + 34.198 \; R^2 = 0.9873$

$y = 0.0015x^2 - 0.0891x + 1.5019 \; R^2 = 0.9842$
$y = 0.0022x^2 - 0.1184x + 1.975 \; R^2 = 0.9312$
$y = 0.0012x^2 - 0.068x + 1.1321 \; R^2 = 0.9677$

b

Local
Optic
Soorab-96

E (mmol . m^{-2} . s^{-1})

gs (mol . m^{-2} . s^{-1})

T$_{leaf}$ (^{o}C)

143
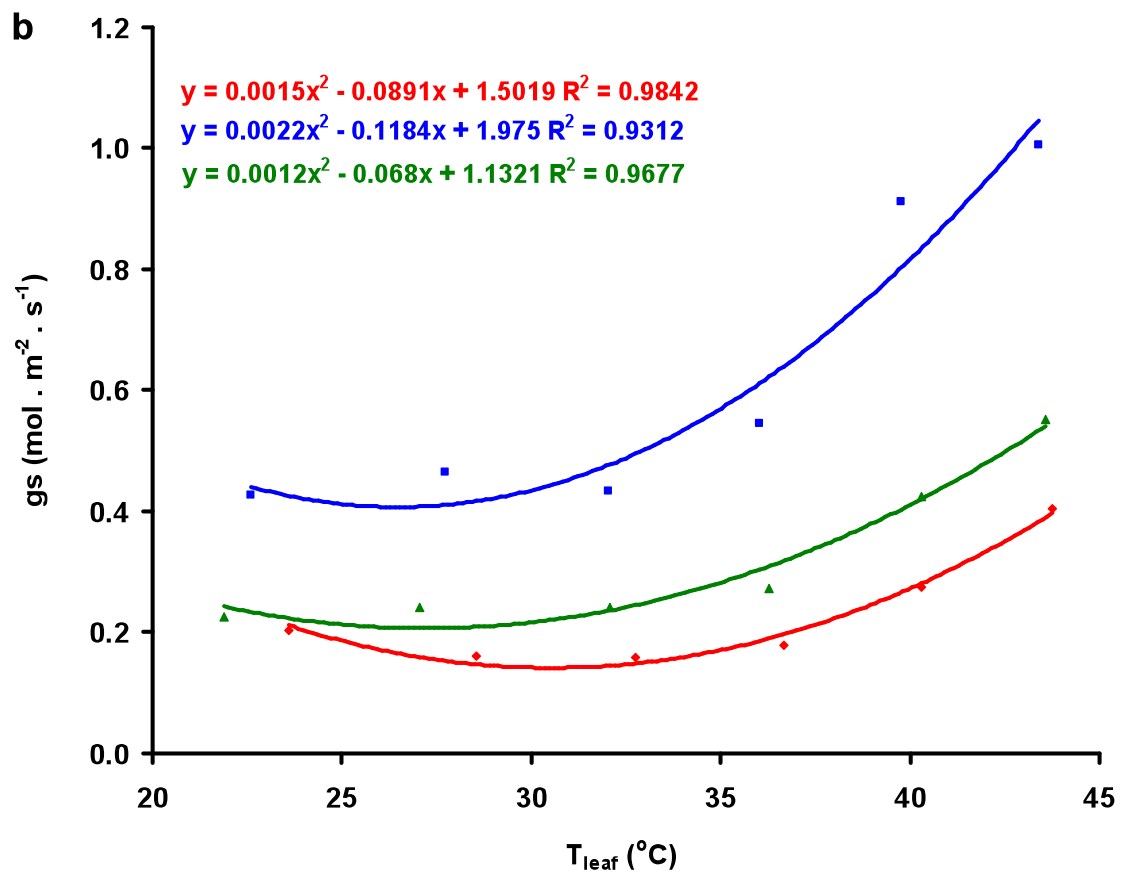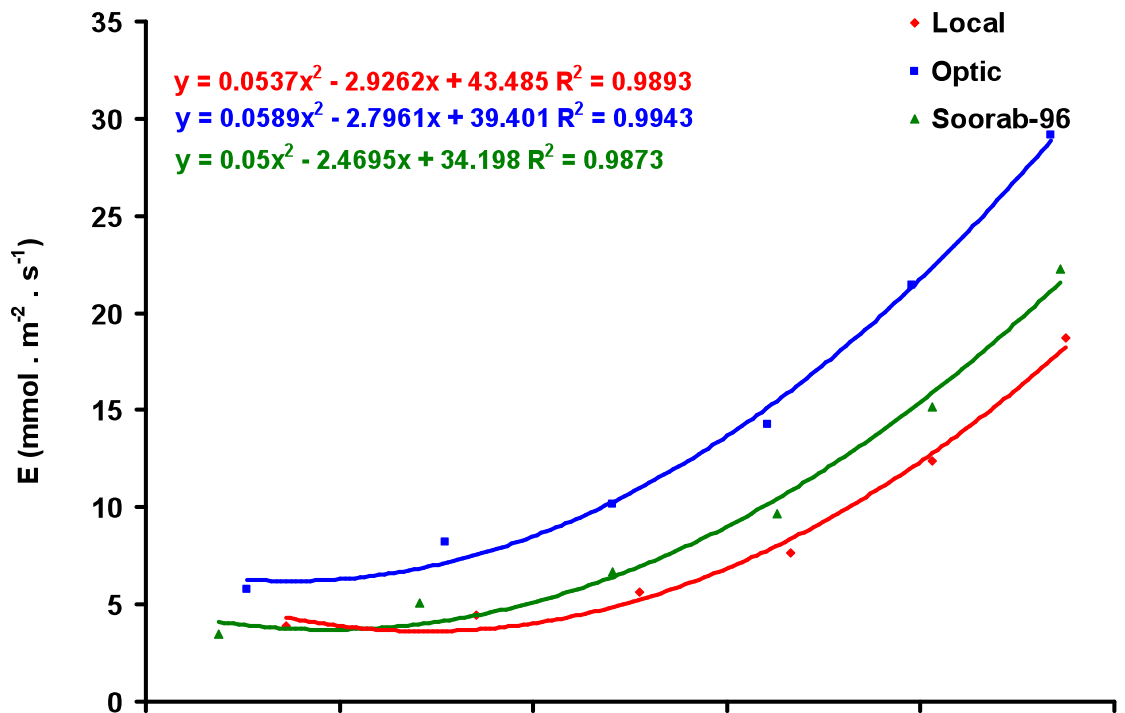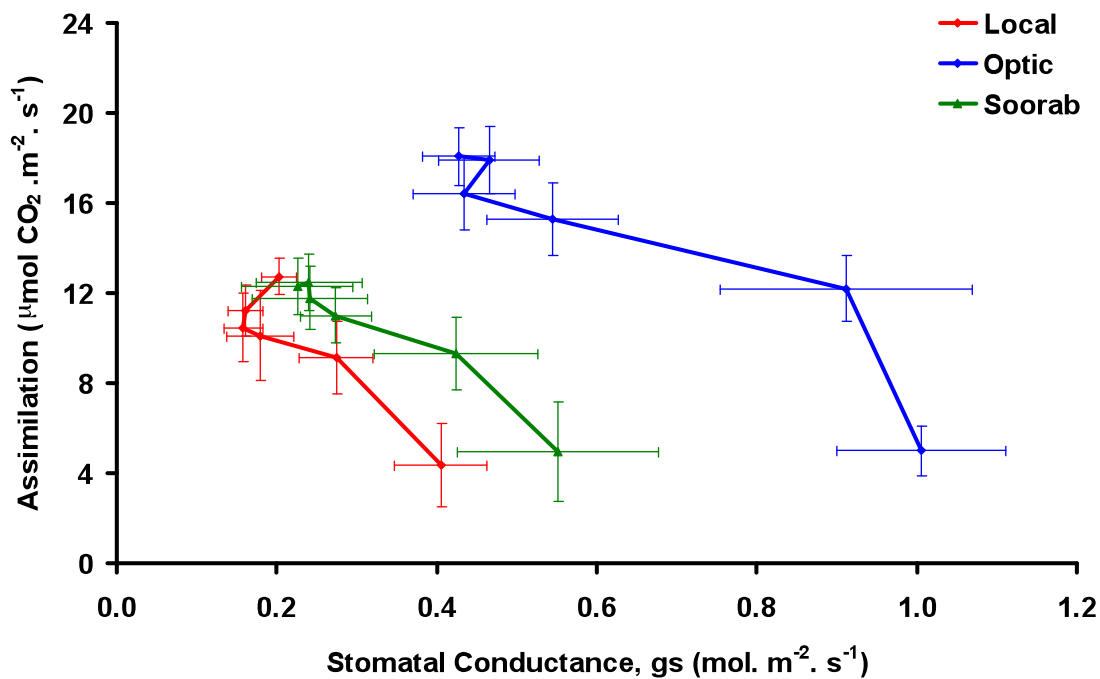
Figure 5-3: Relation of CO$_2$ Assimilation (A) with Stomatal Conductance (gs) During Incremental Heat stress Events.

CO$_2$ assimilation (A) plotted against stomatal conductance **(gs)**. The values represent the average ($\pm$ SE) for 5 replicates obtained from independent leaves of each genotype. It was difficult to fit a trend line representative of all data points.

5.1.2 Leaf Absorptance

To test whether the dramatic suppression in CO_2 assimilation rates were attributable to the efficiency of the light harvesting processes leaf absorbtance and chlorophyll fluorescence excitation spectra were measured immediately before and after heat stress (see Section 2.2.3 for experimental details).

5.1.2.1 Light Absorptance

Measurements before (T_{leaf} 25ºC) and after twenty minutes of thermal stress period (T_{leaf} 44ºC) indicated no major changes in leaf absorbtance measured using an Perkin Elmer λ800 spectro-photometer fitted with a Lab-sphere PELA-1020 Integrated Sphere (2 nm slit widths; Figure 5-4a).

5.1.2.2 Chlorophyll Fluorescence Excitation Spectra

The efficiency of light capture and exciton energy transferred from the Chl*b*-containing peripheral Light Harvesting Complexes (LHCs) to the Chl*a* containing PSII core units can be assessed from room temperature Chl*a* excitation spectra. Fluorescence emission (at 680 nm) emanates from Chl*a* in the core PSII units which are excited directly through Chl*a* absorption (from 420-445 nm), or through Chl*b* absorption in the peripheral LHCs (from 460-490 nm) and energy transfer to Chl*a* in the PSII core. The ratio of the Chl*a* fluorescence emission excited directly through Chl*a* and through Chl*b* therefore provides an estimate of the efficiency of light absorption and energy transfer from the peripheral Chl*a* / Chl*b*-containing LHCs to the Chl*a*-containing PSII units. These spectra indicate that excitation of PSII core complexes through Chl*a* and Chl*b* is similar before and after heat stress, implying the observed decline in A_{sat} is not attributable to a decrease in the rate of energization of the PSII reaction centers (Figure 5-4b).

Figure 5-4: Normalized Absorptance and Fluorescence Excitation Spectra Before and After Heat Stress in Single Leaves of Barley Genotypes.

Top Panel (a): normalized absorptance spectra; bottom panel (b): normalized Chl*a* fluorescence excitation spectra. Leaf absorptance was measured before (23 ºC) and after a 20 minute heat stress (44 ºC) period. The efficiency of light absorption and exciton delivery to PSII reaction centres was assessed from Chl*a* excitation spectra. The arrows indicate the peaks in PSII Chl*a* emission that arise from direct excitation into Chl*a* and Chl*b* (peripheral LHC complexes; see Section 2.2.3.1 for experimental details).

a

b

147
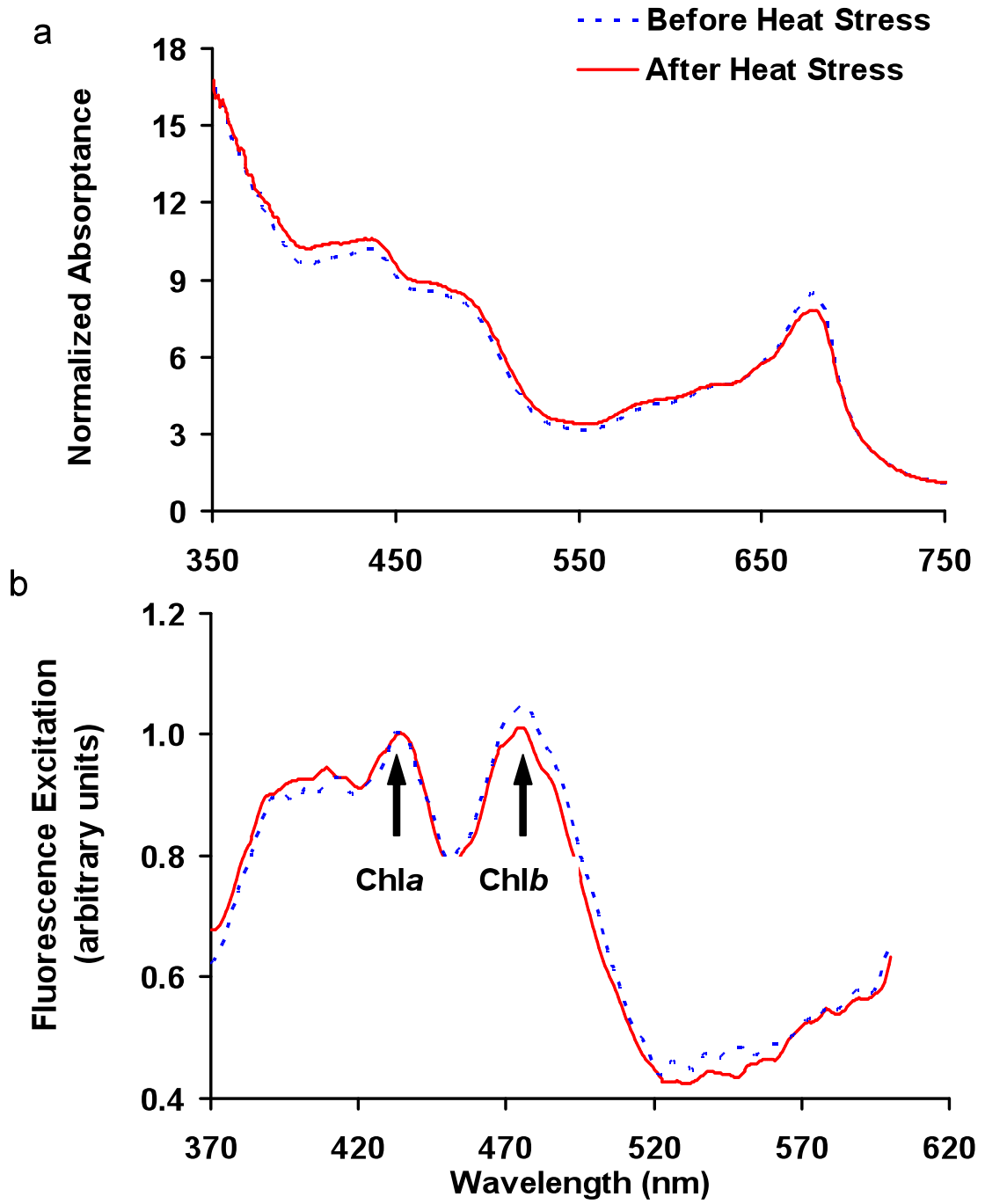
5.2 *'Temperature Jump' Heat Stress Experiments*

Further experiments were designed to mimic heat stress events that might occur in arid areas where higher air temperatures persist for at least three hours during hot peak summer days (12:00 noon to 3:00 PM). Investigations were also undertaken to establish the basis of CO_2 assimilation rate suppression, *i.e.* whether this suppression could be attributable to injury to the photosynthetic electron transport chain or to the kinetic properties of the enzymes of the kinetics of the C3 cycle. To address these questions 3 hours heat stress periods were implied. The effects of 3 hour heat stress increases in T_{leaf} were assessed for the key parameters of photosynthesis. This included carboxylation efficiency (Φ CO_2), PSII photochemistry (Φ PSII; *i.e.* Fv/Fm), whole chain of photosynthetic electron transport rates (ETRs), and metabolite pool levels of the C3 cycle.

5.2.1 Gas Exchange Measurements

5.2.1.1 Light Saturated CO_2 Assimilation Rates (A_{sat}) and   Carboxylation Efficiency (Φ CO_2)

The efficiency of the C3 cycle can be estimated from plots of CO_2 assimilation rates and external (C_a) and internal (C_i) CO_2 concentrations (A/C_a and A/C_i plots; see Material and Methods Section 2.1.3.1.1). From these plots the parameters A_{sat} (light saturated CO_2 assimilation) and the carboxylation coefficient (the efficiency of CO_2 fixation, Φ CO_2) can be estimated.

Figure 5-5a presents the results from A/C_a measurements on fully expanded 4th emergent leaves of the barley genotypes Local, Optic, and Soorab-96. With all three genotypes increasing T_{leaf} to 40.0 ($\pm$ 0.2 ºC) for 3 hours severely impaired A_{sat} to less than 15 % of their initial rates, and a similar decline was observed in Φ CO_2. To investigate this observation further, measurements of A/C_a responses were monitored on the same piece of attached leaf for up to 5 days post-heat stress to assess recovery of photosynthetic competence. Measurement of A_{sat} and Φ CO_2 showed leaves from landrace Local significantly recovered approximately 40 % of their lost capacity 5 days after stress. No significant recovery was observed in the other two lines Optic and Soorab-96 (Figure 5-5 a and b; $p<0.05$).

Before collecting data presented in figure 5-5 a & b, it was made sure that there is no significant effect of 'Temperature Jump' heat stress application's set up on the photosynthetic efficiency of barley leaves. The data presented in Figure 5-6 a & b confirmed that there was no significant differences ($p<0.05$) for CO_2 assimilation and carboxylation efficiency of barley genotypes, collected immediately before, immediately after and 5 days after, by keeping the type, age, and piece of leaves at control temperature levels i.e. T_{leaf} 25.0 ($\pm$ 0.2 ºC) for 3 hours using a modified thermal cycler, ('Temperature Jump' Heat Stress experiments, see Material and Methods Section 2.2.2.2). Data for stomatal conductance, transpiration rates, quantum efficiency, Φ PSII, NPQ ETR_{ss} and ETR_{max} showed similar trends in all three genotypes (for brevity data not presented).

5.2.1.2 Phenotypic Differences in Leaves After Heat Stress

Figure 5-7 presents images of leaves from the three barley genotypes before and 5 days after heat stress (T_{leaf} 40.0 $\pm$0.2 ºC for 3 hours). In all replicates Optic showed the greatest level of heat stress damage and Local the least, implying leaves of landrace Local posses the capacity to partially recovered from thermal damage.

Figure 5-5: Effects of Three Hours Heat Stress on Barley Leaf Function.

Top panel (a): light saturated CO_2 assimilation rates (A_{sat}); bottom panel (b): carboxylation efficiency ($\Phi\ CO_2$). Parameters were measured with IRGAs and extracted from CO_2 response curves (see Materials and Methods Section 2.1.3.1.1) at T_{leaf} 25 ºC ($\pm$ 0.5 ºC) and saturating light levels (550 µmol $.m^{-2}$ $.s^{-1}$ PAR) immediately before, immediately after, and then 5 days after subjecting a marked region of an attached barley leaf to heat stress. Heat stress was imposed by increasing T_{leaf} to 40.0 ºC ($\pm$ 0.2 ºC) for three hours using a modified thermal cycler (see Materials and Methods Section 2.2.2.2). The presented values are the averages and standard errors of 5 replicates. ANOVA tests were performed by using a General Linear Model. Tables for ANOVA and grouping information along with Figures for residual and interaction plots are presented in Appendix (Figures A 5-1 & A 5-2).

a

T_{leaf} 40 °C for 3 Hours

■ **Local**
■ **Optic**
■ **Soorab**

LSD 0.05

A_{sat} (μ mol CO_2. m^{-2}. s^{-1})

20
15
10
5
0

b

LSD 0.05

Φ CO_2 (mol CO_2. m^{-2}. s^{-1})

0.08
0.06
0.04
0.02
0.00

Before   **Immediately After**   **5 Days Recovery**

151
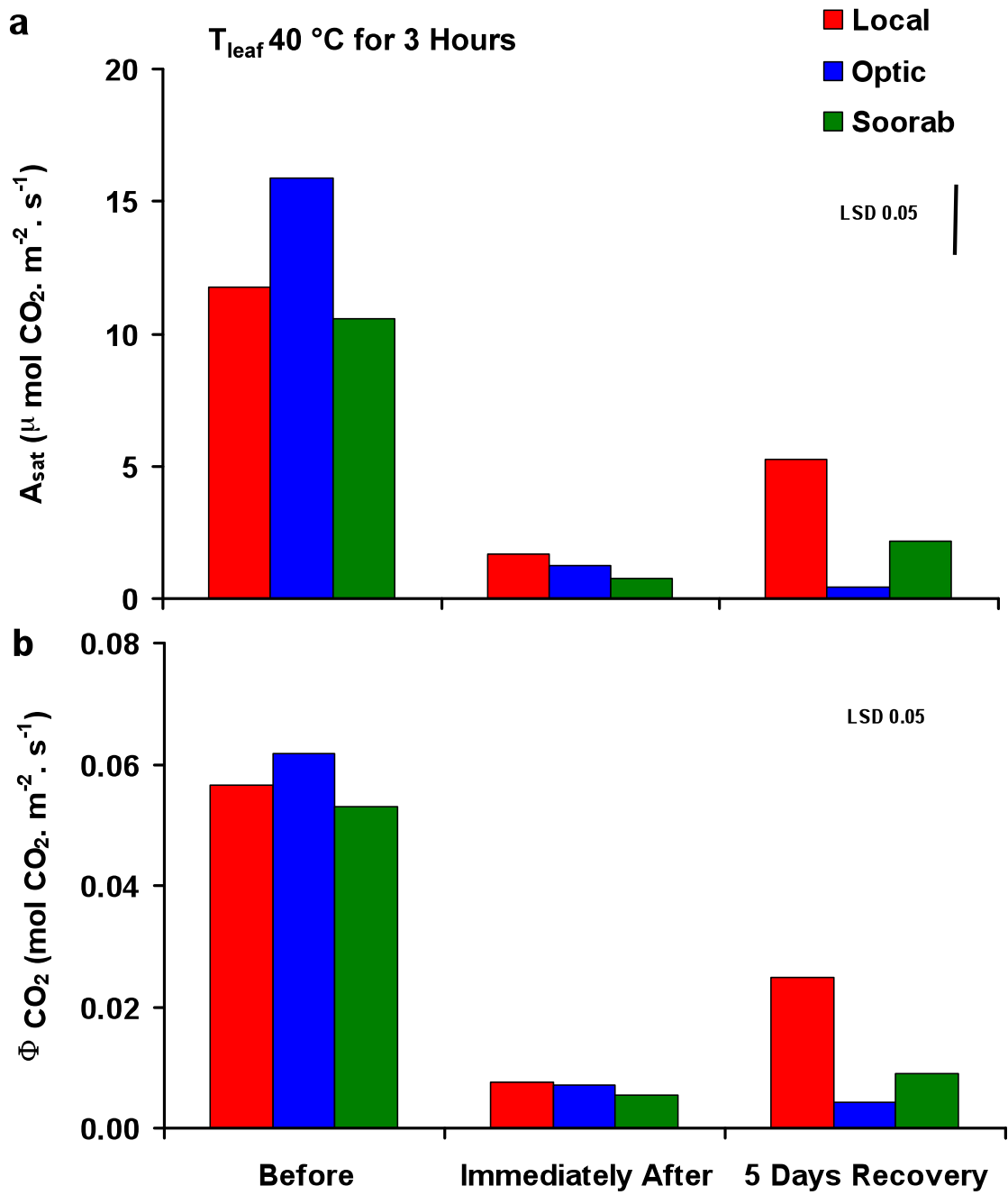
Figure 5-6: Effects of Three Hours Control Leaf Temperatures on Barley Leaf Function.

Top panel (a): light saturated CO_2 assimilation rates (A_{sat}); bottom panel (b): carboxylation efficiency ($\Phi\ CO_2$). Parameters were measured with IRGAs and extracted from CO_2 response curves (see Materials and Methods Section 2.1.3.1.1) at T_{leaf} 25 °C ($\pm$ 0.5 °C) and saturating light levels (550 µmol $.m^{-2}\ .s^{-1}$ PAR) immediately before, immediately after, and then 5 days after subjecting a marked region of an attached barley leaf to heat stress (see Materials and Methods Section 2.2.2.2). The presented values are the averages and standard errors of 5 replicates. ANOVA tests were performed by using a General Linear Model. Tables for ANOVA and grouping information along with Figures for residual and interaction plots are presented in Appendix (Figures A 5-3 & A 5-4).

a T_{leaf} 25 °C for 3 Hours

Legend:
- Local (red)
- Optic (blue)
- Soorab (green)

y-axis: A_{sat} (μ mol CO_2. m^{-2}. s^{-1})

LSD 0.05

b

y-axis: Φ CO_2 (mol CO_2. m^{-2}. s^{-1})

LSD 0.05

x-axis: Before   Immediately After   5 Days Recovery

153
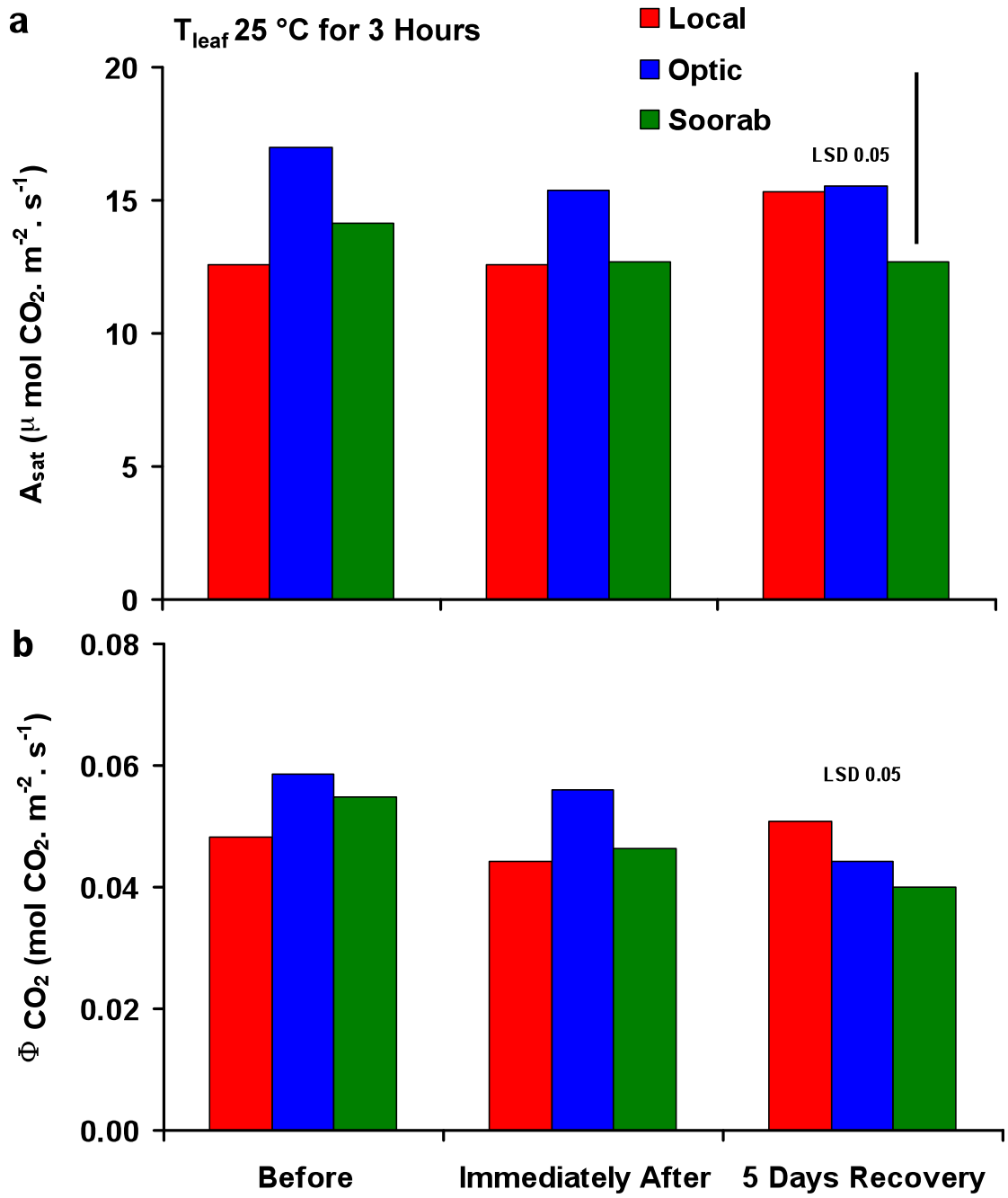
Figure: 5-7: Images of Leaves from Three Barley Genotypes, Before and 5 Days After Heat Stress Recovery.

The paired images were taken from the fully expanded 4th emergent leaf approximately 80 mm from the base of the leaf blade immediately before (control) and 5 days after elevating T_{leaf} to 40.0 ºC (± 0.2 ºC) for three hours using a modified thermal cycler (see Materials & Methods Section 2.2.2.2). After heat stress, plants were returned to the growth room (25 ºC) to recover. In all cases leaves from line Optic showed far more extensive damage subjecting to heat stress after 5 days than landrace Local (n = 5).

5.2.1.3 Transpiration (E) and stomatal Conductance (gs)

To confirm that the suppression in A_{sat} arising from a 3-hour heat stress period was not attributable to stomatal function, parallel measurements of E and **gs** were also made on the plants used in the experiments described in Section 5.2.1.1. Data shown in Figures 5-8 a & b were collected from CO_2 response curves (see Material and Methods Section 2.1.3.1.1) and showed no differences before or immediately after heat stress for stomatal conductance (**gs**) and transpiration rates (E) in all three genotypes.
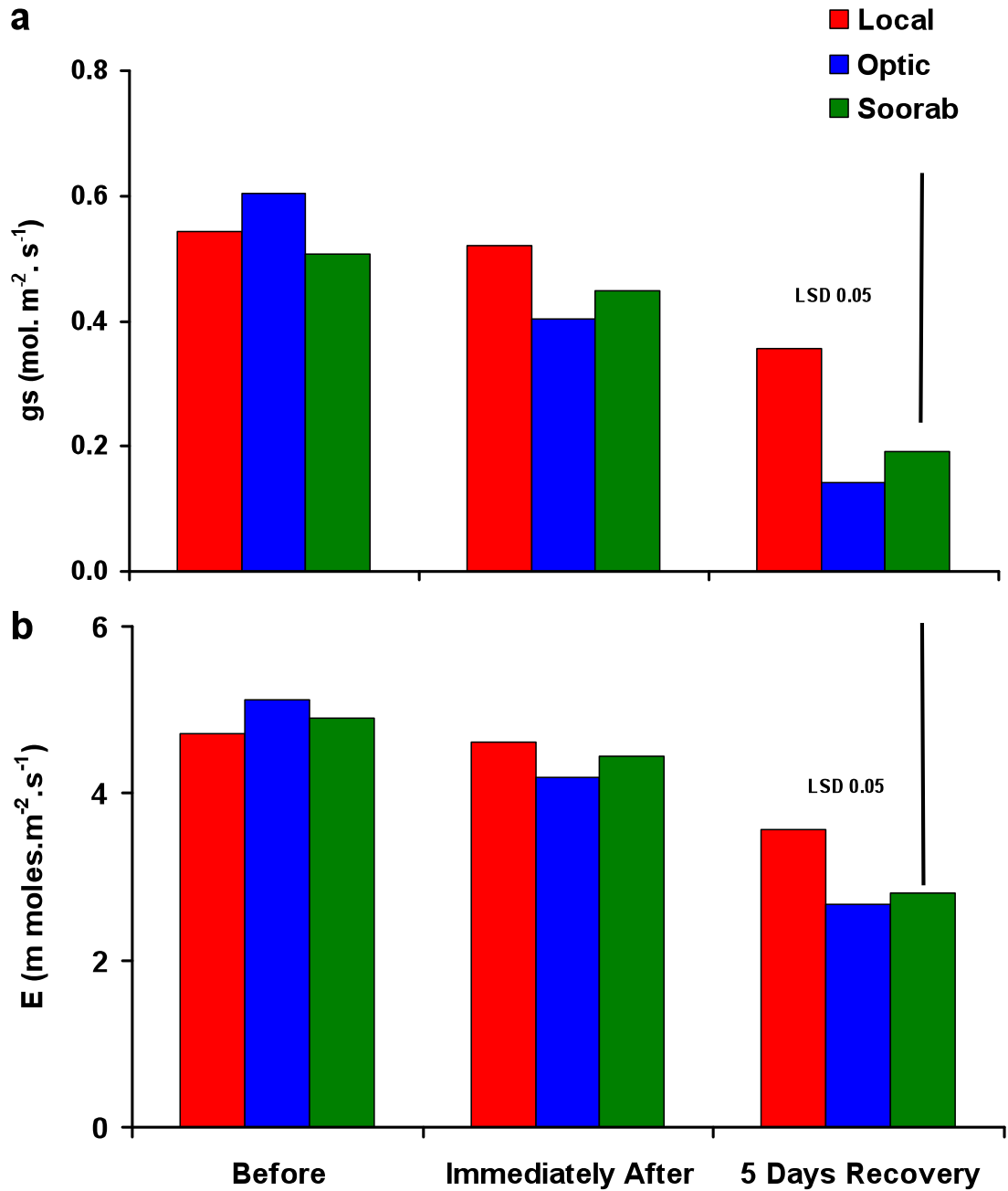
Figure 5-8: Effects of Three Hours Heat Stress on Stomatal Conductance and Transpiration Rates of Barley Leaves.

Top panel (a): stomatal conductance (**gs**); bottom panel (b): transpiration (E). Stomatal conductance and transpiration rates were measured immediately before, immediately after, and 5 days after subjecting an attached leaf to heat stress (see Materials and Methods Section 2.2.2.2). The presented values are the averages and standard errors of 5 replicates. ANOVA tests were performed by using a General Linear Model. Tables for ANOVA and grouping information along with Figures for residual and interaction plots are presented in Appendix (Figures A 5-5& A 5-6).

5.2.1.4 Relationship of CO$_2$ Assimilation (A) And Apparent Photorespiration with Stomatal Conductance (gs) under Temperature Jump Heat Stress Events

The relationship between CO$_2$ assimilation and apparent photorespiration in barley genotypes before, immediately after, and five days after heat stress showed a very similar pattern with stomatal conductance. Both these values for parameters collected immediately after heat stress declined significantly (*c.f.* before) without any significant change in stomatal conductance. After five days, however, stomatal conductance also declined significantly in Optic and Soorab with a similar type of decline observed in CO$_2$ assimilation and apparent photorespiration of these genotypes (*c.f.* before), landrace Local showed a least decline in gs and significant recovery in A$_{sat}$ after 5 days ($p<0.05$; Figure 5-9 a & b).
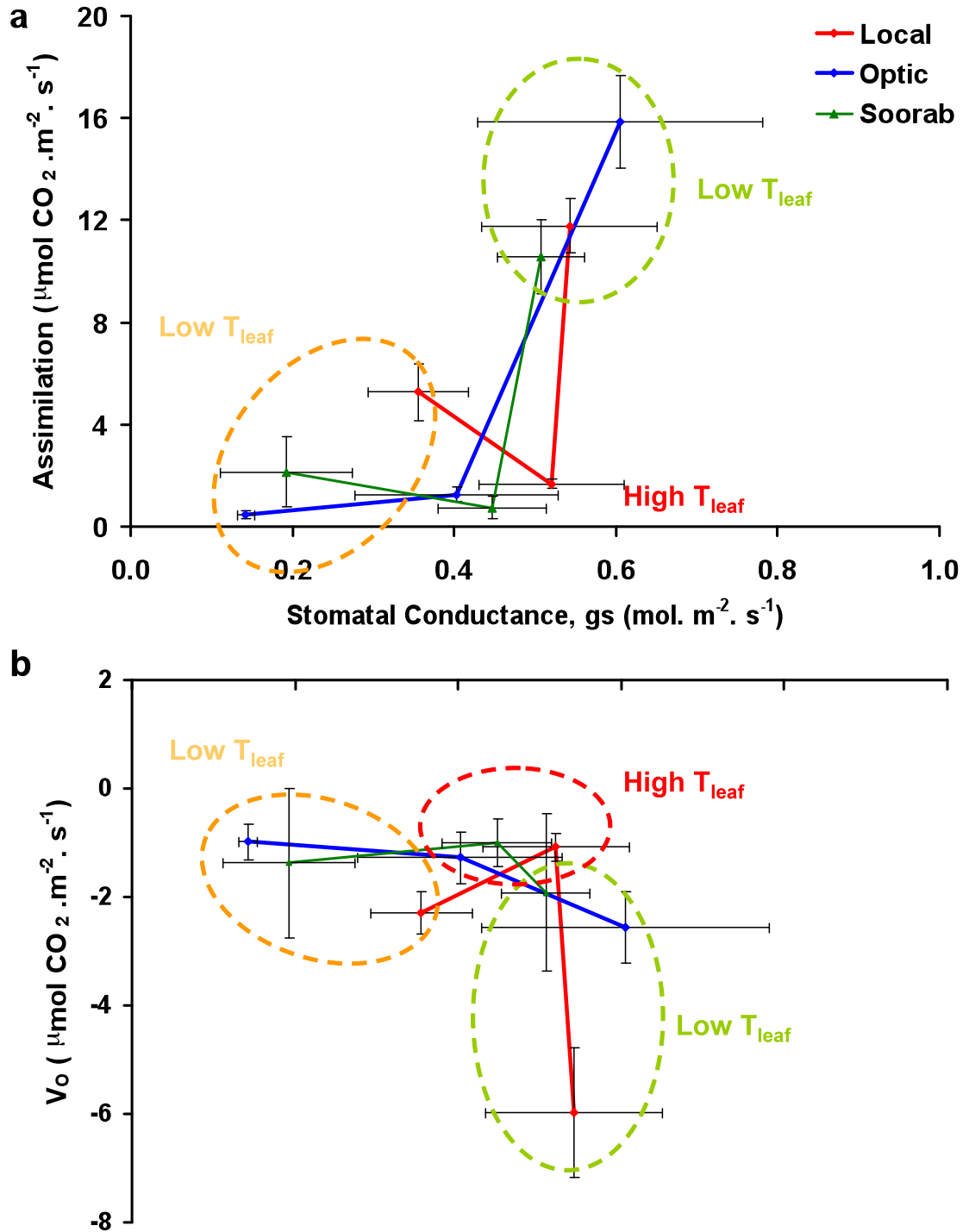
Figure 5-9: CO₂ Assimilation and Photorespiration *Versus* Stomatal Conductance of Barley Leaves.

Top panel (a): (A *vs.* **gs**); bottom panel (b): (V$_o$ *vs.* **gs**) (E). CO₂ assimilation, photorespiration and stomatal conductance were measured at T$_{leaf}$ 23°C (± 0.5 °C) and saturating light levels (550 µmol .m^{-2} .s^{-1} PAR) immediately before, immediately after, and 5 days after subjecting an attached leaf to heat stress. The presented values are the averages and standard errors of 5 replicates. Fitting a Trend line was difficult due to variation in data points.

5.2.1.5 Effects of Temperature Jump Heat Stress on the Ratio of Stomatal Conductance Before, Immediately After and 5 Days after

To see the differences in stomatal behavior of three barley genotypes the ratio of **gs** were calculated by immediately after compared with values of before and 5days after compared with before. It is clear from data that the ratio of immediately after over before is showing no significant differences for all genotypes, however, ratio of 5days after over before was significantly suppressed in Optic and Soorab-96, but not in Local ($p<0.05$; Figure 5-10a).

5.2.1.6 Stomatal Densities in Leaves of Local and Optic

Throughout the gas exchange experiments line Optic often showed higher rates of stomatal conductance and transpiration rates than the other two lines. To investigate this stomatal densities from upper and lower leaf surfaces of landrace Local and line Optic were calculated. Numbers of stomata per unit area were counted under a light microscope at 100x magnification. Line Optic showed a significantly higher number (45 %) of stomata per unit area than Local on both surfaces (Figure 5-10b; $p<0.05$), confirming that there is a positive correlation between stomatal density vs. stomatal conductance and CO_2 assimilation. But the gas exchange measurements will not affected by the observed differences in stomatal densities, as these data is direct measurements of water vapour and CO_2 gas through IRGA not on the basis of estimation.
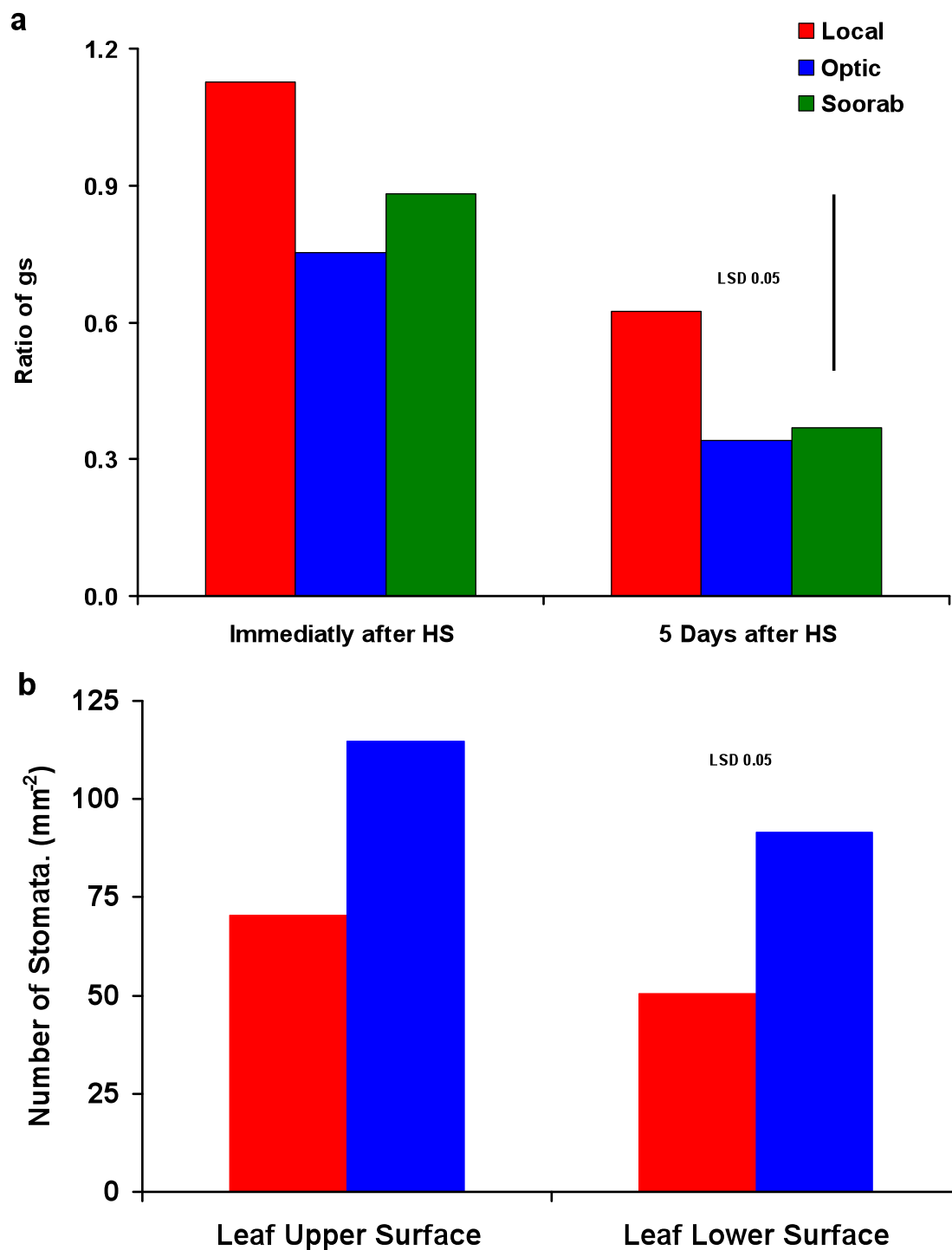
Figure 5-10: Ratio of (gs) and Stomatal Densities of Barley Leaves.

Top panel (a): Ratio of stomatal conductance (gs) before (numerator), immediately after (denominator) and five days After Heat Stress (denominator); bottom panel (b): Stomatal densities were calculated by dividing total number of stomata per unit area observed under a light microscope at 100x magnification. ANOVA tests were performed by using a General Linear Model.

5.2.2 Fluorescence Measurements

Measurements of A_{sat} and Φ CO_2 provide evidence that heat stress rapidly suppresses photosynthesis, but they did not indicate which photosynthetic processes are affected. For example, a decline in the steady state rates of A_{sat} and Φ CO_2 could arise from thermal impairment of the light harvesting capacity of a leaf, primary photochemical events in the reaction centers of PSI and PSII, steady state photosynthetic Electron Transport Rates (ETR_{ss}), the capacity of the light reactions to generate ATP and NADPH, the kinetic properties of enzymes of the C3 cycle, or the concentration of CO_2 in the chloroplast (the site of RuBisCO; see Figure 5-11)

In Sections 5.1.2 and 5.1.1.2 it was shown that A_{sat} and Φ CO_2 were suppressed by 20 minutes exposure to T_{leaf} of > 40 ºC, and this was not attributable to changes in the light harvesting capacity or **gs** of leaves. To investigate whether the suppression in A_{sat} and Φ CO_2 could be attributable to primary photochemical events or photosynthetic electron transport, pulse modulated chlorophyll fluorescence techniques were used (Baker, 2008).

5.2.2.1 Quantum Efficiency (Fv/Fm) and Non Photochemical Quenching (NPQ)

The effects of 3 hours heat stress events on PSII photochemistry and Non Photochemical Quenching (NPQ) were assessed using saturating light pulses and modulated fluorescence techniques. Raising T_{leaf} produced a significant ($p<0.05$) but relatively modest approximately 40 to 50% suppression of the maximum quantum efficiency of PSII (Φ_{PSII}; *i.e.* Fv/Fm of fully dark adapted leaves), and a 40 to 60 % suppression in the Non- Photochemical Quenching parameter (Figure 5-12 a and b, respectively). No major differences among the lines were observed in the initial responses of leaves to heat stress.
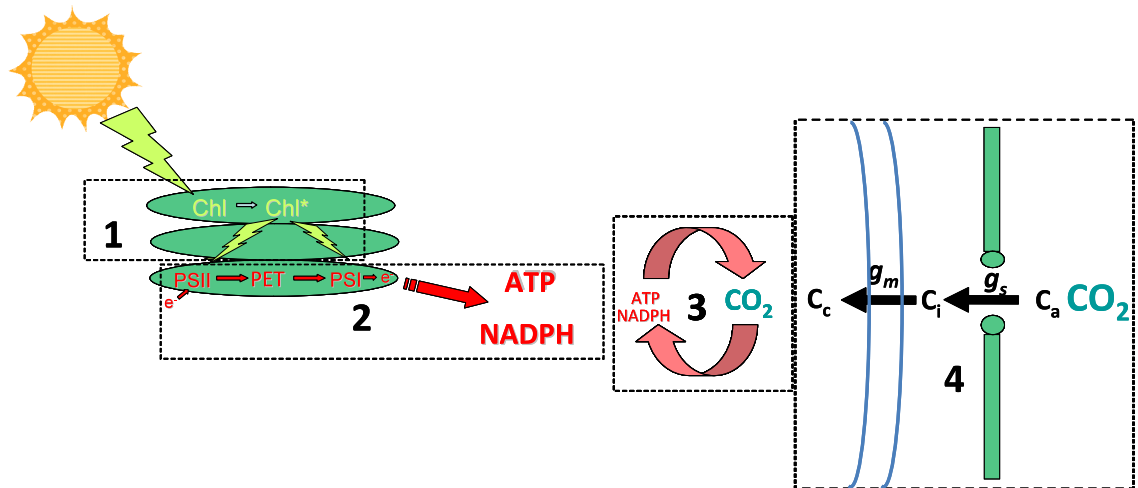
Limitation of Carbon Assimilation Rates

1. Light Harvesting Capacity
2. Photosynthetic Electron Transport / Chemiosmosis
3. C3 Cycle Kinetics
4. CO_2 Supply / g_s / g_m

Figure 5-11: Schematic Diagram of the Processes Affecting Leaf CO_2 Assimilation Rates.

CO_2 assimilation rates can be impaired by injury to any of the four phases shown above. (1), capture and delivery of excitation energy by the Light Harvesting Complexes (LHCs) to the Reaction Centers (RCs); (2), primary photochemistry in PSI and PSII and photosynthetic Electron Transport Rates (ETRs); (3), the kinetic properties of the enzymes of the C3 cycle: (4), the delivery of CO_2 from the air to the chloroplast stroma. This is controlled by the CO_2 concentration gradient for CO_2 diffusion from the air to the intracellular leaf space (C_a-C_i) and the stomatal conductance (**gs**) and by the CO_2 diffusion gradient from the intracellular leaf space to the chloroplast ($C_i - C_c$) and the mesophyll conductance **gm**.

Figure 5-12: Effects of Three Hours Heat Stress on Barley Leaf (PS-II) Photochemistry.

Top panel (a): quantum efficiency (Φ PSII); bottom panel (b): Non Photochemical Quenching (NPQ). Φ PSII and NPQ of dark adapted barley leaves were measured by pulse amplitude modulated fluorescence (see Materials and Methods Section 2.2.3.2) at T_{leaf} 25 ºC ($\pm$ 0.5 ºC) immediately before, immediately after, and then 5 days after subjecting a marked region of an attached barley leaf to heat stress (see Materials & Methods Section 2.2.2.2). The presented values are the averages and standard errors of 5 replicates. ANOVA tests were performed by using a General Linear Model. Tables for ANOVA and grouping information along with Figures for residual and interaction plots are presented in Appendix (Figures A 5-7 & A 5-8).

a

b
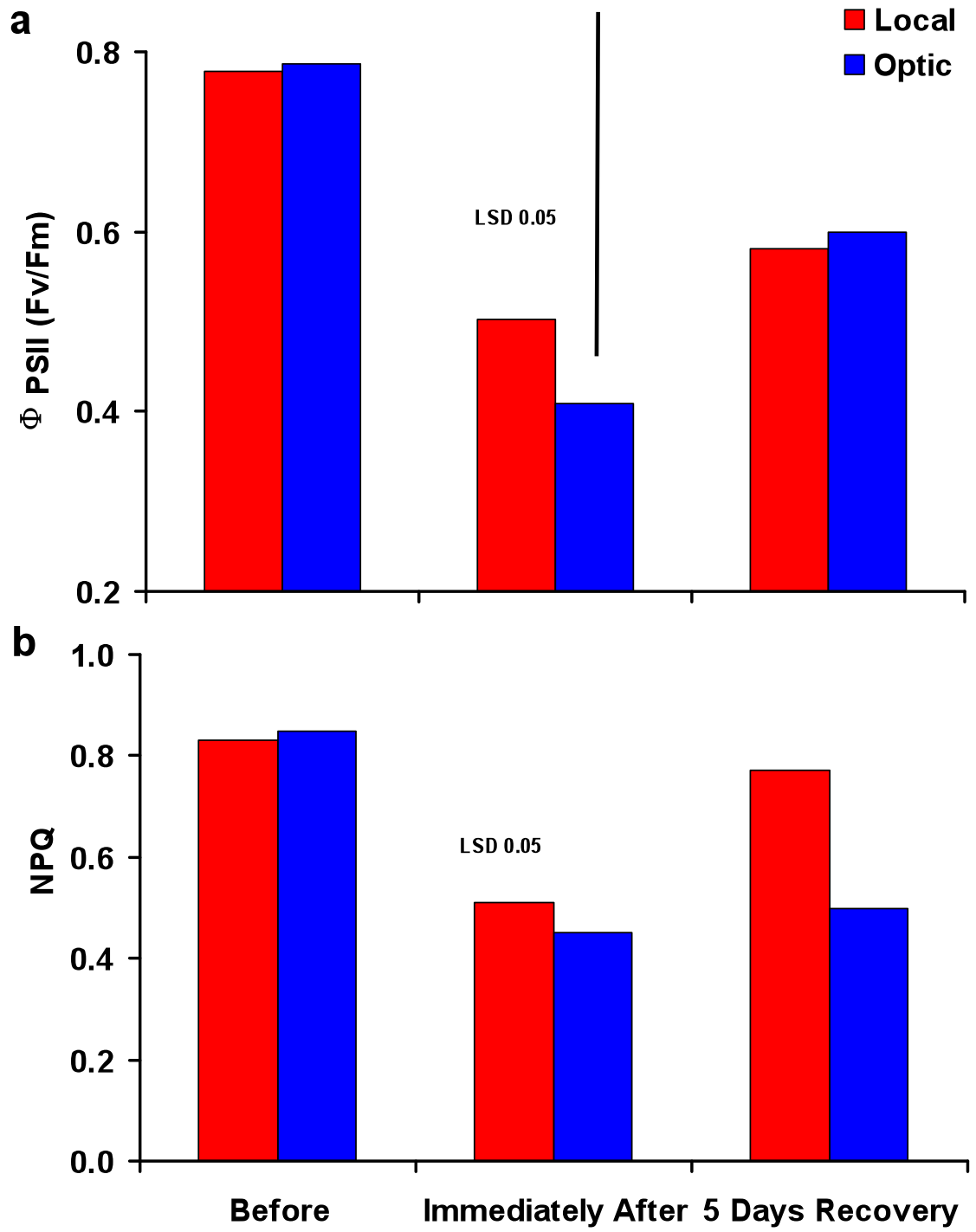
5.2.2.2 Steady State and Maximum Electron Transport Rates

To observe the thermal stress effects on photosynthetic electron transport data for maximum (ETR_{max}) and steady state (ETR_{ss}) electron transport rates were collected using a WALZ MINI-PAM fluorimeter fitted with a 2030-B Leaf Clip and an external actinic light (550 μmol m^{-2} .s^{-1} delivered by a 50W quartz halogen bulb). Data shown in Figure 5-13 a & b indicates that increasing T_{leaf} severely impaired steady state ETR and maximal ETR in Optic and Local to approximately 20-30 % of their pre-stressed values. This suppression, however, is not as severe as it was for A_{sat} and the Φ CO_2 of the C3 cycle (approximately 15; Figure 5-10).   In landrace Local both ETR_{ss} and ETR_{max} appear to show a approximately 40 % recovery after five days but no clear recovery was observed in line Optic ($p<0.05$).

Figure 5-13: Effects of Three Hours Heat Stress on Barley Leaf Photosynthetic Electron Transport Rates.

Steady state and maximum electron transport rates of fully dark adapted barley leaves were collected by a pulse amplitude modulated fluorescence (see Materials and Methods Section 2.2.3.2) at T_{leaf} 25 ºC (± 0.5 ºC) immediately before, immediately after, and then 5 days after subjecting a marked region of an attached barley leaf to heat stress (see Materials and Methods Section 2.2.2.2). The presented values are the averages and standard errors of 5 replicates. ANOVA tests were performed by using a General Linear Model. Tables for ANOVA and grouping information along with Figures for residual and interaction plots are presented in Appendix (Figures A 5-9 & A 5-10).
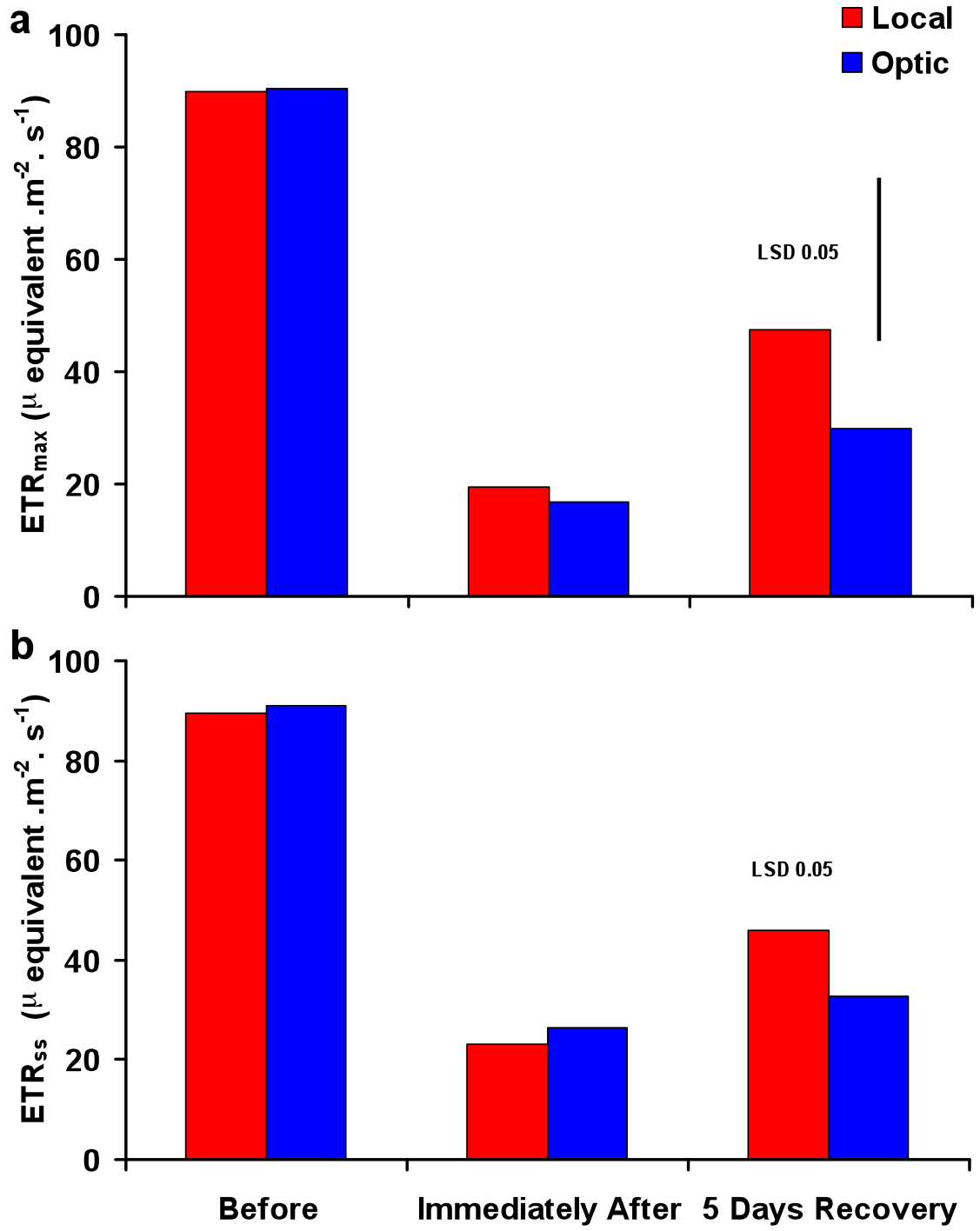
5.2.3 C3 Cycle Metabolites

Data for ETR_{max} showed a suppression of approximately 75 % in photosynthetic electron transport after heat stress compared with a >85 % suppression in CO_2 assimilation rates, confirming that the observed dramatic suppression could not be attributable entirely on the suppression of photosynthetic electron transport rates.

On the basis of these observations further investigations were carried out to pinpoint the exact site of primary thermal damage. In this regard C3 cycle metabolites were isolated and quantified using reverse-phase liquid chromatography linked to triple mass spectrometry (Arrivault *et al.*, 2009; see Material and Methods Section 2.2.5). Just before freezing in liquid nitrogen electron transport rates (ETR) were measured in each leaf sample from the centre of the marked region using pulse amplitude modulated fluorescence (see Materials and Methods Section 2.2.5.1). These measurements confirmed electron transport rates (ETR) were high in control leaves (*ca.* 95 μ equivalent $.m^{-2} .s^{-1}$) and declined to (*ca.* 24 μ equivalent $.m^{-2} .s^{-1}$) after thermal stress (data not shown).

The results of the metabolite profiling are given in Table 5-1, and are summarized in the diagrams of the metabolic pathways in Figure 5-14. Metabolite levels were quantified by comparison with authentic standards, and were corrected for ion suppression when internal standards were available (Arrivault *et al.*, 2009).

5.2.3.1 Effect of Heat Stress on Metabolite Pool Levels of Cytosol, Mitochondria and Plastid

Figure 5-14a shows a cartoon summary of the compartmentation of metabolite pathways in green leaves and Fig 5-14b the effects of heat stress on key metabolite levels involved in the C3 cycle; these are mostly found in plastids (Arrivault *et al.*, 2009). Metabolites with known location are marked (Stitt *et al.*, 1980, 1982; Gerhardt *et al.*, 1987).

Considering the all metabolite pools of C3 cycle, starch and sucrose synthesis pathways, heat stress caused some significant changes in control and heat stressed leaf samples of the two barley genotypes Local and Optic. The metabolite pools of ADP, $NADP^+$, and AMP showed a significant increase of approximately 50 to 80 % (Table-5-1: Fig 5-14a; $p<0.05$) in their pool levels after heat stress. The reduced forms of NADPH and NADH were not assayed, but the trends shown by $NADP^+$ after heat stress treatment makes it

168

likely that there has been significant increase in net synthesis of both co-factors as well. Amino acids pool levels increased approximately 50 %. R5P, X5P, Ru5P, NAD, and DHAP pools levels were not changed in the control and heat stressed samples (Table-5-1: Fig 5-14a & 5-14b; $p<0.05$). However, 3PGA, S7P, F6P, G1P, G6P, and Glucose pools decreased significantly approximately 50 % to 85% (Table-5-1: Fig 5-14b; $p<0.05$); all the pools mentioned above are believed to prevail in plastids (Taiz and Zeiger, 2003). Furthermore, ADPG and starch pool levels in plastids, and UPDG and sucrose in cytosol were found to remain unchanged. Some metabolites reported to be found mostly in mitochondrion such as, succinate (which is involved in amino acid synthesis pathways) were found to increase, whereas others such as fumarate, citrate, isocitrate, and malate remain unchanged. Only the levels of 2-oxoglutarate, which acts as the carbon acceptor for inorganic nitrogen assimilation, were decreased significantly from 50 to 60 % after heat stress (Table 5-1; Figure 5-14a; $p<0.05$).

Table 5-1: Metabolites in the Leaves of Local and Optic Barley Genotypes Before and Immediately after Heat Stress of 40.0 ±0.2 ºC for 3 hours (mean ± SE n=5).

Amount (nmol .g^{-1} F Wt), * (μmol .g^{-1} F Wt)				
Metabolite	**Local Control**	**Local Stressed**	**Optic Control**	**Optic Stressed**
Aconitate	34.2 ± 4.6	35.1± 5.6	28.8 ± 5.4	18.8 ± 5.4
ADP	0.9 ± 0.5	4.3*± 1.1	2.8 ± 1.1	8.5*± 1.5
AMP	3.1 ± 0.4	6.4*± 3.2	7.4 ± 2.8	6.1 ± 2.1
ADPG	2.6 ± 0.5	0.4*± 0.2	1.5 ± 0.2	0.3*± 0.2
Amino acids*	8.1 ± 0.3	19.6*± 1.1	10.9 ± 1.1	19.9*± 2.9
Aspartate	0.4 ± 0.01	1.5*± 0.1	0.8 ± 0.1	1.7*± 0.4
Citrate*	4.3 ± 0.9	5.8 ± 0.9	8.6 ± 0.2	7.2 ± 1.3
DHAP	21.2 ± 2.6	5.5*± 1.3	29.9 ± 2.8	13.9*± 4.9
F6P	173.2 ±18.7	34.9*± 6.3	202.2 ± 10.8	77.4*± 30.6
Fructose*	1.7 ± 0.6	0.8*± 0.1	1.8 ± 0.3	1.5*± 0.4
Fummarate*	165.5 ±23.1	124.8 ± 13.5	155.0 ± 10.1	181.3 ± 28.3
G1P	33.9 ± 2.6	17.9*± 3.0	36.0 ± 1.5	40.6*± 8.8
G6P	143 ±11.0	45.5*± 9.2	149.6 ± 6.9	72.8*± 18.7
Glucose*	2.7 ± 0.8	1.1*± 0.1	1.6 ± 0.3	1.6 ± 0.4
Glutamate*	4± 0.4	3.5 ± 0.3	4.7 ± 0.2	3.6 ± 0.3
Glycerate*	1.2 ±0.2	0.1*± 0.01	1.4 ± 0.3	0.4*± 0.02
Isocitrate*	2.3 ± 0.3	1.5 ± 0.1	1.9 ± 0.2	1.9 ± 0.2
Malate*	36.0 ± 6.4	23.0 ± 2.8	32.2 ± 3.5	39.7 ± 5.9
NAD	11.1 ± 1.6	23.0*± 1.3	9.8 ± 1.6	25.7*± 3.7
NADP	0.9 ± 0.2	1.9*± 0.3	1.1 ± 0.3	1.4 ± 0.2
2-OG	207.6 ±34.8	85.3*±23.4	166.2 ± 27.3	68.8*± 30.5
3 PGA	294.7 ±33.03	37.7*±6.62	389.0 ± 28.3	64.7*± 12.6
R5P	2.3 ± 0.3	1.4 ± 0.3	2.6 ± 0.2	1.7 ± 0.4
S7P	98.0* ±16.7	13.2*± 4.2	145.6*± 10.4	35.6*± 23.4
Succinate	101.8 ±14.7	344.7*±58.3	133.3 ± 10.8	235.3*± 40.4
Sucrose*	14.5 ± 4.2	8.6*± 1.1	15.6 ± 1.3	16.3 ± 1.7
Starch*	1.4 ± 0.4	0.3*± 0.1	3.7 ± 1.2	6.1*± 1.4
UDPG	24.4 ± 1.9	24.9 ± 3.1	24.8 ± 0.6	32.1 ± 4.1
X5P+Ru5P	198.4 ±25.6	118.1 ± 34.7	316.1 ± 33.9	255.6 ± 53.9

Metabolites were measured by 2D Liquid Chromatography-triple Mass Spectrometry (2D-LC/MS^3), except fructose, glucose, sucrose, and starch, which were measured by enzymatic essay. Values in cells filled with ▬ and asterisked show a significant decrease after heat stress and values in cells filled with ▬ and asterisked show a significant increase after heat stress. The presented values are the averages and standard errors of 5 replicates. ANOVA tests were performed by using a General Linear Model. Tables for ANOVA and grouping information along with Figures for residual and interaction plots are presented in Appendix (Figures A 5-11 to 5-17).

Figure 5-14: of Thermal Induced Changes in Barley Leaf Metabolite Pools.

Top panel (a): trend of metabolite pool levels in cytosol, mitochondrion, and plastids after heat stress; bottom panel (b): trend of metabolite pool levels found in plastids after heat stress. Metabolites were measured by (2D-LC/MS^3), except fructose, glucose, sucrose, and starch, which were measured by enzymatic essay. Differences between the values observed before and after heat stress are shown as ⬇ ,significantly decreased; ⬆ , significantly increased; ⬌ , no significant change.
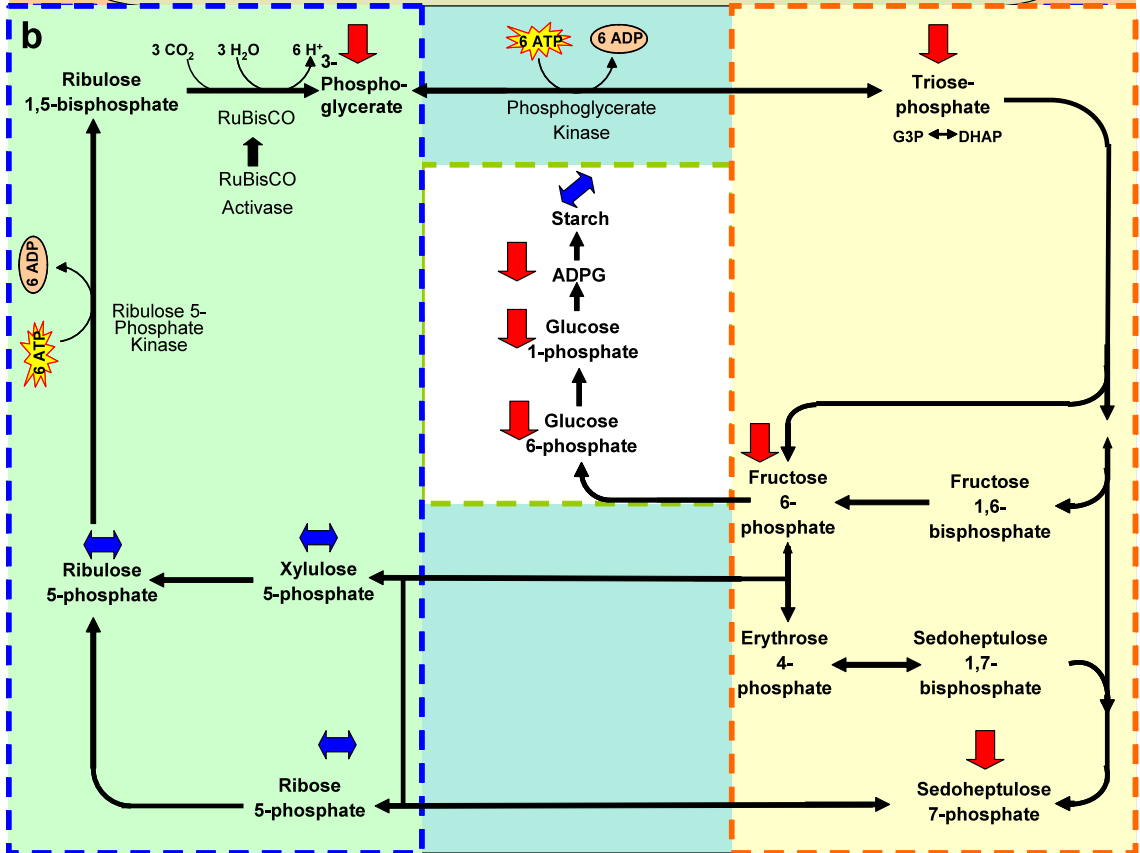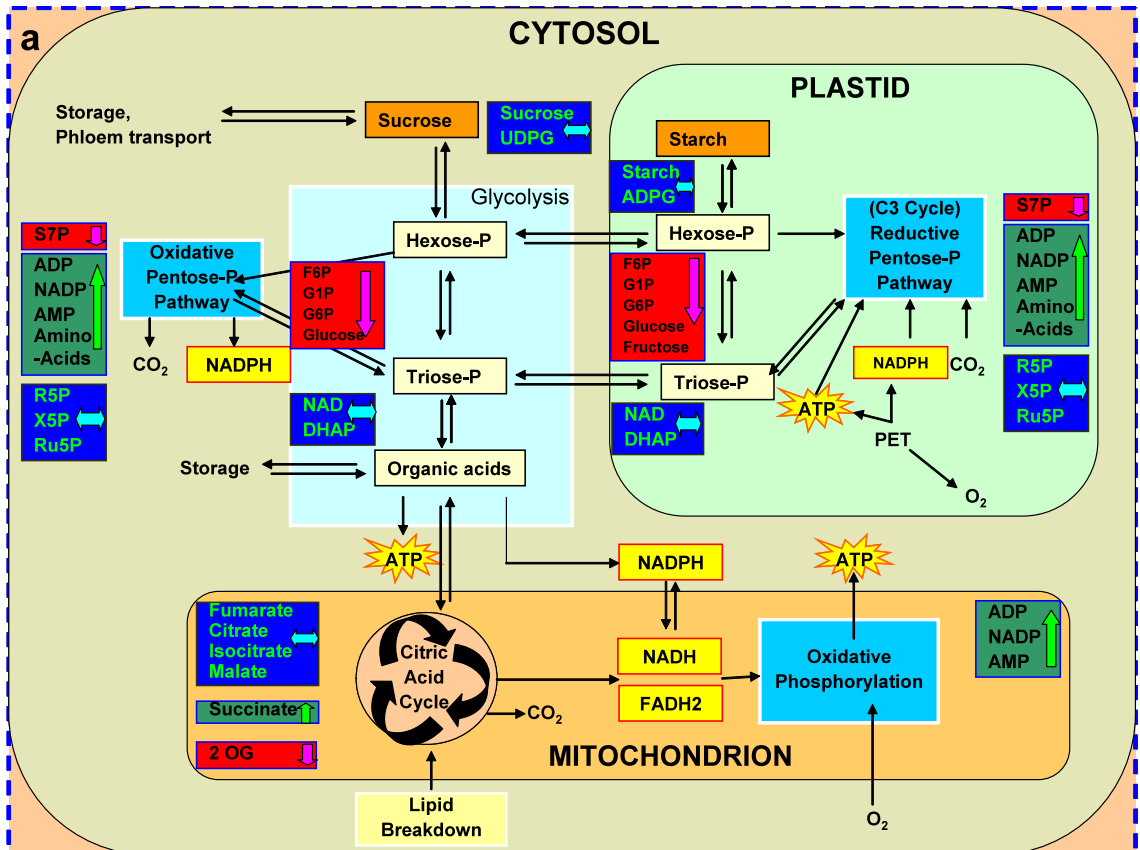
5.3 *Discussion*

Plants growing in arid regions often experience low shoot water concentrations, low turgor pressures, and high salinity in the rhizosphere, but in addition may also suffer from high shoot temperatures. In this Chapter a series of experiments was undertaken to asses the effects of high leaf temperatures (T_{leaf}) on photosynthesis in barley genotypes Local, Soorab, and Optic.

Two experimental approaches were used. One approach relied on the continious measurement of photosynthetic parameters whilst leaf temperature was gradually increased from control (25 °C) to damaging temperatures (40 °C) over a period of approximately 180 minutes (see Section 2.2.2.1); these experiments are referred to as 'Incremental Heat Stress'. The second approach relied on measuring a range of photosynthetic parameters at 25 °C on the same piece of leaf before and immidiately after a 3 hours heat stress event (typically 40 °C); these experiments are referred to as the 'Temperature Jump' experiments.

The incremental heat stress experiments indicated that a brief elevation of leaf temperature to approximately 40 °C for just 20 minutes severely impaired light saturated CO_2 assimilation rates (A_{sat}) in all three barley genotypes (Figures 5-1 & 5-5). A decline in CO_2 assimilation rates in cereals at high temperature (> 35 °C) has already been reported by many workers (Cen and Sage, 2005; Kirschbaum and Farquhar, 1984; Yamori *et al.*, 2005; Ziska, 2001), but there is some contention on exactly which photosynthetic processes are affected.

To pinpoint the possible site of injury attributable for the decrease in A_{sat}, four distinct processes (Figure 5-11) that control the rate of net CO_2 assimilation were studied: (1), capture of excitation energy by the Light Harvesting Complexes (LHCs) and its delivery to the Reaction Centers (RCs): (2), primary photochemistry, and *in vivo* photosynthetic electron transport rates that result in the production of ATP and NADPH: (3), the kinetic properties of the enzymes of the C3 cycle; this includes the enzymes involved in the carboxylation, phosphorylation, and reduction, and the RUBP regeneration phases: (4), the delivery of CO_2 from the air to the chloroplast stroma, and this is controlled by the CO_2 concentration gradient for CO_2 diffusion from the air to the intracellular leaf space (C_a-C_i) and the stomatal conductance (**gs**), and by the CO_2 diffusion gradient from

the intracellular leaf space to the chloroplast ($C_i - C_c$) and the mesophyll conductance (**gm;** Bernacchi *et al.*, 2002).

The results show that neither **gs** nor the delivery of excitation energy to the reaction centres (Figure 5-2 & 5-4) are affected by heat stress, and therefore the observed changes in A_{sat} are not attributable to these (see Figure 5-11).

Measurements showed the maximum quantum efficiency of PSII (Φ_{PSII}) is suppressed by heat stress but only by 50 % (Figure 5-12), whereas the corresponding decreases in A_{sat} was 85 %. This suggests that although Φ_{PSII} was affected, unlike others (Baker, 2008; Goss and Jakob, 2010; Song *et al.*, 2010) the results presented here suggest it can not account for the observed decrease in $A_{sat.}$ Similarly, *in vivo* measurements on photosynthetic electron transport also showed a decrease of 70 % (Figure 5-13) after heat stress. It is important to realize that this method estimates electron transport from water through to the oxidation of NADPH by the C3 cycle, and this itself is dependent on the carbon flux through this pathway. A decrease in the efficiency of the C3 cycle, therefore, would feed back and result in a decrease in ETR. Non-the-less, the observed suppression of A_{sat} was greater than that of photosynthetic electron transport and it is concluded that the decrease in A_{sat} is unlikely to have arisen from thermal injury to components of the photosynthetic electron transport chain.

Heat stress also affected the metabolite pool levels of the C3 cycle and their intermediates. Metabolite pool levels immediately after the RuBisCO-catalysed carboxylation step were significantly depleted (3PGA by *ca.* 85 %, triose phosphate by up to 75 %, S7P by up to 85 %), whereas those that feed into RuBisCO (*i.e.* metabolites of the RUBP regeneration phase X5P/R5P, Ri5P, Ru5P) were unaffected. These findings suggest that heat stress impairs the activity of C3 cycle enzymes between R5P and 3PGA (Figure 5-14). This includes the activities of the enzymes Phosphoribulokinase [EC 2.7.1.19], RuBisCO itself [EC 4.1.1.39], and RuBisCO Activase [4.1.1.39]. Alternatively, low carbon assimilation after heat stress may have arisen from low levels of ATP which is required for the generation of RuBP and 1,3PGA. ATP levels were not measured directly, but large increases in ADP concentration was observed in heat stressed tissues indicating that endogenous levels of ATP may have been low.

As the C3 pathway is cyclic, it is not easy to explain why after heat stress the metabolic pools of the carboxylation, reduction/phosphorylation, and initial parts of the regeneration phase are depleted, whereas those of the later stages of the regeneration phase (X5P, R5P and Ru5P) are unaffected. Taken simply, as many of the metabolites are in equilibrium, one might expect carbon to be evenly distributed throughout the metabolite pools. This is not the case, however, and presumably this has arisen from the complexities associated with perturbations in the regulation of a highly non-linear metabolic pathway (equilibrium reactions, changing substrate concentrations, feedback competitive and non- competitive inhibition, allosteric effects, *etc.*). In addition, it is unclear to what extent hexose and triose phosphate transport out of the chloroplast was affected by heat stress.

Visual inspection of leaves after five days recovery showed Optic to have the greatest level of heat stress damage and Local the least implying leaves of line Local have the capacity to partially recover from thermal damage. To investigate this observation further, measurements of A_{sat} and $\Phi\ CO_2$ were monitored on the same piece of attached leaf for up to 5 days post heat stress (Figure 5-5). Measurement of A_{sat} and $\Phi\ CO_2$ showed leaves from line Local significantly recovered part of their lost capacity 5 days after stress ($p<0.05$; Figure 5-5 and 5-7); whereas no significant recovery was observed in Soorab-96 or Optic

From these results it concluded that the thermal suppression of CO_2 assimilation is probably arises from a decrease in the activity of C3 cycle enzymes closely associated with the carboxylation step itself (i.e. RuBisCO, RuBisCO Activase, or Ribulose 5-phosphate kinase), and these findings are broadly similar with those published by others (Salvucci and Crafts-Brandner, 2004a; Salvucci and Crafts-Brandner, 2004b; Salvucci *et al.,* 2001). There are other possibilities, however, the supply of CO_2 from the intracellular air spaces to the chloroplast stroma (*i.e.* **gm**) may be severely affected, or the capacity of heat stressed leaves to generate ATP may cause the observed low assimilation rates.

Chapter 6: General Discussion

At the outset of this study the intention was to compare and contrast the responses of four barley genotypes for their ability to tolerate drought and salinity. It quickly became apparent, however, that for plants growing in controlled environmental conditions the direct application of drought stress on plants is not easy to administer in a physiologically significant way. There are many studies in the literature where drought effects have been imposed by merely withholding watering on plants that have been grown at approximately 20 ºC in low light (*e.g.* 200 μmol $.m^{-2}$ $.s^{-1}$ PPFD, approximately $\frac{1}{8}$ of full sunlight), and humidities that result in small transpiration vapour pressure deficits (*i.e.* VPDs of < 2.0 kPa). Under these conditions it is difficult to assess the relative effects of combinations of stress factors that are likely to be experienced by crops growing in arid regions where air temperatures routinely exceed 35 ºC, daily light levels are above 1500 μmol $.m^{-2}$ $.s^{-1}$ PPFD for several hours (thereby increasing leaf temperature), and VPDs can exceed 5.0 kPa. In addition, salinity levels in the soil are often moderately high and this imposes additional stresses (Byerlee *et al.*, 1993; Khan *et al.*, 2009). It was hoped that by studying the effects of high temperatures and moderate levels of salinity (up to 150 mM NaCl) it would be possible to identify physiological traits in genotypes that are known to perform well in agricultural systems in arid regions, thereby providing a basis for the identification of the molecular mechanisms that gives rise to tolerance. Four barley genotypes were chosen for the study providing a spectrum of tolerance, namely Local, Soorab-96, Awaran-2002 (all grown commercially in Pakistan), and Optic (north European line; see Table 2-1 for details).

6.1 *Comparison of Salt Stress in Barley Genotypes*

The expected increases in salinity of agricultural land due to evaporation and irrigation, and the impending need to establish arable production in hitherto un-exploited land, will lead to a demand for crops that can yield well under saline conditions. Barley is considered to be one of the more halotolerant cereals when compared with wheat and rice (Munns and Tester, 2008).

During the salt screening experiments genotypes were grown in a hydroponics system where germination, growth, development, and yield parameters were assessed. The hydroponics system is very labor intensive but was considered to be a better approach as the water and ion concentrations at the root surface are homogenous, unlike solid support media (soil, sand, *etc.*), and it is easier to asses root physiology. Growing plants in hydroponics in glass house conditions, however, does not mimic natural field conditions well as salinity varies within the soil from patch to patch, and controlled physical factors (i.e. day and night temperatures, humidity and light intensity) may cause complex interactions in natural field conditions.

As reported by others, the work presented in this thesis also showed that salinity caused significant alterations in agronomic and physiological traits of barley genotypes (Chapter 3 and 4; Hernández *et al.*, 1995; Takemura *et al.*, 2000). It is well established that the metabolic processes of halophytes (plants adapted to saline habitats) are no more tolerant of high concentrations of NaCl than are those of non-halophytes (glycophytes). For example, *in vitro* activities of enzymes extracted from the halophytes *Atriplex spongeosa* and *Suaeda maritima* were just as sensitive to NaCl as were those extracted from beans or peas (reviewed by Munns *et al.*, 1983). Generally, Na^+ starts to inhibit most enzymes at a concentration above 50 mM. The concentration at which Cl^- becomes toxic is even less well defined, but is probably in the range of 150 mM and above. Even K^+ may inhibit enzymes at concentrations of approaching 200 mM (Greenway and Osmond, 1972). Halophytes, therefore, are thought to demonstrate halotolerance by preventing toxic levels of ions from accumulating in the cytoplasm (Tester and Davenport, 2003). Maintenance of ionic balance is achieved through two main mechanisms: minimizing the entry of salt into the plant: minimizing the concentration of salt in the cytoplasm. Halophytes demonstrate both types of mechanisms; they 'exclude' salt from the plant well, but effectively compartmentalize in vacuoles the salt that inevitably does get in. Thus, halophytes utilize ion transport mechanisms to maintain low cytoplasmic ion levels, and regain turgor.

Sometimes plants are classified as 'Includers' and 'Excluders' to describe their strategies for coping with high salinity (James *et al.*, 2006; Munns *et al.*, 1983), but this is somewhat confusing as all plants exclude salt from their tissues at some concentrations. Similarly, all plants take up salt. The key difference between glycophytes and halophytes is the reason why they do this. Glycophytes are principally

concerned only with maintaining low internal Na^+ and Cl^- levels. For this reason, upon exposure to low levels of NaCl (<150 mM), they attempt to prevent Na^+ and Cl^- uptake into the plant, and may be considered as excluders. At some low external NaCl concentration, however, these exclusion mechanism breakdown and salt begins to accumulate to toxic levels in the cytoplasm; at this point glycophytes may be considered as includers. The key point here is that at these relatively low external NaCl concentrations (i.e. <150 mM NaCl) osmotic stress is minimal and it is the ionic component of salinity that causes death. In hydroponic solutions 150 mM NaCl exerts a water potential of approximately 300 mosmol or -0.74 MPa, and water potentials of highly productive well-watered salt free soils are typically within the -0.5 to -0.8 MPa range (Ashraf, 1994). The four barley genotypes used in this study were all severely affected by 100 mM NaCl (equivalent to a water potential of approximately -0.5 MPa), and only landrace Local survived to harvest in 150 mM NaCl. It seems unlikely, therefore, that the water potentials experience by these barley genotypes in 100 and 150 mM NaCl were sufficient to cause the observed damage. In contrast, halophytes withstand higher salt concentrations, in some cases full strength sea water (*ca.* 500 mM NaCl or even higher) sea water has a water potential of *ca.* -2.5 MPa (Ali *et al.*, 2007). For this reason halophytes often experience both ionic stress and loss of turgor (often referred to as water stress). Upon exposure to salinity, therefore, halophytes take up Na^+ and Cl^- and compartmentalize this in their vacuoles to establish low vacuolar solute potentials, which if sufficiently low will reverse the water potential gradient between this compartment and the rhizosphere and thus result in water uptake and the re-establishment of turgor. Here halophytes operate as includers. Once a favorable turgor pressure has been gained, however, water balance has been achieved and halophytes no longer take up Na^+ and Cl^- and operate as excluders.

The better halotolerance of landrace Local can be attributable to its ability to prevent salt entry through the roots (between 50 to 100 mM NaCl) compared with the halo-sensitive genotype Optic (Figures 4-9 to 4-15). There is a great deal in the recent literature on the mechanism relating to Na^+ exclusion from leaf blades (Munns and Tester, 2008). Na^+ exclusion by roots ensures that Na^+ does not accumulate to toxic concentrations within leaves. A failure to maintain effective Na^+ exclusion mechanisms will manifest as toxic effects after days or weeks, depending on the species, and causes the premature death of older leaves.

The findings discussed in Chapter 4 of this study are consistent with this hypothesis, as landrace Local showed a major increase in shoot Na^+ and minor increase in root Na^+ when external NaCl was increased from 100 to 150 mM NaCl, and this corresponded to a major suppression in growth. In contrast, line Optic showed a major increase in shoot Na^+ and moderate increase in root Na^+ between 50 and 100 mM NaCl, which also corresponded to a major decline in growth.

There is an opinion that the success of cereals growing under different salinity regimes is related to their short life cycles. It has been reported that the difference in time to maturity between salt stressed and the non-stressed plants reflects an underlying halotolerance strategy such that the salt-stressed plants are ready for harvest 1 to 2 weeks before non-stressed controls (Francois *et al*., 1986). The data presented in this thesis do not support this contention, however, as there was no correlation between the duration of life cycle (Awaran < Optic = Local < Soorab) and tolerance of 100 mM NaCl (Local > Soorab > Optic > Awaran).

Landrace Local could prove a very useful resource for studying abiotic stress tolerance mechanisms and could be used in breeding programmes, but unfortunately its inherited shortcomings (lower yield compared with Optic and reported susceptibility towards diseases) are not desirable for its widespread adoption. In contrast, line Awaran (due to its early maturity) and line Optic (due to its better yield) are preferred by breeders but their susceptibility to abiotic stress limits their range. Soorab-96 has relatively better salinity tolerance compared with Optic and Awaran but it has a significantly longer life cycle decreasing land usage for other crop. Clearly, there is potential to exploit landrace Local in breeding programmes for abiotic stress with the high yielding lines to improve barley production in arid regions.

Photosynthesis rates declined in parallel with the observed decline in growth and yield parameters as salt concentration was increased. CO_2 assimilation rates (A), the Carboxylation Coefficient (Φ CO_2, a measure of the efficiency of the carboxylation processes), the Quantum Efficiency (α), and rate of dark respiration (Rd) declined in all genotypes, however, landrace Local performed significantly better compared with the elite lines. Recent reviews in the literature reported that **gs** is a major factor in salinity induced decline in CO_2 assimilation (James *et al*., 2008). Data are presented in Chapter

4 also showing a correlation between CO_2 assimilation and **gs** (Figure 4-5). Establishing a cause-and-effect relationship between CO_2 assimilation and **gs** is complicated as CO_2 assimilation is a complex and highly dynamic process with several feed back control steps. For example, a direct effect of salinity on the kinetic properties of an enzyme in the C3 cycle will result in an immediate decline in CO_2 assimilation leading to an increase in Cc, followed by an increase in Ci; an increase in the internal CO_2 concentration of the leaf will be sensed by the guard cells leading to stomatal closure. Alternatively, a direct effect of salinity on **gs** will lead to a decrease in Ci and be followed by a decrease in Cc; lower levels of CO_2 in the chloroplast will result in a decline in CO_2 assimilation. In these two cases the primary site of injury is different but the observations are the same, a decline in CO_2 assimilation and **gs**. In conclusion, it is difficult to untangle the cause-and-effect relationship between CO_2 assimilation and **gs** in a system at steady state after several weeks of prolonged exposure to a stress.

What is unclear, however, is the effect of high salinity upon mesophyll conductance (**gm**), and the extent to which this impairs CO_2 assimilation rates (Flexas *et al*., 2004). Whilst it was possible to estimate **gm** using the 'Constant J' method in control (non-stressed) plants, the imposition of even moderate salt stress resulted in a failure to solve the non-linear equations. Presumably, this occurred because the model of photosynthesis upon which the Constant J method is based (and indeed all three published methods for estimating **gm**, see Loreto *et al*., 1992) breaks down when salt stress is applied. Both of the fluorescence-based methods for estimating **gm** are determined by parallel measurements from A/Ci curves where CO_2 assimilation (*i.e.* electron transport, J) is limited by either CO_2 supply or the regeneration of Ru1,5-BP, or both; one explanation for the apparent breakdown of the model is that with salt stress other factors are also limiting CO_2 assimilation.

Cause-and-effect relationships between photosynthesis and growth rate can be difficult to untangle. It is always difficult to know whether a reduced rate of photosynthesis is the cause of a growth reduction, or the result. With the onset of salinity stress, a reduced rate of photosynthesis is certainly not the sole cause of a growth reduction because of the rapidity of the change in leaf expansion rates (Cramer and Bowmann, 1991; Fricke *et al*., 2004; Passioura and Munns, 2000), and also because of the increase in stored carbohydrate, which indicates unused assimilate (Munns *et al*., 2000). However, with time, feedback inhibition from sink to source may fine tune the rate of photosynthesis to

match the reduced demand arising from growth inhibition (Paul and Foyer, 2001). Reduced leaf expansion resulting in a buildup of unused photosynthate in growing tissues may generate feedback signals that down regulate photosynthesis.

One important clarification that should be made is that the photosynthetic parameters measured in this study were made on healthy living green tissues and expressed on a unit leaf area basis. They do not, therefore, reflect the cumulative effect of salt stress on the total amount of living green tissues that will have directly contributed to the overall plant photosynthesis rate and the measured plant growth parameters. It is recommended that some attention is paid to estimating the amount of living and dead tissues in further studies. In practice, however, this may not be easy to do as the living tissues will represent a spectrum of 'healthy' and 'stressed' leaves, which will, therefore, exhibit a range of photosynthesis rates. Integrating these rates over the whole plant and over an extended period of several weeks to test for strong correlations between growth and photosynthesis rates will be difficult.

In these studies plants were not in ψ_{H2O} equilibrium with the growth media, and the measured plant ψ_{H2O} were always more negative than the hydroponic solutions. When exposed to NaCl at concentrations above 50 mM Optic tissues ψ_s were always more negative than those in Local presumably due to high proline and Na^+ levels; this resulted in a higher ψ_P which helped plants re-establish more positive ψ_{H2O}. It is generally viewed that saline solutions cause tissue desiccation by drawing water from cells through osmosis. This causes a loss of turgor that has major implications for long term survival (see Section 1.2.1.1.5). The response of dehydrated plants, therefore, is to re-establish turgor pressure by accumulating small osmotically active solutes in the vacuole (*e.g.* Na^+) and cytoplasm (compatible solutes such as proline; Hong *et al.*, 2000; Hoque *et al.*, 2007). It might be predicted, therefore, that genotypes that re-establish high turgor pressures by accumulating high levels of electrolyte and compatible solutes should subsequently perform better than those that do not. In these studies, the salt-sensitive line Optic accumulated higher levels of Na^+ and proline in tissues that did Local, and this indeed resulted in higher turgor pressures. These findings contradict the observation that Local is the more halotolerant of the two and strongly suggest that it is the ionic component of salinity stress, not the osmotic component, which suppresses growth over this range of NaCl concentrations. One point that should be emphasized relates to the errors in the measurement of $^{tissue}\psi_{H2O}$ that can arise with the pressure

chamber method if the solute potential of the xylem ($^{xylem}\psi_s$) is not taken into account. In Section 4.2.2 it was stated that the method relies on $^{xylem}\psi_s$ being zero, and clearly this will not be the case in plants exposed to increasing salt stress. This point is often overlooked in the literature, and published values are, therefore, often unreliable. Values for $^{leaf}\psi_{H2O}$ presented here have been corrected for this error by directly measuring $^{xylem}\psi_s$, and this has resulted in very different estimates of $^{tissue}\psi_{H2O}$ and ψ_P. The validity of the corrected method presented here could be assessed using other methods. For example, $^{tissue}\psi_{H2O}$ could be determined using psychrometric methods which do not rely on assumptions on xylem solute potential (Toole and Moya, 1981). Direct measurements of ψ_P are also possible using microelectrode techniques (Fricke and Peters, 2002); unfortunately, neither of these techniques were available.

There is clear evidence that compared with line Optic landrace Local maintained low shoot and root levels of Na^+ at higher NaCl concentration. This observation also supports the contention that osmoregulation is not a critical response for the survival of salinity tolerant plants; if it were, one would expect halotolerant plants like Local to take up and sequester more Na^+ in their vacuoles than the halosensitive line Optic in an attempt to regain turgor (osmoregulate) and this does not appear to be the case. Instead, it is line Optic that accumulates the highest levels of Na^+, but presumably the cells cannot sequester it all in their vacuoles, hence cellular metabolism is compromised and growth and survival are affected. It seems likely that the halotolerant landrace Local maintains low intracellular levels of Na^+ by showing reduced rates of Na^+ uptake, increased rates of Na^+ efflux, or both. Proline concentrations increased in both lines, as they were expected to; however, this increase was significantly higher in the halosensitive line Optic.

During the early stages of development (up to 21 days) the accumulation of Na^+ in seedlings (see Section 4.4) upon exposure to moderate levels of salinity (100 mM NaCl and below) indicate that there were no genotypic differences; increasing external NaCl from 0 to 50 mM causes an increase in tissue Na^+ levels, but above 50 mM NaCl mechanisms are activated that prevent further accumulation; presumably this occurs through Na^+ exclusion or Na^+ efflux at the root / rhizosphere surface, or both. Above 100 mM NaCl, however, these mechanisms appears to fail in the line Optic and Na^+ levels in the seedlings increase. In contrast, landrace Local manages to maintain low and constant tissue Na^+ levels over the 50 to 150 mM external NaCl concentration

range. Further studies should be undertaken to establish how Local maintains Na^+ balance; this may involve better Na^+ discrimination (i.e. reduced uptake), and/or better Na^+ efflux (*via* Na^+/H^+ antiporters and/or P- type Na^+ -ATPases; see Figure 1-2). One approach will be to embark on a series of biophysical studies using electrophysiological techniques to establish genotypic differences in Na^+ transport capacity.

6.1.1 Epigenetic Base of Halotolerance in Barley

Another interesting observation is the ability of barley to 'remember' that their preceding generations were exposed to higher salt concentrations (see Section 4.6; Bajehbaj, 2010; Mohammadi, 2009). It is conceivable that the differences in halotolerance observed between the landrace Local and the other elite lines arose from the degree of salt stress experienced by parental lines that produced the seed used in this study; these seed stocks were supplied from the Agriculture Research Institute, Quetta, Pakistan and were harvested from field grown plants.

From the results discussed in Chapter 3 and 4 it is clear that there is also a genetic basis that confers an improved performance in landrace Local when exposed to high salinity. The basis of the genetic and epigenetic halotolerance factors needs to be investigated further. Although the genome of barley has not been completely sequenced, over 800,000 cDNAs have been; work has begun on the genome sequence and with high throughput DNA sequencing technology, it should be only a matter of two or three years before this information is available to the scientific community. Further, barley is a diploid plant of the family Triticae which makes genetic studies and loci mapping relatively simple. There are now over 3,000 SNP markers for barley, and chips are available (BOPA Chips, Illumina Corp) for high throughput mapping (Szucs *et al*., 2009). Finally, there are already several TILLING populations of barley and others are being developed, and this resource provides a sound basis for identifying knockout (null) lines for phenotyping. The epigenetic basis of halotolerance presumably involves changes in chromatin structure and the degree of DNA acetylation and methylation (Finnegan, 2010), and this also requires further investigation.

The conclusion is that barley germplasm is available that could significantly improve halotolerance in cereals. What needs to be established is which genes are responsible for the observed halotolerance and to what extent epigenetic factors are important. It is important to stress that any studies on salinity tolerance in different genotypes should not ignore epigenetic factors, otherwise conclusions could be misleading.

6.2 *Comparison of Thermal Stress in Barley Genotypes*

Leaf temperature (T_{leaf}) of well watered plants in high air temperatures (>35 °C) is often 5-10 °C below air temperature (T_{air}) due to transpiration rates (Vitale *et al*., 2007), but as the rate slows T_{leaf} rises. Unfortunately most of the published research work (Barnabas *et al*., 2008; Haldimann and Feller, 2005; Parent *et al*., 2010) to asses the effects of high temperature on plants has recorded only air temperature, not leaf temperature, and consequently precise conclusion are difficult to draw. In this study attempts were made to mimic hot, arid conditions measuring and controlling leaf temperatures (see Section 2.2.2.2). It seems likely that leaves will experience the greatest heat stress as they are exposed to direct sunlight and show high absorbtance. The literature contains many reports on the effects of high T_{leaf} on photosynthesis rates (Bukhov *et al*., 1999; Crafts-Brandner and Salvucci, 2002; June *et al*., 2004; Sharkey and Schrader, 2006). Various photosynthetic parameters are affected by heat stress and show positive correlations with plant growth. Any constraint in photosynthesis can limit plant growth at high temperatures. Photochemical reactions in the thylakoid membranes, and carbon metabolism in the stroma of the chloroplast have been suggested as the primary sites of injury at high temperatures (Wang *et al*., 2010; Wise *et al*., 2004). The ratio of variable fluorescence to maximum fluorescence (Fv/Fm) and the base fluorescence (F_0) are physiological parameters that have been shown to correlate with heat tolerance (Yamada *et al*., 1996). There is a good evidence that increasing T_{leaf} and light levels lead to an acclimation in PSII that improves thermotolerance as long as the upper thermal limits of survival are not exceeded (Salvucci and Crafts-Brandner, 2004b; Marchand *et al*., 2005). In addition to leaves, the floral parts of the plant are also possible targets for thermal injury (Gross and Kigel, 1994). The effects of high spike temperature on reproduction and yield, however, were not considered in this study. Imposing heat stress evenly on these plant organs is difficult and reliable estimates of spike temperature will require thermal imaging technology. It is suggested that the effects of high spike temperature on yield should be studied as this may prove to be a more significant factor than $T_{leaf.}$

Brief elevation of >38 °C of leaf temperature severely suppressed CO_2 assimilation rates in barley leaves. Leaf temperatures of this magnitude are not uncommon for water limited plants growing in habitats of high irradiance (Bucks *et al*., 1984; Drake, 1976;

Mattson and Haack, 1987). The results presented in this thesis revealed that several processes which contribute to CO_2 assimilation, for example Φ_{PSII} and ETR, are affected but it appears that the processes most closely associated with the C3 cycle are affected the most (Section 5.2.3.1). Possible sites of primary injury include the kinetic properties of the individual enzymes involved in the C3 cycle itself (K_m, V_{max}, *etc.*), as well as the supply of substrates to drive CO_2 assimilation (CO_2, ATP, and NADPH).

Interpreting the response of *in vivo* electron transport rates to high T_{leaf} is difficult, because of the large number of individual steps involved, and because it is linked to the carboxylation processes and even CO_2 supply. As a result, it has been difficult to pinpoint specific limiting steps that control the temperature response of electron transport (Sage and Cubien, 2007). The mechanism causing the decline in the electron transport rate above the thermal optimum remains uncertain (June *et al.*, 2004). One leading proposal is that cyclic electron transport is activated at elevated temperatures at the expense of linear electron transport, thereby causing a shortage of NADPH (Bukhov *et al.*, 1999; Sharkey and Schrader, 2006). Electron flow through PSII decreases above the thermal optimum in a pattern that mimics a decline in whole chain electron transport of wheat (Yamasaki *et al.*, 2002); in contrast, electron flow rate through PSI is stable between the thermal optimum for photosynthesis and 40 °C, indicating it has high capacity to support enhanced cyclic electron flow at elevated temperature (Berry and Björkman 1980; Yamasaki *et al*. 2002). The data presented in Chapter 5, however, clearly shows that ADP levels increase with thermal stress, which suggests no stimulation in cyclic electron transport. These studies also show that $NADP^+$ increases, however, and this is consistent with a decline in ETR (Yamasaki et al., 2002).

In this study the *in vivo* measurements of steady state and maximum electron transport showed a significant decline after heat stress. It is important to realize that no conclusions can be drawn on the effects of heat stress on the photosynthetic electron transport chain *in vivo* by fluorescence measurements because these rates are coupled to the carboxylation processes including CO_2 supply to the chloroplast. Consequently, a measured decline in *in vivo* ETR may be attributable to a direct effect of heat stress on components of the electron transport chain or carboxylation processes further down stream.

In Chapter 5 data are presented that show CO_2 assimilation was impaired by 85 % by heat stress, but concomitant measurements on the coupled *in vivo* ETR were impaired by only 70 %. There are several explanations for this apparent discrepancy. First, not all

of the electrons passing through the electron transport chain are used to reduce CO_2, a significant fraction may be used to reduce oxygen (Mehler reaction), nitrate (nitrate and nitrite reductase) and sulphate, or feed the antioxidant mechanisms in the chloroplast (thioredoxin, glutathione, *etc.*). For example, if approximately 18 % and 82 % of the electrons are used for the above alternative electron sinks and CO_2 reduction, (respectively) in non-stressed tissues, and the corresponding inhibition after heat stress is 0 % and 85 % (respectively), this would give the observed inhibition in ETR approximately 70 %. The consumption of electrons before and after heat stress by these alternative electron sinks was not measured in these studies and so it is not possible to confirm this hypothesis at this time. Another explanation for the discrepancy between heat-stress induced inhibition of CO_2 assimilation and *in vivo* ETR could be related to precision of measurement of the two different methods. There is general agreement, however, that CO_2 assimilation and *in vivo* ETR measurements correlate well (Baker, 2008; Genty *et al.*, 1989). The theoretical maximum efficiency is reported to be 10 electrons per CO_2 molecule fixed (Zhu *et al.*, 2008), and values of 10 to 13 were routinely measured in this study. There is no evidence, therefore to assume the discrepancies are attributable to this source of error.

It is suggested, therefore, that direct effects of heat stress on the electron transport chain (if any) should be obtained when ETR is uncoupled from CO_2 assimilation by adding an electron acceptor like methyl viologen (Bugg *et al.*, 1980). Attempts to measure ETR after application of methyl viologen to intact leaves did not work at the recommended concentrations (100 μ mol $.l^{-1}$) probably due to slow uptake. Application of 500 μ mol $.l^{-1}$, however, completely suppressed (>90 %) CO_2 assimilation but unfortunately also suppressed the ETR; it is not clear why. It is suggested that appropriate concentrations of methyl viologen along with *in vitro* measurements of ETR from stressed and controlled leaf samples might produce interpretable results on the effects of heat stress on ETR.

No evidence was found that to support the view that the rapid thermally-induced decline in CO_2 assimilation was attributable to a decrease in g_s ; indeed the opposite was found, in the short-term (*ca*. 20 minutes) stomata open at high T_{leaf}. It is quite conceivable that CO_2 concentration in the stroma (C_c) was low due to thermally-induced decreases in mesophyll conductance (g_m; Bernacchi *et al.*, 2002). Attempts were made to estimate g_m in control and heat stressed tissues using both the 'Constant J' and 'Variable J'

fluorescence methods (Loreto *et al*., 1992). Whilst reliable estimates for g_m were obtained from control leaves, no sensible values were collected from moderately or severely heat stressed leaves; it appears that the model for photosynthesis upon which these two measurements are based breaks down upon mild heat stress making estimates of g_m impracticable. What is clear, however, is that the values obtained from control leaves (*ca*. $0.12 - 0.45$ mol $.m^{-2}$ $.s^{-1}$) are of a comparable magnitude to the measured values of stomatal conductance (g_s; *ca*. $0.2 - 1.2$ mol $.m^{-2}$ $.s^{-1}$), suggesting that even in control leaves CO_2 assimilation rates (A) are suppressed at least as much by g_m as by g_s. From comparison of the corresponding A/Ca and A/Ci curves from non-stressed leaves (Figure 2-3) the limitations of g_s on CO_2 assimilation is *ca*. 15 %, and it is reasonable to assume, therefore, that g_m exerts a similar limitation on CO_2 assimilation. Clearly, the limitations that g_m imposes on photosynthesis rates needs to be established both in unstressed plants, as well as plants exposed to a range of environmental stress factors.

One of the interesting observations from the incremental heat stress experiments (Section 5.1.1.2) is the rapid response of stomata to increasing leaf temperature. In the experiments reported here as T_{leaf} was increased from 23°C to 36°C (T_{air} from 25 °C to 40 ºC) the driving force for transpiration, the vapour pressure deficit (VPD), more than doubled (from 2.80 to 5.92 KPa) but g_s remained unchanged. In contrast, once T_{leaf} exceeded the threshold level of 36 °C / 5.92 KPa, it appears that a signalling mechanism was activated that induces stomatal opening and a corresponding increase in transpiration rate. Presumably stomatal opening is affected to reduce T_{leaf} and prevent heating to 40 °C which severely damages the leaves of Local and Soorab-96, and is lethal for Optic. The plants used in this study were well watered, but it is well established that the stomata of cereal crops grown in the field partially close during the hottest part of the day to conserve water (Robredo *et al*., 2007). It seems reasonable to conclude that stomatal aperture is regulated by a signalling mechanism for the conservation of tissue water when below a threshold level, and a separate signalling mechanism to prevent T_{leaf} rising to >36 °C. To our knowledge, this temperature-dependent signalling mechanism is novel and has not been studied before. It would be interesting to establish whether the increase in g_s with T_{leaf} reported here is triggered directly by leaf temperatures exceeding 36 ºC. It would also be interesting to investigate the response of stomata in a range of plants that are partially water limited and experiencing high leaf temperatures. In arid zones field crops are probably faced with

this dilemma, to reduce transpiration and conserve water and risk the rapid onset of thermal damage, or to maintain transpiration to reduce T_{leaf} but suffer the consequences of loss of turgor. Clearly, for water limited heat stressed plants, maintaining high values of g_s (and thereby high transpiration rates) to prevent T_{leaf} rising to lethal levels will soon result in further leaf desiccation and a reduction in transpiration rate, and this will inevitably lead to high T_{leaf} and tissue necrosis anyway. High temperature-induced stomatal opening, therefore, appears to offset the time when lethal T_{leaf} occurs; unless some amelioration occurs during this period (*i.e.*-watering), the result will be the same, thermally-induced leaf necrosis. Increased water availability clearly lessen these effects but perhaps the onset of rapid thermal damage to the shoot tissues rather than water concentration in the shoot *per se* is the primary reason why some plants perform badly in these habitats. Strategies that focus on the genetic basis for heat tolerance or the capacity to recover from thermal injury may prove to be a fruitful avenue for developing crops with multiple traits for production in arid marginal lands.

The suppression of CO_2 assimilation induced by brief elevation of T_{leaf} to 40 °C does not arise from changes in the excitation rate of photochemical efficiency of PSII. This precludes the involvement of protective mechanisms that are reported to regulate the fate of absorbed light energy such as the Xanthophyll cycle, state transitions, or photoinhibition (Baker, 2008; Goss and Jakob, 2010; Song *et al.*, 2010). The activation of such mechanisms would have been reflected in the various fluorescence parameters determined from induction and dark recovery experiments (not presented) carried out in this study. Although high leaf temperatures did affect some of these fluorescence parameters, they were relatively minor compared with the suppression observed in CO_2 assimilation. Of particular interest is the modest effect of elevated leaf temperatures on Φ_{PSII}. It is well established that the D1 protein that constitutes part of the hererodimeric core of the PSII reaction centre is prone to damage (Allakhverdiev *et al.*, 2008; Kern *et al.*, 2009; Lindahl *et al.*, 2000). Some evidence was found to support the contention that primary photochemical processes and ETR were affected but these may have arisen because the major electron sink (CO_2 assimilation) was suppressed and not as a direct cause of thermal stress *per se*.

At the thermal optimum, the activation state of RuBisCO declines in response to shading or elevated CO_2 (Woodrow and Berry, 1988). In both cases, RuBisCO deactivation is considered a regulatory response to a shift in limitation away from

RuBisCO capacity to either RuBP or Pi regeneration capacity (Mott *et al.,* 1984; von Caemmerer and Quick 2000). The identification of RuBisCO Activase as the main regulatory protein for RuBisCO provided a mechanistic explanation for the patterns of RuBisCO deactivation in response to shade or CO_2 enrichment (Portis 2003). RuBisCO Activase consumes ATP and reducing power in a reaction sequence that frees tightly bound phosphorylated sugars from RuBisCO's catalytic sites. Removal of the sugar phosphates allows for spontaneous carbamylation of a lysine residue, which then activates the catalytic site, or frees the carbamylated catalytic site of bound inhibitors. ADP is an important inhibitor of RuBisCO Activase, and Activase requires ATP and reducing power to exist in its most active configuration. The active form of RuBisCO Activase comprises of aggregates of 8 to 16 subunits, which are assembled from inactive dimers and monomers using ATP and reducing power in a thioredoxin-dependent reaction (Zhang *et al.*, 2002).

Away from the thermal optimum, the activation state of RuBisCO declines, particularly at elevated temperature. At suboptimal temperatures, the decrease in the activation state is inconsistent, and has been linked to an inhibition on CO_2 assimilation by a Pi regeneration capacity (Hendrickson *et al.*, 2004; Cen and Sage, 2005). The reduction in the activation state above the thermal optimum is widely observed and is proposed to limit CO_2 assimilation (Portis, 2003; Haldimann and Feller, 2004, 2005; Salvucci and Crafts-Brandner 2004 a, b & c). Early evidence in support of a limiting role of the RuBisCO activation state was a rise in RuBP metabolite pools and RuBP/PGA ratios, which indicate a constriction at the carboxylation step at elevated temperatures (Kobza and Edwards 1987). Later studies showed RuBisCO Activase to be heat labile at temperatures corresponding to those where CO_2 assimilation and the activation state of RuBisCO decline (Crafts-Brandner and Salvucci, 2000; Salvucci and Crafts-Brandner 2004a). Similar results are reported in Chapter 5 of this thesis. After heat stress the metabolite pool levels of C3 cycle intermediates immediately after the carboxylation phase showed a significant decrease as did those in the starch synthesis pathway. In contrast, the metabolite pool levels of those compounds that feed into the carboxylation phase were unchanged. From these findings it can be concluded that the thermal suppression of CO_2 is probably closely associated with a decrease in the activity of C3 cycle enzymes closely associated with the carboxylation step itself (see also Section 5.3 for further explanation).

The data presented here are consistent with reports of an indirect thermally-induced decrease in the activity of Ribulose-1,5-Bisphosphate Carboxylase/Oxygenase (RuBisCO) due to inactivation of RuBisCO Activase and/or activity of phosphoribulokinase (Ribulose 5-Phosphate Kinase, [EC 2.7.1.19]; Kurek *et al*., 2007; Salvucci and Crafts-Brandner, 2004b; Salvucci *et al*., 2001).

6.3 *Conclusions and Future Work*

6.3.1 Salt Stress

- Evidence was found for a genetic basis for the observed differences in halotolerance between the different genotypes, with landrace Local performing best at all stages of development.
- Halotolerance appears to be at least partially related to the ability of genotypes to Na^+ exclude from the plant and to regulate Na^+ transport from the root to the shoot.
- It is recommended that comparative studies at the electrophysiological level are undertaken to characterize Na^+ transport in these genotypes.
- There is evidence for an epigenetic basis for halotolerance in barley.
- In barley salt stress arises from ionic stress not osmotic stress.
- There was no evidence that older leaves are used as a repository for Na^+.

6.3.2 Thermal Stress

- $T_{leaf} > 38\,°C$ results in rapid and major suppression of CO_2 assimilation.
- The observed decline in CO_2 assimilation can not be attributable to **gs** or light harvesting capacity.
- Declines in ETR and PSII activities were measured but are unlikely to be responsible for decline in CO_2 assimilation.
- Further studies on the effects of heat stress on *in vitro* ETR are required to confirm this.
- The observed decrease in CO_2 assimilation appears to be attributable to suppression in the rate of conversion of Ru5P to 3PGA mediated by the C3 cycle enzymes phosphoribulokinase [EC 2.7.1.19]; RuBisCO [EC 4.1.1.39]; or RuBisCO Activase.

- *In vitro* measurements on the effects of heat stress on the activity of these enzymes should be made to pinpoint the site of thermal injury in barley.

- Robust methods need to be developed for assessing the importance of mesophyll conductance **gm** in thermal injury.

- Significant differences in the recovery after heat shock in barley genotypes are observed and appear to have a genetic basis. Studies should be undertaken to identify the underlying mechanisms responsible for this recovery in landrace Local.

- The effects of thermal stress on flowering process in barley need to be explored.

6.3.3 General Conclusions

- Landrace Local and other landraces offer a unique and under explored resource for breeding stress tolerance into elite barley lines.

- It is unclear to what extent epigenetic factors affect stress tolerance and a better understanding is required to avoid false conclusions from being drawn. This will include de-imprinting seeds by growing the parental lines in control conditions for several generations before embarking on genetic studies.

7 References.

Adams SR, Cockshull KE, Cave CRJ (2001) Effect of Temperature on the Growth and Development of Tomato Fruits 10.1006/anbo.2001.1524. Ann Bot **88:** 869-877

Al-Khatib M, McNeilly T, Collins JC (1992) The potential of selection and breeding for improved salt tolerance in lucerne (Medicago sativa L.). Euphytica **65:** 43-51

Ali MR, Shalimuddin M, Bagum SA (2007) Identification of Salt Tolerant Barley Genotypes for Coastal Region Of Bangladesh. Bangladesh J. Bot. 36: 151-155

Ali Q, Athar H-u-R, Ashraf M (2008) Modulation of growth, photosynthetic capacity and water relations in salt stressed wheat plants by exogenously applied 24-epibrassinolide. Plant Growth Regulation **56:** 107-116

Allakhverdiev S, Kreslavski V, Klimov V, Los D, Carpentier R, Mohanty P (2008) Heat stress: an overview of molecular responses in photosynthesis. Photosynthesis Research **98:** 541-550

Amtmann A, Sanders D (1998) Mechanisms of Na^+ Uptake by Plant Cells Advances in Botanical Research. In JA Callow, ed, Incorporating Advances in Plant Pathology, Ed Volume 29. Academic Press, pp 75-112

Amzallag Gn, Seligmann H, Lerner Hr (1993) A Developmental Window for Salt-Adaptation In Sorghum bicolor. Journal of Experimental Botany **44:** 645-652

Apse MP, Aharon GS, Snedden WA, Blumwald E (1999) Salt Tolerance Conferred by Overexpression of a Vacuolar Na^+/H^+ Antiport in Arabidopsis 10.1126/science.285.5431.1256. Science **285:** 1256-1258

Arrivault S, Guenther M, Ivakov A, Feil R, Vosloh D, Dongen JTv, Sulpice R, Stitt M (2009) Use of reverse-phase liquid chromatography, linked to tandem mass spectrometry, to profile the Calvin cycle and other metabolic intermediates in Arabidopsis rosettes at different carbon dioxide concentrations. The Plant Journal **59:** 826-839

Asch F, Dingkuhn M, Dorffling K (2000) Salinity increases CO_2 assimilation but reduces growth in field-grown, irrigated rice. In Plant and Soil, Vol 218. Springer Netherlands, pp 1-10

Ashraf M (1994) Breading for salinity tolerance in plants. CRC Crit. Rev.in plant sci **13**: 17042

Ashraf M, Foolad MR (2005) Pre Sowing Seed Treatment--A Shotgun Approach to Improve Germination, Plant Growth, and Crop Yield Under Saline and Non Saline Conditions Advances in Agronomy. *In* DL Sparks, ed, Ed Volume 88. Academic Press, pp 223-271

Ashraf M, Foolad MR (2007) Roles of glycine betaine and proline in improving plant abiotic stress resistance. Environmental and Experimental Botany **59:** 206-216

Ashraf M, Harris PJC (2004) Potential biochemical indicators of salinity tolerance in plants. Plant Science **166:** 3-16

Athar HR, Ashraf M (2009) Strategies for Crop Improvement Against Salinity and Drought Stress: An Overview. *In* Salinity and Water Stress, pp 1-16

Attumi A-AM (2007) A Study of Salt Tolerance in *Arabidopsis thaliana* and *Hordeum vulgare*. University of Glasgow, UK, Glasgow

Ayaz FA, Kadioglu A, Turgut R (2000) Water stress effects on the content of low molecular weight carbohydrates and phenolic acids in Ctenanthe setosa (Rose.) Eichler, Can. J. plant Sci. **80**: 373-378

Badger MR, Sharkey TD, Caemmerer S (1984) The relationship between steady-state gas exchange of bean leaves and the levels of carbon-reduction-cycle intermediates. Planta **160:** 305-313

Bajehbaj AA (2010) The effects of NaCl priming on salt tolerance in sunflower germination and seedling grown under salinity conditions. African Journal of Biotechnology **9:** 1764-1770

Baker NR (2008) Chlorophyll Fluorescence: A Probe of Photosynthesis *In Vivo* doi:10.1146/annurev.arplant.59.032607.092759. Annual Review of Plant Biology **59:** 89-113

Bañon S, Fernandez JA, Franco JA, Torrecillas A, Alarcón JJ, Sánchez-Blanco MJ (2004) Effects of water stress and night temperature preconditioning on water relations and morphological and anatomical changes of Lotus creticus plants. Scientia Horticulturae **101:** 333-342

Barbour MM, Warren CR, Farquhar GD, Forrester G, Brown H (2010) Variability in mesophyll conductance between barley genotypes, and effects on transpiration efficiency and carbon isotope discrimination. Plant Cell Environ

Bari G, Hamid A (1988) Salt tolerance of rice varieties and mutant strains. Pakistan J. Sci.Ind. Res., 31: 282-284

Barnabas B, Jager K, Feher A. (2008) The effect of drought and heat stress on reproductive processes in cereals. Plant, Cell and Environment **31:** 11–38.

Barrett CB (2010) Measuring Food Insecurity 10.1126/science.1182768. Science **327:** 825-828

Bassett TJ (2010) Reducing hunger vulnerability through sustainable development. *In* PNAS, Vol 107, pp 5697-5698

Batelli G, Verslues PE, Agius F, Qiu Q, Fujii H, Pan S, Schumaker KS, Grillo S, Zhu J-K (2007) SOS2 promotes salt tolerance in part by interacting with the vacuolar H^+-ATPase and upregulating its transport activity 10.1128/MCB.00430-07. Mol. Cell. Biol.: MCB.00430-00407

Bates LS, Waldren RP, Teare ID (1973) Rapid determination of free proline for water-stress studies. Plant and Soil **39:** 205-207

Battisti DS, Naylor RL (2009) Historical Warnings of Future Food Insecurity with Unprecedented Seasonal Heat 10.1126/science.1164363. Science **323:** 240-244

Beddington J (2010) Food security: contributions from science to a new and greener revolution 10.1098/rstb.2009.0201. Philosophical Transactions of the Royal Society B: Biological Sciences **365:** 61-71

Benlloch-Gonzalez M, Fournier JM, Benlloch M (2010) K^+ deprivation induces xylem water and K+ transport in sunflower: evidence for a co-ordinated control 10.1093/jxb/erp288. J. Exp. Bot. **61:** 157-164

Berger R (1985a) Methods of enzymatic analysis. Vol. VI. ldquometabolites 1: Carbohydratesrdquo. 3rd Edition. Weinheim; Deerfield Beach, Florida; Basel: Verlag Chemie, 1984 701 (724) S., 295 DM (Serienpreis); 350 DM (Einzelpreis). Acta Biotechnologica **5:** 382

Berger R (1985b) Methods of Enzymatic Analysis. Vol. VII, Metabolites II: Tri- and Dicarboxylic Acids, Purines, Pyrimidines and Perivates, Coenzymes, Inorganic Compounds (3rd edn). Acta Biotechnologica **5:** 347-357

Bernacchi CJ, Portis AR, Nakano H, von Caemmerer S, Long SP (2002) Temperature Response of Mesophyll Conductance. Implications for the Determination of Rubisco Enzyme Kinetics and for Limitations to Photosynthesis *in Vivo* 10.1104/pp.008250. Plant Physiol. **130:** 1992-1998

Berry J, Bjorkman O (1980) Photosynthetic Response and Adaptation to Temperature in Higher Plants doi:10.1146/annurev.pp.31.060180.002423. Annual Review of Plant Physiology **31:** 491-543

Bhatnagar-Mathur P, Vadez V, Sharma K (2008) Transgenic approaches for abiotic stress tolerance in plants: retrospect and prospects. In Plant Cell Reports, Vol 27. Springer Berlin / Heidelberg, pp 411-424

Björkman O, Demmig B (1987) Photon yield of O2 evolution and chlorophyll fluorescence characteristics at 77 K among vascular plants of diverse origins. Planta **170:** 489-504

Bloem MW, Semba RD, Kraemer K (2010) Castel Gandolfo Workshop: An Introduction to the Impact of Climate Change, the Economic Crisis, and the Increase in the Food Prices on Malnutrition 10.3945/jn.109.112094. J. Nutr. **140:** 132S-135

Blum A (1996) Crop responses to drought and the interpretation of adaptation. Plant Growth Regulation **20:** 135-148

Blumwald E, Aharon GS, and Apse MP (2000) Sodium transport in plant cells. *Biochem.Biophys.Acta 1465:140-151.* **1465:** 140-151

Bohnert HJ, Gong Q, Li P, Ma S (2006) Unraveling abiotic stress tolerance mechanisms - getting genomics going. Current Opinion in Plant Biology Genome studies and molecular genetics: Part 1: Model legumes / edited by Nevin D Young and Randy C Shoemaker; Part 2: Maize genomics / edited by Susan R Wessler. Plant biotechnology / edited by John Salmeron and Luis R Herrera-Estrella **9:** 180-188

Bossio D, Geheb K, Critchley W (2010) Managing water by managing land: Addressing land degradation to improve water productivity and rural livelihoods. Agricultural Water Management Comprehensive Assessment of Water Management in Agriculture **97:** 536-542

Brown RaN, L. (2000) Leading wildlife academic programs into the new millennium. Wildlife Society Bulletin **28:** 495-502

Buchanan BB, Gruissem W, Jones RL (2000) Biochemistry and Molecular Biology of Plants. AmericanSociety of Plant Physiologists, Rockville, MD .

Bucks DA, F.S. Nakayama, O.F. French (1984) Water management for guayule rubber production. ASABE. **27** (6): 1763-1770.

Bugg MW, Whitmarsh J, Rieck CE, Cohen WS (1980) Inhibition of photosynthetic electron transport by diphenyl ether herbicides. JournalPlant Physiology **65:** 47-50

Bukhov NG, Wiese C, Neimanis S, Heber U (1999) Heat sensitivity of chloroplasts and leaves: Leakage of protons from thylakoids and reversible activation of cyclic electron transport. In Photosynthesis Research, Vol 59. Springer Netherlands, pp 81-93

Bureau U-C (2004) Global population at a glance: 2002 and beyond. *In* International Brief, Washington, DC: US Census Bureau.

Byerlee D, Husain T (1993) Agricultural Research Strategies for Favoured and Marginal Areas: the Experience of Farming Systems Research in Pakistan doi:10.1017/S0014479700020603. Experimental Agriculture **29:** 155-171

von Caemmerer S, Quick WP (2000) Rubisco: physiology invivo. In Photosynthesis: Physiology and Metabolism (eds R.C. Leegood, T.D. Sharkey & S. von Caemmerer), pp. 85–113. Kluwer Academic, Dordrecht, the Netherlands.

von Caemmerer S, Farquhar G, Berry J (2009) Biochemical Model of C$_3$ Photosynthesis. In A Laisk, L Nedbal, Govindjee, eds, Photosynthesis *in silico* **29:** pp 209-230

Caliński, Tadeusz and Kageyama, Sanpei (2000) Block designs: A Randomization approach, Volume I: Analysis. Lecture Notes in Statistics. **150**. New York: Springer-Verlag. ISBN 0-387-98578-6

Camejo D, Rodríguez P, Angeles Morales M, Miguel Dell'Amico J, Torrecillas A, Alarcón JJ (2005) High temperature effects on photosynthetic activity of two tomato cultivars with different heat susceptibility. Journal of Plant Physiology **162:** 281-289

Carr MKV (1972) The Climatic Requirements of the Tea Plant: A Review doi:10.1017/S0014479700023449. Experimental Agriculture **8:** 1-14

Cen Y-P, Sage RF (2005) The Regulation of Rubisco Activity in Response to Variation in Temperature and Atmospheric CO2 Partial Pressure in Sweet Potato 10.1104/pp.105.066233. Plant Physiol. **139:** 979-990

Chandler PM, Robertson M (1994) Gene Expression Regulated by Abscisic Acid and its Relation to Stress Tolerance doi:10.1146/annurev.pp.45.060194.000553. Annual Review of Plant Physiology and Plant Molecular Biology **45:** 113-141

Cheikh N, Jones RJ (1994) Disruption of Maize Kernel Growth and Development by Heat Stress. Plant Physiol. **106:** 45-51

Chi W-T, Fung Rwm, Liu H-C, Hsu C-C, Charng Y-Y (2009) Temperature-induced lipocalin is required for basal and acquired thermotolerance in *Arabidopsis*. Plant, Cell & Environment **32:** 917-927

Chinnusamy V, Jagendorf A, Zhu J-K (2005) Understanding and Improving Salt Tolerance in Plants. Crop Sci **45:** 437-448

Colmer TD, Munns R, Flowers TJ (2005) Improving salt tolerance of wheat and barley: future prospects doi:10.1071/EA04162. Australian Journal of Experimental Agriculture **45:** 1425-1443

Cooper PJM, Gregory PJ, Tully D, Harris HC (1987) Improving Water use Efficiency of Annual Crops in the Rainfed Farming Systems of West Asia and North Africa doi:10.1017/S001447970001694X. Experimental Agriculture **23:** 113-158

Cornic G (2000) Drought stress inhibits photosynthesis by decreasing stomatal aperture - not by affecting ATP synthesis. Trends in Plant Science **5:** 187-188

Corwin DL, Kaffka SR, Hopmans JW, Mori Y, van Groenigen JW, van Kessel C, Lesch SM, Oster JD (2003) Assessment and field-scale mapping of soil quality properties of a saline-sodic soil. Geoderma The assessment of soil quality **114:** 231-259

Crafts-Brandner SJ, Salvucci ME (2002) Sensitivity of Photosynthesis in a C4 Plant, Maize, to Heat Stress 10.1104/pp.002170. Plant Physiol. **129:** 1773-1780

Cramer GR (2002) Response of abscisic acid mutants of *Arabidopsis* to salinity doi:10.1071/PP01132. Functional Plant Biology **29:** 561-567

Cramer GR, Bowman DC (1991) Kinetics of Maize Leaf Elongation 10.1093/jxb/42.11.1417 Journal of Experimental Botany **42** 1417-1426

Cramer G, Ali Ergül , Grimplet J, Tillett R, Tattersall E, Bohlman M, Vincent D, Sonderegger J, Evans J, Osborne C, Quilici D, Schlauch K, Schooley D, Cushman J (2007) Water and salinity stress in grapevines: early and late changes in transcript and metabolite profiles. In Functional & Integrative Genomics, **7:** pp 111-134

De Las Rivas J, Barber J (1997) Structure and Thermal Stability of Photosystem II Reaction Centers Studied by Infrared Spectroscopyâ€ Biochemistry **36:** 8897-8903

De Ronde JA, Cress WA, Krüger GHJ, Strasser RJ, Van Staden J (2004) Photosynthetic response of transgenic soybean plants, containing an *Arabidopsis* P5CR gene, during heat and drought stress. Journal of Plant Physiology **161:** 1211-1224

Demirevska-Kepova K, Holzer R, Simova-Stoilova L, Feller U (2005) Heat stress effects on ribulose-1,5-bisphosphate carboxylase/oxygenase, Rubisco binding protein and Rubisco activase in wheat leaves. Biologia Plantarum **49:** 521-525

Derek Eamus, Daniel T, Taylor, Catriona MO, Macinnis-NG, & SS, Lionel De Silva (2007) Comparing model predictions and experimental data for the response of stomatal conductance and guard cell turgor to manipulations of cuticular conductance, leaf-to-air vapour pressure difference and temperature: feedback mechanisms are able to account for all observations. Plant, Cell & Environment **31:** 269-277

Diamant S, Eliahu N, Rosenthal D, Goloubinoff P (2001) Chemical Chaperones Regulate Molecular Chaperones in Vitro and in Cells under Combined Salt and Heat Stresses. The Journal of Biological Chemistry**:** 39586-39591

Drake BG (1976) Estimating water status and biomass of plant communities by remote sensing. In Lange, O.L., L. Kappen, and E. D. Shultze (Eds.). Water and Plant Life. Springer-Verlag, Berlin, Germany**:** 572-575

Egamberdieva D, Renella G, Wirth S, Islam R (2010) Secondary salinity effects on soil microbial biomass. Biology and Fertility of Soils **46:** 445-449

Ehlers JD, Hall AE (1998) Heat tolerance of contrasting cowpea lines in short and long days. Field Crops Research **55:** 11-21

Evans JR, Loreto F (2000) Acquisition and diffusion of CO_2 in higher plant leaves. In Photosynthesis: Physiology and Metabolism (eds R.C. Leegood, T.D. Sharkey & S. von Caemmerer), pp. 321–351. Kluwer Academic, Dordrecht, the Netherlands.

Fageria NK (1992) Maximizing crop yields. Marcel Deker, New York

FAO (1991) An international action program on water and sustainable agricultural development. A Strategy for the Implementation of the Mar del Pints Action Plan of the 1990s. Rome, Italy: FAO. Food blance sheets (Rome)

FAO (2009) The State of Agricultural Commodity Markets 2009. *In*, http://www.fao.org/docrep/012/i0854e/i0854e00.htm

Farooq M, Wahid A, Kobayashi N (2009) Plant drought stress: effects, mechanisms and management. Agron. Sustain. Dev. **29:** 185-212

Farquhar GD, Caemmerer S, Berry JA (1980) A biochemical model of photosynthetic CO_2 assimilation in leaves of C3 species. Planta **149:** 78-90

Farquhar GD, Sharkey TD (1982) Stomatal conductance and photosynthesis. Annu.Rev.Plant Physiol **33**

Feder ME, Hofmann GE (1999) Heat-Shock Proteins, Molecular Chaperones, And The Stress Response: Evolutionary and Ecological Physiology doi:10.1146/annurev.physiol.61.1.243. Annual Review of Physiology **61:** 243-282

Fernández-Ballester G G-SF, Cerdá A, Martínez V. (2003) Tolerance of citrus rootstock seedlings to saline stress based on their ability to regulate ion uptake and transport. Tree Physiol. **23:** 265-271

Finnegan EJ (2010) DNA Methylation: a Dynamic Regulator of Genome Organization and Gene Expression in Plants. In EC Pua, MR Davey, eds, Plant Developmental Biology - Biotechnological Perspectives. Springer Berlin Heidelberg, pp 295-323

Fischer Gn, Shah M, N. Tubiello F, van Velhuizen H (2005) Socio-economic and climate change impacts on agriculture: an integrated assessment, 1990 to 2080 10.1098/rstb.2005.1744. Philosophical Transactions of the Royal Society B: Biological Sciences **360:** 2067-2083

Fischer RAT, Edmeades GO (2010) Breeding and Cereal Yield Progress 10.2135/cropsci2009.10.0564. Crop Sci **50:** S-85-98

Flexas J, Medrano H (2002) Drought-inhibition of Photosynthesis in C3 Plants: Stomatal and Non-stomatal Limitations Revisited 10.1093/aob/mcf027. Ann Bot **89:** 183-189

Flexas J, Bota J, Loreto F, Cornic G, Sharkey TD (2004) Diffusive and Metabolic Limitations to Photosynthesis under Drought and Salinity in C_3 Plants. Plant Biology **6:** 269-279

Flowers TJ (2004) Improving crop salt tolerance 10.1093/jxb/erh003. J. Exp. Bot. **55:** 307-319

Flowers TJ, Troke PF, Yeo AR (1977) The Mechanism of Salt Tolerance in Halophytes doi:10.1146/annurev.pp.28.060177.000513. Annual Review of Plant Physiology **28:** 89-121

Francois LE, Maas EV, Donovan TJ, Youngs VL (1986) Effect of salinity on grain yield and quality, vegetative growth, and germination of semi-dwarf and durum wheat. Agron. J. **78**: 1053-1058.

Fricke W, Akhiyarova G, Wei W, Alexandersson E, Miller A, Kjellbom PO, Richardson A, Wojciechowski T, Schreiber L, Veselov D, Kudoyarova G, Volkov V (2006) The short-term growth response to salt of the developing barley leaf 10.1093/jxb/erj095 Journal of Experimental Botany **57** 1079-1095

Fricke W, Akhiyarova G, Veselov D, Kudoyarova G (2004) Rapid and tissue specific changes in ABA and in growth rate in response to salinity in barley leaves 10.1093/jxb/erh117 Journal of Experimental Botany **55** 1115-1123

Fricke W, Peters WS (2002) The Biophysics of Leaf Growth in Salt-Stressed Barley. A Study at the Cell Level 10.1104/pp.001164. Plant Physiol. **129:** 374-388

Fu H-H, Luan S (1998) AtKUP1: A Dual-Affinity K+ Transporter from Arabidopsis 10.1105/tpc.10.1.63. Plant Cell 10: 63-74

Fukuda A, Nakamura A, Tanaka Y (1999) Molecular cloning and expression of the Na+/H+ exchanger gene in Oryza sativa. Biochimica et Biophysica Acta (BBA) - Bioenergetics **1446**: 149-155

Gardner B, Hardie I, Parks PJ (2010) United States Farm Commodity Programs and Land Use 10.1093/ajae/aap039. American Journal of Agricultural Economics **92:** 803-820

Gardens E (2009) Gardens feeling the heat. *In* Garden Evolution, Gardening for every one. http://www.gardenevolution.co.uk/?p=33

Gaxiola RA, Rao R, Sherman A, Grisafi P, Alper SL, Fink GR (1999) The Arabidopsis thaliana proton transporters, AtNhx1 and Avp1, can function in cation detoxification in yeast Proceedings of the National Academy of Sciences of the United States of America **96:** 1480-1485

Gaxiola RA, Li JS, Undurraga S, Dang LM, Allen GJ (2001) Drought- and salttolerant plants result from overexpression of the AVP1 H$^+$-pump. Proc. Natl. Acad. Sci. USA **98:**11444–49

Gerhardt R, Stitt M, Heldt HW (1987) Subcellular Metabolite Levels in Spinach Leaves : Regulation of Sucrose Synthesis during Diurnal Alterations in Photosynthetic Partitioning 10.1104/pp.83.2.399. Plant Physiol. **83:** 399-407

Ghars MA, Parre E, Debez A, Bordenave M, Richard L, Leport L, Bouchereau A, Savouré A, Abdelly C (2008) Comparative salt tolerance analysis between Arabidopsis thaliana and Thellungiella halophila, with special emphasis on K^+/Na^+ selectivity and proline accumulation. Journal of Plant Physiology **165:** 588-599

Genty B, Briantais J-M, Baker NR (1989) The relationship between the quantum yield of photosynthetic electron transport and quenching of chlorophyll fluorescence. Biochimica et Biophysica Acta (BBA) - General Subjects **990:** 87-92

Gibon Y, Vigeolas H, Tiessen A, Geigenberger P, Stitt M (2002) Sensitive and high throughput metabolite assays for inorganic pyrophosphate, ADPGlc, nucleotide phosphates, and glycolytic intermediates based on a novel enzymic cycling system. Plant J. **30**

Gibson LR, Mullen RE (1996) Influence of Day and Night Temperature on Soybean Seed Yield. Crop Sci **36:** 98-104

Glenn EP, Brown JJ, Blumwald E (1999) Salt Tolerance and Crop Potential of Halophytes. Critical Reviews in Plant Sciences **18:** 227 - 255

Gomez J, Sanchez-Martinez D, Stiefel V, Rigau J, Puigdomenech P, Pages M (1988) A gene induced by the plant hormone abscisic acid in response to water stress encodes a glycine-rich protein. **334:** 262-264

Goss R, Jakob T (2010) Regulation and function of xanthophyll cycle-dependent photoprotection in algae. Photosynthesis Research **106**, (1-2): 103-122

Grafen A, Hails R (2002) Modern statistics for the life sciences Oxford University Press, USA ISBN: 0199252319

Grattan SR (2010) Irragation Water salinity and crop production. *In* FWQP Reference Sheet, Vol 9

Greenway H, Munns R (1980) Mechanisms of Salt Tolerance in Nonhalophytes doi:10.1146/annurev.pp.31.060180.001053. Annual Review of Plant Physiology **31:** 149-190

Greenway H. Osmond CB (1972) Salt responses of enzymes from species differing in salt tolerance. Plant Physiology **49:** 256–259.

Griffiths H, Parry M (2002) Plant Responses to Water Stress 10.1093/aob/mcf159. Ann Bot **89:** 801-802

Grieve CM, Francois LE, Maas EV (1994) Salinity Affects the Timing of Phasic Development in Spring Wheat. Crop Sci. **34:** 1544-1549

Gross Y, Kigel J (1994) Differential sensitivity to high temperature of stages in the reproductive development of common bean (Phaseolus vulgaris L.). Field Crops Research **36:** 201-212

Guilioni L, Wery J, Tardieu F (1997) Heat Stress-induced Abortion of Buds and Flowers in Pea: Is Sensitivity Linked to Organ Age or to Relations between Reproductive Organs? 10.1006/anbo.1997.0425. Ann Bot **80:** 159-168

Guo Y-P, Zhou H-F, Zhang L-C (2006) Photosynthetic characteristics and protective mechanisms against photooxidation during high temperature stress in two citrus species. Scientia Horticulturae **108:** 260-267

Haimeirong, Haimeirong, Kubota F, Yoshimura Y (2002) Estimation of Photosynthetic Activity from the Electron Transport Rate of Photosystem 2 in a Film-Sealed Leaf of Sweet Potato, Ipomoea batatas Lam. Photosynthetica **40:** 337-341

Hajibagheri MA, Yeo AR, Flowers TJ, Collins JC (1989) Salinity resistance in *Zea mays* fluxes of potassium, sodium and chloride, cytoplasmic concentrations and microsomal membrane lipids, Plant, Cell and Envir. **12**: 753-757.

Hall A (1992) Breeding for heat tolerance. Plant Breed Rev **10:** 129-168

Hall A (2001) Crop responses to environment. CRC Press LLC, U.S.

Haldimann P, Feller U (2005) Growth at moderately elevated temperature alters the physiological response of the photosynthetic apparatus to heat stress in pea (Pisum sativum L.) leaves. Plant, Cell & Environment **28:** 302-317

Hanson BR, Ayars JE (2002) Strategies for reducing subsurface drainage in irrigated agriculture through improved irrigation. Irrigation and Drainage Systems **16:** 261-277

Harley PC, Sharkey TD (1991) An improved model of C3 photosynthesis at high CO_2: Reversed O_2 sensitivity explained by lack of glycerate reentry into the chloroplast. In Photosynthesis Research, Vol 27. Springer Netherlands, pp 169-178

Haro R, Ba nuelos MA, Senn MAE, Barrero-Gil J, Rodr´ıguez-Navarro A (2005) HKT1 mediates sodium uniport in roots. Pitfalls in the expression of HKT1 in yeast. Plant Physiol **139:**1495–506

Hasegawa PM, Bressan RA, Zhu J-K, Bohnert HJ (2000) Plant cellular and molecular responses to high salinity. Annu. Rev. Plant Physiol. Plant Mol. Biol. **51:** 463–99

Hendrickson L, Ball MC, Wood JT, Chow WS, Furbank RT (2004) Low temperature effects on photosynthesis and growth of grapevine. Plant, Cell & Environment **27:** 795-809

Hernández JA, Olmos E, Corpas FJ, Sevilla F, del Río LA (1995) Salt-induced oxidative stress in chloroplasts of pea plants. Plant Science **105:** 151-167

Hernandez F, Sancho JV, Pozo OJ (2005) Critical review of the application of liquid chromatography/mass spectrometry to the determination of pesticide residues in biological samples. Anal. Bioanal. Chem **382:** 934-946

Hirayama T, Shinozaki K (2010) Research on plant abiotic stress responses in the post-genome era: past, present and future. The Plant Journal **61:** 1041-1052

Hoagland DR, Arnon DI (1950) The water culture method of growing plants without soil. *In Experiment Station circular* California Agricultural., pp 347-360

Hong Z, Lakkineni K, Zhang Z, Verma DPS (2000) Removal of Feedback Inhibition of Delta 1-Pyrroline-5-Carboxylate Synthetase Results in Increased Proline Accumulation and Protection of Plants from Osmotic Stress 10.1104/pp.122.4.1129. Plant Physiol. **122:** 1129-1136

Hoque MA, Banu MNA, Okuma E, Amako K, Nakamura Y, Shimoishi Y, Murata Y (2007) Exogenous proline and glycinebetaine increase NaCl-induced ascorbate-glutathione cycle enzyme activities, and proline improves salt tolerance more than glycinebetaine in tobacco Bright Yellow-2 suspension-cultured cells. Journal of Plant Physiology **164:** 1457-1468

Howarth CJ (2005) Genetic improvement of growth and survival at high temperature. Abiotic stresses: plant resistance through breeding …, 2005 - cadair.aber.ac.uk

Huang Y, Zhang G, Wu F, Chen J, Zhou M (2006) Differences in Physiological Traits Among Salt-Stressed Barley Genotypes. Communications in Soil Science and Plant Analysis **37:** 557 - 570

Hübner S, Höffken M, Oren E, Haseneyer G, Stein N, Graner A, Schmid K, Fridman E (2009) Strong correlation of wild barley (*Hordeum spontaneum*) population structure with temperature and precipitation variation. Molecular Ecology **18:** 1523-1536

Hussain MK, Rehman OU (1995) Breeding sunflower for salt tolerance: association of shoot growth and mature plant traits for salt tolerance in cultivated sunflower (*Helianthus annuus* L.), Helia. **18**: 69-76.

Hussain MK, Rehman OU (1997) Evaluation of sunflower (*Helianthus annuus* L.) germplasm for salt tolerance at the shoot stage. Helia. **20**: 69-78.

Husain S, Munns R, Condon AGT (2003) Effect of sodium exclusion trait on chlorophyll retention and growth of durum wheat in saline soil doi:10.1071/AR03032. Australian Journal of Agricultural Research **54:** 589-597

Huxman TE, Barron-Gafford G, Gerst KL, Angert AL, Tyler AP, Venable DL (2008) Photosynthetic Resource-Use Efficiency And Demographic Variability In Desert Winter Annual Plants Doi:10.1890/06-2080.1. Ecology **89:** 1554-1563

Iglesias-Acosta M, Martínez-Ballesta MC, Teruel JA, Carvajal M (2010) The response of broccoli plants to high temperature and possible role of root aquaporins. Environmental and Experimental Botany **68**: 83-90

Izanloo A, Condon AG, Langridge P, Tester M, Schnurbusch T (2008) Different mechanisms of adaptation to cyclic water stress in two South Australian bread wheat cultivars 10.1093/jxb/ern199. J. Exp. Bot. **59**: 3327-3346

James RA, Rivelli AR, Munns R, Caemmerer Sv (2002) Factors affecting CO2 assimilation, leaf injury and growth in salt-stressed durum wheat doi:10.1071/FP02069. Functional Plant Biology **29**: 1393-1403

James RA, Munns R, von Caemmerer S, Trejo C, Miller C, Condon TAG (2006) Photosynthetic capacity is related to the cellular and subcellular partitioning of Na+, K+ and Cl- in salt-affected barley and durum wheat. Plant, Cell & Environment **29**: 2185-2197

James RA, von Caemmerer S, (Tony) Condon AG, Zwart AB, Munns R (2008) Genetic variation in tolerance to the osmotic stress componentof salinity stress in durum wheat doi:10.1071/FP07234. Functional Plant Biology **35**: 111-123

Jamil M, Rha ES (2004) The effect of salinity (NaCl) on the germination and seedling of sugar beet (*Beta vulgaris* L.) and cabbage (*Brassica oleracea capitata* L.), Korean J. plant Res. **7**: 226-232.

Jeannette S, Craig R, Lynch JP (2002) Salinity tolerance of phaseolus species during germination and early seedling growth, Crop Sci. **42**: 1584-1594

Jiang Y, Huang B (2000) Effects of Drought or Heat Stress Alone and in Combination on Kentucky Bluegrass. Crop Sci **40**: 1358-1362

John P, Moorea, Ma¨ ite Vicre′ -Gibouinb, and JMF, Driouichb A (2008) Adaptations of higher plant cell walls to water loss:drought vs desiccation. Physiologia Plantarum **134**: 237–245

Jones RA (1993) Developing Crops Better Adapted To Saline Environments: Progress, Puzzles And Constraints. Acta Hort. (ISHS) **323**: 461-476

June T, Evans JR, Farquhar GD (2004) A simple new equation for the reversible temperature dependence of photosynthetic electron transport: a study on soybean leaf doi:10.1071/FP03250. Functional Plant Biology **31**: 275-283

Kalra N, Chander S, Pathak H, Aggarwal PK, Gupta NC, Sehgal M, Chakraborty D (2007) Impacts of climate change on agriculture. Outlook on Agriculture **36**: 109-118

Kamei, A., Seki, M., Umezawa, T., Ishida, J., Satou, M., Akiyama, K., Zhu, J. K., and Shinozaki, K. (2005). Analysis of gene expression profiles in Arabidopsis salt overly sensitive mutants sos2-1 and sos3 -1. *Plant, Cell & Environment* **28:** 1267-1275.

Karim MA, Fracheboud Y, Stamp P (1999) Photosynthetic activity of developing leaves of (*Zea mays*) is less affected by heat stress than that of developed leaves. Physiologia Plantarum **105:** 685-693

Khan MA, Ahmed S, Begum I, Alvi AS, M. S. Mughal (1999) Development of barley as a feed/fodder crop for the Mediterranean environment of highland Balochistan, Pakistan. Cah. Opt. Mediterr**:** 229-233

Khan MAA, S.; Begum, I.; Jalil, S.A.; Alvi, A. (1997) Evaluation of exotic barley germplasm for biotic and abiotic stresses in Mediterranean highland Baluchistan. RACHIS (ICARDA); Barley and Wheat Newsletter **16:** 32-40

Khan MJ, Razzaq A, Khattak MK, Garcia L (2009) Effect of different pre-sowing water application depths on wheat yield under spate irrigation in Dera Ismael Khan District of Pakistan. Agricultural Water Management **96:** 1467-1474

Kern J, Zouni A, Guskov A, KrauÃŸ N (2009) Lipids in the Structure of Photosystem I, Photosystem II and the Cytochrome b6f Complex. In Lipids in Photosynthesis, pp 203-242

Kirschbaum M, Farquhar G (1984) Temperature Dependence of Whole-Leaf Photosynthesis in (*Eucalyptus pauciflora*) Sieb. Ex Spreng doi:10.1071/PP9840519. Functional Plant Biology **11:** 519-538

Kishore GM, Shewmaker C (1999) Biotechnology: Enhancing human nutrition in developing and developed worlds Proceedings of the National Academy of Sciences of the United States of America **96:** 5968-5972

Kishore P, Sangam S, Amrutha RN, Laxmi P, Naidu K, Rao K, Rao S, Reddy K, Theriappan P, Sreenivasulu N (2005) Regulation of proline biosynthesis, degradation, uptake and transport in higher plants: its implications in plant growth and abiotic stress tolerance. Curr Sci **88:** 428-434

Kobza J, Edwards GE (1987) Influences of leaf temperature on photosynthetic carbon metabolism in wheat. Plant Physiology **83:** 69–74.

Kramer PJ, Boyer JS (1995) Water Relations of Plants and Soils. Academic Press, San Diego, CA-USA.

Kurek I, Chang TK, Bertain SM, Madrigal A, Liu L, Lassner MW, Zhu G (2007) Enhanced Thermostability of Arabidopsis Rubisco Activase Improves Photosynthesis and Growth Rates under Moderate Heat Stress 10.1105/tpc.107.054171. Plant Cell **19:** 3230-3241

Lakhdar A, Rabhi M, Ghnaya T, Montemurro F, Jedidi N, Abdelly C (2009) Effectiveness of compost use in salt-affected soil. Journal of Hazardous Materials **171:** 29-37

Lang T (2010) Crisis? What Crisis? The Normality of the Current Food Crisis. Journal of Agrarian Change **10:** 87-97

Langridge P, Paltridge N, Fincher G (2006) Functional genomics of abiotic stress tolerance in cereals 10.1093/bfgp/eli005. Briefings in Functional Genomics and Proteomics **4:** 343-354

LaRosa PC, Hasegawa PM, Rhodes D, Clithero JM, Watad A-EA, Bressan RA (1987) Abscisic Acid Stimulated Osmotic Adjustment and Its Involvement in Adaptation of Tobacco Cells to NaCl 10.1104/pp.85.1.174. Plant Physiol. **85:** 174-181

Läuchli A (1984) Salt exclusion: An adaptation of legumes for crops and pastures under saline conditions. In Salinity tolerance in plants. Strategies for crop improvement. R C Staples and GH Toenniessen John Wiley and Sons,, New York

Laurie S, Feeney KA, Maathuis FJM, Heard PJ, Brown SJ, Leigh RA (2002) A role for HKT1 in sodium uptake by wheat roots. Plant J. **32:**139–49

Lawlor DW (1995) The effects of water deficit on photosynthesis. In Environmental and Plant Metabolism: Flexibility and Acclimation(ed. N. Smirnoff). BIOS Scientific Publishers, **:** 129-160.

Lee H, Cheng Y-C, Fleming GRWshl-lceetriapcboaaodcuandtec (2009) Quantum Coherence Accelerating Photosynthetic Energy Transfer. *In* Ultrafast Phenomena XVI, pp 607-609

Lessani H, Marschner H (1978) Relation Between Salt Tolerance and Long-Distance Transport of Sodium and Chloride in Various Crop Species doi:10.1071/PP9780027. Functional Plant Biology **5:** 27-37

Li C, Zhang G, Lance R (2007) Recent Advances in Breeding Barley for Drought and Saline Stress Tolerance. *In* Advances in Molecular Breeding Toward Drought and Salt Tolerant Crops, pp 603-626

Lindahl M, Spetea C, Hundal T, Oppenheim AB, Adam Z, Andersson B (2000) The Thylakoid FtsH Protease Plays a Role in the Light-Induced Turnover of the Photosystem II D1 Protein 10.1105/tpc.12.3.419. Plant Cell **12**: 419-432

Liu W, Fairbairn DJ, Reid RJ, Schachtman DP (2001) Chracterization of twoHKT1homologues from Eucalyptus camaldulensis that display intrinsic osmosensing capability. Plant Physiol. **127:** 283-294

Lobell DB, Asner GP (2003) Climate and management contributions to recent trends in U.S. agricultural yields. Science **299:** 1032

Loreto F, Peter C, Harley, Marco GD, Sharkey TD (1992) Estimation of Mesophyll Conductance to CO_2 Flux by Three Different Methods Plant Physiol **98**

Lu X-Y, Huang X-L (2008) Plant miRNAs and abiotic stress responses. Biochemical and Biophysical Research Communications **368:** 458-462

Lunn JE, Feil R, Hendriks JH, Gibon Y, Morcuende R, Osuna D, Scheible WR, Carillo P, Hajirezaei MR, Stitt M (2006) Sugar-induced increases in trehalose 6-phosphate are correlated with redox activation of ADPglucose pyrophosphorylase and higher rates of starch synthesis in Arabidopsis thaliana. Biochem. J. **397:** 139-148

Luo B, Groenke K, Takors R, Wandrey C, Oldiges M (2007) Simultaneous determination of multiple intracellular metabolites in glycolysis, pentose phosphate pathway and tricarboxylic acid cycle by liquid chromatography-mass spectrometry. Journal of Chromatography A **1147:** 153-164

Maas EV, Grieve CM (1987) Sodium-induced calcium deficiency in salt-stressed corn. Plant, Cell and Environment **10:** 559-564

Maccaferri M, Sanguineti MC, Giuliani S, Tuberosa R (2009) Genomics of Tolerance to Abiotic Stress in the Triticeae. *In* Genetics and Genomics of the Triticeae, pp 481-558

Maeshima M (2001) Tonoplast Transporters: Organization and Function doi:10.1146/annurev.arplant.52.1.469. Annual Review of Plant Physiology and Plant Molecular Biology **52:** 469-497

Maestri E, Klueva N, Perrotta C, Gulli M, Nguyen HT, Marmiroli N (2002) Molecular genetics of heat tolerance and heat shock proteins in cereals. Plant Molecular Biology **48:** 667-681

Magnotta S, Gogarten J (2002) Multi site polyadenylation and transcriptional response to stress of a vacuolar type H^+-ATPase subunit A gene in Arabidopsis thaliana. BMC Plant Biology **2:** 3

Mahmood A, Latif T, Khan MA (2009) Effect Of Salinity On Growth, Yield And Yield Components In Basmati Rice Germplasm. Pak. J. Bot. 41: 3035-3045

Makino A, Nakano H, Mae T (1994) Effects of growth temperature on the responses of ribulose-1,5-bisphosphate carboxylase, electron-transport components, and sucrose synthesis enzymes to leaf nitrogen in rice, and their relationships to photosynthesis. Plant Physiology **105:** 1231–1238.

Malcolm CV, 1933- (1982) Wheatbelt salinity : a review of the salt land problem in south western Australia / by C.V. Malcolm ; editor: C.H. Trotman. Western Australian Dept. of Agriculture, [Perth, W.A.]:

Mann CC (1999) FUTURE FOOD:Crop Scientists Seek a New Revolution 10.1126/science.283.5400.310. Science **283:** 310-314

Marchand FL, Mertens S, Kockelbergh F, Beyens L, Nijs I (2005) Performance of High Arctic tundra plants improved during but deteriorated after exposure to a simulated extreme temperature event. Global Change Biology **11:** 2078-2089

Marchione TJ, Messer E (2010) Food Aid and the World Hunger Solution: Why the U.S. Should Use a Human Rights Approach. Food and Foodways: Explorations in the History and Culture of **18:** 10 - 27

Mass EV, Grieve CM (1987) Sodium-induced calcium deficiency in salt-stressed corn. Plant Cell Environ **10**: 559-564

Massoud F (1974) Salinity and alkalinity as soil degradation hazards. FAO; FAO/UNEP Expert Consultation on Soil Degradation, Rome (Italy), **Tab., ann.. 19 ref:** 22

Masood MS, Seiji Y, Shinwari ZK, Anwar R (2004) Mapping Quantitative Trait Loci (QTLS) for Salt Tolerance in Rice (*Oryza Sativa*) using RFLPs. Pak. J. Bot. **36:** 825-834

Mattson WJ, Haack RA (1987) The Role of Drought in Outbreaks of Plant-Eating Insects. BioScience **37:** 110-118 CR - Copyright © 1987 American Institute of Biological Sciences and University of California Press

Mazorra LM, Nunez M, Hechavarria M, Coll F, SÃ¡nchez-Blanco MJ (2002) Influence of Brassinosteroids on Antioxidant Enzymes Activity in Tomato Under Different Temperatures. Biologia Plantarum **45:** 593-596

Merlo L, Geigenberger P, Hajirezaei M, Stitt M (1993) Changes of carbohydrates, metabolites and enzyme activities in potato tubers during development, and within a single tuber along a stolon-apex gradient. J. Plant Physiol. **142:** 392-402

Mohammadi GR (2009) The Influence of NaCl Priming on Seed Germination and Seedling Growth of Canola (Brassica napus L.) Under Salinity Conditions. American-Eurasian J. Agric. & Environ. Sci. **5:** 697-700

Momcilovic I, Ristic Z (2007) Expression of chloroplast protein synthesis elongation factor, EF-Tu, in two lines of maize with contrasting tolerance to heat stress during early stages of plant development. J Plant Physiol. **1:** 90-99

Morpurgo R (1991) Correlation between Potato Clones Grown *in vivo* and *in vitro* under Sodium Chloride Stress Conditions. Plant Breeding **107:** 80-82

Mott KA, Jensen RG, Oleary JW, Berry JA (1984) Photosynthesis and ribulose 1,5-bisphosphate concentrations in intact leaves of Xanthium strumarium L. Plant Physiology **76:** 968–971.

Moya JL, Gomez-Cadenas A, Primo-Millo E, Talon M (2003) Chloride absorption in salt-sensitive Carrizo citrange and salt-tolerant Cleopatra mandarin citrus rootstocks is linked to water use 10.1093/jxb/erg064. J. Exp. Bot. **54:** 825-833

Munns R (1993) Physiological processes limiting plant growth in saline soils: some dogmas and hypotheses. Plant, Cell and Environment **16:** 15-24

Munns R, Passioura JB, Guo J, Chazen O, Cramer GR (2000) Water relations and leaf expansion: importance of time scale 10.1093/jexbot/51.350.1495 Journal of Experimental Botany 51: 1495-1504

Munns R (2005) Genes and salt tolerance: bringing them together. New Phytologist **167:** 645-663

Munns R (2009) Strategies for Crop Improvement in Saline Soils. *In* Salinity and Water Stress, Tasks for Vegetation Science, 2009, Volume 44, II, pp 99-110

Munns R, Greenway H, Kirst GO (1983) Halotolerant eukaryotes. In Physiological Plant Ecology. III. Responses to the Chemical and Biological Environment (eds O. L. Lange, P. S. Nobel, C. B. Osmond & H. H. Zeigler.), Encyclopedia of Plant Physiology, New Series, **12:** 59–135

Munns R, Termaat A (1986) Whole-Plant Responses to Salinity doi:10.1071/PP9860143. Functional Plant Biology **13:** 143-160

Munns R, Schachtman DP, Condon AG (1995) The significance of a two-phase growth response to salinity in wheat end barley. Aust.J.plant physiol **22**: 559-571

Munns R, James RA, Läuchli A (2006) Approaches to increasing the salt tolerance of wheat and other cereals. J. Exp. Bot. **57:**1025–43

Munns R, Tester M (2008) Mechanisms of Salinity Tolerance doi:10.1146/annurev.arplant.59.032607.092911. Annual Review of Plant Biology **59:** 651-681

Nevo E, Gorham J, Beiles A (1992) Variation for 22Na Uptake in Wild Emmer Wheat, *Triticum* dicoccoides in Israel: Salt Tolerance Resources for Wheat Improvement 10.1093/jxb/43.4.511. J. Exp. Bot. **43:** 511-518

Nollen EAA, Morimoto RI (2002) Chaperoning signaling pathways: molecular chaperones as stress-sensing `heat shock' proteins. J Cell Sci **115:** 2809-2816

Ona A, Gabriele P, Albinas A, Algis K (2010) Cultivar and plant density influence on weediness in spring barley. Zemdirbyste-Agriculture **97:** 53-60

Orabi J, Jahoor A, Backes G (2009) Genetic diversity and population structure of wild and cultivated barley from West Asia and North Africa. Plant Breeding **128:** 606-614

Paul MJ, Foyer CH (2001) Sink regulation of photosynthesis 10.1093/jexbot/52.360.1383 Journal of Experimental Botany 52 1383-1400

Panchuk II, Volkov RA, Schoffl F (2002) Heat Stress- and Heat Shock Transcription Factor-Dependent Expression and Activity of Ascorbate Peroxidase in Arabidopsis 10.1104/pp.001362. Plant Physiol. **129:** 838-853

Parent B, Turc O, Gibon Y, Stitt M, Tardieu F (2010) Modelling temperature-compensated physiological rates, based on the coordination of responses to temperature of developmental processes 10.1093/jxb/erq003 Journal of Experimental Botany **2:** 2-17

Parida AK, Das AB (2005) Salt tolerance and salinity effects on plants: a review. Ecotoxicology and Environmental Safety **60:** 324-349

Passioura JB, Munns R (2000) Rapid environmental changes that affect leaf water status induce transient surges or pauses in leaf expansion rate. Aust. J. Plant Physiol. **27:**941–48

Pimental, D., Huang, X., Cordova, A., and Pimental, M. (1997). Impact of population growth on food supplies and environment. *Population and Environment* **19:** 9-14.

Porter JR (2005) Rising temperatures are likely to reduce crop yields. Nature **436:** 174

Portis A (2003) Rubisco activase Rubisco's catalytic chaperone. In Photosynthesis Research, Vol 75. Springer Netherlands, pp 11-27

Pretty J (2008) Agricultural sustainability: concepts, principles and evidence 10.1098/rstb.2007.2163. Philosophical Transactions of the Royal Society B: Biological Sciences **363:** 447-465

Radin JW, Lu Z, Percy RG, Zeiger E (1994) Genetic variability for stomatal conductance in Pima cotton and its relation to improvements of heat adaptation Proceedings of the National Academy of Sciences of the United States of America **91:** 7217-7221

Rahman MA, Chikushi J, Yoshida S, Karim AJMS (2009) Growth and Yield Components of Wheat Genotypes Exposed to High Temperature Stress Under Control Environment. Bangladesh J. Agril. Res. **34:** 361-372

Rashid A, Hollington PA, Harris D, Khan P (2006) On-farm seed priming for barley on normal, saline and saline-sodic soils in North West Frontier Province, Pakistan. European Journal of Agronomy **24:** 276-281

Razzaque MA, Talukder NM, Islam MS, Bhadra AK, RK. D (2009) The effect of salinity on morphological characteristics of seven rice (Oryza sativa) genotypes differing in salt tolerance. Pak J Biol Sci. **12:** 406-412

Rees DJ, Qureshi ZA, Mehmood S, Raza SH (1991) Catchment basin water harvesting as a means of improving the productivity of rain-fed land in upland Balochistan doi:10.1017/S0021859600076188. The Journal of Agricultural Science **116:** 95-103

Rengasamy P (2006) World salinization with emphasis on Australia 10.1093/jxb/erj108. J. Exp. Bot. **57:** 1017-1023

Riadh K, Wided M, Hans-Werner K, Chedly A (2010) Responses of Halophytes to Environmental Stresses with Special Emphasis to SalinityAdvances in Botanical Research. *In* J-CKaM Delseny, ed, Ed Volume 53. Academic Press, pp 117-145

Robredo A, Pérez-López U, de la Maza HS, González-Moro B, Lacuesta M, Mena-Petite A, Muñoz-Rueda A (2007) Elevated CO2 alleviates the impact of drought on barley improving water status by lowering stomatal conductance and delaying its effects on photosynthesis. Environmental and Experimental Botany **59:** 252-263

Rodriguez-Navarro A, Quintero FJ, and Garciadeblas B (1994) Na^+-ATPases and Na^+/H^+ antiporters in fungi. *Biochimica et Biophysica Acta* **1187:** 203-205

Sade N, Vinocur BJ, Diber A, Shatil A, Ronen G, Nissan H, Wallach R, Karchi H, Moshelion M (2009) Improving plant stress tolerance and yield production: is the tonoplast aquaporin SlTIP2;2 a key to isohydric to anisohydric conversion? New Phytologist **181:** 651-661

Sage RF, Sharkey TD (1987) The effect of temperature on the occurrence of O2 and CO_2 insensitive photosynthesis in fieldgrown plants. **Plant Physiology 84:** 658–664

Sage RF, Sharkey TD, Seemann JR (1990) Regulation of Ribulose-1,5-Bisphosphate Carboxylase Activity in Response to Light Intensity and CO_2 in the C3 Annuals *Chenopodium album* L. and *Phaseolus vulgaris* L. 10.1104/pp.94.4.1735. Plant Physiol. **94:** 1735-1742

Sage RF, Kubien DS (2007) The temperature response of C3 and C4 photosynthesis. Plant, Cell & Environment **30:** 1086-1106

Sairam RK, Tyagi A (2004) Physiology and molecular biology of salinity stress tolerance in plants. Current Science **86:** 407-421

Sajid Aqeel Ahmad M, Javed F, Ashraf M (2007) Iso-osmotic effect of NaCl and PEG on growth, cations and free proline accumulation in callus tissue of two indica rice (<i>Oryza sativa</i> L.) genotypes. In Plant Growth Regulation, Vol 53. Springer Netherlands, pp 53-63

Sakamoto A, Murata N (2002) The role of glycine betaine in the protection of plants from stress: clues from transgenic plants. Plant, Cell & Environment **25:** 163-171

Salvucci ME, Crafts-Brandner SJ (2004a) Inhibition of photosynthesis by heat stress: the activation state of Rubisco as a limiting factor in photosynthesis. Physiologia Plantarum **120**: 179-186

Salvucci ME, Crafts-Brandner SJ (2004b) Relationship between the Heat Tolerance of Photosynthesis and the Thermal Stability of Rubisco Activase in Plants from Contrasting Thermal Environments 10.1104/pp.103.038323. Plant Physiol. **134:** 1460-1470

Salvucci ME, Crafts-Brandner SJ (2004c) Mechanism for deactivation of Rubisco under moderate heat stress. Physiologia Plantarum **122:** 513-519

Salvucci ME, Osteryoung KW, Crafts-Brandner SJ, Vierling E (2001) Exceptional Sensitivity of Rubisco Activase to Thermal Denaturation *in Vitro* and *in Vivo* 10.1104/pp.010357. Plant Physiol. **127:** 1053-1064

Sambrook J, Russell DW (2001) Molecular Cloning - A Laboratory Manual,. Cold Spring Habour Laboratory Press, New York

Sanders DW (1992) International activities in assessing and monitoring soil degradation doi:10.1017/S0889189300004392. American Journal of Alternative Agriculture **7:** 17-24

Schoffl F, Prandl R, Reindl A (1998) Regulation of the Heat-Shock Response 10.1104/pp.117.4.1135. Plant Physiol. **117:** 1135-1141

Schrader SM, Kane HJ, Sharkey TD, von Caemmerer S (2006) High temperature enhances inhibitor production but reduces fallover in tobacco Rubisco. Functional Plant Biology **33:** 921–929.

Schulte D, Close TJ, Graner A, Langridge P, Matsumoto T, Muehlbauer G, Sato K, Schulman AH, Waugh R, Wise RP, Stein N (2009) The International Barley Sequencing Consortium--At the Threshold of Efficient Access to the Barley Genome 10.1104/pp.108.128967. Plant Physiol. **149:** 142-147

Seligmann H, Amzallag GN (1995) Adaptive determinism during salt-adaptation in Sorghum bicolor. Biosystems **36:** 71-77

Serrano R and Gaxiola R (1994) Microbial models and salt stress tolerance in plants. *Crit.Rev.in plant.Sci.* **13(2):** 121-138

Shalhevet J (1994) Using water of marginal quality for crop production: major issues. Agricultural Water Management **25:** 233-269

Sharkey TD, Schrader SM (2006) High temperature stress. In Physiology and Molecular Biology of Stress Tolerance in Plants (eds K.V.M. Rao,A.S. Raghavendra & K.J. Reddy), pp. 101–129. Springer, Dordrecht, the Netherlands.

Sharkey Td, Bernacchi Cj, Farquhar Gd, Singsaas El (2007) Fitting photosynthetic carbon dioxide response curves for C3 leaves. Plant, Cell & Environment **30:** 1035-1040

Shi H, Zhu J-K (2002) Regulation of expression of the vacuolar Na$^+$/H$^+$ antiporter gene AtNHX1 by salt stress and abscisic acid. Plant Molecular Biology **50:** 543-550

Shinozaki K, Yamaguchi-Shinozaki K (1996) Molecular responses to drought and cold stress. Current Opinion in Biotechnology **7:** 161-167

Siddiqi EH, Ashraf M, Hussain M, Jamil A (2009) Assessment of Inter-Cultivar Variation for Salt Tolerance in Safflower (Carthamus Tinctorius L.) using Gas Exchange Characteristics as Selection Criteria. Pak. J. Bot. **41:** 2251-2259

Singh NK, LaRosa PC, Handa AK, Hasegawa PM, Bressan RA (1987) Hormonal regulation of protein synthesis associated with salt tolerance in plant cells Proceedings of the National Academy of Sciences of the United States of America **84:** 739-743

Sirault XRR, James RA, Furbank RT (2009) A new screening method for osmotic component of salinity tolerance in cereals using infrared thermography doi:10.1071/FP09182. Functional Plant Biology **36:** 970-977

Smertenko A, Draber P, Viklicky V and Opatrny Z (1997) Heat stress affects the organization of microtubules and cell division in *Nicotiana tabacum* cells. Plant, Cell and Environment **20:** 1534-1542

Sohrabi Y, Heidari G, Esmailpoor B (2008) Effect of salinity on growth and yield of Desi and Kabuli chickpea cultivars. Pakistan journal of biological sciences **11**: 664-667

Sokal RR, Rohlf FJ (1994) Biometry: The principles and practice of statistics in biological research. 3rd ed. WH Freeman & Co, 1994

Semenov MA, Halford NG (2009) Identifying target traits and molecular mechanisms for wheat breeding under a changing climate 10.1093/jxb/erp164 Journal of Experimental Botany **60** 2791-2804

Song L, Chow WS, Sun L, Li C, Peng C (2010) Acclimation of photosystem II to high temperature in two Wedelia species from different geographical origins: implications for biological invasions upon global warming 10.1093/jxb/erq220. J. Exp. Bot.: erq220

Stitt M, Wirtz W, Heldt HW (1980) Metabolite levels during induction in the chloroplast and extrachloroplast compartments of spinach protoplasts. Biochimica et Biophysica Acta (BBA) - Bioenergetics **593:** 85-102

Stitt M, Wirtz W, Heldt HW (1983) Regulation of Sucrose Synthesis by Cytoplasmic Fructosebisphosphatase and Sucrose Phosphate Synthase during Photosynthesis in Varying Light and Carbon Dioxide 10.1104/pp.72.3.767. Plant Physiol. **72:** 767-774

Stone P (2001) The effects of heat stress on cereal yield and quality. In: *Crop Responses and Adaptations to Temperature Stress.* (ed. A.S.Basra), pp. 243–291. Food Products Press, Binghamton, NY, USA.

Sung D-Y, Kaplan F, Lee K-J, Guy CL (2003) Acquired tolerance to temperature extremes. Trends in Plant Science **8:** 179-187

Suzuki N, Mittler R (2006) Reactive oxygen species and temperature stresses: A delicate balance between signaling and destruction. Physiologia Plantarum **126:** 45-51

Szucs Pt, Blake VC, Bhat PR, Chao S, Close TJ, Cuesta-Marcos A, Muehlbauer GJ, Ramsay L, Waugh R, Hayes PM (2009) An Integrated Resource for Barley Linkage Map and Malting Quality QTL Alignment 10.3835/plantgenome2008.01.0005. The Plant Genome **2:** 134-140

Taffouo VC, Kouamou JK, Ngalangue LM, Ndjeudji BAN, Akoa A (2009) Effects of Salinity Stress on Growth, Ions Partitioning and Yield of Some Cowpea (Vigna unguiculata L. Walp.) Cultivars. International Journal of Botany **5**: 135-143

Taiz L (1992) The Plant Vacuole. J Exp Biol **172:** 113-122

Taiz L, Zeiger E (2003) Plant physiology. 3rd edn.10.1093/aob/mcg079. Sinauer Associates, Inc, Publishers, Sunderland USA

Takemura T, Hanagata N, Sugihara K, Baba S, Karube I, Dubinsky Z (2000) Physiological and biochemical responses to salt stress in the mangrove, Bruguiera gymnorrhiza. Aquatic Botany **68:** 15-28

Terashima I, Hanba YT, Tazoe Y, Vyas P, Yano S (2006) Irradiance and phenotype: comparative eco-development of sun and shade leaves in relation to photosynthetic CO_2 diffusion 10.1093/jxb/erj014 Journal of Experimental Botany **57:** 343-354

Tester M, Davenport RJ (2003) Na^+ transport and Na^+ tolerance in higher plants. Ann. Bot. **91:**503–27

Tezara W, Mitchell VJ, Driscoll SD, Lawlor DW (1999) Water stress inhibits plant photosynthesis by decreasing coupling factor and ATP. **401:** 914-917

Thomas VC (2009) Principles of Water Resources: History, Development, Management and Policy. Technology & Engineering, Published by John Villy and Sons, USA: ISBN 978-0-470-13631-7 (pbk…).

Todorov DT, Karanov EN, Smith AR, Hall MA (2003) Chlorophyllase Activity and Chlorophyll Content in Wild Type and eti 5 Mutant of Arabidopsis thaliana Subjected to Low and High Temperatures. Biologia Plantarum **46:** 633-636

Toenniessen GH, O'Toole JC, DeVries J (2003) Advances in plant biotechnology and its adoption in developing countries. Current Opinion in Plant Biology **6:** 191-198

Toole J, Moya T (1981) Comparison of pressure chamber and psychrometer estimates of leaf water potential in rice. In Plant and Soil, Vol 62. Springer Netherlands, pp 313-317

To´th SZ, Schansker G, Kissimon J, Kova´cs L, Garab G, Strasser R (2005) Biophysical studies of photosystem II-related recovery processes after a heat pulse in barley seedlings (Hordeum vulgare L.). Journal of Plant Physiology **162**: 181-194

Tricker P, Trewin H, Kull O, Clarkson G, Eensalu E, Tallis M, Colella A, Doncaster C, Sabatti M, Taylor G (2005) Stomatal conductance and not stomatal density determines the long-term reduction in leaf transpiration of poplar in elevated CO<sub>2</sub>. In Oecologia, Vol 143. Springer Berlin / Heidelberg, pp 652-660

Tsukaguchi T, Kawamitsu Y, Takeda H, Suzuki K, Egawa Y (2003) Water status of flower buds and leaves as affected by high temperature in heat tolerant and heat-sensitive cultivars of snap bean (Phaseolus vulgaris L. Plant Prod Sci **6:** 4-27

Turner A, Beales J, Faure S, Dunford RP, Laurie DA (2005) The Pseudo-Response Regulator Ppd-H1 Provides Adaptation to Photoperiod in Barley 10.1126/science.1117619. Science **310:** 1031-1034

USDA NRCS (2002) Soil Conservationists. Salinity Management Guide - Salt Management. *In*. Available at. http://www.launionsweb.org/salinity.htm

USDA-ARS (2008) Research Databases. Bibliography on Salt Tolerance. George E. Brown, Jr. Salinity Lab. US Dep. Agric., Agric. Res. Serv. Riverside, CA.

Vinocur B, Altman A (2005) Recent advances in engineering plant tolerance to abiotic stress: achievements and limitations. Curr Opin Biotechnol. **16:** 123-132

Visioli G, Maestri E, Marmiroli N (1997) Differential display-mediated isolation of a genomic sequence for a putative mitochondrial LMWHSP specifically expressed in condition of induced thermotolerance in Arabidopsis thaliana (L.). Plant Molecular Biology **34:** 517-527

Vitale L, Di Tommasi P, Arena C, Fierro A, Virzo De Santo A, Magliulo V (2007) Effects of water stress on gas exchange of field grown Zea mays L. in Southern Italy: an analysis at canopy and leaf level. Acta Physiologiae Plantarum **29:** 317-326

Vogel JL, Parsell DA, Lindquist S (1995) Heat-shock proteins Hsp104 and Hsp70 reactivate mRNA splicing after heat inactivation. Current Biology **5:** 306-317

Wahid A, Close T (2007) Expression of dehydrins under heat stress and their relationship with water relations of sugarcane leaves. Biologia Plantarum **51:** 104-109

Wahid A, Gelani S, Ashraf M, Foolad MR (2007) Heat tolerance in plants: An overview. Environmental and Experimental Botany **61:** 199-223

Waines JG, Ehdaie B (2007) Domestication and Crop Physiology: Roots of Green-Revolution Wheat 10.1093/aob/mcm180. Ann Bot **100:** 991-998

Walia H, Wilson C, Condamine P, Liu X, Ismail Am, Close Tj (2007) Large-scale expression profiling and physiological characterization of jasmonic acid-mediated adaptation of barley to salinity stress. Plant, Cell and Environment **30:** 410-421

Wang W, Vinocur B, Shoseyov O, Altman A (2004) Role of plant heat-shock proteins and molecular chaperones in the abiotic stress response. Trends in Plant Science **9:** 244-252

Wang R, Chen S, Deng L, Fritz E, Hu̎ttermann A, Polle A (2007) Leaf photosynthesis, fluorescence response to salinity and the relevance to chloroplast salt compartmentation and anti-oxidative stress in two poplars. In Trees - Structure and Function, **21:** pp 581-591

Wang L-J, Fan L, Loescher W, Duan W, Liu G-J, Cheng J-S, Luo H-B, Li S-H (2010) Salicylic acid alleviates decreases in photosynthesis under heat stress and accelerates recovery in grapevine leaves. BMC Plant Biology **10:** 34

Warren C, Dreyer E (2006) Temperature response of photosynthesis and internal conductance to CO2: results from two independent approaches 10.1093/jxb/erl067 Journal of Experimental Botany **57:** 3057-3067

Way DA and Oren R (2010) Differential responses to changes in growth temperature between trees from different functional groups and biomes: a review and synthesis of data 10.1093/treephys/tpq015. Tree Physiol **30:** 669-688

White PJ, Broadley MR (2001) Chloride in Soils and its Uptake and Movement within the Plant: A Review 10.1006/anbo.2001.1540. Ann Bot **88:** 967-988

Wilhelm EP, Mullen RE, Keeling PL, Singletary GW (1999) Heat Stress during Grain Filling in Maize: Effects on Kernel Growth and Metabolism. Crop Sci **39:** 1733-1741

Willits DH, Peet MM (1998) The effect of night temperature on greenhouse grown tomato yields in warm climates. Agricultural and Forest Meteorology **92:** 191-202

Woodrow IE, Berry JA (1988) Enzymatic regulation of photosynthetic CO_2 fixation in C3 plants. Annual Review of Plant Physiology and Plant Molecular Biology **39,** 533–594.

Wise Rr, Olson Aj, Schrader Sm, Sharkey Td (2004) Electron transport is the functional limitation of photosynthesis in field-grown Pima cotton plants at high temperature. Plant, Cell & Environment **27:** 717-724

Xu Z, Zhou G (2008) Responses of leaf stomatal density to water status and its relationship with photosynthesis in a grass 10.1093/jxb/ern185 Journal of Experimental Botany 59 3317-3325

Yamada M, Hidaka T, Fukamachi H (1996) Heat tolerance in leaves of tropical fruit crops as measured by chlorophyll fluorescence. Scientia Horticulturae **67:** 39-48

Yamane Y, Kashino Y, Koike H, Satoh K (1998) Effects of high temperatures on the photosynthetic systems in spinach: Oxygen-evolving activities, fluorescence characteristics and the denaturation process. Photosynthesis Research **57:** 51-59

Yamasaki T, Yamakawa T, Yamane Y, Koike H, Satoh K, Katoh S (2002) Temperature Acclimation of Photosynthesis and Related Changes in Photosystem II Electron Transport in Winter Wheat 10.1104/pp.010919. Plant Physiol. **128:** 1087-1097

Yamori W, Noguchi K, Terashima I (2005) Temperature acclimation of photosynthesis in spinach leaves: analyses of photosynthetic components and temperature dependencies of photosynthetic partial reactions. Plant, Cell & Environment **28:** 536-547

Yamori W, Suzuki K, Noguchi K, Nakai M, Terashima I (2006) Effects of Rubisco kinetics and Rubisco activation state on the temperature dependence of the photosynthetic rate in spinach leaves from contrasting growth temperatures. Plant,Cell & Environment 29, 1659–1670.

Yang X, Liang Z, Lu C (2005) Genetic Engineering of the Biosynthesis of Glycinebetaine Enhances Photosynthesis against High Temperature Stress in Transgenic Tobacco Plants 10.1104/pp.105.063164. Plant Physiol. **138:** 2299-2309

Yan L, Loukoianov A, Tranquilli G, Helguera M, Fahima T, Dubcovsky J (2003) Positional cloning of the wheat vernalization gene VRN1 10.1073/pnas.0937399100 Proceedings of the National Academy of Sciences of the United States of America **100** 6263-6268

Yan L, Loukoianov A, Blechl A, Tranquilli G, Ramakrishna W, SanMiguel P, Bennetzen JL, Echenique V, Dubcovsky J (2004) The Wheat VRN2 Gene Is a Flowering Repressor Down-Regulated by Vernalization 10.1126/science.1094305. Science **303:** 1640-1644

Yensen NP (2006) Halophyte Uses For The Twenty-First Century. *In* Ecophysiology of High Salinity Tolerant Plants, pp 367-396

Yeo A (1998) Molecular biology of salt tolerance in the context of whole-plant physiology 10.1093/jxb/49.323.915. J. Exp. Bot. **49:** 915-929

Yoshida N, Castro MJL, Cirelli AFn (2010) Degradation of monensin on soils: influence of organic matter and water content. Chemistry and Ecology **26:** 27 - 33

Zadoks Jc, Chang Tt, Konzak Cf (1974) A decimal code for the growth stages of cereals. Weed Research **14:** 415-421

Zaragoza-Castells J, Sánchez-Gómez D, Hartley IP, Matesanz S, Valladares F, Lloyd J, Atkin OK (2008) Climate-dependent variations in leaf respiration in a dry-land, low productivity Mediterranean forest: the importance of acclimation in both high-light and shaded habitats. Functional Ecology **22:** 172-184

Zhang HX, Blumwald E (2001) Transgenic salt-tolerant tomato plants accumulate salt in foliage but not in fruit. Nature Biotechnology **19**: 765-768

Zhang CG, Chromy BA, McCutchen-Maloney SL (2001) Hostpathogen interactions: a proteomic view. Expert Review of Proteomics **2:** 187-202

Zhang X-H, Ewy RG, Widholm JM, Portis AR (2002) Complementation of the Nuclear Antisense rbcS-Induced Photosynthesis Deficiency by Introducing an rbcS Gene into the Tobacco Plastid Genome 10.1093/pcp/pcf158 Plant and Cell Physiology **43** 1302-1313

Zhang J-H, Huang W-D, Liu Y-P, Pan Q-H (2005) Effects of Temperature Acclimation Pretreatment on the Ultrastructure of Mesophyll Cells in Young Grape Plants (*Vitis vinifera* L. cv. Jingxiu) Under Cross-Temperature Stresses. Journal of Integrative Plant Biology **47:** 959-970

Zhang J-L, Flowers T, Wang S-M (2010) Mechanisms of sodium uptake by roots of higher plants. Plant and Soil **326:** 45-60

Ziska LH (2001) Growth temperature can alter the temperature dependent stimulation of photosynthesis by elevated carbon dioxide in Abutilon theophrasti. Physiologia Plantarum 111, 322–328.

Zhu J-K (2003) Regulation of ion homeostasis under salt stress. Current Opinion in Plant Biology **6:** 441-445

Zhu X-G, Long SP, Ort DR (2008) What is the maximum efficiency with which photosynthesis can convert solar energy into biomass? Current Opinion in Biotechnology Food biotechnology / Plant biotechnology **19:** 153-159

Zohary, Daniel, Hopf M (2000) Domestication of Plants in the Old World: The Origin and Spread of Cultivated Plants in West Asia, Europe, and the Nile Valley. Oxford University Press

1 Appendix

Table A 3-1: Composition of 1/4 Strength Hoagland's Nutrient Solution (SHNS) Ingredients.

Source (Hoagland and Arnon, 1950). *Applied concentration.

http://bbc.botany.utoronto.ca/efp/cgi-bin/efpWeb.cgi

Macronutrient Compound's name	Formula and Stock solution	¼ SHNS to use*, ml/l	
Mono-potassium phosphate	1 M KH_2PO_4 (fw 136.09)	0.25	
Potassium nitrate	1 M KNO_3 (fw 101.11)	1.25	
Calcium nitrate	1 M $Ca(NO_3)_2$ (fw 236.2)	1.25	
Magnesium sulphate	1 M $MgSO_4$ x $7H_2O$	0.5	
Micronutrient Compound's name	**Formula**	**g/l**	**¼ SHNS to use***
Boric acid	H_3BO_3 (fw 61.83)	2.86	0.25 ml/l
Manganese chloride-4 hydrate	$MnCl_2$ x $4H_2O$ (fw 197.9)	1.81	.....
Zinc sulphate - 7 hydrate	$ZnSO_4$ x $7H_2O$ (fw 287.5)	0.22	.....
Cupric sulphate 5 hydrate	$CuSO_4$ x $5H_2O$ (fw 249.7)	0.08	.....
Sodium molybdate	Na_2MoO_4 x $2H_2O$ (fw 241.9)	0.12	.....
FeNa-EDTA, ferric monosodium Ethylenediaminetetra acetic acid	Fe Na EDTA (fw 367.05)	42.5 mM	.....

1.1 *Statistical Analysis*

Statistical analysis was performed using the General Linear Model ANOVA routine in MINITAB (version 16). Experiments presented in Chapters 3 & 4.

Factor 1, Line (Fixed), 4 levels:

Line 1;   Local
Line 2;   Optic
Line 3;   Soorab-96
Line 4;   Awaran-2002

Factor 2, Salinity (Fixed), 4 levels:

Level 1;   0 mM NaCl
Level 2;   50 mM NaCl
Level 3;   100 mM NaCl
Level 4;   150 mM NaCl

Experiments presented in Chapter 5.

Factor 1, Line (Fixed), 3 levels:

Line 1;   Local
Line 2;   Optic
Line 3;   Soorab-96

Factor 2, Temperature (Fixed), 3 levels

Level 1;   before
Level 2;   immediately after
Level 3;   5 days after

Analysis of Variance and Grouping Information tables are presented for each analysis. In addition, residual plots are presented to confirm the data are normally distributed, along with group average Interaction Plots. Where appropriate data were log base 10 transformed to conform to a normal distribution.

Figure A 3-1: General Linear Model: Germination % of versus Line, NaCl Concentration.

```
Factor              Type   Levels  Values
Line                fixed      4   1 (Local), 2 (Optic), 3 (Soorab-96), 4
                                   (Awaran-2002)
NaCl Concentration  fixed      4   0, 50, 100, 150

Analysis of Variance for Germination % of Control, using Adjusted SS for Tests

Source                   DF    Seq SS   Adj SS   Adj MS       F       P
Line                      3   29006.2  29006.2   9668.7  117.03  0.000
NaCl Concentration        3   63424.9  63424.9  21141.6  255.90  0.000
Line*NaCl Concentration   9   26999.6  26999.6   3000.0   36.31  0.000
Error                   144   11896.9  11896.9     82.6
Total                   159  131327.7

S = 9.08943   R-Sq = 90.94%   R-Sq(adj) = 90.00%


Grouping Information Using Bonferroni Method and 95.0% Confidence

        NaCl
Line  Concentration   N   Mean   Grouping
2          0         10  100.0   A
4          0         10  100.0   A
3          0         10  100.0   A
1          0         10  100.0   A
1         50         10   99.0   A
1        100         10   96.9   A B
2         50         10   96.8   A B
1        150         10   94.9   A B
3         50         10   84.0     B C
4         50         10   78.0       C
3        100         10   60.0         D
3        150         10   60.0         D
4        100         10   50.0         D
2        100         10   48.1         D
4        150         10   30.0           E
2        150         10   14.9             F

Means that do not share a letter are significantly different.
```

LSD = 14.69

Residual Plots for Germination % of Control
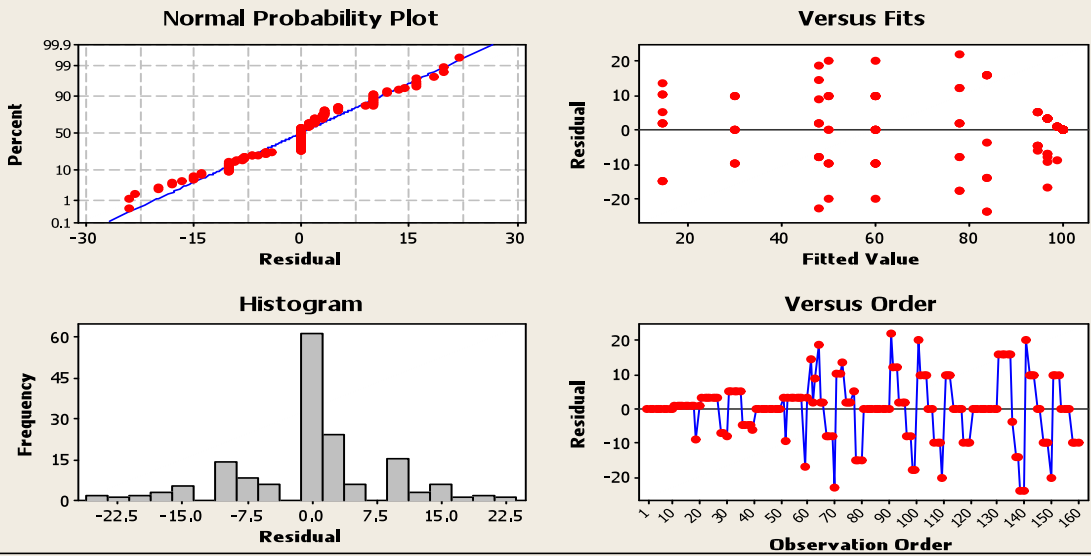
Interaction Plot for Germination % of Control
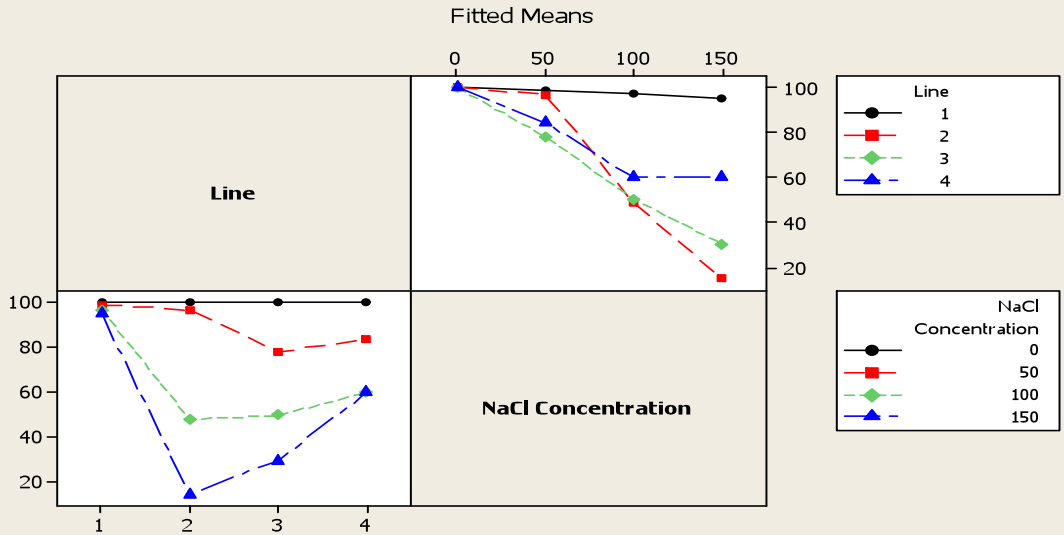
Figure A 3-2: General Linear Model: Seedling Shoot Length versus Line, NaCl Concentration.

```
Factor                Type   Levels  Values
Line                  fixed       4  1, 2, 3, 4
NaCl Concentration    fixed       4  0, 50, 100, 150


Analysis of Variance for Seedling Shoot Length, using Adjusted SS for Tests

Source                   DF   Seq SS   Adj SS  Adj MS      F      P
Line                      3   26.784   26.784   8.928   8.38  0.000
NaCl Concentration        3  248.791  248.791  82.930  77.82  0.000
Line*NaCl Concentration   9   12.970   12.970   1.441   1.35  0.224
Error                    80   85.250   85.250   1.066
Total                    95  373.795


S = 1.03229   R-Sq = 77.19%   R-Sq(adj) = 72.92%

Grouping Information Using Bonferroni Method and 95.0% Confidence

      NaCl
Line  Concentration  N  Mean  Grouping
1       50           6  4.8   A
1        0           6  4.6   A
4       50           6  4.2   A
3        0           6  4.2   A
2        0           6  4.2   A
1      100           6  3.9   A
3       50           6  3.8   A
2       50           6  3.8   A
4        0           6  3.8   A
4      100           6  1.5      B
2      100           6  1.2      B
3      100           6  1.2      B
1      150           6  1.1      B
4      150           6  0.2      B
3      150           6  0.1      B
2      150           6  0.1      B
```

Means that do not share a letter are significantly different.

LSD = 2.10

222

Residual Plots for Seedling Shoot Length
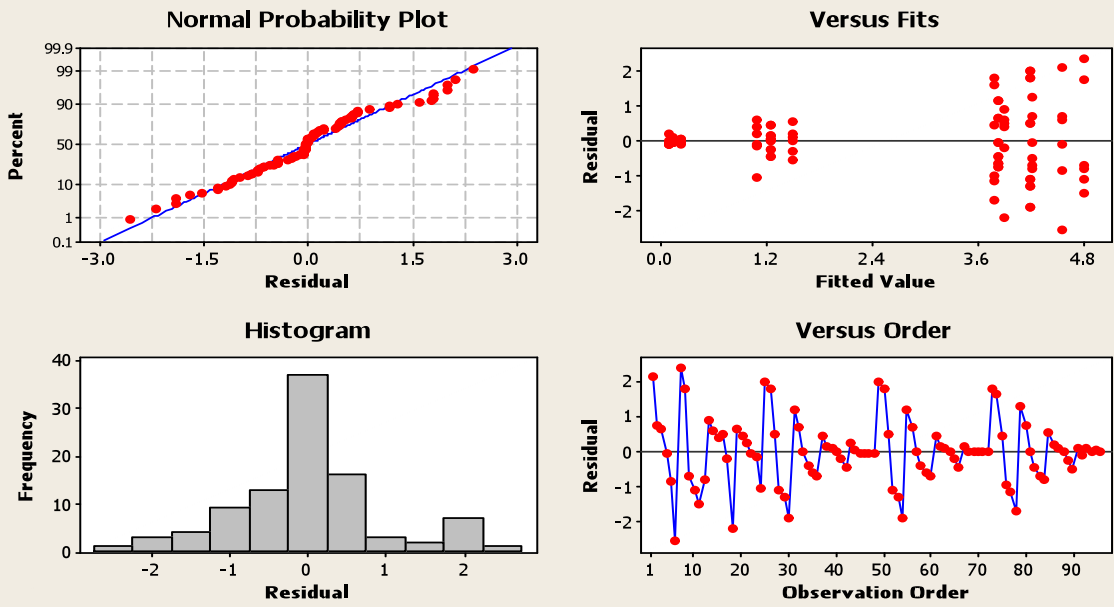
Interaction Plot for Seedling Shoot Length
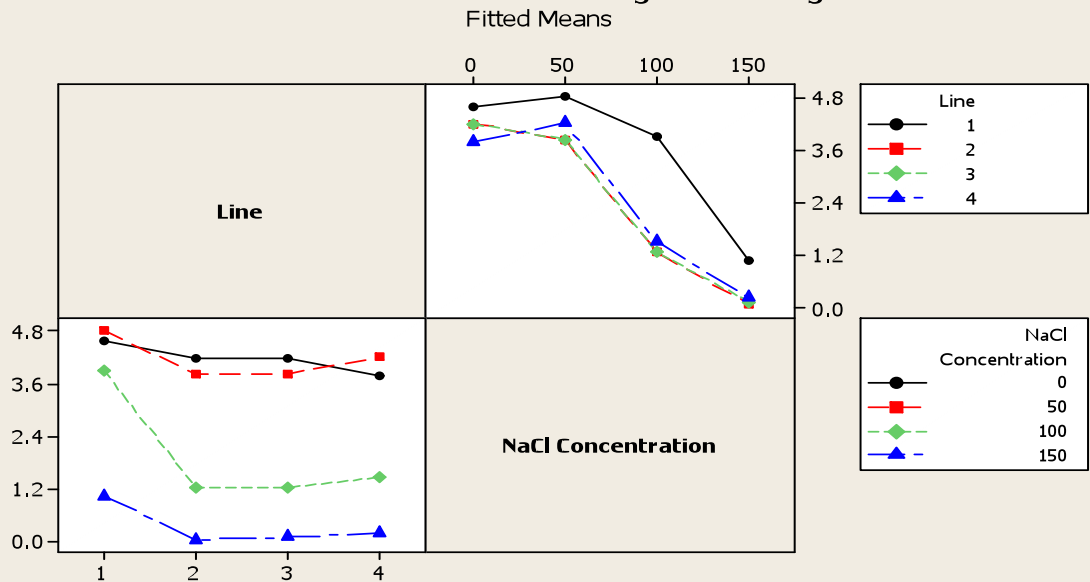
Figure A 3-3: General Linear Model: Log Shoot (Length) versus Line, NaCl Concentration.

```
Factor    Type   Levels  Values
Line      fixed       4  1 (Local), 2 (Optic), 3 (Soorab-96), 4
                          (Awaran-2002)
NaCl Con  fixed       4  0, 50, 100, 150


Analysis of Variance for Log S (Length), using Adjusted SS for Tests

Source          DF   Seq SS    Adj SS   Adj MS        F      P
Line             3  0.14293   0.14293  0.04764    18.83  0.000
NaCl Con         3  1.46701   1.46701  0.48900   193.23  0.000
Line*NaCl Con    9  0.16488   0.16488  0.01832     7.24  0.000
Error           32  0.08098   0.08098  0.00253
Total           47  1.85580


S = 0.0503055   R-Sq = 95.64%   R-Sq(adj) = 93.59%


Grouping Information Using Bonferroni Method and 95.0% Confidence

      NaCl
Line  Con  N  Mean  Grouping
1       0  3  1.9   A
2       0  3  1.9   A B
1      50  3  1.9   A B
3      50  3  1.9   A B
2      50  3  1.9   A B
1     100  3  1.8   A B
4     100  3  1.8   A B
2     100  3  1.8   A B
3     100  3  1.8   A B C
4      50  3  1.8   A B C
3       0  3  1.7   A B C
4       0  3  1.7     B C
1     150  3  1.6       C
4     150  3  1.4         D
3     150  3  1.4         D
2     150  3  1.3         D


Means that do not share a letter are significantly different.
```

LSD = 28.18

Residual Plots for Log S (Length)
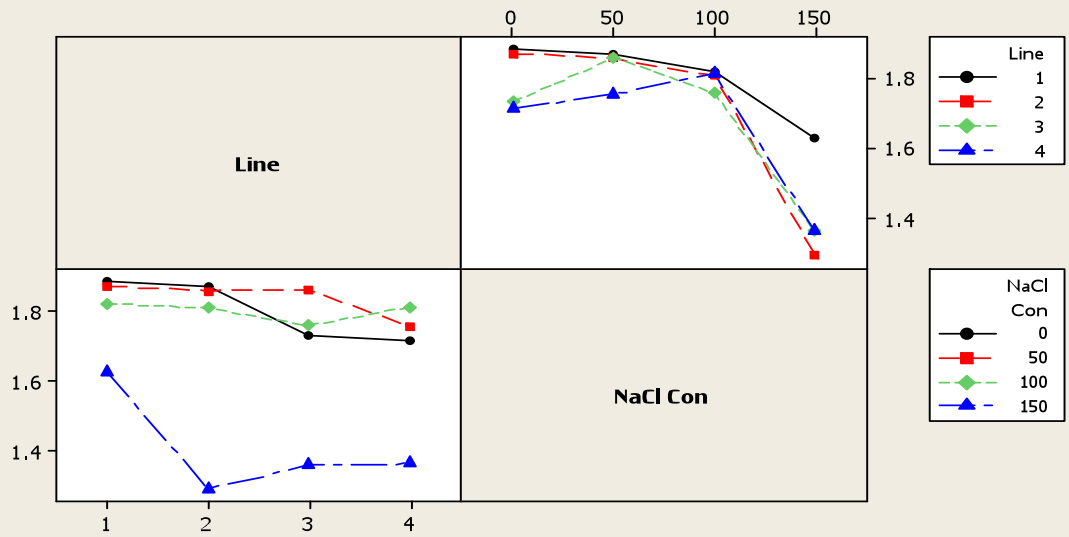
Figure A 3-4: General Linear Model: Root (Length) versus Line, NaCl Concentration.

```
Factor     Type   Levels  Values
Line       fixed      4   1 (Local), 2 (Optic), 3 (Soorab-96), 4
                              (Awaran-2002)
NaCl Con   fixed      4   0, 50, 100, 150
```

Analysis of Variance for R (Length), using Adjusted SS for Tests

```
Source         DF   Seq SS   Adj SS   Adj MS      F      P
Line            3  1069.73  1069.73   356.58   7.22  0.001
NaCl Con        3  3877.26  3877.26  1292.42  26.17  0.000
Line*NaCl Con   9  1269.27  1269.27   141.03   2.86  0.014
Error          32  1580.59  1580.59    49.39
Total          47  7796.85
```

S = 7.02805   R-Sq = 79.73%   R-Sq(adj) = 70.23%

Grouping Information Using Bonferroni Method and 95.0% Confidence

```
      NaCl
Line  Con   N  Mean  Grouping
1     100   3  60.0  A
1      50   3  58.0  A
2       0   3  56.0  A B
3      50   3  54.2  A B
4      50   3  53.7  A B
1       0   3  53.3  A B
3       0   3  48.5  A B C
2     100   3  48.3  A B C
4       0   3  47.0  A B C
3     100   3  44.7  A B C
4     100   3  42.3  A B C
1     150   3  41.3  A B C
2      50   3  41.3  A B C
2     150   3  33.7    B C D
4     150   3  30.7      C D
3     150   3  14.4        D
```

Means that do not share a letter are significantly different.

LSD= 22.6

Residual Plots for Log R (Length)
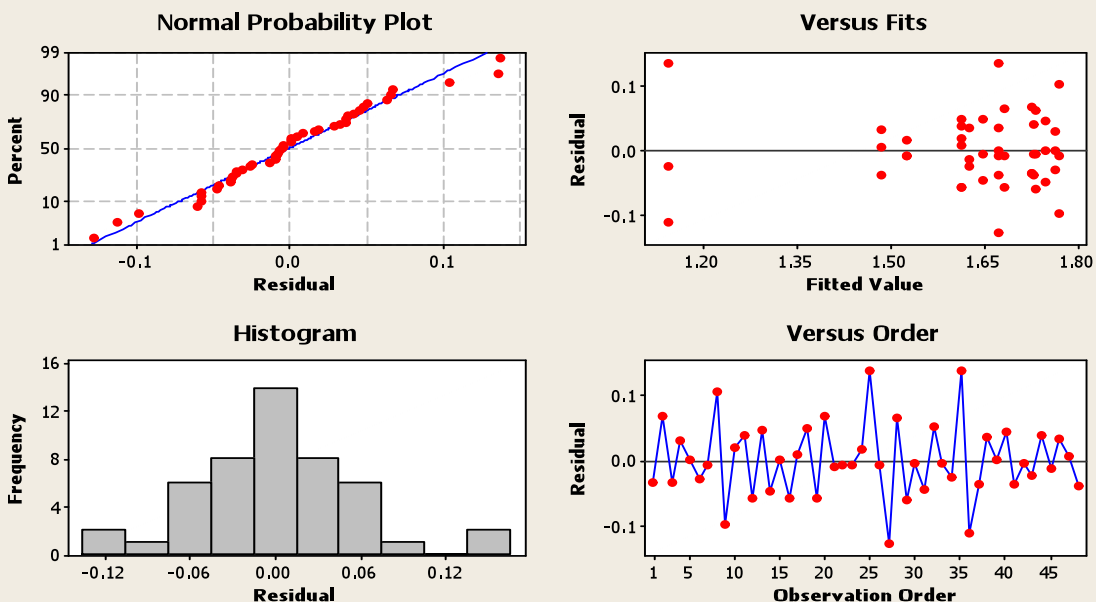
Interaction Plot for Log R (Length)
Fitted Means
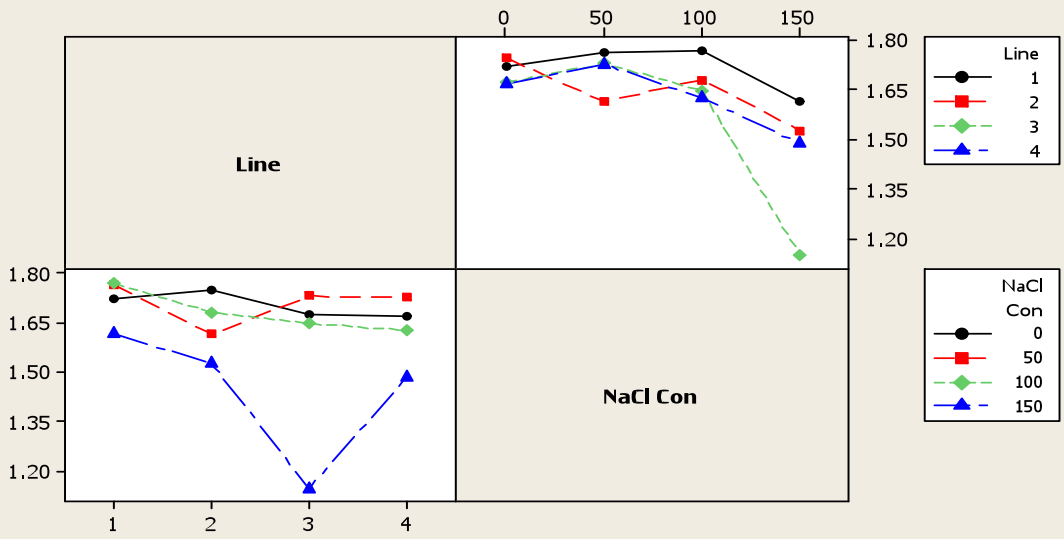
Figure A 3-5: General Linear Model: Shoot Fresh Wt versus Line, NaCl Concentration.

```
Factor     Type   Levels  Values
Line       fixed       4  1 (Local), 2 (Optic), 3 (Soorab-96), 4
                          (Awaran-2002)
NaCl Con   fixed       4  0, 50, 100, 150


Analysis of Variance for Shoot Fresh Wt, using Adjusted SS for Tests

Source          DF   Seq SS    Adj SS   Adj MS      F       P
Line             3  138.079   138.079   46.026  13.32   0.000
NaCl Con         3  378.682   378.682  126.227  36.53   0.000
Line*NaCl Con    9   76.090    76.090    8.454   2.45   0.030
Error           32  110.586   110.586    3.456
Total           47  703.436


S = 1.85898   R-Sq = 84.28%   R-Sq(adj) = 76.91%


Grouping Information Using Bonferroni Method and 95.0% Confidence

      NaCl
Line   Con   N  Mean  Grouping
3       50   3  12.3  A
1       50   3  10.5  A B
3        0   3  10.4  A B
1      100   3  10.1  A B C
1        0   3   9.8  A B C
2        0   3   9.6  A B C
3      100   3   8.1  A B C
4       50   3   8.1  A B C
2       50   3   7.0  A B C D
4        0   3   6.7  A B C D E
1      150   3   6.7  A B C D E F
2      100   3   5.4    B C D E F
4      100   3   4.1      C D E F
2      150   3   1.5                G
4      150   3   0.8                G
3      150   3   0.7                G
```
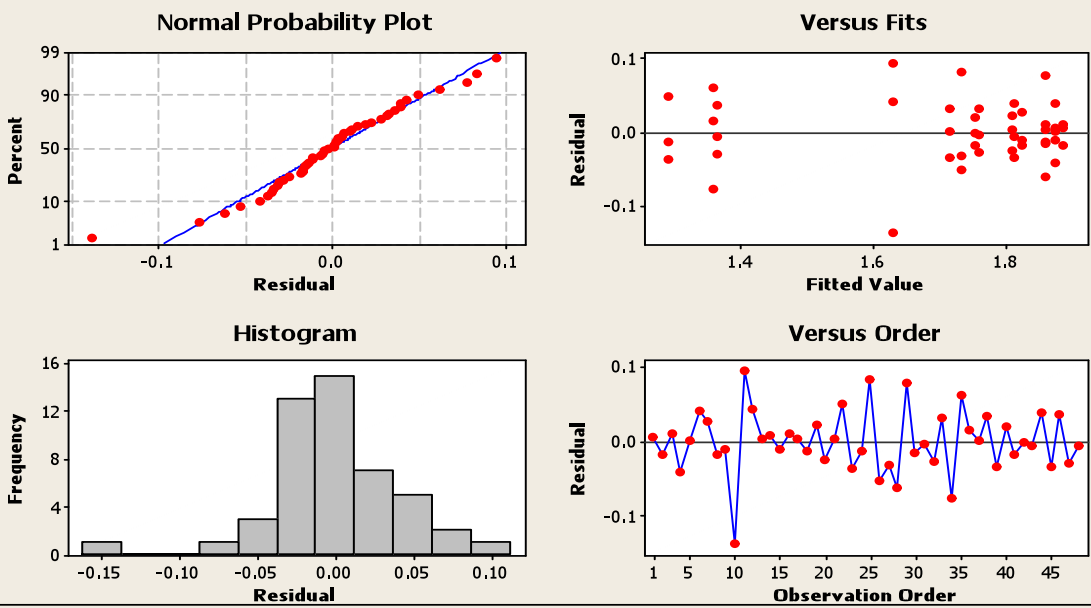
Means that do not share a letter are significantly different.

LSD= 5.97

Residual Plots for Shoot Fresh Wt

Interaction Plot for Shoot Fresh Wt
Fitted Means
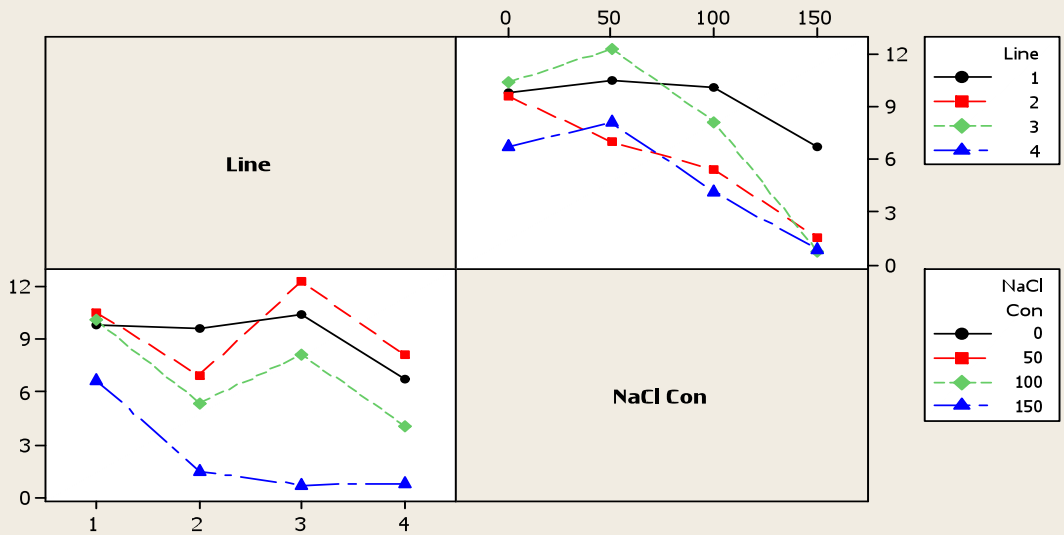
Figure A 3-6: General Linear Model: Root Fresh Wt versus Line, NaCl Concentration.

```
Factor     Type   Levels  Values
Line       fixed      4   1 (Local), 2 (Optic), 3 (Soorab-96), 4
                              (Awaran-2002)
NaCl Con   fixed      4   0, 50, 100, 150


Analysis of Variance for Root Fresh Wt, using Adjusted SS for Tests

Source          DF   Seq SS    Adj SS  Adj MS      F      P
Line             3   70.855    70.855  23.618   7.22  0.001
NaCl Con         3  134.528   134.528  44.843  13.71  0.000
Line*NaCl Con    9   16.027    16.027   1.781   0.54  0.831
Error           32  104.679   104.679   3.271
Total           47  326.090


S = 1.80865   R-Sq = 67.90%   R-Sq(adj) = 52.85%


Grouping Information Using Bonferroni Method and 95.0% Confidence

       NaCl
Line   Con   N   Mean  Grouping
1       50   3   7.6   A
1        0   3   7.0   A
3       50   3   6.6   A B
2        0   3   6.5   A B C
3        0   3   5.7   A B C
1      100   3   5.6   A B C
2      100   3   4.5   A B C
2       50   3   4.5   A B C
3      100   3   4.4   A B C
4       50   3   3.7   A B C
1      150   3   3.6   A B C
4        0   3   3.4   A B C
4      100   3   2.3   A B C
3      150   3   1.0       C D
4      150   3   0.8         D
2      150   3   0.7         D


Means that do not share a letter are significantly different.
```
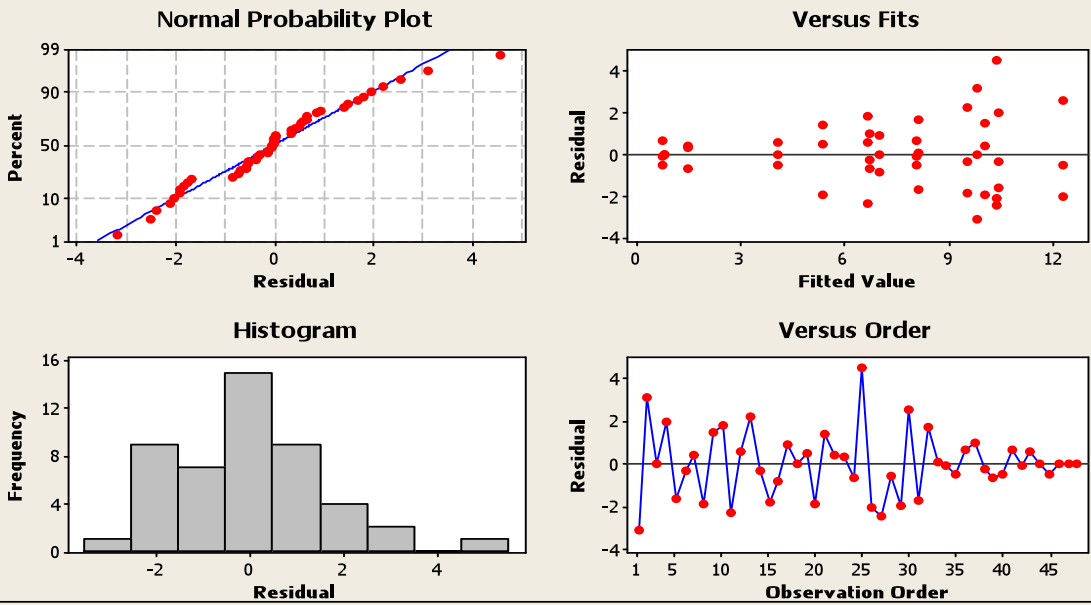
LSD= 3.81

Residual Plots for Root Fresh Wt

Interaction Plot for Root Fresh Wt
Fitted Means

231
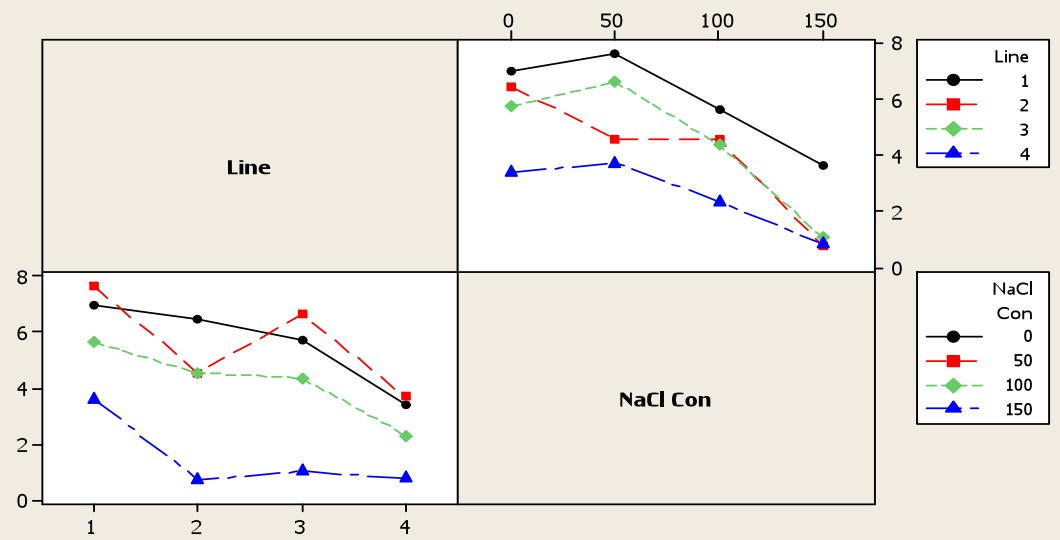
Figure A 3-7: General Linear Model: Shoot Dry Wt versus Line, NaCl Concentration.

```
Factor    Type   Levels  Values
Line      fixed      4   1 (Local), 2 (Optic), 3 (Soorab-96), 4
                             (Awaran-2002)
NaCl Con  fixed      4   0, 50, 100, 150


Analysis of Variance for Shoot Dry Wt, using Adjusted SS for Tests

Source         DF   Seq SS   Adj SS   Adj MS      F      P
Line            3  0.57070  0.57070  0.19023   4.62  0.009
NaCl Con        3  3.71955  3.71955  1.23985  30.14  0.000
Line*NaCl Con   9  0.78424  0.78424  0.08714   2.12  0.057
Error          32  1.31650  1.31650  0.04114
Total          47  6.39100


S = 0.202832   R-Sq = 79.40%   R-Sq(adj) = 69.74%


Grouping Information Using Bonferroni Method and 95.0% Confidence

       NaCl
Line   Con  N  Mean  Grouping
3       50  3   1.3  A
4       50  3   1.0  A B
1       50  3   1.0  A B
1      100  3   0.9  A B
3        0  3   0.8  A B
4        0  3   0.8  A B
2        0  3   0.8  A B
3      100  3   0.8  A B C
1        0  3   0.8  A B C
2       50  3   0.6    B C
2      100  3   0.5    B C
1      150  3   0.5    B C
4      100  3   0.4    B C
2      150  3   0.1        D
4      150  3   0.1        D
3      150  3   0.1        D


Means that do not share a letter are significantly different.
```
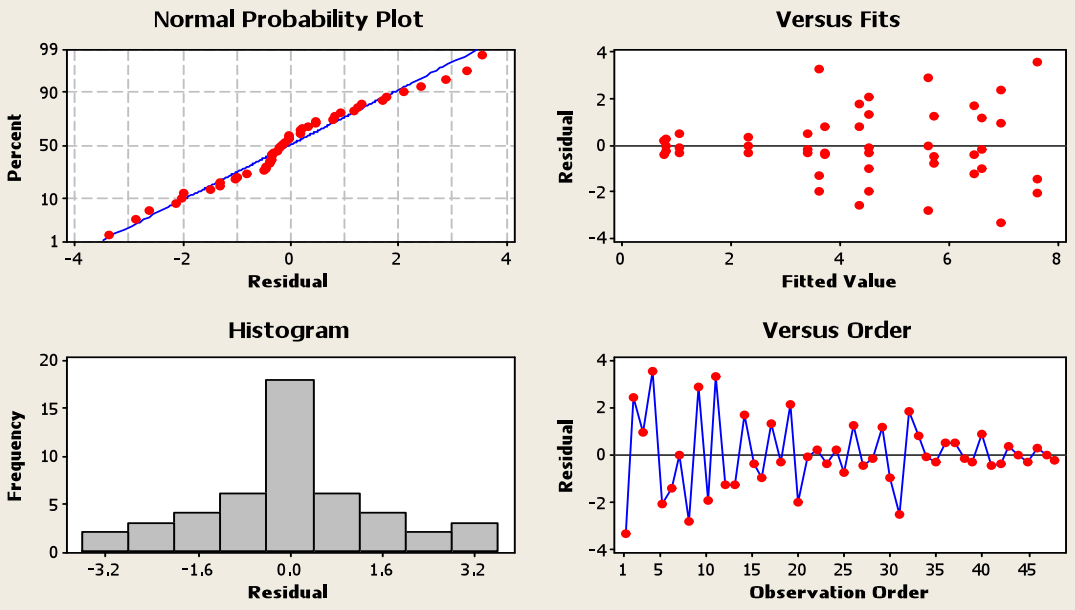
LSD= 0.64

Residual Plots for Shoot Dry Wt
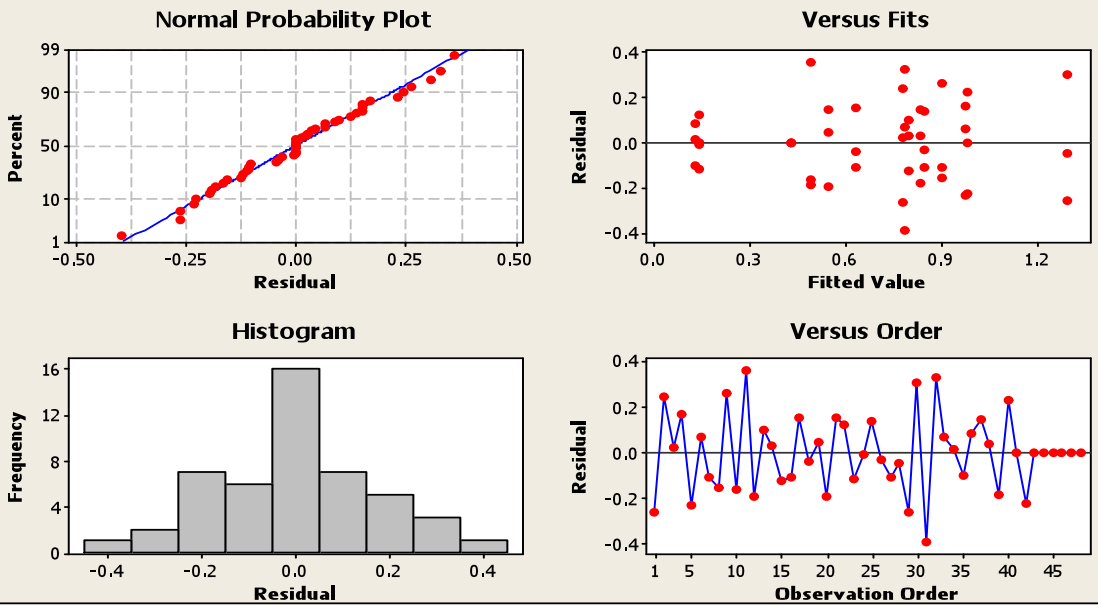
Interaction Plot for Shoot Dry Wt
Fitted Means

233
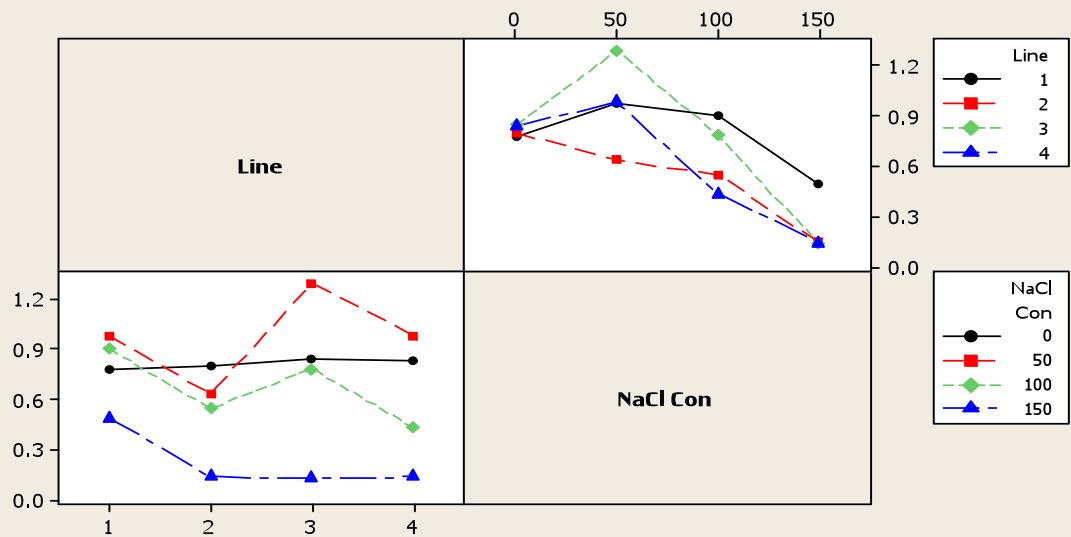
Figure A 3-8: General Linear Model: Root Dry Wt versus Line, NaCl Concentration.

```
Factor     Type    Levels  Values
Line       fixed        4  1 (Local), 2 (Optic), 3 (Soorab-96), 4
                           (Awaran-2002)
NaCl Con   fixed        4  0, 50, 100, 150


Analysis of Variance for Root Dry Wt, using Adjusted SS for Tests

Source          DF   Seq SS   Adj SS   Adj MS      F      P
Line             3  0.29966  0.29966  0.09989   9.84  0.000
NaCl Con         3  0.37487  0.37487  0.12496  12.31  0.000
Line*NaCl Con    9  0.09789  0.09789  0.01088   1.07  0.410
Error           32  0.32487  0.32487  0.01015
Total           47  1.09728


S = 0.100758   R-Sq = 70.39%   R-Sq(adj) = 56.52%

Grouping Information Using Tukey Method and 95.0% Confidence

      NaCl
Line  Con   N  Mean  Grouping
1      50   3   0.5  A
1     100   3   0.4  A B
2       0   3   0.4  A B
1       0   3   0.3  A B C
3      50   3   0.3  A B C D
2     100   3   0.3  A B C D
2      50   3   0.3  A B C D
4      50   3   0.3  A B C D
3     100   3   0.2  A B C D
1     150   3   0.2  A B C D
3       0   3   0.2    B C D
4     100   3   0.1    B C D
4       0   3   0.1    B C D
3     150   3   0.1      C D
4     150   3   0.1        D E
2     150   3   0.0          E

Means that do not share a letter are significantly different.
```

LSD= 0.22

Residual Plots for Root Dry Wt
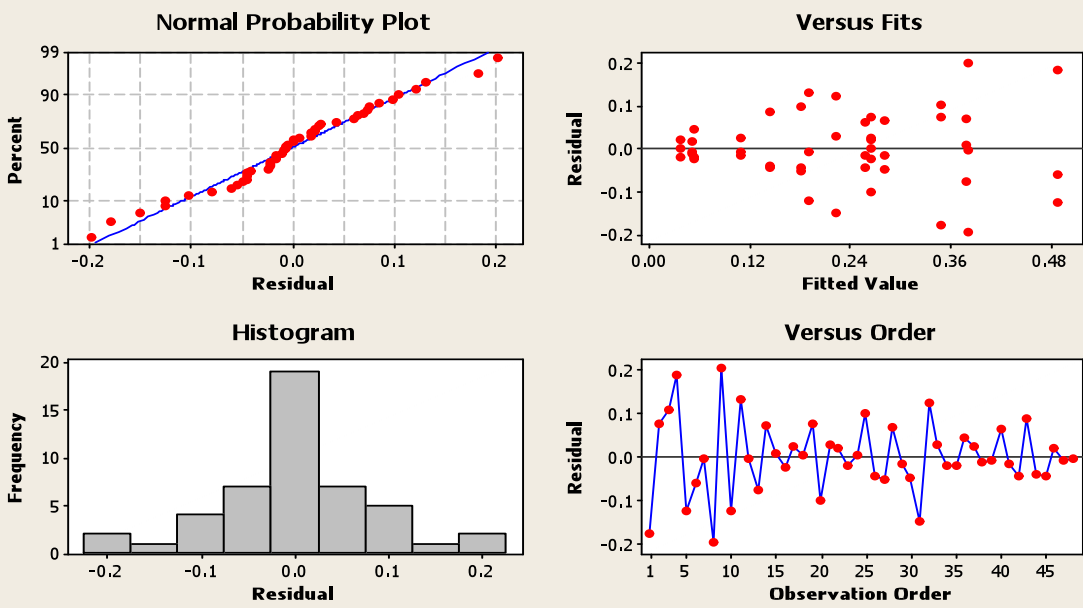
Interaction Plot for Root Dry Wt
Fitted Means
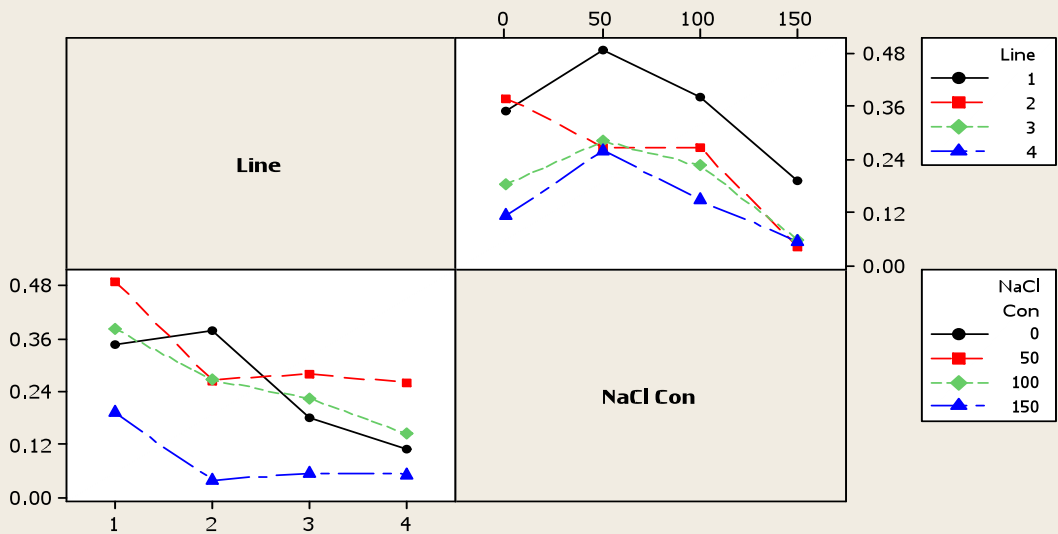
Figure A 3-9: General Linear Model: Local versus Tillering days, NaCl Concentration.

```
Factor          Type    Levels  Values
Tillering days  fixed       5   45, 60, 75, 90, 105
NaCl con        fixed       4   0, 50, 100, 150


Analysis of Variance for Local, using Adjusted SS for Tests

Source                   DF   Seq SS    Adj SS  Adj MS      F      P
Tillering days            4   37.360    37.360   9.340   7.50  0.000
NaCl con                  3  156.510   156.510  52.170  41.90  0.000
Tillering days*NaCl con  12   21.040    21.040   1.753   1.41  0.180
Error                    80   99.600    99.600   1.245
Total                    99  314.510

Grouping Information Using Tukey Method and 95.0% Confidence

Tillering  NaCl
days       con   N  Mean  Grouping
105         50   5   7.0  A
 90         50   5   6.6  A B
105          0   5   5.8  A B C
 75         50   5   5.8  A B C
 60         50   5   4.6  A B C D
 90          0   5   4.4    B C D E
 45         50   5   4.4    B C D E
 75          0   5   4.2    B C D E
105        100   5   4.2    B C D E
 60          0   5   3.8      C D E
 60        100   5   3.8      C D E
 75        100   5   3.8      C D E
 90        100   5   3.8      C D E
 45          0   5   3.0        D E
 45        150   5   2.4        D E
105        150   5   2.4        D E
 45        100   5   2.4        D E
 90        150   5   2.2        D E
 75        150   5   2.0          E
 60        150   5   2.0          E


Means that do not share a letter are significantly different.
```

LSD= 2.58

Residual Plots for Local

Interaction Plot for Local
Fitted Means
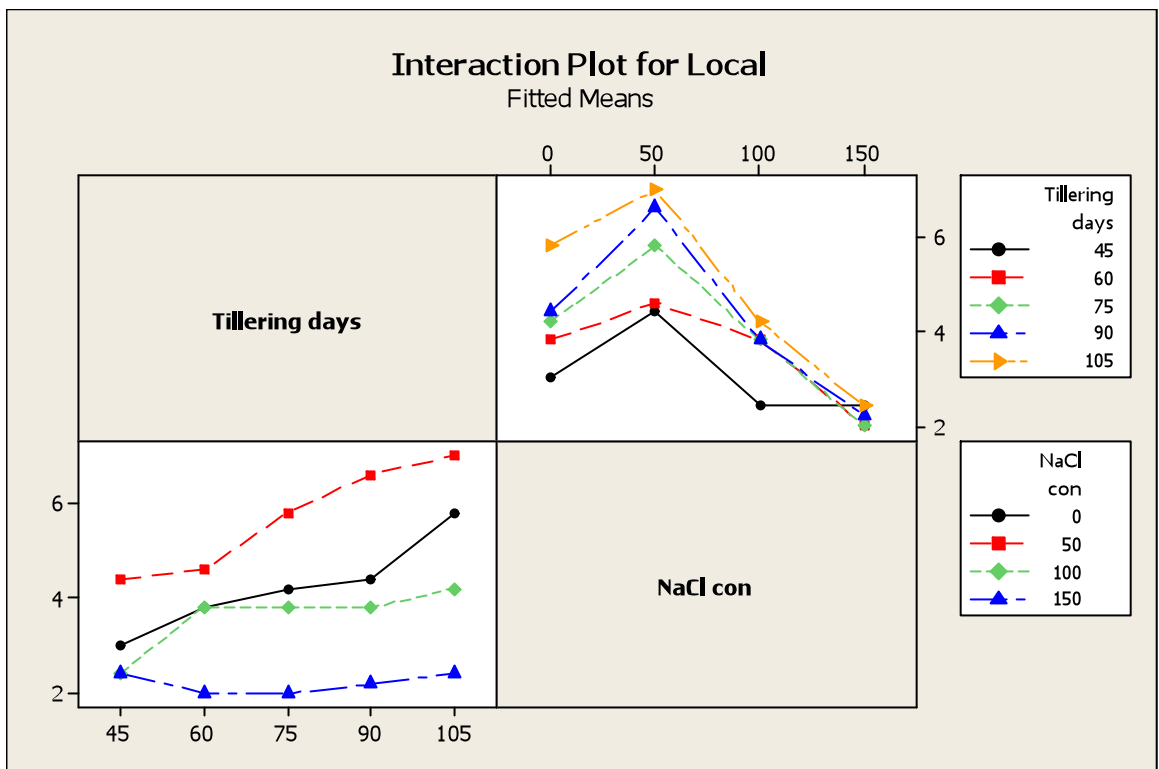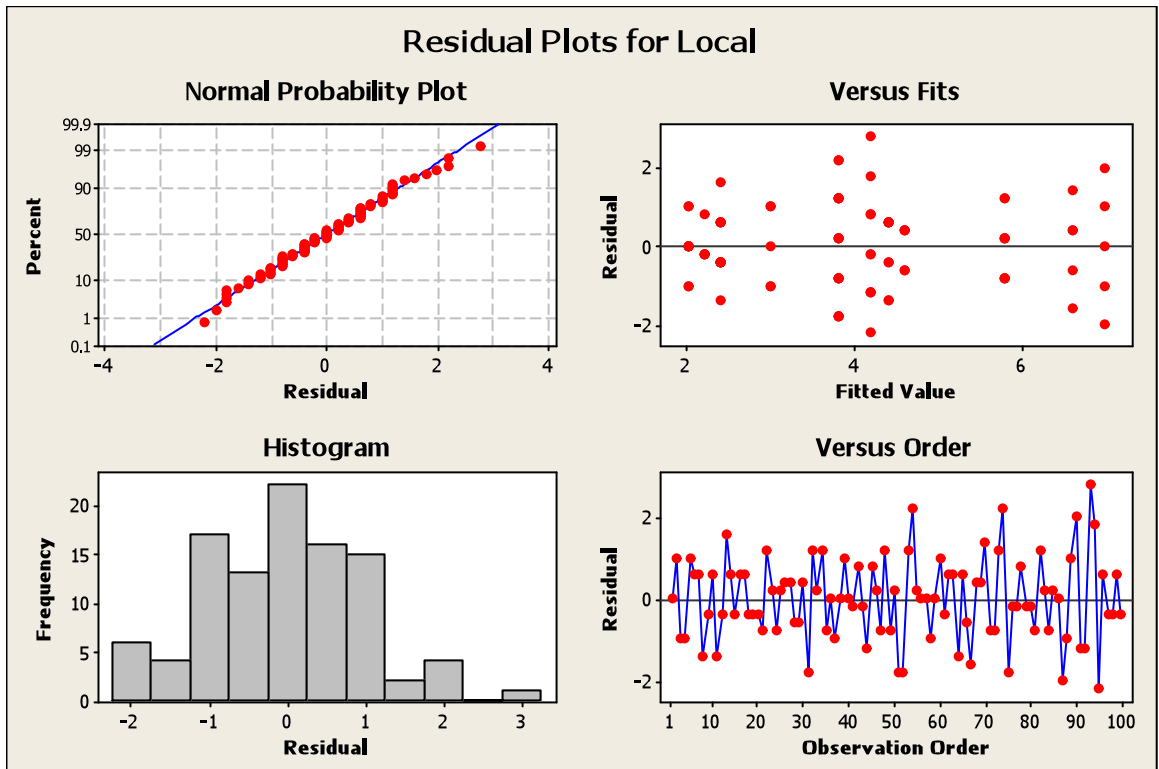
Figure A 3-10: General Linear Model: Optic versus Tillering days, NaCl Concentration.

```
Factor          Type   Levels  Values
Tillering days  fixed      5   45, 60, 75, 90, 105
NaCl con        fixed      4   0, 50, 100, 150


Analysis of Variance for Optic, using Adjusted SS for Tests

Source                   DF   Seq SS   Adj SS   Adj MS        F      P
Tillering days            4    9.640    9.640    2.410     6.10  0.000
NaCl con                  3  280.430  280.430   93.477   236.65  0.000
Tillering days*NaCl con  12   82.120   82.120    6.843    17.32  0.000
Error                    80   31.600   31.600    0.395
Total                    99  403.790


S = 0.628490   R-Sq = 92.17%   R-Sq(adj) = 90.32%

Grouping Information Using Tukey Method and 95.0% Confidence

Tillering  NaCl
days       con   N  Mean  Grouping
105          0   5   7.6  A
 90          0   5   6.2  A B
 75          0   5   5.2    B C
105         50   5   4.4      C D
 90         50   5   4.2      C D E
 75         50   5   4.2      C D E
 60          0   5   4.0      C D E
 45        100   5   4.0      C D E
 60         50   5   3.4        D E F
 45          0   5   3.0        D E F
 75        100   5   3.0        D E F
 60        100   5   2.8          E F
 45         50   5   2.8          E F
 90        100   5   2.4            F G
105        100   5   2.0            F G
 60        150   5   1.0              G H
 75        150   5   1.0              G H
 45        150   5   1.0              G H
105        150   5   0.0                H
 90        150   5  -0.0                H
```

Means that do not share a letter are significantly different.

LSD= 2.58

Residual Plots for Optic
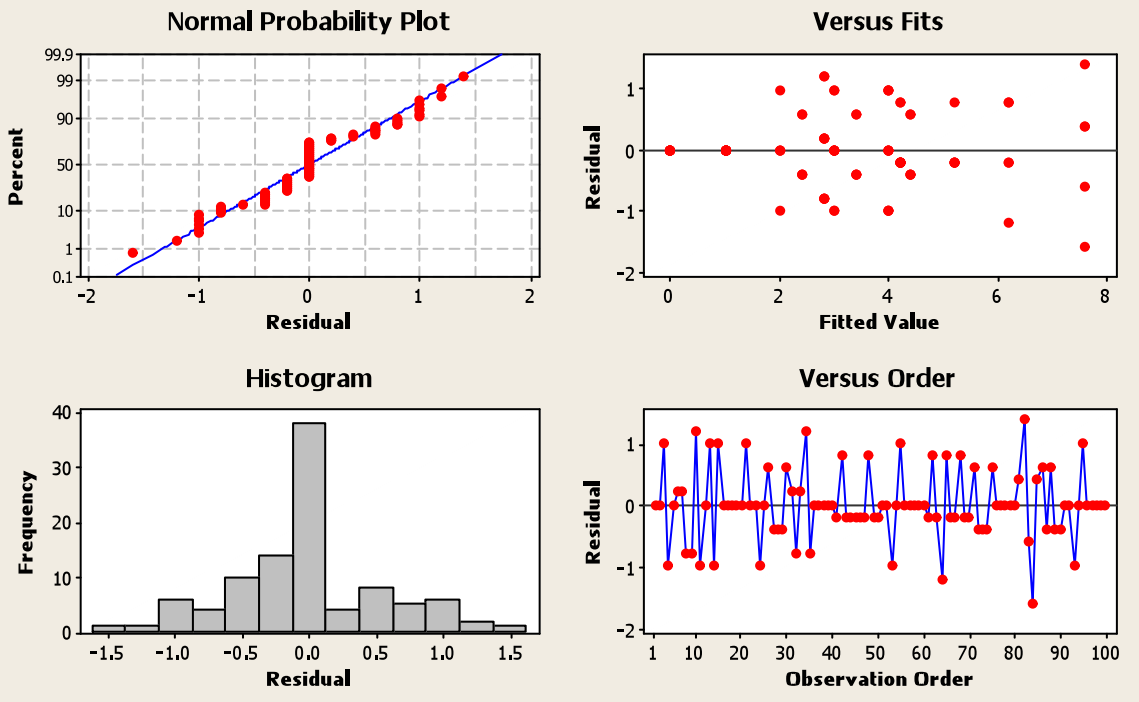
Interaction Plot for Optic
Fitted Means
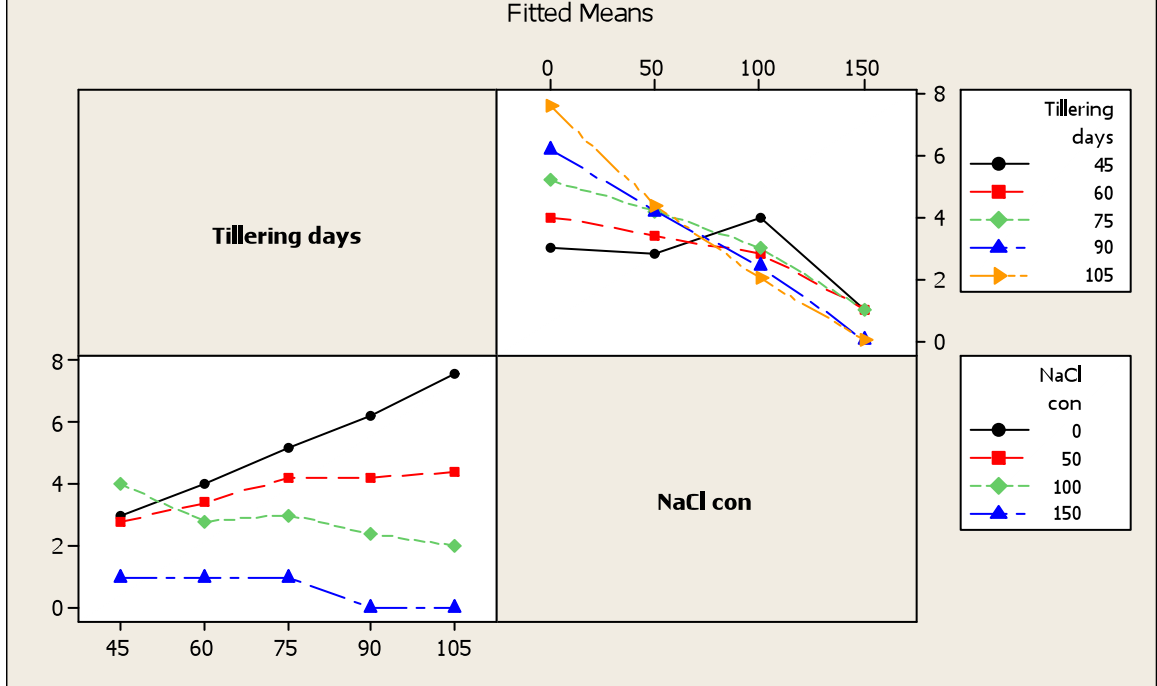
Figure A 3-11: General Linear Model: Soorab versus Tillering days, NaCl Concentration.

```
Factor          Type    Levels  Values
Tillering days  fixed        5  45, 60, 75, 90, 105
NaCl con        fixed        4  0, 50, 100, 150


Analysis of Variance for Soorab, using Adjusted SS for Tests

Source                   DF    Seq SS    Adj SS   Adj MS      F      P
Tillering days            4    78.700    78.700   19.675  23.15  0.000
NaCl con                  3   197.960   197.960   65.987  77.63  0.000
Tillering days*NaCl con  12    90.340    90.340    7.528   8.86  0.000
Error                    80    68.000    68.000    0.850
Total                    99   435.000


S = 0.921954   R-Sq = 84.37%   R-Sq(adj) = 80.66%

Grouping Information Using Tukey Method and 95.0% Confidence

Tillering  NaCl
days        con   N  Mean  Grouping
105          50   5   8.4  A
105           0   5   6.2    B
 90          50   5   5.2    B C
 75          50   5   5.2    B C
 60          50   5   4.8    B C
 90           0   5   4.6    B C
 75           0   5   4.6    B C
 60           0   5   4.2    B C D
 75         100   5   3.6      C D E
 90         100   5   3.4      C D E
105         100   5   3.4      C D E
 60         100   5   3.4      C D E
 45          50   5   2.4        D E
 75         150   5   2.0          E F
 90         150   5   2.0          E F
 45           0   5   1.8          E F
 60         150   5   1.6          E F
 45         150   5   1.6          E F
 45         100   5   1.6          E F
105         150   5   0.0            F
```
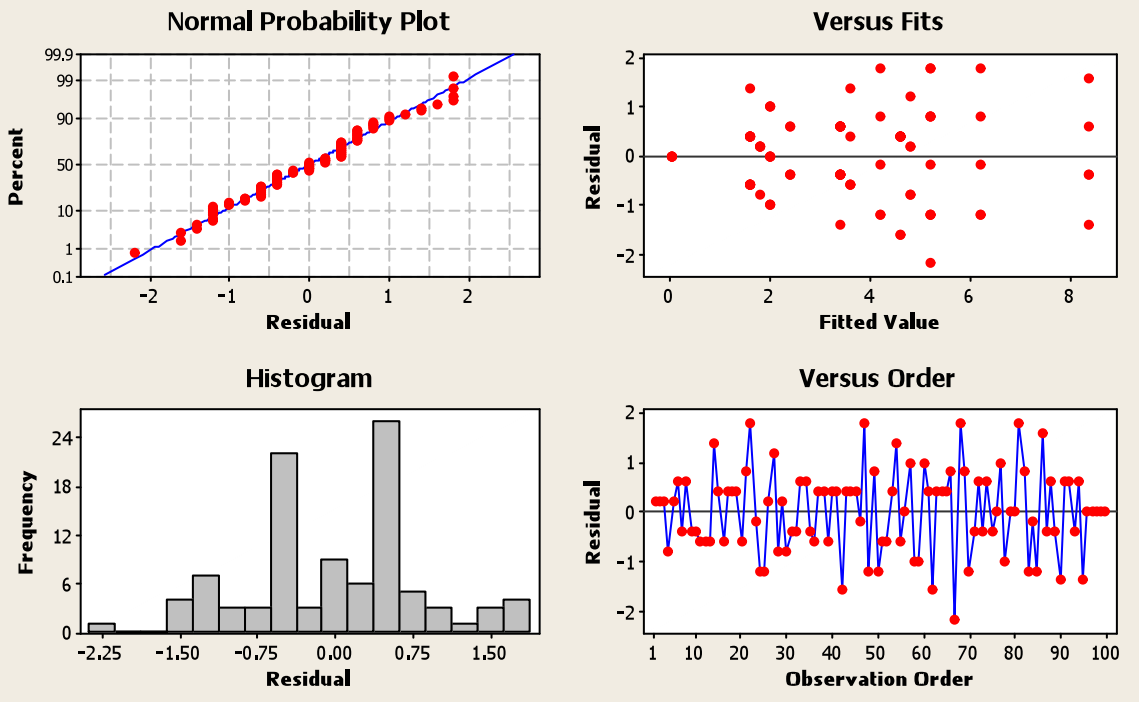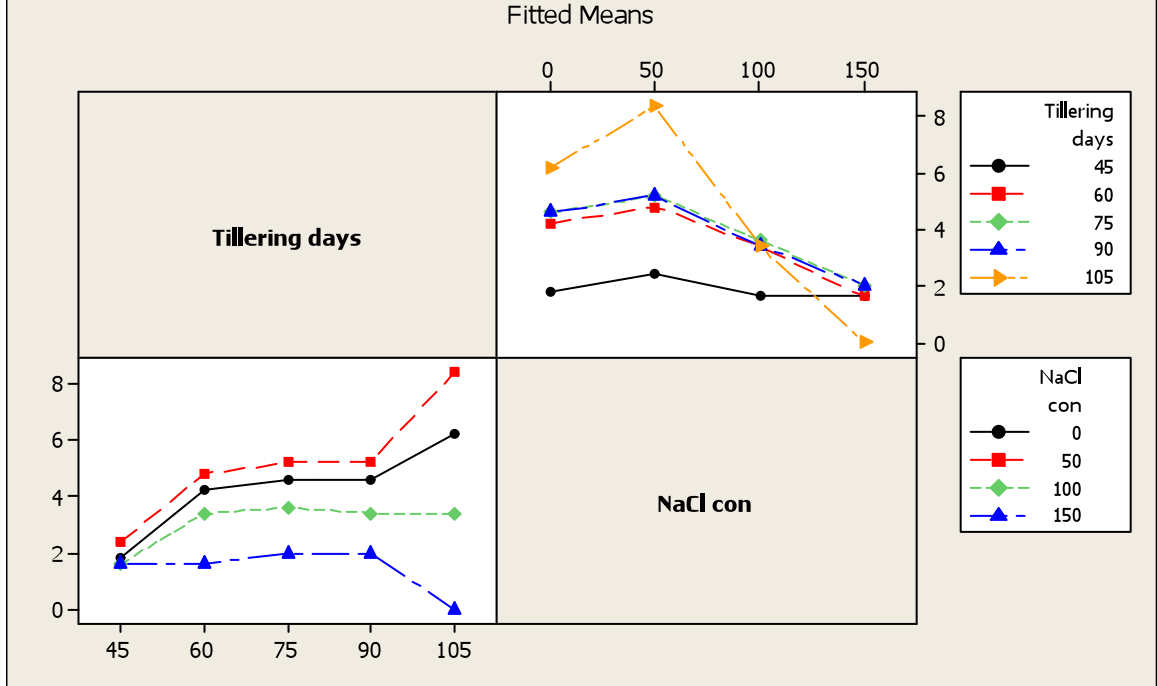
Means that do not share a letter are significantly different.

LSD= 2.13

Residual Plots for Soorab

Interaction Plot for Soorab

Figure A 3-12: General Linear Model: Soorab versus Tillering days, NaCl Concentration.

```
Factor          Type   Levels  Values
Tillering days  fixed       5  45, 60, 75, 90, 105
NaCl con        fixed       4  0, 50, 100, 150


Analysis of Variance for Awaran, using Adjusted SS for Tests

Source                  DF   Seq SS   Adj SS  Adj MS       F      P
Tillering days           4    1.360    1.360   0.340    0.89  0.471
NaCl con                 3  153.950  153.950  51.317  135.04  0.000
Tillering days*NaCl con 12   50.400   50.400   4.200   11.05  0.000
Error                   80   30.400   30.400   0.380
Total                   99  236.110


S = 0.616441   R-Sq = 87.12%   R-Sq(adj) = 84.07%

Grouping Information Using Tukey Method and 95.0% Confidence

Tillering  NaCl
days        con  N  Mean  Grouping
105          50  5   4.8  A
 90          50  5   4.2  A B
105           0  5   4.2  A B
 90           0  5   3.8  A B C
 75          50  5   3.8  A B C
 75           0  5   3.4  A B C D
 60          50  5   3.4  A B C D
 60           0  5   2.8    B C D E
 45          50  5   2.6      C D E F
 45           0  5   2.4      C D E F G
 45         150  5   2.2        D E F G
 45         100  5   2.0        D E F G
 60         150  5   1.8          E F G
 60         100  5   1.6          E F G
 75         100  5   1.4          E F G H
 90         100  5   1.2            F G H
105         100  5   1.0              G H
 75         150  5   0.0                H
105         150  5   0.0                H
 90         150  5  -0.0                H

Means that do not share a letter are significantly different.
```
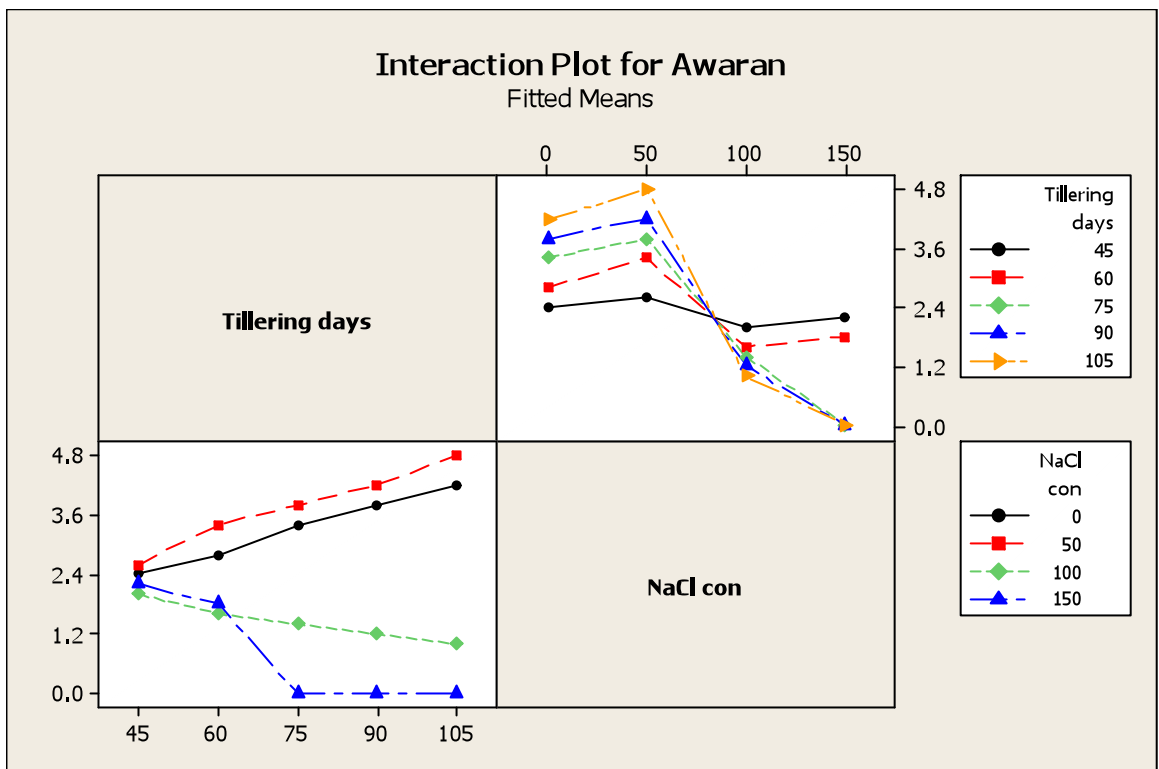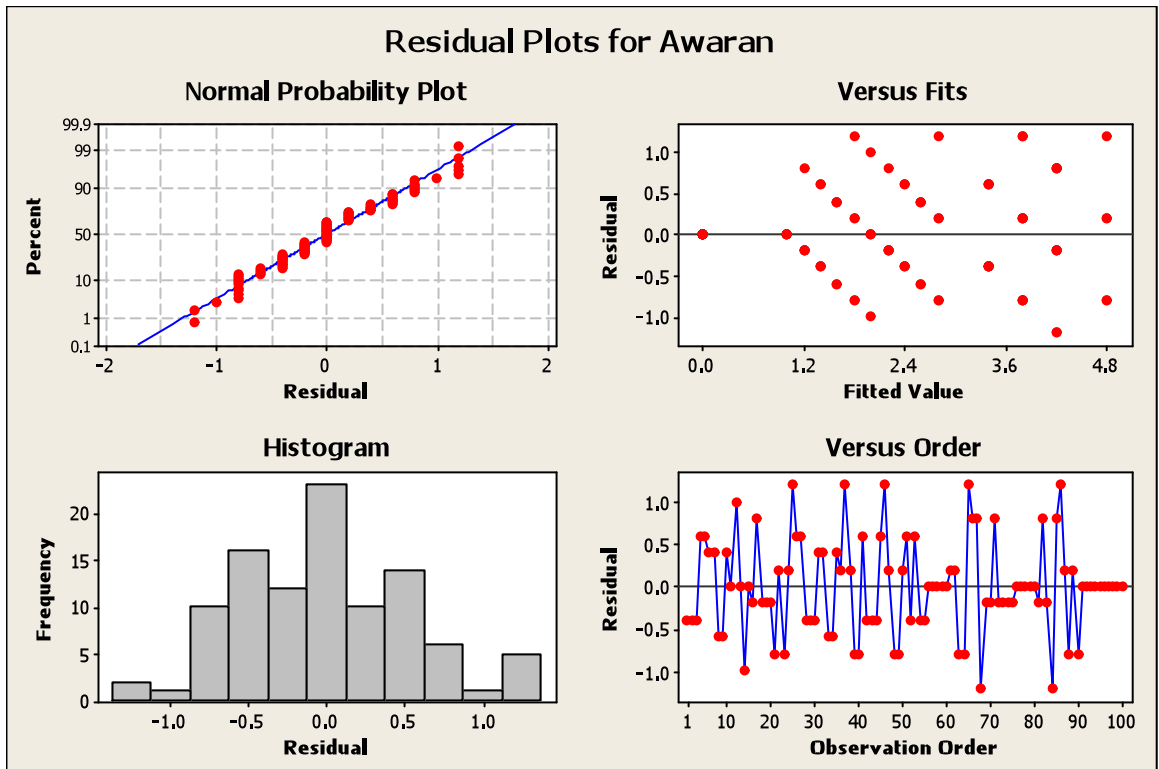
LSD= 1.42

Residual Plots for Awaran

Interaction Plot for Awaran
Fitted Means

Figure A 3-13: General Linear Model: Ears /plant versus Line, NaCl Concentration.

```
Factor     Type   Levels  Values
Line       fixed      4   1 (Local), 2 (Optic), 3 (Soorab-96), 4
                              (Awaran-2002)
Treatment  fixed      4   0, 50, 100, 150


Analysis of Variance for Ears /plant, using Adjusted SS for Tests

Source          DF   Seq SS   Adj SS   Adj MS       F      P
Line             3   39.995   39.995   13.332   16.37  0.000
Treatment        3  381.979  381.979  127.326  156.38  0.000
Line*Treatment   9   45.112   45.112    5.012    6.16  0.000
Error           64   52.109   52.109    0.814
Total           79  519.195


S = 0.902336   R-Sq = 89.96%   R-Sq(adj) = 87.61%


Grouping Information Using Bonferroni Method and 95.0% Confidence

Line  Treatment  N  Mean  Grouping
3       50       5   7.8  A
1       50       5   7.0  A B
2        0       5   6.4  A B C
3        0       5   5.0    B C D
1        0       5   5.0    B C D
4       50       5   4.8      C D
2       50       5   4.4      C D E
4        0       5   4.0        D E
1      100       5   3.4        D E F
3      100       5   3.2        D E F
2      100       5   2.6          E F G
1      150       5   1.7            F G H
4      100       5   1.0              G H
4      150       5   0.0                H
2      150       5  -0.0                H
3      150       5  -0.0                H


Means that do not share a letter are significantly different.
```
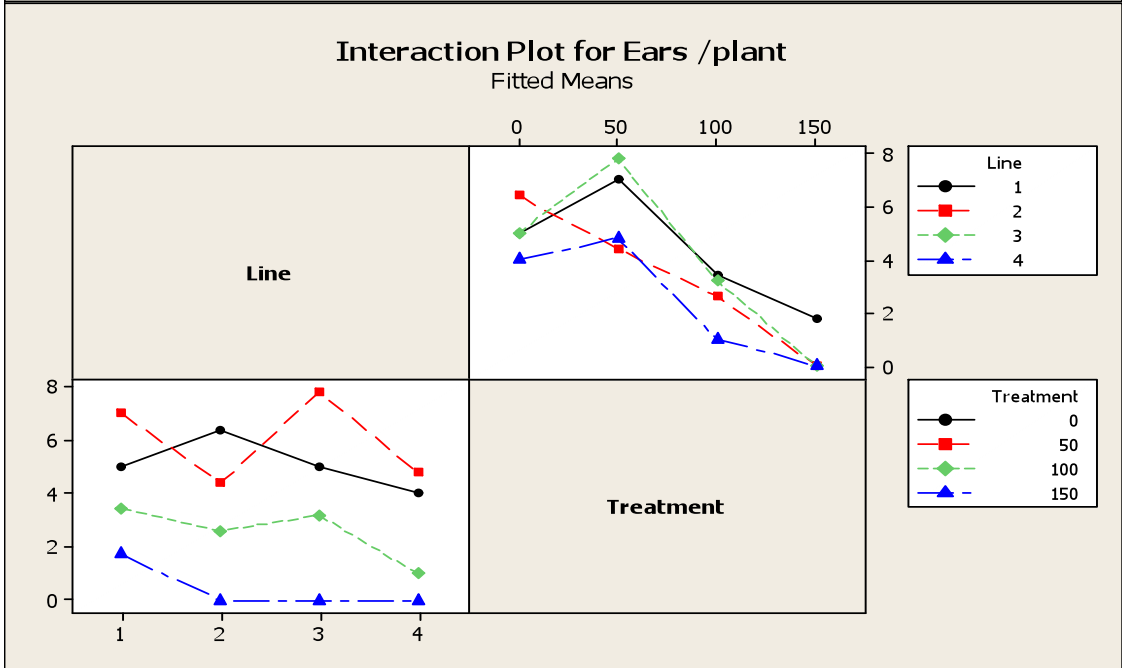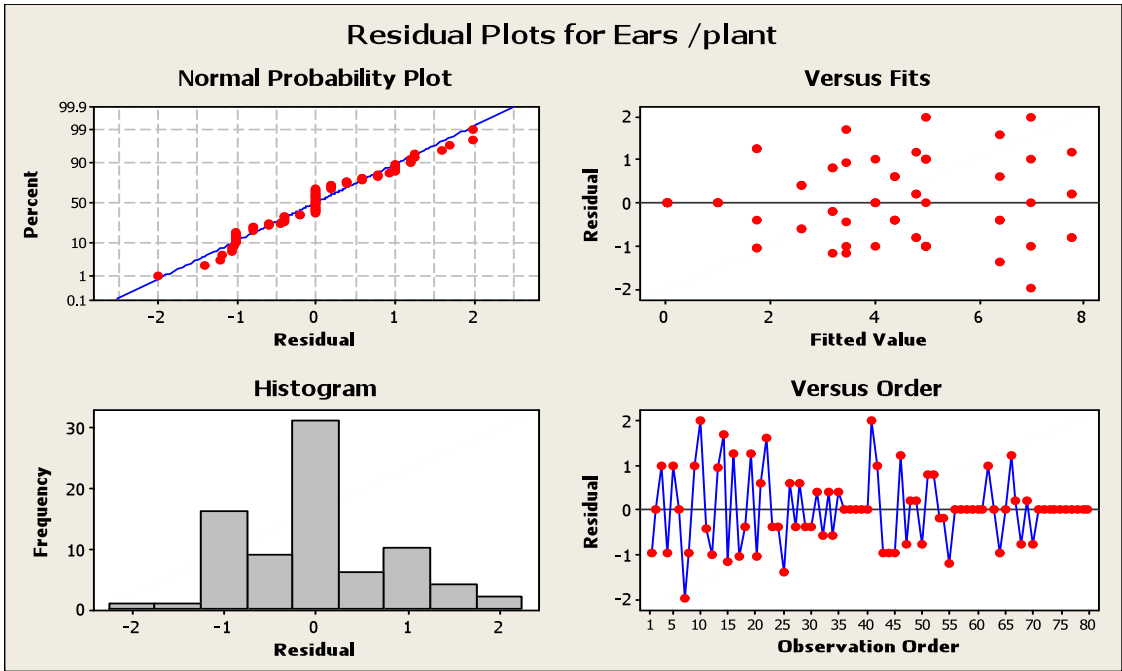
LSD= 2.12

Residual Plots for Ears /plant

Interaction Plot for Ears /plant
Fitted Means

Figure A 3-14: General Linear Model: Grains/Plant versus Line, NaCl Concentration.

```
Factor      Type   Levels  Values
Line        fixed       4  1 (Local), 2 (Optic), 3 (Soorab-96), 4
                           (Awaran-2002)
Treatment   fixed       4  0, 50, 100, 150

Analysis of Variance for Grains/Plant, using Adjusted SS for Tests

Source          DF    Seq SS    Adj SS   Adj MS       F      P
Line             3     768.4     768.4    256.1    0.86  0.469
Treatment        3   98493.7   98493.7  32831.2  109.72  0.000
Line*Treatment   9   12991.6   12991.6   1443.5    4.82  0.000
Error           64   19151.0   19151.0    299.2
Total           79  131404.7

S = 17.2984   R-Sq = 85.43%   R-Sq(adj) = 82.01%

Grouping Information Using Tukey Method and 95.0% Confidence

Line  Treatment  N   Mean  Grouping
3       50       5  114.6  A
2        0       5  106.2  A B
4       50       5  102.0  A B C
1       50       5   91.1  A B C
3        0       5   72.2    B C D
1        0       5   68.4    B C D E
4        0       5   68.2    B C D E
2       50       5   66.2      C D E
1      100       5   51.8        D E F
3      100       5   41.0        D E F
4      100       5   32.0          E F G
2      100       5   30.1          E F G
1      150       5   15.1            F G
4      150       5    0.0              G
3      150       5   -0.0              G
2      150       5   -0.0              G

Means that do not share a letter are significantly different.
```
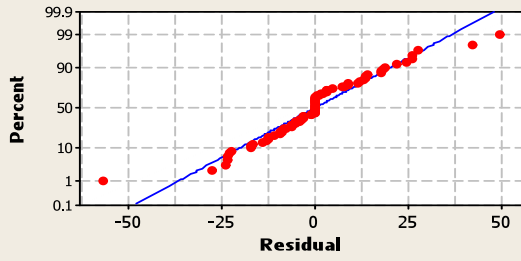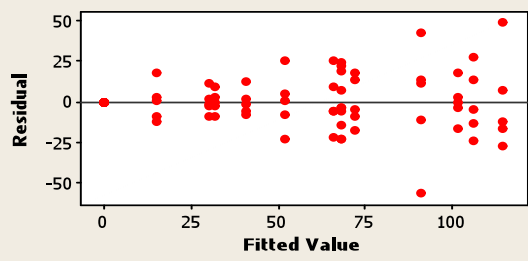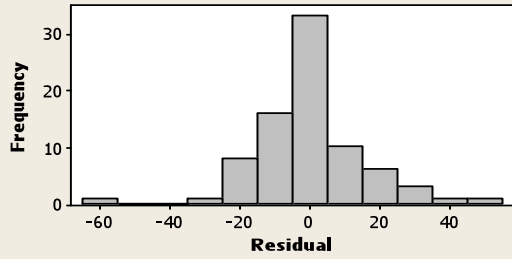
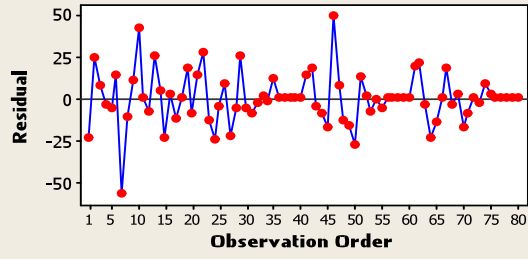**LSD= 28.98**

Residual Plots for Grains/Plant
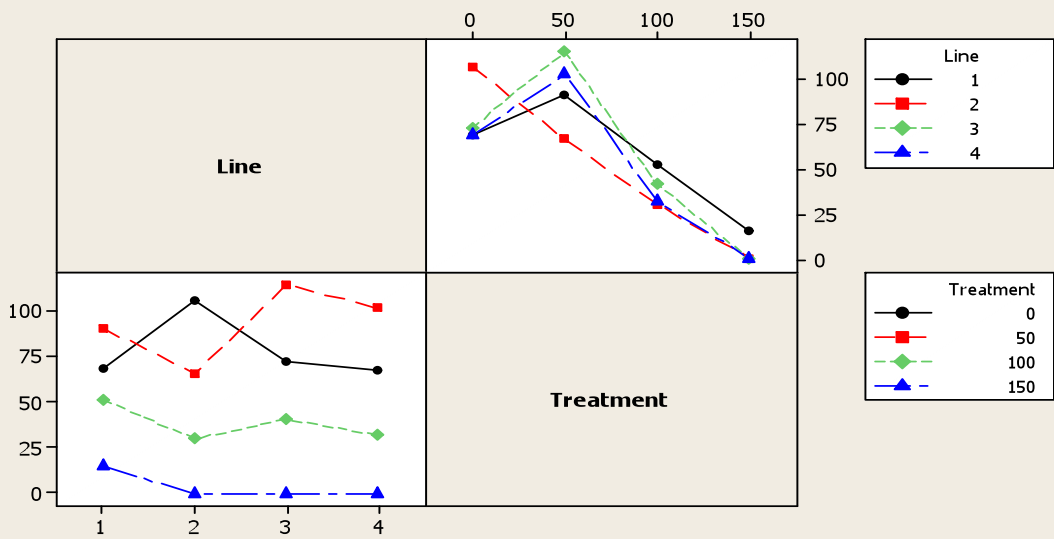
Interaction Plot for Grains/Plant

Figure A 3-15: General Linear Model: Grain Wt/plant versus Line, NaCl Concentration.

```
Factor     Type   Levels  Values
Line       fixed       4  1 (Local), 2 (Optic), 3 (Soorab-96), 4
                           (Awaran-2002)
Treatment  fixed       4  0, 50, 100, 150


Analysis of Variance for Grain Wt/plant, using Adjusted SS for Tests

Source          DF   Seq SS   Adj SS  Adj MS       F      P
Line             3    0.806    0.806   0.269    0.84  0.476
Treatment        3  204.088  204.088  68.029  213.35  0.000
Line*Treatment   9   23.264   23.264   2.585    8.11  0.000
Error           64   20.407   20.407   0.319
Total           79  248.566


S = 0.564682   R-Sq = 91.79%   R-Sq(adj) = 89.87%


Grouping Information Using Tukey Method and 95.0% Confidence

Line  Treatment  N  Mean   Grouping
3       50       5   5.0   A
4       50       5   4.6   A B
2        0       5   4.1   A B C
1       50       5   3.6     B C D
1        0       5   3.2       C D
2       50       5   2.9       C D E
3        0       5   2.7         D E
4        0       5   2.7         D E
1      100       5   1.7           E F
2      100       5   1.1             F G
3      100       5   0.9             F G
4      100       5   0.4               G
1      150       5   0.2               G
4      150       5   0.0               G
2      150       5   0.0               G
3      150       5  -0.0               G


Means that do not share a letter are significantly different.
```
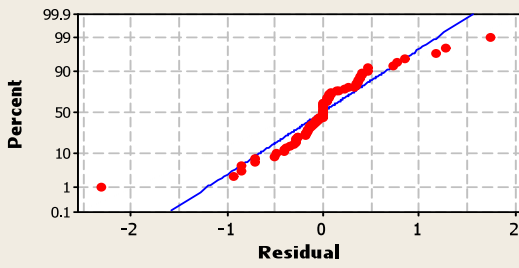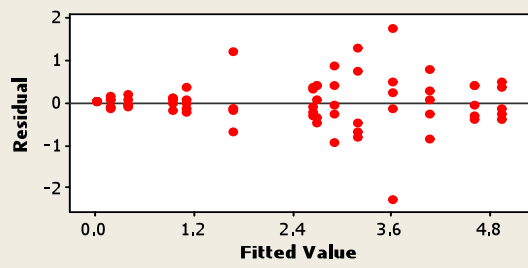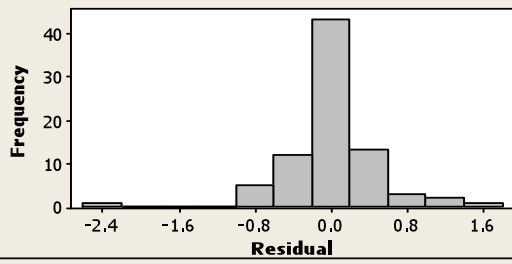
LSD= 1.27

Residual Plots for Grain Wt/plant
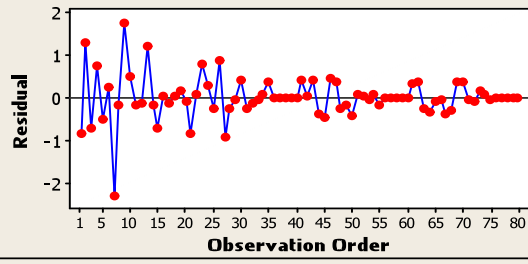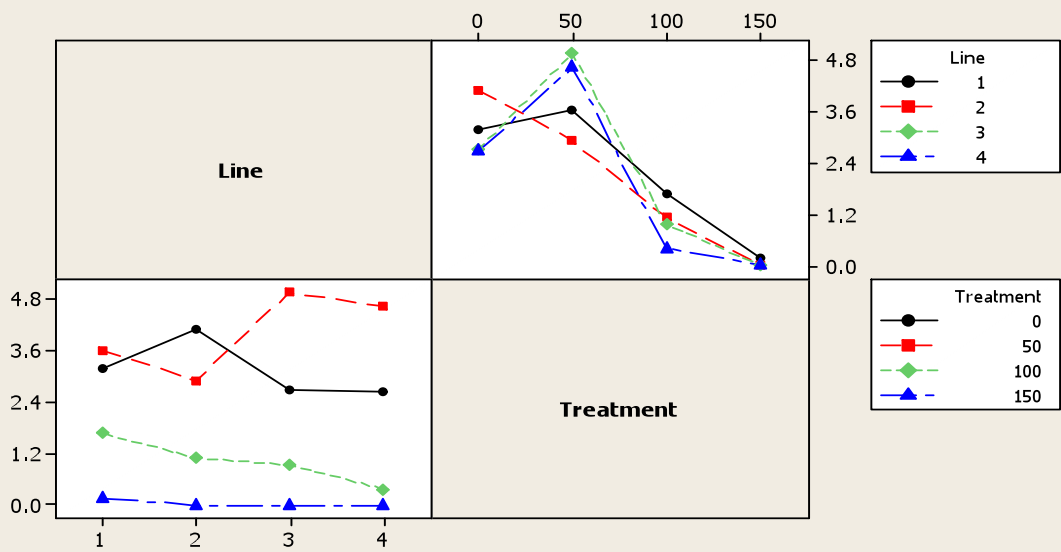
Interaction Plot for Grain Wt/plant

Figure A 3-16: General Linear Model: 1000 Grain Wt versus Line, NaCl Concentration.

```
Factor      Type    Levels  Values
Line        fixed        4  1 (Local), 2 (Optic), 3 (Soorab-96), 4
                            (Awaran-2002)
Treatment   fixed        4  0, 50, 100, 150


Analysis of Variance for 1000 grain wt, using Adjusted SS for Tests

Source            DF    Seq SS    Adj SS   Adj MS       F      P
Line               3     819.8     819.8    273.3    6.35  0.001
Treatment          3   18154.9   18154.9   6051.6  140.70  0.000
Line*Treatment     9    1517.3    1517.3    168.6    3.92  0.001
Error             64    2752.6    2752.6     43.0
Total             79   23244.6


S = 6.55819   R-Sq = 88.16%   R-Sq(adj) = 85.38%


Grouping Information Using Bonferroni Method and 95.0% Confidence

Line  Treatment  N   Mean  Grouping
1         0      5   47.2  A
4        50      5   46.1  A
3        50      5   44.8  A
4         0      5   40.7  A
1        50      5   40.2  A
2        50      5   40.2  A
2         0      5   40.1  A
3         0      5   38.0  A B
2       100      5   32.1  A B
1       100      5   32.1  A B
3       100      5   23.3    B C
4       100      5   12.4      C D
2       150      5   11.3      C D
1       150      5   11.3      C D
3       150      5    0.0        D
4       150      5    0.0        D


Means that do not share a letter are significantly different.
```
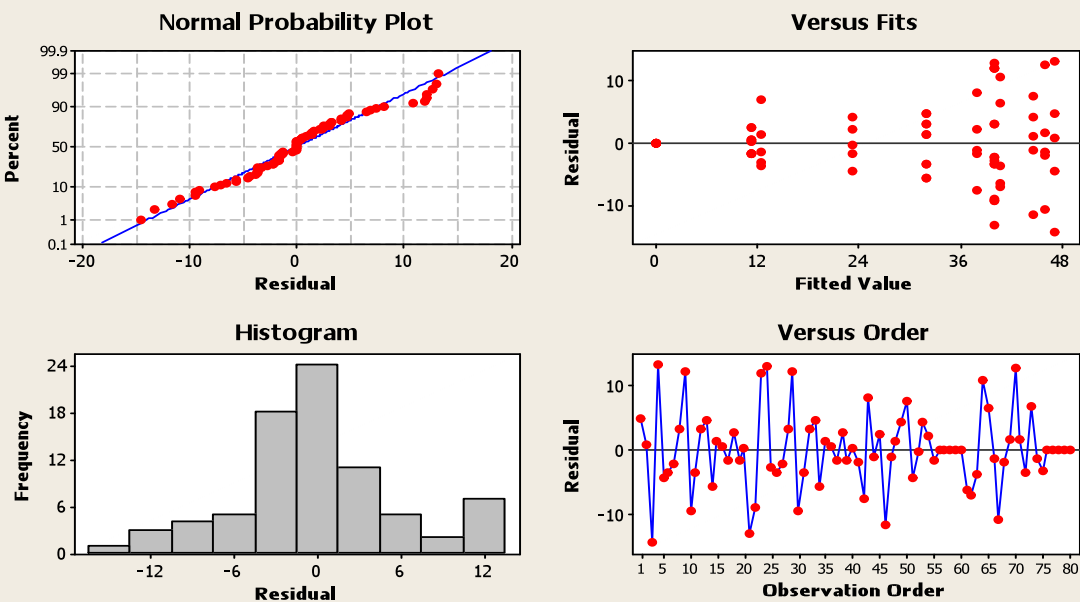
LSD= 15.45

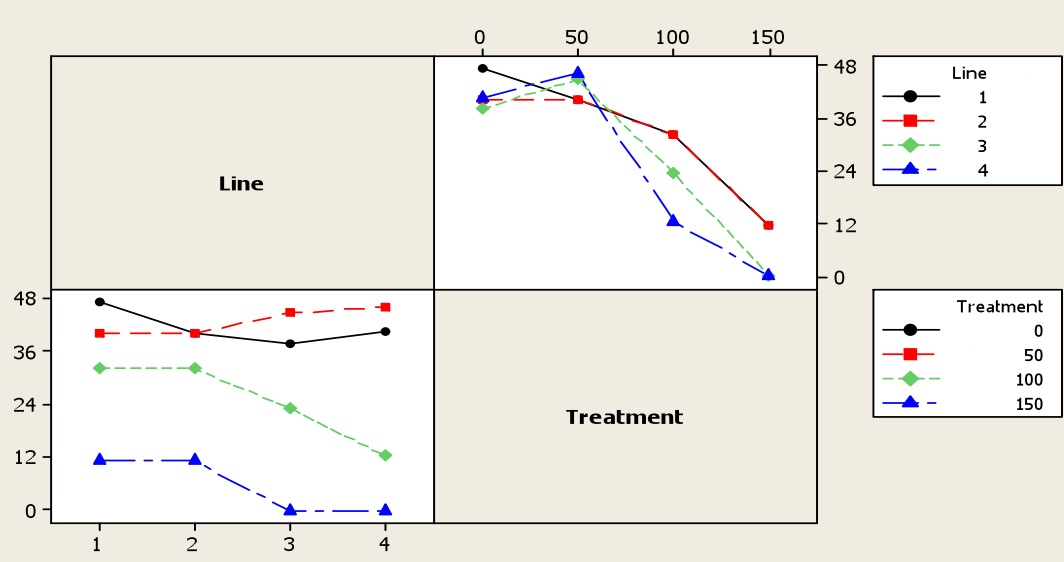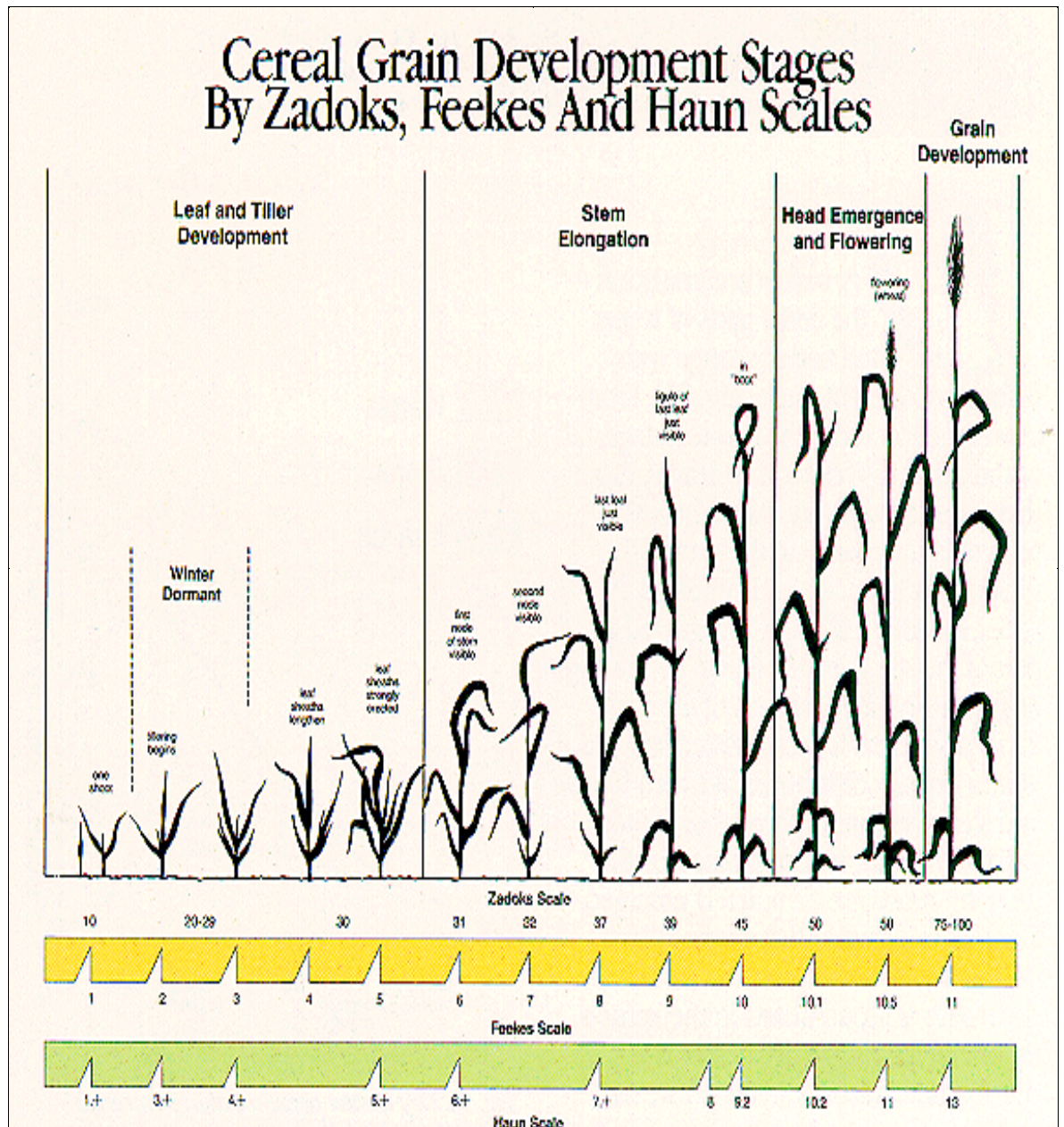Residual Plots for 1000 grain wt

Interaction Plot for 1000 grain wt
Fitted Means

Figure A 3-17: Cereal Grain Development Stages by Zadoks, Feekes and Haun.

Source: http://plantsci.missouri.edu/cropsys/growth.html#Field_staging_form

Table A 3-2: Cereal Grain Development Stages by Zadoks, Feekes and Haun.

Source: http://plantsci.missouri.edu/cropsys/growth.html#Field_staging_form

----

Zadoks Scale	Feekes Scale	Haun Scale	Description
			Germination
00	-	-	Dry Seed
01	-	-	Start of imbibition
03	-	-	Imbibition complete
05	-	-	Radicle emerged from seed
07	-	-	Coleoptile emerged from seed
09	-	0.0	Leaf just at coleoptile tip
			Seedling Growth
10	1	-	First leaf through coleoptile
11	-	1.0	First leaf extended
12	-	1.+	Second leaf extending
13	-	2.+	Third leaf extending
14	-	3.+	Fourth leaf extending
15	-	4.+	Fifth leaf extending
16	-	5.+	Sixth leaf extending
17	-	6.+	Seventh leaf extending
18	-	7.+	Eighth leaf extending
19	-	-	Nine or more leaves extended
			Tillering
20	-	-	Main shoot only
21	2	-	Main shoot and one tiller
22	-	-	Main shoot and two tillers
23	-	-	Main shoot and three tillers
24	-	-	Main shoot and four tillers
25	-	-	Main shoot and five tillers
26	3	-	Main shoot and six tillers

27	-	-	Main shoot and seven tillers
28	-	-	Main shoot and eight tillers
29	-	-	Main shoot and nine tillers

Stem Elongation

30	4-5	-	Psuedo stem erection
31	6	-	First node detectable
32	7	-	Second node detectable
33	-	-	Third node detectable
34	-	-	Fourth node detectable
35	-	-	Fifth node detectable
36	-	-	Sixth node detectable
37	8	-	Flag leaf just visible
39	9	-	Flag leaf ligule/collar just visible

Booting

40	-	-	---
41	-	8-9	Flag leaf sheath extending
45	10	9.2	Boot just swollen
47	-	-	Flag leaf sheath opening
49	-	10.1	First awns visible

Inflorescence Emergence

50	10.1	10.2	First spikelet of inflorescence visible
53	10.2	-	1/4 of inflorescence emerged
55	10.3	10.5	1/2 of inflorescence emerged
57	10.4	10.7	3/4 of inflorescence emerged
59	10.5	11.0	Emergence of inflorescence completed

Anthesis

60	10.51	11.4	Beginning of anthesis
65	-	11.5	Anthesis 1/2 completed

69	-	11.6	Anthesis completed

Milk Development

70	-	-	---
71	10.54	12.1	Kernel watery-ripe
73	-	13.0	Early milk
75	11.1	-	Medium milk
77	-	-	Late milk

Dough Development

80	-	-	---
83	-	14.0	Early dough
85	11.2	-	Soft dough
87	-	15.0	Hard dough

Ripening

90	-	-	---
91	11.3	-	Kernel hard (difficult to divide by thumbnail)
92	11.4	16.0	Kernel hard (can no longer be dented by thumbnail)
93	-	-	Kernel loosening in daytime
94	-	-	Overripe, straw dead and collapsing
95	-	-	Seed dormant
96	-	-	Viable seed giving 50% germination
97	-	-	Seed not dormant
98	-	-	Secondary dormancy induced
99	-	-	Secondary dormancy lost

Figure A 3-18: General Linear Model: Local versus Dev. Stage, NaCl Concentration

```
Factor              Type   Levels  Values
Dev. Stage          fixed      4   1, 2, 3, 4
NaCl Concentration  fixed      4   0, 50, 100, 150


Analysis of Variance for Local, using Adjusted SS for Tests

Source                      DF   Seq SS   Adj SS  Adj MS       F      P
Dev. Stage                   3  26053.7  26053.7  8684.6  840.44  0.000
NaCl Concentration           3   1657.8   1657.8   552.6   53.48  0.000
Dev. Stage*NaCl Concentration 9    349.5    349.5    38.8    3.76  0.003
Error                       32    330.7    330.7    10.3
Total                       47  28391.7


S = 3.21455   R-Sq = 98.84%   R-Sq(adj) = 98.29%

Grouping Information Using Tukey Method and 95.0% Confidence

Dev.   NaCl
Stage  Concentration  N   Mean  Grouping
4         50          3  100.0  A
4          0          3   89.0    B
4        100          3   80.3    B C
4        150          3   79.3    B C D
3         50          3   76.0      C D
3          0          3   70.0        D E
3        100          3   60.3          E F
3        150          3   59.0            F
2         50          3   55.0            F
2          0          3   51.0            F G
2        100          3   42.0              G H
2        150          3   38.0                H
1          0          3   26.0                  I
1         50          3   26.0                  I
1        100          3   23.0                  I
1        150          3   22.3                  I

Means that do not share a letter are significantly different.
```

LSD= 15.45

Residual Plots for Local

Interaction Plot for Local
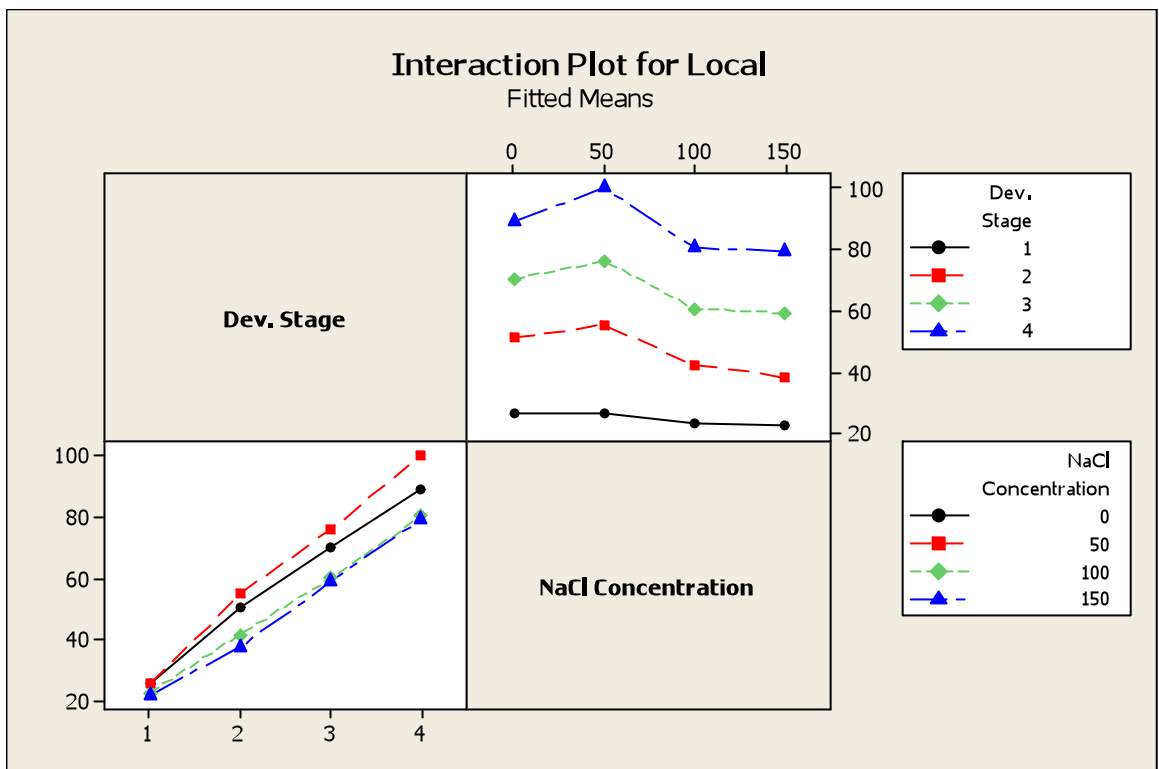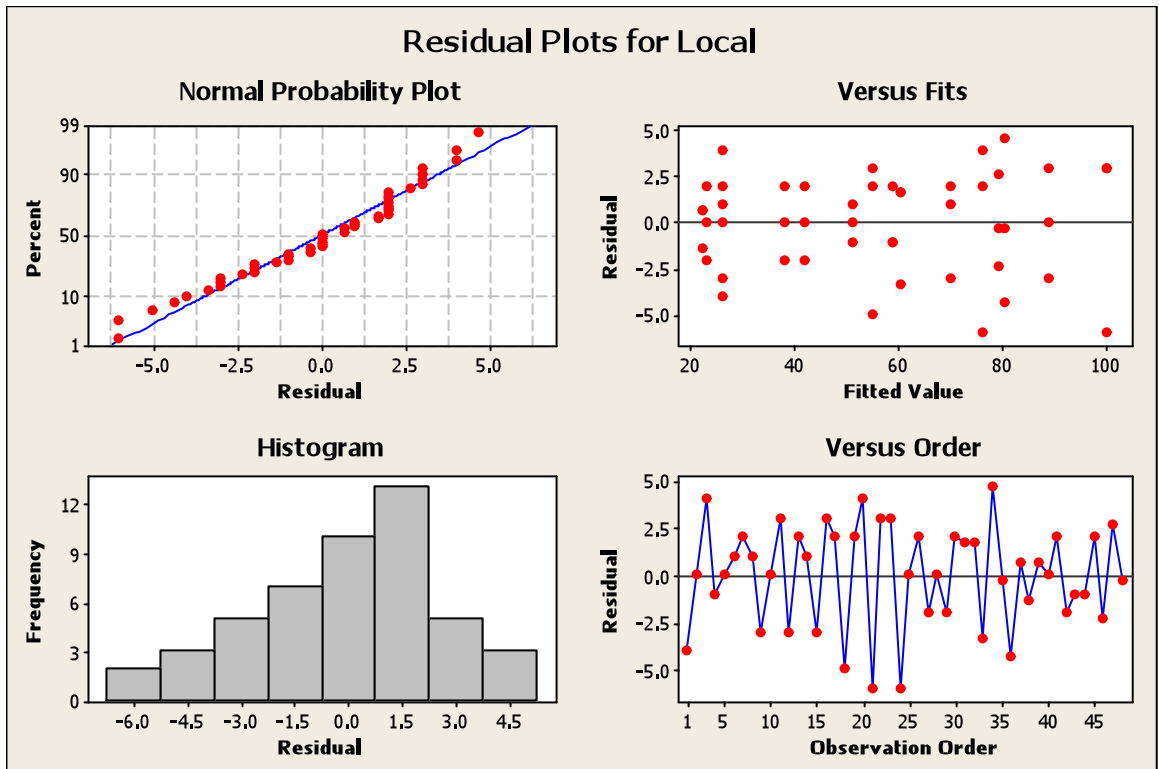
Figure A 3-19: General Linear Model: Optic versus Dev. Stage, NaCl Concentration

```
Factor              Type   Levels  Values
Dev. Stage          fixed       4  1, 2, 3, 4
NaCl Concentration  fixed       4  0, 50, 100, 150


Analysis of Variance for Optic, using Adjusted SS for Tests

Source                     DF   Seq SS   Adj SS  Adj MS       F      P
Dev. Stage                  3   9900.4   9900.4  3300.1  526.27  0.000
NaCl Concentration          3  11290.4  11290.4  3763.5  600.16  0.000
Dev. Stage*NaCl Concentration  9  12145.7  12145.7  1349.5  215.21  0.000
Error                      32    200.7    200.7     6.3
Total                      47  33537.3


S = 2.50416   R-Sq = 99.40%   R-Sq(adj) = 99.12%

Grouping Information Using Tukey Method and 95.0% Confidence

Dev.   NaCl
Stage  Concentration  N  Mean  Grouping
4         50          3  82.3  A
4          0          3  78.0  A
4        100          3  77.0  A
3         50          3  65.3   B
3          0          3  64.0   B
3        100          3  63.3   B
2        150          3  53.0    C
2        100          3  52.7    C
2         50          3  51.3    C
2          0          3  50.0    C
1          0          3  22.0     D
1        150          3  21.3     D
1         50          3  21.0     D
1        100          3  20.7     D
3        150          3   0.0      E
4        150          3  -0.0      E

Means that do not share a letter are significantly different.
```

LSD= 7.58

Residual Plots for Optic

Interaction Plot for Optic
Fitted Means
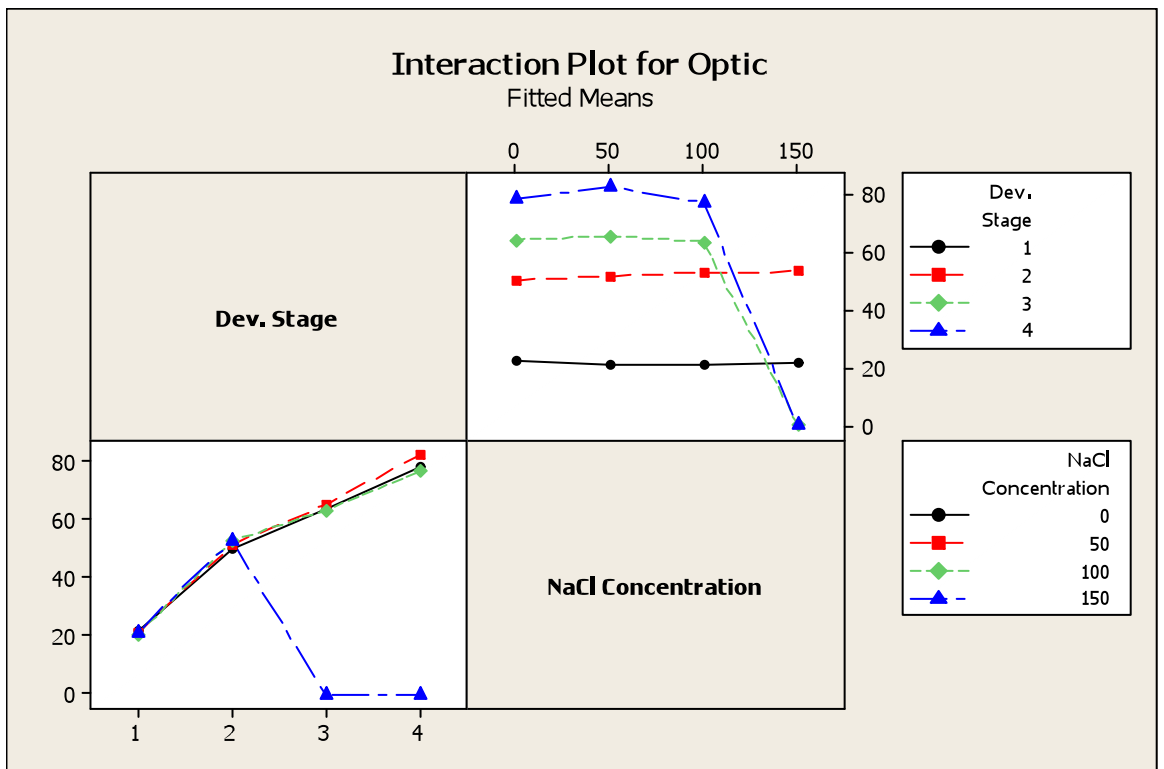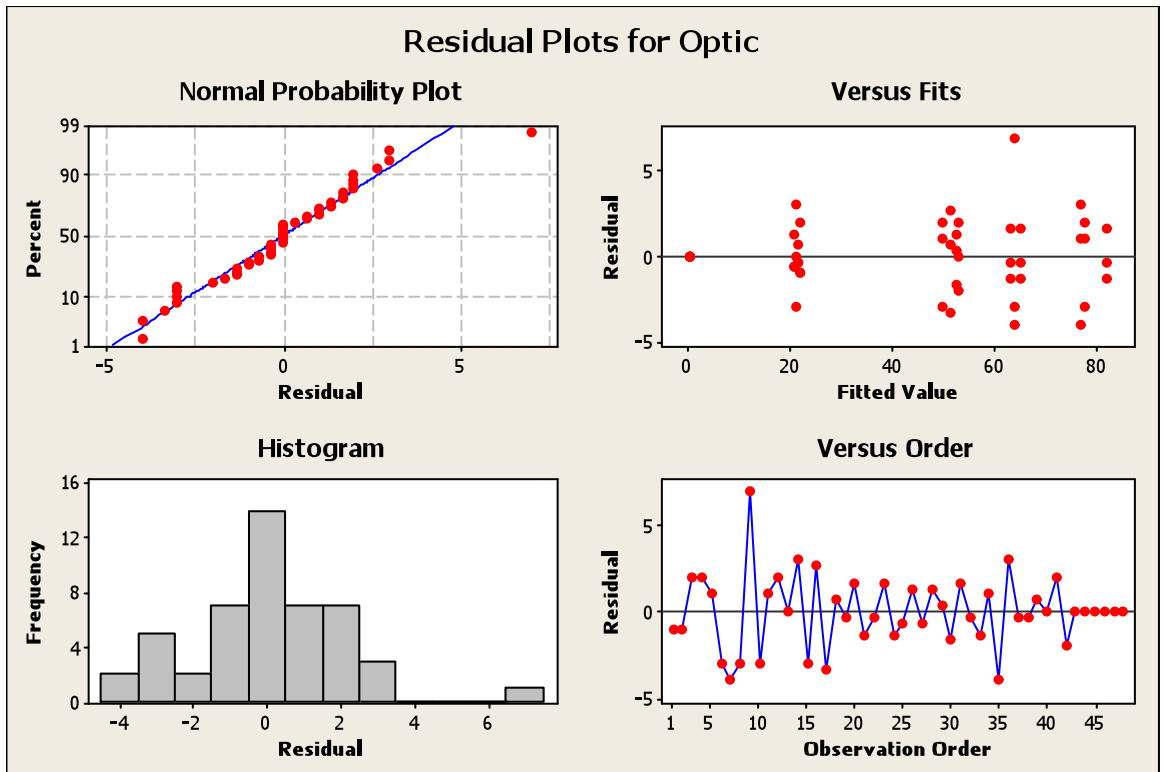
Figure A 3-20: General Linear Model: Soorab versus Dev. Stage, NaCl Concentration

```
Factor               Type    Levels  Values
Dev. Stage           fixed        4  1, 2, 3, 4
NaCl Concentration   fixed        4  0, 50, 100, 150


Analysis of Variance for Soorab, using Adjusted SS for Tests

Source                      DF   Seq SS   Adj SS   Adj MS        F      P
Dev. Stage                   3  26862.6  26862.6   8954.2  1043.21  0.000
NaCl Concentration           3  30047.7  30047.7  10015.9  1166.90  0.000
Dev. Stage*NaCl Concentration 9 27526.5  27526.5   3058.5   356.33  0.000
Error                       32    274.7    274.7      8.6
Total                       47  84711.5


S = 2.92973   R-Sq = 99.68%   R-Sq(adj) = 99.52%

Grouping Information Using Tukey Method and 95.0% Confidence

Dev.    NaCl
Stage   Concentration  N   Mean  Grouping
4         50           3  126.3  A
4        100           3  123.3  A
4          0           3  120.0  A
3        100           3  103.7    B
3         50           3  103.0    B
3          0           3   96.0    B
2        100           3   78.7      C
2         50           3   70.3      C D
2          0           3   67.0        D
2        150           3   64.7        D
1        150           3   29.0          E
1          0           3   28.0          E
1        100           3   28.0          E
1         50           3   27.7          E
4        150           3   -0.0            F
3        150           3   -0.0            F

Means that do not share a letter are significantly different.
```

LSD= 8.86

Residual Plots for Soorab
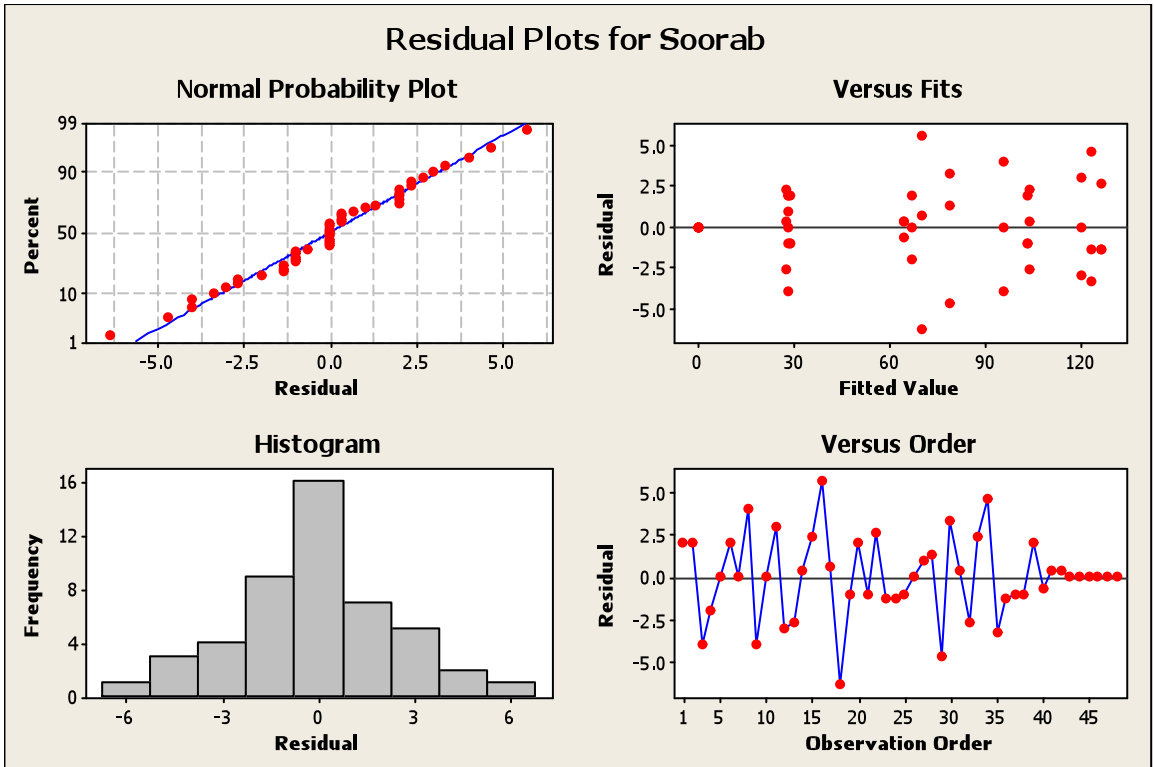
Interaction Plot for Soorab
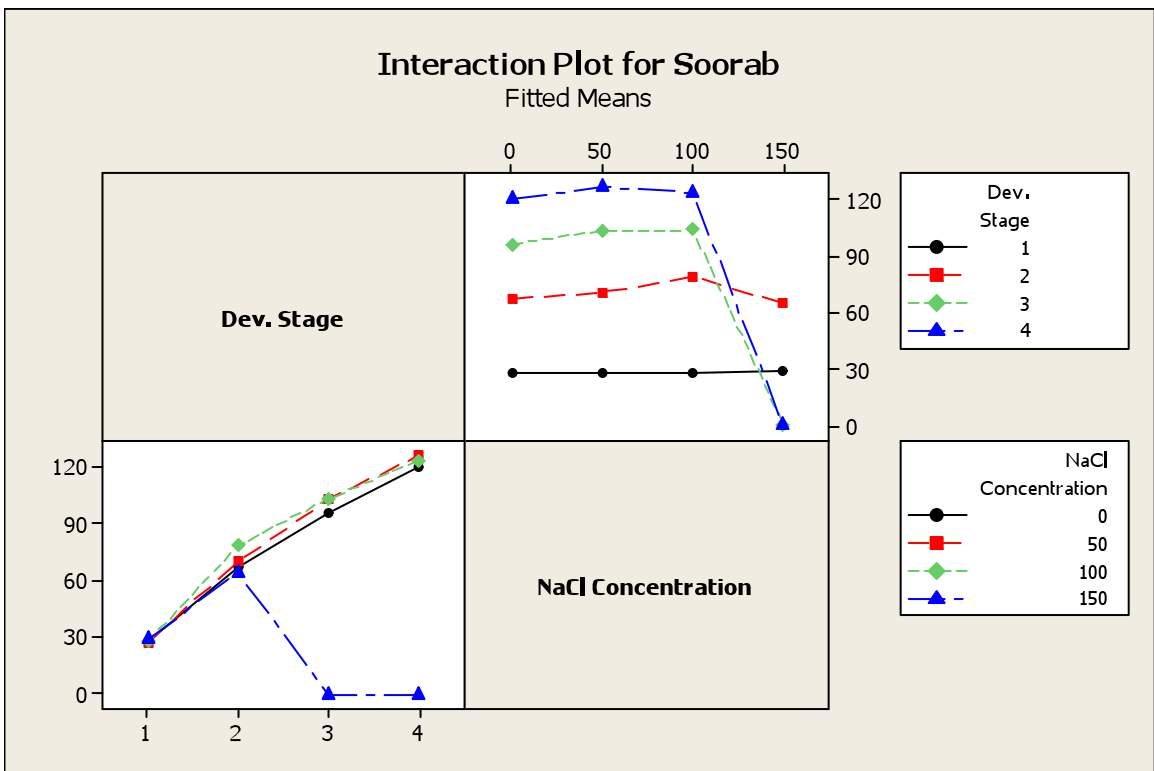
Figure A 3-21: General Linear Model: Awaran versus Dev. Stage, NaCl Concentration

```
Factor               Type   Levels  Values
Dev. Stage           fixed       4  1, 2, 3, 4
NaCl Concentration   fixed       4  0, 50, 100, 150


Analysis of Variance for Awaran, using Adjusted SS for Tests

Source                       DF   Seq SS   Adj SS   Adj MS        F      P
Dev. Stage                    3   4672.7   4672.7   1557.6   519.19  0.000
NaCl Concentration            3   9184.1   9184.1   3061.4  1020.45  0.000
Dev. Stage*NaCl Concentration 9   7787.0   7787.0    865.2   288.41  0.000
Error                        32     96.0     96.0      3.0
Total                        47  21739.8


S = 1.73205   R-Sq = 99.56%   R-Sq(adj) = 99.35%

Grouping Information Using Tukey Method and 95.0% Confidence

Dev.   NaCl
Stage  Concentration  N  Mean  Grouping
4          50         3  70.3  A
4           0         3  68.0  A
4         100         3  58.7    B
3           0         3  58.0    B
3          50         3  56.7    B
2          50         3  44.7      C
3         100         3  44.7      C
2           0         3  44.0      C
2         150         3  37.0        D
2         100         3  31.3          E
1           0         3  23.0            F
1          50         3  22.7            F
1         150         3  21.3            F
1         100         3  20.7            F
3         150         3   0.0              G
4         150         3  -0.0              G

Means that do not share a letter are significantly different.
```

LSD= 8.86

Residual Plots for Awaran

Interaction Plot for Awaran
Fitted Means
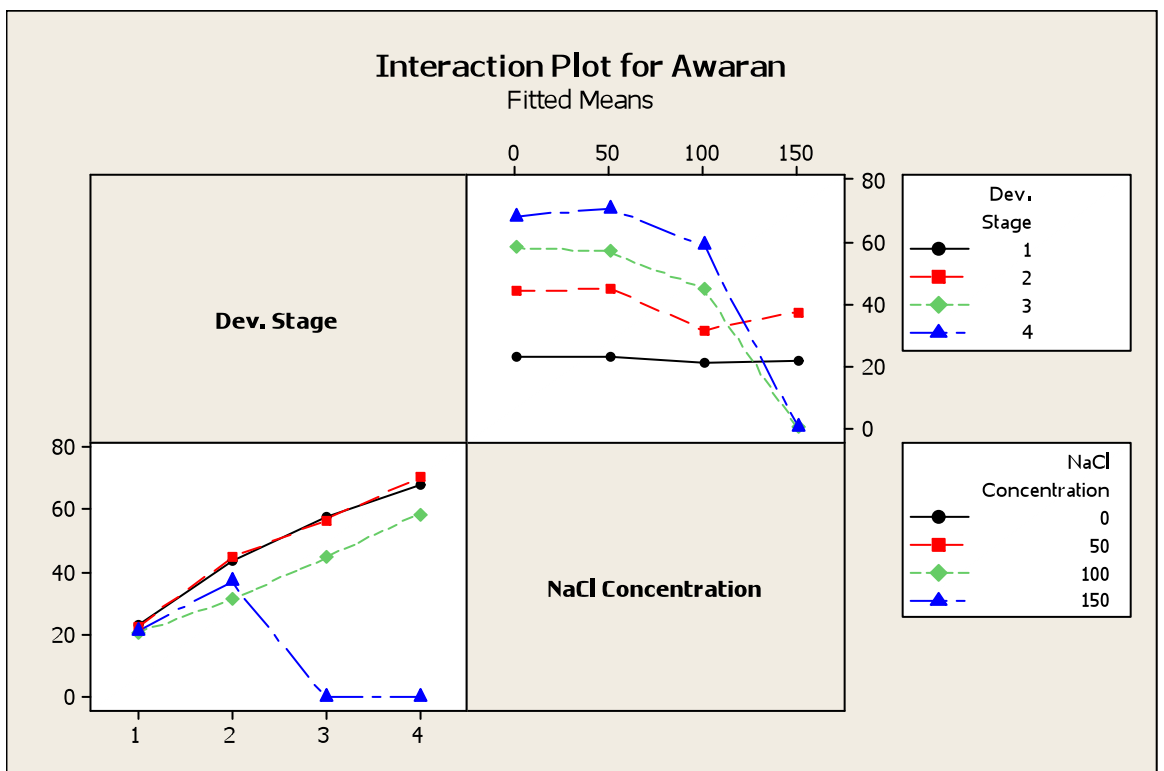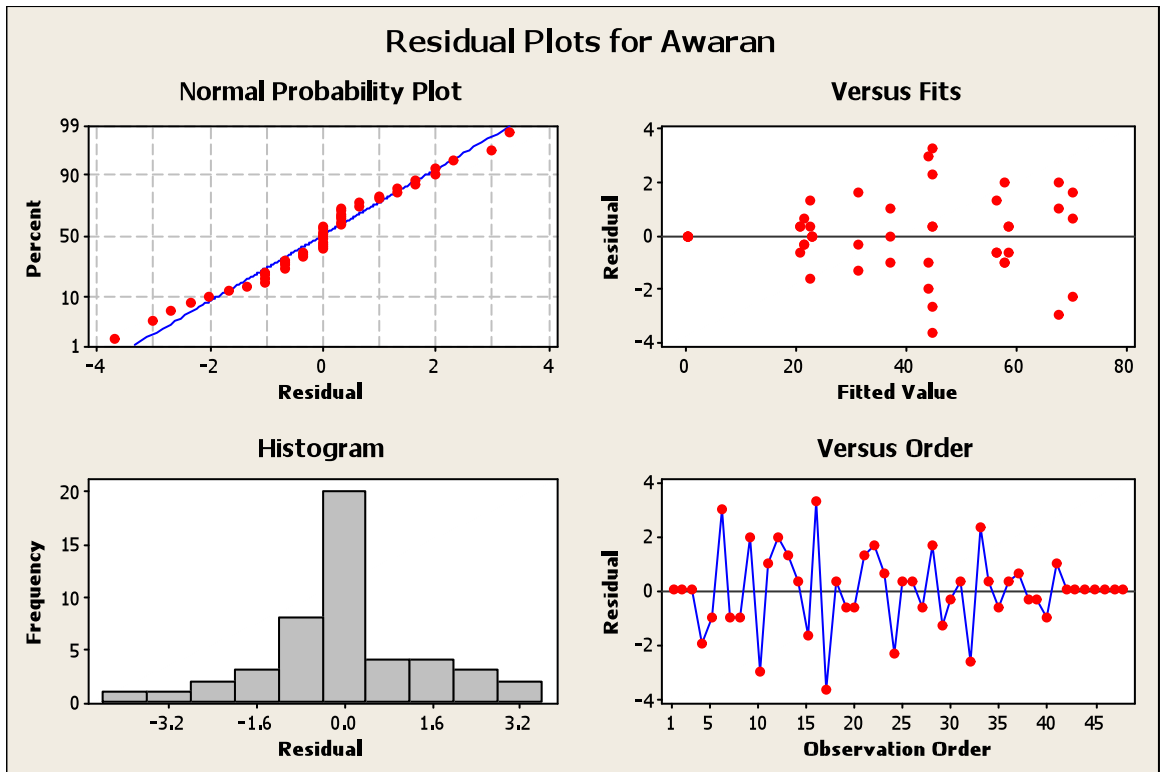
Figure A 4-1: General Linear Model: gs versus Line, NaCl Concentration.

```
Factor    Type   Levels  Values
Line      fixed       2  1 (Local), 2 (Optic)
NaCl Con  fixed       4  0, 50, 100, 150

Analysis of Variance for gs, using Adjusted SS for Tests

Source           DF   Seq SS   Adj SS   Adj MS       F      P
Line              1  0.15225  0.15225  0.15225   81.15  0.000
NaCl Con          3  1.02397  1.02397  0.34132  181.92  0.000
Line*NaCl Con     3  0.08557  0.08557  0.02852   15.20  0.000
Error            72  0.13509  0.13509  0.00188
Total            79  1.39689

S = 0.0433157   R-Sq = 90.33%   R-Sq(adj) = 89.39%

Grouping Information Using Tukey Method and 95.0% Confidence

      NaCl
Line  con   N  Mean  Grouping
2       0   3   0.5  A
1       0   3   0.5  A
1      50   3   0.5  A
2      50   3   0.4  A B
1     100   3   0.3    B C
1     150   3   0.3    B C
2     100   3   0.2      C
2     150   3   0.1        D

Means that do not share a letter are significantly different.
```

LSD= 0.16
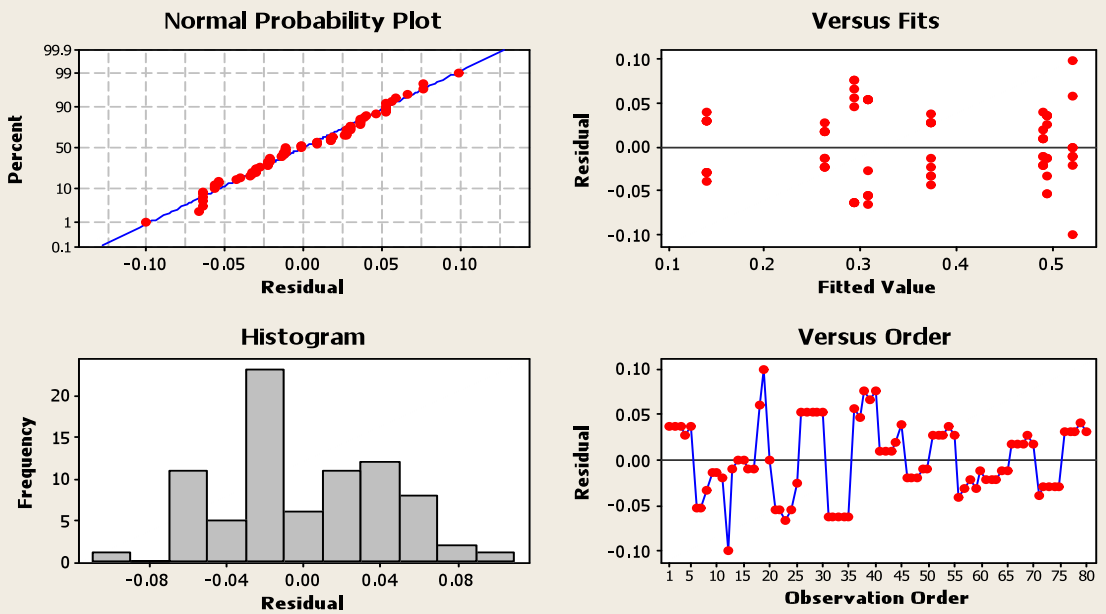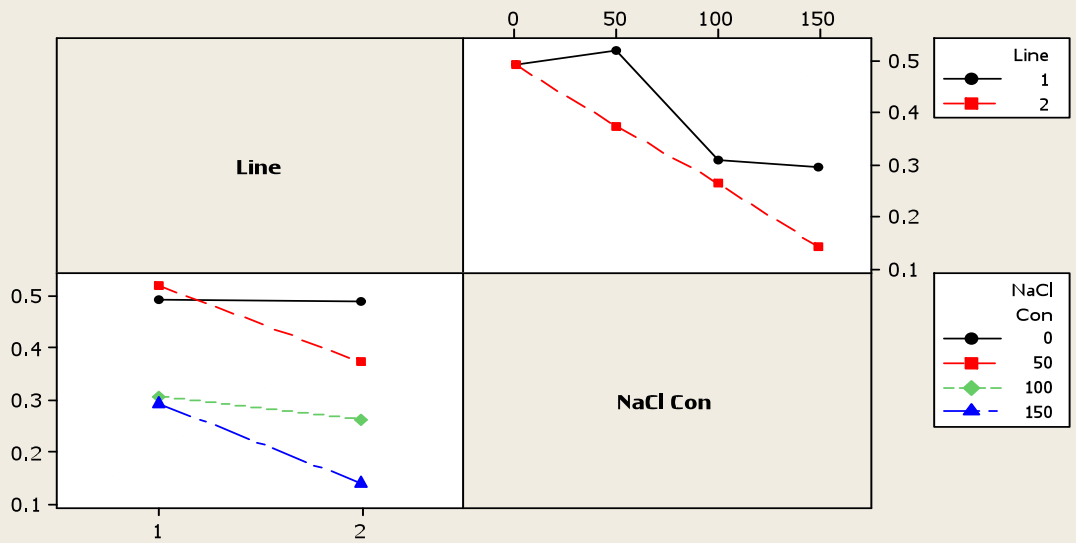
Figure A 4-2: General Linear Model: A$_{sat}$ versus Line, NaCl Concentration.

```
Factor    Type   Levels  Values
Line      fixed      2   1, 2
NaCl con  fixed      4   0, 50, 100, 150


Analysis of Variance for Asat, using Adjusted SS for Tests

Source         DF   Seq SS   Adj SS  Adj MS      F      P
Line            1    52.81    52.81   52.81   4.88  0.042
NaCl con        3  1385.13  1385.13  461.71  42.69  0.000
Line*NaCl con   3   147.59   147.59   49.20   4.55  0.017
Error          16   173.05   173.05   10.82
Total          23  1758.58


S = 3.28872   R-Sq = 90.16%   R-Sq(adj) = 85.85%

Grouping Information Using Bonferroni Method and 95.0% Confidence

      NaCl
Line  con  N  Mean  Grouping
2      50  3  20.6  A
1      50  3  18.9  A
1       0  3  18.8  A
2       0  3  18.4  A
1     100  3  17.8  A
2     100  3   6.5     B
1     150  3   1.6     B
2     150  3  -0.3     B

Means that do not share a letter are significantly different.
```

LSD= 10.05

Residual Plots for Asat

Normal Probability Plot

Versus Fits

Histogram

Versus Order

Interaction Plot for Asat
Fitted Means
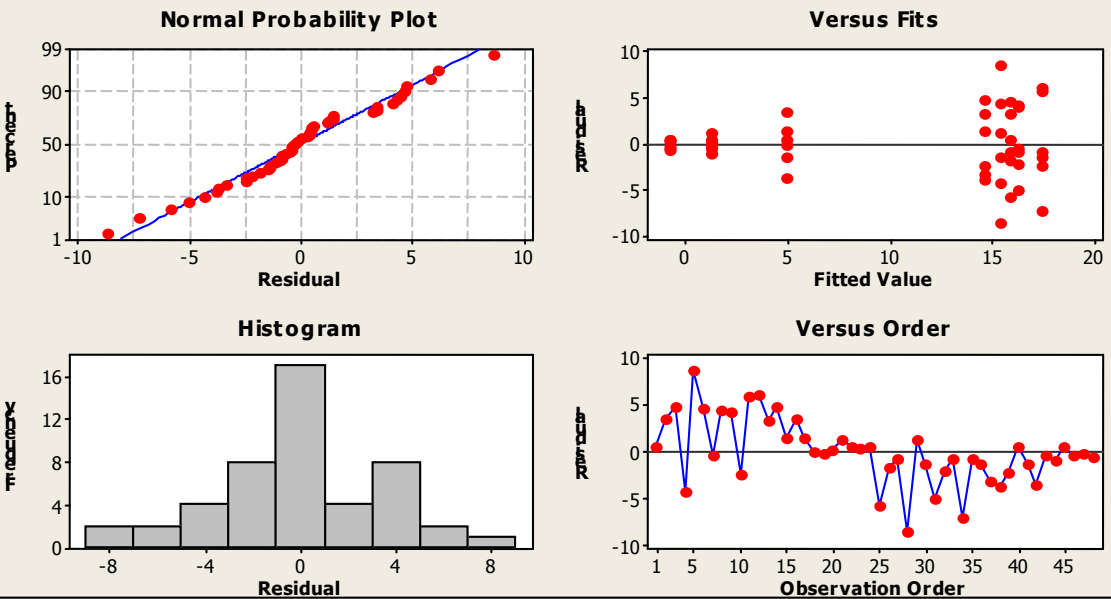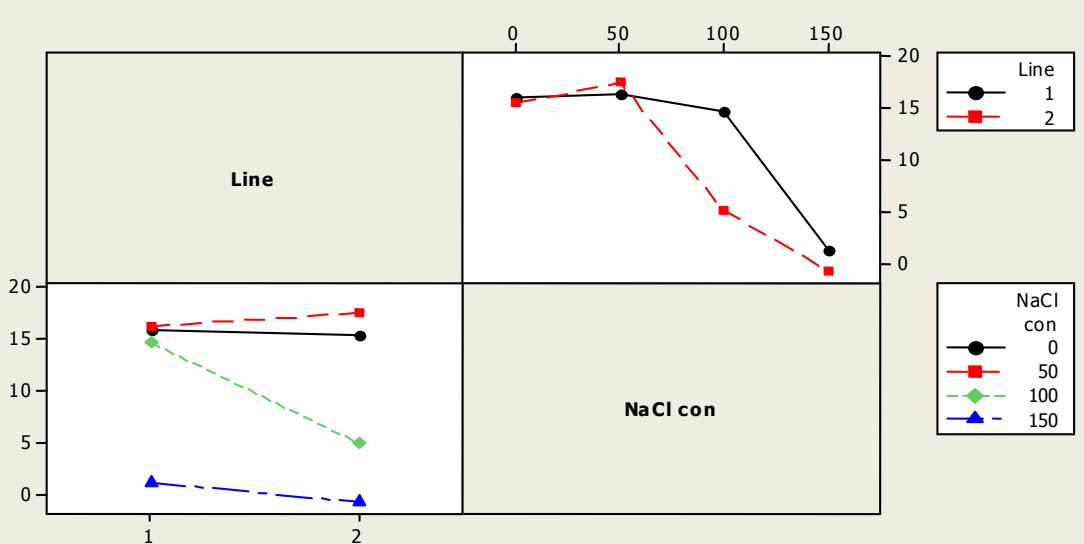
Line

NaCl con

Figure A 4-3: General Linear Model: A$_{180}$ versus Line, NaCl Concentration.

```
Factor     Type    Levels  Values
Line       fixed       2  1 (Local), 2 (Optic)
NaCl con   fixed       4  0, 50, 100, 150


Analysis of Variance for A180, using Adjusted SS for Tests

Source          DF  Seq SS  Adj SS  Adj MS      F      P
Line             1   37.20   37.20   37.20   5.38  0.034
NaCl con         3  743.71  743.71  247.90  35.88  0.000
Line*NaCl con    3   67.31   67.31   22.44   3.25  0.050
Error           16  110.54  110.54    6.91
Total           23  958.77


S = 2.62847   R-Sq = 88.47%   R-Sq(adj) = 83.43%


Grouping Information Using Bonferroni Method and 95.0% Confidence

      NaCl
Line  con   N  Mean  Grouping
2      50   3  14.3  A
1      50   3  13.6  A
1       0   3  13.1  A
2       0   3  12.5  A
1     100   3  11.4  A
2     100   3   3.4     B
1     150   3   0.9     B
2     150   3  -1.2     B


Means that do not share a letter are significantly different.
```

LSD= 8.03

Residual Plots for A180
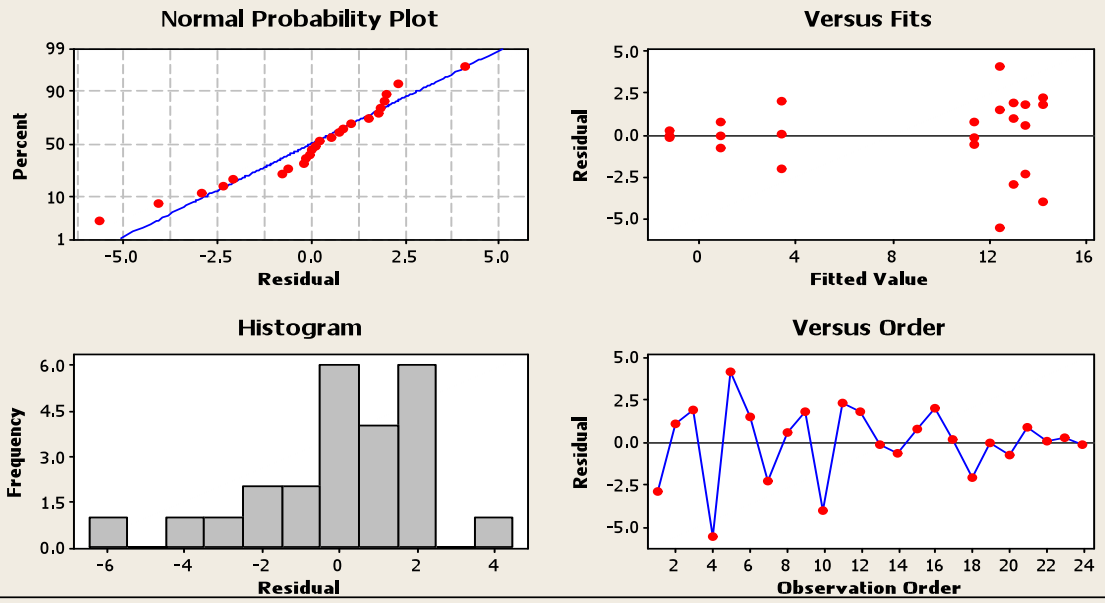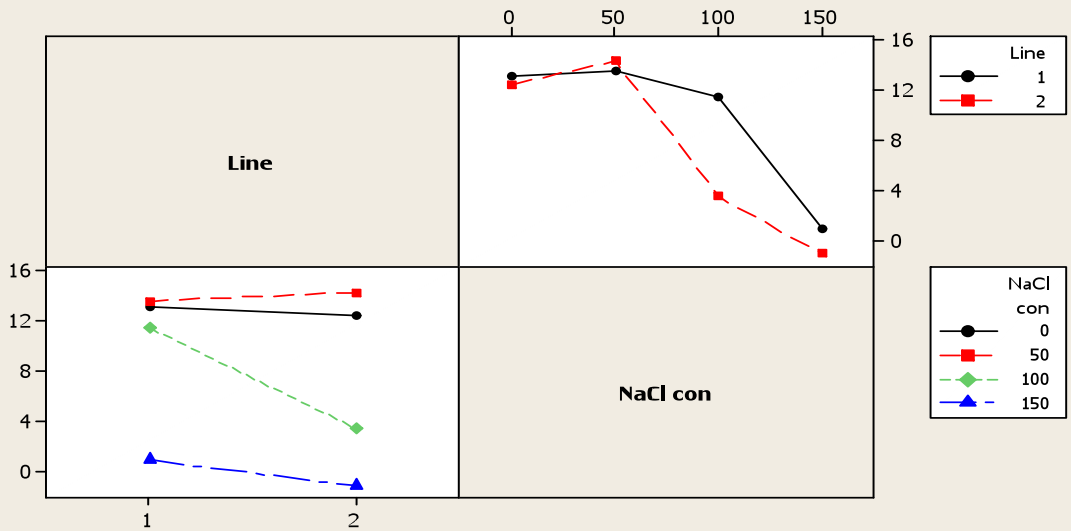
Figure A 4-4: General Linear Model: Log QE versus Line, NaCl Concentration.

```
Factor    Type   Levels  Values
Line      fixed      2   1 (Local), 2 (Optic)
NaCl con  fixed      4   0, 50, 100, 150


Analysis of Variance for Log QE, using Adjusted SS for Tests


Source          DF   Seq SS   Adj SS   Adj MS      F      P
Line             1  0.08863  0.08863  0.08863   3.27  0.089
NaCl con         3  3.09730  3.09730  1.03243  38.08  0.000
Line*NaCl con    3  0.11375  0.11375  0.03792   1.40  0.280
Error           16  0.43375  0.43375  0.02711
Total           23  3.73342


S = 0.164648   R-Sq = 88.38%   R-Sq(adj) = 83.30%


Grouping Information Using Bonferroni Method and 95.0% Confidence


      NaCl
Line  con   N  Mean  Grouping
2      50   3  -0.9  A
1      50   3  -1.0  A
1       0   3  -1.0  A
2       0   3  -1.0  A
1     100   3  -1.0  A
2     100   3  -1.4  A B
1     150   3  -1.8    B C
2     150   3  -1.9      C


Means that do not share a letter are significantly different.
```

LSD= 0.31
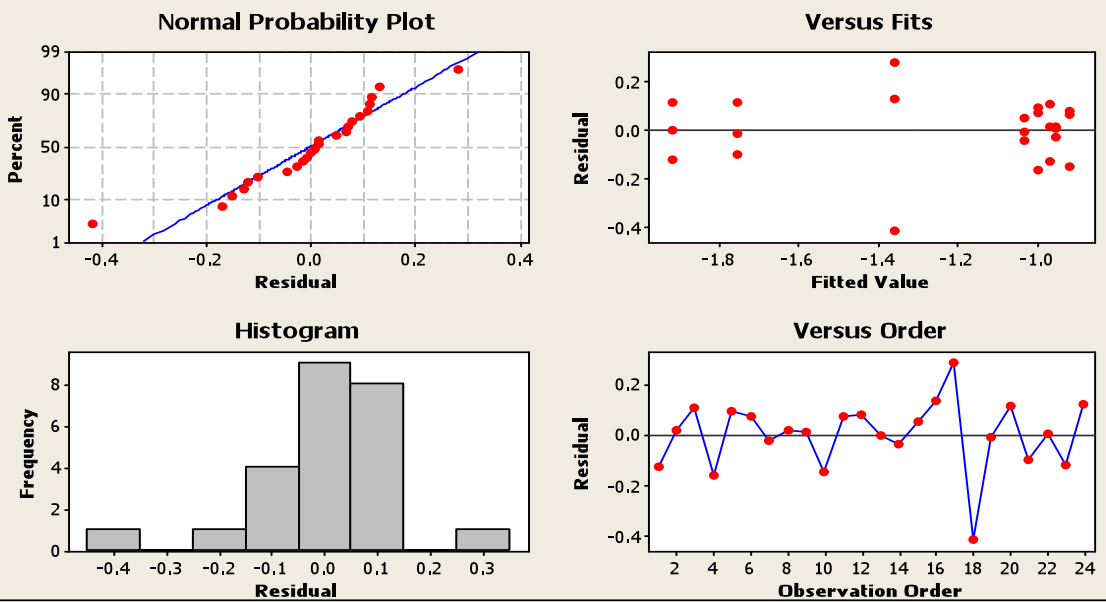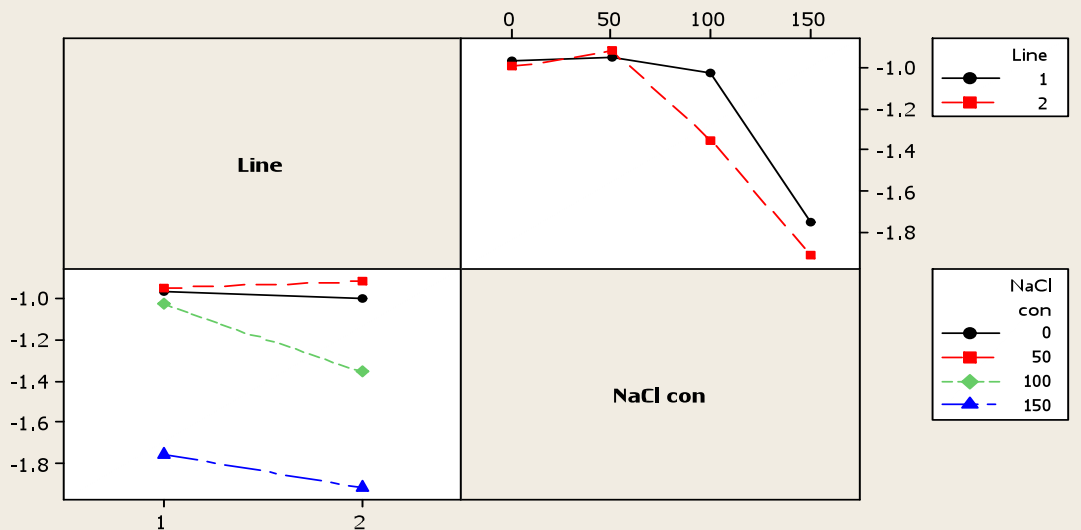
Figure A 4-5: General Linear Model: Carboxylation Efficiency versus Line, NaCl Concentration.

```
Factor     Type   Levels  Values
Line       fixed       2  1 (Local), 2 (Optic)
NaCl con   fixed       4  0, 50, 100, 150


Analysis of Variance for Carboxylation Efficiency, using Adjusted SS for Tests

Source        DF     Seq SS      Adj SS      Adj MS       F      P
Line           1  0.0000739   0.0000739   0.0000739    0.15  0.705
NaCl con       3  0.0321979   0.0321979   0.0107326   21.56  0.000
Line*NaCl con  3  0.0008433   0.0008433   0.0002811    0.56  0.646
Error         16  0.0079631   0.0079631   0.0004977
Total         23  0.0410782


S = 0.0223091   R-Sq = 80.61%   R-Sq(adj) = 72.13%


Grouping Information Using Tukey Method and 95.0% Confidence

      NaCl
Line  con   N  Mean  Grouping
2      50   3  0.1   A
2       0   3  0.1   A
1      50   3  0.1   A
1       0   3  0.1   A
1     100   3  0.1   A B
2     100   3  0.1   A B C
1     150   3  0.0     B C
2     150   3  0.0       C

Means that do not share a letter are significantly different.
```

LSD= 0.06

Residual Plots for Carboxylation Efficiency

Interaction Plot for Carboxylation Efficiency
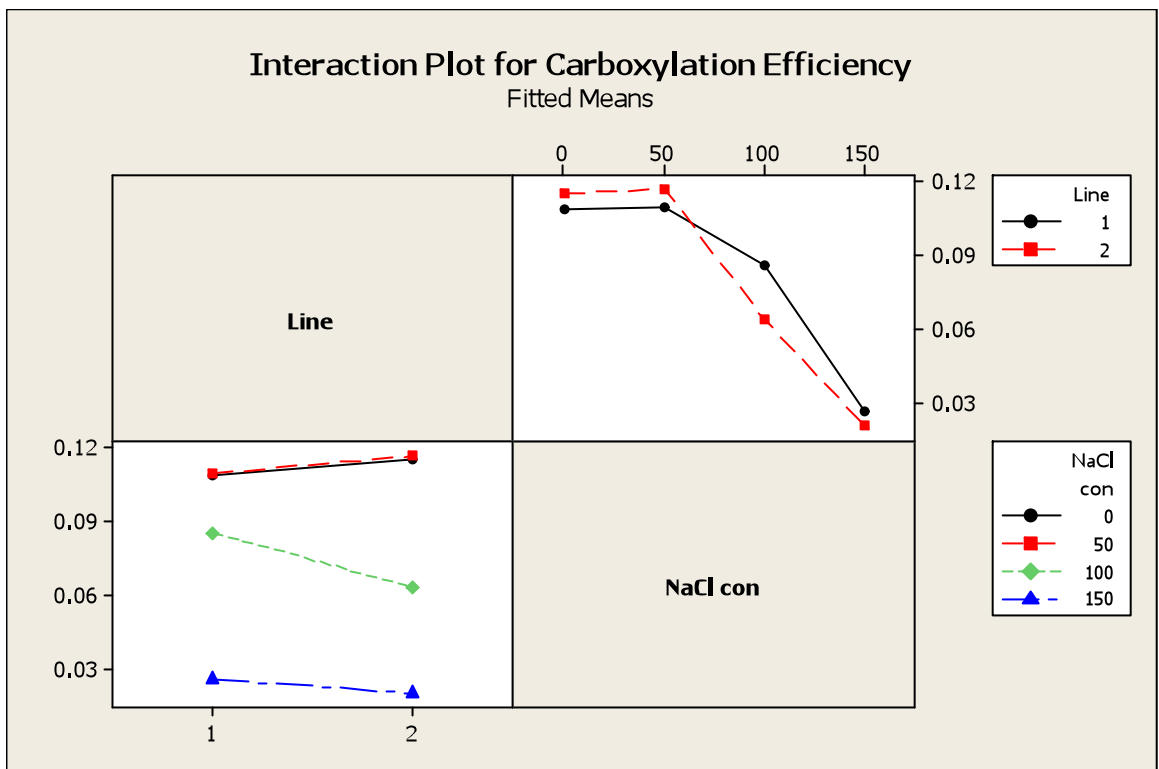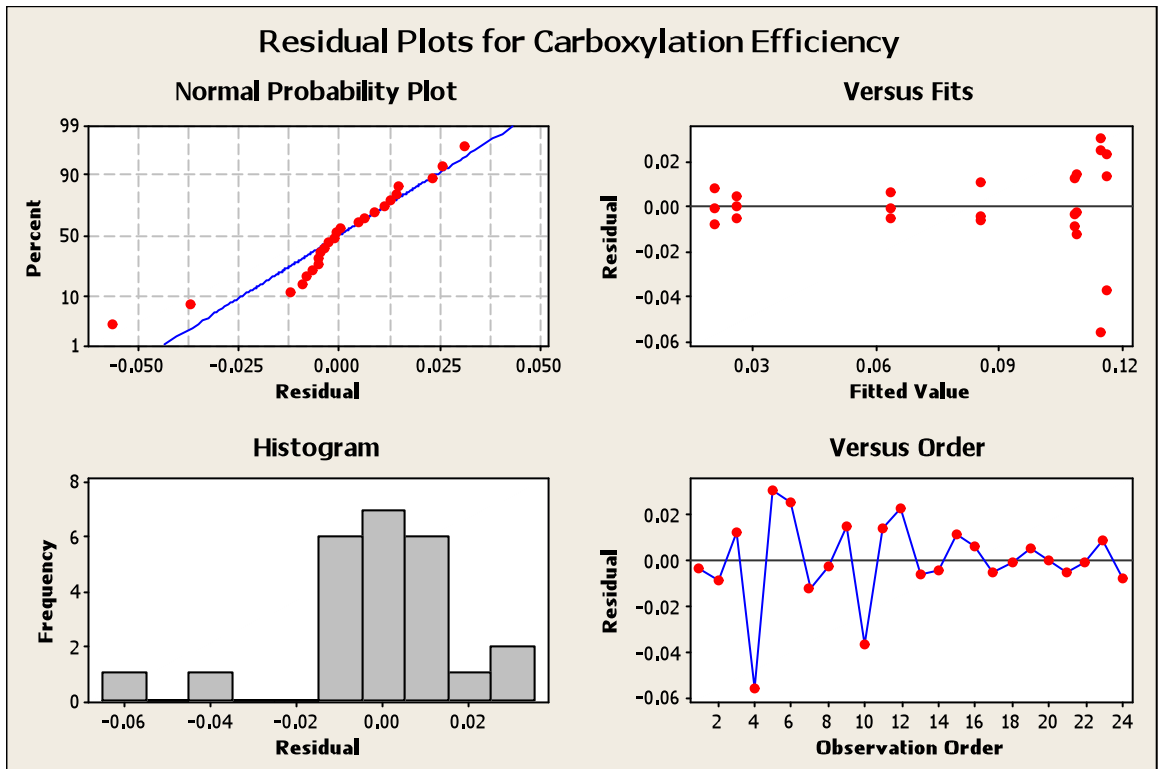
Figure A 4-6: General Linear Model: V_o versus Line, NaCl Concentration.

```
Factor    Type   Levels  Values
Line      fixed      2  1 (Local), 2 (Optic)
NaCl con  fixed      4  0, 50, 100, 150


Analysis of Variance for Vo, using Adjusted SS for Tests

Source          DF   Seq SS  Adj SS  Adj MS     F      P
Line             1    0.695   0.695   0.695  0.23  0.635
NaCl con         3   75.217  75.217  25.072  8.43  0.001
Line*NaCl con    3    1.024   1.024   0.341  0.11  0.950
Error           16   47.614  47.614   2.976
Total           23  124.550


S = 1.72506   R-Sq = 61.77%   R-Sq(adj) = 45.05%


Grouping Information Using Sidak Method and 95.0% Confidence

      NaCl
Line  con  N  Mean  Grouping
2     150  3  -2.2  A
1     150  3  -2.3  A
2     100  3  -3.9  A B
1     100  3  -4.6    B
2       0  3  -6.0    B
1      50  3  -6.5    B
2      50  3  -6.7    B
1       0  3  -6.7    B


Means that do not share a letter are significantly different.
```

LSD= 2.24

Residual Plots for Vo

Normal Probability Plot

Versus Fits

Histogram

Versus Order

Interaction Plot for Vo
Fitted Means
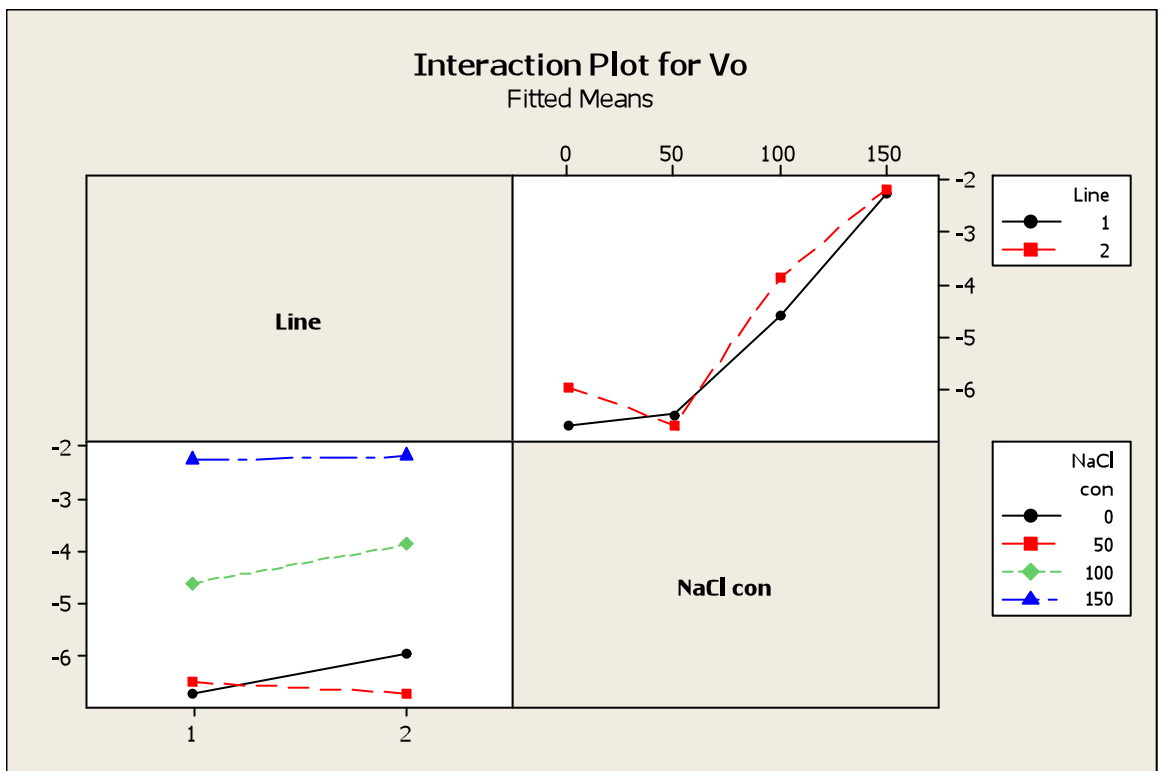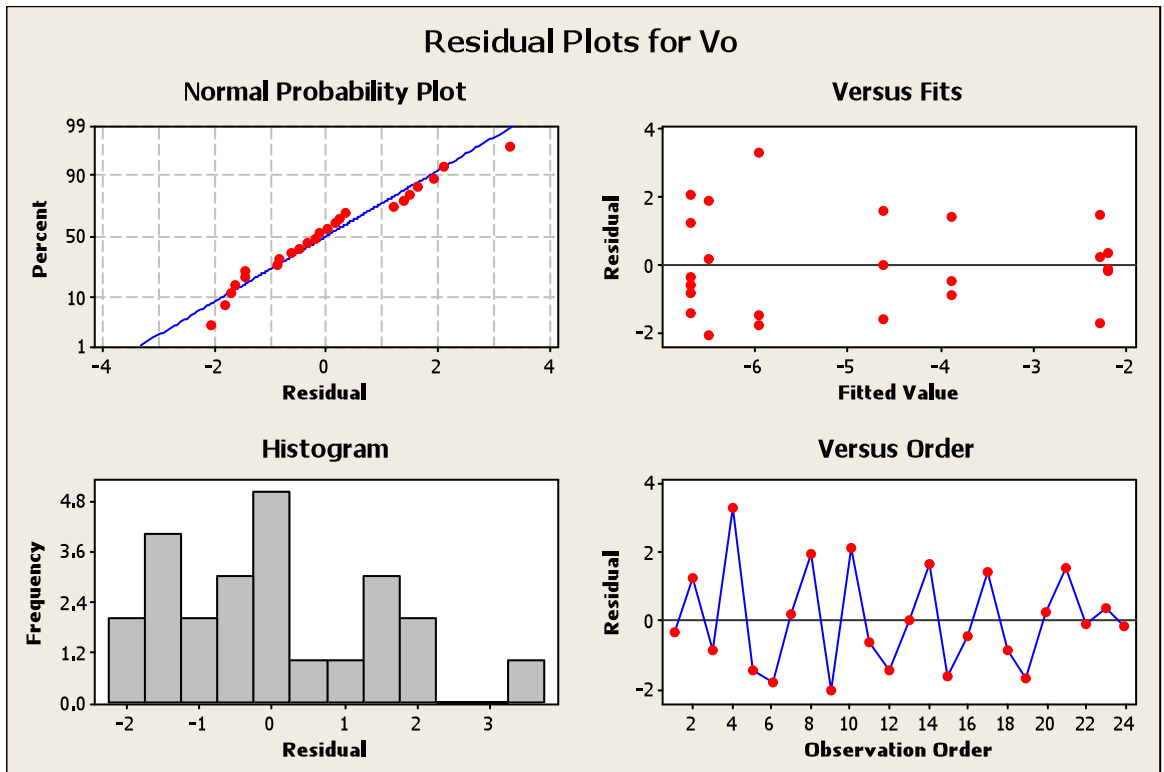
Figure A 4-7: General Linear Model: Rd versus Line, NaCl Concentration.

```
Factor     Type    Levels  Values
Line       fixed        2  1 (Local), 2 (Optic)
NaCl con   fixed        4  0, 50, 100, 150


Analysis of Variance for Rd, using Adjusted SS for Tests

Source          DF   Seq SS  Adj SS  Adj MS     F      P
Line             1   0.7486  0.7486  0.7486  1.53  0.233
NaCl con         3   6.0871  6.0871  2.0290  4.16  0.023
Line*NaCl con    3   0.6222  0.6222  0.2074  0.43  0.738
Error           16   7.8068  7.8068  0.4879
Total           23  15.2648


S = 0.698518   R-Sq = 48.86%   R-Sq(adj) = 26.48%


Grouping Information Using Bonferroni Method and 95.0% Confidence

       NaCl
Line   con   N  Mean  Grouping
1       50   3  -0.5  A
2        0   3  -0.5  A
1        0   3  -0.5  A
2       50   3  -0.6  A
1      100   3  -1.1  A
1      150   3  -1.3  A
2      150   3  -1.8  A
2      100   3  -1.9  A

Means that do not share a letter are significantly different.


LSD= 1.12
```

Residual Plots for Rd
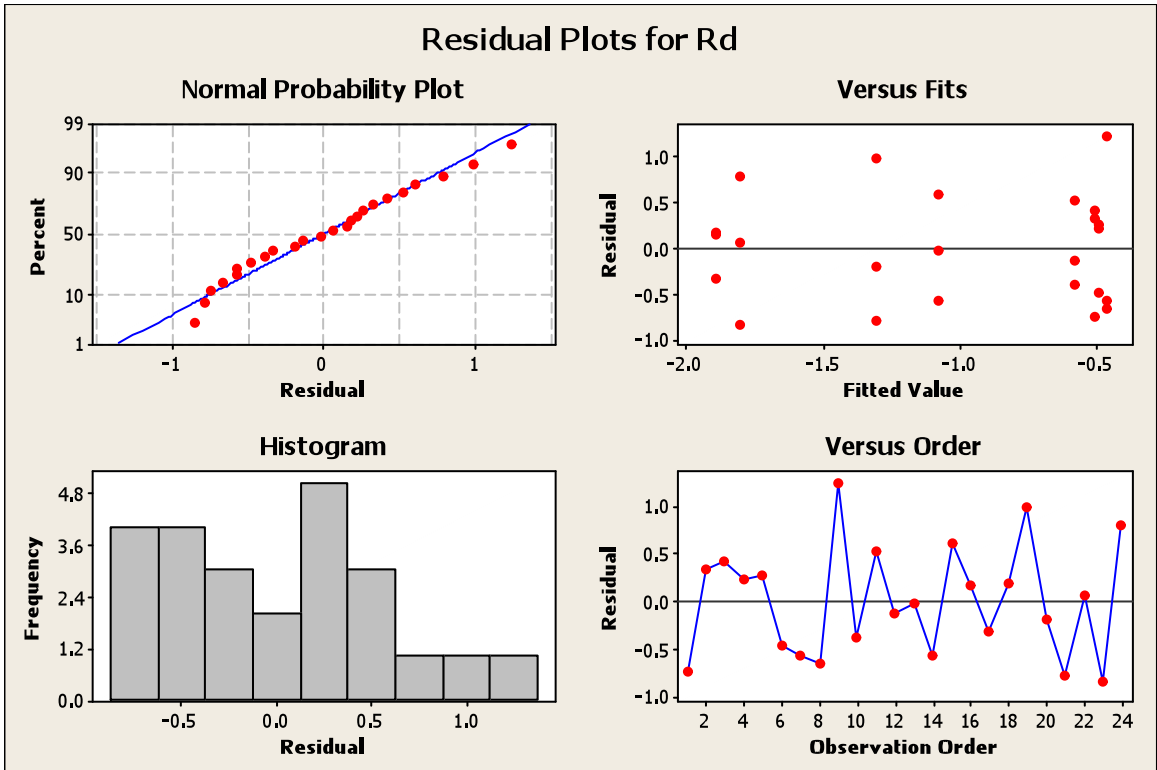
Interaction Plot for Rd
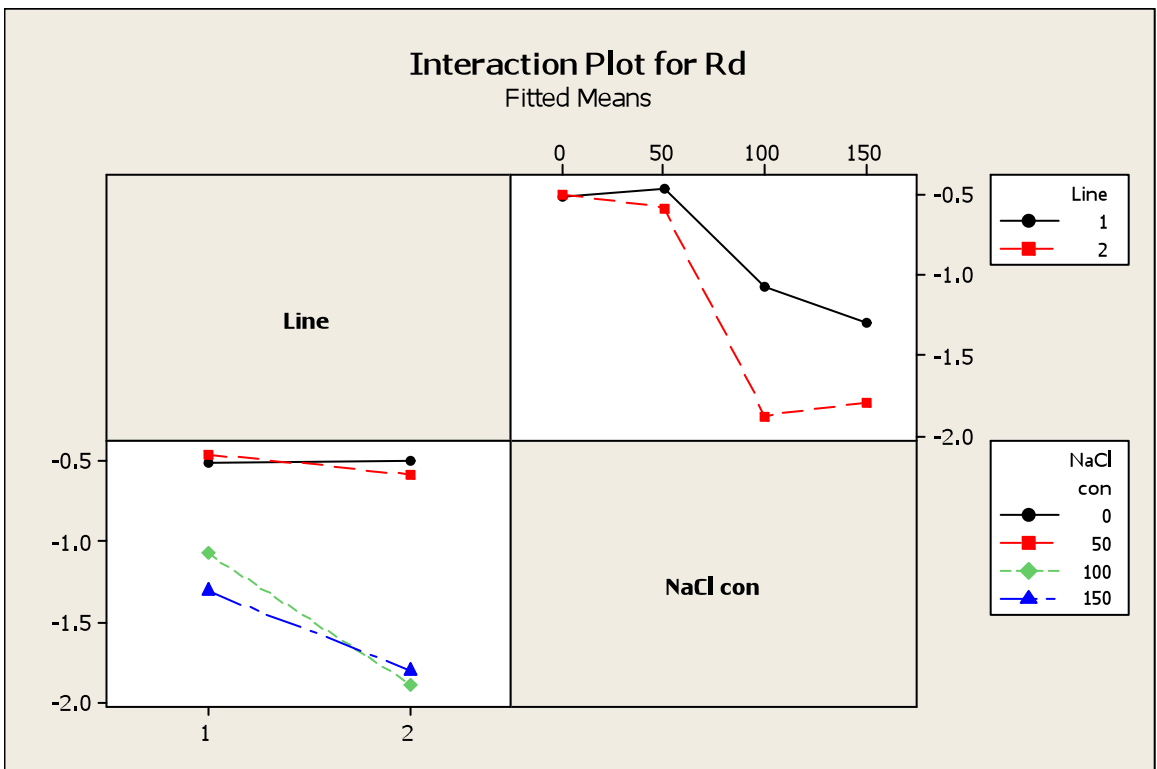
Table A 4-1: General Linear Model: Ci/Ca versus Line, NaCl Con

```
Factor    Type   Levels  Values
Line      fixed      2   1, 2
NaCl Con  fixed      4   0, 50, 100, 150


Analysis of Variance for Ci/Ca, using Adjusted SS for Tests

Source          DF   Seq SS    Adj SS    Adj MS     F      P
Line             1  0.10746   0.10746   0.10746   3.28   0.089
NaCl Con         3  0.01304   0.01304   0.00435   0.13   0.939
Line*NaCl Con    3  0.12865   0.12865   0.04288   1.31   0.306
Error           16  0.52419   0.52419   0.03276
Total           23  0.77335


S = 0.181003   R-Sq = 32.22%   R-Sq(adj) = 2.56%

Grouping Information Using Tukey Method and 95.0% Confidence

NaCl
Con   N  Mean  Grouping
150   6   0.7  A
  0   6   0.7  A
100   6   0.6  A
 50   6   0.6  A

Means that do not share a letter are significantly different.
```

LSD= 0.3

Table A 4-2: General Linear Model: Asat versus gs; line through 0

```
Quadratic

     A=a+bgs+cgs² ' a=0
     Fits well    R²              Local= 0.984
                  R²              Local= 0.967


Analysis of Variance regression of fits.for

Local               c         b           a

                    -75.499   77.432      0
     SE             3.775     1.589       -
     R²             0.984
     Df.            153
     N=             155

Optic               c         b           a

                    -49.009   68.467      0
     SE             5.892     2.266       -
     R²             0.967
     Df.            158
     N=             160


Test for slope differences


     Graffen and Hails (2002)

T    =      Coeff(Local) – Coeff (Optic) x t 155
            ─────────────────────────────────────
                    SE Coeff (Local)
```

```
b SE difference = 5.642
c SE difference = 7.017

p<0.001

Thus slopes are different
```

Figure A 4-8: General Linear Model: Relative Water Content % Control versus Line, NaCl Concentration.

```
Factor    Type   Levels  Values
Line      fixed       2  1 (Local), 2 (Optic)
NaCl Con  fixed       4  0, 50, 100, 150


Analysis of Variance for RWC % Control, using Adjusted SS for Tests

Source          DF   Seq SS    Adj SS  Adj MS      F      P
Line             1    733.2     733.2   733.2   1.48  0.241
NaCl Con         3  27340.8   27340.8  9113.6  18.40  0.000
Line*NaCl Con    3    408.1     408.1   136.0   0.27  0.843
Error           16   7924.9    7924.9   495.3
Total           23  36407.0

S = 22.2555   R-Sq = 78.23%   R-Sq(adj) = 68.71%


Grouping Information Using Bonferroni Method and 95.0% Confidence

      NaCl
Line  Con  N   Mean  Grouping
2       0  3  100.0  A
1       0  3  100.0  A
1      50  3   92.7  A
2      50  3   73.2  A B
1     100  3   72.0  A B
2     100  3   53.6  A B
1     150  3   13.3    B
2     150  3    7.0    B

Means that do not share a letter are significantly different.
```

LSD= 67.96

Residual Plots for RWC % Control

Interaction Plot for RWC % Control
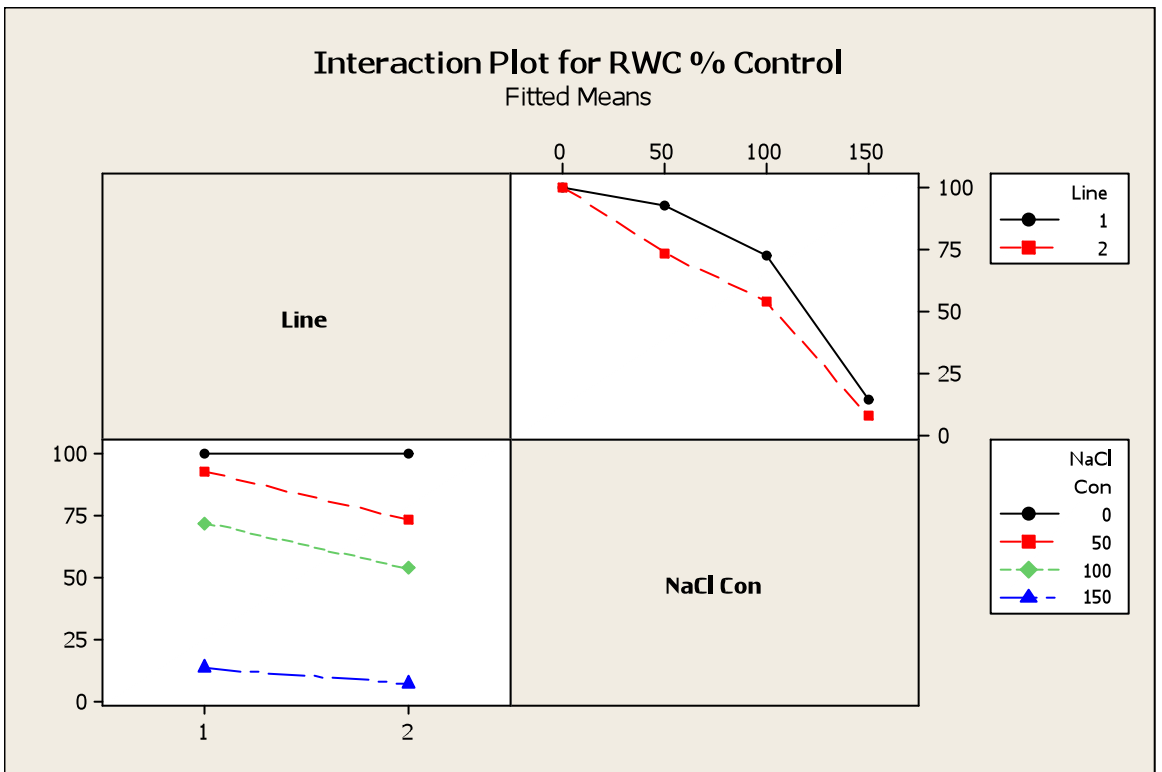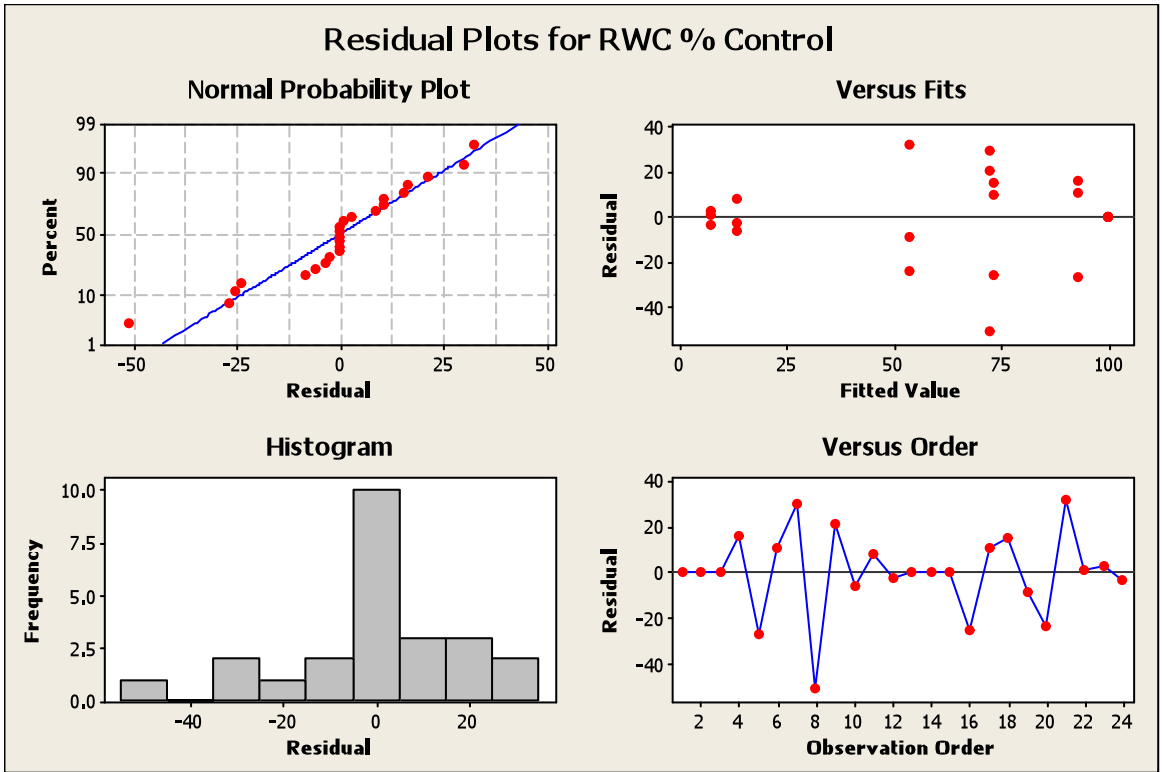
Figure A 4-9: General Linear Model: Log Water Use Efficiency versus Line, NaCl Concentration.

```
Factor    Type    Levels  Values
Line      fixed       2   1 (Local), 2 (Optic)
NaCl Con  fixed       4   0, 50, 100, 150

Analysis of Variance for Log WUE, using Adjusted SS for Tests

Source          DF    Seq SS    Adj SS    Adj MS      F      P
Line             1  0.041380  0.041380  0.041380   6.34  0.014
NaCl Con         3  0.253717  0.253717  0.084572  12.97  0.000
Line*NaCl Con    3  0.016352  0.016352  0.005451   0.84  0.479
Error           72  0.469561  0.469561  0.006522
Total           79  0.781010

S = 0.0807569   R-Sq = 39.88%   R-Sq(adj) = 34.03%

Grouping Information Using Bonferroni Method and 95.0% Confidence

        NaCl
Line    Con   N   Mean  Grouping
1        50   3   0.27  A
1       100   3   0.26  A
2         0   3   0.23  A
1         0   3   0.23  A
2        50   3   0.22  A B
2       100   3   0.20  A B
1       150   3   0.18    B
2       150   3   0.17    B

Means that do not share a letter are significantly different.
```
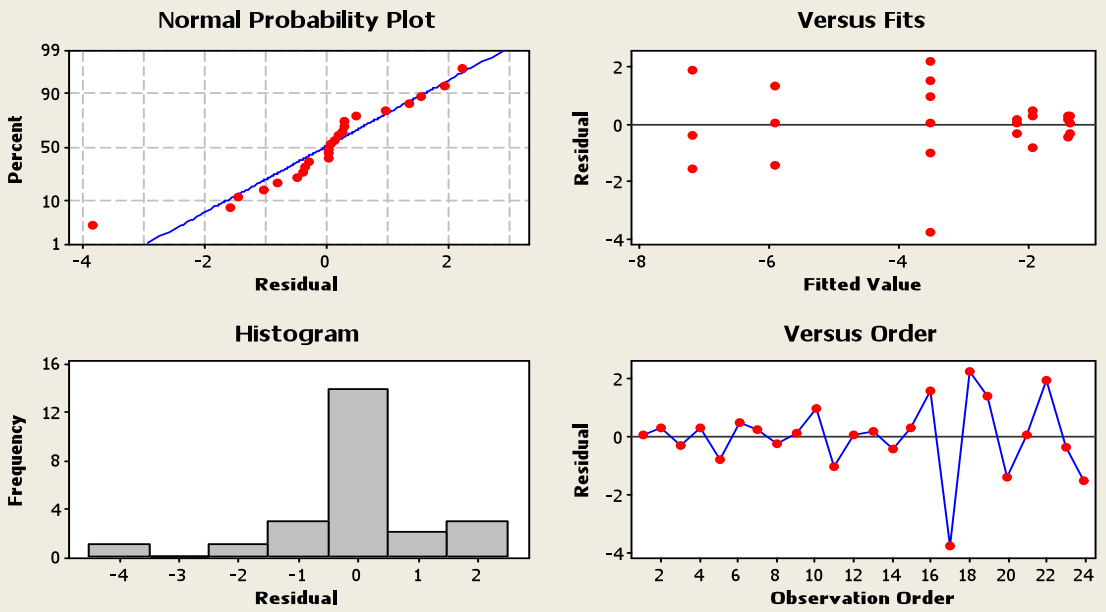
LSD = 0.13

Residual Plots for Log WUE
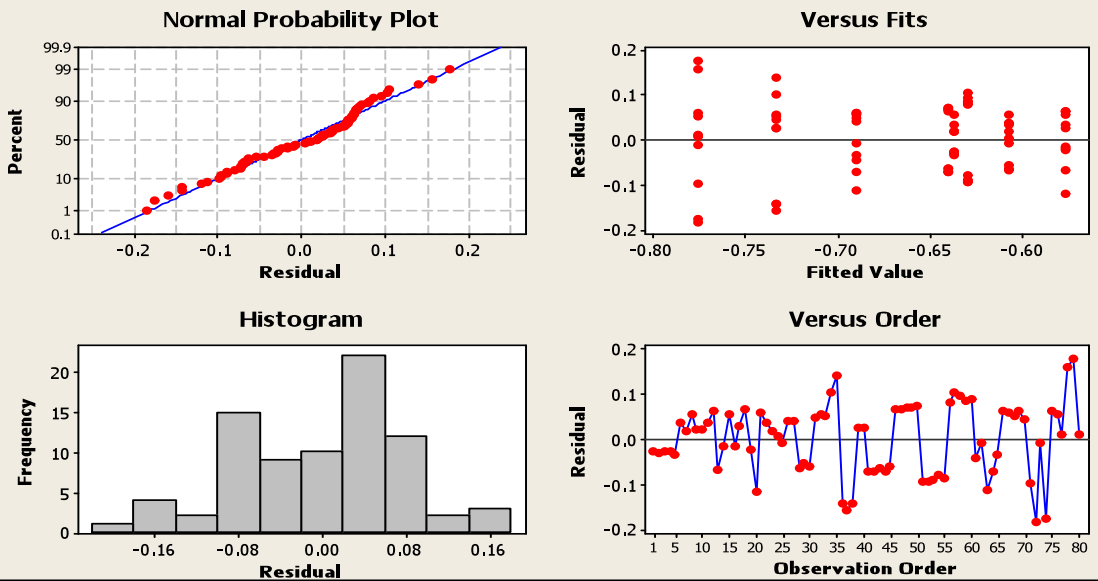
Interaction Plot for Log WUE
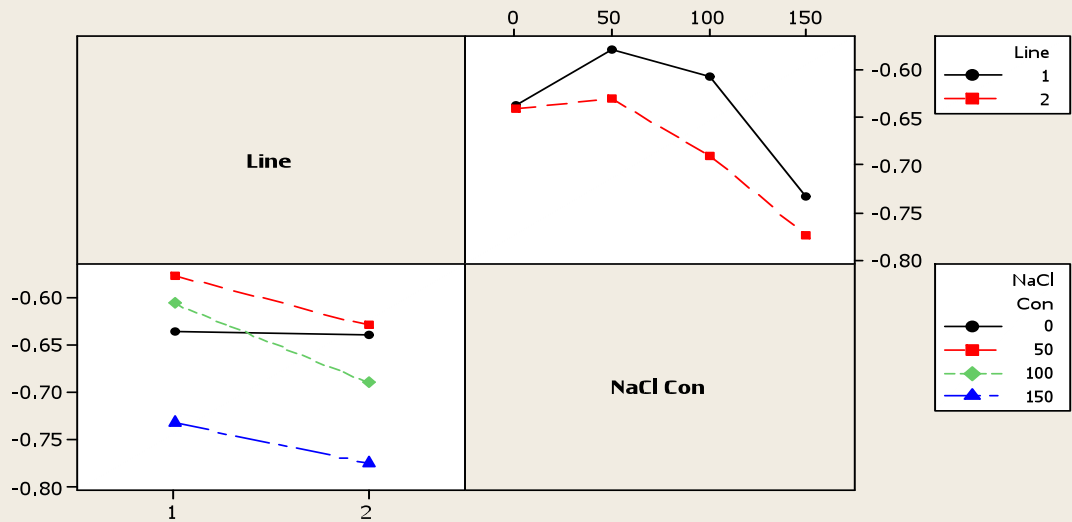
Figure A 4-10: General Linear Model: Water Potential versus Line, NaCl Concentration.

```
Factor     Type    Levels  Values
Line       fixed       2   1 (Local), 2 (Optic)
NaCl Con   fixed       4   0, 50, 100, 150

Analysis of Variance for Water Potential, using Adjusted SS for Tests

Source          DF   Seq SS   Adj SS   Adj MS      F      P
Line             1   3.5658   3.5658   3.5658  15.47  0.001
NaCl Con         3  23.5175  23.5175   7.8392  34.01  0.000
Line*NaCl Con    3   5.8486   5.8486   1.9495   8.46  0.001
Error           16   3.6876   3.6876   0.2305
Total           23  36.6196

S = 0.480080   R-Sq = 89.93%   R-Sq(adj) = 85.52%

Grouping Information Using Bonferroni Method and 95.0% Confidence

      NaCl
Line  Con   N  Mean  Grouping
2       0   3  -0.7  A
1       0   3  -0.8  A B
1     100   3  -1.5  A B C
1      50   3  -1.6  A B C
2      50   3  -1.6  A B C
2     100   3  -2.3    B C
1     150   3  -2.3      C
2     150   3  -4.7          D

Means that do not share a letter are significantly different.
```

LSD= 1.45

Residual Plots for Water Potential
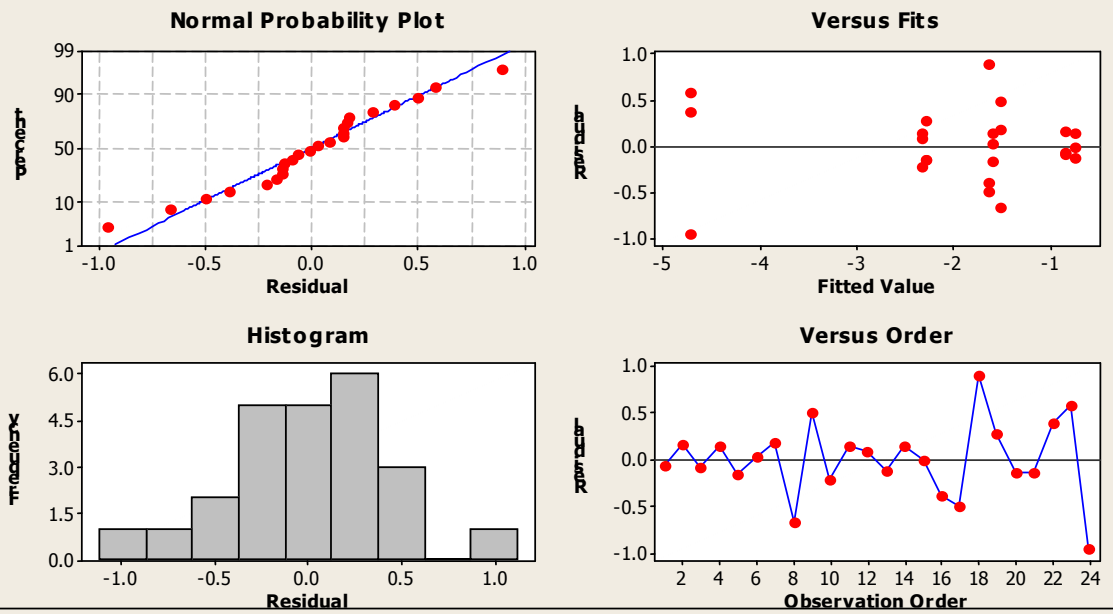
Interaction Plot for Water Potential
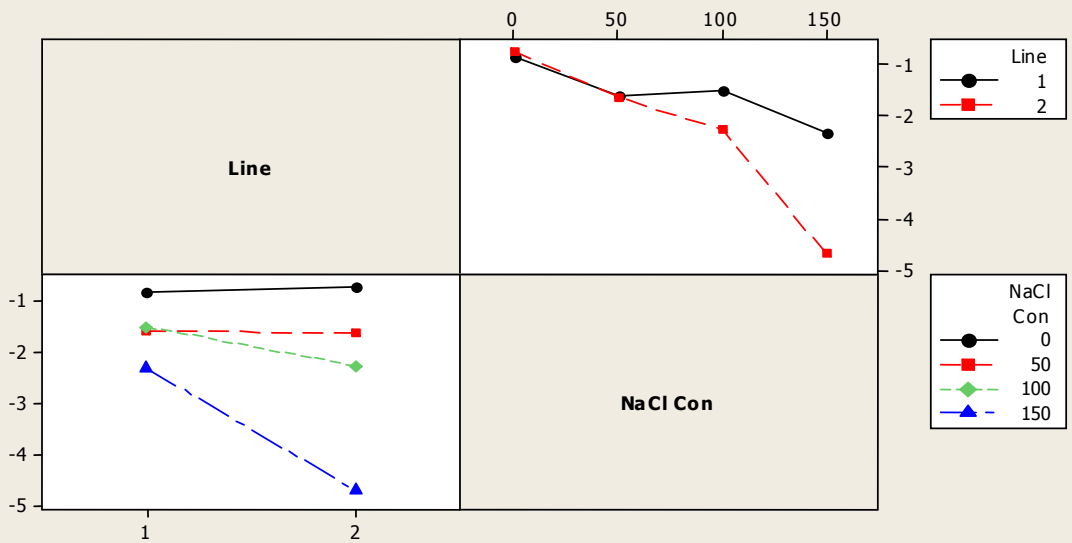
Figure A 4-11: General Linear Model: Log Turgor Pressure versus Line, NaCl Concentration.

```
Factor     Type   Levels  Values
Line       fixed       2  1, 2
NaCl Con   fixed       4  0, 50, 100, 150

Analysis of Variance for Log Turgor Pressure, using Adjusted SS for Tests

Source         DF   Seq SS  Adj SS  Adj MS     F      P
Line            1   1.2299  1.2299  1.2299  2.51  0.133
NaCl Con        3   0.7988  0.7988  0.2663  0.54  0.660
Line*NaCl Con   3   1.0537  1.0537  0.3512  0.72  0.556
Error          16   7.8413  7.8413  0.4901
Total          23  10.9237

S = 0.700060   R-Sq = 28.22%   R-Sq(adj) = 0.00%


Grouping Information Using Sidak Method and 95.0% Confidence

      NaCl
Line  Con   N  Mean  Grouping
2     150   3   0.3  A
2     100   3   0.3  A
1     100   3  -0.3  A
2       0   3  -0.3  A
1       0   3  -0.3  A
2      50   3  -0.4  A
1      50   2  -0.5  A
1     150   3  -0.8  A

Means that do not share a letter are significantly different.
```

LSD= 2.47

Residual Plots for Log Turgor Pressure

Interaction Plot for Log Turgor Pressure
Fitted Means
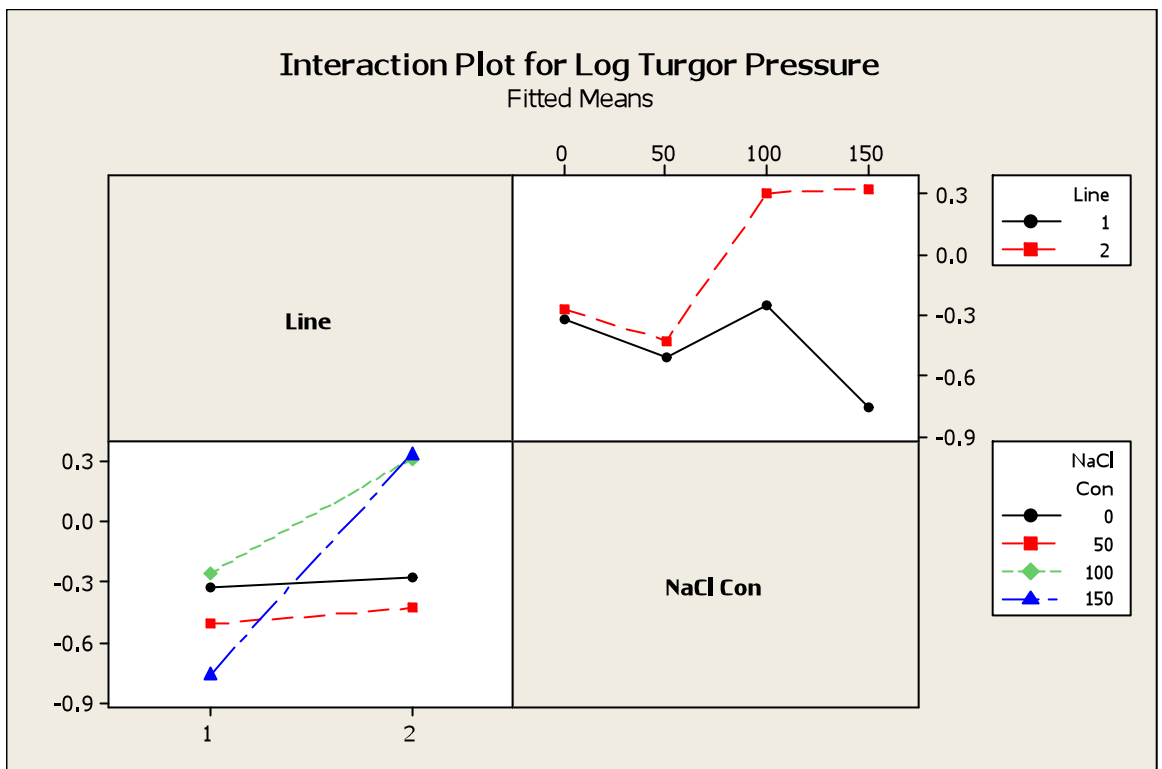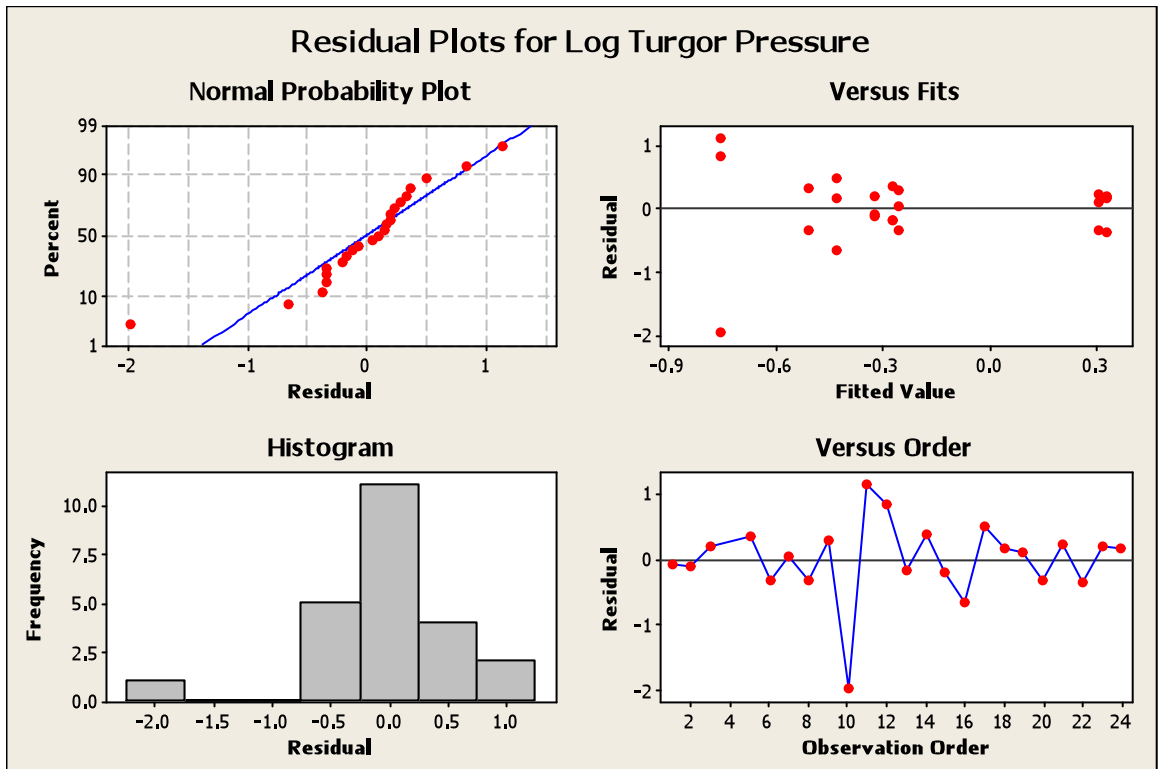
Figure A 4-12: General Linear Model: Solute Potential versus Line, NaCl Concentration.

```
Factor     Type    Levels  Values
Line       fixed        2  1 (Local), 2 (Optic)
NaCl Con   fixed        4  0, 50, 100, 150

Analysis of Variance for Solute Potential, using Adjusted SS for Tests

Source           DF   Seq SS   Adj SS   Adj MS      F       P
Line              1   30.940   30.940   30.940  13.79   0.002
NaCl Con          3   53.111   53.111   17.704   7.89   0.002
Line*NaCl Con     3   14.450   14.450    4.817   2.15   0.134
Error            16   35.908   35.908    2.244
Total            23  134.409

S = 1.49808   R-Sq = 73.28%   R-Sq(adj) = 61.60%




Grouping Information Using Bonferroni Method and 95.0% Confidence

      NaCl
Line  Con   N  Mean  Grouping
1       0   3  -1.3  A
2       0   3  -1.4  A B
1      50   3  -1.9  A B
1     100   3  -2.2  A B
1     150   3  -3.5  A B C
2      50   3  -3.5  A B C
2     100   3  -5.9    B C
2     150   3  -7.2      C

Means that do not share a letter are significantly different.
```

LSD= 4.57

Residual Plots for Solute Potential

Figure A 4-13: General Linear Model: Log Proline Concentration versus Line, NaCl Concentration.

```
Factor    Type    Levels  Values
Line      fixed        2  1 (Local), 2 (Optic)
NaCl Con  fixed        4  0, 50, 100, 150

Analysis of Variance for Log Proline Con, using Adjusted SS for Tests

Source         DF   Seq SS   Adj SS   Adj MS      F      P
Line            1  0.56790  0.56790  0.56790  17.43  0.001
NaCl Con        3  3.99392  3.99392  1.33131  40.85  0.000
Line*NaCl Con   3  0.24494  0.24494  0.08165   2.51  0.096
Error          16  0.52145  0.52145  0.03259
Total          23  5.32821

S = 0.180528   R-Sq = 90.21%   R-Sq(adj) = 85.93%

Grouping Information Using Bonferroni Method and 95.0% Confidence

      NaCl
Line  Con   N  Mean  Grouping
2     150   3  1.5   A
2     100   3  1.3   A B
1     150   3  1.2   A B C
2      50   3  1.2   A B C
1     100   3  0.8     B C
1      50   3  0.7       C D
1       0   3  0.3         D
2       0   3  0.2         D

Means that do not share a letter are significantly different.
```

LSD= 3.46

290

Residual Plots for Log Proline Con
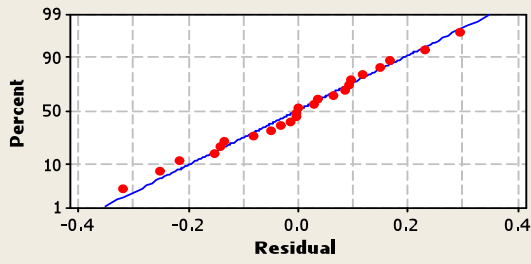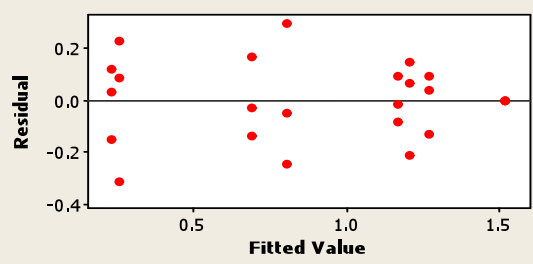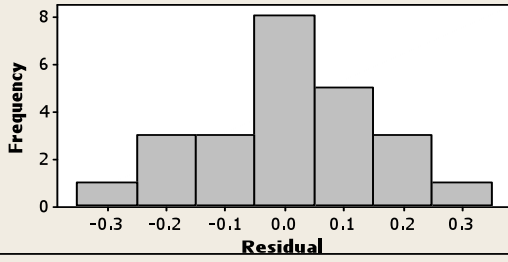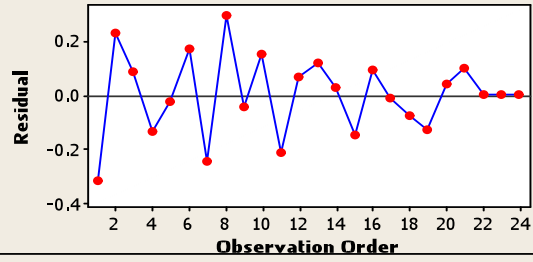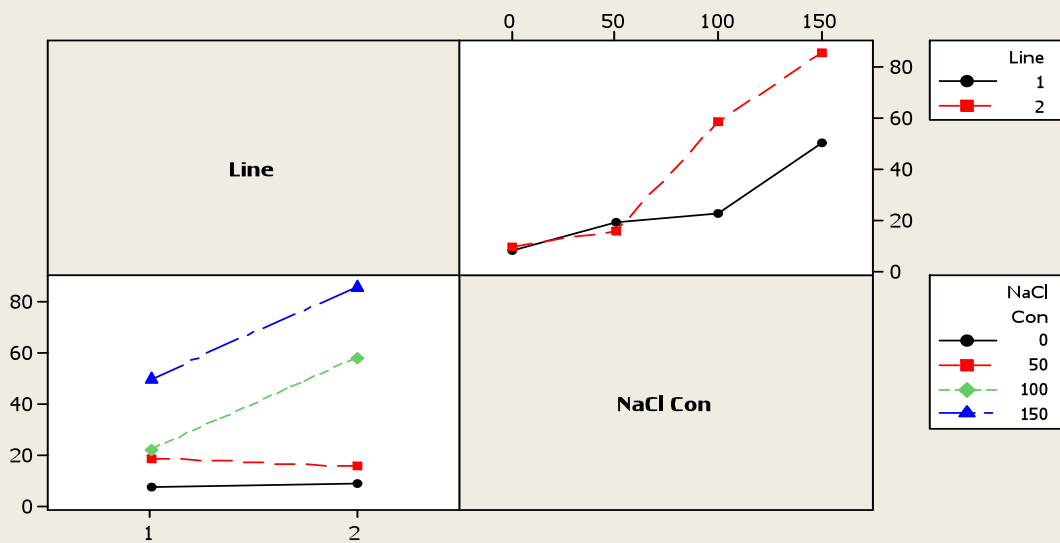
Interaction Plot for Log Proline Con
Fitted Means
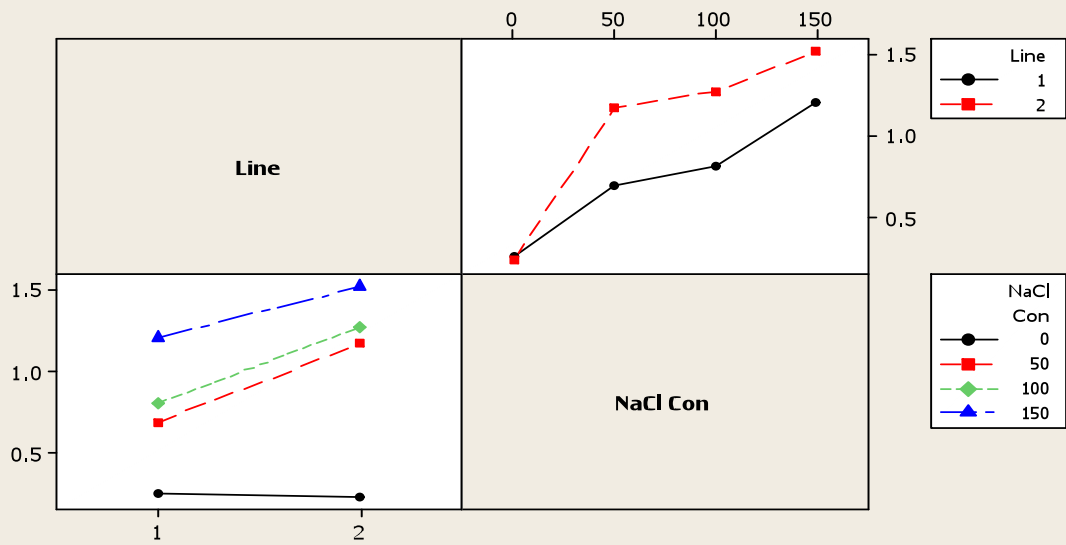
Figure A 4-14: General Linear Model: Log Shoot K versus Line, NaCl Concentration.

```
Factor    Type   Levels  Values
Line      fixed      2   1 (Local), 2 (Optic)
NaCl Con  fixed      4   0, 50, 100, 150


Analysis of Variance for Log Shoot K, using Adjusted SS for Tests

Source         DF   Seq SS   Adj SS   Adj MS      F      P
Line            1  0.61102  0.61102  0.61102   9.39  0.007
NaCl Con        3  2.54168  2.54168  0.84723  13.02  0.000
Line*NaCl Con   3  0.50104  0.50104  0.16701   2.57  0.091
Error          16  1.04088  1.04088  0.06505
Total          23  4.69461


S = 0.255059   R-Sq = 77.83%   R-Sq(adj) = 68.13%

Grouping Information Using Tukey Method and 95.0% Confidence

      NaCl
Line  Con   N  Mean  Grouping
1       0   3  1.8   A
2       0   3  1.7   A
1     100   3  1.4   A
1      50   3  1.4   A
2      50   3  1.3   A
1     150   3  1.3   A
2     100   3  1.1   A B
2     150   3  0.5     B


Means that do not share a letter are significantly different.
```
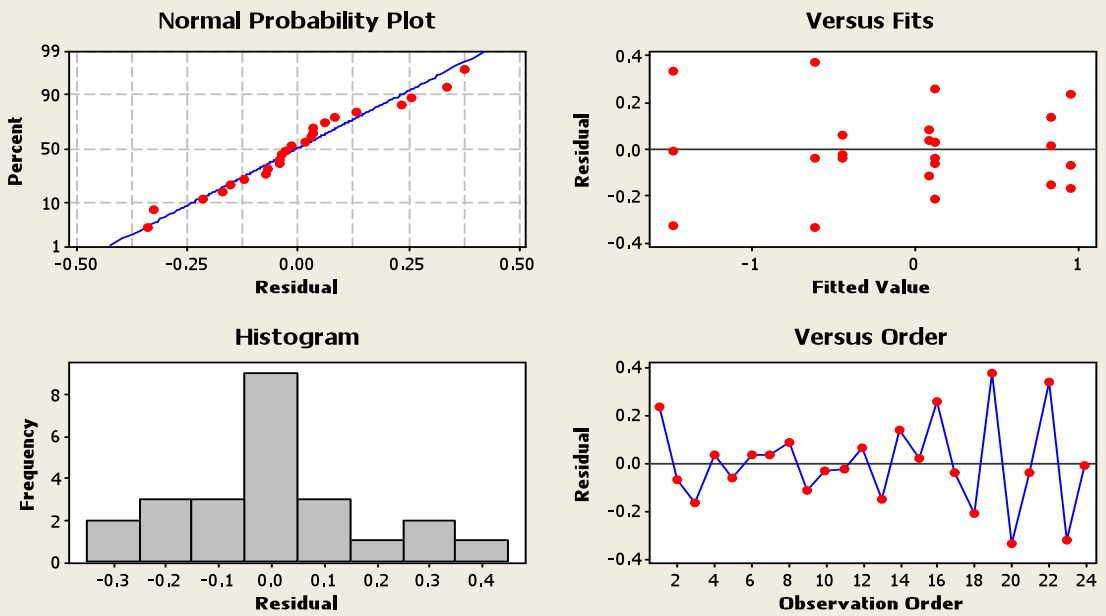
LSD= 5.12

Residual Plots for Log Shoot K

Interaction Plot for Log Shoot K
Fitted Means
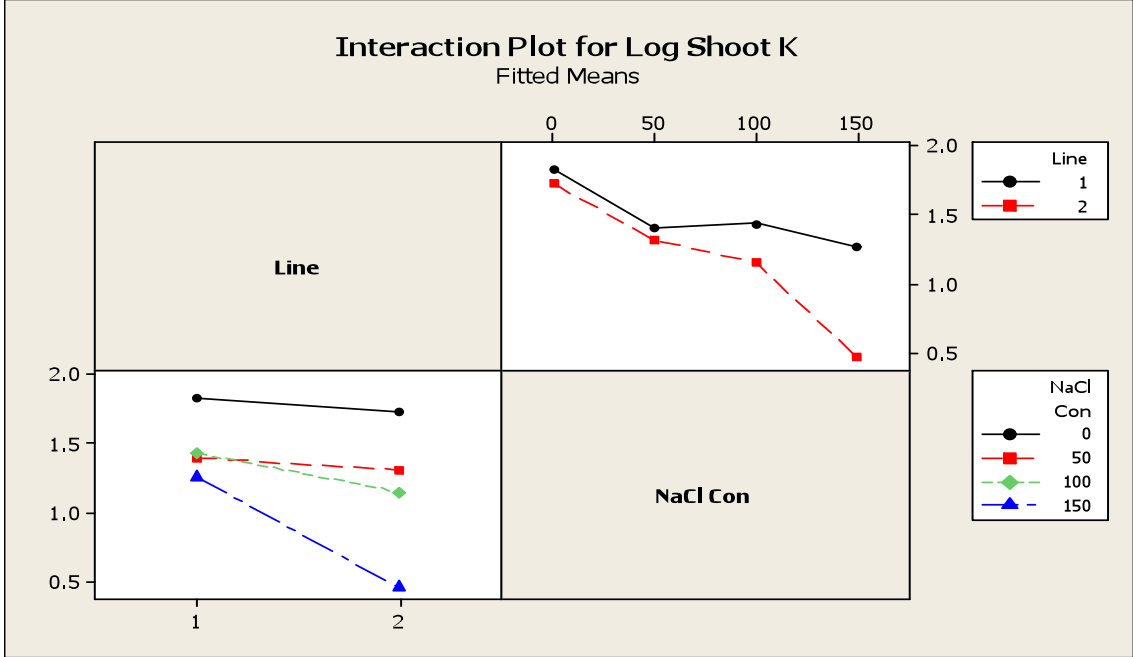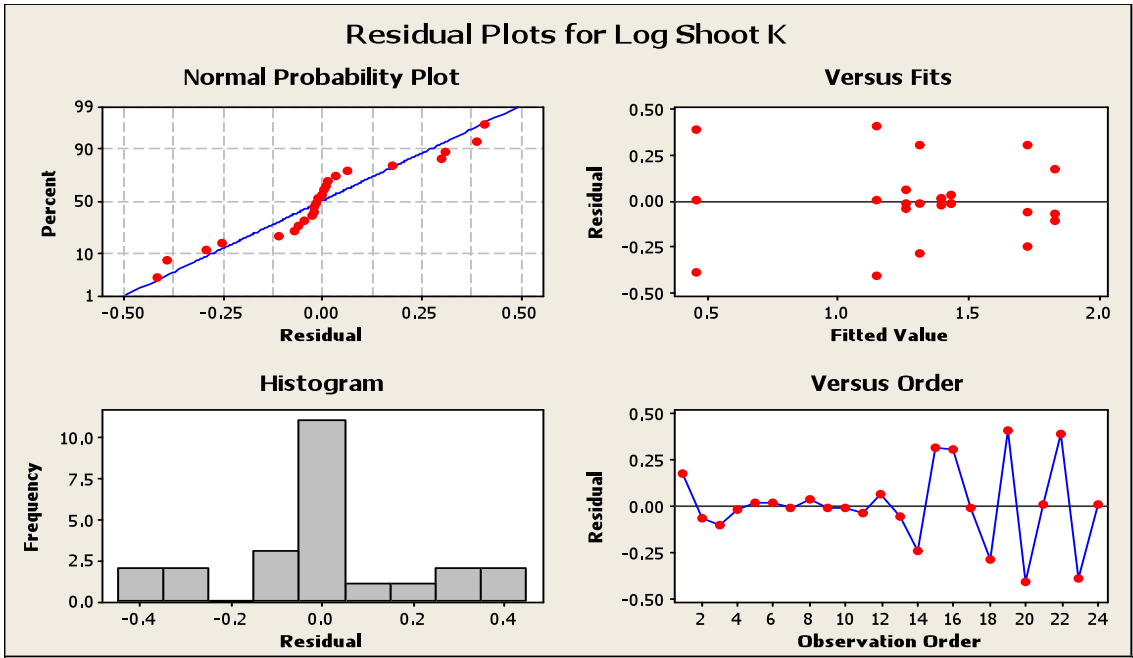
Figure A 4-15: General Linear Model: Shoot Na versus Line, NaCl Concentration.

```
Factor     Type    Levels  Values
Line       fixed        2  1 (Local), 2 (Optic)
NaCl Con   fixed        4  0, 50, 100, 150

Analysis of Variance for Shoot Na, using Adjusted SS for Tests

Source          DF   Seq SS    Adj SS   Adj MS       F      P
Line             1   1834.9    1834.9   1834.9   53.52  0.000
NaCl Con         3  12769.1   12769.1   4256.4  124.14  0.000
Line*NaCl Con    3   2044.2    2044.2    681.4   19.87  0.000
Error           16    548.6     548.6     34.3
Total           23  17196.9


S = 5.85559   R-Sq = 96.81%   R-Sq(adj) = 95.41%


Grouping Information Using Tukey Method and 95.0% Confidence

      NaCl
Line  Con   N  Mean  Grouping
2     150   3  85.7  A
2     100   3  58.2    B
1     150   3  50.0    B
1     100   3  22.2      C
1      50   3  18.8      C
2      50   3  15.4      C
2       0   3   9.1      C
1       0   3   7.5      C

Means that do not share a letter are significantly different.
```
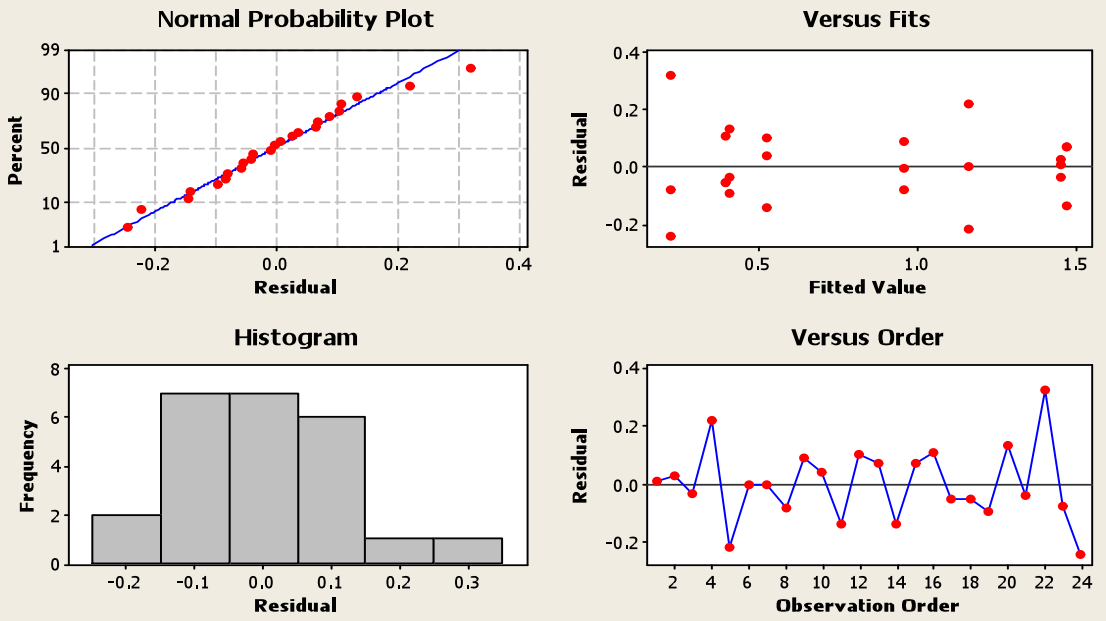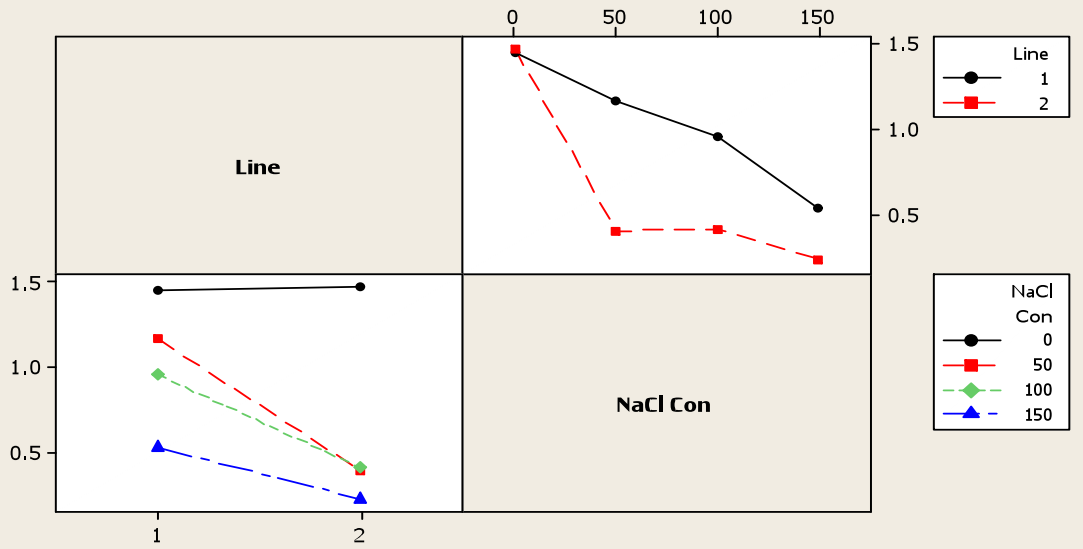
LSD= 16.56

Residual Plots for Shoot Na
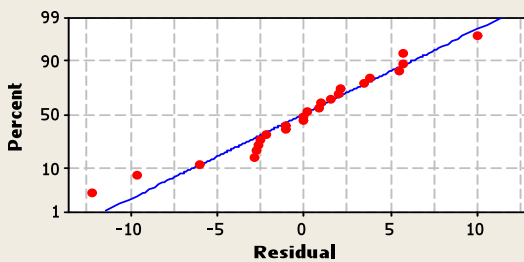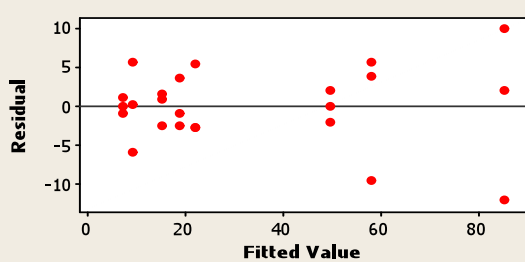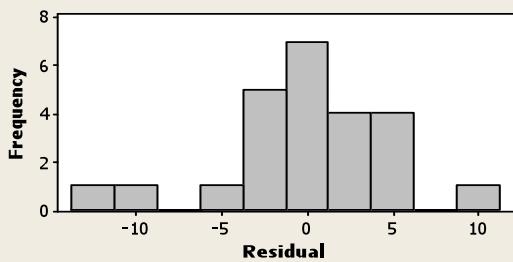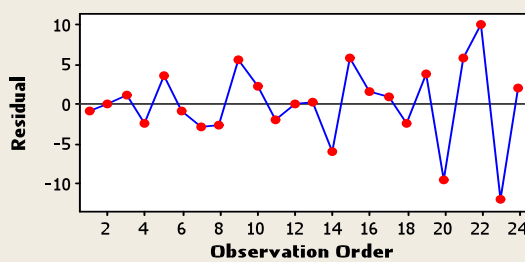
Figure A 4-16: General Linear Model: Log Shoot K/Na versus Line, NaCl Concentration.

```
Factor     Type   Levels  Values
Line       fixed      2   1 (Local), 2 (Optic)
NaCl Con   fixed      4   0, 50, 100, 150

Analysis of Variance for Log S K/Na, using Adjusted SS for Tests

Source         DF   Seq SS    Adj SS   Adj MS     F      P
Line            1   1.2875    1.2875   1.2875   27.07  0.000
NaCl Con        3  10.8144   10.8144   3.6048   75.80  0.000
Line*NaCl Con   3   1.0796    1.0796   0.3599    7.57  0.002
Error          16   0.7610    0.7610   0.0476
Total          23  13.9424

S = 0.218082   R-Sq = 94.54%   R-Sq(adj) = 92.15%

Grouping Information Using Tukey Method and 95.0% Confidence

       NaCl
Line   Con   N   Mean  Grouping
1        0   3   9.9   A
2        0   3   7.2   A
2       50   3   1.5      B
1       50   3   1.3      B
1      100   3   1.3      B
1      150   3   0.4      B
2      100   3   0.3      B
2      150   3   0.0      B

Means that do not share a letter are significantly different.
```
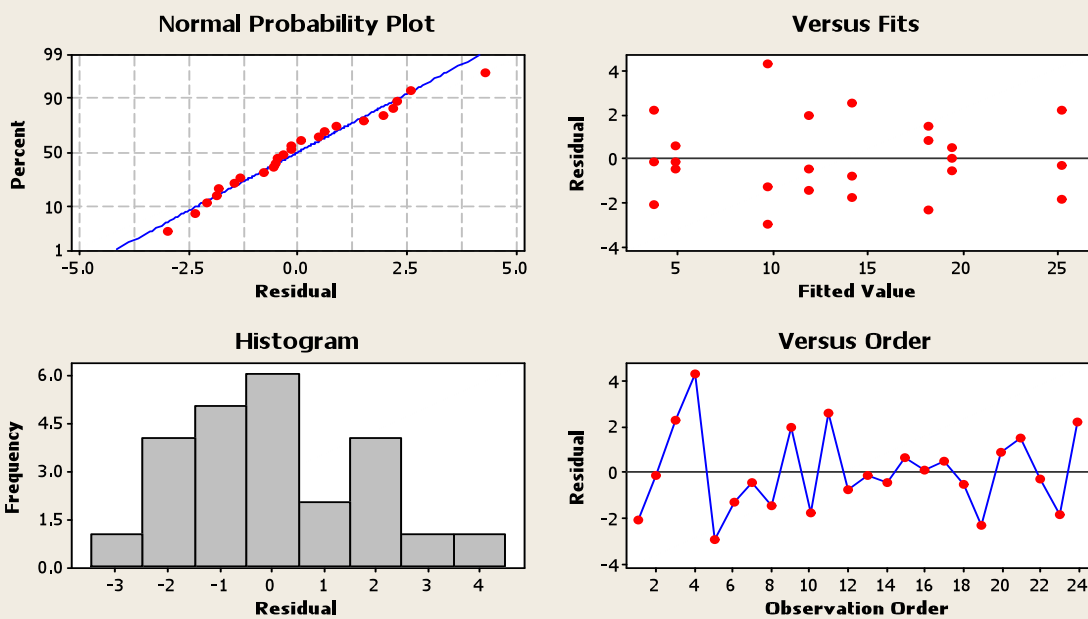
LSD= 5.68

Residual Plots for Log S K/Na
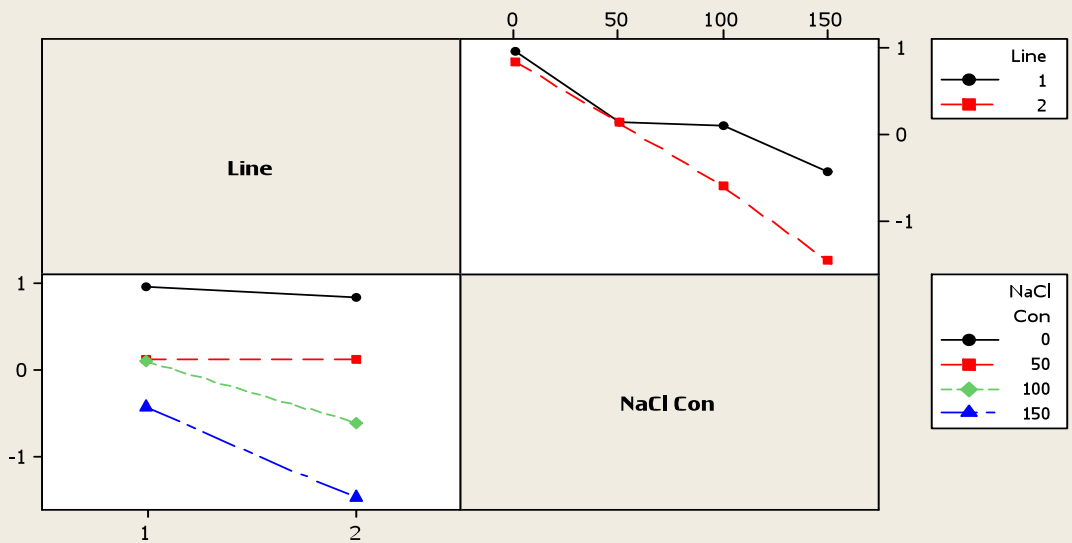
Figure A 4-17: General Linear Model: Log Root K versus Line, NaCl Concentration.

```
Factor     Type   Levels  Values
Line       fixed       2  1 (Local), 2 (Optic)
NaCl Con   fixed       4  0, 50, 100, 150


Analysis of Variance for Log Root K, using Adjusted SS for Tests

Source          DF   Seq SS   Adj SS   Adj MS       F      P
Line             1  0.95864  0.95864  0.95864   39.32  0.000
NaCl Con         3  3.76042  3.76042  1.25347   51.41  0.000
Line*NaCl Con    3  0.51380  0.51380  0.17127    7.02  0.003
Error           16  0.39009  0.39009  0.02438
Total           23  5.62295


S = 0.156143   R-Sq = 93.06%   R-Sq(adj) = 90.03%



Grouping Information Using Tukey Method and 95.0% Confidence

      NaCl
Line  Con   N  Mean  Grouping
2       0   3  30.3  A
1       0   3  28.3  A
1      50   3  15.9    B
1     100   3   9.2    B C
1     150   3   3.5      C
2     100   3   2.6      C
2      50   3   2.5      C
2     150   3   2.0      C

Means that do not share a letter are significantly different.
```

LSD= 2.75

Residual Plots for Log Root K

Interaction Plot for Log Root K

Figure: A 4-18: General Linear Model: Root Na versus Line, NaCl Concentration.

```
Factor     Type    Levels  Values
Line       fixed      2  1 (Local), 2 (Optic)
NaCl Con   fixed      4  0, 50, 100, 150

Analysis of Variance for Root Na, using Adjusted SS for Tests

Source          DF   Seq SS  Adj SS  Adj MS      F      P
Line             1   301.94  301.94  301.94  65.11  0.000
NaCl Con         3   771.97  771.97  257.32  55.49  0.000
Line*NaCl Con    3    88.64   88.64   29.55   6.37  0.005
Error           16    74.20   74.20    4.64
Total           23  1236.76

S = 2.15351   R-Sq = 94.00%   R-Sq(adj) = 91.38%


Grouping Information Using Tukey Method and 95.0% Confidence

      NaCl
Line  Con  N  Mean  Grouping
2     150  3  25.3  A
2      50  3  19.5  A B
2     100  3  18.2    B
1     150  3  14.2    B C
1     100  3  11.9      C
1      50  3   9.7      C D
2       0  3   4.8        D E
1       0  3   3.6          E

Means that do not share a letter are significantly different.
```
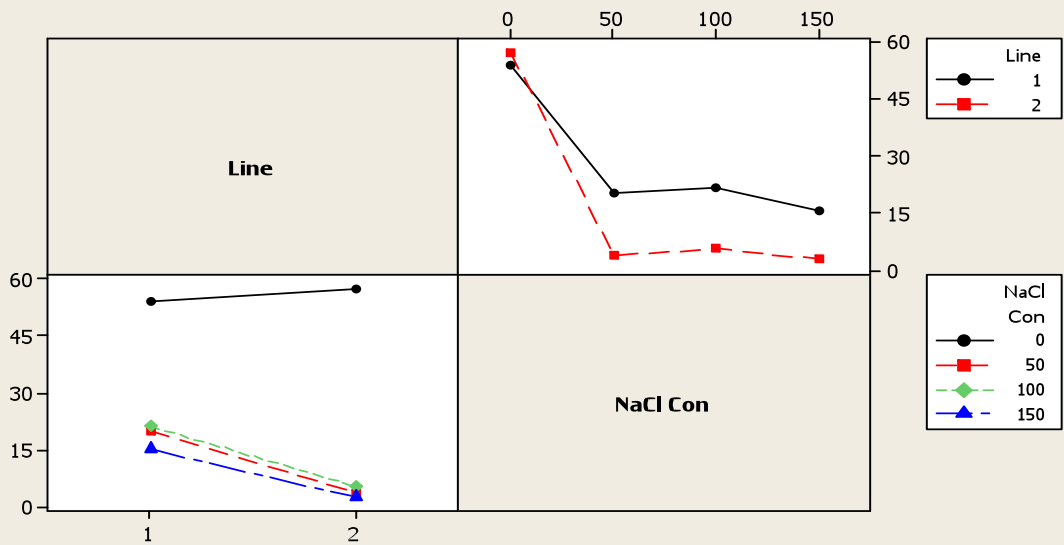
LSD= 6.12
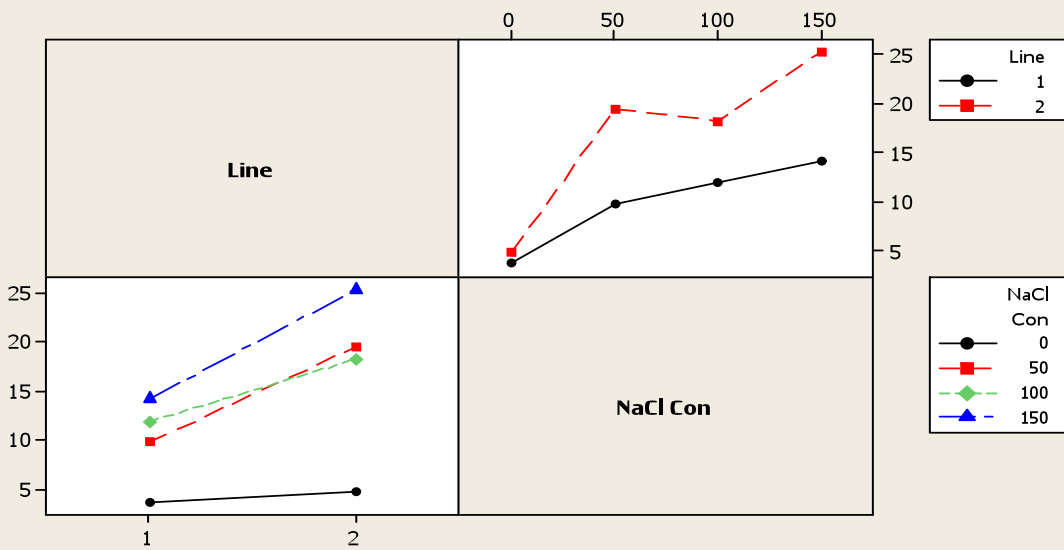
Figure A 4-19: General Linear Model: Log Root K/Na versus Line, NaCl Concentration.

```
Factor    Type   Levels  Values
Line      fixed       2  1 (Local), 2 (Optic)
NaCl Con  fixed       4  0, 50, 100, 150


Analysis of Variance for Log Root K/Na, using Adjusted SS for Tests

Source          DF   Seq SS   Adj SS  Adj MS       F      P
Line             1   2.4206   2.4206  2.4206   74.79  0.000
NaCl Con         3  10.4016  10.4016  3.4672  107.13  0.000
Line*NaCl Con    3   0.6749   0.6749  0.2250    6.95  0.003
Error           16   0.5179   0.5179  0.0324
Total           23  14.0150


S = 0.179905   R-Sq = 96.31%   R-Sq(adj) = 94.69%

Grouping Information Using Tukey Method and 95.0% Confidence

      NaCl
Line  Con  N  Mean  Grouping
1       0  3  10.5  A
2       0  3   6.3  A B
1      50  3   1.6    B
1     100  3   0.8    B
1     150  3   0.3    B
2     100  3   0.1    B
2      50  3   0.1    B
2     150  3   0.1    B

Means that do not share a letter are significantly different.
```

LSD= 3.23

Residual Plots for Log Root K/Na

Interaction Plot for Log Root K/Na
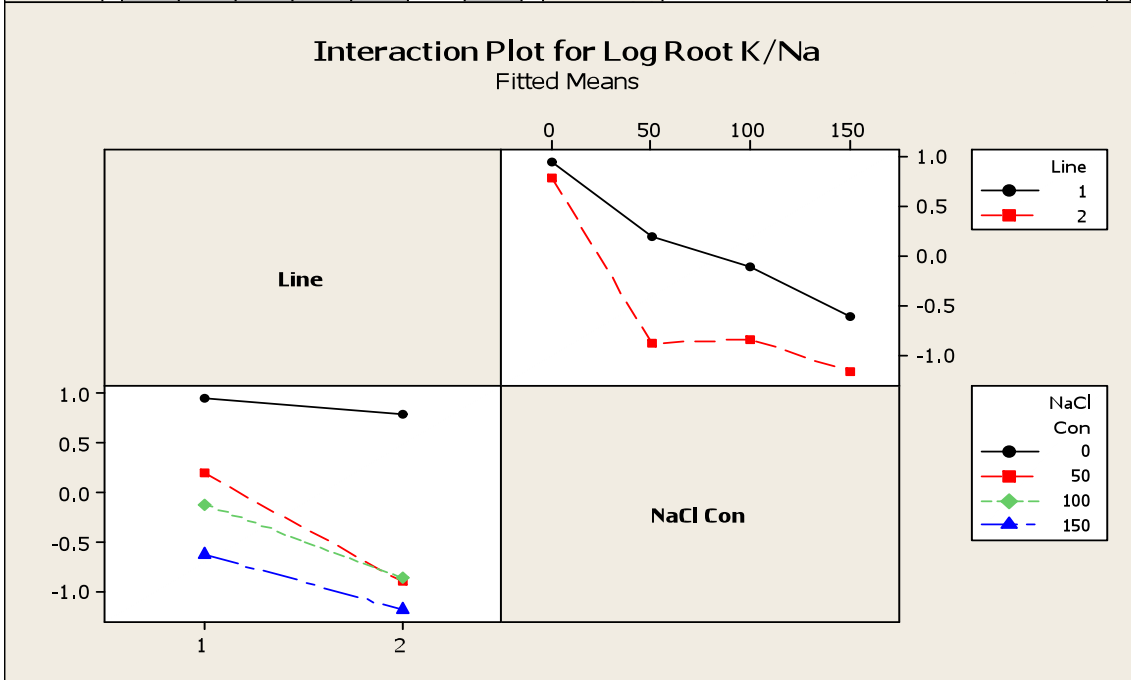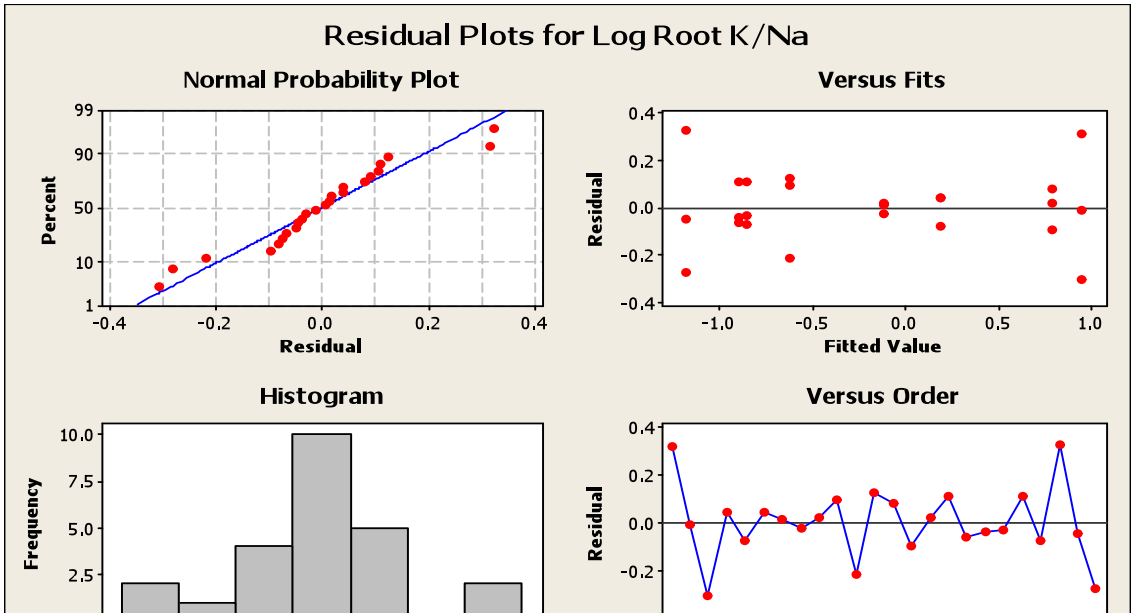
Figure A 4-20: General Linear Model: Green Leaf K versus Line, NaCl Concentration.

```
Factor    Type    Levels  Values
Line      fixed        2  1 (Local), 2 (Optic)
NaCl Con  fixed        4  0, 50, 100, 150

Analysis of Variance for GL K, using Adjusted SS for Tests

Source          DF   Seq SS   Adj SS   Adj MS       F      P
Line             1    653.2    653.2    653.2   69.22  0.000
NaCl Con         3   8929.2   8929.2   2976.4  315.41  0.000
Line*NaCl Con    3    405.9    405.9    135.3   14.34  0.000
Error           16    151.0    151.0      9.4
Total           23  10139.3

S = 3.07193   R-Sq = 98.51%   R-Sq(adj) = 97.86%

Grouping Information Using Tukey Method and 95.0% Confidence

      NaCl
Line  Con   N  Mean  Grouping
2       0   3  57.5  A
1       0   3  54.0  A
1     100   3  21.3    B
1      50   3  20.2    B
1     150   3  15.3    B
2     100   3   5.3      C
2      50   3   3.6      C
2     150   3   2.5      C

Means that do not share a letter are significantly different.
```

LSD= 8.69

Residual Plots for GL K

Normal Probability Plot

Versus Fits

Histogram

Versus Order
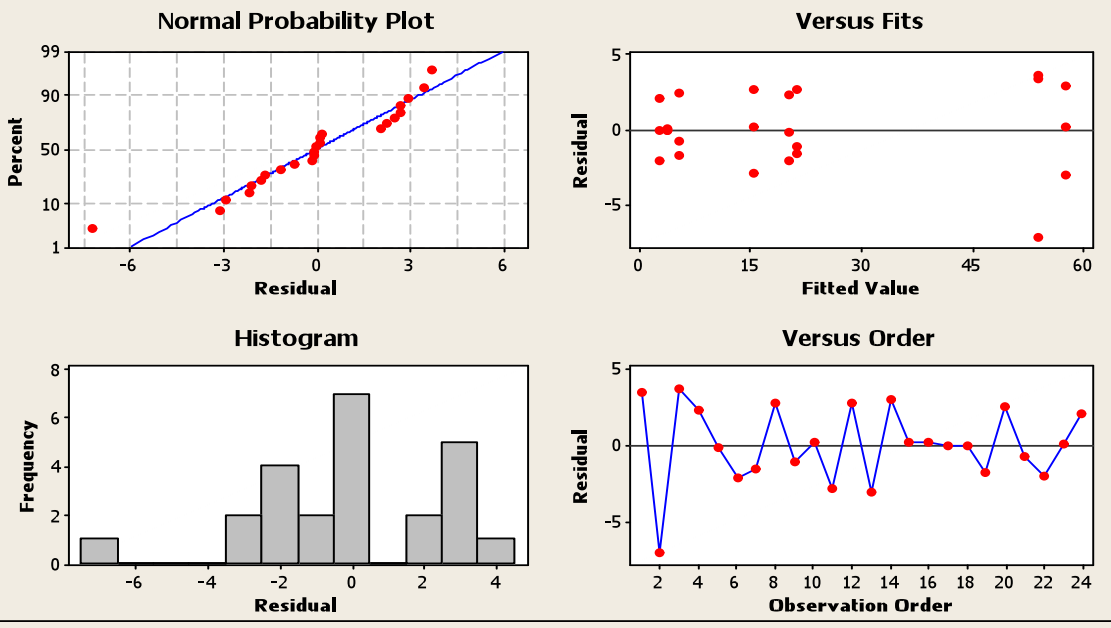
Interaction Plot for GL K
Fitted Means

Line

NaCl Con

Figure A 4-21: General Linear Model: Log Green Leaf Na versus Line, NaCl Concentration.

```
Factor    Type    Levels  Values
Line      fixed        2  1 (Local), 2 (Optic)
NaCl Con  fixed        4  0, 50, 100, 150

Analysis of Variance for Log GL Na, using Adjusted SS for Tests

Source        DF   Seq SS   Adj SS   Adj MS       F      P
Line           1  0.43053  0.43053  0.43053   86.35  0.000
NaCl Con       3  3.48533  3.48533  1.16178  233.00  0.000
Line*NaCl Con  3  0.27638  0.27638  0.09213   18.48  0.000
Error         16  0.07978  0.07978  0.00499
Total         23  4.27202

S = 0.0706124   R-Sq = 98.13%   R-Sq(adj) = 97.32%

Grouping Information Using Tukey Method and 95.0% Confidence

      NaCl
Line  Con   N  Mean  Grouping
2     150   3  73.7  A
2     100   3  49.9    B
1     150   3  43.3    B
2      50   3  24.5      C
1      50   3  14.5        D
1     100   3  12.8        D E
2       0   3   5.0          E
1       0   3   4.9          E

Means that do not share a letter are significantly different.


LSD= 10.46
```

Residual Plots for Log GL Na
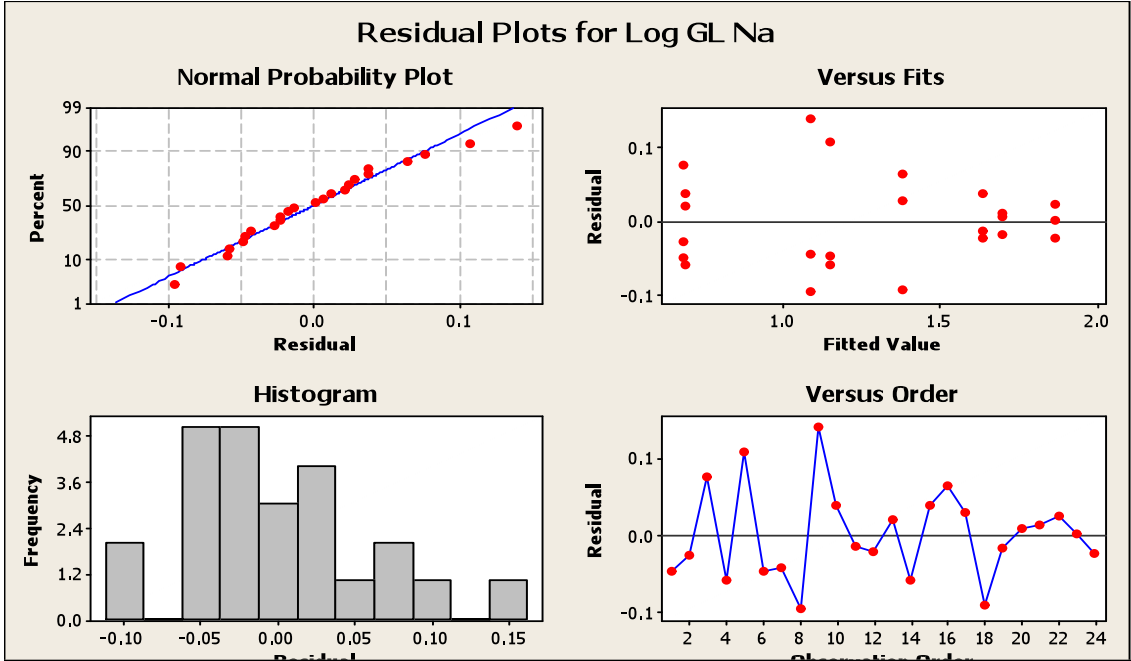
Interaction Plot for Log GL Na
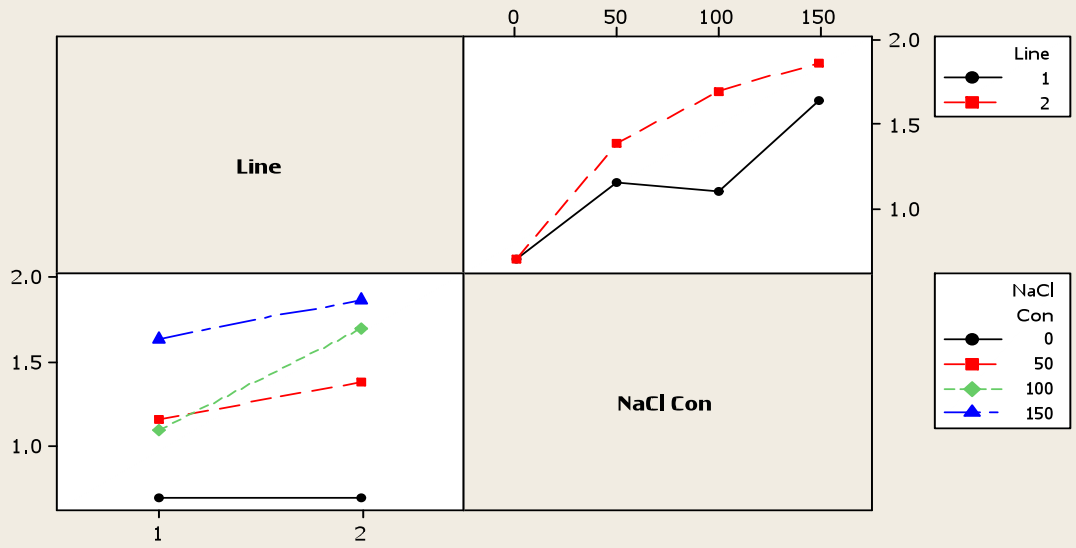
Figure A 4-22: General Linear Model: Log Green Leaf K/Na versus Line, NaCl Concentration.

```
Factor     Type   Levels  Values
Line       fixed       2  1 (Local), 2 (Optic)
NaCl Con   fixed       4  0, 50, 100, 150


Analysis of Variance for Log GL K/Na, using Adjusted SS for Tests

Source         DF   Seq SS   Adj SS  Adj MS      F      P
Line            1   4.2225   4.2225  4.2225  88.40  0.000
NaCl Con        3  13.9658  13.9658  4.6553  97.46  0.000
Line*NaCl Con   3   1.5383   1.5383  0.5128  10.73  0.000
Error          16   0.7643   0.7643  0.0478
Total          23  20.4909
S = 0.218557   R-Sq = 96.27%   R-Sq(adj) = 94.64%


Grouping Information Using Tukey Method and 95.0% Confidence

      NaCl
Line  Con   N  Mean  Grouping
2       0   3  11.7  A
1       0   3  11.1  A
1     100   3   1.8    B
1      50   3   1.4    B
1     150   3   0.4    B
2      50   3   0.1    B
2     100   3   0.1    B
2     150   3   0.0    B


Means that do not share a letter are significantly different.
```
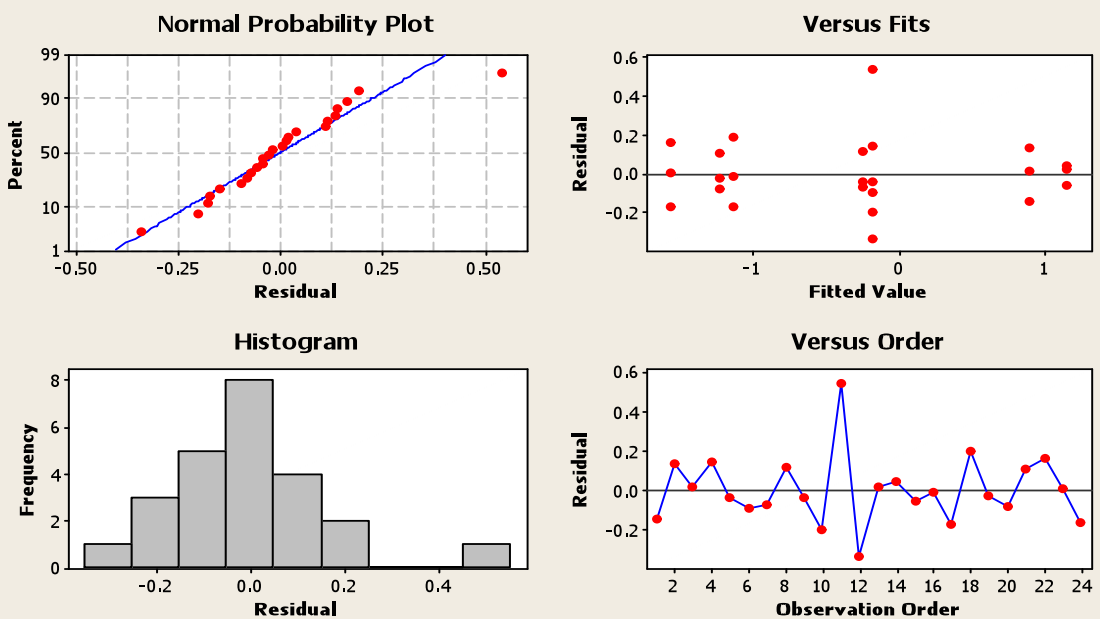
LSD= 2.75

Residual Plots for Log GL K/Na

Interaction Plot for Log GL K/Na
Fitted Means
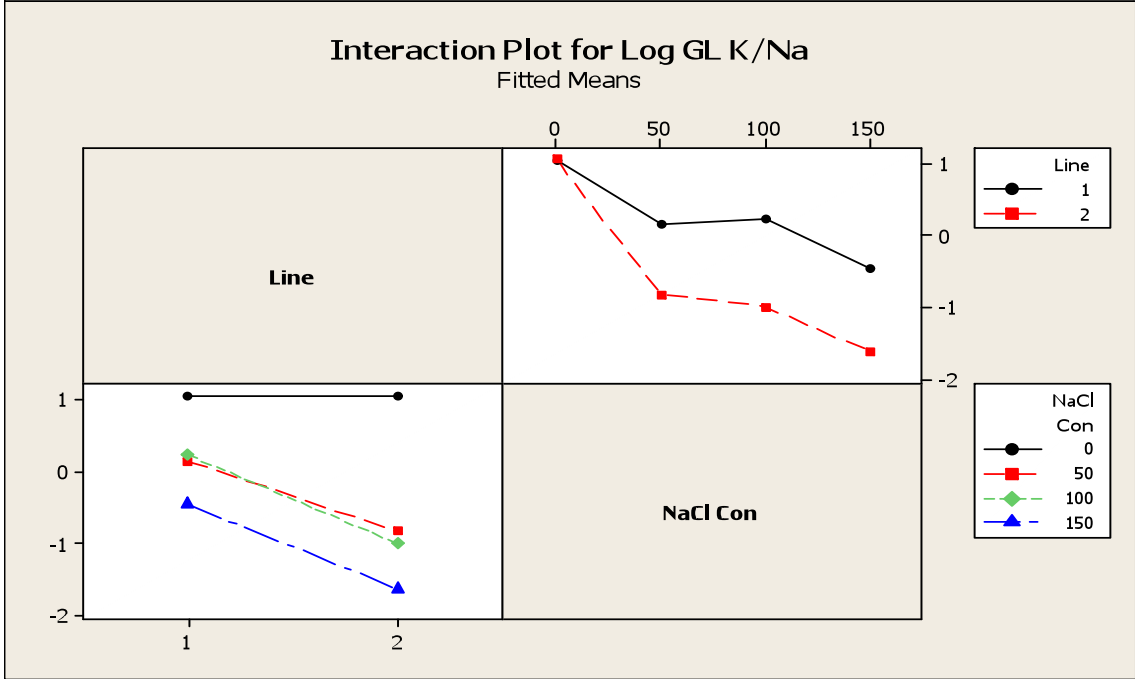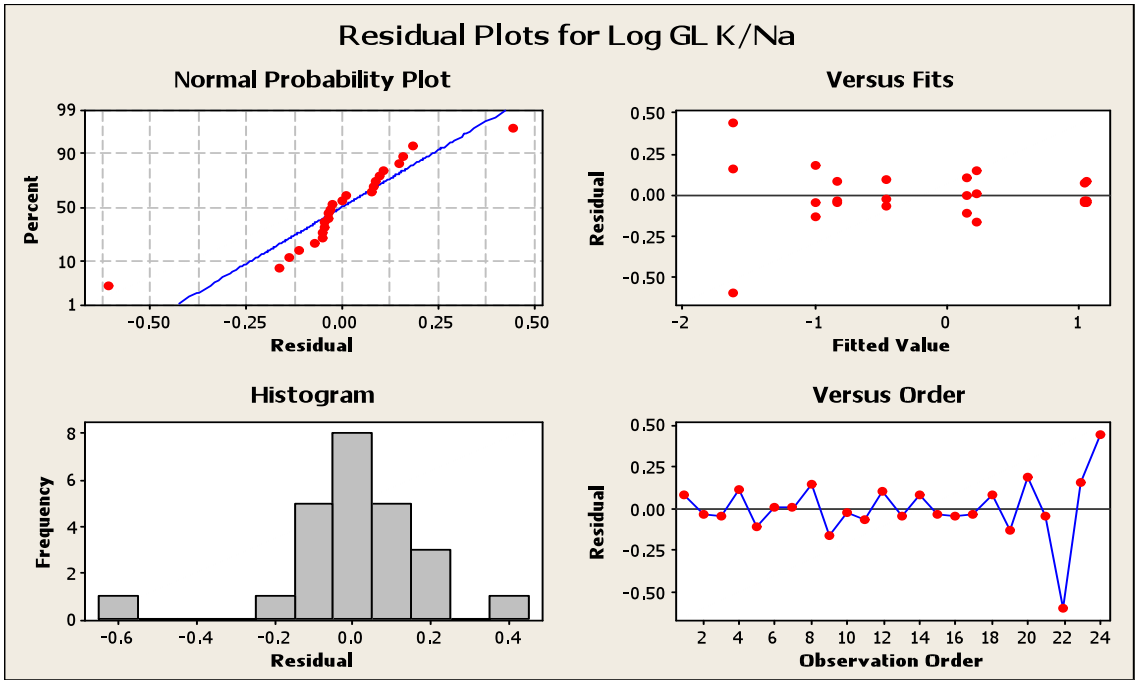
Figure A 4-23: General Linear Model: Log Desiccated Leaf K versus Line, NaCl Concentration.

```
Factor     Type   Levels  Values
Line       fixed       2  1 (Local), 2 (Optic)
NaCl Con   fixed       4  0, 50, 100, 150

Analysis of Variance for Log DL K, using Adjusted SS for Tests

Source        DF   Seq SS   Adj SS   Adj MS      F      P
Line           1  1.97056  1.97056  1.97056  42.28  0.000
NaCl Con       3  3.41210  3.41210  1.13737  24.40  0.000
Line*NaCl Con  3  1.36171  1.36171  0.45390   9.74  0.001
Error         16  0.74569  0.74569  0.04661
Total         23  7.49006

S = 0.215883   R-Sq = 90.04%   R-Sq(adj) = 85.69%

Grouping Information Using Tukey Method and 95.0% Confidence

      NaCl
Line  Con   N  Mean  Grouping
2       0   3  64.7  A
1       0   3  46.7  A B
1     150   3  45.9  A B
1     100   3  17.1  A B
1      50   3  15.2  A B
2     100   3   4.4    B
2      50   3   3.3    B
2     150   3   1.8    B

Means that do not share a letter are significantly different.
```
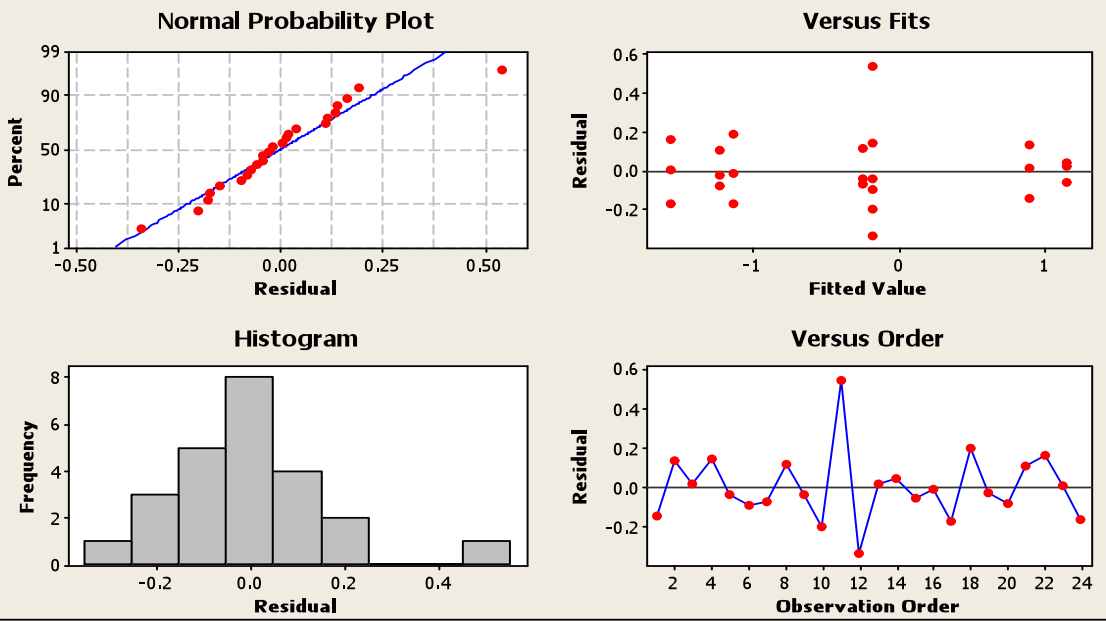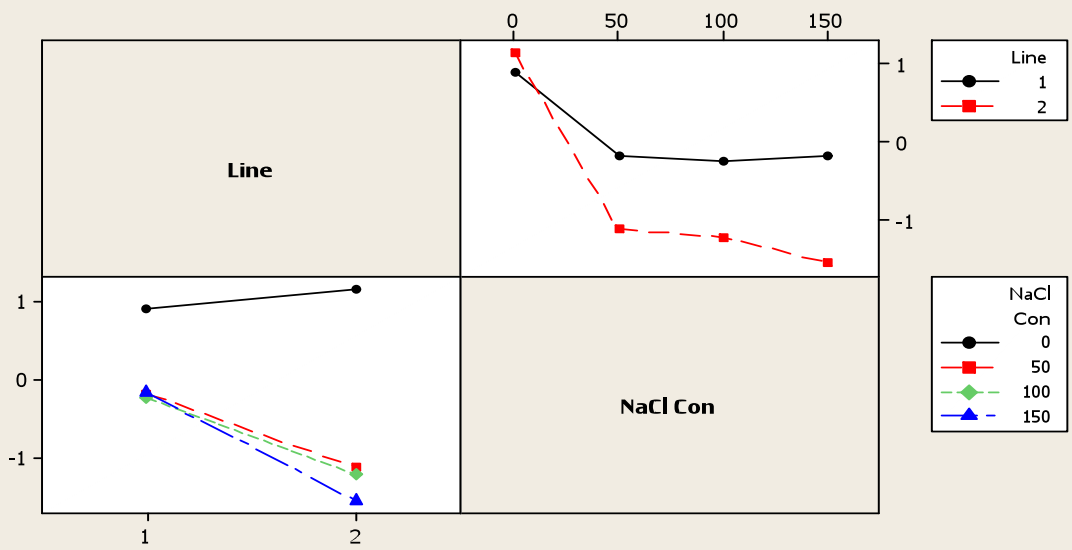
LSD = 4.08

Residual Plots for Log DL K
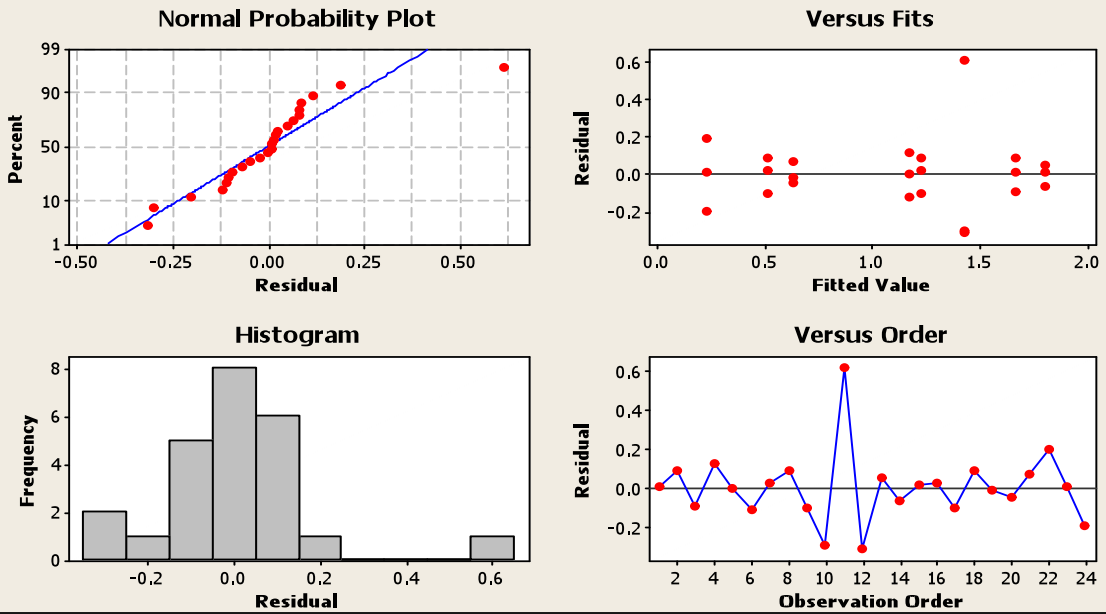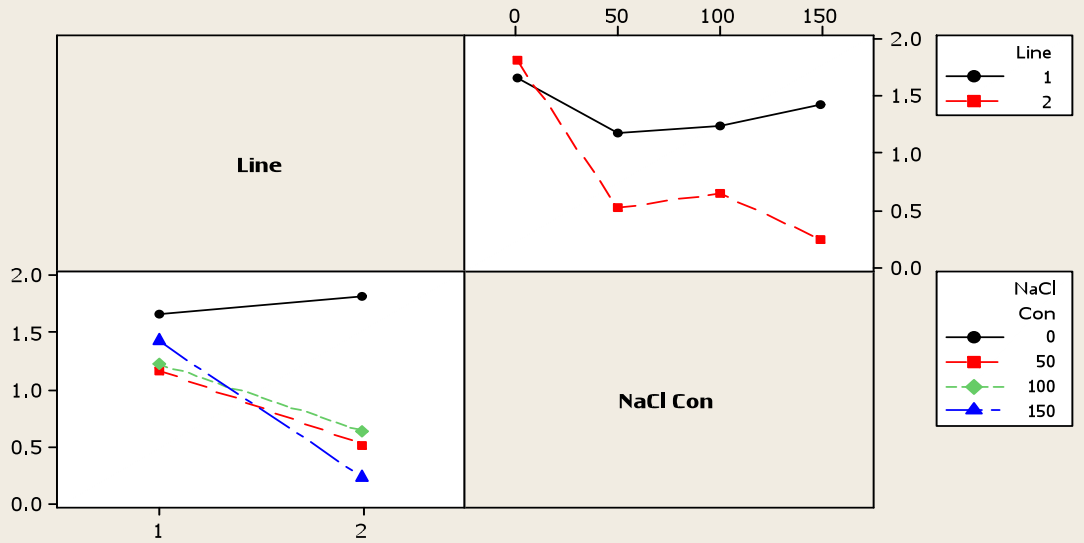
Figure A 4-24: General Linear Model: Desiccated Leaf Na versus Line, NaCl Concentration.

```
Factor     Type   Levels  Values
Line       fixed       2  1 (Local), 2 (Optic)
NaCl Con   fixed       4  0, 50, 100, 150

Analysis of Variance for DL Na, using Adjusted SS for Tests

Source         DF   Seq SS  Adj SS  Adj MS      F      P
Line            1   2763.7  2763.7  2763.7  84.57  0.000
NaCl Con        3   8557.0  8557.0  2852.3  87.28  0.000
Line*NaCl Con   3   1524.7  1524.7   508.2  15.55  0.000
Error          16    522.9   522.9    32.7
Total          23  13368.3

S = 5.71656   R-Sq = 96.09%   R-Sq(adj) = 94.38%

Grouping Information Using Tukey Method and 95.0% Confidence

      NaCl
Line  Con   N  Mean  Grouping
2     100   3  73.5  A
2     150   3  61.8  A
2      50   3  45.4    B
1     150   3  41.0    B
1     100   3  30.0    B C
1      50   3  22.5      C
1       0   3   6.1        D
2       0   3   4.6        D

Means that do not share a letter are significantly different.
```

LSD= 16.57

Residual Plots for Log DL K/Na
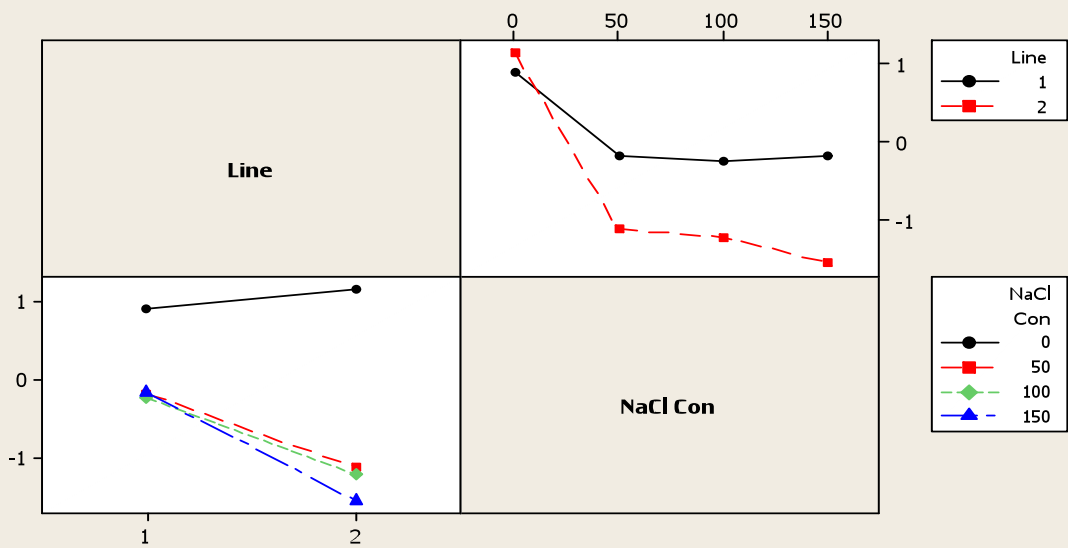
Figure A 4-25: General Linear Model: Log Desiccated Leaf K/Na versus Line, NaCl Concentration.

```
Factor     Type   Levels  Values
Line       fixed       2  1 (Local), 2 (Optic)
NaCl Con   fixed       4  0, 50, 100, 150


Analysis of Variance for Log DL K/Na, using Adjusted SS for Tests

Source          DF   Seq SS    Adj SS  Adj MS       F      P
Line             1   3.5123    3.5123  3.5123   80.76  0.000
NaCl Con         3  14.2965   14.2965  4.7655  109.57  0.000
Line*NaCl Con    3   2.2432    2.2432  0.7477   17.19  0.000
Error           16   0.6959    0.6959  0.0435
Total           23  20.7478


S = 0.208549   R-Sq = 96.65%   R-Sq(adj) = 95.18%


Grouping Information Using Tukey Method and 95.0% Confidence

      NaCl
Line  Con   N  Mean  Grouping
2       0   3  14.1  A
1       0   3   8.1    B
1     150   3   1.0      C
1      50   3   0.7      C
1     100   3   0.6      C
2      50   3   0.1      C
2     100   3   0.1      C
2     150   3   0.0      C


Means that do not share a letter are significantly different.
```
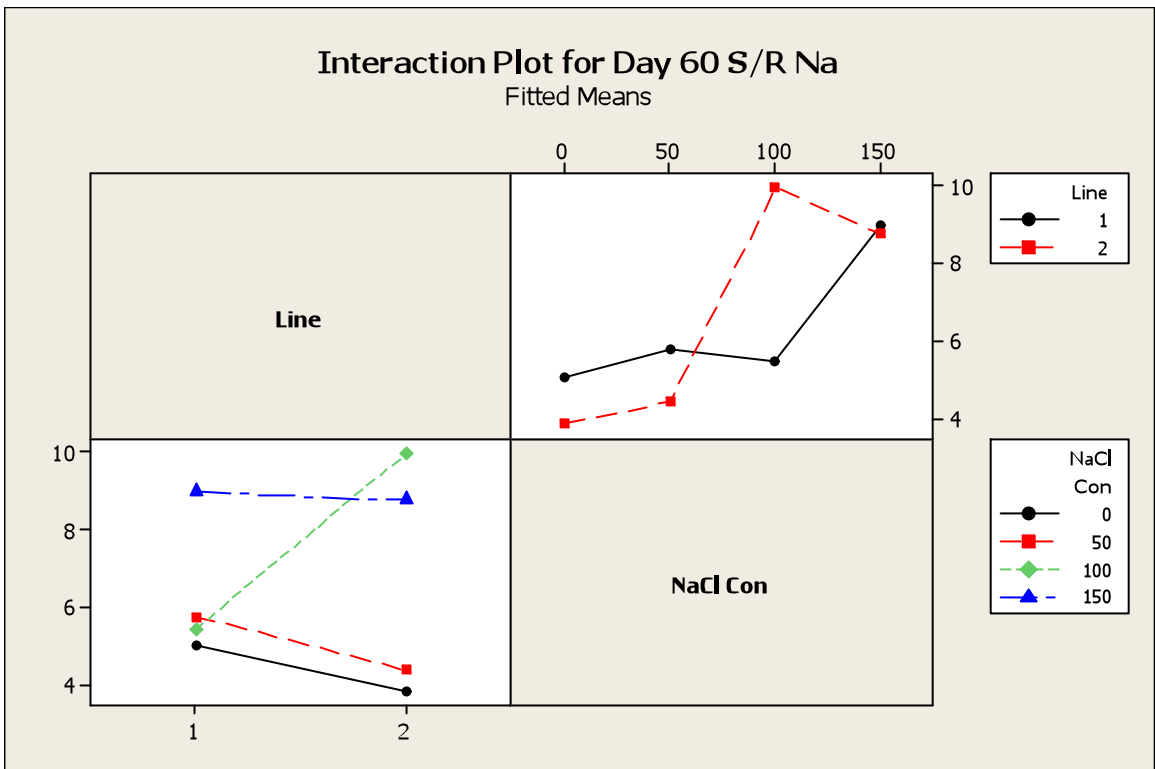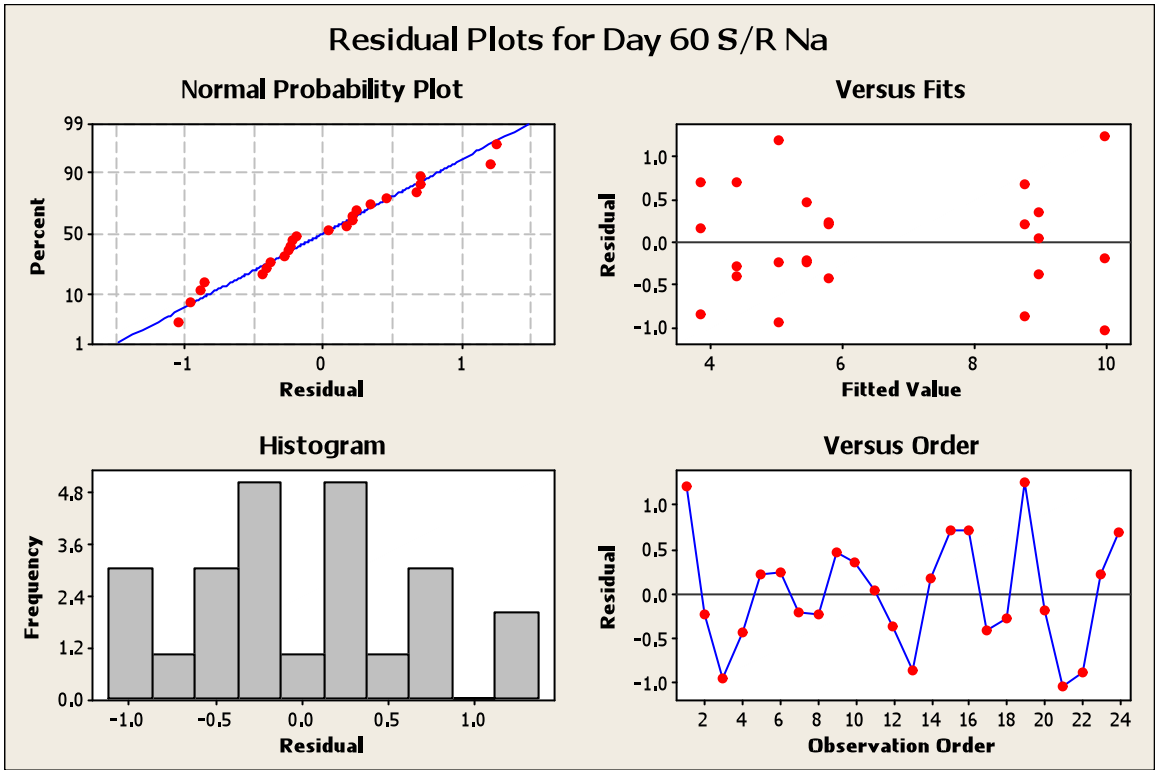
LSD= 3.24

Residual Plots for Log DL K/Na

Figure A 4-26: General Linear Model: Day 60 S/R K versus Line, NaCl Concentration

```
Factor    Type   Levels  Values
Line      fixed       2  1, 2
NaCl Con  fixed       4  0, 50, 100, 150


Analysis of Variance for Day 60 S/R K, using Adjusted SS for Tests

Source         DF   Seq SS   Adj SS   Adj MS       F      P
Line            1    0.282    0.282    0.282    0.56  0.463
NaCl Con        3   44.092   44.092   14.697   29.45  0.000
Line*NaCl Con   3  326.132  326.132  108.711  217.84  0.000
Error          16    7.985    7.985    0.499
Total          23  378.490


S = 0.706429   R-Sq = 97.89%   R-Sq(adj) = 96.97%


Grouping Information Using Bonferroni Method and 95.0% Confidence

      NaCl
Line  Con   N  Mean  Grouping
1     150   3  15.4  A
2      50   3  12.5    B
2     100   3  10.6    B
1     100   3   7.2      C
2       0   3   6.2      C D
1       0   3   6.1      C D
2     150   3   4.1        D E
1      50   3   3.7          E

Means that do not share a letter are significantly different.
```

LSD= 2.16

Residual Plots for Day 60 S/R K

Interaction Plot for Day 60 S/R K
Fitted Means
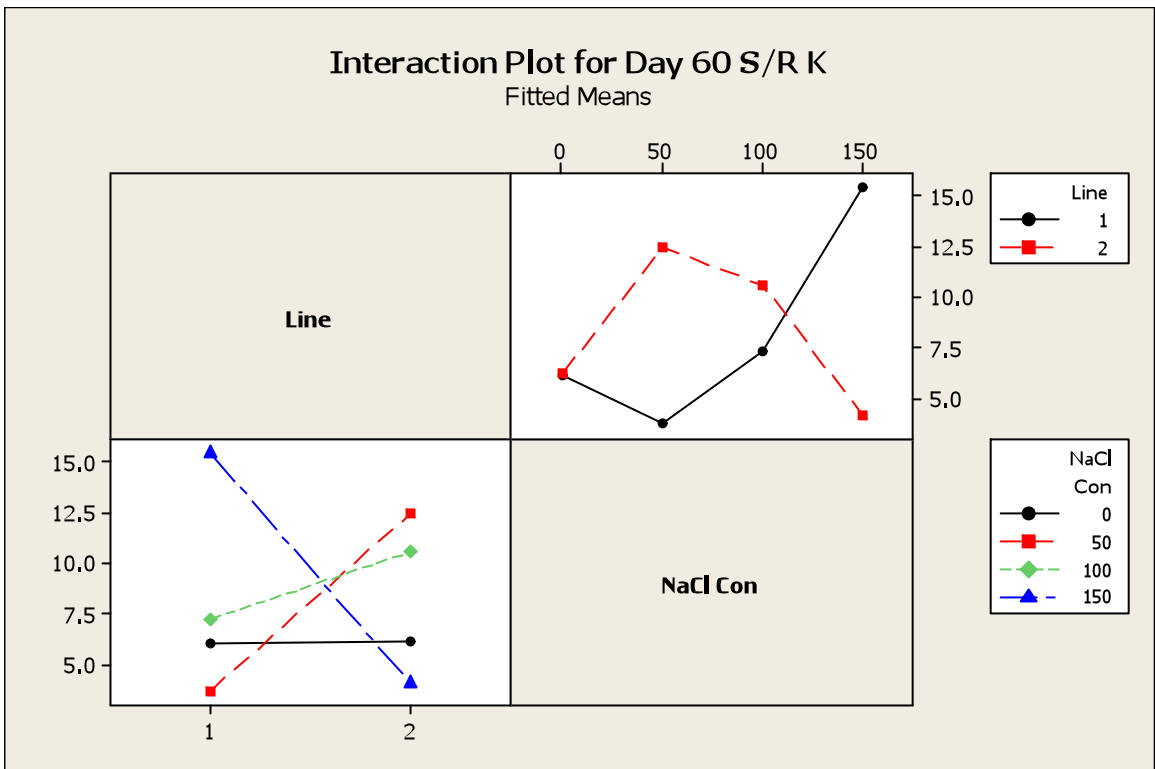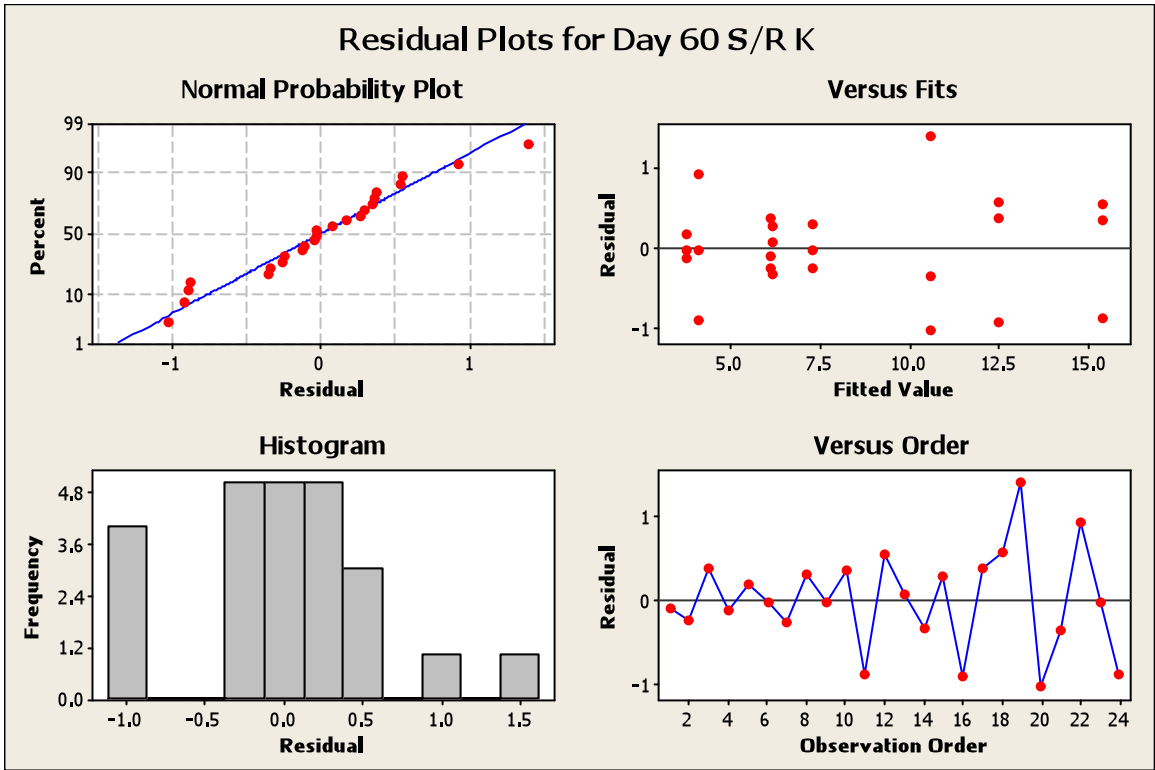
Figure A 4-27: General Linear Model: Day 60 S/R Na versus Line, NaCl Con

```
Factor    Type   Levels  Values
Line      fixed       2  1, 2
NaCl Con  fixed       4  0, 50, 100, 150


Analysis of Variance for Day 60 S/R Na, using Adjusted SS for Tests

Source         DF   Seq SS   Adj SS   Adj MS      F      P
Line            1    1.153    1.153    1.153   1.97  0.179
NaCl Con        3   79.855   79.855   26.618  45.54  0.000
Line*NaCl Con   3   34.565   34.565   11.522  19.71  0.000
Error          16    9.352    9.352    0.585
Total          23  124.926


S = 0.764537   R-Sq = 92.51%   R-Sq(adj) = 89.24%

Grouping Information Using Sidak Method and 95.0% Confidence

      NaCl
Line  Con   N  Mean  Grouping
2     100   3  10.0  A
1     150   3   9.0  A
2     150   3   8.8  A
1      50   3   5.8    B
1     100   3   5.4    B
1       0   3   5.0    B
2      50   3   4.4    B
2       0   3   3.8    B

Means that do not share a letter are significantly different.
```

LSD= 2.32

Residual Plots for Day 60 S/R Na

Interaction Plot for Day 60 S/R Na

Figure A 4-28: General Linear Model: Shoot Na$^+$ versus Line, NaCl Concentration.

```
Factor     Type    Levels  Values
Line       fixed        2  1 (Local), 2 (Optic)
NaCl Con   fixed        4  0, 50, 100, 150


Analysis of Variance for Na Shoot, using Adjusted SS for Tests

Source           DF   Seq SS    Adj SS   Adj MS      F      P
Line              1    931.7     931.7    931.7  16.62  0.000
NaCl Con          3  12270.1   12270.1   4090.0  72.95  0.000
Line*NaCl Con     3   1114.9    1114.9    371.6   6.63  0.001
Error            32   1794.2    1794.2     56.1
Total            39  16110.8

S = 7.48780   R-Sq = 88.86%   R-Sq(adj) = 86.43%


Grouping Information Using Tukey Method and 95.0% Confidence

      NaCl
Line  Con   N  Mean  Grouping
2     150   5  79.4  A
2     100   5  60.4    B
1     150   5  52.4    B
1     100   5  51.8    B C
2      50   5  36.9      C D
1      50   5  32.6        D E
1       0   5  21.8        D E
2       0   5  20.7          E

Means that do not share a letter are significantly different.
```

LSD= 15.3

Residual Plots for Na Shoot

Normal Probability Plot

Versus Fits

Histogram

Versus Order
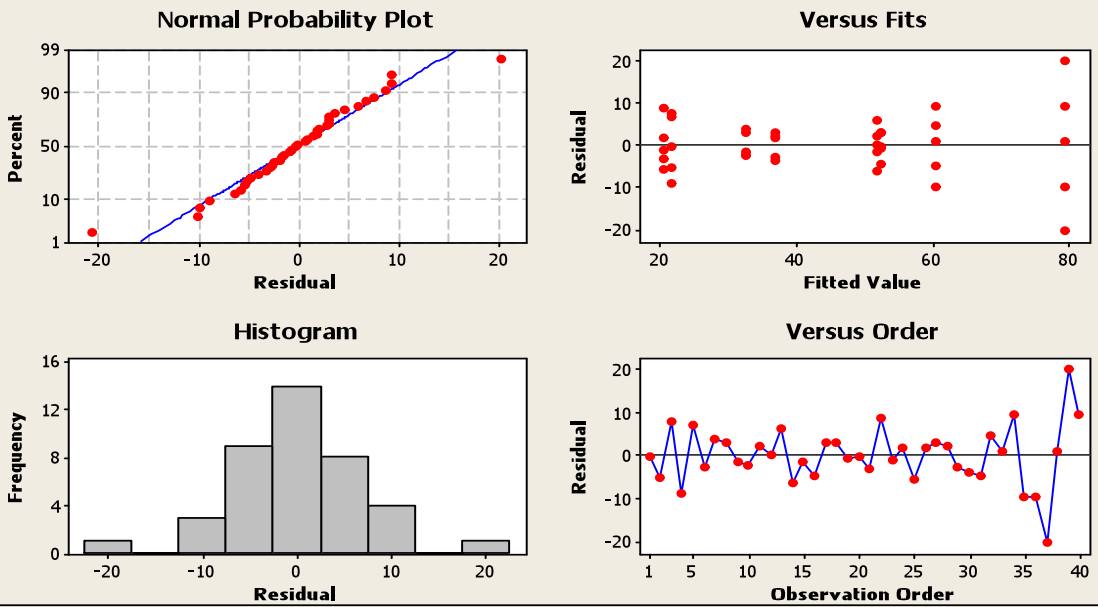
Interaction Plot for Na Shoot
Fitted Means
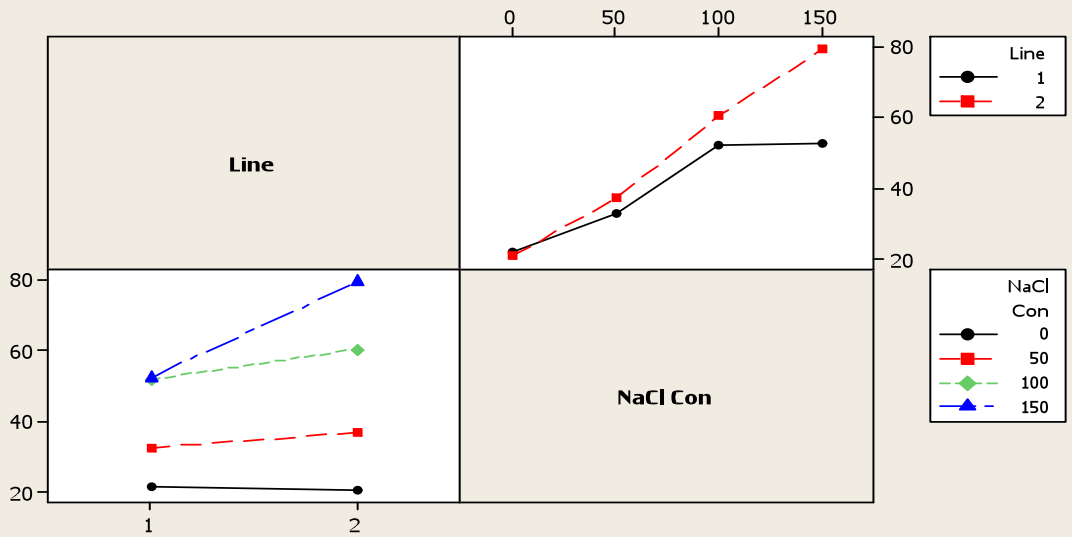
Figure A 4-29: General Linear Model: Log K Shoot versus Line, NaCl Con

```
Factor     Type   Levels  Values
Line       fixed       2  1, 2
NaCl Con   fixed       4  0, 50, 100, 150


Analysis of Variance for Log K Shoot, using Adjusted SS for Tests

Source         DF   Seq SS   Adj SS   Adj MS       F      P
Line            1  0.00148  0.00148  0.00148    0.30  0.590
NaCl Con        3  3.99800  3.99800  1.33267  266.17  0.000
Line*NaCl Con   3  0.13687  0.13687  0.04562    9.11  0.000
Error          32  0.16022  0.16022  0.00501
Total          39  4.29657


S = 0.0707594   R-Sq = 96.27%   R-Sq(adj) = 95.46%

Grouping Information Using Tukey Method and 95.0% Confidence

      NaCl
Line  Con   N  Mean  Grouping
2       0   5  1.8   A
1       0   5  1.8   A
2      50   5  1.3    B
1     100   5  1.2    B C
1      50   5  1.2      C
2     100   5  1.1      C D
1     150   5  1.0        D E
2     150   5  0.9          E

Means that do not share a letter are significantly different.
```

LSD= 1.3

Residual Plots for Log K Shoot

Interaction Plot for Log K Shoot
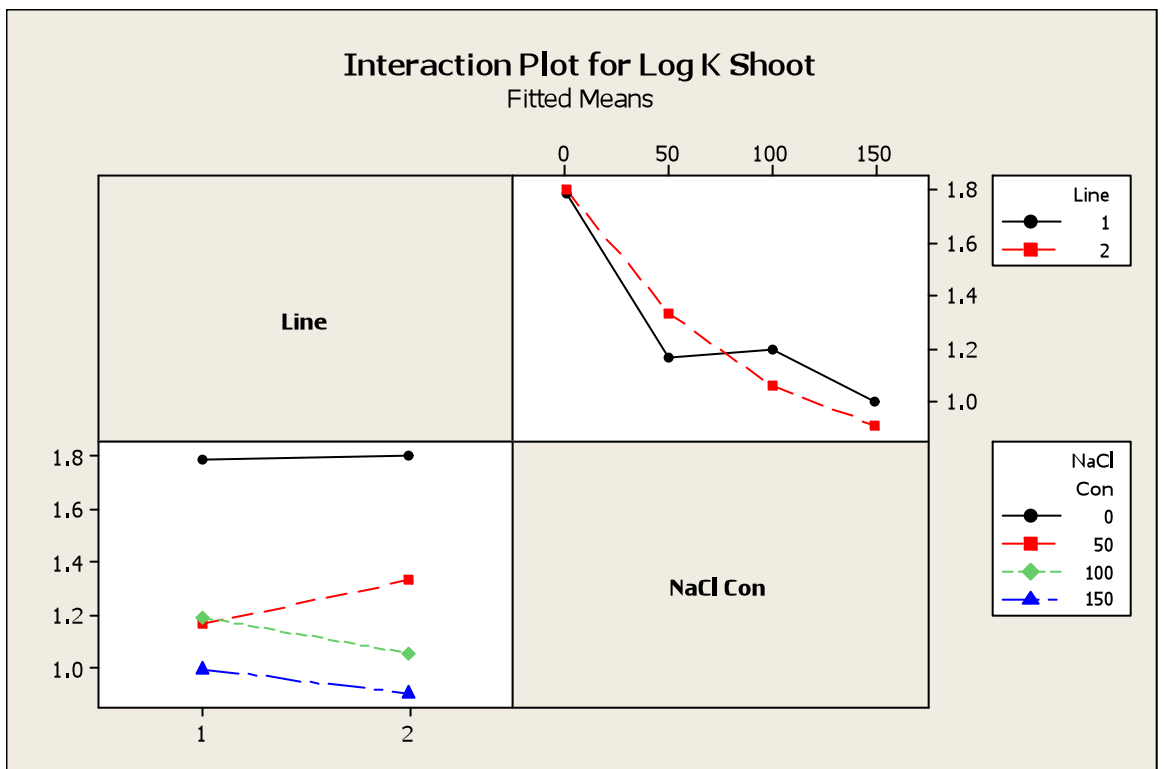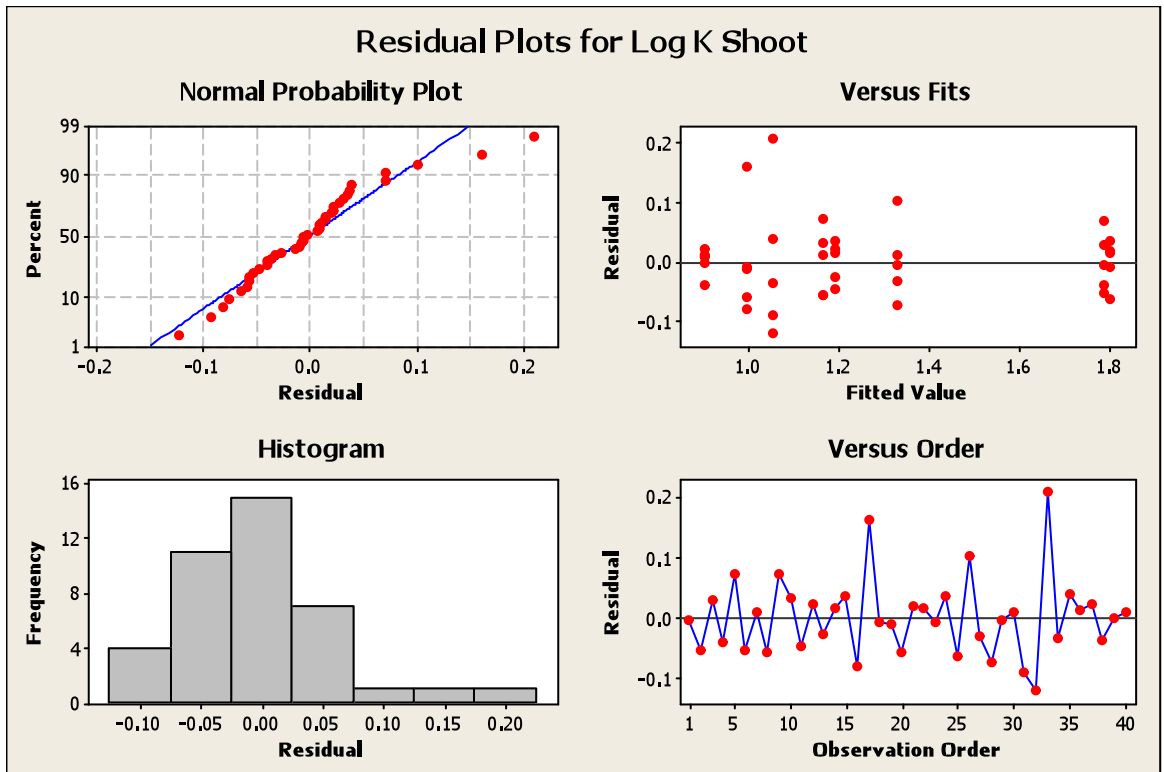
Figure A 4-30: General Linear Model: Log Root Na$^+$ versus Line, NaCl Concentration.

```
Factor     Type    Levels  Values
Line       fixed       2   1 (Local), 2 (Optic)
NaCl Con   fixed       4   0, 50, 100, 150

Analysis of Variance for Log Na Root, using Adjusted SS for Tests

Source          DF   Seq SS    Adj SS    Adj MS      F      P
Line             1  0.06854   0.06854   0.06854   3.64   0.066
NaCl Con         3  1.40269   1.40269   0.46756  24.80   0.000
Line*NaCl Con    3  0.04931   0.04931   0.01644   0.87   0.466
Error           32  0.60322   0.60322   0.01885
Total           39  2.12376


S = 0.137298   R-Sq = 71.60%   R-Sq(adj) = 65.38%


Grouping Information Using Tukey Method and 95.0% Confidence

      NaCl
Line  Con   N  Mean  Grouping
2     150   5  38.4  A
2     100   5  30.0  A B
1     150   5  28.0  A B C
1     100   5  26.6  A B C
2      50   5  18.3    B C
1      50   5  12.7      C
2       0   5  11.7      C
1       0   5  11.6      C


Means that do not share a letter are significantly different.
```

LSD= 1.8

Residual Plots for Log Na Root
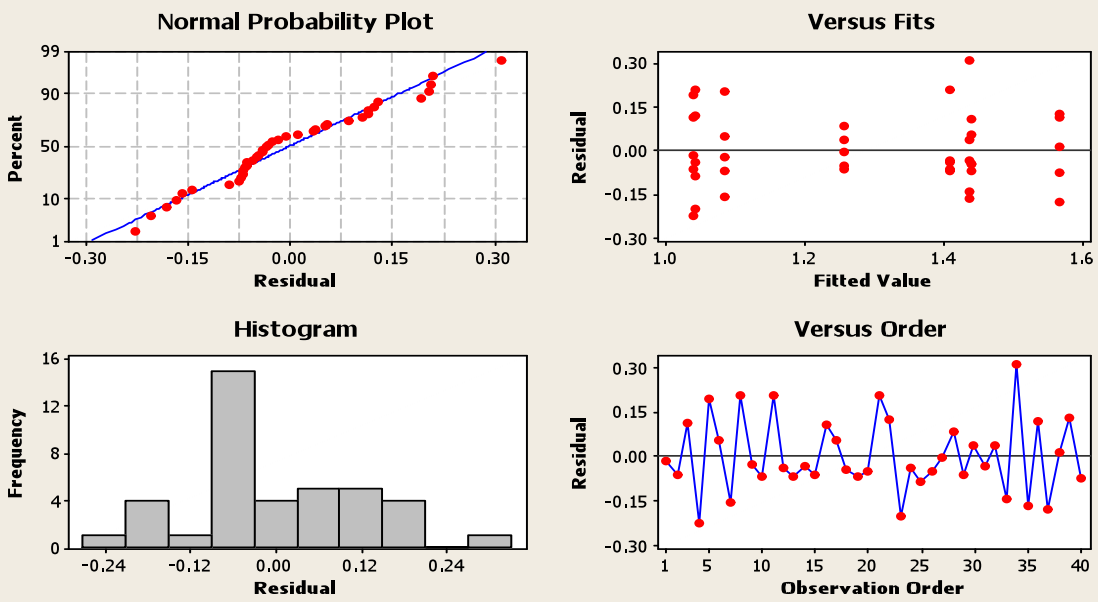
Interaction Plot for Log Na Root
Fitted Means
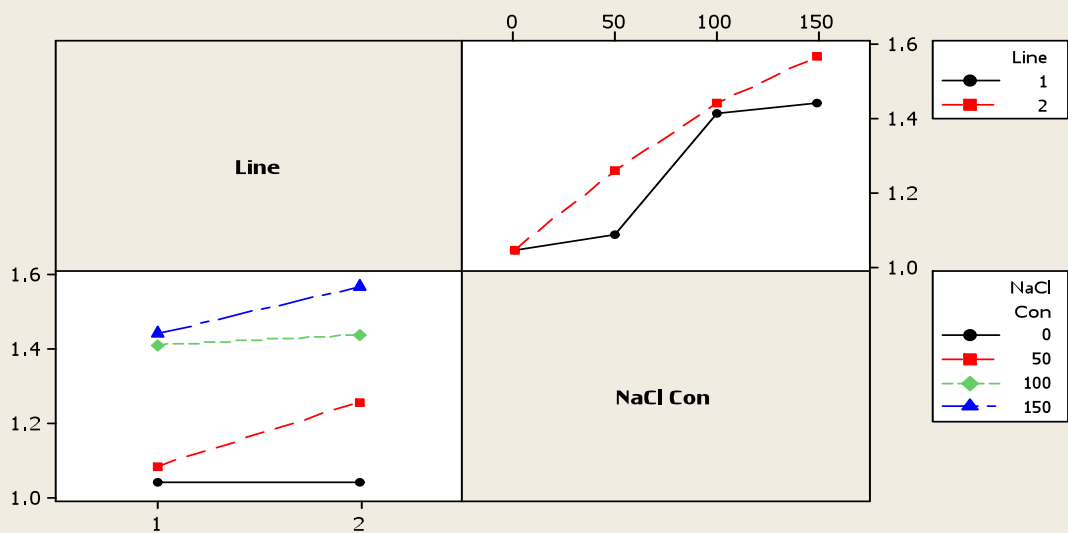
Figure A 4-31: General Linear Model: K Root versus Line, NaCl Con

```
Factor    Type   Levels  Values
Line      fixed       2  1, 2
NaCl Con  fixed       4  0, 50, 100, 150


Analysis of Variance for K Root, using Adjusted SS for Tests

Source          DF   Seq SS   Adj SS  Adj MS       F      P
Line             1     7.70     7.70    7.70    1.26  0.270
NaCl Con         3  2894.77  2894.77  964.92  158.02  0.000
Line*NaCl Con    3    48.13    48.13   16.04    2.63  0.067
Error           32   195.40   195.40    6.11
Total           39  3146.00


S = 2.47108   R-Sq = 93.79%   R-Sq(adj) = 92.43%


Grouping Information Using Tukey Method and 95.0% Confidence

      NaCl
Line  Con   N  Mean  Grouping
2       0   5  28.0  A
1       0   5  25.1  A
1      50   5  16.9    B
2      50   5  14.9    B
1     100   5   9.6      C
2     100   5   7.4      C D
1     150   5   5.3      C D
2     150   5   3.0        D

Means that do not share a letter are significantly different.
```
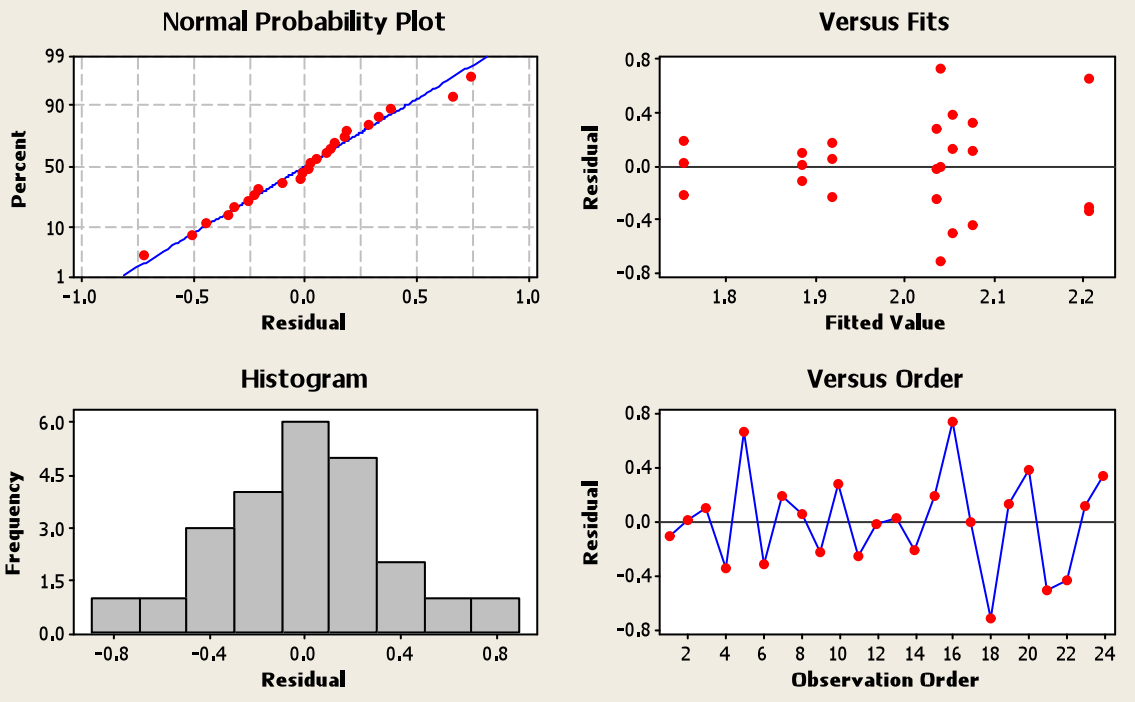
LSD= 5.07

Residual Plots for K Root
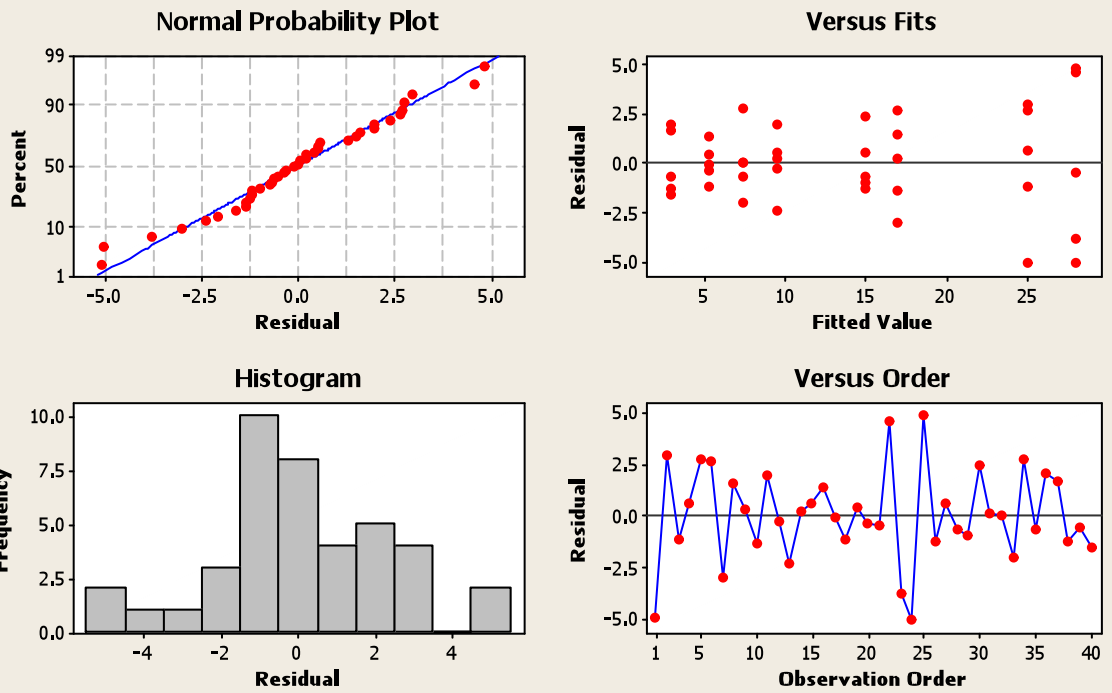
Interaction Plot for K Root
Fitted Means
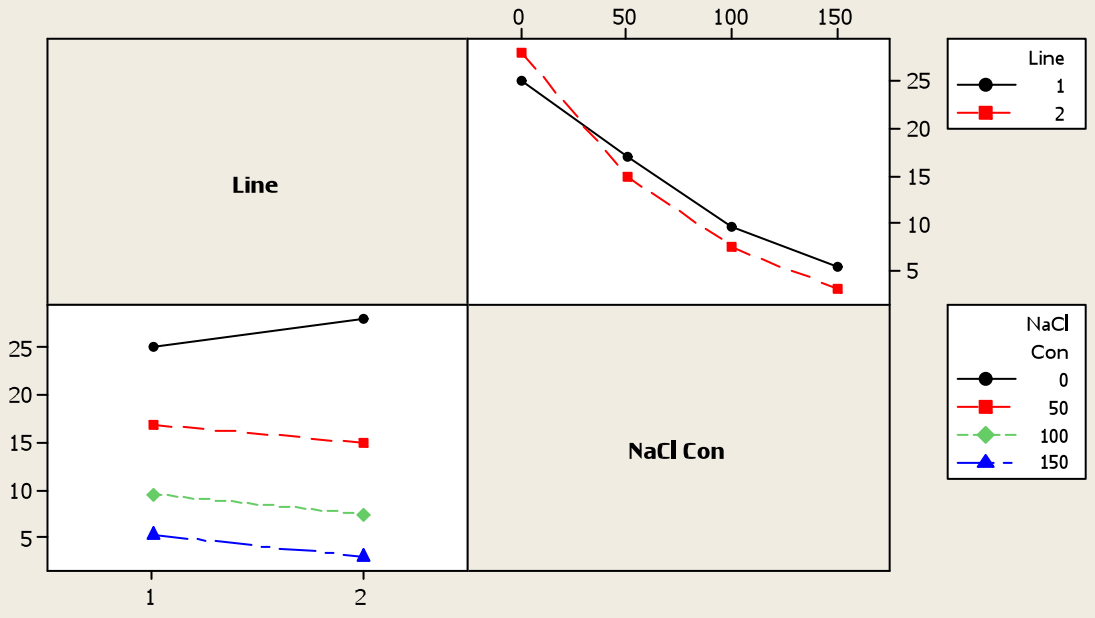
Figure A 4-32: General Linear Model: Day 24 S/R K versus Line, NaCl Con

```
Factor     Type    Levels  Values
Line       fixed      2    1, 2
NaCl Con   fixed      4    0, 50, 100, 150


Analysis of Variance for Day 24 S/R K, using Adjusted SS for Tests

Source          DF  Seq SS  Adj SS  Adj MS      F      P
Line             1  0.4620  0.4620  0.4620   5.93  0.027
NaCl Con         3  5.9710  5.9710  1.9903  25.54  0.000
Line*NaCl Con    3  1.0242  1.0242  0.3414   4.38  0.020
Error           16  1.2468  1.2468  0.0779
Total           23  8.7040


S = 0.279150   R-Sq = 85.68%   R-Sq(adj) = 79.41%


Grouping Information Using Tukey Method and 95.0% Confidence

      NaCl
Line  Con  N  Mean  Grouping
2     150  3  2.7   A
1       0  3  2.5   A
2       0  3  2.2   A B
1     150  3  2.0   A B
1     100  3  1.7     B
2     100  3  1.6     B C
2      50  3  1.5     B C
1      50  3  0.9       C

Means that do not share a letter are significantly different.
```

LSD= 0.87

Residual Plots for Day 24 S/R K
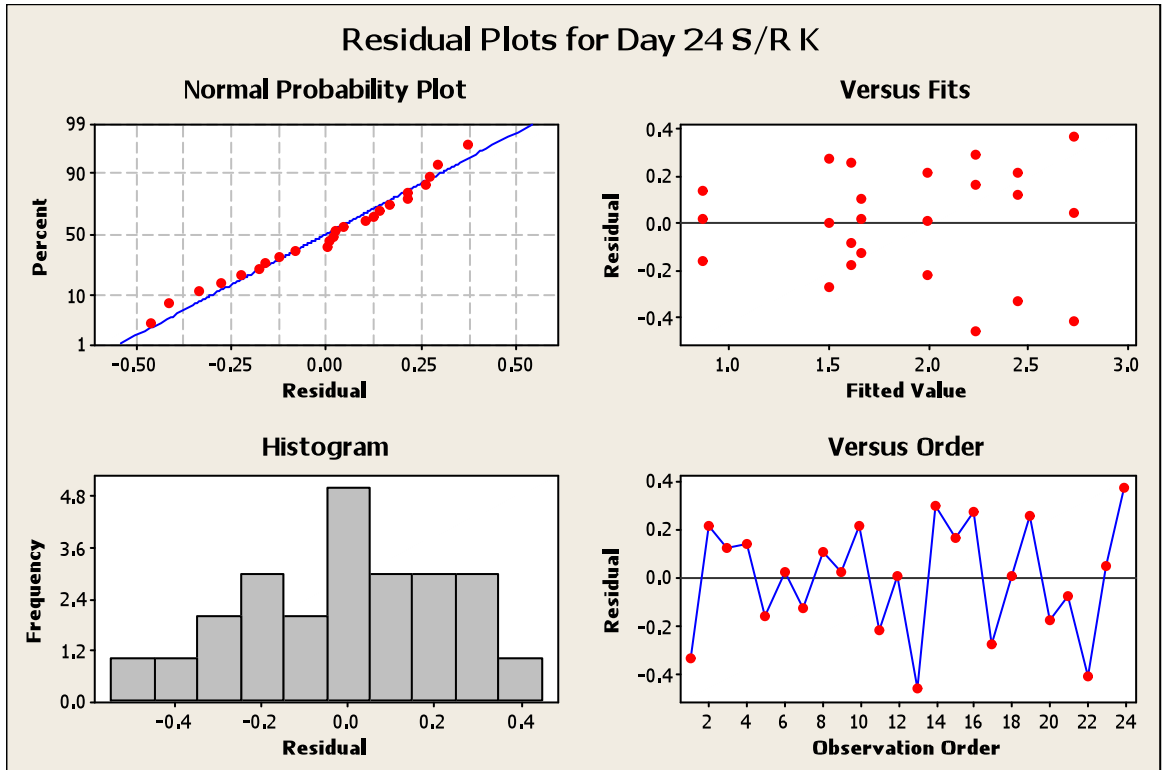
Interaction Plot for Day 24 S/R K
Fitted Means
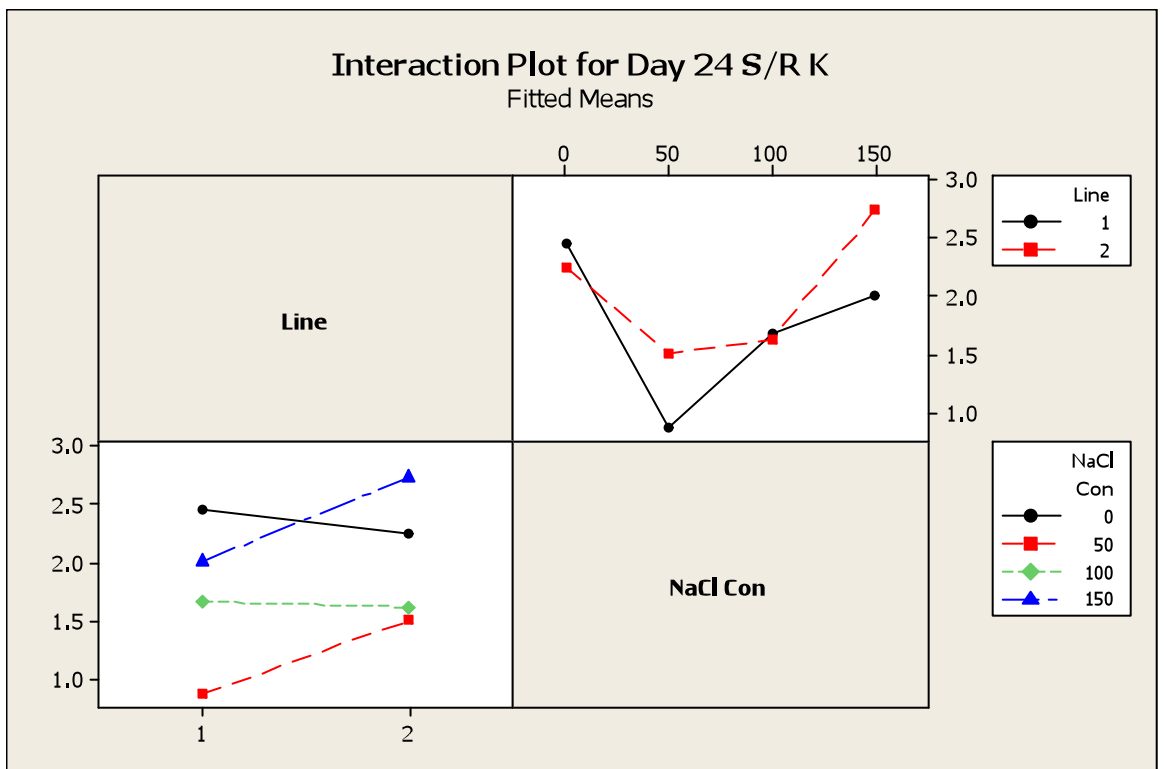
Figure A 4-33: General Linear Model: Day 24 S/R Na versus Line, NaCl Con

```
Factor     Type    Levels  Values
Line       fixed        2  1, 2
NaCl Con   fixed        4  0, 50, 100, 150


Analysis of Variance for Day 24 S/R Na, using Adjusted SS for Tests

Source          DF  Seq SS  Adj SS  Adj MS     F      P
Line             1  0.0060  0.0060  0.0060  0.03  0.856
NaCl Con         3  0.3057  0.3057  0.1019  0.58  0.639
Line*NaCl Con    3  0.0914  0.0914  0.0305  0.17  0.914
Error           16  2.8296  2.8296  0.1768
Total           23  3.2327


S = 0.420535   R-Sq = 12.47%   R-Sq(adj) = 0.00%

Grouping Information Using Tukey Method and 95.0% Confidence

      NaCl
Line  Con   N  Mean  Grouping
1      50   3   2.2  A
2     150   3   2.1  A
2     100   3   2.1  A
2      50   3   2.0  A
1     150   3   2.0  A
1     100   3   1.9  A
1       0   3   1.9  A
2       0   3   1.8  A

Means that do not share a letter are significantly different.
```

LSD= 0.87

Residual Plots for Day 24 S/R Na

Interaction Plot for Day 24 S/R Na
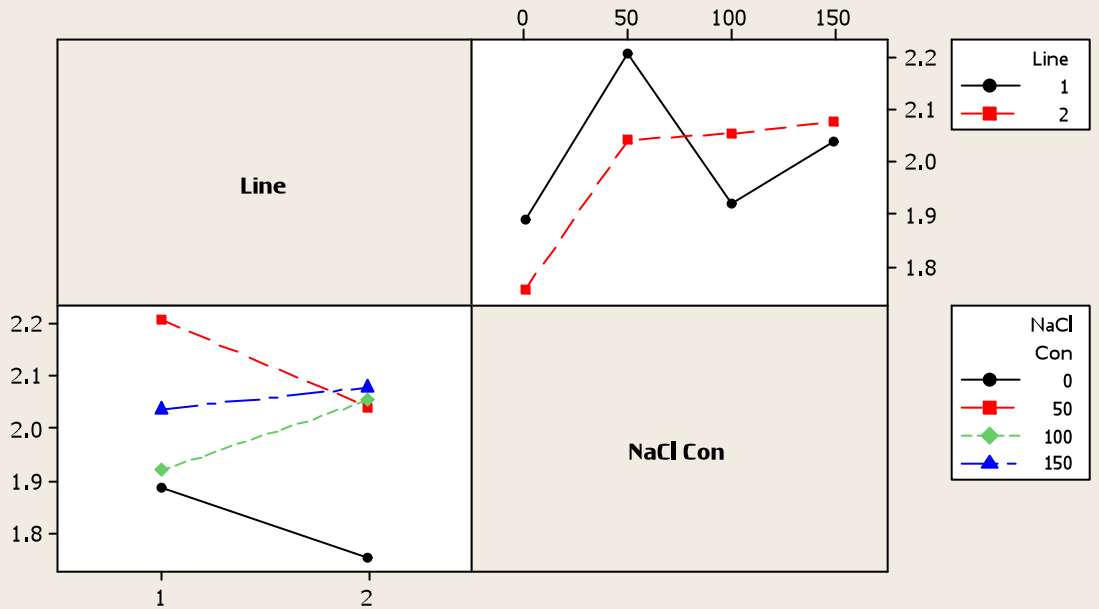
Figure A 4-34: General Linear Model: Survival % versus Line, NaCl Concentration.

```
Factor    Type   Levels  Values
Line      fixed       2  1 (Local), 2 (Optic)
NaCl Con  fixed       3  125, 150, 175


Analysis of Variance for Survival %, using Adjusted SS for Tests

Source          DF   Seq SS    Adj SS   Adj MS      F      P
Line             1   3707.6    3707.6   3707.6  33.14  0.000
NaCl Con         2  18148.1   18148.1   9074.1  81.10  0.000
Line*NaCl Con    2   1142.0    1142.0    571.0   5.10  0.025
Error           12   1342.6    1342.6    111.9
Total           17  24340.3


S = 10.5775   R-Sq = 94.48%   R-Sq(adj) = 92.19%


Grouping Information Using Bonferroni Method and 95.0% Confidence

      NaCl
Line  Con   N  Mean  Grouping
1     125   3  91.7  A
1     150   3  88.9  A
2     125   3  61.1  A B
2     150   3  41.7    B
1     175   3   8.3      C
2     175   3  -0.0      C


Means that do not share a letter are significantly different.
```

LSD= 31.54

332

Residual Plots for Survival %
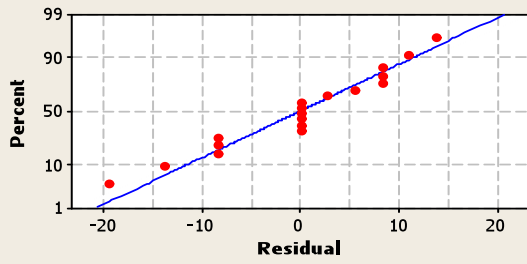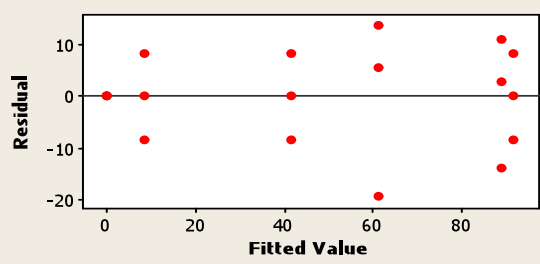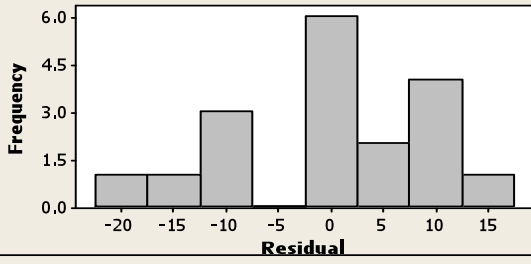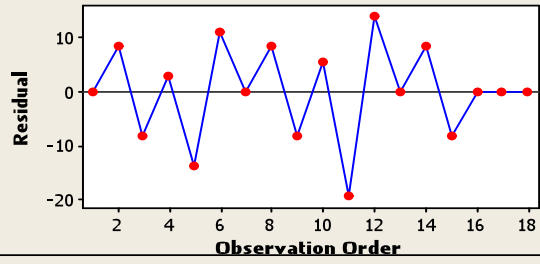
Interaction Plot for Survival %
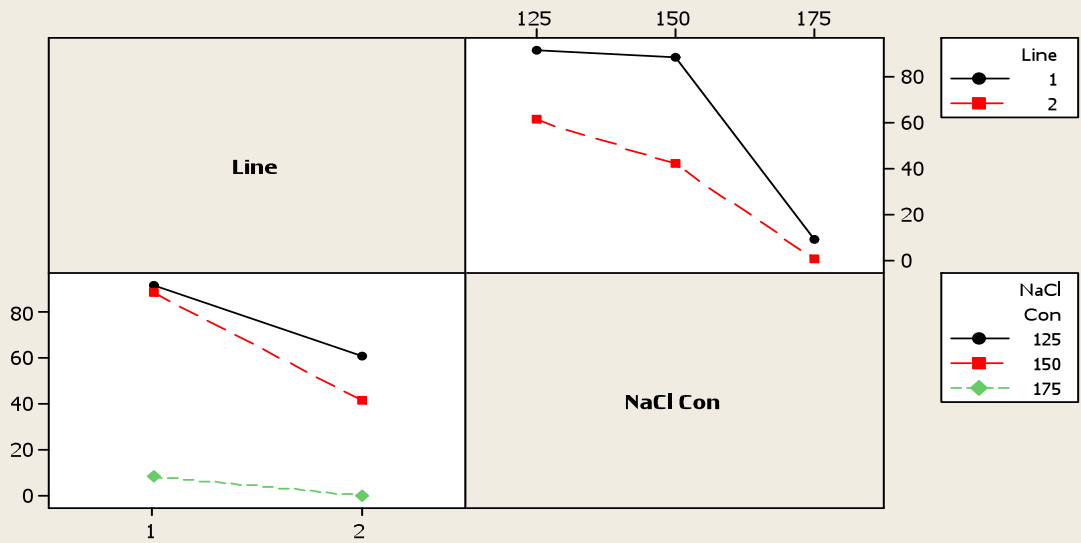
Figure A 4-35: General Linear Model: Seedling Shoot Length versus Line, NaCl Concentration.

```
Factor        Type   Levels  Values
Line          fixed       2  1 (Local), 2 (Optic)
Treatment_1   fixed       4  1, 2, 3, 4

Analysis of Variance for Seedling Length, using Adjusted SS for Tests

Source             DF   Seq SS   Adj SS   Adj MS        F       P
Line                1    15.74    15.74    15.74     6.14   0.016
Treatment_1         3  2343.42  2343.42   781.14   304.47   0.000
Line*Treatment_1    3   173.13   173.13    57.71    22.49   0.000
Error              72   184.72   184.72     2.57
Total              79  2717.02


S = 1.60175   R-Sq = 93.20%   R-Sq(adj) = 92.54%


Grouping Information Using Bonferroni Method and 95.0% Confidence

Line  Treatment  N  Mean  Grouping
1     2          10  6.0  A
2     2          10  5.2  A
1     1          10  1.3     B
2     1          10  0.3     B

Means that do not share a letter are significantly different.
```

LSD= 1.54

Residual Plots for Seedling Shoot Length
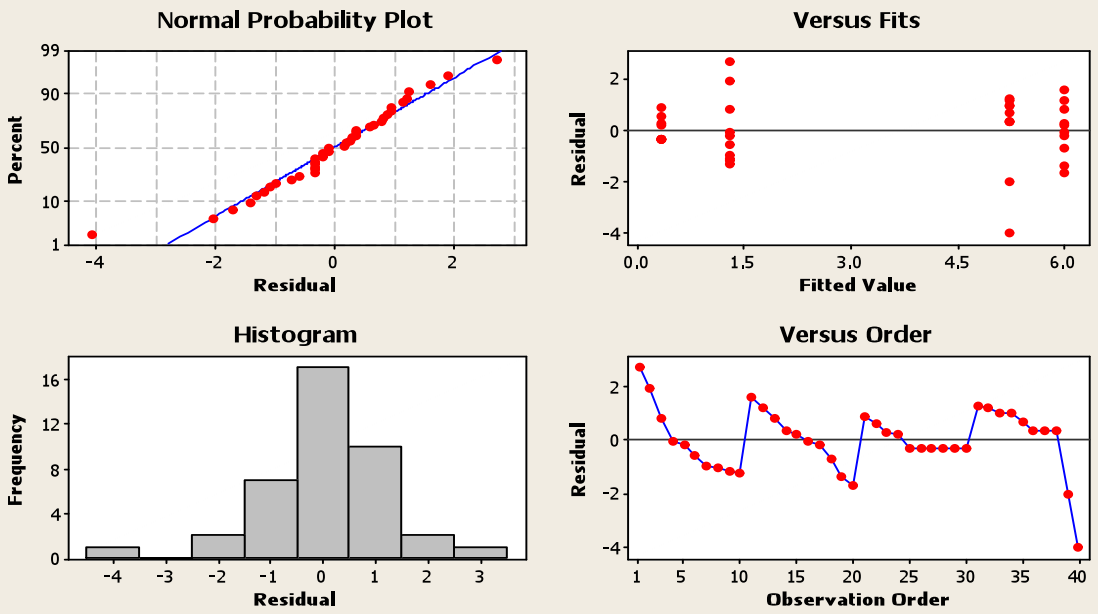
Interaction Plot for Seedling Shoot Length
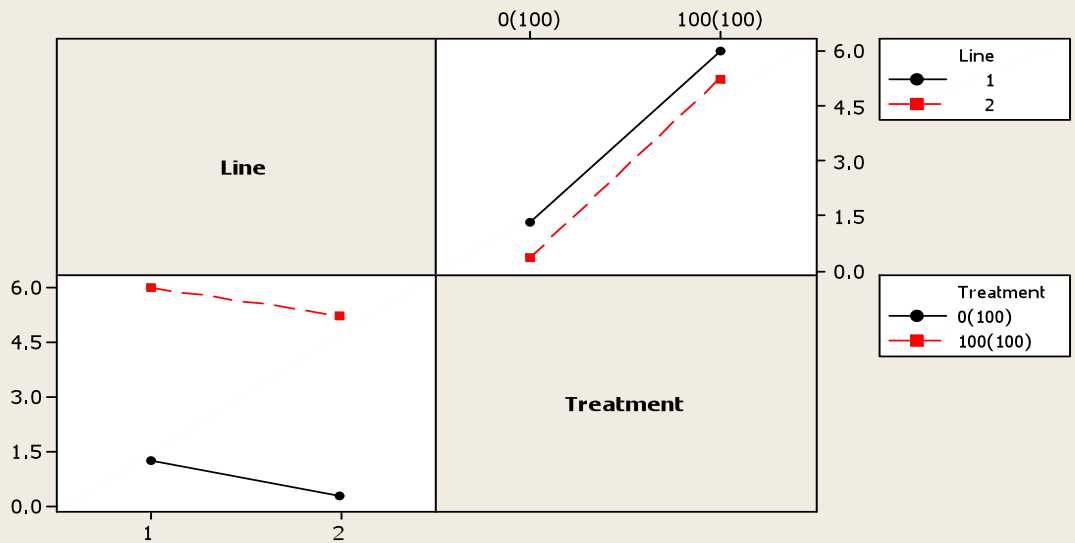
Figure A 5-1: General Linear Model: Log A_{sat} versus Line, HS Treatment.

```
Factor         Type    Levels  Values
Line           fixed       3  1 (Local), 2 (Optic), 3 (Soorab-96)
HS Treatment   fixed       3  0, 3, 120


Analysis of Variance for Log Asat, using Adjusted SS for Tests

Source               DF   Seq SS  Adj SS  Adj MS      F       P
Line                  2   1.0677  1.0124  0.5062   5.27   0.013
HS Treatment          2   7.3473  7.0120  3.5060  36.49   0.000
Line*HS Treatment     4   2.7143  2.7143  0.6786   7.06   0.001
Error                24   2.3062  2.3062  0.0961
Total                32  13.4355


S = 0.309989   R-Sq = 82.83%   R-Sq(adj) = 77.11%


Grouping Information Using Tukey Method and 95.0% Confidence

       HS
Line  Treatment  N  Mean  Grouping
2        0       4   1.2  A
1        0       4   1.1  A
3        0       4   1.0  A
3      120       2   0.7  A B
1      120       4   0.6  A B
1        3       4   0.2    B
2        3       4   0.1    B C
3        3       3  -0.1    B C
2      120       4  -0.6      C


Means that do not share a letter are significantly different.
```

LSD = 5.49

Residual Plots for Asat
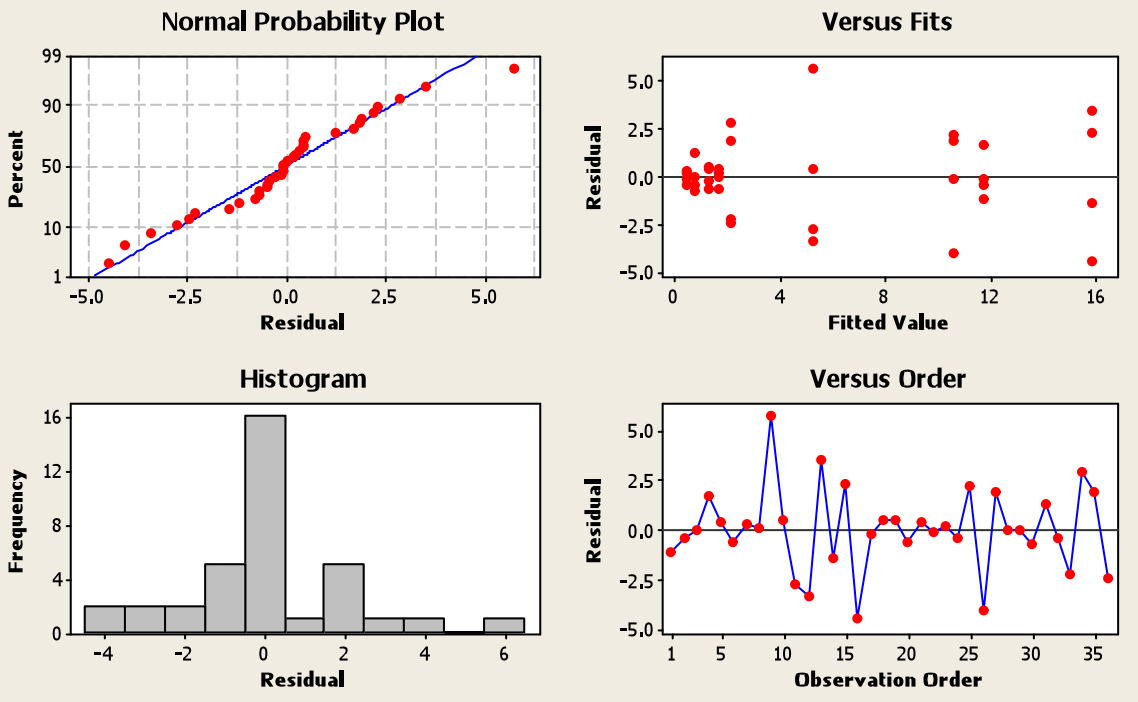
Interaction Plot for Log Asat
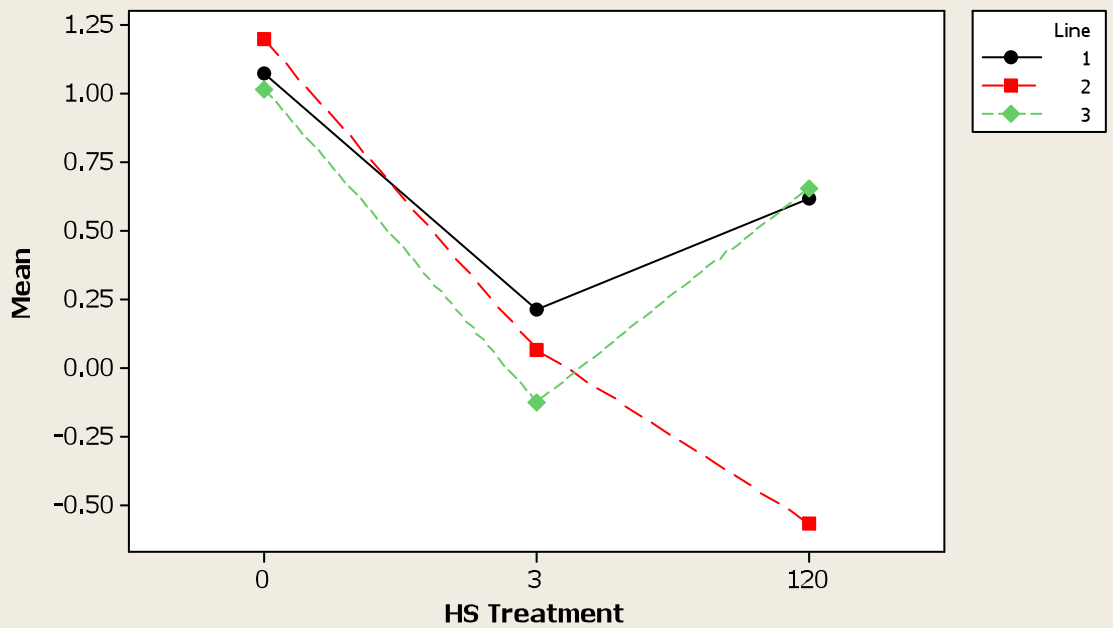
Figure A 5-2: General Linear Model: Log Carboxylation Efficiency versus Line, HS Treatment.

```
Factor         Type   Levels  Values
Line           fixed       3  1 (Local), 2 (Optic), 3 (Soorab-96)
HS Treatment   fixed       3  0, 3, 120

Analysis of Variance for Log Carboxylation Efficiency, using Adjusted SS for
    Tests

Source              DF   Seq SS   Adj SS   Adj MS      F      P
Line                 2   0.8271   0.8271   0.4136   3.86  0.033
HS Treatment         2   7.3396   7.3396   3.6698  34.28  0.000
Line*HS Treatment    4   0.9168   0.9168   0.2292   2.14  0.103
Error               27   2.8907   2.8907   0.1071
Total               35  11.9741

S = 0.327204   R-Sq = 75.86%   R-Sq(adj) = 68.71%



Grouping Information Using Tukey Method and 95.0% Confidence

      HS
Line  Treatment  N  Mean  Grouping
2        0       4  1.8   A
1        0       4  1.8   A
3        0       4  1.7   A
1      120       4  1.4   A B
1        3       4  0.9     B C
2        3       4  0.8     B C
3      120       4  0.7     B C
2      120       4  0.6     B C
3        3       4  0.5       C

Means that do not share a letter are significantly different.
```

LSD = 0.018

Residual Plots for Log Carboxylation Efficien
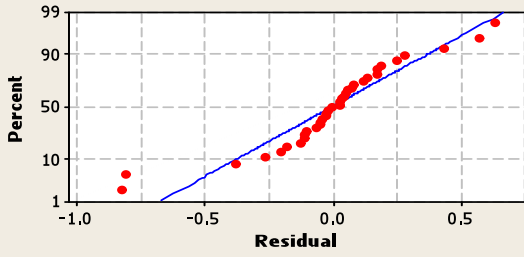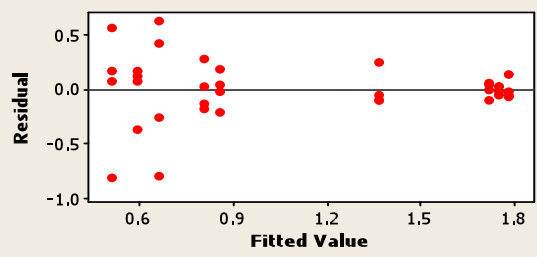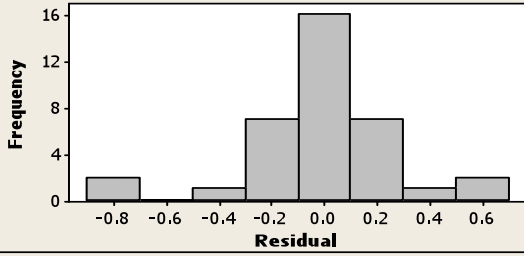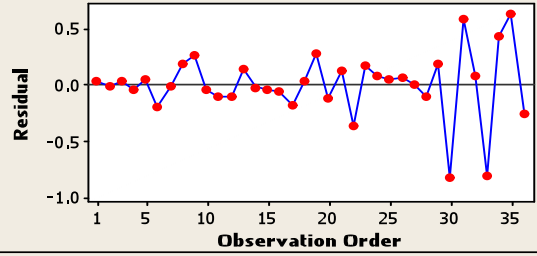
Interaction Plot for Log Carboxylation Efficien
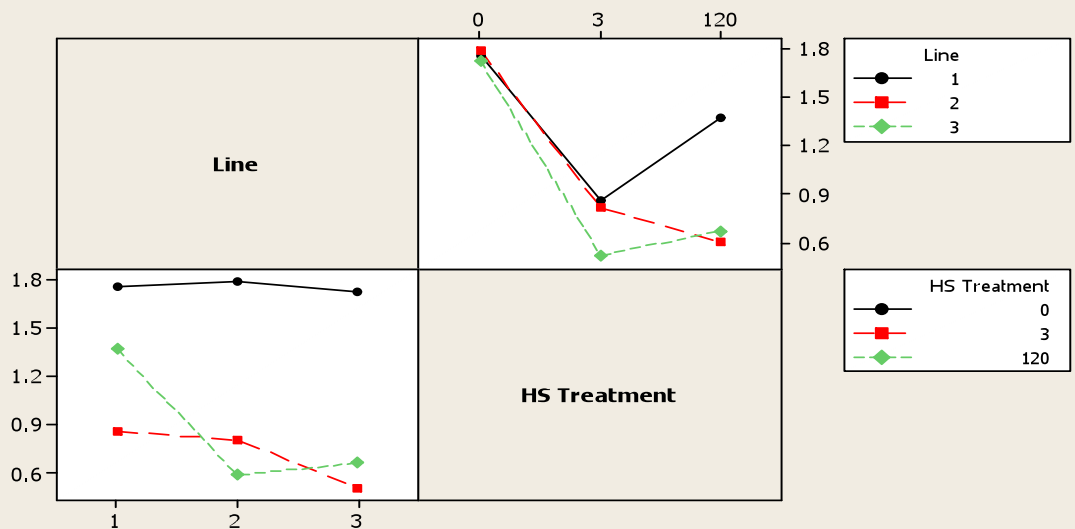
Figure A 5-3: General Linear Model: Asat@25 oC versus Line, HS Treatment

```
Factor         Type    Levels  Values
Line           fixed        3  1 (Local), 2 (Optic), 3 (Soorab-96)
HS Treatment   fixed        3  0, 3, 120


Analysis of Variance for Asat@25 oC, using Adjusted SS for Tests

Source             DF    Seq SS    Adj SS  Adj MS     F      P
Line                2    42.602    42.602  21.301  3.32  0.059
HS Treatment        2     6.036     6.036   3.018  0.47  0.633
Line*HS Treatment   4    17.956    17.956   4.489  0.70  0.603
Error              18   115.593   115.593   6.422
Total              26   182.187


S = 2.53414   R-Sq = 36.55%   R-Sq(adj) = 8.35%

Grouping Information Using Tukey Method and 95.0% Confidence

       HS
Line   Treatment  N   Mean  Grouping
2         0       3   17.0  A
2        120      3   15.5  A
2         3       3   15.4  A
1        120      3   15.3  A
3         0       3   14.2  A
3        120      3   12.7  A
3         3       3   12.7  A
1         0       3   12.6  A
1         3       3   12.6  A

Means that do not share a letter are significantly different.
```
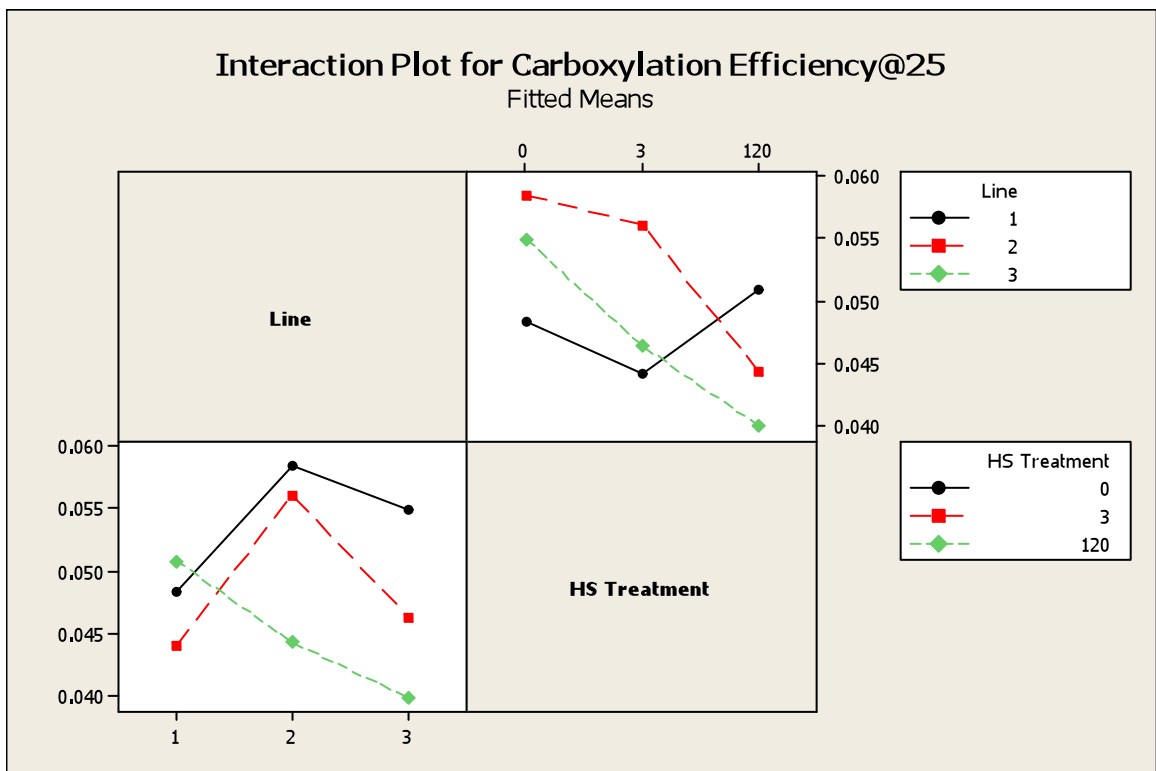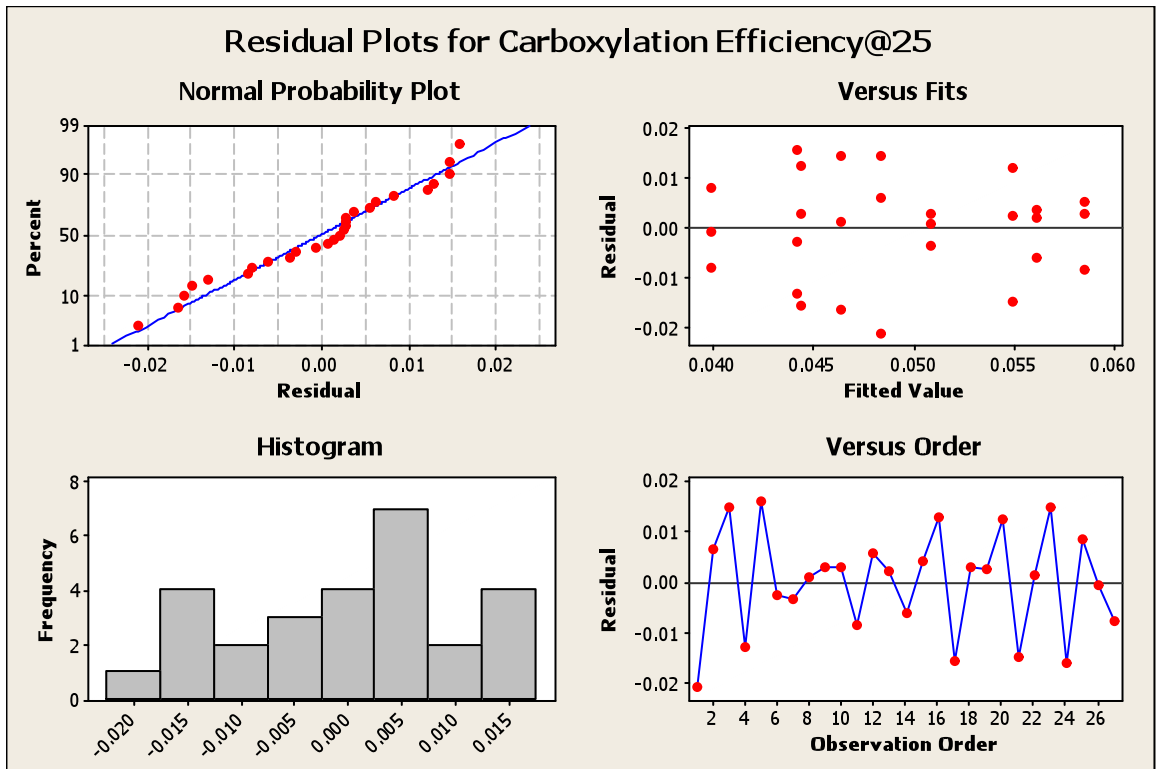
LSD = 7.25

Residual Plots for Asat@25 oC

Interaction Plot for Asat@25 oC
Fitted Means
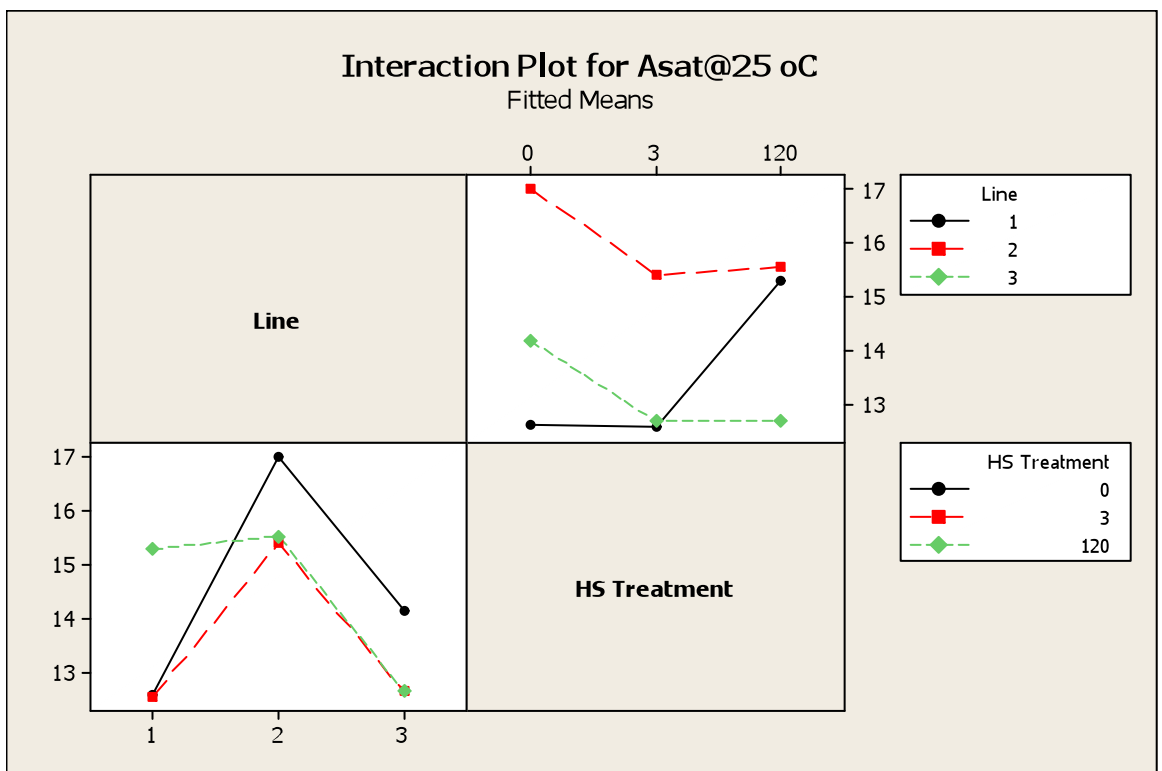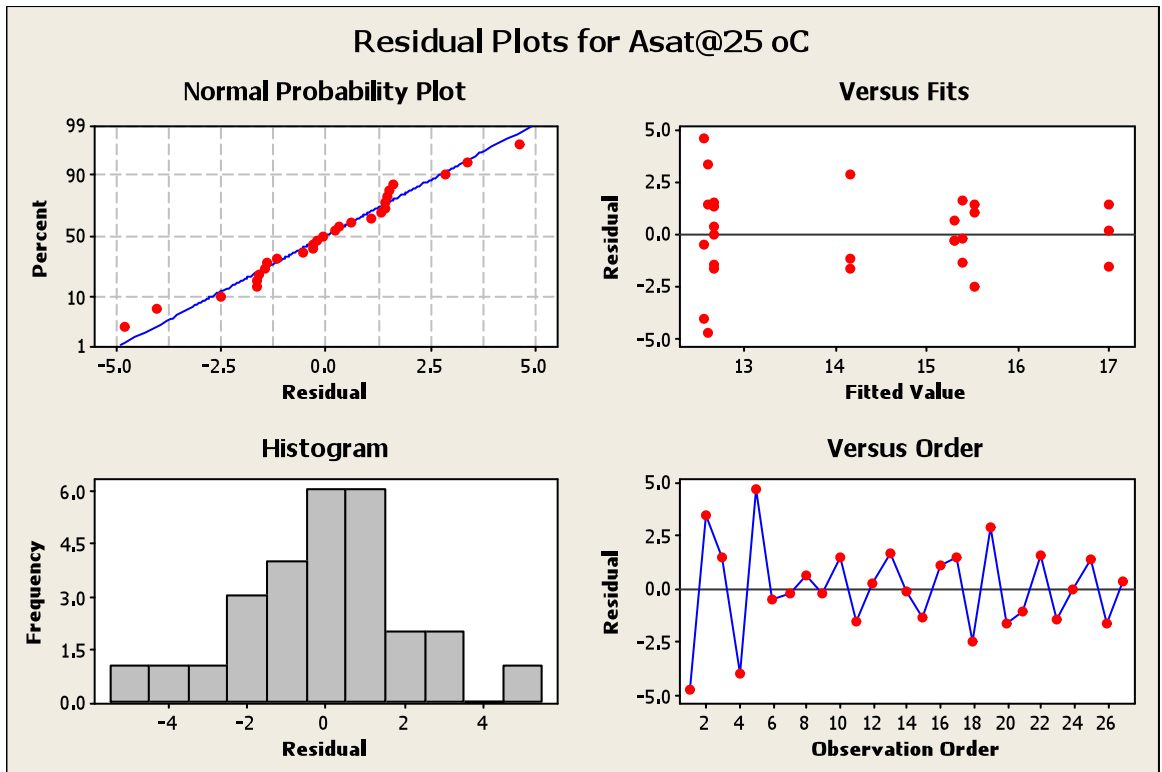
Figure A 5-4: General Linear Model: Carboxylation Efficiency @25 oC versus Line, HS Treatment.

```
Factor          Type   Levels  Values
Line            fixed       3  1 (Local), 2 (Optic), 3 (Soorab-96)
HS Treatment    fixed       3  0, 3, 120


Analysis of Variance for Carboxylation Efficiency@25, using Adjusted SS for
     Tests

Source               DF      Seq SS      Adj SS      Adj MS      F      P
Line                  2   0.0001880   0.0001880   0.0000940   0.62  0.550
HS Treatment          2   0.0003581   0.0003581   0.0001791   1.18  0.331
Line*HS Treatment     4   0.0003971   0.0003971   0.0000993   0.65  0.632
Error                18   0.0027380   0.0027380   0.0001521
Total                26   0.0036812


S = 0.0123332   R-Sq = 25.62%   R-Sq(adj) = 0.00%

Grouping Information Using Tukey Method and 95.0% Confidence

      HS
Line  Treatment  N  Mean  Grouping
2        0       3   0.1  A
2        3       3   0.1  A
3        0       3   0.1  A
1      120       3   0.1  A
1        0       3   0.0  A
3        3       3   0.0  A
2      120       3   0.0  A
1        3       3   0.0  A
3      120       3   0.0  A

Means that do not share a letter are significantly different.
```

LSD = 0.034

Residual Plots for Carboxylation Efficiency@25

Interaction Plot for Carboxylation Efficiency@25
Fitted Means

Figure A 5-5: General Linear Model: gs versus Line, HS Treatment

```
Factor        Type   Levels  Values
Line          fixed       3  1, 2, 3
HS Treatment  fixed       3  0, 3, 120


Analysis of Variance for gs, using Adjusted SS for Tests

Source              DF   Seq SS    Adj SS    Adj MS    F      P
Line                 2  0.06421   0.06421   0.03210  0.50  0.615
HS Treatment         2  0.65549   0.65549   0.32774  5.06  0.014
Line*HS Treatment    4  0.08218   0.08218   0.02054  0.32  0.864
Error               27  1.74985   1.74985   0.06481
Total               35  2.55172


S = 0.254577   R-Sq = 31.42%   R-Sq(adj) = 11.11%

 Grouping Information Using Tukey Method and 95.0% Confidence

      HS
Line  Treatment  N  Mean  Grouping
2         0      4  0.6   A
1         0      4  0.5   A
1         3      4  0.5   A
3         0      4  0.5   A
3         3      4  0.4   A
2         3      4  0.4   A
1       120      4  0.4   A
3       120      4  0.2   A
2       120      4  0.1   A

Means that do not share a letter are significantly different.
```

LSD = 0.40

Residual Plots for gs
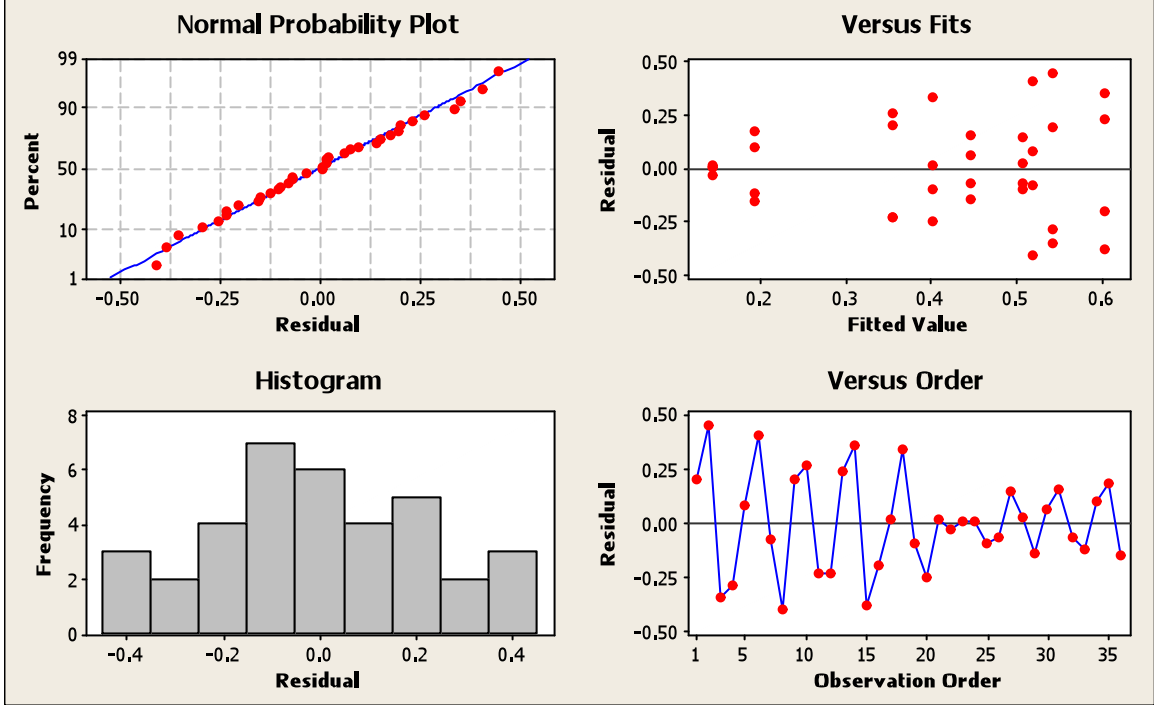
Interaction Plot for gs

345
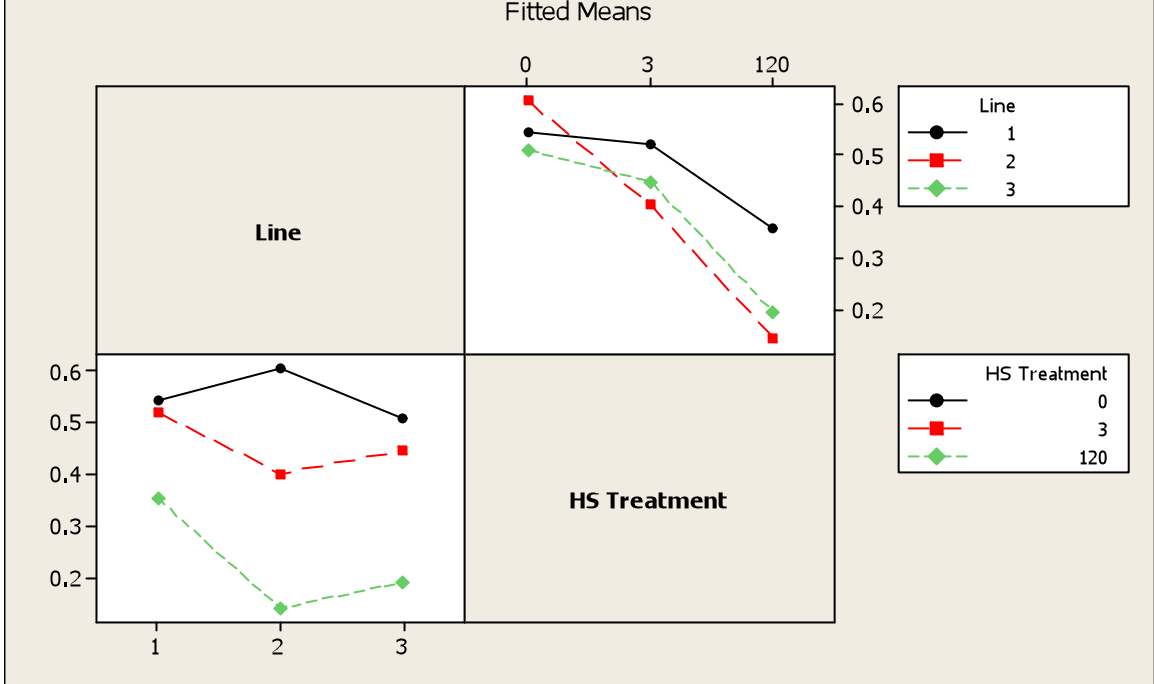
Figure A 5-6: General Linear Model: E versus Line, HS Treatment

```
Factor        Type   Levels  Values
Line          fixed       3  1, 2, 3
HS Treatment  fixed       3  0, 3, 120


Analysis of Variance for E, using Adjusted SS for Tests

Source             DF  Seq SS  Adj SS  Adj MS     F      P
Line                2   0.633   0.633   0.316  0.18  0.835
HS Treatment        2  23.372  23.372  11.686  6.68  0.004
Line*HS Treatment   4   1.929   1.929   0.482  0.28  0.891
Error              27  47.211  47.211   1.749
Total              35  73.145


S = 1.32232   R-Sq = 35.46%   R-Sq(adj) = 16.33%

Grouping Information Using Tukey Method and 95.0% Confidence

       HS
Line  Treatment  N  Mean  Grouping
2         0      4   5.1  A
3         0      4   4.9  A
1         0      4   4.7  A
1         3      4   4.6  A
3         3      4   4.4  A
2         3      4   4.2  A
1       120      4   3.6  A
3       120      4   2.8  A
2       120      4   2.7  A

Means that do not share a letter are significantly different.
```
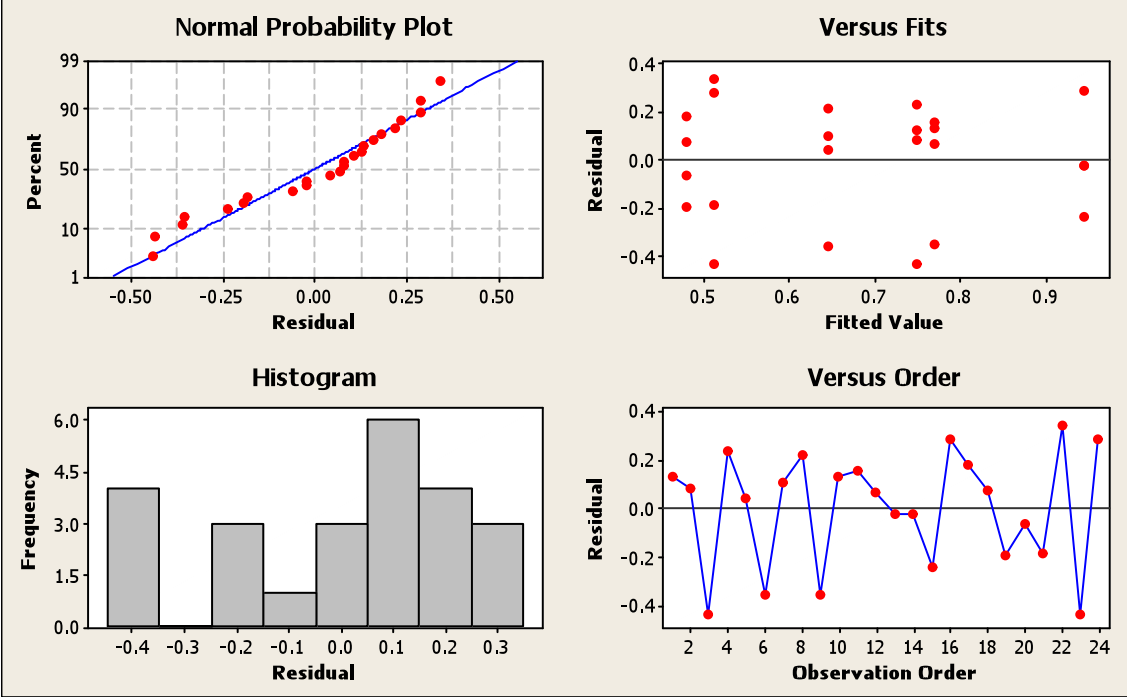
LSD = 3.14

Residual Plots for E

Interaction Plot for E
Fitted Means
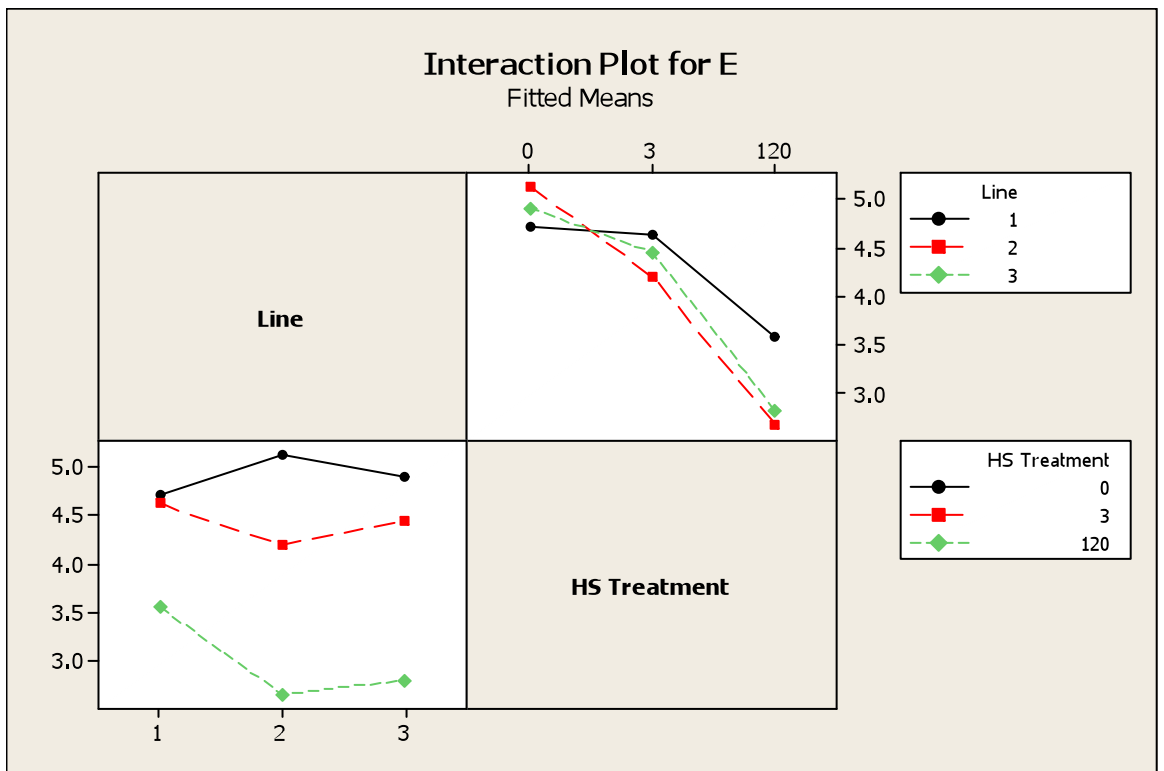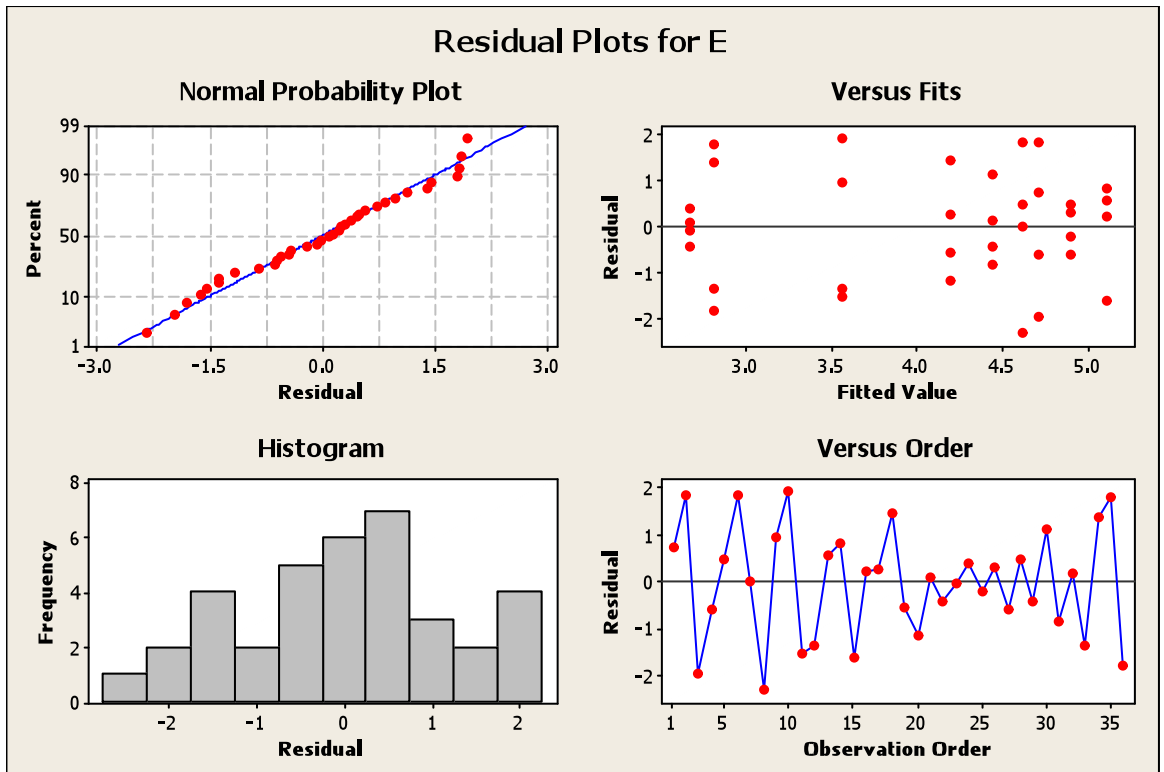
Figure A 5-7: General Linear Model: Log (PSII) Efficiency versus Line, HS Treatment.

```
Factor        Type   Levels  Values
Line          fixed      2  1 (Local), 2 (Optic)
HS Treatment  fixed      3  0, 3, 120


Analysis of Variance for Log (PSII) Efficiency, using Adjusted SS for Tests

Source             DF   Seq SS   Adj SS   Adj MS     F      P
Line                1  0.01586  0.01586  0.01586  0.22  0.645
HS Treatment        2  0.57956  0.57956  0.28978  4.02  0.036
Line*HS Treatment   2  0.01525  0.01525  0.00763  0.11  0.900
Error              18  1.29880  1.29880  0.07216
Total              23  1.90948


S = 0.268618   R-Sq = 31.98%   R-Sq(adj) = 13.09%


Grouping Information Using Tukey Method and 95.0% Confidence

       HS
Line  Treatment  N  Mean  Grouping
2        0       4  -0.1  A
1        0       4  -0.1  A
1        3       4  -0.4  A
1      120       4  -0.4  A
2      120       4  -0.5  A
2        3       4  -0.5  A

Means that do not share a letter are significantly different.
```

LSD = 0.39

Residual Plots for (PSII) Efficiency
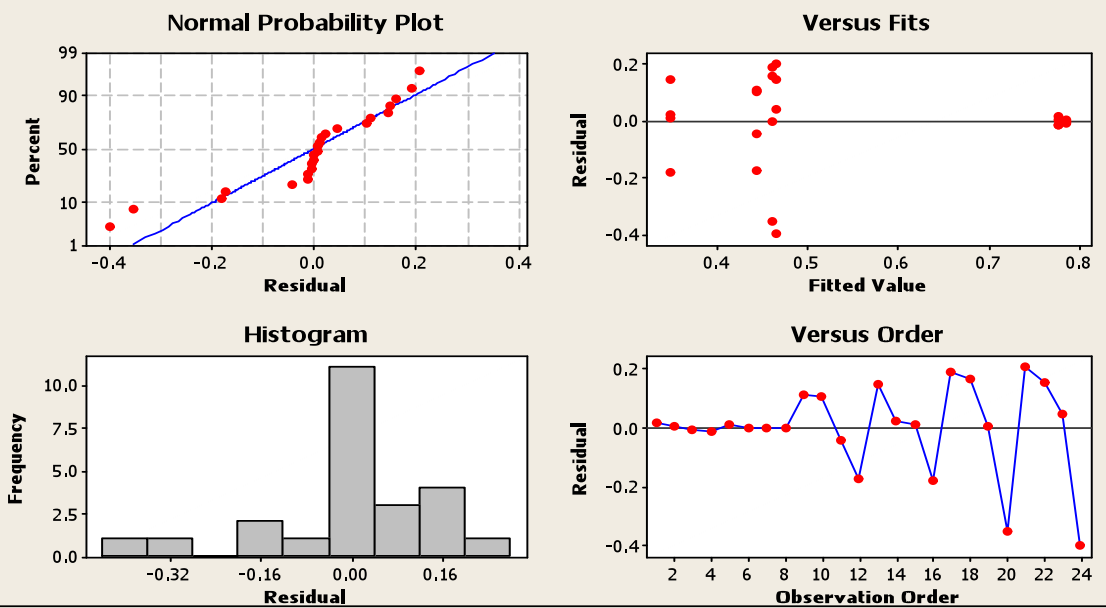
Interaction Plot for (PSII) Efficiency
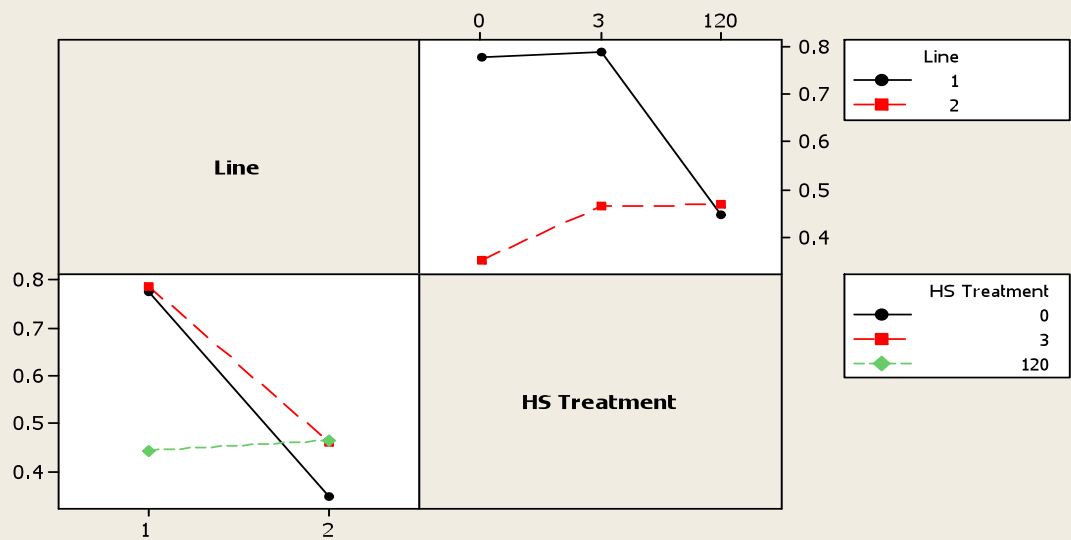
Figure A 5-8: General Linear Model: NPQ versus Line, HS Treatment.

```
Factor        Type   Levels  Values
Line          fixed       2  1 (Local), 2 (Optic)
HS Treatment  fixed       3  0, 3, 120


Analysis of Variance for NPQ, using Adjusted SS for Tests

Source             DF   Seq SS   Adj SS   Adj MS     F     P
Line                1  0.03540  0.03540  0.03540  0.50  0.491
HS Treatment        2  0.34582  0.34582  0.17291  2.42  0.117
Line*HS Treatment   2  0.23091  0.23091  0.11546  1.62  0.226
Error              18  1.28639  1.28639  0.07147
Total              23  1.89852


S = 0.267331   R-Sq = 32.24%   R-Sq(adj) = 13.42%

Grouping Information Using Tukey Method and 95.0% Confidence

      HS
Line  Treatment  N  Mean  Grouping
2        0       4   0.9  A
1       120      4   0.8  A
1        0       4   0.8  A
1        3       4   0.6  A
2       120      4   0.5  A
2        3       4   0.5  A

Means that do not share a letter are significantly different.
```
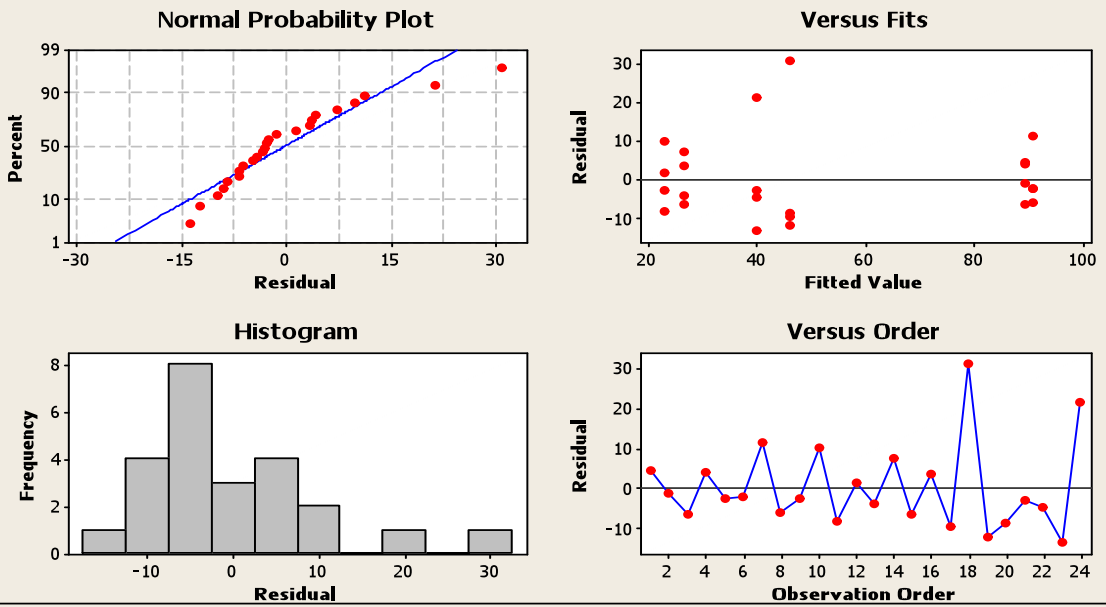
LSD = 0.6

Residual Plots for NPQ

Interaction Plot for NPQ
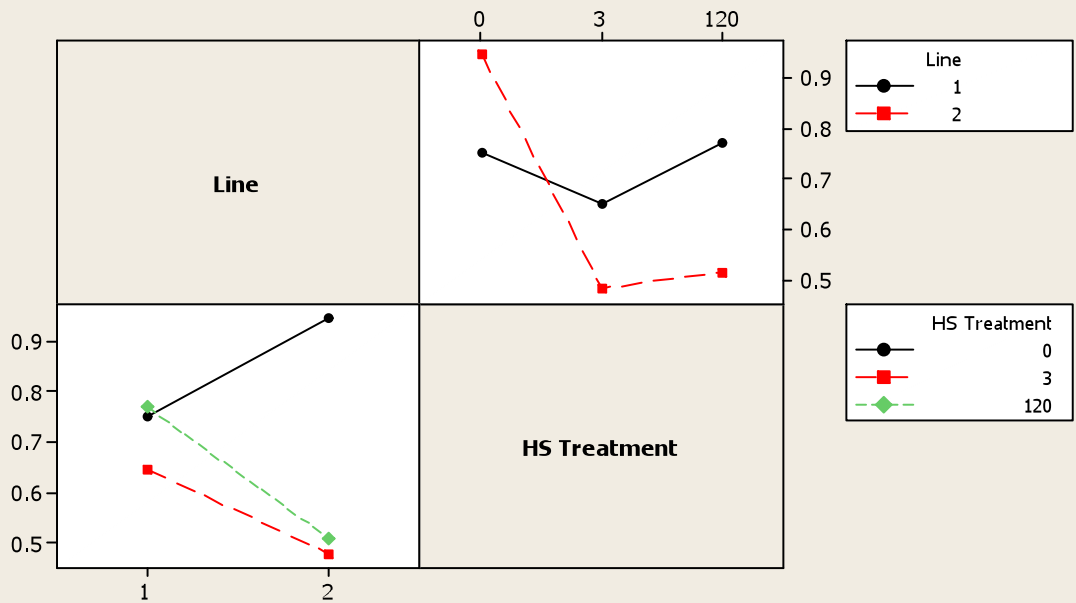
Figure A 5-9: General Linear Model: ETRss versus Line, HS Treatment.

```
Factor        Type   Levels  Values
Line          fixed      2   1 (Local), 2 (Optic)
HS Treatment  fixed      3   0, 3, 120


Analysis of Variance for ETRSS, using Adjusted SS for Tests

Source             DF    Seq SS    Adj SS    Adj MS      F      P
Line                1      50.8      50.8      50.8   0.31  0.583
HS Treatment        2   21597.9   21597.9   10798.9  66.40  0.000
Line*HS Treatment   2      54.8      54.8      27.4   0.17  0.846
Error              18    2927.6    2927.6     162.6
Total              23   24631.1


S = 12.7533   R-Sq = 88.11%   R-Sq(adj) = 84.81%


Grouping Information Using Tukey Method and 95.0% Confidence

       HS
Line   Treatment  N  Mean   Grouping
2         0       4  90.4   A
1         0       4  89.7   A
1        120      4  44.2     B
2        120      4  37.5     B
1         3       4  19.6     B
2         3       4  16.9     B

Means that do not share a letter are significantly different.
```
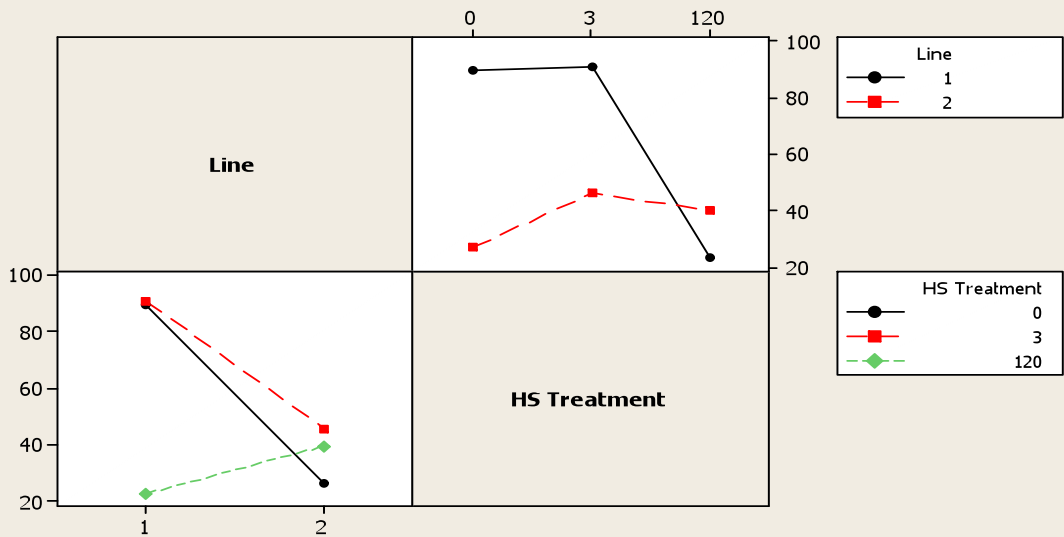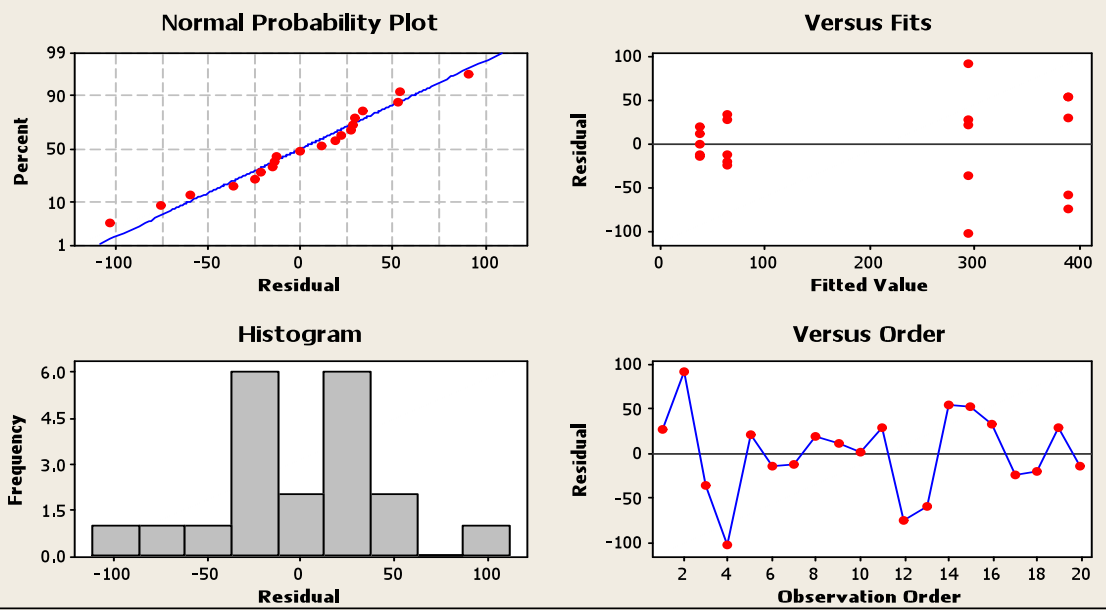
LSD = 28.59
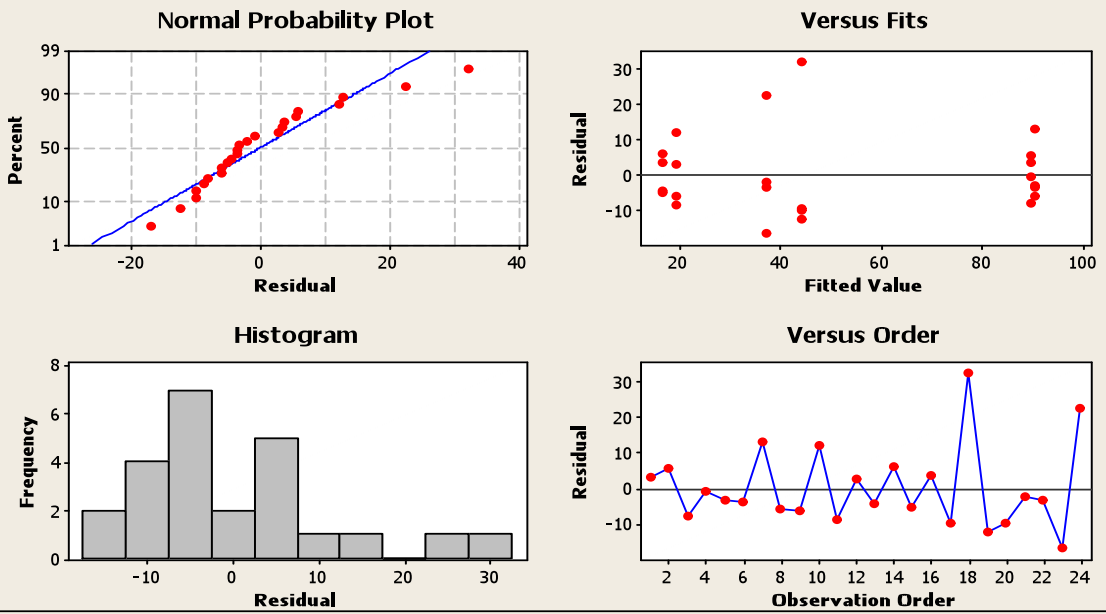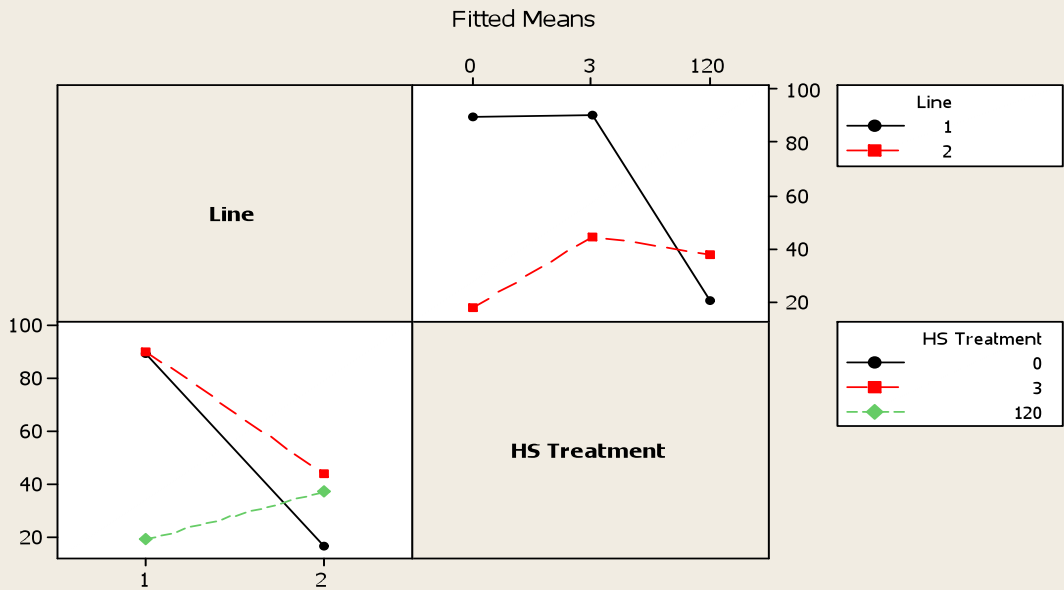
Figure A 5-10: General Linear Model: ETRmax versus Line, HS Treatment.

```
Factor        Type    Levels  Values
Line          fixed      2    1 (Local), 2 (Optic)
HS Treatment  fixed      3    0, 3, 120


Analysis of Variance for ETRMAX, using Adjusted SS for Tests

Source              DF   Seq SS    Adj SS   Adj MS      F      P
Line                 1      1.6       1.6      1.6   0.01  0.918
HS Treatment         2  18318.5   18318.5   9159.2  65.12  0.000
Line*HS Treatment    2    104.5     104.5     52.3   0.37  0.695
Error               18   2531.8    2531.8    140.7
Total               23  20956.4


S = 11.8598   R-Sq = 87.92%   R-Sq(adj) = 84.56%



Grouping Information Using Tukey Method and 95.0% Confidence

      HS
Line  Treatment  N  Mean  Grouping
2        0       4  91.0  A
1        0       4  89.6  A
1      120       4  46.1    B
2      120       4  39.8    B
2        3       4  26.5    B
1        3       4  23.1    B

Means that do not share a letter are significantly different.
```

LSD = 26.63

Residual Plots for ETRMAX

Interaction Plot for ETRMAX
Fitted Means

355

Figure A 5-11: General Linear Model: 3 PGA versus Line, HS Treatment.

```
Factor      Type   Levels  Values
Line        fixed       2  1 (Local), 2 (Optic)
Treatment   fixed       2  1, 2


Analysis of Variance for 3 PGA, using Adjusted SS for Tests

Source          DF  Seq SS  Adj SS  Adj MS       F      P
Line             1   18379   18379   18379    7.02  0.017
Treatment        1  422308  422308  422308  161.28  0.000
Line*Treatment   1    5658    5658    5658    2.16  0.161
Error           16   41895   41895    2618
Total           19  488240


S = 51.1709   R-Sq = 91.42%   R-Sq(adj) = 89.81%



Grouping Information Using Tukey Method and 95.0% Confidence

Line  Treatment  N   Mean  Grouping
2     1          5  389.0  A
1     1          5  294.8    B
2     2          5   64.8      C
1     2          5   37.8      C

Means that do not share a letter are significantly different.
```
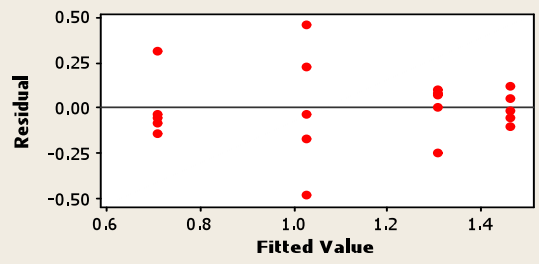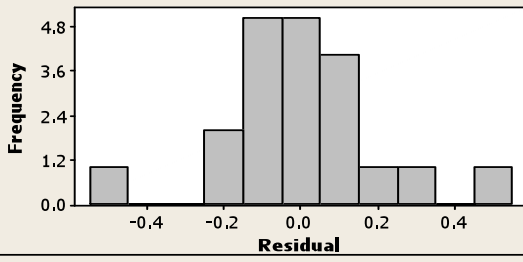
LSD = 90.63

Residual Plots for 3 PGA
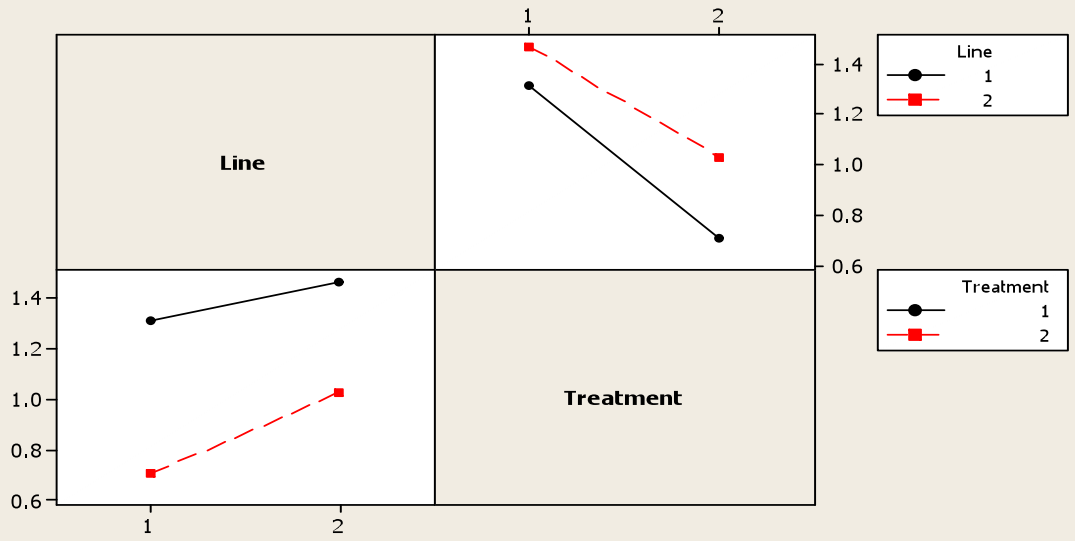
Interaction Plot for 3 PGA
Fitted Means
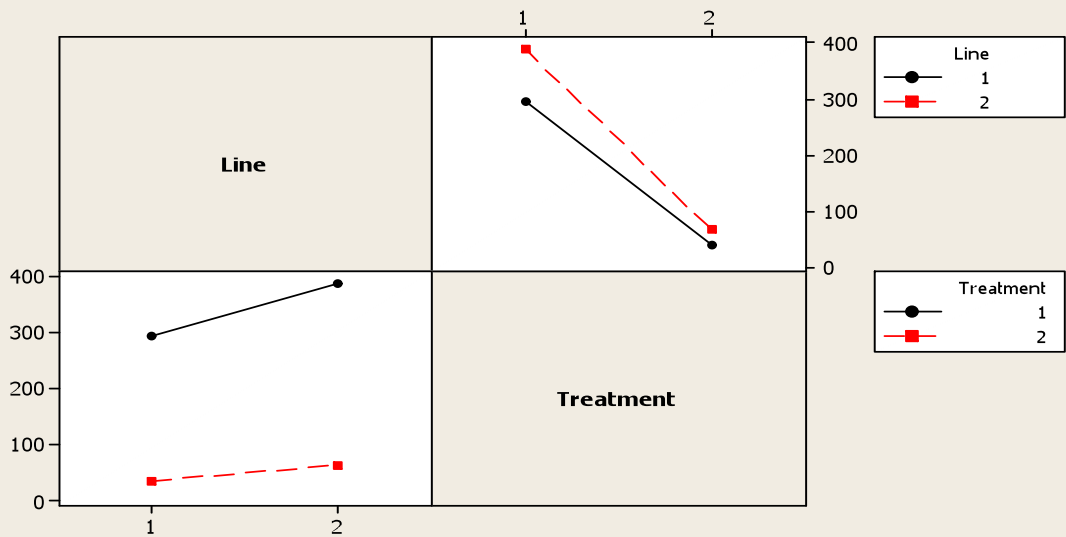
Figure A 5-12: General Linear Model: Log DHAP versus Line, HS Treatment.

```
Factor      Type   Levels  Values
Line        fixed       2  1 (Local), 2 (Optic)
Treatment   fixed       2  1, 2

Analysis of Variance for Log DHAP, using Adjusted SS for Tests

Source          DF   Seq SS   Adj SS   Adj MS      F      P
Line             1  0.28770  0.28770  0.28770   5.87  0.028
Treatment        1  1.35725  1.35725  1.35725  27.69  0.000
Line*Treatment   1  0.03296  0.03296  0.03296   0.67  0.424
Error           16  0.78416  0.78416  0.04901
Total           19  2.46207

S = 0.221382   R-Sq = 68.15%   R-Sq(adj) = 62.18%


Grouping Information Using Tukey Method and 95.0% Confidence

Line  Treatment  N  Mean  Grouping
2     1          5  29.9  A
1     1          5  21.2  A B
2     2          5  13.9    B C
1     2          5   5.5      C

Means that do not share a letter are significantly different.
```

LSD = 12.85

Residual Plots for Log DHAP
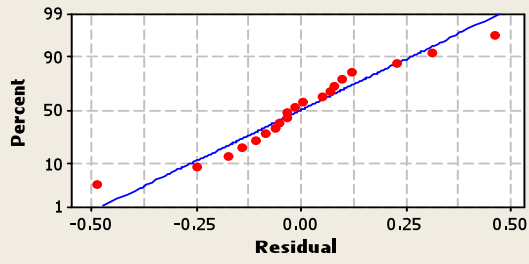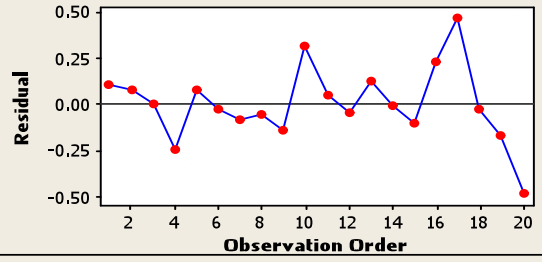
Interaction Plot for Log DHAP
Fitted Means

Figure A 5-13: General Linear Model: S7P versus Line, HS Treatment.

```
Factor      Type   Levels  Values
Line        fixed       2  1 (Local), 2 (Optic)
Treatment   fixed       2  1, 2

Analysis of Variance for S7P, using Adjusted SS for Tests

Source          DF  Seq SS  Adj SS  Adj MS      F      P
Line             1    6130    6130    6130   5.15  0.037
Treatment        1   47400   47400   47400  39.86  0.000
Line*Treatment   1     796     796     796   0.67  0.425
Error           16   19028   19028    1189
Total           19   73354


S = 34.4851   R-Sq = 74.06%   R-Sq(adj) = 69.20%


Grouping Information Using Tukey Method and 95.0% Confidence

Line  Treatment  N   Mean  Grouping
2     1          5  145.6  A
1     1          5   98.0  A B
2     2          5   35.6    B C
1     2          5   13.2      C

Means that do not share a letter are significantly different.
```
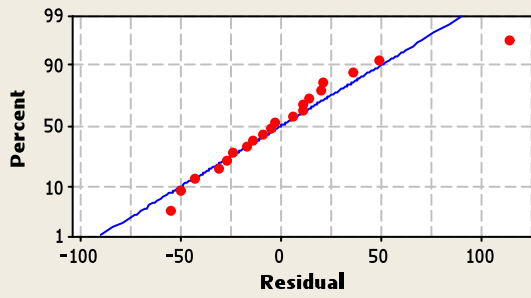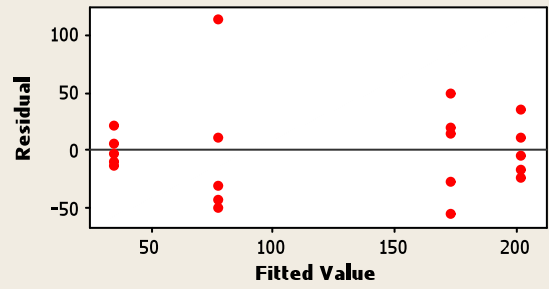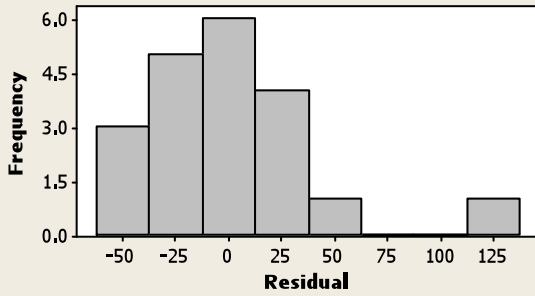
LSD = 62.45

Residual Plots for S7P
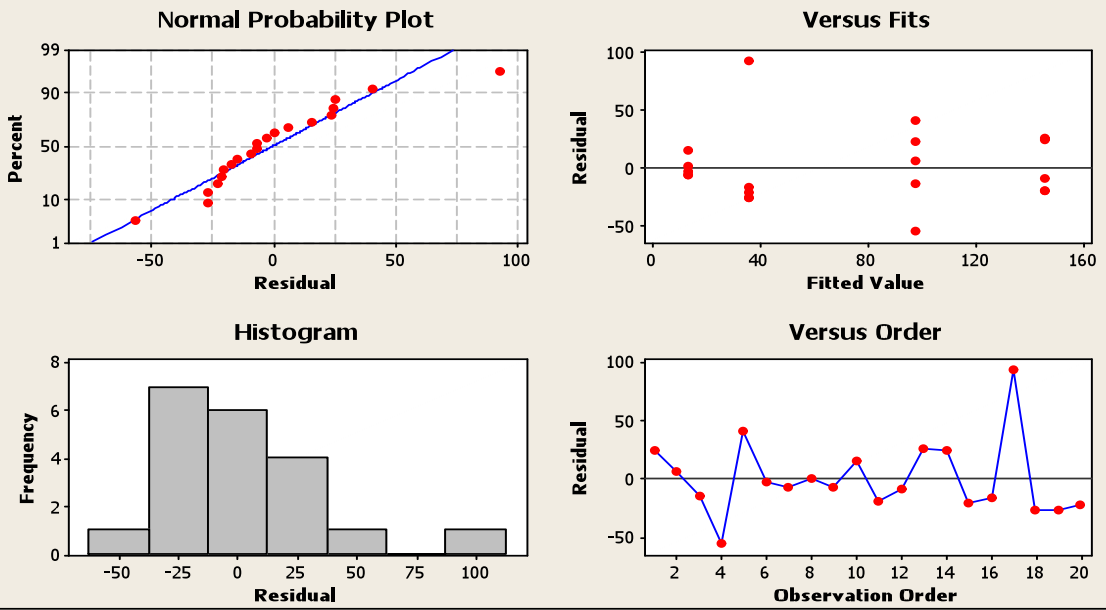
Interaction Plot for S7P
Fitted Means
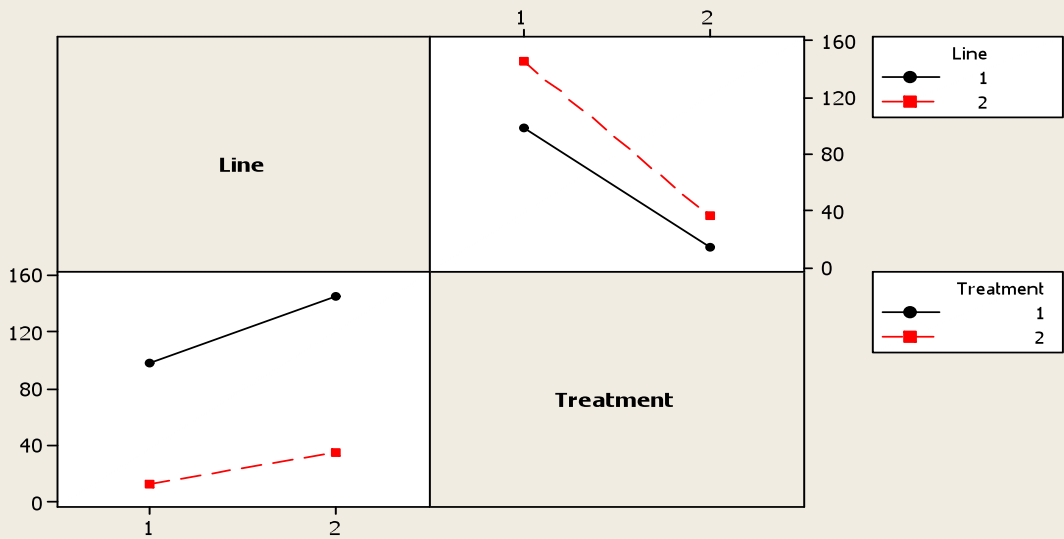
Figure A 5-14: General Linear Model: F6P versus Line, Treatment

```
Factor      Type   Levels  Values
Line        fixed      2   1, 2
Treatment   fixed      2   1, 2


Analysis of Variance for F6P, using Adjusted SS for Tests

Source          DF  Seq SS  Adj SS  Adj MS      F      P
Line             1    6400    6400    6400   3.55  0.078
Treatment        1   86584   86584   86584  48.05  0.000
Line*Treatment   1     227     227     227   0.13  0.727
Error           16   28831   28831    1802
Total           19  122042


S = 42.4490   R-Sq = 76.38%   R-Sq(adj) = 71.95%

Grouping Information Using Tukey Method and 95.0% Confidence

Line  Treatment  N   Mean  Grouping
2     1          5  202.2  A
1     1          5  173.2  A
2     2          5   77.4     B
1     2          5   34.9     B

Means that do not share a letter are significantly different.
```
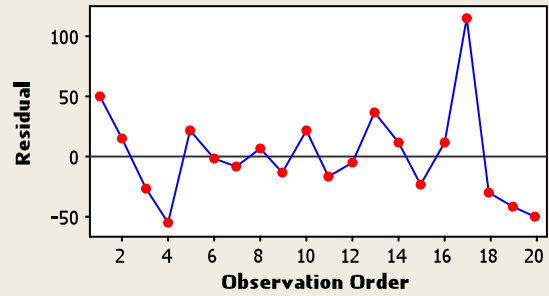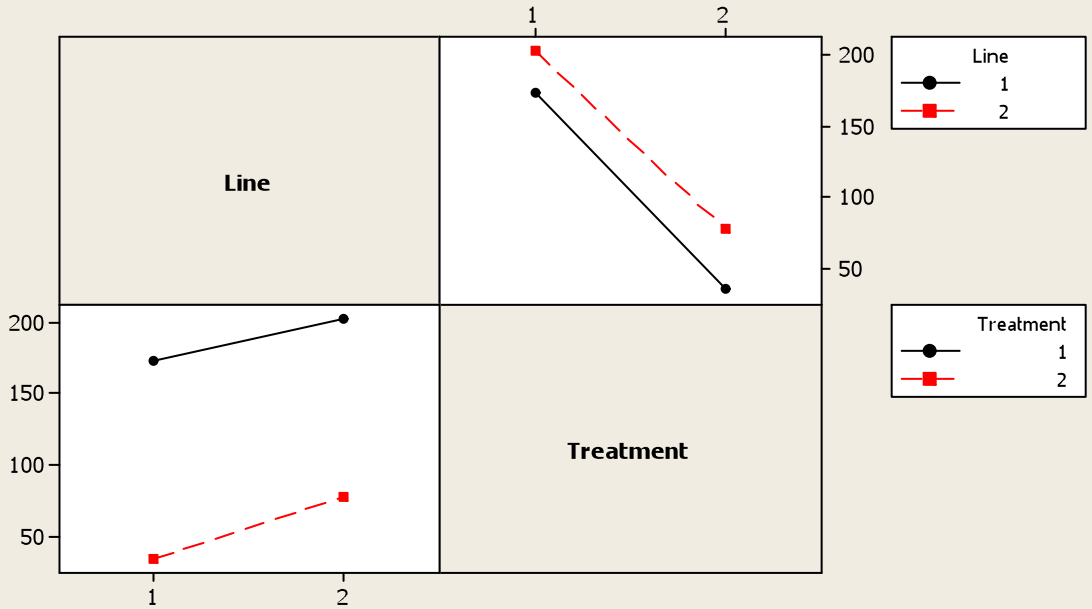
LSD = 76.9

Residual Plots for F6P

Interaction Plot for F6P

363

Figure A 5-15: General Linear Model: Log G1P versus Line, HS Treatment.

```
Factor      Type   Levels  Values
Line        fixed      2  1 (Local), 2 (Optic)
Treatment   fixed      2  1, 2

Analysis of Variance for Log G1P, using Adjusted SS for Tests

Source          DF   Seq SS   Adj SS   Adj MS     F      P
Line             1  0.16092  0.16092  0.16092   6.53  0.021
Treatment        1  0.10774  0.10774  0.10774   4.37  0.053
Line*Treatment   1  0.11084  0.11084  0.11084   4.50  0.050
Error           16  0.39411  0.39411  0.02463
Total           19  0.77360


S = 0.156945   R-Sq = 49.06%   R-Sq(adj) = 39.50%


Grouping Information Using Tukey Method and 95.0% Confidence

Line  Treatment  N  Mean  Grouping
2     2          5  40.6  A
2     1          5  36.0  A B
1     1          5  33.9  A B
1     2          5  17.9    B

Means that do not share a letter are significantly different.
```
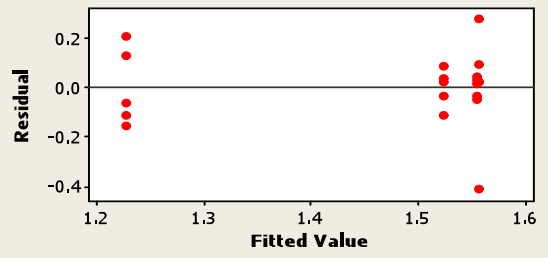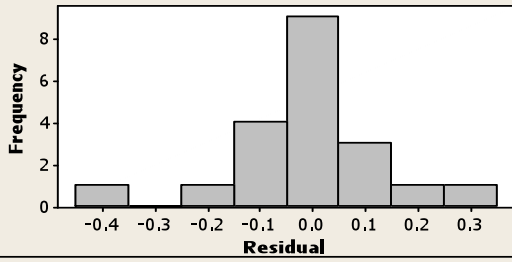
LSD = 19.8

Residual Plots for Log G1P
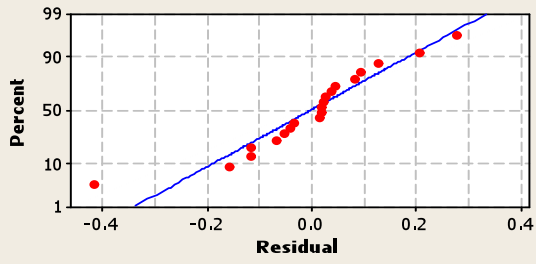
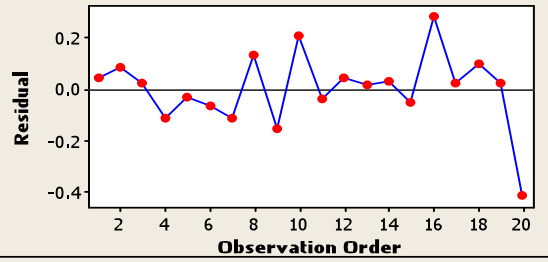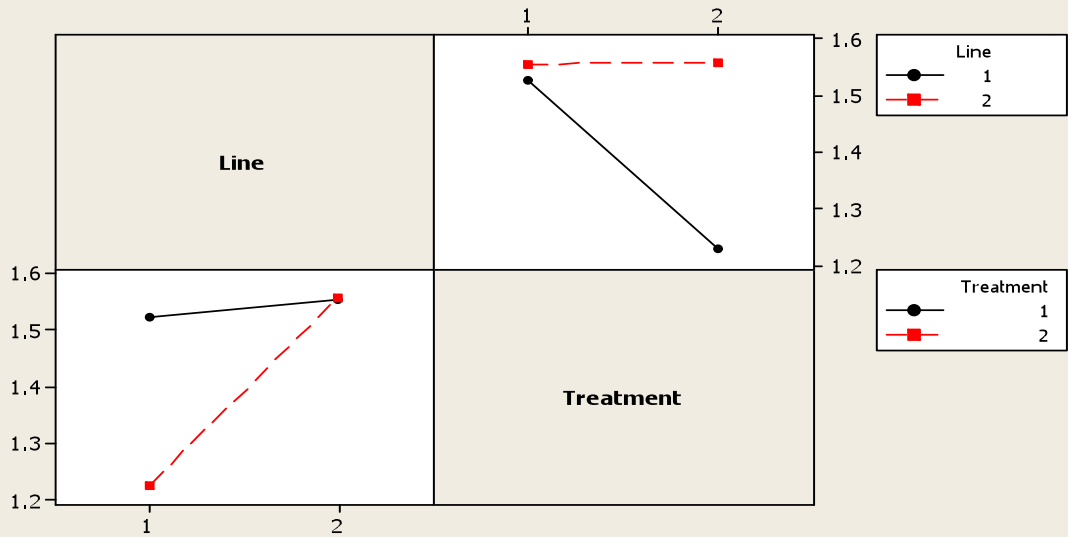Interaction Plot for Log G1P
Fitted Means

Figure A 5-16: General Linear Model: G6P versus Line, Treatment

```
Factor      Type   Levels  Values
Line        fixed       2  1, 2
Treatment   fixed       2  1, 2


Analysis of Variance for G6P, using Adjusted SS for Tests

Source          DF  Seq SS  Adj SS  Adj MS      F      P
Line             1    1442    1442    1442   1.91  0.185
Treatment        1   37978   37978   37978  50.44  0.000
Line*Treatment   1     536     536     536   0.71  0.411
Error           16   12046   12046     753
Total           19   52002


S = 27.4385   R-Sq = 76.84%   R-Sq(adj) = 72.49%


Grouping Information Using Tukey Method and 95.0% Confidence

Line  Treatment  N   Mean  Grouping
2     1          5  149.6  A
1     1          5  143.0  A
2     2          5   72.8    B
1     2          5   45.5    B

Means that do not share a letter are significantly different.
```
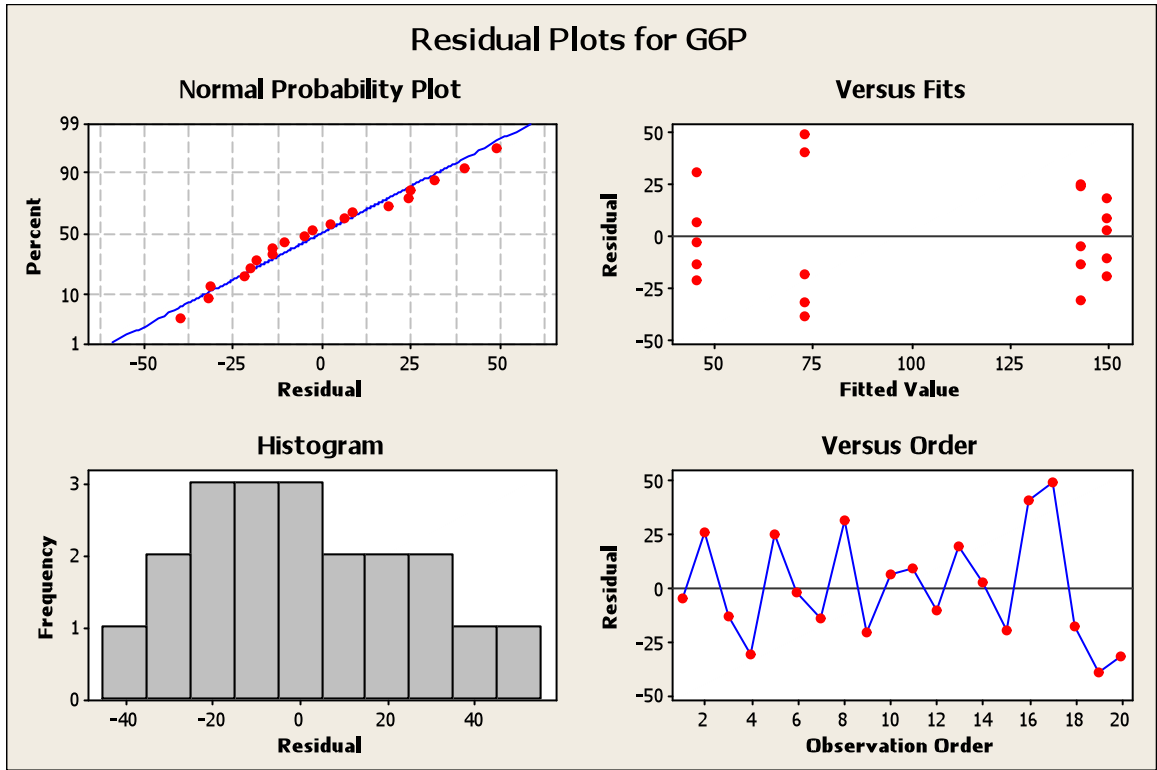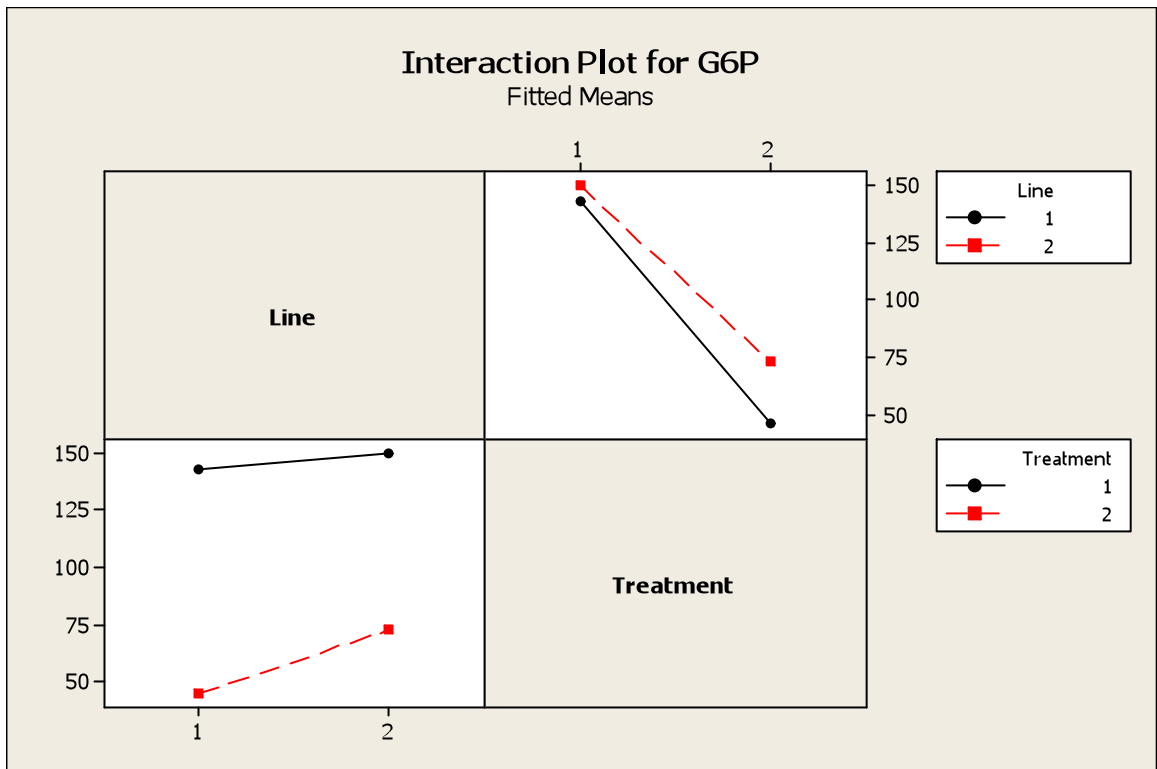
LSD = 50.05

Residual Plots for G6P

Interaction Plot for G6P

Figure A 5-17: General Linear Model: Log ADPG versus Line, HS Treatment.

```
Factor      Type   Levels  Values
Line        fixed       2  1 (Local), 2 (Optic)
Treatment   fixed       2  1, 2

Analysis of Variance for Log ADPG, using Adjusted SS for Tests

Source          DF  Seq SS  Adj SS  Adj MS      F      P
Line             1  0.2277  0.2277  0.2277   2.10  0.166
Treatment        1  4.6631  4.6631  4.6631  43.10  0.000
Line*Treatment   1  0.0001  0.0001  0.0001   0.00  0.971
Error           16  1.7310  1.7310  0.1082
Total           19  6.6219

S = 0.328917   R-Sq = 73.86%   R-Sq(adj) = 68.96%


Grouping Information Using Tukey Method and 95.0% Confidence

Line  Treatment  N  Mean  Grouping
1     1          5  2.6   A
2     1          5  1.5   A B
1     2          5  0.4     B
2     2          5  0.3     B

Means that do not share a letter are significantly different.
```
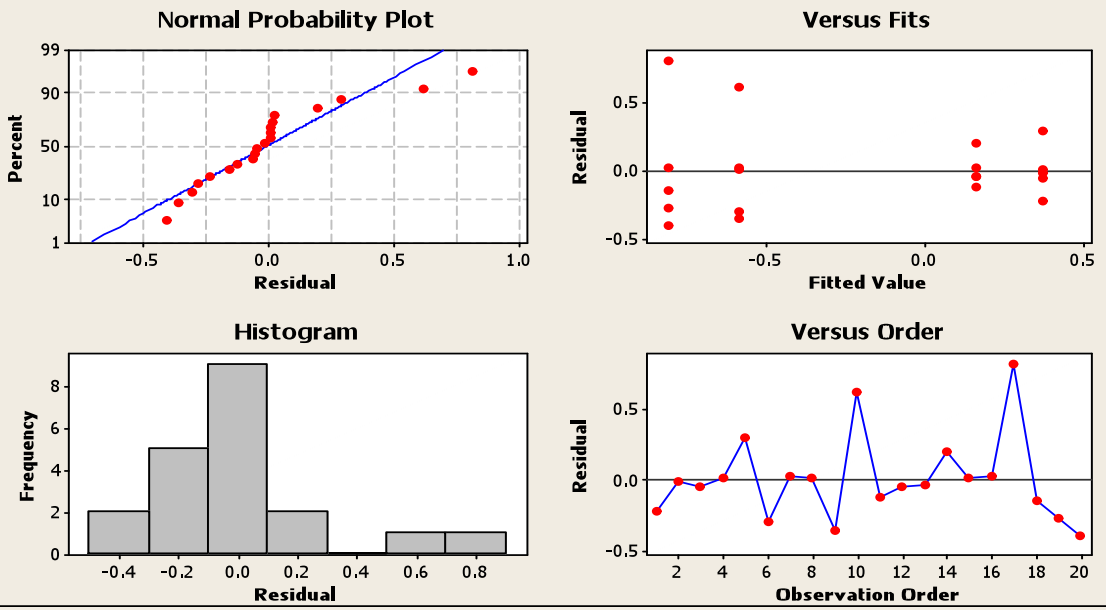
LSD = 1.29

Residual Plots for Log ADPG

Interaction Plot for Log ADPG
Fitted Means